NAC INTERNATIONAL

Atlanta Corporate Headquarters
3930 East Jones Bridge Road, Suite 200
Norcross, GA 30092
Phone 770-447-1144
Fax 770-447-1797
www.nacintl.com

August 20, 2008

U.S. Nuclear Regulatory Commission
11555 Rockville Pike
Rockville, MD 20852-2738

Attn: Document Control Desk

Subject: Responses to Request for Additional Information (RAI) on the Amendment Application for CoC No. 9225 for the NAC-LWT Cask to Incorporate PWR Mixed-Oxide (MOX) Fuel Rods as Authorized Contents (TAC L24181)

Docket No. 71-9225

Reference:
1. Model No. NAC-LWT Package, U.S. Nuclear Regulatory Commission (NRC) Certificate of Compliance (CoC) No. 9225, Revision 48, July 2008
2. Safety Analysis Report (SAR) for the NAC Legal Weight Truck Cask, Revision 38, NAC International, November 2007
3. Submittal of a Request for an Amendment of Certificate of Compliance (CoC) No. 9225 for the NAC-LWT Cask to Incorporate PWR Mixed-Oxide (MOX) Fuel Rods as Authorized Contents, NAC International, January 25, 2008
4. Request for Additional Information for Review of the Certificate of Compliance No. 9225, Revision for the Model No. NAC-LWT Package, NRC, July 15, 2008

NAC International (NAC) herewith provides responses to the RAI (Reference 4) on NAC's application (Reference 3) for an amendment to the CoC (Reference 1) to incorporate various changes to the NAC-LWT contents and the operating procedures as described in Reference 3.

This submittal has been prepared in accordance with discussions between NRC staff and NAC, and includes eight copies of this transmittal letter, eight copies of the RAI questions with the NAC responses presented in the standard NAC RAI response format, and eight copies of the Revision LWT-08E changed SAR pages for Reference 2. The changed NAC-LWT SAR pages incorporate the requested information.

Based on the August 13, 2008 teleconference with SFST personnel, in addition to the responses to Reference 4, NAC has included changed SAR pages in Revision LWT-08E in Chapter 1, Section 1.1, and Chapter 3, Section 3.4.4.3 and Section 3.4.4.7, stating that PWR rods, as well as PWR MOX/UO_2 rods may include Integral Fuel Burnable Absorber (IFBA) rods. The presence of IFBA rods does not provide a significant contribution to fuel rod gas generation or cask cavity pressure.

ED20080111

NM550/
NMSS

Consistent with NAC administrative practice, this proposed revision is numbered to uniquely identify the applicable changed pages. Revision bars mark the SAR text changes (on Revision LWT-08E pages) that are proposed. Upon final approval, the changed pages will be reformatted, assigned the next appropriate revision number, and incorporated into the NAC-LWT SAR. A List of Effective Pages is included for clarity.

Responses to two RAI questions (5-5 and 5-6) include submittal of NAC proprietary data input files for the MOX shielding analyses on electronic media. The CD containing the NAC proprietary information is included in a separate sealed envelope labeled "NAC PRORIETARY Enclosure." Also enclosed is a Proprietary Information Affidavit executed by Thomas A. Danner, NAC Vice President, Engineering, in accordance with 10 CFR 2.390. The affidavit covers the MOX shielding data input files on CD media that is provided in this submittal.

The approval of the PWR MOX fuel rod contents will permit the transport of irradiated PWR MOX and PWR UO_2 fuel rods to receiving facilities for the completion of post-irradiation examinations (PIE) to evaluate the performance of PWR MOX fuel rods in commercial PWR reactor facilities. It is the intent of the PWR MOX fuel supplier (MOX Services) to complete the transport of the irradiated MOX rods as soon as possible after discharge from the reactor. Per the original amendment request (Reference 3), the PWR MOX fuel rods will be acceptable for loading and transport 90 days after reactor discharge, which would allow the initial group of PWR MOX fuel rods to be transported as soon as October 2008. In order to meet the earliest transport date and the current cask loading window, NAC requests approval of the amendment by September 15, 2008. This will allow mobilization of equipment and preparation of site-specific loading procedures to support the planned October 2008 loading date.

If you have any comments or questions, please contact me on my direct line at 678-328-1274.

Sincerely,

Anthony L. Patko
Director, Licensing
Engineering

Enclosures

NAC INTERNATIONAL

NAC INTERNATIONAL
AFFIDAVIT PURSUANT TO 10 CFR 2.390

Thomas A. Danner (Affiant), Vice President, Engineering, of NAC International, hereinafter referred to as NAC, at 3930 East Jones Bridge Road, Norcross, Georgia 30092, being duly sworn, deposes and says that:

1. Affiant has reviewed the information described in Item 2 and is personally familiar with the trade secrets and privileged information contained therein, and is authorized to request its withholding.

2. The information to be withheld includes the following NAC proprietary input files that are being provided on the enclosed CD in support of the technical review to incorporate PWR Mixed-Oxide (MOX) fuel rods as authorized contents in the NAC-LWT cask.

   - NAC Proprietary MOX Shielding Input Files

   The information on this CD includes detailed analysis methods and/or results that are being used for the NAC-LWT transport cask. NAC is the owner of the information on the CD. Thus, the above-identified information is considered NAC Proprietary.

3. NAC makes this application for withholding of proprietary information based upon the exemption from disclosure set forth in: the Freedom of Information Act ("FOIA"); 5 USC Sec. 552(b)(4) and the Trade Secrets Act; 18 USC Sec. 1905; and NRC Regulations 10 CFR Part 9.17(a)(4), 2.390(a)(4), and 2.390(b)(1) for "trade secrets and commercial financial information obtained from a person, and privileged or confidential" (Exemption 4). The information for which exemption from disclosure is herein sought is all "confidential commercial information," and some portions may also qualify under the narrower definition of "trade secret," within the meanings assigned to those terms for purposes of FOIA Exemption 4.

4. Examples of categories of information that fit into the definition of proprietary information are:

   a. Information that discloses a process, method, or apparatus, including supporting data and analyses, where prevention of its use by competitors of NAC, without license from NAC, constitutes a competitive economic advantage over other companies.

   b. Information that, if used by a competitor, would reduce their expenditure of resources or improve their competitive position in the design, manufacture, shipment, installation, assurance of quality or licensing of a similar product.

   c. Information that reveals cost or price information, production capacities, budget levels or commercial strategies of NAC, its customers, or its suppliers.

   d. Information that reveals aspects of past, present or future NAC customer-funded development plans and programs of potential commercial value to NAC.

e. Information that discloses patentable subject matter for which it may be desirable to obtain patent protection.

The information that is sought to be withheld is considered to be proprietary for the reasons set forth in Items 4.a, 4.b, and 4d.

5. The information to be withheld is being transmitted to the NRC in confidence.

6. The information sought to be withheld, including that compiled from many sources, is of a sort customarily held in confidence by NAC, and is, in fact, so held. This information has, to the best of my knowledge and belief, consistently been held in confidence by NAC. No public disclosure has been made, and it is not available in public sources. All disclosures to third parties, including any required transmittals to the NRC, have been made, or must be made, pursuant to regulatory provisions or proprietary agreements, which provide for maintenance of the information in confidence. Its initial designation as proprietary information and the subsequent steps taken to prevent its unauthorized disclosure are as set forth in Items 7 and 8 following.

7. Initial approval of proprietary treatment of a document/information is made by the Vice President, Engineering, the Project Manager or the Director, Licensing – the persons most likely to know the value and sensitivity of the information in relation to industry knowledge. Access to proprietary documents within NAC is limited via "controlled distribution" to individuals on a "need-to-know" basis. The procedure for external release of NAC proprietary documents typically requires the approval of the Project Manager based on a review of the documents for technical content, competitive effect and accuracy of the proprietary designation. Disclosures of proprietary documents outside of NAC are limited to regulatory agencies, customers and potential customers and their agents, suppliers, licensees and contractors with a legitimate need for the information, and then only in accordance with appropriate regulatory provisions or proprietary agreements.

8. NAC has invested a significant amount of time and money in the research, development, engineering and analytical costs to develop the information that is sought to be withheld as proprietary. This information is considered to be proprietary because it contains detailed descriptions of analytical approaches, methodologies, technical data and evaluation results not available elsewhere. The precise value of the expertise required to develop the proprietary information is difficult to quantify, but it is clearly substantial.

9. Public disclosure of the information to be withheld is likely to cause substantial harm to the competitive position of NAC, as the owner of the information, and reduce or eliminate the availability of profit-making opportunities. The proprietary information is part of NAC's comprehensive spent fuel storage and transport technology base, and its commercial value extends beyond the original development cost to include the development of the expertise to determine and apply the appropriate evaluation process. The value of this proprietary information and the competitive advantage that it provides to NAC would be lost if the information were disclosed to the public. Making such information available to other parties,

including competitors, without their having to make similar investments of time, labor and money would provide competitors with an unfair advantage and deprive NAC of the opportunity to seek an adequate return on its large investment.

STATE OF GEORGIA, COUNTY OF GWINNETT

Mr. Thomas A. Danner, being duly sworn, deposes and says:

That he has read the foregoing affidavit and the matters stated herein are true and correct to the best of his knowledge, information and belief.

Executed at Norcross, Georgia, this 20th day of August 2008.

Thomas A. Danner
Vice President, Engineering
NAC International

Subscribed and sworn before me this 20th day of August, 2008.

Notary Public

NAC INTERNATIONAL

RESPONSE TO THE

UNITED STATES
NUCLEAR REGULATORY COMMISSION

REQUEST FOR ADDITIONAL INFORMATION

JULY 15, 2008

FOR REVIEW OF THE CERTIFICATE OF COMPLIANCE NO. 9225, REVISION FOR THE MODEL NO. NAC-LWT PACKAGE TO ADD MOX RESEARCH REACTOR FUEL

(TAC NO. L24181, DOCKET NO. 71-9225)

AUGUST 20, 2008

TABLE OF CONTENTS

NAC INTERNATIONAL RESPONSE TO REQUEST FOR ADDITIONAL INFORMATION

EDITORIAL REVIEW

0-1 Provide editorial changes or clarifications on the following items.

1. Page 1-1: The two bullet items (at the bottom of the page) that are marked with revision bars do not seem to be relevant to the current revision. Provide correction or explanation.

2. Page 5.1.1-1: The bullet item "up to 25 PWR or BWR UO_2 high burnup (up to 80,000 MWd/MTU) rods" which is marked with a revision bar does not seem to be relevant to this amendment request. Provide an explanation and necessary analyses if needed.

3. Page 5.1.1-1: The statement "The 25 high burnup PWR and BWR rods may be transported in three configurations: ..." which is marked with a revision bar seems also to indicate that this amendment is seeking approval of 25 high burnup PWR or BWR rods packages. Clarify if this amendment is seeking approval to transport 25 high burnup PWR and BWR rods per package design.

4. Page 6-1: Add the CSI value to the package contents that includes the PWR MOX spent fuel rods package.

This information is needed pursuant to the requirements of 10 CFR 71.33.

NAC International Response

1. The NAC-LWT cask is permitted to transport up to 55 segmented TPBARs. This payload, included in SAR Table 1.1-1, was submitted to the NRC in 2006 and was approved via CoC Revision No. 43 in December 2006. This particular payload had not been included in the Section 1 description in previous submittals. To correct for this editorial item, the up to 55 segmented TPBARs were added to the 300 TPBAR cask configuration description on Page 1-1 of the SAR.

NAC International Response to RAI 0-1 (cont'd)

2. The line was modified to include "UO_2" into the payload description. The MOX amendment requested MOX PWR rods to be included as permissible payload. Without the text modification, there was no clear differentiation as to the type of fuel material for which 25 rods may be transported. No change in payload is requested within the 25-rod context.

3. The existing approved content for the NAC-LWT cask is 25 high burnup PWR and BWR rods. Modification to this line was made to clarify that 25 high burnup PWR and BWR rods (i.e., the 25 UO_2 not 16 MOX/UO_2 payload) may be transported in three configurations.

4. The paragraph on page 6-1 listing all CSIs is replaced by a tabular listing. The RAI response tabular listing of CSIs includes the CSI of 0 for the MOX contents. Previous text included an editorial error in that a semicolon rather than a comma separated MOATA from spiral fuel leading to the question on the appropriate CSIs for a number of payloads, including MOX.

NAC INTERNATIONAL RESPONSE TO REQUEST FOR ADDITIONAL INFORMATION

CHAPTER 1 – GENERAL INFORMATION REVIEW

1-1 Provide Transport Index (TI) values in the SAR for the package of the PWR MOX spent fuel rods, the package of the mixed PWR MOX and UO_2 spent fuel rods, and up to 9 depleted burnable poison rods in the PWR MOX spent fuel package.

Chapter 1 of the SAR must include information on the TIs of all proposed PWR MOX spent fuel with/without depleted burnable poison rods packages. The revised SAR, however, does not contain this piece of information for the proposed packages.

This information is needed pursuant to the requirements of 10 CFR 71.33.

NAC International Response

Page 1-2, last paragraph, states:
"The estimated Transport Index (TI) for shielding for the prior listed contents is shown in Table 5.1.1-1. The actual TI for individual shipments will be determined in accordance with 10 CFR 71.4 by the licensee."

This text provides the TIs by reference and is considered by NAC to be sufficient to meet 10 CFR 71 requirements. As Table 5.1.1-1 does not include a reference to the BPRA component of the combined MOX/UO_2 payload, the table is modified to include this component.

Fuel Type	-	PWR MOX or UO_2 rods (including up to 9 BPRAs)
	-	5.0 wt % maximum ^{235}U initial enrichment for UO_2 rods 7.0 wt % fissile Pu for MOX rods
	-	62,500 MWd/MTHM maximum average burnup
	-	2.3 kW/cask maximum decay heat
	-	Minimum cool time 90 days (120 days for Power Grade MOX)
Fuel Form	-	Undamaged rods in a rod holder
Quantity	-	Up to 16 (any combination of UO_2 or MOX) fuel rods plus up to 9 BPRAs
Source of Fuel	-	Commercial PWR nuclear power reactor
Transport Index	-	28

NAC INTERNATIONAL RESPONSE TO REQUEST FOR ADDITIONAL INFORMATION

CHAPTER 3 THERMAL REVIEW

3-1 Delete the second sentence reference in Section 3.4.1.7 to the BWR decay heat of 2.1 kW as being "per rod," since it is actually the total BWR heat loading.

10 CFR 71.7 requires that "information provided to the Commission by a licensee, certificate holder, or an applicant for a license or CoC.....must be complete and accurate in all material respects."

NAC International Response

In order to clarify that the heat loads reported in Section 3.4.1.7 of the LWT SAR are a maximum for the rod contents and not a per rod heat load, the second sentence of Section 3.4.1.7 has been revised to read as follows: "The decay heat for the PWR fuel rod contents is 2.3 kW with a corresponding peaking factor of 1.1. The decay heat for the BWR fuel rod contents is 2.1 kW with a peaking factor of 1.22."

NAC INTERNATIONAL RESPONSE TO REQUEST FOR ADDITIONAL INFORMATION

CHAPTER 3 THERMAL EVALUATION

3-2 Specify the allowable component temperatures that are mentioned in Section 3.4.1.15, which refers to Table 3.4-10 for normal conditions of transport (NCT). Additionally, specify the allowable temperatures that are mentioned in Section 3.5.3.15, which refers to Table 3.5.3.5 for hypothetical accident conditions (HAC).

These sections should clearly identify the NCT and HAC allowable temperatures for the important to safety components of the O-ring seals (including identification as to which seals are being used), the lead gamma shield, the ethylene glycol & water neutron shield (noting that is assumed to fail for HAC and is not required to be met for that condition), and any other vital component temperatures (e.g., fuel cladding) for the NAC-LWT transportation package. Section 3.3, "Technical Specifications of Components," lists the safe operating range of the aforementioned components important to safety, but does not discuss the cladding allowable temperature limit.

10 CFR 71.7 requires that "information provided to the Commission by a licensee, certificate holder, or an applicant for a license or CoC.....must be complete and accurate in all material respects."

NAC International Response

The last paragraph of Section 3.4.1.15 has been revised to clarify that the bounding temperatures for NAC-LWT cask safety components under normal conditions of transport (NCT) are maintained within their allowable limits. The last paragraph of Section 3.4.1.15 has been revised to read as follows:

"Maximum temperatures for package components with the NAC-LWT cask configured for high burnup PWR and BWR fuel rods are summarized in Table 3.4-10. As the analyzed BWR fuel rod content condition is bounding, the temperatures presented in Table 3.4-10, Condition 1 (helium cavity gas backfill) provide bounding temperatures for the PWR MOX fuel rod content configuration. As shown in Table 3.4-10, maximum calculated component temperatures for all

NAC International Response to RAI 3-2 (cont'd)

critical safety components including the fuel rod cladding, the lid metallic containment seal, the Alternate B port cover metallic containment seals, the lead gamma shield and the liquid neutron shield are maintained within their allowable temperature limits as further defined in Section 3.3. Note that for the transport of PWR MOX fuel rods, metallic containment seals will be installed on the lid and Alternate B port cover in accordance with the NAC-LWT cask leaktight transport configuration specified for the PWR MOX fuel rod contents."

In addition, Table 3.4-10 has been revised (changes highlighted) as follows:

Table 3.4-10 PWR and BWR High Burnup Fuel Rods Maximum Component Temperatures – Normal Transport Condition

Conditions: 100°F Ambient Temperature Solar Insolation
2.1 Kilowatts Decay Heat Load
Condition 1: NAC-LWT (Transported in an ISO Container)
Cavity Gas: Helium

Component	Component Temperature (°F)	Allowable Temperature (°F)
Liquid Neutron Shield	306	N/A
Outer Shell	308	800
Lead Gamma Shield	375	600
Inner Shell	385	800
Lid Metallic Containment Shell	385	800
Port Cover Containment Shell	385	550
Basket (maximum)	387	800(1)
Cladding (maximum)	671	752(2)
Aluminum PWR Insert	394	700(3)
Stainless Steel Can Weldment	500	800(2)
Average Cavity Gas	506	N/A

(1) Allowable temperatures greater than 800°F for stainless steel can be used provided stress limits in ASME III, Subsection NH, are employed in the stress evaluations.

(2) The maximum allowable temperature under NCT for PWR, BWR and PWR MOX fuel rod cladding is 752°F (400°C) per ISG-11, Revision 3.

(3) The aluminum insert is not a structural component. The primary consideration in establishing the safe operating range of the aluminum is maintaining the integrity of the aluminum. According to MIL-HDBK-5F, it can be shown that aluminum at 700°F retains component performance.

NAC International Response to RAI 3-2 (cont'd)

Table 3.4-10 PWR and BWR High Burnup Fuel Rods Maximum Component Temperatures – Normal Transport Condition (cont'd)

Condition 2: NAC-LWT (Transported via Truck Trailer)
Cavity Gas: Air

Component	Temperature (°F)
Inner Shell	274
Basket (maximum)	280
Aluminum PWR Insert	286
Stainless Steel Can Weldment	538
Cladding (maximum)	896
Average Cavity Gas	541

Similarly, Section 3.5.3.13 has been revised to show that the maximum temperatures for the critical safety components of the NAC-LWT cask with PWR MOX fuel rod contents under the HAC are maintained within their allowable temperature limits. Section 3.5.3.13 is revised to read as follows:

"The PWR/BWR Rod Transport Canister and 5 × 5 insert used for the transport of 16 PWR MOX high burnup rods is the same design as the one used for the BWR and PWR high burnup rods. The heat load used in the evaluation of the BWR high burnup rods, which includes the effect of the peaking factor, bounds that of the PWR MOX high burnup rods (see Section 3.4.1.15). As presented in Section 3.4.1.15, the reduced conductivity of the PWR MOX fuel rods does not affect the heat transfer through the canister or insert or, in the case of the transient, it does not affect the ability to absorb and retain heat. The initial temperatures of the fuel rods are conservative since the heat load used in the steady-state evaluation is for 25 rods of the design basis heat load (see Section 3.4.1.7), rather than the 16 PWR MOX high burnup rods. Therefore, the maximum component temperatures under the hypothetical accident condition (HAC) are identical to the results reported in Table 3.5-1 for the PWR assembly contents, which were used as the boundary condition for the analysis for PWR and BWR high burnup fuel rod contents and, therefore, are applicable to the PWR MOX fuel rod contents. Table 3.5-1 shows that the lid metallic seal, Alternate B port cover metallic face seal and lead gamma shield are below their respective temperature limits. In addition, the bounding temperatures for the PWR and BWR rod

NAC International Response to RAI 3-2 (cont'd)

contents reported in Table 3.5-4, which are bounding for the PWR MOX fuel rod contents, show that the can weldment and fuel rod cladding temperatures under the HAC are below their respective limits."

Table 3.5-1 has been revised (changes highlighted) to incorporate the metallic face seal used on the Alternate B port cover used for the transport of MOX fuel rod contents, as follows:

Table 3.5-1 Maximum Component Temperatures (°F) During the Fire Accident (Design Basis PWR Fuel, 2.5 kW Heat Load)

Component	Component Temperature (°F)	Temperature Limit (°F)
O-rings: TFE	558	735
Metallic	571(3)	800
Cask radial outer surface	1460	----(1)
Neutron shield region	1435	----(1)
Radial lead gamma shield	578	600
Bottom lead gamma shield	564	600
Inner stainless steel shell	505	800
Fuel basket outer wall	507	700(2)
Fuel rod cladding	703	1058
Alternate Port Cover	--	--
Bolt head	886	900
Bolt threads	807	900
Alternate Port Cover O-ring – bore	565(4)	550
Alternate Port Cover O-ring – face	547	550
Alternate B Port Cover metallic face seal	547	800

Notes:

(1) No upper limit established. The loss of the liquid neutron shield is assumed under HAC

(2) The primary consideration in establishing the safe operating range of the aluminum is maintaining the integrity of the aluminum. According to MIL-HDBK-5F, it can be shown that aluminum at 700°F retains component performance.

(3) The maximum port cover seal temperature is conservatively used to bound the maximum temperature of the metallic seal.

(4) Should the bore seal fail post-fire accident, containment would not be breached.

NAC International Response to RAI 3-2 (cont'd)

In addition, Table 3.5-4 has been revised (changes highlighted) as follows:

Table 3.5-4 PWR and BWR High Burnup Fuel Rods Fire Accident Maximum Temperatures (°F)

NAC-LWT (Transported via Truck Trailer)
Cavity Gas: Air

Component	Component Temperature (°F)	Temperature Limit (°F)
Stainless steel Can Weldment	692	800
Fuel Rod Cladding	1,014	1,058[1]

[1] The maximum allowable temperature under HAC for PWR, BWR and PWR MOX fuel rod cladding is 1,058°F per ISG-11, Revision 3.

NAC INTERNATIONAL RESPONSE TO REQUEST FOR ADDITIONAL INFORMATION

CHAPTER 5 SHIELDING REVIEW

5-1 Provide justification that the SAS2H sequence of SCALE-5.0 is valid for calculating the source terms of the PWR MOX spent fuel with burnup up to 70 GWd/MTHM.

On page 5.3.18-1 of the SAR, the applicant states: "Source terms are generated based on a limiting description of PWR rods using the SCALE 5.0 SAS2H code. The limiting description of a PWR MOX rod bounds MOX rods from all PWR assembly array sizes."

Based on various publications, the SAS2H sequence of the SCALE-5.0 code is neither benchmarked nor validated for MOX fuel with burnup greater than 20 GWd/MTHM. Using this code to determine the source terms of spent MOX fuel, therefore, may not be acceptable because of lack of knowledge in the extended burnup range. The applicant is requested to provide justification for using this code beyond its validated range.

This information is needed pursuant to the requirements of 10 CFR 71.47 and 71.51.

NAC International Response

NAC acknowledges that the amount of available validation information on MOX fuel materials is limited. To address this concern, NAC generated its licensing calculations based on a conservative maximum burnup of 70 GWd/MTHM, while requesting a maximum of 62.5 GWd/MTHM. Based on SAS2H results, this conservatism produces approximately 5% increases in heat load and gamma source (for gammas capable of penetrating the cask shields) and an increase of 20-25% in neutron source. As neutron source is most likely to be affected by uncertainties in the code libraries at high burnups, a significant margin is built into the analysis. Further, the fuel rod evaluated in the NAC-LWT cask shielding calculations is based on a hybrid that contains approximately 2.6 kg of HM, while PWR fuel rods within NAC's assembly database range up to 2.4 kg HM. The increased mass is the result of applying a 150-inch fuel height to a CE14×14 fuel rod type that is actually less than 140 inches in active height. The CE14×14 rod radius was chosen as the licensing basis because it is the largest diameter fuel pellet, which, in turn, produced maximum fuel mass per unit length. The increased fuel mass

NAC International Response to RAI 5-1 (cont'd)

results in an 8% overestimation of total source when compared to the highest mass fuel rod within NAC's PWR fuel rod database. (Note that the NAC LWR fuel rod database does not include South Texas extended active length fuel rods.)

These conservatisms, in combination with the limited MOX validation information, and information available on benchmarking on SCALE SAS2H for high burnup PWR rods, whose primary fissile isotopes are plutonium (MOX) near end of life, justify the acceptability of SCALE to generate the required MOX source terms.

Section 5.3.18.1 is revised to include the above listed discussion to justify the use of SCALE for this application.

NAC INTERNATIONAL RESPONSE
TO
REQUEST FOR ADDITIONAL INFORMATION

CHAPTER 5 SHIELDING REVIEW

5-2 Pertinent to the limiting MOX fuel assembly as described in Section 5.3.18.1, the following information is requested:

1. Clarify if there are any water holes or tubes in the MOX fuel assembly.

2. If yes, provide information on the number of water holes, number of tubes, and number of instrument tube(s) for the fuel assembly that was used in SAS2H depletion calculations.

3. If there are holes and tubes in the assembly modeled in the source term calculation, provide justification on why these tubes were not included in the model.

4. If the answer to item 1 is yes, redo the source term and shielding analyses for the PWR MOX spent fuel package because the calculation model provided in Figure 5.3.18-1 does not include any tubes or water holes. Consequently, the source term calculation may have produced erroneous results.

On page 5.3.18-1 of the SAR, the applicant described the limiting PWR MOX fuel assembly used as the design basis for shielding analyses of the package. However, the SAR provides no information on the number of water holes and/or the number of tubes in the fuel assembly. The SAS2H model presented in Figure 5.3.18-5 does not include any water holes or tubes. If there is indeed no water hole or tube in the assembly, the 176 rods simply cannot make up a square pitch assembly. Consequently, the source term calculations may have produced erroneous results.

This information is needed pursuant to the requirements of 10 CFR 71.47 and 71.51.

NAC International Response

MOX fuel assemblies are identical to standard PWR fuel assemblies in configuration. This includes the use of guide tubes and central instrument tubes (where applicable). The sample source term input provided in Figure 5.3.18-1 demonstrates the use of an input level 2 model

NAC International Response to RAI 5-2 (cont'd)

with the fuel geometry described by a SCALE SAS2 Path B model. The model is centered on a guide tube model surrounded by one-fifth of the fuel assembly. This type of input is required as the maximum mass per unit length fuel type is a CE type fuel assembly with five guide tubes, each occupying four lattice positions. The MOX analysis approach is identical to the one taken in currently licensed NAC-LWT PWR evaluations. As the geometry modeling approach and method are identical to previously reviewed evaluations, and referenced as such in Section 5.3.18.1, NAC did not provide additional detail for the geometry portion of the SAS2H depletion model.

To provide additional information, Table 5.3.18-1 is revised as requested for the MOX depletion model. Specific data added are the number and dimension of the guide tubes.

Note that Figure 5.3.18-5 represents the MCNP model, with Figure 5.3.18-1 illustrating the SAS2H model. Figure 5.3.18-1 contains an inner water zone representing the water rod within the 14×14 lattice (in particular, one out of five water rods occupying four fuel rod lattice positions).

No revisions to the source-generating models are required, as water rods appropriate to the modeled fuel pin are included in the existing evaluations.

NAC INTERNATIONAL RESPONSE TO REQUEST FOR ADDITIONAL INFORMATION

CHAPTER 5 SHIELDING REVIEW

5-3 Pertinent to the spent fuel source terms versus the burnup equation:

1. Prove that the equation is valid for spent MOX fuel.

2. Provide justification that 1.0 for gamma and 4.22 for neutron are adequate values for parameter b for PWR MOX spent fuels.

On page 5.3.18-2 of the SAR, the applicant introduces an equation to relate the gamma and neutron source terms to the assembly burnup. However, it is not clear how these values are obtained. The staff's understanding is that this equation and these two values are derived via regression analyses from data consisting of UO_2 spent fuel assemblies only. The data set does not include any MOX spent fuel. Hence, this equation and these values, 1.0 for gamma and 4.22 for neutron, may not be adequate for the PWR MOX spent fuels because of the vast differences between the nuclear characteristics of UO_2 fuel and MOX spent fuel. The applicant is requested to prove that this equation is still valid and the selected values for parameter b are adequate for the MOX spent fuel.

This information is needed pursuant to the requirements of 10 CFR 71.47 and 71.51.

NAC International Response

The SAR text in Section 5.3.18.1 is revised to include documentation on the SAS2H calculated factors for the parameter "b" for high and low quality MOX material compositions from 31 to 69 GWd/MTHM (values required to bound the burnup shape of an 62.5 GWd/MTHM burned rod). The revised factors are then used to calculate updated "average source to source at average burnup" values. The results are shown in the following table and document that the factors used in the analysis produce conservative dose rates. For MOX material, both short (90 days) and long (2 years) cool times were evaluated to demonstrate that while factors increase with cool time, the 1.0 (gamma) and 4.22 (neutron) factors are conservative. Note that for extended cool time, the source magnitude decreases significantly and the licensing basis for the MOX material is 90 days.

NAC International Response to RAI 5-3 (cont'd)

Table 5-3.1 Fuel Axial Source Profile Parameters

Description	Source	Exponent b	Average Source to Average Burnup
Design Basis (1.08 Peak)	Neutron	4.22	1.1269
	Gamma	1.00	1.000
MOX WG (1.08 Peak) 90 days cool time	Neutron	2.702	1.0485
	Gamma	0.333	0.997
MOX WG (1.08 Peak) 2 years cool time	Neutron	3.284	1.0752
	Gamma	0.766	0.998
MOX PG (1.08 Peak) 90 days cool time	Neutron	1.708	1.0140
	Gamma	0.325	0.997
MOX PG (1.08 Peak) 2 years cool time	Neutron	1.960	1.0213
	Gamma	0.735	0.998

Note: This table also appears in the LWT SAR as Table 5.3.18-6.

NAC INTERNATIONAL RESPONSE TO REQUEST FOR ADDITIONAL INFORMATION

CHAPTER 5 SHIELDING REVIEW

5-4 Pertinent to the shielding analyses:

1. Provide justification for the conclusion that a tight array of load as assumed in the model produces conservative shielding evaluation results.

2. Provide a cask shielding analysis with source term loaded in the outer layer 16 cells of the 5 x 5 lattice.

On page 5.3.18-3 of the SAR, the applicant states: "The fuel rod lattice ([a] 5 x 5 array of tubes containing up to 16 fuel rods) detail is conservatively omitted in the model." The review of the sample input file seems to indicate that the model has a homogenized fuel region that is equivalent to the total area of a 4 x 4 array of fuel tubes in the insert. This indicates that the fuel rods were homogenized into the actual volume of 4 x 4 tubes. The assumption that all rods were loaded in a tight lattice rather than loaded in the outer layer 16 cells of the 25 tube array may not produce conservative results because the model may have overestimated the shielding effect caused by shadowing among the rods in the array.

This information is needed pursuant to the requirements of 10 CFR 71.47 and 71.51.

NAC International Response

The source region within the shielding models is described in Section 5.3.18.2 under the "Source Models" section. The relevant text is duplicated below as an introduction to further discussions. "The combination of 16 fuel rods, either UO_2 or MOX fissile material based, are loaded into a 5×5 tube array insert constructed from stainless steel. The insert in turn is located within a canister, placed into the LWT PWR basket insert. The 16 fuel rods are homogenized within the cross sectional area of the canister internal spacer."

The can weldment inside width is 3.56 inches. The width is translated into a 9.04-cm wide square surface "10" shown in the MCNP input file (Figure 5.3.18-5). A sketch of the geometry is included in Figure 5.3.18-4. This cross-section is used as the basis for the material

NAC International Response to RAI 5-4 (cont'd)

homogenization, resulting in an average density of less than 2 g/cm^3. The homogenization approach represents typical NAC-LWT cask transport deep penetration shielding evaluations where the fuel region does not represent a significant shield and is homogenized to allow maximum computer time to be spent optimizing particles transported through the shield to the detector surfaces. The homogenized source model does not represent a tight lattice and is appropriate for the problem solved.

To address concern that an exterior (outer layer) placement of 16 rods may produce higher dose rates, a revised shielding model explicitly placing the 16 minimum fuel mass fuel rods in the outer insert slot locations is evaluated. A VISED sketch of the revised cask internal model is shown in Figure 5-4.1. As shown in Table 5-4.1, for a sample 80 GWd/MTHM, 90-day cooled source, the discrete model produces lower dose rates than the homogenized source model. Reduced dose rates are the result of the high-density fuel rod actually providing more shielding for the now-compacted source region than the homogenized source. The SAR analysis model description in Section 5.3.18.2 and results in Section 5.3.18.3 are revised to include the additional model description and dose comparison.

NAC International Response to RAI 5-4 (cont'd)

Figure 5-4.1 VISED Sketch of Discrete Pin Model

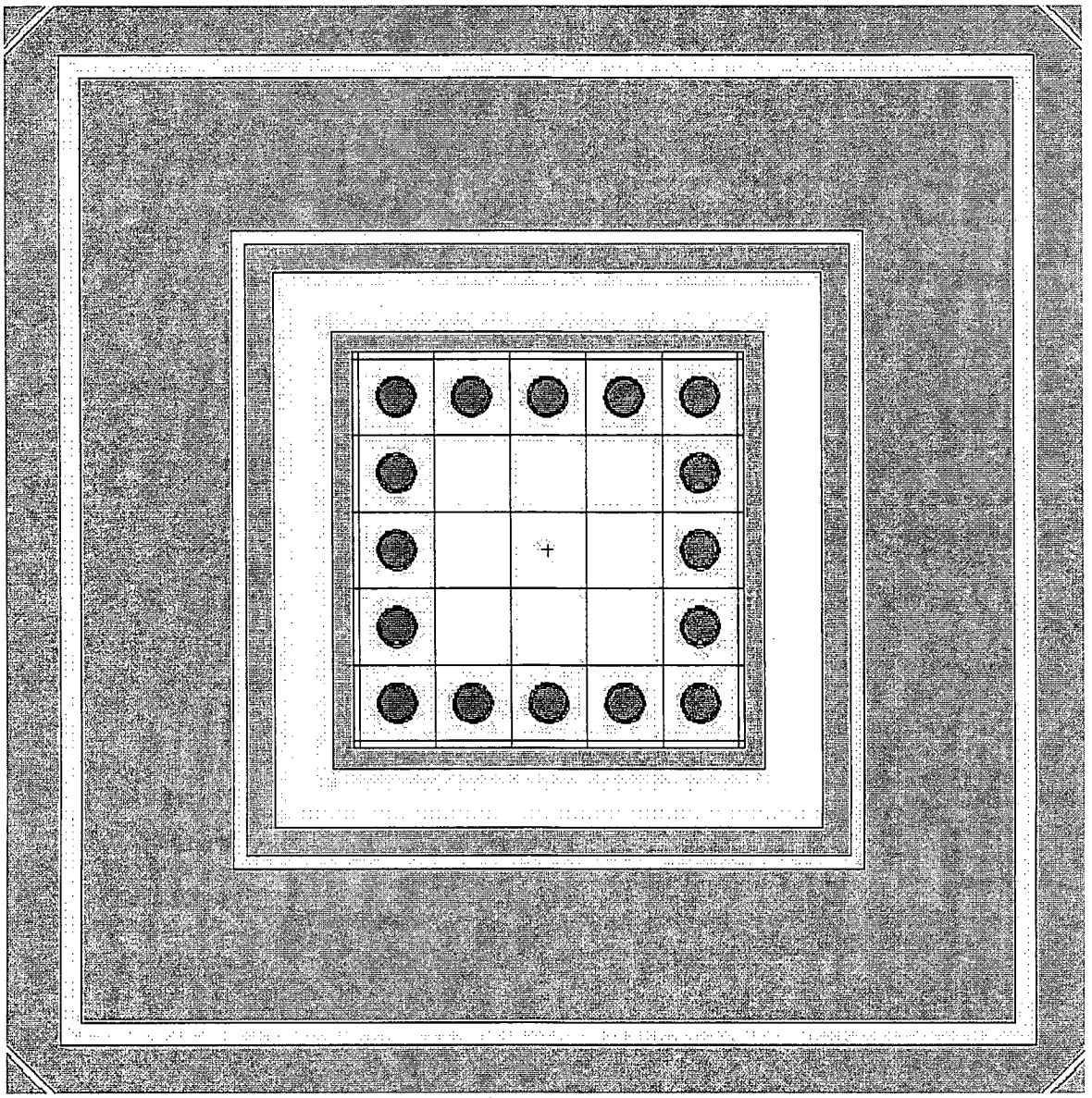

NAC International Response to RAI 5-4 (cont'd)

Table 5-4.1 MOX/UO_2 Fuel Material Configuration/Homogenization Study

Fuel	Surface Average (mrem/hr)			2m Average (mrem/hr)		
	Discrete	Homogenized	Difference	Discrete	Homogenized	Difference
LEU	36.3	39.8	9.7%	2.76	3.03	10.0%
FG	45.8	49.8	8.7%	3.38	3.71	9.8%
MS	44.7	48.9	9.4%	3.30	3.64	10.2%
PG	59.2	64.0	8.2%	4.23	4.61	8.8%
WG	44.0	48.2	9.6%	3.26	3.59	10.1%

Note: This table also appears in the LWT SAR as Table 5.3.18-15.

NAC INTERNATIONAL RESPONSE TO REQUEST FOR ADDITIONAL INFORMATION

CHAPTER 5 SHIELDING REVIEW

5-5 Pertinent to the MOX fuel package shielding model:

1. Provide details on how the mixed MOX and UO_2 spent fuel rods are homogenized in the Monte Carlo shielding analysis model and provide justification on why this simplification produces reliable shielding results.

2. Provide a sample input file for the MOX spent fuel source evaluation model.

3. Provide a sample input file for the mixed MOX and UO_2 fuel transportation package shielding evaluation model.

4. Provide the input file of the model that produced the results presented in Table 5.3.18-14 and Table 5.3.18-15.

On page 5.3.18-3 of the SAR, the applicant states: "The combination of 16 fuel rods, either UO_2 or MOX fissile material based, are loaded into a 5 × 5 tube array insert constructed from stainless steel. ... The 16 rods are homogenized within the cross sectional area of the canister spacer." It is not clear, however, how the rods with different material compositions are homogenized. The staff's review of the sample input file, Figure 5.3.18-5, "Sample MCNP Input File for PWR MOX Fuel (Response Method Benchmark Case)" found that the composition of material with material ID card 1 is for pure UO_2 fuel rather than MOX fuel as the title of the figure indicates. It is not clear which model produced the results presented in Table 5.3.18-14 and Table 5.3.18-15.

This information is needed pursuant to the requirements of 10 CFR 71.47 and 71.51.

NAC International Response

Response to Items 1 and 3:

As stated in Section 5.3.18.3, "Subcritical Multiplication," which has been relabeled "Fuel Material Effects" as part of the RAI response, dose rates were calculated based on UO_2 (LEU)

NAC International Response to RAI 5-5 (cont'd)

fuel material definition. The input file contains the shipment geometry and source for the MOX/UO_2 payload requested. The input file was used to address MOX source issues and is, therefore, appropriately titled MOX shielding. Section 5.3.18.3 was created to evaluate the fuel material difference and to address anticipated NRC concerns as to the validity of using UO_2 rather than MOX as the fuel material. In particular, Table 5.3.18-13 contains a comparison of dose results generated with the various material compositions and demonstrates that there is no significant effect of material composition of the source region. The section was labeled "Subcritical Multiplication," but includes all material/isotope effects. To clarify the evaluation content of this section, the section content is revised to point out that the material substitution accounts for any other isotope effects. As the source region is only 3.5 inches wide, and the neutron spectrum is fast in the dry cask, there is no expected effect of material composition.

To address the concern that this information is insufficient to address regulatory compliance, NAC added evaluations of the discrete pin model with a mixed loading of eight UO_2 and eight MOX rods. A VISED sketch of this geometry is included in Figure 5-5.1. Analysis results demonstrating that there is no effect of mixing materials are included in Table 5-5.1. The results of these evaluations are included in SAR Section 5.3.18.3, revised in response to this RAI. Also included in the SAR is a sample MOX input file for the mixed fuel loading (Figure 5.3.18-9).

Response to Item 2:

A sample source term generation input file was included in the initial MOX submittal as SAR Figure 5.3.18-1.

Response to Item 4:

The referenced tables contain dose results for various sources and conditions (normal and accident). There is, therefore, no single input file to provide. The shielding evaluation was performed via response function as discussed in Section 5.3.18.3, "Dose Response Method." There are, therefore, individual dose runs for each energy line. Input files used in the generation of the dose rate tables are provided as a NAC International PROPRIETARY enclosure in electronic format packaged in a separate sealed envelope labeled RAI 5-5, Item 4, "NAC PROPRIETARY Enclosure."

NAC International Response to RAI 5-5 (cont'd)

Figure 5-5.1 VISED Sketch of Discrete Pin Model – Mixed Loading

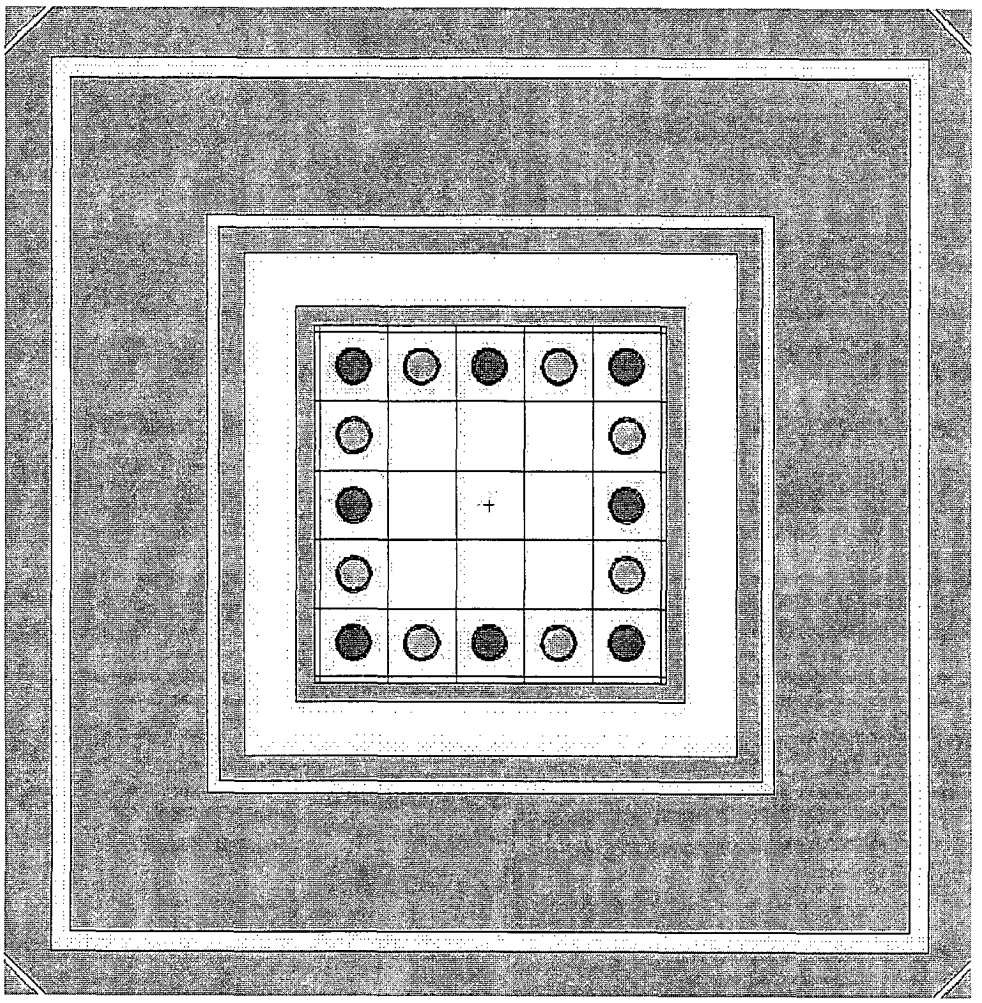

NAC International Response to RAI 5-5 (cont'd)

Table 5-5.1 Mixed Loading/Material Composition Effect Study for PWR MOX Fuel

Fuel Model	Fuel Material	Source	Dose Rate [mrem/hr]	FSD
LEU 16 Rods (MCNP Run)	UO_2	UO_2	36.3	1.2%
WG 16 Rods (MCNP Run)	WG	WG	44.0	1.0%
Numerical Avg. of LEU/WG 16 Rods	--	--	40.0	0.8%
Mixed Loading (MCNP Run)	UO_2/WG	UO_2/WG	40.0	1.1%
Mixed Loading (MCNP Run)	UO_2	UO_2/WG	39.7	1.1%

Note: This table also appears in the LWT SAR as Table 5.3.18-14.

NAC INTERNATIONAL RESPONSE TO REQUEST FOR ADDITIONAL INFORMATION

CHAPTER 5 SHIELDING REVIEW

5-6 Pertinent to the response function method for dose rate calculation:

1. Provide where and how the response function was used to calculate the dose rates at the various points of interest with respect to the cask.

2. Provide justification that the response function is reliable and accurate for dose rate calculations for the MOX spent fuel transportation package.

3. Provide justification that the response function is reliable and accurate for dose rate calculations for the mixed UO_2 and MOX spent fuel transportation package.

4. Provide information on how many sets of response function data were used in determining the dose rates of the various points of interest in respect to the cask.

On page 5.3.18-4 of the SAR, the applicant states: "A sample input file is provided in Figure 5.3.18-5. The sample input provides a complete source description used in the response function benchmark analyses." As this approach completely decoupled the dependence of the particle transport to the material composition of the media that the particles traverse and interact with, the reliability and the accuracy of this approach can be assessed only on a case-by-case basis. It is especially true for MOX fuel because of the large cross sections of the fission, (n, 2n), (gamma, n), (n, gamma), and (n, alpha) reactions and the secondary radiation generated by these nuclear reactions.

Furthermore, the staff needs help to understand if the response function is trying to determine the dose rates at various points of interest by interpolation based on a pre-calculated data set. If so, the correctness of the selected interpolation scheme must be taken into account in the actual application.

This information is needed pursuant to the requirements of 10 CFR 71.47 and 71.51.

NAC International Response

The response function method was used to calculate all relevant licensing dose rates, including normal condition cask surface, 1 meter, 2 meter, and accident condition 1-meter dose rates. The dose response method function in a SAR subsection in Section 5.3.18.3 is revised to provide additional information on the method applied. The revised section includes text stating that for the UO_2 material composition, 198 response function sets were calculated for the radial and axial normal and accident condition models. No interpolation was done on a precalculated data set. Additional text has been added to the SAR to detail the response method.

Further response functions were generated as part of the RAI response set to provide documentation that fuel material isotopic composition (i.e., MOX or UO_2) is irrelevant to the safety conclusion of the shielding evaluations performed in Section 5.3.18. As documented in RAI responses 5-4 and 5-5 and initial submittal Table 5.3.18-13, there is no significant effect of fuel material choice on dose rates. This was expected as deep penetration NAC-LWT cask shielding problems are driven by material interaction within the shields and not within the small diameter payload volume. While MOX materials contain significant differences in isotope cross-sections, within the confines of the NAC-LWT cask evaluations, the small fissile material mass, the absence of moderator to reduce neutron energy to thermal or epithermal levels for increased material interaction, and the high neutron leakage (large height to diameter ratio) all contribute to the negligible effect of material properties.

Note that spent fuel packages licensed by the US NRC are typically analyzed based on shielding models relying on fresh fuel compositions. This approach is only valid when considering that spent fuel isotopics, in particular, the inclusion of plutonium generated during in-core use, do not significantly affect the conclusions of the evaluations.

To further document the acceptability of the response function approach, additional evaluations are performed comparing the result of the response approach (i.e., multiplication of source spectra by dose response at a given energy line) with a direct solution approach containing the full energy spectrum. The relevant input files are included within the NAC International PROPRIETARY enclosure provided with this RAI response in a separate sealed envelope labeled RAI 5-6, "NAC International PROPRIETARY Enclosure." The additional comparisons

NAC International Response to RAI 5-6 (cont'd)

are based on the discrete fuel rod model to allow mixed fuel to be explicitly accounted for. Results of the comparisons are shown in Figures 5-6.1, 5-6.2 and 5-6.3, and demonstrate that the results of the response and direct solutions are equivalent, independent of the source modeling employed (i.e., discrete fuel rods or homogenized). Differences between response method and direct calculation results are associated with significantly higher statistical uncertainties produced by the direct calculation approach.

NAC International Response to RAI 5-6 (cont'd)

Figure 5-6.1 Comparison of Direct Solution and Response Function Results at Cask Surface for Normal Conditions Model for Discrete Rod Mixed Loading of 8 UO_2 Rods and 8 WG Rods

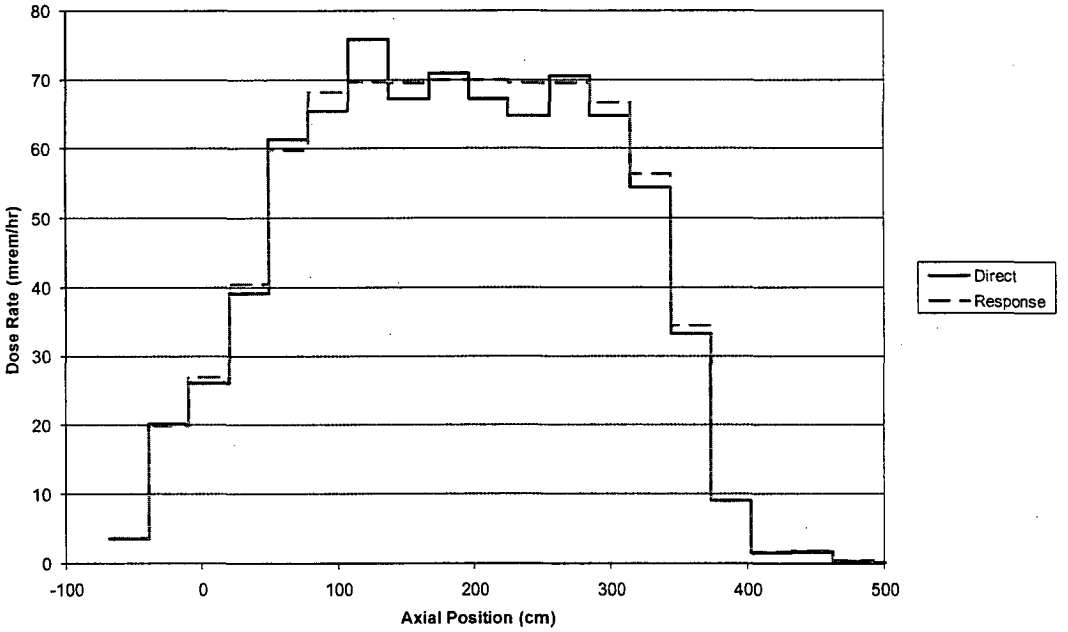

Note: This figure also appears in the LWT SAR as Figure 5.3.18-10.

Figure 5-6.2 Comparison of Direct Solution and Response Function Results at Cask Surface for Normal Conditions Model for Homogenized WG Material

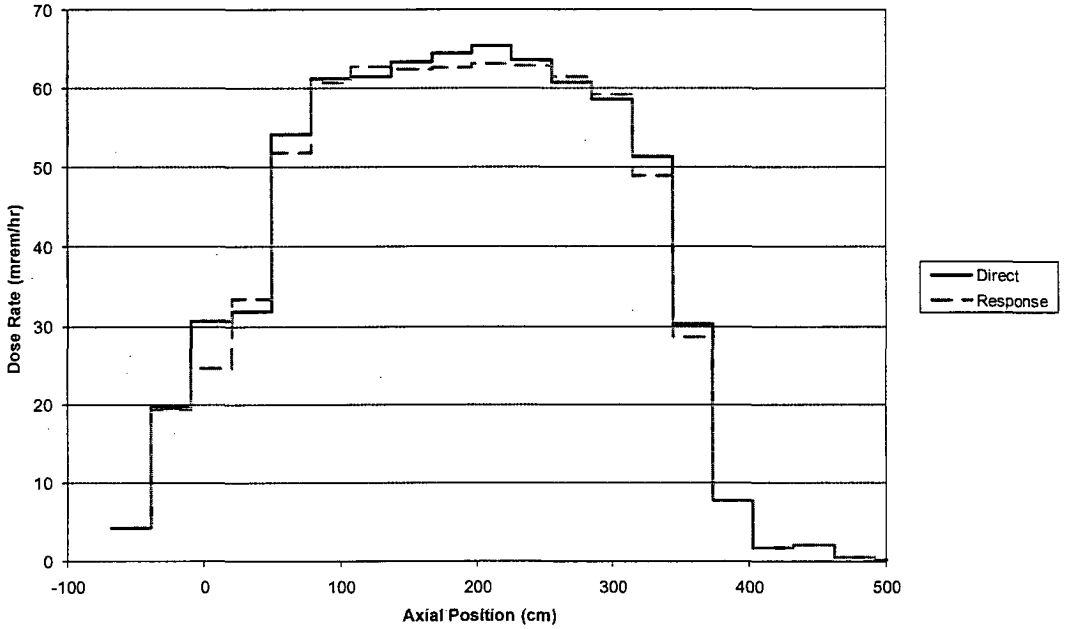

Note: This figure also appears in the LWT SAR as Figure 5.3.18-11.

NAC International Response to RAI 5-6 (cont'd)

Figure 5-6.3 Comparison of Direct Solution and Response Function Results at Cask Surface for Normal Conditions Model for Homogenized LEU Material

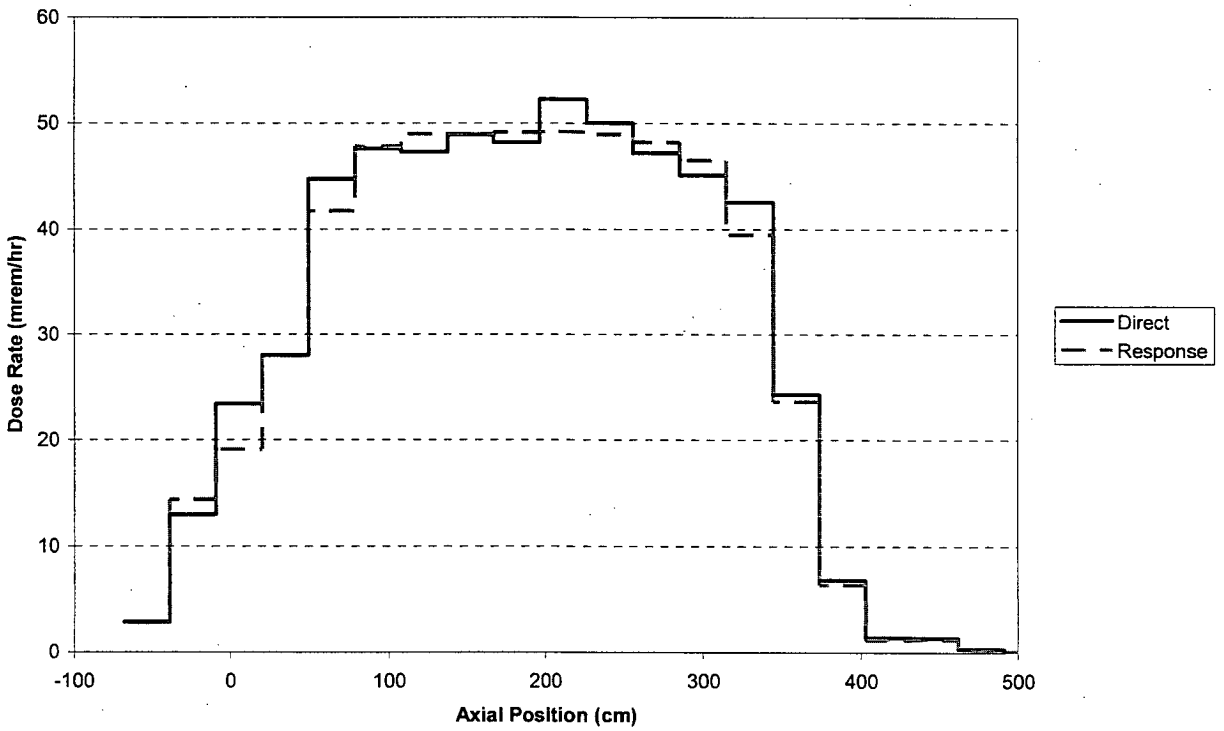

Note: This figure also appears in the LWT SAR as Figure 5.3.18-12.

NAC INTERNATIONAL RESPONSE TO REQUEST FOR ADDITIONAL INFORMATION

CHAPTER 6 CRITICALITY REVIEW

6-1 Provide geometry data and corresponding input file for the square pitch PWR MOX spent fuel package criticality model.

Appendix A of the SAR provides two output files for the hexagonal pitch lattice loading pattern of the PWR MOX spent fuel rod packages. However, Section 6.7.1.3 of the SAR indicates that 3.6 cm square pitch loading pattern is the most reactive configuration.

This information is needed pursuant to the requirements of 10 CFR 71.33.

NAC International Response

SAR discussion on Page 6.7.1-9, Maximum Reactivity Rod Pitch Evaluation subsection of Section 6.7.1.3, establishes that square pitch and hexagonal pitch configurations are not statistically different and that the hexagonal pitch case will be used to move forward with the moderator density ratio evaluations. The difference in maximum reactivity between the hexagonal and square model for a realistic plutonium composition (MS in Table 6.7.1-4) is less than 0.001 Δk. Even for the hypothetical all ^{241}Pu composition, the change in reactivity is approximately 0.003 Δk (as compared to a maximum margin versus allowable > 0.1 for a hypothetical infinite cask array under voided neutron shield accident conditions).

Also note the large conservatism in the calculations, as fuel rods are located within a square pitch basket insert with a nominal pitch of 11/16 inch (1.7463 cm), which produces a significantly lower reactivity system (even without considering that the model removed the parasitic absorber steel fuel tubes from the model).

To address the specific request, the MS 3.8-cm pitch input file producing maximum reactivity (Figure 6.6.15-3) is added to SAR Appendix 6.6. This case contains the relevant geometry data requested.

NAC INTERNATIONAL RESPONSE
TO
REQUEST FOR ADDITIONAL INFORMATION

CHAPTER 6 CRITICALITY REVIEW

6-2 For the mixed PWR MOX and UO_2 spent fuel package:

1. Provide criticality safety evaluations for both NCT and HAC scenario.
2. Provide the MCNP code benchmark evaluation.
3. Provide the upper safety limit (USL) evaluation.

On page 6.7.1-11 of the SAR, the applicant states: "Evaluations of a mixed shipment of enriched UO_2 rods and MOX rods are not required, as the reactivity of the evaluated MOX rods are significantly higher than those of the UO_2 rods. Mixed shipments are, therefore, permitted."

The staff reviewed this discussion regarding the acceptability of the mixed MOX and UO_2 fuel rods and found it not adequate for the following reasons:

1. The UO_2 and the MOX fuel system behave very differently because these two systems have significantly different energies of average lethargy causing fission (EALCFs). In addition, the UO_2 system has a lower EALCF under the flooded condition in comparison with that of a MOX system. On the other hand, the UO_2 system has a higher EALCF under dry conditions in comparison with that of a MOX system. As such, the behavior of the mixed UO_2 and MOX system is not clear.
2. The computer code the applicant used has never been benchmarked for fission systems of enriched UO_2 and MOX fuel. The reliability and accuracy of the results are not assessable.

This information is needed pursuant to the requirements of 10 CFR 71.55, 71.59, 71.71, and 71.73.

NAC International Response

The MCNP code benchmark evaluations for MOX and UO_2 fuel rod configurations are included in SAR Section 6.7.2. No benchmarks for mixed heterogeneous UO_2 and MOX rod systems have been located by NAC staff to augment the relevant discussions. Per Section 6.7.2, the USL for arrays of UO_2 rods is 0.9376 and 0.9331 for MOX rods for a Δk of 0.0045 between the two fuel types. The evaluations demonstrate that MCNP, with its associated cross-sections, accurately predicts system reactivities containing either fuel rod type. As the MOX rods cannot discern that a neutron interacting with them originated in a uranium fuel rod or a MOX rod, the question of a mixed heterogeneous rod critical benchmark does not seem relevant to document the safety of the NAC-LWT cask MOX transport system.

Review staff stated: "The UO_2 and the MOX fuel system behave very differently because these two systems have significantly different energies of average lethargy causing fission (EALCFs). In addition, the UO_2 system has a lower EALCF under the flooded condition in comparison with that of a MOX system. On the other hand, the UO_2 system has a higher EALCF under dry conditions in comparison with that of a MOX system. As such, the behavior of the mixed UO_2 and MOX system is not clear."

The focus of the evaluations and, therefore, the expected review is done for a wet (flooded) system, as no reasonable extrapolation of the data provided would indicate a safety concern for a dry system at the requested fissile material levels. While it is recognized that code performance and bias are potentially affected by the difference in the energy level of neutron-causing fission, the benchmarks accounted for the basic phenomena, and the computer code demonstrated capability for tracking particles at their relevant energy levels.

Analyses have demonstrated that the UO_2 payload, calculated to be at maximum reactivity flooded with an EALCF of 0.13 eV, is significantly lower in reactivity than the MOX payload with an EALCF of 0.13 eV. NAC concluded that insertion of the lower reactivity UO_2 rods and corresponding replacement of higher reactivity MOX rods do not increase system reactivity.

NAC International Response to RAI 6-2 (cont'd)

Given the significant margin (Δk of 0.13) between maximum calculated reactivity for a hypothetical fuel material (all ^{241}Pu) at maximum reactivity pitch, without inclusion of the tube insert that retains the rods in a fixed position, the evaluations demonstrate that the system meets regulatory requirements. No mixed fuel evaluations are, therefore, performed and no mixed bias is discussed. SAR Section 6.7.1.3 is revised to include a discussion on margins and conservative modeling in the Maximum Reactivities and Comparison to USL subsection.

NAC INTERNATIONAL RESPONSE TO REQUEST FOR ADDITIONAL INFORMATION

CHAPTER 7 OPERATING PROCEDURES REVIEW

7-1 Provide information on how to identify the cooling time of the fuel rods and add this information to the operating procedure as it is applicable.

On page 7.1-53 of the SAR, operating procedure number 17 requires the operators to verify that the fuel rods and burnable poison rods comply with the content type, form, and quality conditions of the CoC. The procedure, however, does not include verification of the cooling time or radiation level of the rods as a parameter. Because this parameter is very critical to shielding safety, it should be added as a requirement.

This information is needed pursuant to the requirements of 10 CFR 71.47 and 71.51.

NAC International Response

NAC has revised Step 17 in MOX fuel rod loading procedure (Section 7.1.12) to read as follows: "Identify the PWR MOX fuel rods (and standard PWR rods and BPRs, as applicable) to be loaded into the PWR/BWR Rod Transport Canister. Verify that the fuel rods and BPRs comply with the content type, form, heat load, minimum cooling time and quantity conditions of the NAC-LWT CoC. Load the screened or free flow ...."

In addition, NAC has proposed the following conditions be added to the NAC-LWT CoC as follows:

5.(b)(1) Type and form of material (continued)
Add new item (xvii) as follows:

(xvii) PWR MOX (mixed oxide) undamaged fuel rods consisting of uranium and plutonium dioxide pellets within zirconium alloy type cladding. The plutonium enrichment is 7.0 weight percent maximum and 2.0 weight percent minimum, the maximum active fuel rod length is 153.5 inches, and the maximum pellet diameter is 0.3765 inch. The maximum burnup is 62,500 MWd/MTU and the minimum cool time is 90 days.

NAC International Response to RAI 7-1(cont'd)

5.(b)(2) Maximum quantity of material per package (continued)
Add new item (xviii) as follows:

(xviii) For intact PWR MOX fuel rods as described in Item 5.(b)(1)(xvii):

Up to 16 PWR MOX rods or a combination of PWR MOX and high burnup PWR fuel rods as described in Item 5.(b)(1)(viii). Maximum decay heat not to exceed 2.3 kW per package. Individual PWR MOX and PWR UO_2 fuel rods shall be placed in a 5×5 insert loaded into a screened or free flow rod canister in accordance with NAC International Drawing No. 315-40-104, Assembly 97. Up to nine nonstainless burnable poison rods (BPRs) may be loaded in the spare locations in the 5×5 insert. The PWR/BWR fuel rod canister shall be transported in the PWR basket and the PWR insert installed in the cask cavity.

Therefore, the loading verification procedure specified in the SAR Section 7.1.12, Step 17 will appropriately verify that the PWR MOX and other authorized contents comply with the CoC prior to transport. Note that due to ALARA, the specific radiation level of a fuel rod or element is never measured prior to loading, and the contents are shown to be enveloped within the authorized conditions of the CoC by the detailed analyses provided in the SAR.

August 2008

Revision LWT-08E

NAC-LWT

Legal Weight Truck Cask System

SAFETY ANALYSIS REPORT

Volume 1 of 2

Docket No. 71-9225

NAC INTERNATIONAL

Atlanta Corporate Headquarters: 3930 East Jones Bridge Road, Norcross, Georgia 30092 USA
Phone 770-447-1144, Fax 770-447-1797, www.nacintl.com

List of Effective Pages

LIST OF EFFECTIVE PAGES

Chapter 1

76 drawings in the
Chapter 1 List of Drawings

Chapter 1 Appendices 1-A
through 1-G

Chapter 2

LIST OF EFFECTIVE PAGES (Continued)

LIST OF EFFECTIVE PAGES (Continued)

Chapter 1

1.1 Introduction

The NAC-LWT spent-fuel shipping cask has been developed by NAC International (NAC) as a safe means of transporting radioactive materials authorized as approved contents. The cask design is optimized for legal weight over the road transport, with a gross weight of less than 80,000 pounds. The cask provides maximum safety during the loading, transport, and unloading operations required for spent-fuel shipment. The NAC-LWT cask assembly is composed of a package that provides a containment vessel that prevents the release of radioactive material. The actual containment boundary provided by the package consists of a 4.0-inch thick bottom plate, a 0.75-inch thick, 13.375-inch inner diameter shell, an upper ring forging, and an 11.3-inch thick closure lid. The cask lid closure is accomplished using twelve, 1-inch diameter bolts. The cask has an outer shell, 1.20 inches thick, to protect the containment shell and also to enclose the 5.75-inch thick lead gamma shield. Neutron shielding is provided by a 5.0-inch thick neutron shield tank with a 0.24-inch (6mm) thick outer wall, containing a water/ethylene glycol mixture and 1.0 minimum weight percent (wt %) boron (58 wt % ethylene glycol; 39 wt % demineralized water; 3 wt % potassium tetraborate [$K_2B_4O_7$]). The neutron shield tank system includes an expansion tank to permit the expansion and contraction of the shield tank liquid without compromising the shielding or overstressing the shield tank structure. Aluminum honeycomb impact limiters are attached to each end of the cask to absorb kinetic energy developed during a cask drop, and limit the consequences of normal operations and hypothetical accident events.

The NAC-LWT is a legal weight truck cask designed to transport the following contents:

- 1 PWR assembly;
- up to 2 BWR assemblies;
- up to 15 sound metallic fuel rods;
- up to 42 MTR fuel elements;
- up to 42 DIDO fuel assemblies;
- up to 25 high burnup PWR fuel rods (including up to 14 rods classified as damaged);
- up to 25 high burnup BWR fuel rods (including up to 14 rods classified as damaged);
- up to 16 PWR MOX fuel rods (or a combination of 16 PWR MOX and UO_2 PWR rods) and up to 9 BPRs;
- up to 9 damaged metallic fuel rods;
- up to 3 severely damaged metallic fuel rods in filters;
- up to 140 TRIGA intact or damaged fuel elements/fuel debris ("TRIGA" is a Trademark of General Atomics);
- up to 560 TRIGA fuel cluster rods;
- 2 GA IFM packages;
- up to 300 TPBARs (of which two can be prefailed);

- up to 55 TPBARs segmented during post-irradiation examination (PIE), including segmentation debris; ,
- up to 700 PULSTAR fuel elements (intact or damaged);
- up to 42 spiral fuel assemblies;
- up to 42 MOATA plate bundles; or
- up to 4,000 lbs of solid, irradiated and contaminated hardware, which may include fissile material less than a Type A quantity and meeting the exemptions of 10 CFR 71.15, paragraphs (a), (b) and (c). Total allowed mass includes the weight of spacers, shoring and dunnage.

PWR or BWR fuel rods may be placed in a fuel rod insert (also referred to as a rod holder) or in a fuel assembly lattice. The lattice may be irradiated or unirradiated. Up to 14 of the fuel rods may be classified as damaged. Damaged fuel rods must be placed in a rod holder. Damaged fuel rods or rod sections may be encapsulated to facilitate handling prior to placement in the rod holder. PWR rods may include Integral Fuel Burnable Absorber (IFBA) rods.

PWR MOX fuel rods (or a combination of PWR MOX and UO_2 PWR fuel rods) are required to be loaded in a screened or free flow PWR/BWR Rod Transport Canister with a 5 × 5 insert and transported in a leaktight configuration NAC-LWT. PWR MOX/UO_2 rods may include Integral Fuel Burnable Absorber (IFBA) rods.

PULSTAR fuel elements may be configured as intact fuel assemblies, may be placed into a fuel rod insert, i.e., a 4×4 rod holder (intact elements only), or may be loaded into one of two can designs, designated as the PULSTAR screened fuel can or the PULSTAR failed fuel can. Damaged PULSTAR fuel elements and nonfuel components of PULSTAR fuel assemblies must be loaded into cans. PULSTAR fuel cans may only be loaded into the top or base module of the 28 MTR basket assembly. Intact PULSTAR fuel assemblies and intact PULSTAR fuel elements in a TRIGA fuel rod insert may be loaded in any basket module.

Irradiated hardware may be loaded directly into the NAC-LWT cavity or preloaded into a canister or cage. Stainless steel dunnage may be used to limit the movement of the irradiated hardware within the cask cavity. The maximum gamma source term of the irradiated hardware shall be limited to that defined for the authorized PWR content condition as described in Chapter 5.

The NAC-LWT cask provides a testable containment for the contents during both normal operations and hypothetical accident conditions, satisfying the requirements of 10 CFR 71.51. Any number of NAC-LWT casks may be shipped at one time, each on its own vehicle.

NAC-LWT casks may be shipped in a closed International Shipping Organization (ISO) container when containing all fuel contents other than PWR and BWR fuel assemblies. NAC-LWT

casks containing PWR and BWR fuel assemblies are to be transported on an open trailer with a personnel barrier.

The terminology of MTR, DIDO and TRIGA fuel elements will be used independent of whether the element contains low, medium or high enriched uranium (i.e., LEU, MEU or HEU), except when required for analysis or loading purposes.

Chapter 3

Table of Contents

List of Figures

List of Figures (continued)

List of Tables

List of Tables (continued)

3.4.1.4 PWR Rod

Heat transfer of the NAC-LWT containing 25 PWR rods with a total heat load of 1.41 kW configured in the PWR/BWR aluminum basket in the NAC-LWT cask enclosed in an International Shipping Organization (ISO) container was evaluated using ANSYS. The model presented in Figure 3.4-3 was revised to include the PWR/BWR aluminum basket and 25 PWR rods. Results from this evaluation are summarized in Table 3.4-7.

These results show that the temperatures are lower at all locations (except the neutron shield region) than the corresponding temperatures for the design basis PWR fuel presented in Table 3.4-2. Similar to the discussion presented in Section 3.4.1.3.3 for the MTR heat transfer analysis, temperature results from the two dimensional heat transfer analysis are conservative based on the imposed limitations of the model and can be used to evaluate acceptability of component temperatures outside the modeled section. Temperature of components in the lid closure region is less than the hottest basket temperature which is directly influenced by the decay heat of the fuel. It is concluded that the temperature of the safety related O-ring seals is within the allowable range of temperature of -40°F to +735°F. The maximum temperature of the lead gamma shield in the base of the LWT cask is less than the cask inner shell and much lower than the maximum of +600°F.

3.4.1.5 Thermal Evaluation for TRIGA Fuel

The thermal evaluation for TRIGA fuel is performed using classical analysis employing a thermal resistance model. The TRIGA fuel is transported in a basket assembly consisting of 5 modules - a base module, a top module, and three intermediate modules. During transport all 5 modules must be installed in the cask. The three intermediate modules are interchangeable, but the top and base modules are not. Each module contains 7 cells, and each open cell holds up to 4 TRIGA fuel elements. The top module is sized to accept fuel follower control elements, which are longer than the typical element. The center cell of each module is blocked with an 11-gage stainless steel plate so that fuel cannot be loaded in the center cell. The thermal evaluation conservatively assumes that the center cell also contains 4 fuel elements, so although only 120 fuel elements may be loaded into the cask, the thermal evaluation assumes 140 elements. Consequently, the total heat load in the thermal evaluation is conservatively considered to be 1.05 kW (7.5 watt/fuel element × 140 = 1.05 kW).

TRIGA fuel elements may be transported directly in a basket module cell, in a screened failed fuel can, or in a sealed failed fuel can. The fuel cans fit in either a top or base module cell. The

screened failed fuel cans hold up to four (4) TRIGA fuel elements, while the sealed failed fuel can holds up to two (2) damaged elements or equivalent fuel debris.

As described in Section 1.2.3.1, TRIGA fuel elements with minor cladding defects are loaded into screened failed fuel cans (screened cans). The screened can precludes gross particulate material from escaping the cell. The screened failed fuel cans are provided in two lengths. The screened failed fuel can is a square tube of 14-gage, Type 304 stainless steel, that holds four fuel elements. It is provided with a closure lid and an end plate that is screened to allow water draining.

TRIGA fuel debris and damaged fuel elements, which do not have structural integrity, are loaded into sealed failed fuel cans (sealed cans). The sealed cans are used to containerize the TRIGA fuel debris. The cans are provided in two lengths. The shorter can may be used in the base or top basket modules. The longer can may only be used in the top module. The cans are vacuum dried and leak tested prior to loading into a TRIGA fuel basket.

The TRIGA fuel thermal evaluation determines the maximum fuel cladding temperatures based on the maximum basket temperatures determined for the design basis heat load MTR thermal analysis presented in Section 3.4.1.3.1. An intermediate basket module with the shortest TRIGA fuel, which provides the highest heat load density, is used to obtain a bounding evaluation. Based on the maximum basket temperature and heat load density, the maximum fuel cladding temperatures are determined using a thermal resistance model.

The cross-section of the TRIGA and MTR fuel baskets are identical. As shown in Section 1.2.3 and Table 1.2-4, the maximum decay heat load for MTR fuel is 1.26 kW per cask. The maximum decay heat load for TRIGA fuel is 1.05 kW per cask. Therefore, it is conservative to use the maximum basket temperature for MTR fuel as a boundary condition for the thermal resistance model for TRIGA fuel.

Since the total decay heat load for MTR fuel bounds that for TRIGA fuel, the temperatures for cask components for the MTR fuel also bound those for the TRIGA fuel. The cask body temperatures for the MTR fuel are shown in Table 3.4-6.

3.4.1.5.1 TRIGA Model Description

The heat generated from the TRIGA fuel in the basket is transferred to the basket module by thermal conduction and radiation, and then transferred to the cask inner shell from the basket surface by the same heat transfer modes. The heat is finally transferred through the cask and International Shipping Organization (ISO) container to ambient. The thermal resistance model and thermal analysis of TRIGA fuel considers the regions inside a single basket opening of the TRIGA fuel basket. This analysis bounds transport in the cask without an ISO container.

The thermal resistance model is shown in Figure 3.4-5. The maximum temperature of the basket (T_{basket}) is taken from the MTR design basis heat loading thermal analysis. The temperatures for the TRIGA fuel are determined by stepping through each of the resistors in the thermal circuit, from the basket to the fuel cladding. All temperatures calculated are maximums, based on the basket temperature. Each successive maximum temperature calculated is then applied uniformly over the next surface in the resistance model. Fuel may be shipped directly in a basket cell, in a screened failed fuel can, or in a sealed failed fuel can. Since the model assumes the presence of the can, the model is conservative for configurations in which a can is not used.

The gas in the cask cavity is considered to be air in the thermal resistance model. Thermal conductivities of air and stainless steel are obtained from "Fundamentals of Heat and Mass Transfer" (Incropera). Emissivities of stainless steel (basket) and aluminum (fuel clad) are obtained from the Nuclear Systems Material Handbook and from "Scoping Design Analyses for Optimized Shipping Casks Containing 1-, 2-, 3-, 5-, or 10-Year-Old PWR Spent Fuel" (Bucholz), respectively.

Assuming the maximum temperature of the basket (T_{basket}) occurs at all inside surfaces of the webs forming the central cell in the basket module, the temperature of the can (T_{can}) is then determined by considering heat conduction and radiation between the can surface and the inside surface of the basket central cell. Convection in the gap between these surfaces is conservatively ignored.

The heat transfer rate across the gap per unit length (q_{gap}) between the can surface and the inside surface of the basket central cell wall can be represented as follows:

$$q_{gap} = q_{cond} + q_{rad}$$

$$q_{gap} = \frac{A(K_{cond})(T1 - T2)}{L_{gap}} + \frac{A(\sigma)(T1^4 - T2^4)}{\left(\frac{1}{\varepsilon_1} + \frac{1}{\varepsilon_2} - 1\right)}$$

where:

q_{gap} = 7.5 watt × 4/14 = 2.14 watt = 7.302 Btu/hr

A = Can surface area = 3.33 × 4 = 13.32 inch^2

K_{cond} = Air conductivity @ 260°F (400°K) = 1.628 × 10^{-3} Btu/hr-in-°F

L_{gap} = Gap size between can and basket = (3.44-3.33)/2 = 0.055 inch

$T1$ = temperature at can surface (T_{can})

$T2$ = temperature at inside surface of the basket central cell (T_{basket}) = 267°F

σ $= 1.19 \times 10^{-11}$ Btu/hr-in^2-°R

ε_1 = emissivity of web of basket central cell (stainless steel) = 0.36

ε_2 = emissivity of can (stainless steel) = 0.36

The temperature at the can (T_{can}) is calculated to be 287°F.

The maximum temperature of the can (T_{can}) is then applied to all can surfaces for determining the cladding temperature of the fuel. It is assumed that there are four (4) fuel elements inside the can surrounded by air. In the equivalent resistor analogy, the fuel elements do not contact each other, neglecting heat conduction between fuel elements. For a specific fuel element, an assumed circular region equivalent to 1/4 of the area inside the can, is developed to contain a fuel element, which results in a uniform air gap. The fuel cladding temperature is determined using the formula representing a hollow cylinder. Note that convective heat transfer in the gap between the fuel clad and the can is conservatively ignored.

Heat transfer rate per unit length of the basket (Q_{leng}) can be represented as:

$$Q_{leng} = q_{cond} + q_{rad}$$

$$Q_{leng} = \frac{2\pi (K_{cond})(T1 - T2)}{\ln\left(\frac{r_2}{r_1}\right)} + \frac{\sigma(2\pi r_1)(T1^4 - T2^4)}{\left(\frac{1}{\varepsilon_1}\right) + \left(\frac{1-\varepsilon_2}{\varepsilon_2}\right)\left(\frac{r_1}{r_2}\right)}$$

where:

r_1 = fuel cladding outer radius = 0.675 inch

r_2 = radius of equivalent circular region representing ¼ of the area inside a can
= 0.93 inch

K_{cond} = Air conductivity @ 260°F (400°K) = 1.628×10^{-3} Btu/hr-in-°F

σ $= 1.19 \times 10^{-11}$ Btu/hr-in^2-°R

ε_1 = emissivity of fuel cladding (aluminum) = 0.22

ε_2 = emissivity of the can (stainless steel) = 0.36

T1 = fuel cladding temperature (T_{clad})

T2 = can temperature (T_{can}) = 287°F

The fuel cladding temperature (T_{clad}) is solved to be 326°F.

3.4.1.5.2 TRIGA Fuel Thermal Evaluation Results

Using the model described above, and the assumed boundary condition of 267°F for the maximum basket temperature (from Table 3.4-6), the maximum normal transport conditions temperature of the TRIGA fuel is determined as shown in Table 3.4-8.

A conservative temperature of 400°F is established as the maximum allowable temperature for aluminum-clad TRIGA fuel, as described in Section 3.4.1.3.3 for MTR fuel. Stainless steel clad TRIGA fuel is allowed a significantly higher cladding temperature, since the melting temperature of stainless steel is 2,600°F (Mark's) and stainless steel retains its capability to function as a mechanical component at temperatures up to the 800°F range. Therefore, the temperatures calculated for the TRIGA fuel cladding are acceptable.

3.4.1.6 TRIGA Fuel Cluster Rods

The TRIGA fuel cluster rods are 0.542 inches OD with 0.016-inch thick Incoloy 800 cladding. Each rod is inserted into a 6061-T6 aluminum tube (0.75 inch OD, 0.62 inch ID) that is part of the fuel rod insert. Up to sixteen rods and a fuel rod insert are placed into a single cell of the seven cell basket. This TRIGA basket has the same cross sectional dimensions and basket material as the MTR basket presented in Section 3.4.1.3. The thermal evaluation for the TRIGA fuel cluster rods is performed using two-dimensional planar finite element analyses and the general purpose ANSYS computer code. Two transport conditions are evaluated:

Condition 1:

The NAC-LWT is supported in an ISO container with solar insolance applied on the surface of the ISO container, and the NAC-LWT is considered to be insulated from the environment (only for the normal conditions of transport steady state conditions). The gas inside the ISO container is air. The cavity of the NAC-LWT is actually backfilled with helium as required by operational procedures.

Condition 2:

The NAC-LWT is not located in an ISO container and solar insolation is applied to the NAC-LWT cask surface.

For the purpose of performing these thermal analyses, the cavity of the NAC-LWT is considered to be filled with air.

For each of the two conditions listed above, only a single fuel configuration is evaluated: 16 rods in a fuel rod insert in each of the seven cells comprising a basket section. This corresponds to a total heat load of 210 watts for each basket section (30 watts per cell of a basket section which

corresponds to 30/16 or 1.875 watts per rod). Therefore, the heat load in the cask cavity corresponding to five basket sections is 5 times 210 watts or 1.05 kW.

Since the finite element model corresponds to a one inch axial length, the heat generation applied to each rod in the model was 1.875 watts divided by the length of the rod or 22 inches. Although the aluminum inserts will conduct heat in the axial direction, this was conservatively ignored.

3.4.1.6.1 Condition 1 Analysis of TRIGA Fuel Cluster Rods

Thermal analyses of the NAC-LWT cask for Condition 1 are performed using a half symmetry cross sectional model of the cask in an ISO container positioned along the container centerline. The model employed for the ISO container, cask body and the seven-celled basket is the same finite element model used in Section 3.4.1.3.1 for the MTR fuel thermal model (Condition 1). The similarity in modeling includes the finite element mesh and the material properties for conduction, convection and radiation. The 16 rods and fuel rod inserts are modeled in each of the seven cells, as shown in Figure 3.4-7. Figure 3.4-8 and Figure 3.4-9 show details of the fuel region model. The TRIGA fuel cluster rods were conservatively modeled in the center of the aluminum fuel tube, and the fuel rod inserts were modeled without any contact with the sides of the basket. The 0.13 inch aluminum shell, which surrounds the TRIGA fuel cluster, provides a heat transfer path from the rods to the basket surface. This aluminum shell was conservatively not considered in the analysis. The space between the aluminum tubes and the stainless steel basket surface was modeled with the cavity gas, and the modes of heat transfer from fuel rod insert to the basket surface included conduction through the gas and radiation from the surface of the insert to the basket surface.

3.4.1.6.2 Condition 2 Analysis of TRIGA Fuel Cluster Rods

Thermal analyses of the NAC-LWT cask for Condition 2 are performed using a half symmetry cross sectional model of the cask in which the outer surface of the expansion tank is the boundary of the model. The modeling of the normal steady state conditions of the NAC-LWT from the center of the cask to the outer surface of the expansion tank is identical to the model described in Section 3.4.1.3.1 with the following exceptions:

1. The gas in the NAC-LWT cask cavity is considered to be air.
2. The solar insolance and convection to the ambient temperature of 100°F is applied to the outer shell of the expansion tank.

3.4.1.6.3 TRIGA Fuel Cluster Rods Heat Transfer Results

The thermal analysis is performed to demonstrate that the temperature of the TRIGA fuel cluster rod is maintained within acceptable limits. A conservative temperature of 800°F is established as

the maximum allowable TRIGA fuel cladding temperature for normal conditions of transport. For aluminum 6061-T6 aluminum alloy, the allowable temperature is considered to be 400°F.

Temperatures for package components with the NAC-LWT configured for the TRIGA fuel are summarized in Table 3.4-9. In this table, the maximum fuel clad temperature is 295°F, which is significantly below the 800°F value. For the aluminum, the maximum reported temperature is 292°F, which is also well below the 400°F limit.

3.4.1.7 High Burnup PWR or BWR Rods in a Rod Holder

The high burnup rods may be either BWR rods or PWR rods. The decay heat for the PWR fuel rod contents is 2.3 kW with a corresponding peaking factor of 1.1. The decay heat for the BWR fuel rod contents is 2.1 kW with a peaking factor of 1.22. The thermal evaluation employs a two-dimensional planar model to ensure that the peaking factor is conservatively included and the heat load applied to the finite element model is the total heat load factored by the peaking factor. The bounding product of the heat load and the peaking factor corresponds to the BWR. The evaluation of the BWR rod is considered to bound the temperatures corresponding to the PWR rod configuration. All of the fuel rods are considered to be intact for this evaluation. The evaluation of damaged fuel rods is provided in Section 3.4.1.11.

The rod holder for the high burnup rod transport can accommodate two configurations: a 4×4 matrix of pin tubes containing 16 rods and a 5×5 matrix of pin tubes containing 25 rods. Since the decay heat per rod is considered to be the same, the maximum heat load is bounded by the 25-rod configuration. For the 4×4 matrix of pin tubes, an additional stainless steel insert, .31-inch thick, is placed in the can weldment. This permits the can weldment to be employed for the 16-rod transport or the 25-rod transport configuration. For the can weldment, the aluminum basket and the remainder of the cask, the additional insert has a negligible affect on their temperatures. Therefore, the bounding configuration is the 25-rod configuration, since it produces 56% more heat load in the cask basket than the 16-rod configuration. The bounding configuration for the clad temperatures and the pin tubes supporting the fuel rods is also the 25-rod configuration due to the 56% additional heat load. While the additional insert increases the thermal resistance, this is significantly offset by the additional 56% additional decay heat.

Heat transfer analysis of the NAC-LWT containing high burnup rods is performed using two-dimensional planar finite element analyses and the general purpose ANSYS computer code. Two transport conditions are evaluated:

Condition 1:

The NAC-LWT is supported in an ISO container with solar insolance applied on the surface of the ISO container, and the NAC-LWT is considered to be insulated from the environment (only for normal conditions of transport steady state conditions). The gas inside the ISO container is air.

The cavity of the NAC-LWT is backfilled with helium as required by operational procedures.

Condition 2:

The NAC-LWT is not located in an ISO container and solar insolance is applied to the NAC-LWT cask surface.

For the purpose of performing the thermal analyses, the cavity of the NAC-LWT is considered to be filled with air.

3.4.1.7.1 High Burnup PWR and BWR Fuel Rods Thermal Model of the NAC-LWT (Transported in an ISO Container)

Thermal analyses of the NAC-LWT cask for Condition 1 are performed using a half-symmetry, cross-sectional model of the cask in an ISO container. Heat transfer to the environment is limited to surface convection and radiation on both horizontal and vertical surfaces of the ISO container with an emissivity of 0.36. Solar insolance is applied to the vertical surfaces and the top horizontal surface. Heat transfer from the cask to the ISO container is modeled as conduction, convection and radiation. Convective and conductive heat transfer are modeled in the liquid neutron shield, while heat transfer in the cask cavity is limited to conduction and radiation. Axial heat transfer is conservatively ignored in the model.

Bounding configuration of BWR fuels used in analyses is based on U.S. Department of Energy, Office of Civilian Radioactive Waste Management, "Characteristics of Spent Fuel, High-Level Waste, and Other Radioactive Wastes Which May Require Long -Term Isolation," Appendix 2A, December 1987. Thermal properties of UO_2 and zirconium alloy cladding are from 1) Hagrman, D.L., Reymann, G.A., "Matpro-Version 11, A Handbook of Material Properties for Use in the Analysis of Light Water Reactor Rod Behavior," Idaho Falls, ID, EG&G Idaho, Inc., 1997; 2) Rust, J.H., "Nuclear Power Plant Engineering," Atlanta, GA, S.W., Holland Company, 1979. Thermal conductivity for 6061-T651 aluminum alloy is based on ASME Code, Section II, Part D, Table TCD.

The finite element model for the condition 1 is shown in Figure 3.4-10. The fuel cladding and the inner surface of the pin tube are considered to be in point-to-point contact. The outer surface

of the fuel cladding only contacts the pin tube in one point in the model. The pin tubes are conservatively considered separated and a gap of 0.0005 inch between pin tubes is modeled. This condition neglects any pin tube contact due to dead weight loading of the contents. One of the can weldment sides is modeled in contact with the aluminum insert. For the other three sides, a gap 0.042/0.084/0.042 inch between the aluminum insert and the tube of the can weldment is modeled. The details of this modeling are shown in Figure 3.4-11. Likewise, only one surface between the PWR aluminum insert and the PWR basket is considered to be in contact.

Conduction (through helium) and radiation (using emissivity of stainless steel for both surfaces) are modeled from the inner shell of the cask to the basket.

The heat transfer analysis model uses conduction in the remaining volume of the cask cavity. The conductivity of this material corresponds to helium. (see Table 3.2-7). The properties for the remaining materials are contained in Table 3.2-1 through Table 3.2-8.

The air space between the NAC-LWT cask and the ISO container is modeled using air with an effective conductivity. This effective conductivity (Incropera) is:

$$\frac{k_{eff}}{k} = 0.386\left(\frac{Pr}{0.861+Pr}\right)^{1/4}\left(Ra_c^{*}\right)^{1/4}$$

$$Ra_c^{*} = \frac{[\ln(D_0/D_i]^4}{L^3\left(D_i^{-3/5}+D_0^{-3/5}\right)^5}\,Ra_L$$

$$Ra_L = \frac{g\beta(T_i-T_o)L^3}{\alpha\nu}$$

where:

Pr = Prandtl number (Krieth)

ν = kinematic viscosity (Krieth)

α = thermal diffusivity (Krieth)

β = $1/T_f$

T_f = $(T_i+T_o)/2$

T_i = inner surface temperature

T_o = outer surface temperature

D_i = inner diameter (cask surface)

D_o = outer diameter (height of the ISO container)

$L = (D_o - D_i)/2$

3.4.1.7.2 High Burnup PWR and BWR Fuel Rods Thermal Model of the NAC-LWT (Transported via Truck Trailer)

Thermal analyses of the NAC-LWT cask for Condition 2 are performed using a half-symmetry planar cross-sectional model of the cask in which the inner surface of the inner shell is the boundary of the model. The maximum temperature of 274°F (PWR design basis fuel with 2.5 kW heat load and a peaking factor of 1.2 under normal transport condition [Table 3.4-2]) is applied to the boundary of the model. The modeling of the normal steady state condition of the NAC-LWT from the center of the cask to the inner surface of the inner shell is identical to the model described in Section 3.4.1.7.1 with the following exceptions:

1. The gas in the NAC-LWT cask cavity is considered to be air.
2. The constant temperature of 274°F is applied to the outer surface of the model, which corresponds to the inner surface of the cask inner shell. This temperature corresponds to the condition, which imposes solar insolance and convection/radiation boundary at the outer shell of the expansion tank. This is also described in Section 3.4.1.1.

The Condition 2 model of the NAC-LWT cask with high burnup PWR and BWR fuel rods is shown in Figure 3.4-12. This model is also used to calculate both normal and accident condition temperatures for the cask.

3.4.1.7.3 High Burnup PWR and BWR Fuel Rods Heat Transfer Analyses Results

The thermal analysis is performed to demonstrate that the component temperature of NAC-LWT cask loaded with high burnup PWR and BWR rods is maintained within acceptable limits.

Maximum temperatures for package components with the NAC-LWT configured for high burnup PWR and BWR rods are summarized in Table 3.4-10. As shown in Table 3.4-10, component temperatures are all maintained within their allowable temperatures.

3.4.1.8 Thermal Evaluation for DIDO Fuel

3.4.1.8.1 Analytical Models for the DIDO Fuel Contents

Heat transfer analysis of the NAC-LWT containing DIDO fuel is performed using a two-dimensional planar finite element analysis and the general purpose ANSYS computer code. Two transport conditions are evaluated:

Condition 1:

The NAC-LWT is supported in an ISO container with solar insolance on the surface of the ISO container, and the NAC-LWT is considered to be insulated from the environment (only for the normal conditions of transport steady state conditions). The gas inside the ISO container is air. The cavity of the NAC-LWT is backfilled with helium as required by operational procedures.

Condition 2:

The NAC-LWT is not located in an ISO container and solar insolation is applied to the NAC-LWT cask surface. For the purpose of performing the thermal analysis, the cavity of the NAC-LWT is considered to be filled with air.

A single fuel configuration is considered for this evaluation. Each DIDO fuel assembly is limited to having a heat load of 25 W per assembly. The total contents of the NAC-LWT for the DIDO fuel are limited to having six basket modules and each module is limited to having seven DIDO fuel assemblies. This limits the heat load of a basket module to 175 W, and a total NAC-LWT heat load of 1.05 kW. The 1.05 kW total heat load is enveloped by the 1.26 kW total heat load for the NAC-LWT MTR fuel contents contained in Section 3.4.1.3. Since the NAC-LWT cask ambient conditions are the same for the DIDO fuel as for the MTR fuel, the maximum temperature of all cask body components for the DIDO contents are enveloped by the maximum temperatures for the MTR fuel contents. Therefore, the cask inner shell temperature for the MTR fuel contents bounds the maximum cask inner shell temperature for the DIDO fuel contents. The maximum cask inner shell temperature is used as the boundary condition for the finite element model for the DIDO thermal evaluation. For Condition 1 and Condition 2, the maximum inner shell temperatures are 214°F and 181°F, respectively. These values correspond to the design basis heat load values obtained from Table 3.4-6.

Two finite element models are used in the evaluation of the DIDO fuel basket and the DIDO fuel assemblies.

The evaluation of the maximum basket component temperatures for these conditions is performed using a finite element model, which is shown in Figure 3.4-14. This model is used to evaluate both conditions. This model corresponds to the 4.01-inch inside diameter stainless steel tubes, the 1/2-inch thick plates, the 3/4-inch × 3/8-inch aluminum bars (thermal shunts) and the 0.19-inch thick aluminum sheet (heat transfer shell) on the outside of the tubes. The SOLID70, eight-noded brick element is used to represent stainless steel components, the heat transfer shell and the cavity gas between the surfaces of the circular plates and the heat transfer shell and the

inner shell of the cask body. To account for the axial conductance of the thermal shunts, they are modeled as conduction elements using an area corresponding to the dimensions of the aluminum bars. Radiation is conservatively neglected from the outer surface of the heat transfer shell and the inner surface of the cask inner shell. The center tube is assumed not to be in contact with any of the six outer tubes. During transport, the NAC-LWT is in a horizontal position in which the basket modules are in contact with the inner shell of the cask. To represent the contact of the basket module with the cask inner shell, the inner shell temperature was applied to two nodes of the circular plates and the remaining nodes corresponding to the inner surface of the inner shell of the cask body. The 25 W per assembly heat load is represented by applying the heat flux along a concentrated area at the inner tube surface, which would correspond to the contact of the fuel assembly with the 4.01-inch inside diameter stainless steel tube.

For Condition 1, the elements representing the cavity gas between the basket and the inner shell correspond to helium, whereas for Condition 2, these elements use properties for air.

To determine the maximum temperature for the fuel, a separate detailed model of a DIDO fuel assembly is constructed. This model is shown in Figure 3.4-15, which consists of four circular cylinders in contact at a corresponding single point to be transported in the horizontal position. Each cylinder is comprised of a layer of fuel of 0.64 mm (0.025 in.) thickness between two aluminum shells, each being 0.46 mm (0.018 in.) thick. The boundary condition of this model is the maximum basket temperature determined from the detailed basket model and the volumetric heat generation corresponding to 25 W per assembly.

3.4.1.8.2 DIDO Fuel Heat Transfer Analyses Results

The thermal analysis is performed to demonstrate that the temperature of the DIDO fuel is maintained within acceptable limits. A conservative temperature of 400°F is established as the maximum allowable DIDO fuel cladding temperature for normal conditions of transport. The aluminum retains it capability to function as a mechanical component in this temperature range and it is not close to the 1,220°F melting temperature of aluminum (Table 6.4.1, p. 6-60, Marks' Mechanical Handbook for Mechanical Engineers). The material properties presented in MIL-HDBK-5F indicate that 2000 series aluminum retains over 40% of its room temperature yield and ultimate strengths at a long-term temperature of 300°F.

Maximum temperatures for package components with the NAC-LWT configured for DIDO fuel are summarized in Table 3.4-12. The reported temperatures are lower at all locations than the corresponding temperatures for the design basis PWR fuel presented in Table 3.4-2. The DIDO fuel assembly cladding temperatures are maintained below 400°F.

3.4.1.9 Thermal Evaluation for General Atomics IFM

The heat generated from the General Atomics IFM in the Fuel Handling Unit (FHU) is transferred to the basket by thermal conduction and radiation, and is then transferred to the cask inner shell from the basket surface by the same heat transfer modes. The heat is finally transferred through the cask and International Shipping Organization (ISO) container to ambient. The thermal resistance model and thermal analysis of General Atomics IFM consider a single FHU of the fuel. The maximum temperature from the resistor model corresponds to the FHU's stainless steel shell, while the minimum temperature corresponds to the inner surface of the transport cask inner shell. The fuel is actually stored in two FHUs, but the evaluation conservatively considers the total heat load of 13 W to be placed into a container at the center of the cask cavity. The evaluation does not consider the reduction in thermal resistance due to the contact of the FHU with the basket or of the basket with the inner shell of the transport cask. Additional conservatism is included by ignoring heat transfer by radiation across any of the gaps in the system. To ensure that a bounding temperature for the basket is calculated, air properties are used in the analysis for the gas in the cavity. Also, conservatism is included by using the inner shell temperature corresponding to the 1.26 kW condition for the cask body as opposed to 13 W. This analysis, therefore, bounds transport in the cask with and without an ISO container.

A thermal evaluation of the top module is performed by considering a heat load of 13 W in the center of the basket with only one 6.0-inch diameter top module tube. This is conservative because it maximizes the gap between the tube and the cask inner shell. Air is used as the cavity gas as an additional conservatism. The maximum temperature is computed using the resistor analogy.

For concentric cylinders, the thermal resistance (R) for the heat flow through the cylinders is taken from Krieth as:

$$R = \frac{\ln\left(\frac{r_2}{r_1}\right)}{2\pi K L}$$

where:

r_2 = outer radius of cylinder (inch)

r_1 = inner radius of cylinder (inch)

K = thermal conductivity (BTU/hr/in/°F)

The effective resistance from the secondary enclosure can be expressed as to the cask inner shell:

$$R_T = R_1 + R_2 + R_3 + \frac{1}{\frac{1}{R_4} + \frac{1}{R_5}}$$

where:

R_1 = resistor of the outer canister

R_2 = resistor of the gap between outer canister and the basket shell

R_3 = resistor basket shell

R_4 = resistor of the air from the basket shell to inner shell surface (outside of the basket disks)

R_5 = resistor of stainless steel disks supporting the basket shell in series with the air gap between the basket disks and the inner shell

The maximum temperature of the secondary enclosure can be determined by the following equation:

$$T_i = R_t Q + T_{cask}$$

where:

Q = total heat load

T_{cask} = temperature of cask inner shell

The following parameters will be used for this evaluation:

Q = 13 Watts

L = 37.0 inches – length of shortest secondary fuel closure

r_1 = 2.255 inches – minimum inner radius of secondary closure

r_2 = 2.375 inches – minimum outer radius of secondary closure

r_3 = 2.75 inches – inner radius of module fuel cell

r_4 = 3.00 inches – outer radius of module fuel cell

r_5 = 6.688 inches – inner radius of LWT

r_6 = 6.6325 inches – outer radius of the basket disks

K_{ss} = 0.7143 Btu/hr/in/F at 70°F for stainless steel

K_{air} = 0.00161 Btu/hr/in/F at 300°F for air

From Table 3.4-6, the maximum temperature of the LWT inner shell for a 1.26 kW heat load is 214°F, with 100°F ambient temperature with solar insolance. This is used as a bounding temperature for the cask inner shell (T_{cask}) for this evaluation.

$$R_{eff} = \frac{1}{\frac{1}{R_4} + \frac{1}{R_5}} \qquad R_4 = \frac{\ln(6.688/3.0)}{2\pi(0.00161)(37.0-2)}$$

$$R_4 = 2.264$$

$$R_5 = \frac{\ln(6.8125/3.0)}{2\pi(0.7143)(2)} + \frac{\ln(6.688/6.6325)}{2\pi(0.00161)(2)}$$

(Stainless steel disk in series with the air between the basket disk and the inner shell)

$$R_5 = 0.503$$

$$R_{eff} = \frac{1}{\frac{1}{R_4} + \frac{1}{R_5}}$$

$$R_{eff} = 0.412$$

$$R_T = R_1 + R_2 + R_3 + R_{eff}$$

$$R_T = \frac{\ln(2.375/2.255)}{2\pi(0.7143)(37.0)} + \frac{\ln(2.75/2.375)}{2\pi(0.00161)(37.0)} + \frac{\ln(3.0/2.75)}{2\pi(0.7143)(37.0)} + 0.412$$

$$R_T = 0.0003 + 0.392 + 0.0005 + .412 = 0.805$$

The maximum temperature of the secondary enclosure (T_i) is:

$$T_i = 0.805(13 \times 3.415) + 214 = 250^\circ F$$

The maximum temperature of the basket is conservatively considered to be the same as the temperature of the secondary enclosure (250°F). Temperatures of individual components are summarized in Table 3.4-13.

The maximum content temperature for the GA IFM shipment is considered to be bounded by the TRIGA maximum fuel cladding temperature of 326°F contained in Table 3.4-8, which corresponds to a bounding heat load of 1.05 kW (as compared to the approximately 13 watts for the GA IFM).

A conservative temperature of 800°F is established as the maximum allowable temperature for the stainless steel basket and the contents, which is comprised of the steel-clad TRIGA fuel and the HTGR pellets. The steel cladding of the TRIGA fuel is actually an inconel alloy. Mil HDBK-5G (1 November 1994), Section 6.3.2, identifies that alloys of inconel are used for parts

requiring strength for temperatures exceeding 1,000°F, which significantly exceeds 800°F. The HTGR pellets were designed for operational exposure to reactor core temperatures exceeding 1,000°F, which also exceeds 800°F. Therefore, the maximum temperatures for the contents for the GA IFM are acceptable.

3.4.1.10 High Burnup PWR or BWR Fuel Rods in a Fuel Assembly Lattice

The NAC-LWT cask may transport up to 25 intact high burnup PWR or BWR fuel rods that are in a fuel assembly lattice. The decay heat for the PWR rods is 2.3 kW with a corresponding peaking factor of 1.1, and the decay heat for the BWR rods is 2.1 kW with a corresponding peaking factor of 1.22.

The thermal evaluation employs two-dimensional planar half-symmetry models of the fuel lattice with 25 fuel rods, fuel channel (for BWR fuel), PWR insert (for BWR fuel), fuel basket, and the gas inside the cask cavity. The model extends to the inner surface of the cask inner shell. The model for a 7 × 7 BWR fuel lattice with 25 fuel rods is shown in Figure 3.4-16. BWR arrays of 7 × 7, 8 × 8, 9 × 9, and 10 × 10 are analyzed. PWR arrays of 14 × 14, 15 × 15, 16 × 16, and 7 × 17 are analyzed. The BWR model includes a fuel channel and insert, which are absent from the PWR model.

To determine the worst-case fuel rod arrangement, the 25 fuel rods are analyzed in five different arrangements:

1. Centered (top and bottom) in the two-dimensional model (as shown in Figure 3.4-16).
2. Centered horizontally and concentrated at the bottom of the lattice cross-section.
3. Spread out horizontally and concentrated at the bottom of the lattice cross-section.
4. Centered horizontally and concentrated at the top of the lattice cross-section.
5. Spread out horizontally and concentrated at the top of the lattice cross-section.

For the even numbered fuel arrays (i.e., 8 × 8, 10 × 10, 14 × 14, and 16 × 16), only 24 fuel rods are modeled due to the use of the half-symmetry models. For these cases, a higher heat generation rate is applied at each fuel rod so that the total heat load of 2.3 kW for PWR and 2.1 kW for BWR is maintained. The empty fuel rod locations in the lattice are modeled as air. The maximum inner shell temperature (274°F) for the PWR design basis fuel with 2.5 kW heat load (Table 3.4-2) is applied to the boundary of the model.

For each fuel array and fuel rod location configuration, a steady-state thermal analysis is performed using the general purpose ANSYS computer code. The Condition 2 transport case, with the NAC-LWT not located in an ISO container is evaluated. As shown in Table 3.4-10, this

results in higher maximum temperatures for the fuel cladding than transport Condition 1 where the cask is assumed to be inside of the ISO container. Transport Conditions 1 and 2 are described in Section 3.4.1.3.

3.4.1.11 High Burnup PWR and BWR Fuel Rods in a Rod Holder with Damaged Fuel Rods

The NAC-LWT may transport up to 25 PWR or BWR high burnup fuel rods in a rod holder, with up to 14 of the fuel rods classified as damaged. The maximum decay heat for these configurations is 2.3 kW for PWR and 2.1 kW for BWR. The finite element model for the evaluation of the 25 intact fuel rods in a rod holder is described in Section 3.4.1.7. This section provides the thermal evaluation for the configuration containing damaged fuel rods. The analysis conservatively assumes 15 damaged fuel rods, with the remainder of the rod holder containing intact fuel. The model used for this analysis is based on the two-dimensional half-symmetry model described in Section 3.4.1.7 (Condition 2 configuration), as shown in Figure 3.4-12. Modifications were made to the fuel regions to simulate the damaged fuel rods.

The basket design for the high burnup fuel rod transport can accommodate two configurations: a 4×4 matrix of fuel tubes containing 16 rods and a 5×5 matrix of fuel tubes containing 25 rods. Since the decay heat per rod is considered the same, the maximum heat load occurs with the 5×5 matrix and is the configuration evaluated. Thermal analysis is performed for three cases with different locations of the 15 damaged fuel rods. The fuel rod locations are shown in Figure 3.4-17, which shows the matrix region of the thermal model shown in Figure 3.4-12. The nine locations in the half-symmetry model correspond to 15 actual fuel rod locations. The three cases evaluated are:

Case 1: Damaged fuel rods in locations 4 through 12
Case 2: Damaged fuel rods in locations 7 through 15
Case 3: Damaged fuel rods in locations 1 through 9

The inner surface of the inner shell is the boundary of the model. From Table 3.4-2, the maximum inner shell temperature of 274°F for PWR design basis fuel with 2.5 kW heat load for normal transport conditions is applied to the boundary of the model. The maximum temperature of 274°F results from the condition of solar insolation and convection/radiation to surroundings.

To simulate the damaged fuel rods, a 50% compaction of the fuel material in the fuel tubes is considered. It is assumed that the interior region of the fuel rod tube consists of 50% fuel debris and 50% gas. One half of the heat generation rate for the intact fuel rod is conservatively applied to the entire interior region of the fuel rod tube. Since the volume of the interior of the fuel rod

tube is four times that of the volume of an intact fuel rod, the applied heat load for the damaged fuel is two times that of the heat load for an intact fuel rod. In addition, the heat generation rate is multiplied by a peaking factor of 1.22. The material properties in the entire interior of the fuel rod tubes for the damaged fuel are conservatively considered to be the thermal properties of the fuel (rather than 50% fuel and 50% gas), since this results in higher temperatures in the fuel rod tube walls and the surrounding components.

3.4.1.12 Thermal Evaluation for TPBARs

Heat transfer analysis of the NAC-LWT containing TPBARs is performed using a two-dimensional planar finite element analysis and the general purpose ANSYS computer code. The NAC-LWT is transported in an ISO container with solar insolance on the surface of the ISO container during normal conditions of transport. The gas inside the ISO container is air. The cavity of the NAC-LWT is backfilled with helium as required by operational procedures.

There are two TPBAR content conditions requested for certification: the first is for the transport of up to 300 production TPBARs (of which two can be prefailed) in an open consolidation canister; the second is for the transport of up to 55 segmented TPBARs in a welded closed waste container. The 55 segmented TPBARs and debris resulting from PIE are limited to a total heat load of 127 W, based on a minimum of 90 days of cooling (2.31 watts/rod). Therefore, the loaded TPBAR consolidation canister with 300 rods is considered the bounding content condition for this thermal evaluation with each TPBAR limited to a heat load of 2.31 W, which corresponds to a 90-day cooling period (see Appendix 1-C of Chapter 1). This limits the maximum heat load of the NAC-LWT with TPBAR contents to 0.693 kW. The 0.693 kW total heat load is enveloped by the 1.05 kW total heat load for the NAC-LWT TRIGA fuel contents as described in Section 3.4.1.6. Since the NAC-LWT cask ambient conditions are the same for the TPBAR contents as for the TRIGA fuel contents, the maximum temperature of all cask body components for the TPBAR contents are enveloped by the maximum temperatures for the TRIGA fuel contents. Therefore, the cask inner shell temperature of 222°F (Table 3.4-9) for the TRIGA fuel contents bounds the cask inner shell temperature for the TPBAR contents and is used as the bounding condition for the TPBAR thermal evaluation.

The evaluation of the maximum component temperatures for TPBARs is performed using a finite element model as shown in Figure 3.4-18. This model corresponds to the aluminum basket, the consolidation canister containing 300 TPBARs, and the helium inside the cask. The loaded TPBAR consolidation canister bounds the maximum decay heat of the TPBAR waste container containing 55 segmented TPBARs and, therefore, the thermal evaluation bounds all TPBAR content conditions.

Any axial conductance of the contents is conservatively neglected in this two dimensional planar model. The ANSYS PLANE55 and MATRIX50 elements are used. Radiation is considered using radiation matrix elements while convection is conservatively ignored in the following regions.

- Between the outer surfaces of TPBARs.
- Between the inner surface of the consolidation canister and the adjacent TPBARs.
- Between the outer surface of the consolidation canister and the inner surface of the basket.
- Between the outer surface of the basket and the inner surface of the cask inner shell.

A constant temperature of 222°F (Table 3.4-9, Condition 1) was applied to the outer surface of the model, which corresponds to the inner surface of the cask inner shell. During transport, the NAC-LWT is in a horizontal position in which the TPBAR contents are in contact with the inner surface of the basket, while the basket plates are in contact with the inner shell of the cask.

The heat generated by the 300 TPBARs is applied via a heat generation rate to the stainless steel cladding of the TPBARs. A peaking factor of 1.15 is used in the heat generation rate calculation based on a heat load of 2.31 W for each TPBAR.

The thermal analysis demonstrates that the temperature of the TPBARs is maintained within a conservative limit of 300°F for normal conditions of transport. At 300°F, the aluminum retains its capability as a mechanical component.

Maximum component temperatures for the NAC-LWT containing TPBAR contents are summarized in Table 3.4-16. Maximum cask component temperatures for normal conditions are conservatively obtained from the analysis results corresponding to the TRIGA fuel contents, as shown in Table 3.4-9 (Condition 1).

3.4.1.13 PULSTAR Fuel Elements in 28 MTR Basket

Three loading patterns for PULSTAR fuel elements are postulated for the 28 MTR basket configuration.

- Intact fuel assemblies will be directly loaded into 28 MTR basket;
- Intact fuel elements (rods) will be loaded in the fuel rod insert or the PULSTAR cans;
- Damaged fuel elements (rods) or debris will be loaded in the PULSTAR cans.

The heat load in each basket cell is limited to 30 watts. This corresponds to a maximum heat load of 210 watts for each of the four basket modules. The cask cavity is back-filled with helium.

The thermal analysis for the PULSTAR fuel contents in the 28 MTR basket is bounded by the thermal analysis for the TRIGA fuel cluster rods as presented in Section 3.4.1.6. The MTR basket (Section 3.4.1.3) has the same cross-sectional dimensions and basket material as the basket for TRIGA fuel cluster rods. The maximum modular heat load for TRIGA fuel cluster rods is identical to the maximum modular heat load of the PULSTAR fuel contents (210 watts). The bounding condition for the thermal evaluation for the TRIGA fuel cluster rods is "Condition 2" as described in Section 3.4.1.6.2. In the two-dimensional planar model for the TRIGA fuel cluster, the cask cavity is modeled as air. The model conservatively includes an air gap between the fuel cladding and the aluminum tube and between fuel tube assembly and the inner surface of the basket cell, as shown in Figure 3.4-8 and Figure 3.4-9. This is conservative since there is contact between these components, which provides a significant heat transfer path from the fuel to the basket. Note that the aluminum tubes have an insignificant effect on heat transfer, since the air gap controls the heat conduction in the in-plane direction and the model is a two-dimensional planar model, which neglects any heat transfer in axial direction. Since the PULSTAR fuel rod insert is identical to the TRIGA rod insert, the thermal analysis results for TRIGA fuel cluster rods, Condition 2, as presented in Table 3.4-9, are used as the temperature results for the PULSTAR fuel. These temperatures are summarized in Table 3.4-17 for the PULSTAR fuel. The cask body component maximum temperatures with the NAC-LWT configured for the PULSTAR fuel conservatively use the temperatures from Condition 1 and Condition 2 in Table 3.4-17. The maximum temperatures for the cask body and basket are 222°F and 278°F, respectively, which are significantly below the allowable for stainless steel. For the configuration with intact rods or failed rods loaded in a PULSTAR can, the maximum fuel cladding temperature from Table 3.4-17 is conservatively used as the maximum temperature of the fuel can. The maximum fuel cladding temperature is 295°F, which is significantly below the allowable temperature limit of 1,058°F during transport.

3.4.1.14 Thermal Evaluation for ANSTO Fuel

Two types of ANSTO fuel may be loaded in the ANSTO basket in the NAC-LWT cask:

- MOATA plate fuel elements
- Mark III spiral fuel elements

The ANSTO basket consists of six modules with seven fuel tubes in each module. Each fuel tube may be loaded with a MOATA plate bundle or a Mark III spiral fuel assembly. The maximum heat load for a MOATA plate bundle is 0.4 watt (3 watts per assembly is conservatively considered in the thermal evaluation in this section). The maximum heat load is

18 watts per assembly for the Mark III spiral fuel. The corresponding maximum heat load per cask is 0.126 kW for the MOATA plate bundles and 0.756 kW for the Mark III spiral fuel.

The NAC-LWT is supported in an ISO container with solar insolance applied on the surface of the ISO container. The gas inside the ISO container is air. The cavity of the NAC-LWT is actually backfilled with helium as required by operational procedures.

The thermal evaluation for the MOATA plate fuel elements and Mark III spiral fuel is performed using finite element analysis with the ANSYS program. The finite element models for the MOATA plate bundles and Mark III spiral fuel are shown in Figure 3.4-19 and Figure 3.4-20, respectively. Each model corresponds to a quarter-symmetry cross-section of the fuel, the basket and the helium inside the cask cavity. The models are constructed using ANSYS PLANE55 two-dimensional planar elements. The maximum cask inner shell temperature of 222°F for the LWT cask loaded with the TRIGA fuel cluster rods (see Table 3.4-9) is conservatively used as the boundary condition for both models. The heat load used in the evaluation of the TRIGA fuel cluster rods is 1.05 kW per cask (see Section 3.4.1.6), which is significantly higher than the heat load for the MOATA fuel and Mark III spiral fuel. The MOATA plate fuel elements are explicitly modeled with aluminum cladding on both sides of the fuel meat. A volumetric heat generation rate corresponding to 3 watts per assembly is applied to the elements for fuel meat for the MOATA plate fuel.

The MARK III spiral fuel assemblies are modeled as straight plates with effective orthotropic properties. The longitudinal (radial) properties are decreased to reflect the reduction of the length (from the actual curved plates to the straight plates in the model). The material properties for the fuel meat are conservatively used in the transverse (circumferential) direction of the fuel elements in the model (conductivity of the aluminum clad is higher than that for the fuel meat). A volumetric heat generation rate corresponding to 18 watts per assembly is applied to the fuel elements for the Mark III spiral fuel.

The thermal conductivities of the fuel matrix for MTR fuel from Section 3.4.1.3 are used as the conductivities for the fuel meat for the MOATA plate and MARK III spiral fuel elements in the thermal models. These thermal conductivities are conservative since the fuel meat for the MOATA plate fuel and Mark III spiral fuel is composed of uranium and aluminum alloy, which are significantly more conductive than the fuel matrix material for the MTR fuel. Radiation between the basket tube and the cask inner shell is conservatively not considered in the models. For the MOATA fuel, radiation is only considered between fuel plates. For the Mark III spiral fuel, radiation is modeled across the helium gap between the fuel outer tube and the basket tube.

Steady-state thermal analysis is performed to demonstrate that the temperature of the MOATA plate fuel and Mark III spiral fuel is maintained within acceptable limits. A conservative temperature of 400°F is established as the maximum allowable temperature for these aluminum-clad fuel elements, as discussed in Section 3.4.1.3.3 for the MTR fuel.

3.4.1.15 High Burnup PWR MOX Rods in a PWR/BWR Rod Transport Canister

A maximum of 16 PWR MOX fuel rods (or a combination of PWR MOX and standard PWR fuel rods) may be placed in the PWR/BWR Rod Transport Canister, including a 5 × 5 insert. Along with the maximum 16 PWR MOX rod contents, the remaining tubes may be loaded with burnable poison rods or other zirconium alloy-based hardware components with negligible activation and heat load. The maximum decay heat for the PWR MOX rods is 2.3 kW (or 143 W/rod), with a corresponding peaking factor of 1.1.

The thermal evaluation described in Section 3.4.1.7 for the high burnup PWR and BWR rods is a two-dimensional planar model in which the heat load applied to the model is based on the BWR rod decay heat load factored by the peaking factor. The bounding product of the heat load and the peaking factor for the PWR MOX rods is (2.3)(1.1) or 2.53 kW, as compared to (2.1)(1.22) or 2.56 kW for the BWR high burnup rods. The evaluation performed in Section 3.4.1.7 using the BWR high burnup rods is considered to bound the heat load for the 16 PWR MOX rods.

As described in Section 3.4.1.7, the model for the 25-rod configuration (in a 5 × 5 insert) uses a heat load of (25/16) times the product of the BWR rod decay heat and associated peaking factor. With this bounding heat load, it is, therefore, not necessary to evaluate the 16-rod configuration in the Rod Transport Canister with a 5 × 5 insert.

The thermal conductivities of the UO_2 and MOX from MATPRO-Version 11 at 600°F are 0.26 Btu/hr-in-°F and 0.22 Btu/hr-in-°F, respectively. The thermal resistance to the heat rejection of the rod canister is due to the thin tube walls and the gaps modeled between the tubes and rods and the basket insert. The reduction in the conductivity of the rod material has an insignificant effect on the thermal resistance incorporated in the gaps and thin tube walls in the model. The thermal resistance internal to each rod does not affect the rejection of the heat from other rods in the basket. Since the maximum number of PWR MOX rods is limited to 16, there are nine or more other vacant positions in the basket without the heat generation of the PWR MOX rods. The evaluation of any arbitrary configuration of tubes, with and without the PWR MOX rods, is bounded by an evaluation of the model having all tubes containing the design basis heat load of 143 W for each PWR MOX rod.

The evaluation using BWR rods in Section 3.4.1.7 is considered to bound all configurations of PWR MOX rods.

Maximum temperatures for package components with the NAC-LWT cask configured for high burnup PWR and BWR fuel rods are summarized in Table 3.4-10. As the analyzed BWR fuel rod content condition is bounding, the temperatures presented in Table 3.4-10, Condition 1 (helium cavity gas backfill) provide bounding temperatures for the PWR MOX fuel rod content configuration. As shown in Table 3.4-10, maximum calculated component temperatures for all critical safety components including the fuel rod cladding, the lid metallic containment seal, the Alternate B port cover metallic containment seals, the lead gamma shield and the liquid neutron shield are maintained within their allowable temperature limits as further defined in Section 3.3. Note that for the transport of PWR MOX fuel rods, metallic containment seals will be installed on the lid and Alternate B port cover in accordance with the NAC-LWT cask leaktight transport configuration specified for the PWR MOX fuel rod contents.

3.4.2 Maximum Temperatures

Using the models described, temperatures for the cask body and fuel rod cladding are determined for maximum normal operation conditions (2.5 kW decay heat load, 130°F ambient temperature, still air, full insolation). The maximum cask component and fuel rod cladding temperatures for PWR fuel (2.5 kW) are listed in Table 3.4-2. Not all of the cask components are explicitly modeled; their temperatures are obtained by evaluating the analytical model at the component location. Maximum normal operating temperatures for the 1.26 kW MTR fuel and the 1.05 kW TRIGA fuel configurations are shown in Table 3.4-6 and Table 3.4-8, respectively. Maximum normal operating temperatures for high burnup PWR and BWR fuel rods in a rod holder are shown in Table 3.4-10. The maximum component temperatures for DIDO fuel and General Atomics IFM for normal conditions of transport are shown in Table 3.4-12 and Table 3.4-13, respectively. The maximum component temperatures for 25 high burnup PWR and BWR fuel rods in a fuel assembly lattice are shown in Table 3.4-14. The maximum component temperatures for high burnup PWR or BWR fuel with up to 14 damaged fuel rods in a rod holder are shown in Table 3.4-15. Maximum operating component temperatures for the NAC-LWT containing TPBARs are shown in Table 3.4-16. The maximum operating temperatures for the PULSTAR fuel contents in the MTR basket are shown in Table 3.4-17. The maximum component temperatures for the NAC-LWT containing MOATA plate fuel and Mark III spiral fuel are presented in Table 3.4-22.

3.4.3 Minimum Temperatures

As stated in Section 3.4.1, the minimum temperatures in the cask occur with a 0.0 kW decay heat load and the minimum ambient conditions. Under these conditions, a uniform temperature of -40°F will exist in the cask. The maximum thermal stresses in the cask, during normal

operations conditions, occur when the design basis decay heat load of 2.5 kW exists in the cask along with the minimum ambient conditions (-40°F ambient temperature and no insolance). The cask component and fuel rod clad temperatures for the 2.5 kW decay heat load with minimum ambient conditions are listed in Table 3.4-3.

3.4.4 Maximum Internal Pressures

3.4.4.1 Maximum Internal Pressure for Design Basis Fuel in Normal Conditions

The NAC-LWT cask is filled to one atmosphere (14.7 psia) upon loading. It is necessary to evaluate the internal pressure of the cask after thermal equilibrium has been attained. Assuming a maximum normal fuel cladding temperature of 472°F (932°R) from Table 3.4-2, 3 percent fuel rods rupture, and 30 percent of the fission gas and 100 percent of the rod backfill gas escape from the ruptured fuel rods, the cask internal pressure is calculated. Table 3.4-4 reports the fission gas inventories for the design basis PWR fuel assembly. Table 5.1-2 reports the design parameters of the design basis PWR fuel. Using information from Table 5.1-2, the void volume of a single fuel rod is calculated as 2.43 in^3 (39.82 cm^3) by subtracting the volume of the fuel pellets from the volume of an empty fuel rod (the plenum spring volume is disregarded). The total fuel assembly void volume is calculated as 495.16 in^3 (8,123.28 cm^3) by multiplying the single fuel rod volume by 204, the number of fuel rods in the fuel assembly. The total fuel assembly void volume, the fission gas inventory information in Table 3.4-4, and the maximum normal transport temperature (472°F) are applied to the ideal gas law (PV = nRT) to obtain the pressure in the unruptured fuel rods due to the fission gases. This fission gas pressure, 1,771.5 psia, is also reported in Table 3.4-4, based on 100% availability of fission gases, later adjusted to 30%. The releasable fission gas pressure and rod backfill pressure (assumed 565 psia) are summed to obtain the total fuel rod pressure.

The cask pressure is obtained using Dalton's Law of Partial Pressures:

$$P = P_A + P_B$$

where:

P = total pressure

P_A = partial pressure of gas A (cask cavity helium gas backfill)

P_B = partial pressure of gas B (fuel rod backfill and fission gas)

The reported cask and fuel rod backfill pressures are at standard temperature (72°F) and must be corrected to the normal transport temperature. Given that the internal volumes of the NAC-LWT Cask and the fuel rods remain constant, the resultant pressure is proportional to the temperature change according to the ideal gas law:

$$P_2 = P_1\left(\frac{T_2}{T_1}\right)$$

where:

P_1 = 14.7 psia (cask backfill pressure)

T_1 = 72°F (532°R) (cask backfill temperature)

T_2 = 472°F (932°R) (maximum normal operating condition cavity gas temperature)

Thus, the cask backfill pressure at normal operating temperature equals:

$$P_2 = 14.7\ \text{psia}\left(\frac{932°R}{532°R}\right)$$

$$P_2 = 25.8\ \text{psia}$$

For the fuel rod backfill pressure at normal operating temperature:

P_1 = 565 psia (fuel rod backfill pressure)

T_1 = 72°F (532°R) (fuel rod backfill temperature)

T_2 = 472°F (932°R) (maximum normal operating condition cavity gas temperature)

and:

$$P_2 = 565\ \text{psia}\left(\frac{932°R}{532°R}\right)$$

$$P_2 = 989.8\ \text{psia}$$

The partial pressure of the cask backfill distributed over the cask free volume (including 3% failed rods) is calculated by:

$$P_{\text{cask backfill}} = P_{\text{initial}}\left(\frac{V_{\text{cask}}}{V_{\text{total}}}\right)$$

where:

$P_{initial}$ = 25.8 psia (temperature adjusted cask backfill pressure)

V_{cask} = 5.196 ft^3 (147,134 cm^3)

$V_{rod\ void}$ = 244 cm^3 (volume of 3% failed fuel rods)

V_{total} = V_{cask} + $V_{rod\ void}$

V_{total} = 147,378 cm^3

Thus, the cask backfill partial pressure at normal operating temperature, including the volume of failed fuel rods equals:

$$P_{cask\ backfill} = 25.8\ psia \left(\frac{147{,}134 cm^3}{147{,}378 cm^3} \right)$$

$$P_{cask\ backfill} = 25.8\ psia$$

The partial pressure of the failed fuel rod gases in the cask cavity is calculated by:

$$P_{fuelrods} = P_{initial} \left(\frac{V_{rodvoid}}{V_{total}} \right)$$

where:

$P_{initial}$ = 1,521.3 psia (fission gas pressure (0.30 x 1,771.5 psia) plus rod backfill pressure (989.8 psia))

$V_{rod\ void}$ = 244 cm^3

V_{total} = 147,378 cm^3

Thus, the failed fuel rod partial pressure at normal operating temperature, including fission gases and the volume of cask cavity void equals:

$$P_{fuelrods} = 1{,}521.3\ psia \left(\frac{243.7 cm^3}{147{,}378 cm^3} \right)$$

$$P_{fuelrods} = 2.5\ psia$$

Summing the two partial pressures yields the total cask pressure.

$$P_{Total} = P_{cask\ backfill} + P_{fuelrods}$$

$P_{Total} = 25.8 \text{ psia} + 2.5 \text{ psia}$

$P_{Total} = 28.3 \text{ psia}$

3.4.4.2 High Burnup Fuel Rod Canister Maximum Normal Conditions Internal Pressure

The high burnup fuel sealed canister is filled to one atmosphere (14.7 psia) upon loading. The canister internal pressure is calculated assuming that the average helium backfill gas temperature is 600°F (1060 R) and that 3 percent of the fuel rods fail in normal conditions of transport. The temperature of the canister gas is selected to conservatively bound the temperatures given in Table 3.4-10, Table 3.4-14 and Table 3.4-15. On failure, the fuel rods are assumed to release 30% of the fission gas and 100% of the rod backfill gas. To bound both the PWR and BWR analysis, the fuel type with the highest fission source, on a per rod basis, and smallest free gas volume inside the sealed canister is selected. This fuel type is the Exxon 7 × 7 BWR fuel. The fission gas inventory for this fuel is shown in Table 3.4-11, which reports the fission gas inventory for the assembly, and on a per rod basis. The design parameters for the Exxon 7 × 7 fuel rod are:

Parameter	Value
Number of Rods	49
Rod Diameter (in)	0.570
Clad Thickness (in)	0.036
Pellet Diameter (in)	0.4900
Active Fuel Length (in)	150
Rod Length (in)	170

From the values shown, the void volume of a single fuel rod is calculated as 4.82 in^3 (78.99 cm^3) by subtracting the volume of the fuel pellets from the volume of an empty fuel rod (the plenum spring volume is disregarded). For the analysis, 3% of 25 rods is taken to fail, which is 0.75 rods. Conservatively, the number of failed rods is defined as one, which is equal to a 4% fuel rod failure. The equivalent void volume is then equal to one rod, or 4.82 in^3. The fission gas inventory, provided in Table 3.4-11, and the maximum normal transport temperature (600°F) are applied to the ideal gas law (PV = nRT) to obtain the pressure in the unruptured fuel rods due to the fission gases. This fission gas pressure, 4,251 psia (Table 3.4-11), is based on 100% availability of fission gases, which is adjusted to account for the 30 percent release of the fission gas. The releasable fission gas and rod backfill pressures are summed to obtain the total fuel rod pressure.

The ideal gas law is used to analyze the effects of pressure, temperature, volume, and gas inside the cask the ideal gas law states:

$$pV = nRT$$

where:

p = pressure (atm)
V = volume (liters)
n = gram-moles of material
R = gas constant (0.0831 atm-liters/K g-mole)
T = temperature (K)

After the rods rupture, the resultant internal cask pressure is impacted by three sources: the 1-atm inert gas backfill of the canister, the fission product gas escaping from the fuel rods, and the fuel rod inert gas backfill escaping from the ruptured fuel rods. To calculate the resultant internal cask pressure after the fuel rods rupture, partial pressures are calculated using Dalton's law:

$$P = P_a + P_b$$

where:

P = total pressure

P_a = partial pressure of gas A

P_b = partial pressure of gas B

The void volume of the fuel rod is simply the volume contained within the cladding less the fuel volume. The rod is modeled as a cylinder with a 0.570-in outside diameter, a 0.036-in. wall thickness, and a 150-in. active fuel length. The volume of the plenum spring is disregarded. The void volume, which includes the plenum volume, is 4.82 in^3 per rod.

The partial pressure of the canister is calculated by:

$$P_{canister} = P_{initial}\left(\frac{V_{canister}}{V_{total}}\right)$$

where:

$$P_{initial} = P_{atm} * \frac{T_{norm}}{T_{stand}} = 14.7\ \text{psia} * \frac{588.7\ \text{K}}{295.35\ \text{K}} = 29.3\ \text{psia}$$

$P_{initial}$ = 29.3 psia

The minimum free gas volume is calculated as:

$$V_{canister} = 2{,}800\,in^3 - \pi * r_{OD}^2 * L_{rod} * 25\,rods = 2{,}800\,in^3 - \pi * \left(\frac{0.57\,in}{2}\right)^2 * 170\,in. * 25\,rods$$

$$= 2{,}800\,in^3 - 1085\,in^3 = 1715\,in^3$$

$$V_{canister} = 28.1\ liters$$

$$V_{void} = 4.82\,in^3 * (2.54\,cm/in)^3 * 0.001\,liters/cc = 0.079\,liters$$

$$V_{total} = V_{canister} + 25 * 0.04 * V_{void} = 28.1\,liters + 0.04 * 25 * 0.079 = \sim 28.2\,liters$$

$$V_{total} = \sim 28.2\ liters$$

This results in a $P_{canister}$ of 29.3 psia.

Fission product gas inventories were obtained from Table 3.4-11. Using the ideal gas law, the initial pressure of each fission product gas is calculated based upon these inventories, the normal condition temperature (600°F), and the calculated void volume of the fuel (25 rods). The partial pressure of the fuel rod volume is calculated by:

$$P_{fuel\ rods} = P_{initial}\left(\frac{V_{fuel\ rods}}{V_{total}}\right)$$

where:

$$P_{initial} = 0.3 * P_{fission} + P_{backfill}$$

$$P_{fission} = 4251\,psia$$

$$P_{backfill} = P_{initial}^{backfill} * \frac{T_{norm}}{T_{stand}} = 75\,psia * \frac{588.7\,K}{295.35\,K} = 150\,psia$$

$$P_{initial} = \sim 1{,}425\ psia$$

$$V_{fuel\ rods} = \sim 0.079\ liter\ (at\ 4\%\ of\ the\ total\ fuel\ rod\ volume)$$

$$V_{total} = 28.2\ liters = V_{canister} + 25 * 0.04(V_{void})$$

$$P_{fuel\ rods} = 1425\,psia\left(\frac{0.079\,liter}{28.2\,liters}\right) = \sim 4.00\,psia$$

then:

$$P_{total} = P_{canister} + P_{fuel\ rods} = 29.3\,psia + \sim 4.00\,psia = \sim 33.3\,psia\ (2.3\ atm)$$

An additional analysis was performed for BWR high burnup rods (>45 GWd/MTU) with a 56% failure fraction to envelope damaged fuel rod shipments. This evaluation is conservative since damaged rods are likely to have released their gas inventory prior to shipment.

Following the methodology used for calculating the pressure given above and the calculated canister free gas volume of 29.2 liters, the resulting internal canister pressure from a 56% failed fuel fraction is 82.3 psia (~ 5.6 atm). The calculation follows.

$P_{canister} = P_{initial} * V_{canister} / V_{total}$

$P_{initial} = 29.3$ psia

$V_{canister} = 28.1$ liters

$V_{total} = V_{canister} + 14 * V_{void} = (28.1 \text{ liters}) + 14 * (0.079 \text{ liter}) = 29.2$ liters

$P_{canister} = (29.3 \text{ psia}) * (28.1 \text{ liters}) / (29.2 \text{ liters}) = 28.2$ psia

$P_{fuel\ rods} = P_{initial} * V_{fuel\ rods} / V_{total}$

$P_{initial} = 1{,}425$ psia

$V_{fuel\ rods} = 14 * V_{void} = 1.108$ liters

$P_{fuel\ rods} = (1{,}425 \text{ psia}) * (1.108 \text{ liters}) / (29.2 \text{ liters}) = 54.1$ psia

$P_{total} = P_{canister} + P_{fuel\ rods} = 28.2 \text{ psia} + 54.1 \text{ psia} = 82.3 \text{ psia} = 5.6$ atm

3.4.4.3 25-Rod Maximum Cask Cavity Internal Pressure-Normal Conditions

Following the methodology used for calculating pressure in Section 3.4.4.2, the cask free gas volume is calculated as:

$$V_{cask} = 6{,}534 \text{ in}^3 - \pi * r_{OD}^2 * L_{rod} * 25 \text{ rods} = 6{,}534 \text{ in}^3 - \pi * \left(\frac{0.57 \text{ in}}{2}\right)^2 * 170 \text{ in} * 25 \text{ rods}$$

$$= 6{,}534 \text{ in}^3 - 1{,}085 \text{ in}^3$$

$$= 5{,}449 \text{ in}^3$$

$V_{cask} = 89.32$ liters

Using this free gas volume in place of $V_{canister}$ and the temperatures in Section 3.4.4.2, the cask cavity pressure resulting from a 3% fuel rod failure is 31 psia (~2.1 atm). This pressure is based on the assumption that the gases in the canister are released to the cask cavity. There are no design basis events that could result in the release of the gas in the canister to the cask cavity.

An additional analysis was performed for a bounding 25 BWR high burnup rod configuration (>45 GWd/MTU) containing up to 14 damaged rods. The damaged fuel rods are conservatively assumed to release the rod gas inventory during transport.

Following the methodology used for calculating the pressures given above and the cask free gas volume of 90.4 liters, the resulting internal cask pressure from a 56% failed fuel fraction is 46.4 psia (~ 3.2 atm). The calculation is outlined below.

$P_{cask} = P_{initial} * V_{cask} / V_{total}$

$P_{initial} = 29.3$ psia

$V_{cask} = 89.3$ liters

$V_{total} = V_{cask} + 14 * V_{void} = (89.3 \text{ liters}) + 14 * (0.079 \text{ liter}) = 90.4$ liters

$P_{cask} = (29.3 \text{ psia}) * (89.3 \text{ liters}) / (90.4 \text{ liters}) = 28.9$ psia

$P_{fuel\ rods} = P_{initial} * V_{fuel\ rods} / V_{total}$

$P_{initial} = 1{,}425$ psia

$V_{fuel\ rods} = 14 * V_{void} = 1.108$ liters

$P_{fuel\ rods} = (1{,}425 \text{ psia}) * (1.108 \text{ liters}) / (90.4 \text{ liters}) = 17.5$ psia

$P_{total} = P_{cask} + P_{fuel\ rods} = 28.9 \text{ psia} + 17.5 \text{ psia} = 46.4 \text{ psia} = 3.2$ atm

PWR rods may contain Integral Fuel Burnable Absorbers (with rods referred to as IFBA rods). These rods may contain integral neutron absorber comprised of gadolinium, erbium, or boron. Only boron has the potential to impact pressure calculations as the ^{10}B isotope alpha decays upon neutron activation, thereby adding gas to the system. Activation of erbium and gadolinium does not produce additional gases. The effect on system pressure of the additional gas was evaluated based on a 2.4 g ^{10}B/in coating level [ORNL/TM-200/321], considering 100% conversion to gas, and conservatively applying the fixed absorber level to the full active fuel length. A normal condition failure of 3% of the rods (1 rod, rounded to 4%) increases the cask pressurizing gas quantity by less than 0.04 mole, which translates to a pressure change of 0.3 psi. When considering a conservative in-cask failure of 14 rods, the potential increase in pressure rises to 4 psi for the IFBA rods. Given the conservative cask free volume and fission gas generation (both based on significantly larger BWR rods), in combination with a conservative (rounded up) system temperature applied in the analysis, there is no significant effect on system pressure with the inclusion of IFBA rods.

3.4.4.4 Maximum Cask Cavity Internal Pressure for the General Atomics IFM

The combined heat load of the two GA IFM FHUs is 13 watts. This heat load is distributed between two separate canisters, which have a length of approximately 40 inches. As a result, the heat generation, which would result in a temperature differential between the cavity and ambient, is insignificant.

The internal pressure in the LWT cask cavity is due to the fission gas release from the TRIGA fuel or HTGR fuel pellets in conjunction with the cavity being heated by solar insolance. No credit is taken for the pressure retention capability of the FHUs. The internal pressure that may result from the 20 TRIGA fuel rods in the GA IFM is significantly enveloped by that of the 120 TRIGA fuel rods, which are authorized for transport in the NAC-LWT cask. Likewise, the fission gas release by the HTGR elements is considered to be bounded by the current design basis PWR fuel. Since the free volume for the GA IFM shipment is significantly larger than for the design basis PWR fuel assembly with the PWR basket, the pressure increase in the cavity gas due to the GA IFM shipment is considered to be significantly bounded by the design basis condition in the current NAC-LWT cask. Therefore, the current design pressure of 50 psig for the cask cavity envelopes the cask cavity pressure for the GA IFM contents.

3.4.4.5 TPBAR Shipment Cask Cavity Internal Pressure-Normal Conditions

The method employed in the TPBAR (Tritium Producing Burnable Absorber Rod) shipment evaluation is similar to that employed in the fuel rod evaluations where the cask cavity free volume and molar gas quantities are combined with the ideal gas law (PV=nRT) to determine system pressure. The bounding TPBAR content condition consists of up to 300 production TPBARs (of which two can be prefailed) placed in a consolidation canister and loaded into a NAC-LWT with a TPBAR basket installed in the cavity.

A typical TPBAR is composed of a steel clad rod 0.381 inch in diameter, with a maximum length of 154.15 inches, and a minimum internal free volume of 5.727 inch^3. The TPBARs are located in a consolidation canister composed of three primary pieces: canister body, top insert, and bail. A spacer, attached to the NAC-LWT cask lid, assures that rods remain within the canister envelope and provides support to both the basket and canister under end-drop conditions. The TPBAR basket is a modified NAC-LWT PWR basket that increases the cavity free volume from that provided by a standard PWR basket design.

For conservatism in determining the cask internal pressure, the 298 TPBARs that are not prefailed at loading are assumed to undergo cladding failure during normal transport conditions. Prefailed rods have cladding damage that allows reactor coolant or spent fuel pool water to enter

the rod cavity. Cladding failure during transport results in the release of the rod helium backfill gas, helium gas generated during the tritium production, and a portion of the tritium gas produced. For rods not prefailed, the majority of the tritium is locked in the TPBAR structure and is not released during normal or accident conditions of cask transport. Tritium release from intact or in-cask prefailed rods is limited to 55 Ci/rod (0.0019 mole – See Chapter 1, Appendix 1-B) versus a helium release of 0.42 mole per rod after the 90-day cool-down period. A conservative tritium release of 100 Ci per rod is applied in this calculation. After the 90-day cool-down period, the helium release increases according to the decay of tritium.

$$^{3}\mathrm{He[moles]}(t) = 0.398 \times \left(1 - \exp\left(\frac{-\ln(2)t}{12.33}\right)\right)$$

The remaining two rods in the 300 TPBAR shipment are assumed to be prefailed and waterlogged. These rods contain a maximum of 7.5 moles of H_2O and 0.199 moles of T_2O (1.2 grams H_2), 2% of which dissociate into their constituent gases due to elevated temperatures in the cask cavity (see Chapter 1 appendices). The NAC-LWT is vacuum dried prior to transport, removing water from the cask cavity. This process is expected to remove water from the prefailed rod. The water content is conservatively assumed to remain in the rods for the pressure calculated. After dissociation, the total gaseous inventory in each prefailed TPBAR is 7.78 moles.

Cask cavity gases after rod failure are therefore comprised of the cask helium backfill (one atmosphere at loading); the combined helium rod backfill, helium generated during the tritium production, helium production from tritium decay, and the tritium release itself (298 rods); and the molar inventory of the two prefailed, waterlogged rods. The total free volume available for the gas is the cask cavity volume plus the internal free volume of the failed rods, minus the canister, spacer, basket, and rod volumes.

Description (Based on 300 Rods Failing)	Volume [cm³]
Cavity (Empty)	4.10E+05
TPBAR Rod (Based on Exterior Rod Dimension)	-8.64E+04
TPBAR Minimum Free Interior	2.82E+04
TPBAR Consolidation Canister	-1.40E+04
TPBAR Basket	-8.49E+04
Cask Cavity Spacer	-5.55E+03
Cask Free volume (300 Rods Failed)	2.47E+05

The free volume in the canister cavity for intact rods is 2.19×10^5 cm^3. Applying a conservative volume 2.4×10^5 cm^3 to calculate the cask backfill molar quantity yields 9.98 moles of helium. The backfill conditions at sealing used in the calculation are one atmosphere pressure and a temperature of 68°F. The backfill pressure is specified in the operating procedure, while 68°F is conservative for the cask with a heat-generating payload.

Again employing the ideal gas law with a total 152 moles of gas (298 rods releasing 0.42 moles of helium and 0.003 mole of tritium, two waterlogged rods releasing 7.78 moles each, plus the 10.27 moles cask backfill), a conservative free volume of 2.47×10^5 cm^3, and the normal condition average gas temperature of 246°F, yields an operating pressure of 276 psig at the end of a 90-day cooldown. For a period of one year following the 90-day cooldown and considering a fixed gas temperature of 246°F, the pressure increases to 289 psig (MNOP). System pressure at cool times greater than 90 days will be lower due to the decreased heat loads associated with the radioactive decay of the payload.

The TPBAR content condition of 55 segmented TPBARs contained in a sealed waste container is bounded by the pressure analyses performed for the fully loaded TPBAR consolidation canister. The contents include segments, debris and vented shrouds, all placed in a vented inner storage container within the welded waste container. Due to the condition of the TPBAR segments and the cooling period since irradiation, the heat load of the waste container is 0.127 kW, significantly less than the 0.693 kW analyzed for the production TPBAR content condition of 300 TPBARs in an open consolidation canister.

Each of the 55 TPBARs is assumed to contain a maximum of 1.2 grams of tritium at the time of sealing the waste container, and all backfill gases have been vented. For the purpose of the maximum pressure analysis, all of the contained tritium is assumed to decay to He^3, resulting in a total of 66 grams of He^3. Note that the confinement boundary of the welded waste container is assumed to fail during normal transport conditions. Due to the state of the TPBAR segments and the loading of the materials in dry loading conditions, no water will be present in the waste container. Conservatively assuming that the cask free volume and gas temperature for the transport of the waste container is the same as that for the production TPBAR contents listed previously (2.47×10^5 cm^3), the calculated maximum normal operating pressure (MNOP) for the 55 segmented TPBARS in the waste container is less than 65 psia. Therefore, the MNOP for the 55 segmented TPBAR content condition is conservatively bounded by the MNOP of the 300 production TPBARs in the consolidation canister of 289 psig.

Combustible Hazard Assessment

Hydrogen may be released by prefailed, waterlogged TPBARs (TPBARs damaged during in-core use or in-pool storage) primarily in the form of water, tritiated water, and potentially some tritiated methane. Each prefailed TPBAR has the potential to release the tritium assumed to dissociate from tritiated water (0.004 moles) as well as up to 0.15 moles hydrogen gas dissociated from 7.5 moles of H_2O. Both the hydrogen and the tritium gas, as well as the water and tritiated water, will be removed from the cask during vacuum drying prior to helium backfill.

The flammability/ignitability characteristics of tritium (T_2) in the presence of oxygen are substantially the same as for hydrogen (H_2). Hydrogen in air reaches a lower flammability limit at 4% volume.

Tritium escapes intact TPBARs in the form of molecular tritium gas at a rate of less than 0.12 mCi/hr/TPBAR. For a one-year transport period and a 300 TPBAR payload this rate results in a release of less than 0.01 moles of T_2 gas. Given a helium gas back-fill of approximately 10 moles helium (1 atmosphere) no flammability hazard exists for intact TPBARs.

Tritium may be released by event-failed (in-cask failed) TPBARs in the form of tritiated methane (CH_4) or tritiated water. Event-failed TPBARs may release up to 55 Ci of tritium. This translates to approximately 0.002 mole of tritium that may be released from a TPBAR in conjunction with 0.42 mole of helium.

The 55 equivalent TPBARs, in segments and debris, may release up to 100% of the tritium contained in the pellets during transport. The pellets contain approximately 40% of the tritium quantity in the TPBAR. At NAC-LWT normal and accident conditions temperatures, the TPBAR components release tritium primarily as tritiated water with only a small fraction (maximum 2%) as gaseous tritium (see Appendix 1-B of Chapter 1). During a one-year transport, an additional maximum 1% of the tritiated water may undergo radiolysis and dissociate. Conservatively applying a maximum 3% release rate to the 55 equivalent TPBAR total inventory of 66 grams (1.2 grams per rod) yields an inventory of 0.33 moles T_2. Based on an inert gas cask backfill in excess of 10.3 moles, a bounding estimated maximum hydrogen (T_2) volume fraction of 3.1% is calculated. Therefore, no flammability hazard will exist for the 55 segmented TPBAR content condition.

3.4.4.6 Maximum Internal Pressure for PULSTAR Fuel Element Payload

Based on the allowable loading configurations for PULSTAR fuel elements, cask internal pressures are calculated for a payload of 28 intact assemblies and a mixed payload of 14 intact

assemblies and the equivalent of 14 canned assemblies. A payload of 28 4×4 intact rod inserts is bounded by either of these evaluated payloads.

The ideal gas law and Dalton's law of partial pressures are used to calculate internal pressures. Cask, can, and element backfill initial conditions are taken as a pressure of 1 atm and a temperature of 68°F.

PULSTAR fuel element and fuel assembly dimensions are summarized in Table 3.4-18. Elements are UO_2 pellets clad with zirconium alloy. A PULSTAR fuel assembly is a 5×5 rectangular array of elements with aluminum upper and lower fittings.

Based on the PULSTAR fuel element, PULSTAR failed fuel can, MTR basket stack, and NAC-LWT cavity dimensions, volumes are calculated and summarized in Table 3.4-19.

The remaining two inputs to the pressure calculation are the temperature and fission gas inventory. For conservatism, the average gas temperature applied is the maximum TRIGA fuel clad temperature of 295°F. The TRIGA temperatures are applicable to the PULSTAR fuel element evaluation as discussed in Section 3.4.1.13. The fission gas inventory is taken from the SAS2H results discussed in Chapter 5 and is shown in Table 3.4-20.

For a payload of 28 intact PULSTAR fuel assemblies, the partial pressures of the cask, element (rod) backfill, and fission gases are summed. The cask free volume is 217 liters and is calculated by subtracting the basket stack volume and the assembly envelope volume (multiplied by 28) from the cavity volume. The partial pressure of the cask, P_{Cask}, is simply the initial backfill pressure multiplied by the temperature ratio:

$$P_{Cask} = 1\,\text{atm}\frac{419.26\,\text{K}}{293.15\,\text{K}} = 1.430\,\text{atm}$$

The cask partial pressure due to a 100% release of element backfill, $P_{RodBackfill}$, is the initial backfill pressure multiplied by the temperature ratio and the backfill-to-cask volume ratio:

$$P_{RodBackfill} = 1\,\text{atm}\frac{419.26\,\text{K}}{293.15\,\text{K}}\frac{2.7\,\text{liters}}{217.0\,\text{liters}} = 0.018\,\text{atm}$$

Only 3% of this pressure contributes to the total pressure under normal conditions.

The cask partial pressure due to a 100% release of the element fission gases, $P_{FissionGas}$, is calculated using the Ideal Gas Law:

$$P_{FissionGas} = \frac{28 \cdot 0.448 \cdot 0.08205 \cdot 419.26}{217} = 1.989\,\text{atm}$$

Only 30% of the fission gases are released, and only 3% of the resultant pressure contributes to the total pressure under normal conditions.

The total cask pressure is the sum of the partial pressures, adjusted by the relevant release fractions:

$$P_{Total} = P_{Cask} + 0.03 \cdot P_{RodBackfill} + 0.03 \cdot 0.30 \cdot P_{FissionGas}$$

$$P_{Total} = 1.430 + 0.03 \cdot 0.018 + 0.03 \cdot 0.30 \cdot 1.989 = 1.449 \text{ atm}$$

Cask internal pressure for a mixed payload is calculated in a similar fashion, with a smaller cask free volume due to the difference in can and assembly envelope volume, and an assumed 100% failure rate of PULSTAR elements in either the screened or sealed can. The calculated maximum cavity pressure is 1.8 atm. Pressure in the sealed can is based on a 100% failure rate, the can cavity volume, and a payload equivalent in volume to 25 intact PULSTAR fuel elements. Normal condition pressure in the sealed can is 4.4 atm.

A summary of the pressure calculations is given in Table 3.4-21.

3.4.4.7 Maximum Internal Pressure for 16 PWR MOX/UO_2 Fuel Rods in a Rod Holder

Based on the allowable loading of up to 16 PWR MOX/UO_2 fuel rods, cask internal pressures are calculated. Bounding cask free volume, gas temperatures, and rod backfill pressure are directly obtained from the BWR high burnup rod evaluations in Section 3.4.4.3.

Variable	Unit	Value
Cask Free Volume (PWR Basket with Insert/Canister/Rod Holder)	in^3	5908
Normal Condition Cask Average Gas Temperature	°F	600
Normal Condition Cask Backfill Partial Pressure (at temperature)	psia	29.3
PWR Fuel Rod Backfill Pressure	psia	565

These values are combined with a conservative 2.9 in^3 fuel rod free volume and SAS2H calculated fission and actinide gas inventories to determine system pressure. The 2.9 in^3 free rod volume applied here is larger than the UO_2 rod volume previously employed (2.5 in^3) to account for additional volume designed into the MOX rods to counter any potential increase in fission gas release from the PuO_2 / UO_2 MOX fuel mixture.

The ideal gas law and Dalton's law of partial pressures are used to calculate internal pressures by combining cask backfill, rod backfill, and fission/actinide gases. Fill temperature applied to the rod gases is 22°C (standard temperature). Maximum fission and actinide gas inventories were obtained from 80 GWd/MTHM fuel rod, 3% enriched ^{235}U or 3 wt % fissile Pu, SAS2H output

sets. The fuel rod corresponds to the maximum fissile mass defined in the shielding source term calculations. SAS2H runs produced a total gas inventory of 0.29 mole per rod (99+% fission gas), with bounding values obtained from the UO_2 rods (MOX rods produce approximately 98% of the UO_2 rod fission gas). Gas inventories increase as a function of reduced initial fissile material content. A 3% enrichment and/or 3% fissile Pu content is significantly below levels required to reach an 80 GWd/MTHM burnup level.

The resulting normal condition pressure for a failure fraction of 1/16 (bounds the 3% normal condition PWR rod failure fraction in the Standard Review Plan, NUREG-1617, Supplement 1) and 30% fission gas release is 17.2 psig (31.9 psia, or 2.2 atm).

Parametric studies are performed on the number of rods failing and the release fraction under normal conditions with an applied limit of 50 psig (normal condition structural analysis input value). Normal condition failure of up to 13 rods, at 100% gas release, remains below 50 psig. A similar analysis results in a maximum normal condition pressure of 48.5 psig for a normal condition failure of all 16 rods at a 75% fission gas release fraction (100% of backfill gas is released). Given that each of the rods is individually located within a support tube, no normal condition rod failures are expected during transport.

UO_2 or MOX rods included in the payload may be IFBA rods. As presented in Section 3.4.4.3, IFBA rods are expected to contribute in the range of 0.04 mole per rod to system pressure, assuming the absorber material is boron. As the MOX/UO_2 pressure calculations assumed a conservative 100% fission gas release of 0.29 mole per rod, a rod backfill of 0.075 mole, and a cask backfill of approximately 3.6 moles, the release of IFBA boron-generated gases would not significantly affect system pressure.

3.4.5 Maximum Thermal Stresses

The conditions within the range of normal transport conditions and fabrication that result in the limiting combination of thermal gradient and isothermal stresses have been evaluated. The analyses are performed in Sections 2.5 through 2.7. The resulting isothermal temperature plots are presented in Section 2.10.3.

3.4.6 Evaluation of Package Performance for Normal Conditions of Transport

Section 3.4 provides analyses of the NAC-LWT cask thermal performance for normal transport conditions. The analyses demonstrate that the NAC-LWT cask thermal performance meets the criteria of 10 CFR 71 for normal transport conditions.

The maximum fuel rod cladding temperature under normal transport conditions is 472°F. This is well below the temperatures that can cause fuel rod cladding deterioration. Components important to safety remain within their safe operating ranges (Section 3.3) during normal transport conditions. Thermally induced stresses (in combination with pressure and mechanical load stresses) are less than allowable stresses as shown in Section 2.6. Thus, the analyses of Section 3.4 demonstrate that the NAC-LWT cask fulfills the heat rejection criteria established in Section 3.1 for normal transport conditions.

Figure 3.4-1 HEATING5 Normal Transport Conditions Thermal Model

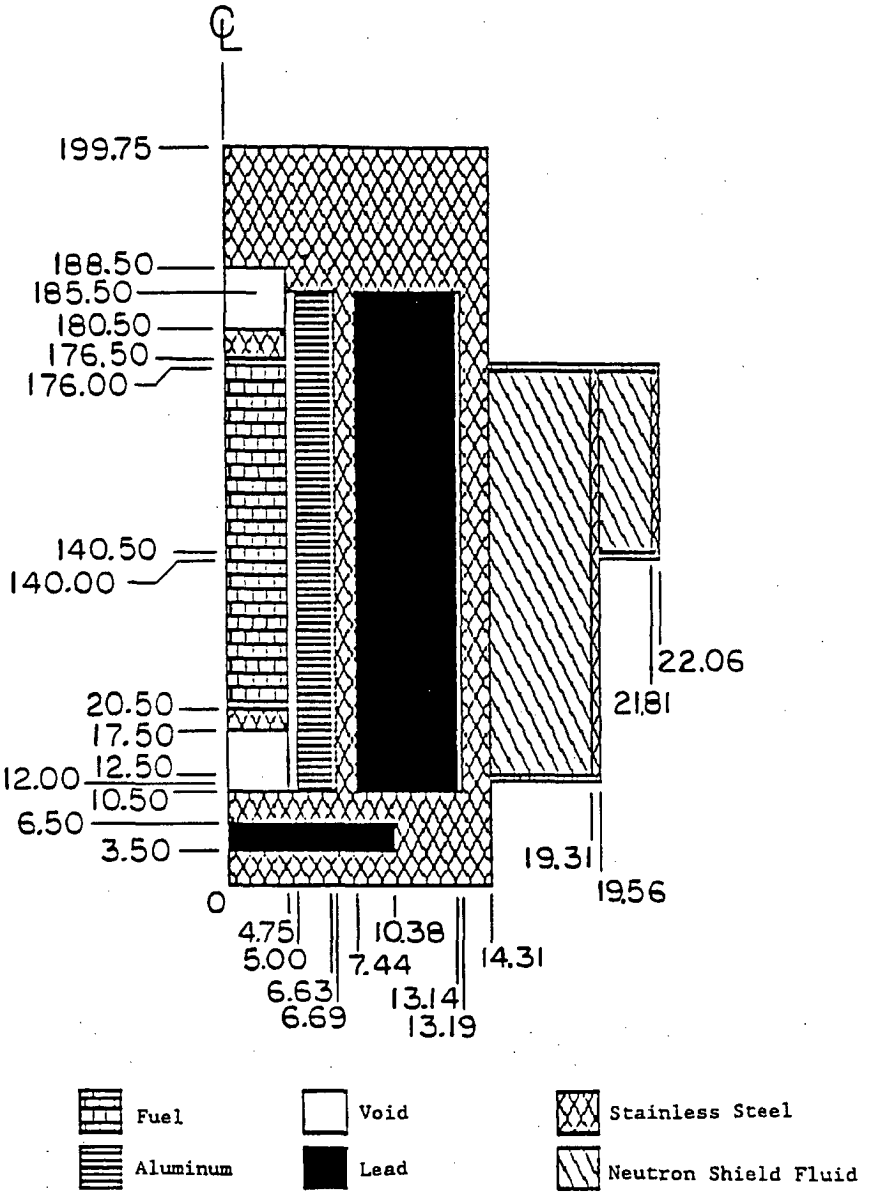

(Dimensions in inches)

Figure 3.4-2 Design Basis PWR Fuel Assembly Axial Flux Distribution

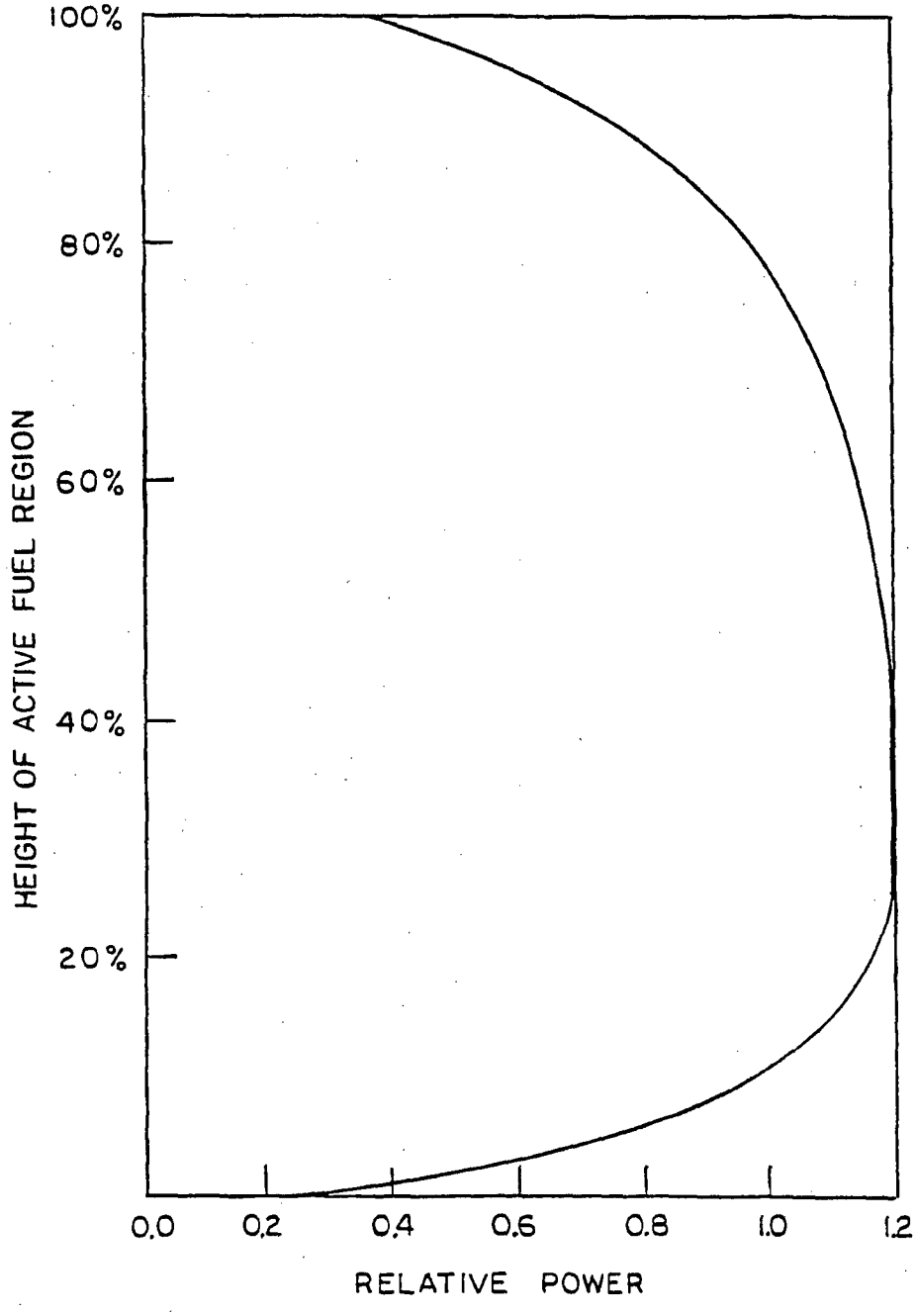

Figure 3.4-3 ANSYS MTR Fuel Design Basis Heat Load Thermal Model (Uniform 30-Watt/Element Configuration Heat Load)

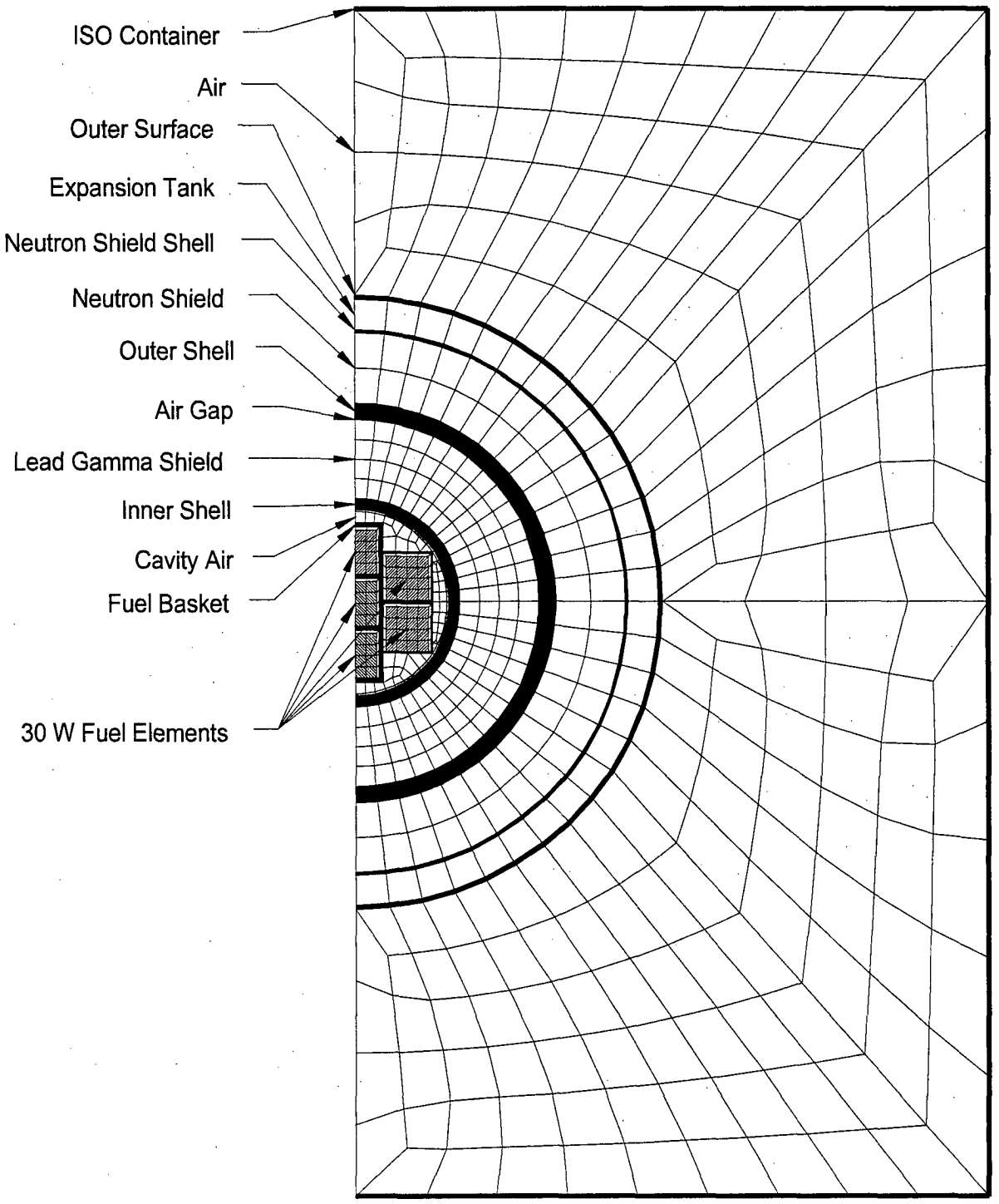

Figure 3.4-4 MTR Fuel Variable Decay Heat ANSYS Thermal Model
(120-Watt / 70-Watt / 20-Watt Configuration Heat Load)

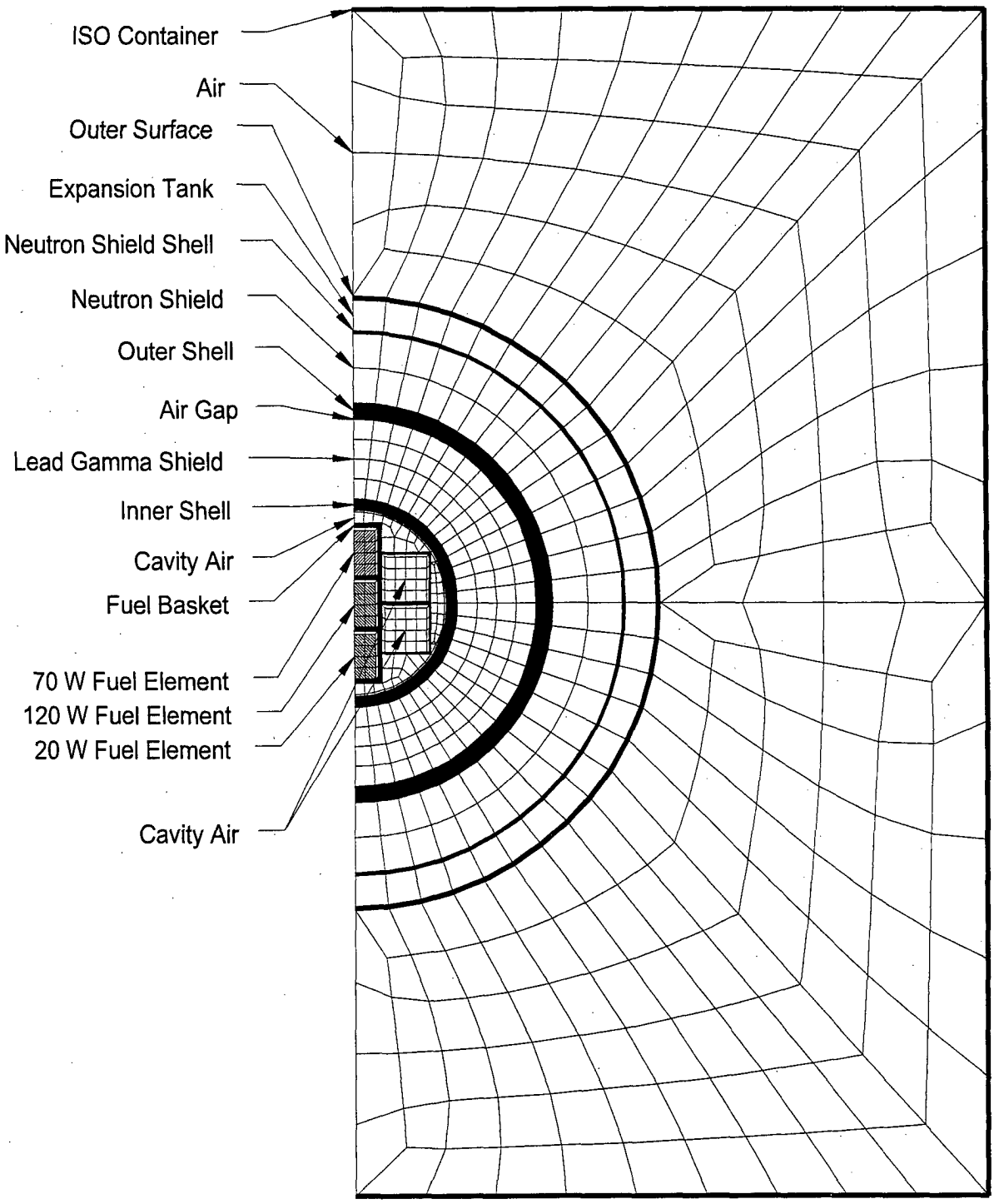

Figure 3.4-5 Thermal Resistance Model for TRIGA Fuel Elements

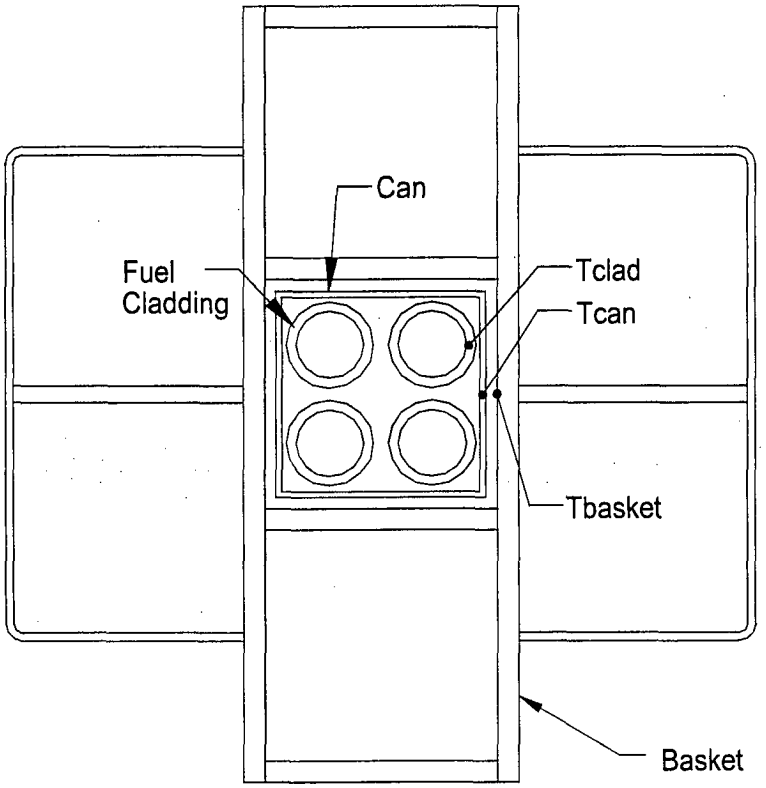

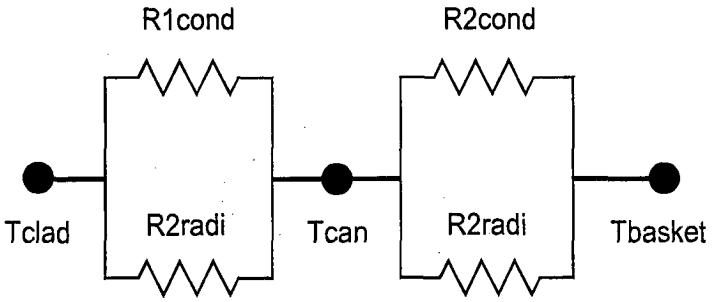

Where:

Rcond =	Thermal resistance for conduction	Tclad =	Maximum fuel cladding temperature
Rradi =	Thermal resistance for radiation		
Tbasket =	Maximum basket temperature		
Tcan =	Maximum can temperature		

Figure 3.4-6 Modeling Details for the MTR Fuel Assembly Resting on the Surface of the NAC-LWT MTR Basket

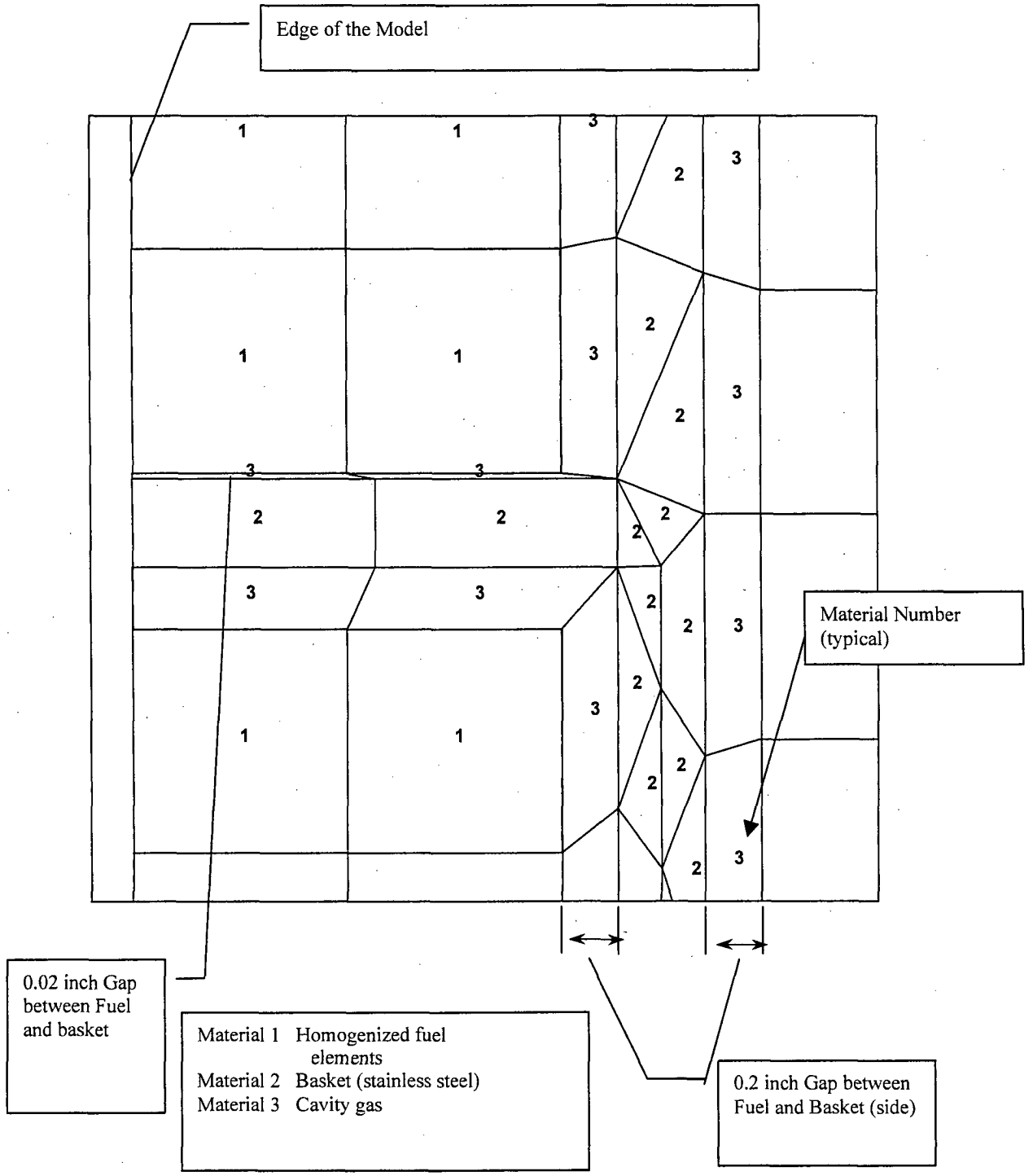

Figure 3.4-7 Finite Element Thermal Model for TRIGA Fuel Cluster Rods

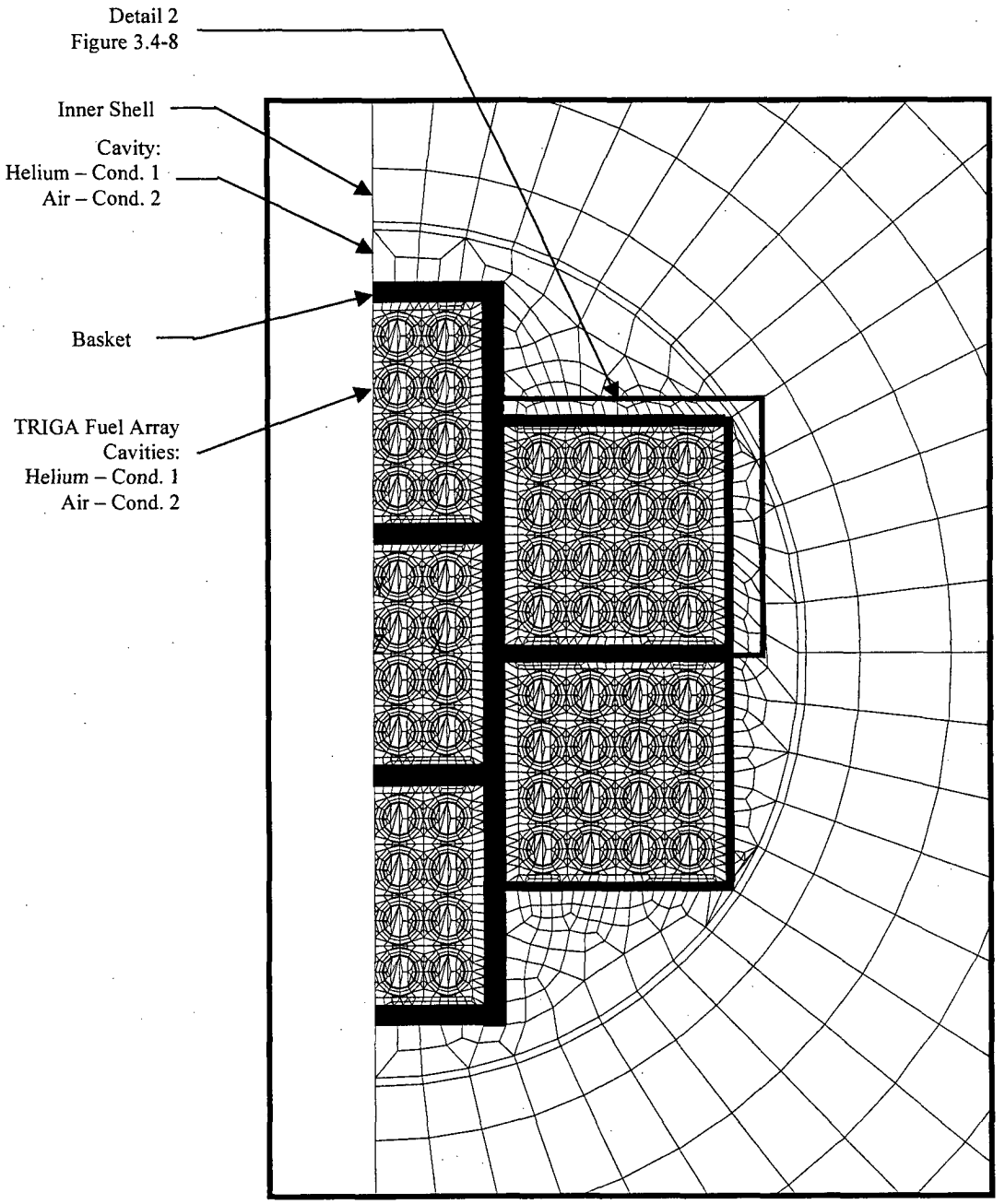

Figure 3.4-8 Details of the TRIGA Fuel Cluster Rods in the Finite Element Model

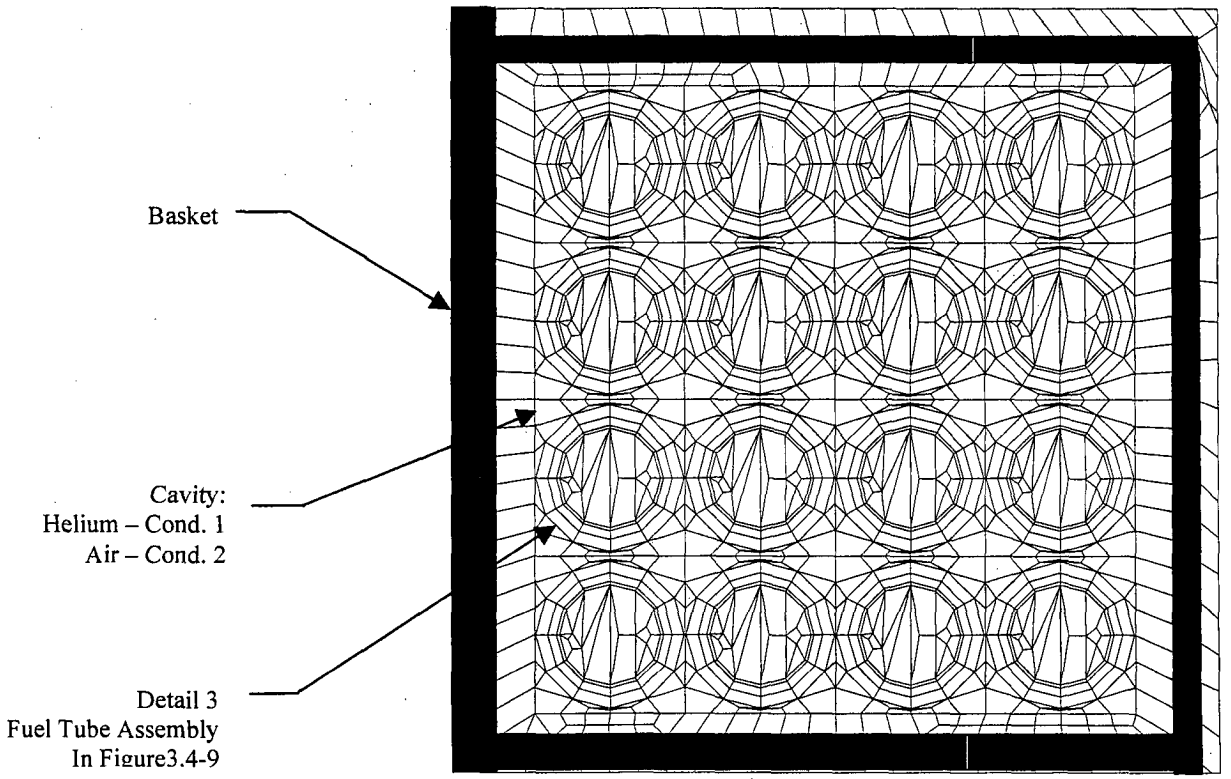

Figure 3.4-9 Individual TRIGA Fuel Cluster Rod Finite Element Model Details

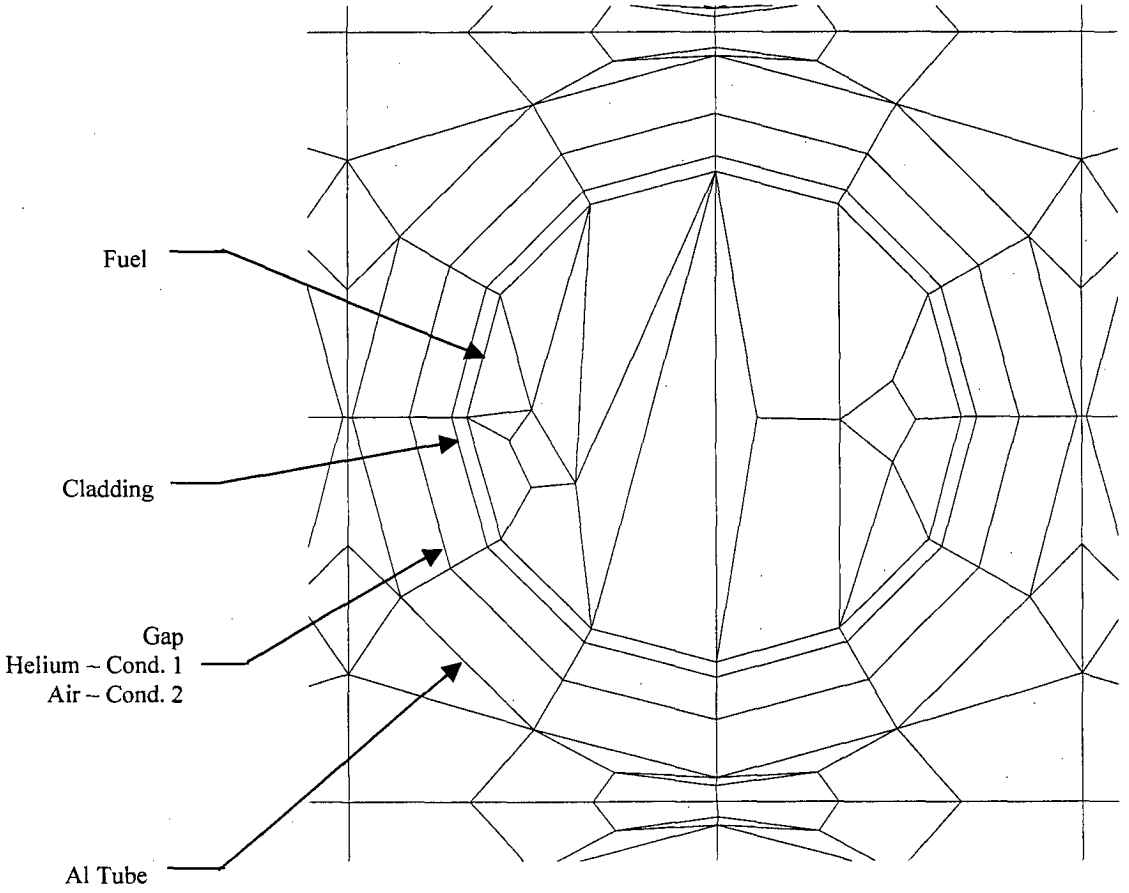

Figure 3.4-10 PWR and BWR High Burnup Fuel Rods Normal Condition ANSYS Thermal Model (Condition 1)

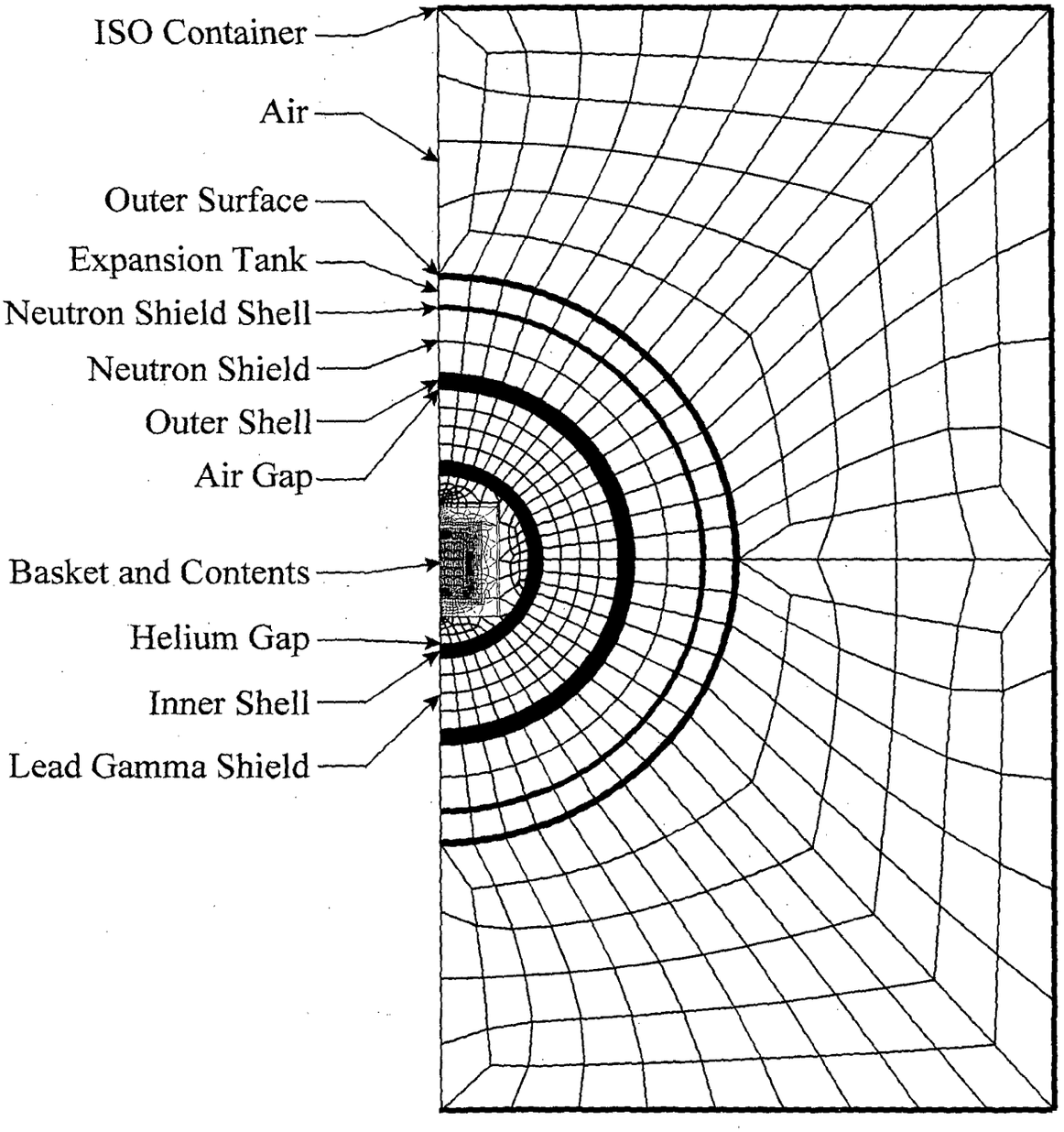

Figure 3.4-11 Close-up of PWR and BWR High Burnup Fuel Rods Normal Condition ANSYS Thermal Model

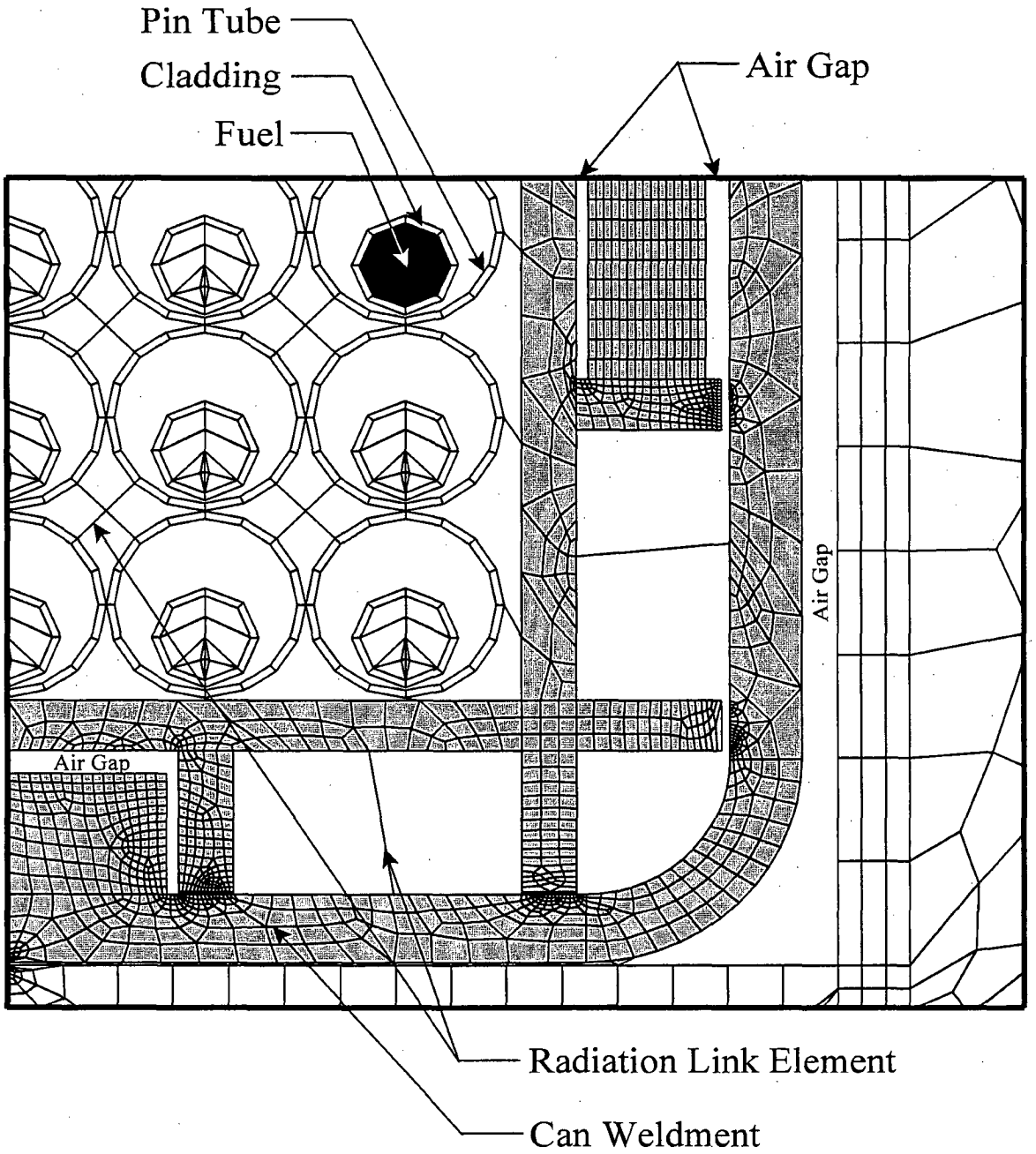

Note: air elements are not shown for clarity.

Figure 3.4-12 PWR and BWR High Burnup Fuel Rods Normal Condition ANSYS Thermal Model (Condition 2)

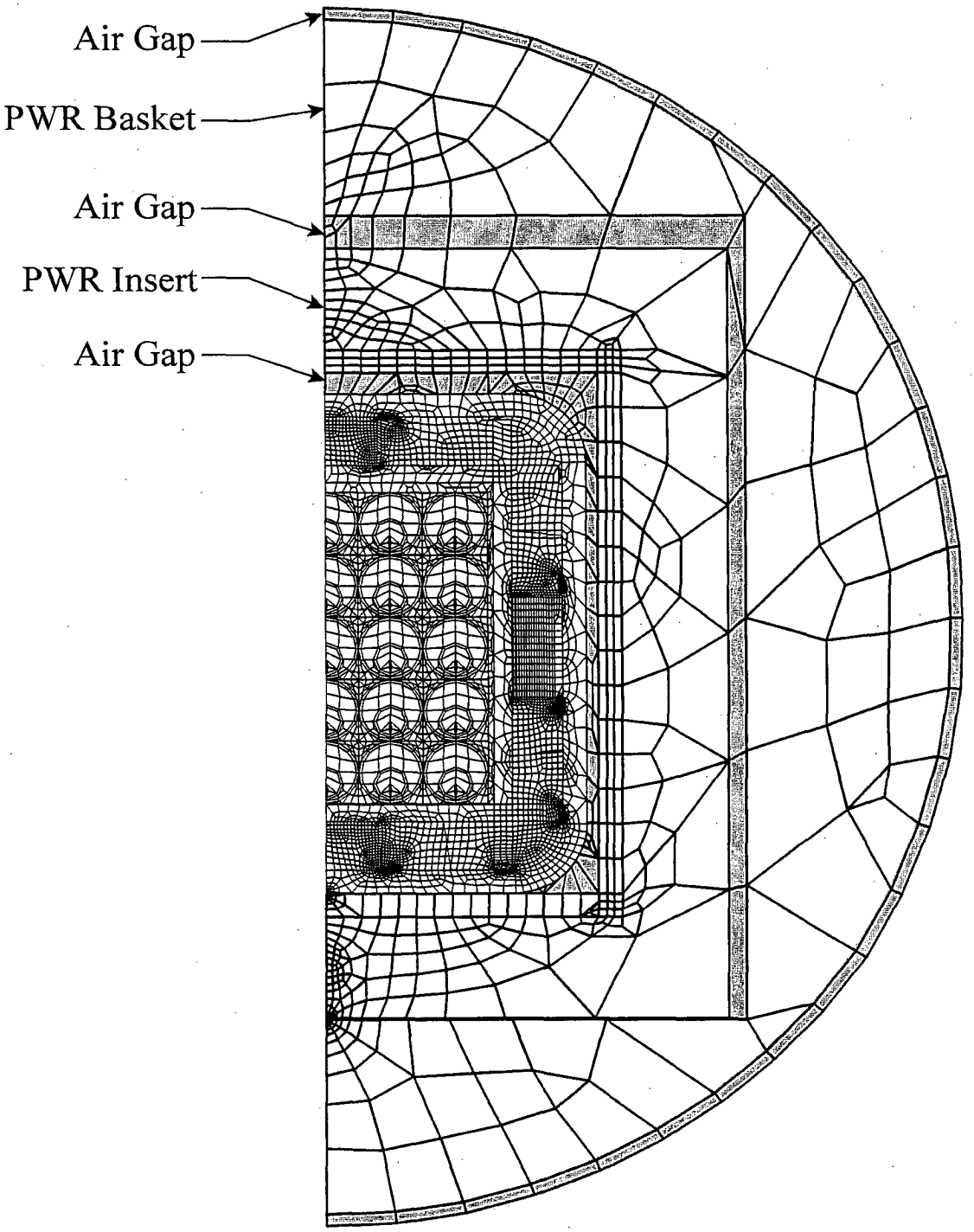

Figure 3.4-13 Finite Element Thermal Model for MTR Fuel Element

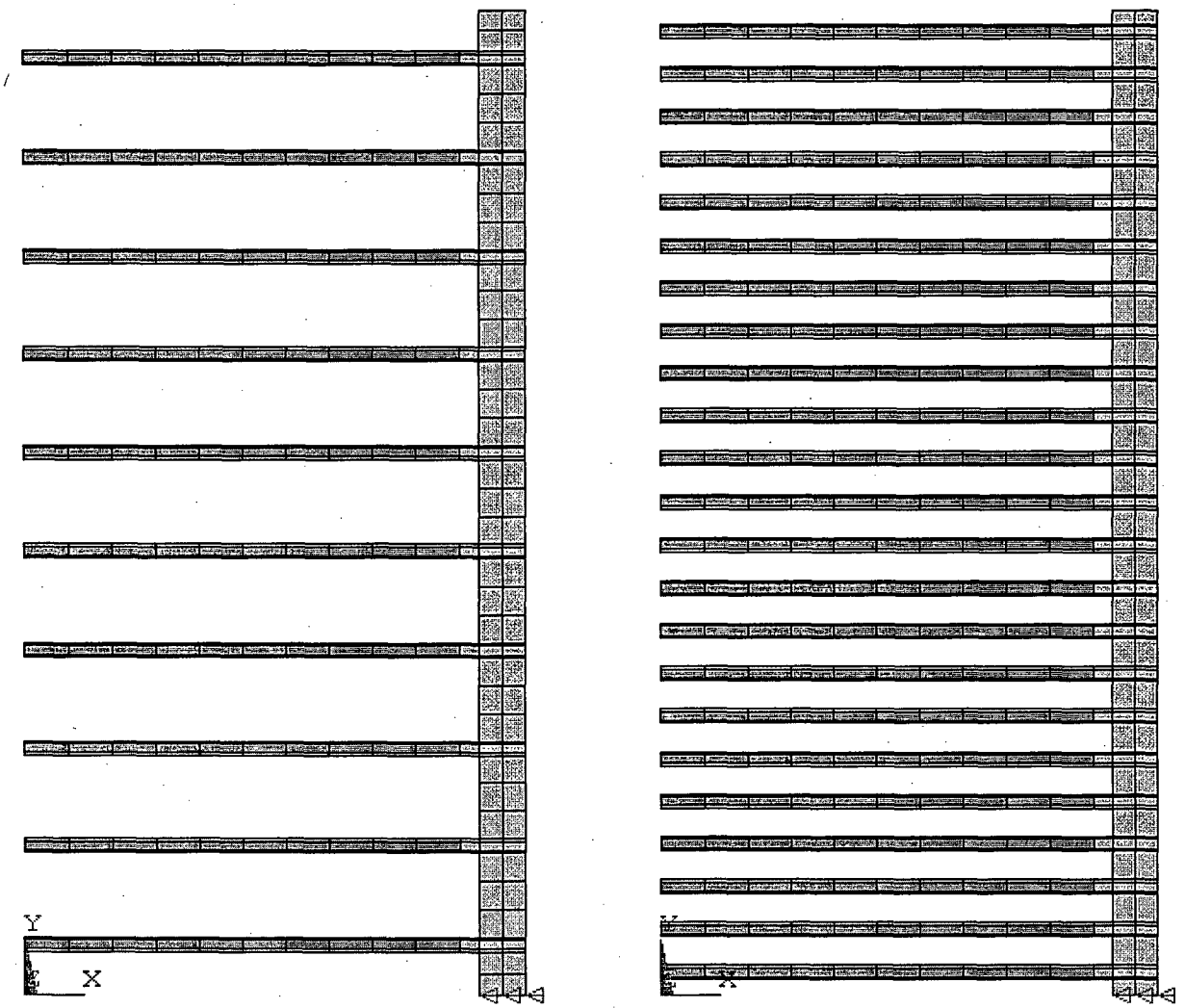

(Air elements omitted for clarity)

Figure 3.4-14 Detailed DIDO Basket Module Finite Element Model

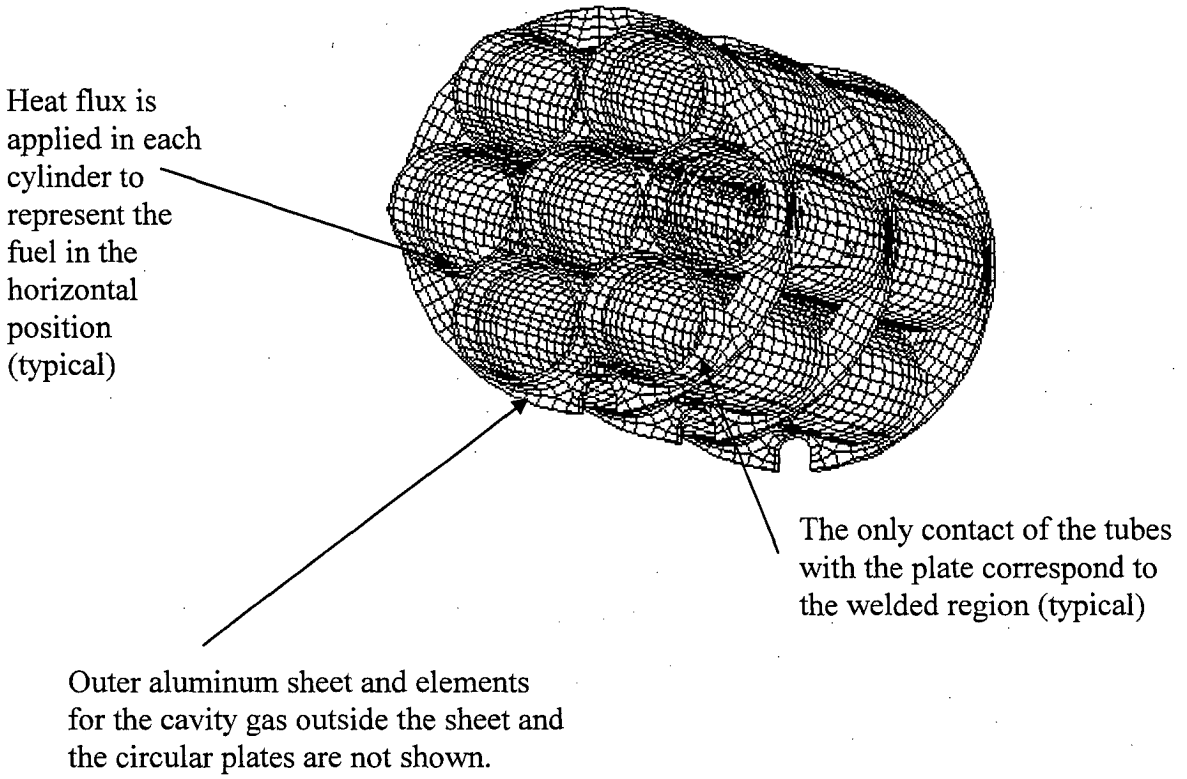

Figure 3.4-15 Detailed DIDO Fuel Assembly Model

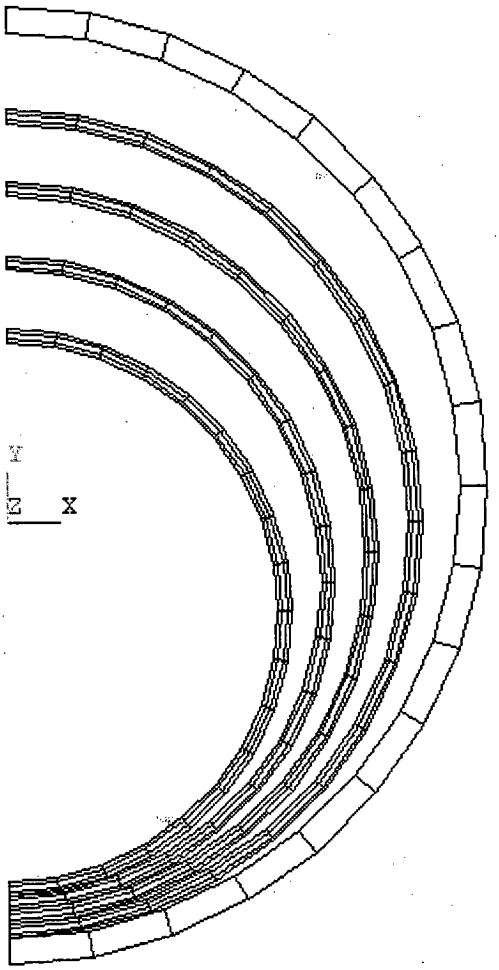

Figure 3.4-16 ANSYS Model for BWR 7 × 7 Fuel Lattice with 25 High Burnup Fuel Rods

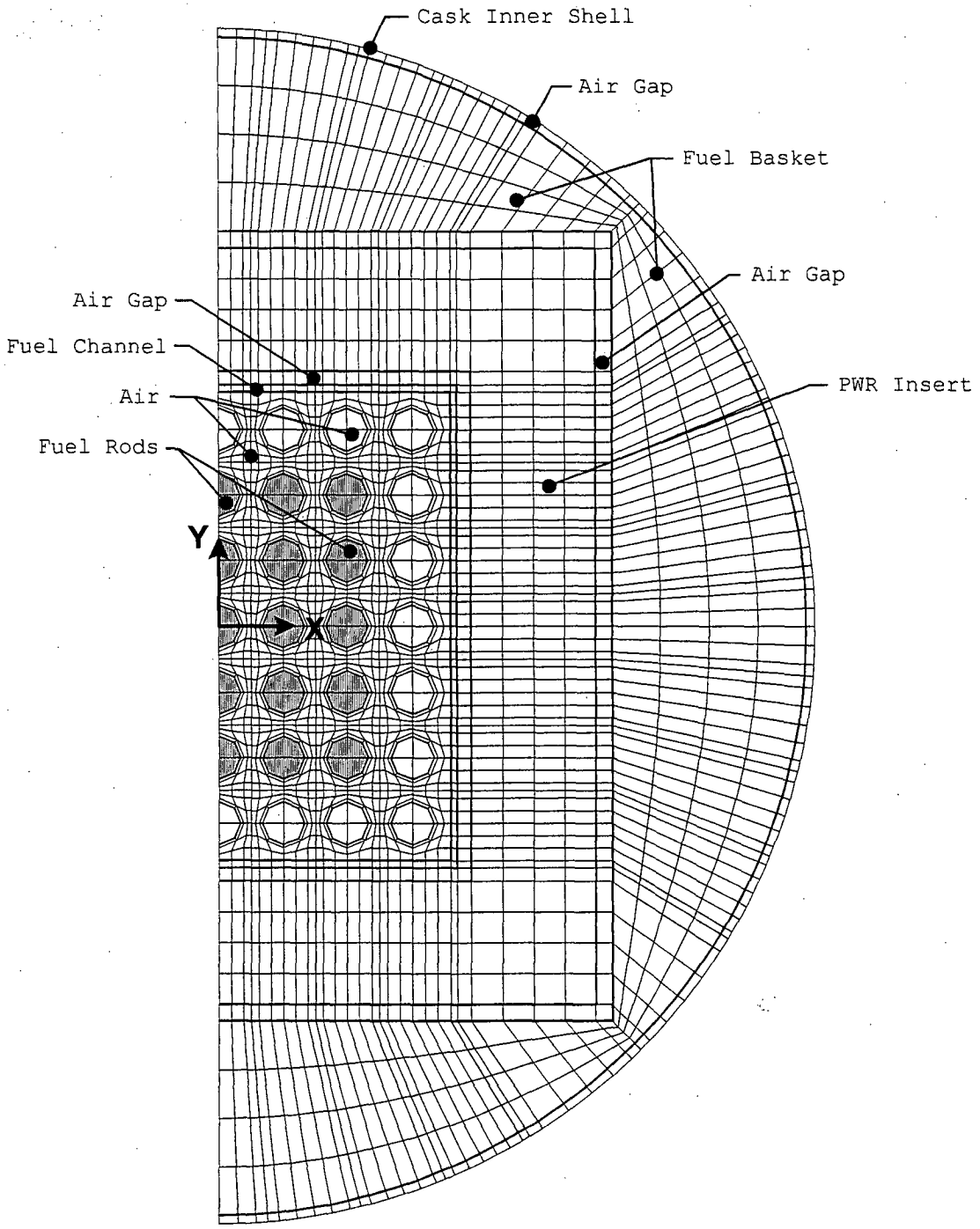

Figure 3.4-17 Fuel Rod Locations in the Thermal Model for Damaged Fuel

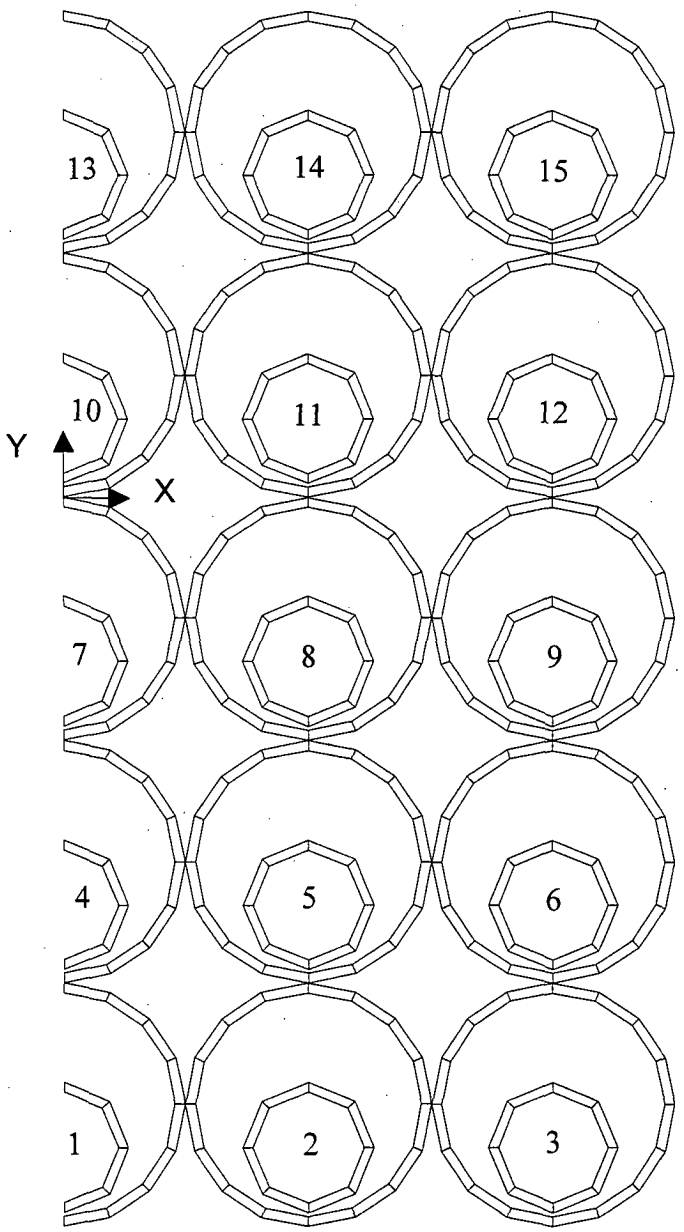

Figure 3.4-18 Finite Element Model for TPBARs

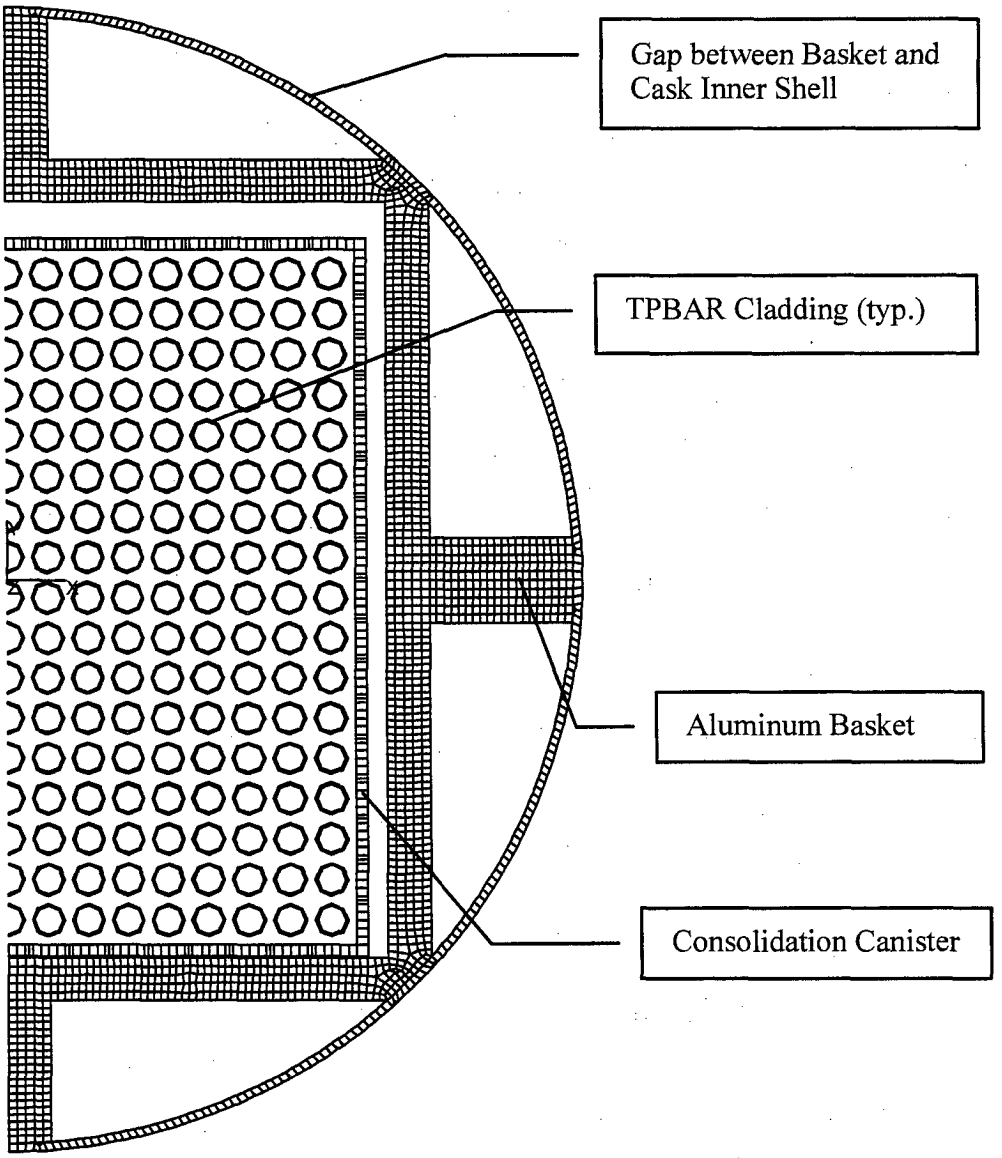

Note: Helium elements, except the gap between the basket and cask inner shell, are not shown for clarity.

Figure 3.4-19 Finite Element Model for MOATA Plate Fuel – ANSTO

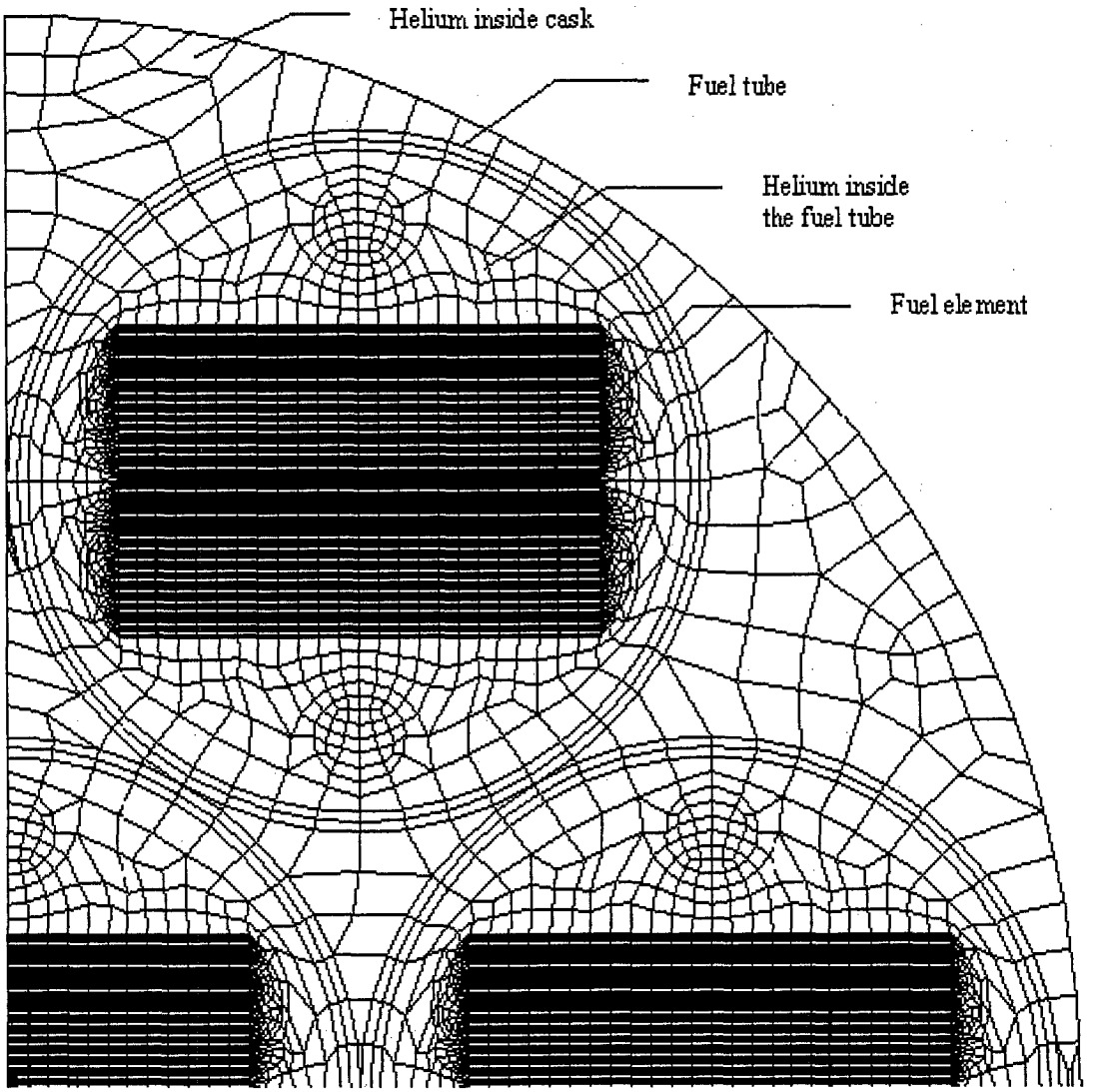

Figure 3.4-20 Finite Element Model for Mark III Spiral Fuel - ANSTO

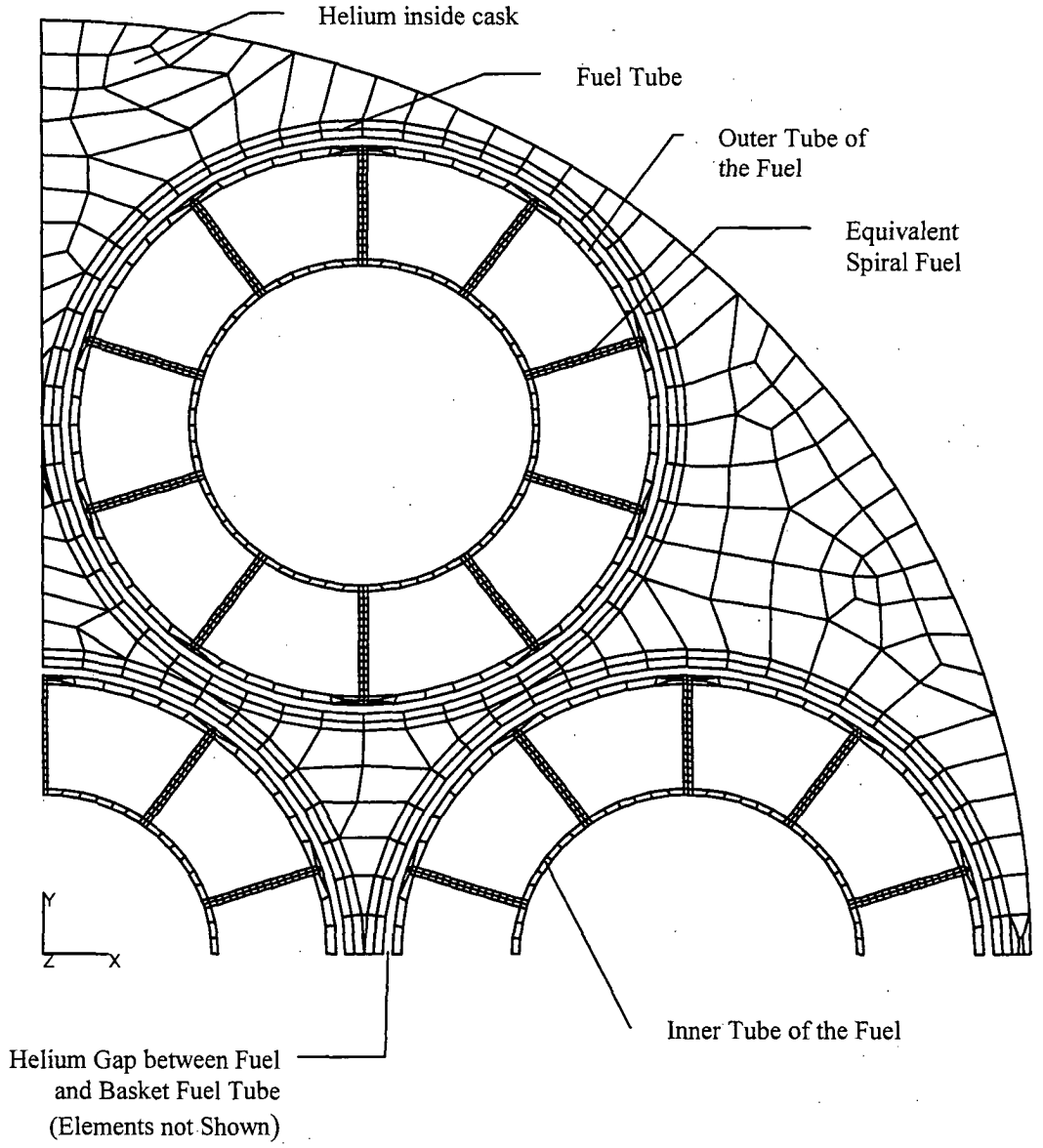

Table 3.4-1 Temperatures for Metallic Fuel Transport

Normal Transport Conditions

Component	Temperature (°F)
O-rings	200
Valves	201
Cask Radial Outer Surface	173
Neutron Shield	252
Radial Lead Gamma Shield	254
Bottom Lead Gamma Shield	210
Inner Stainless Steel Shell	255
Fuel Basket Outer Wall	255
Maximum Fuel Rod Cladding	270

Table 3.4-2 Maximum Component Temperatures – Design Basis PWR Fuel

Normal Transport Conditions

Component	Temperature (°F)
O-rings	227
Valves	231
Cask Radial Outer Surface	229
Neutron Shield	238
Radial Lead Gamma Shield	273
Bottom Lead Gamma Shield	239
Inner Stainless Steel Shell	274
Fuel Basket Outer Wall	276
Maximum Fuel Rod Cladding	472

Table 3.4-3 Limiting Cold Case Component Temperatures – Design Basis PWR Fuel

Normal Transport Conditions

Maximum Decay Heat Load, Minimum Ambient

Component	Temperature (°F)
O-rings	124
Valves	129
Cask Radial Outer Surface	128
Neutron Shield	110
Radial Lead Gamma Shield	167
Bottom Lead Gamma Shield	150
Inner Stainless Steel Shell	167
Fuel Basket Outer Wall	170
Maximum Fuel Rod Cladding	336

Table 3.4-4 Fission Product Gas Inventories and Pressures for Design Basis PWR Fuel Assembly

Fission Product	Inventory per Fuel Assembly (moles)	Initial Pressure (psia)
H-3	0.008	0.615
Kr-80	0.000	0.000
Kr-81	0.000	0.000
Kr-82	0.004	0.308
Kr-83	0.234	17.989
Kr-84	0.687	52.814
Kr-85	0.129	9.917
Kr-86	1.060	81.489
I-127	0.167	12.838
Xe-128	0.010	0.769
I-129	0.704	54.121
Xe-129	0.000	0.000
Xe-130	0.032	2.460
Xe-131	1.641	126.154
Xe-132	4.159	319.728
Xe-134	5.679	436.580
Xe-136	8.529	655.678
Total	**23.044**	**1,771.5**

Table 3.4-5 NAC-LWT Cask Thermal Performance Summary

Normal Transport Conditions

Component	Minimum Temperature °F	Maximum Temperature °F	Safe Operating Range °F
TFE O-rings	-40	227	-40 to +735[1]
Metallic O-rings	-40	227	-40 to +800
Viton® O-rings	-40	227[2]	-40 to +550[3]
Lead gamma shield	-40	273	-40 to +600
Liquid neutron shield	-40	238	-40 to +350

[1] Verified through testing (Certified Test Report D9-3362-1, Applied Technical Services, Inc., Marietta, GA, February 8, 1989)

[2] Normal Transport Condition maximum O-ring temperatures were not calculated. The Viton® O-rings are located in close proximity to the TFE O-rings and there is substantial thermal margin, a new O-ring temperature is not calculated

[3] Verified through testing (Certified Test Report 43939-01, Wyle Laboratories, Inc., Huntsville, AL, February 21, 2000).

Table 3.4-6 MTR Fuel Maximum Component Temperatures – Normal Transport Condition

Conditions: 100°F Ambient Temperature
Solar Insolation
1.26 Kilowatts Decay Heat Load

Condition 1: NAC-LWT (Transported in an ISO Container)
Cavity gas: Helium

Component	Temperature (°F)	
	Design Basis Decay Heat Load [1]	Variable Decay Heat Load [2]
Liquid Neutron Shield	198	198
Outer Shell	199	199
Lead Gamma Shield	212	214
Inner Shell	214	215
Basket (maximum)	256	292
Fuel (maximum)	< 363 [3]	< 363 [3]

Condition 2: NAC-LWT (Transported via Truck Trailer)
Cavity gas: Air

Component	Temperature (°F)	
	Design Basis Decay Heat Load [1]	Variable Decay Heat Load [2]
Liquid Neutron Shield	160	160
Outer Shell	161	160
Lead Gamma Shield	180	180
Inner Shell	181	180
Basket (maximum)	267	312
Fuel (maximum)	< 363 [3]	363

[1] Uniform 30-Watt/Element Configuration Heat Load.
[2] 120-Watt / 70-Watt / 20-Watt Configuration Heat Load.
[3] Fuel not modeled for this condition. Fuel temperature is bounded by the variable decay heat load in air case.

Table 3.4-7 PWR Rods (25 Total) Maximum Component Temperatures – Normal Transport Condition

Conditions: 100°F Ambient Temperature
Cask Inside ISO Container
Solar Insolation
1.41 Kilowatts Decay Heat Load

Component	Temperature (°F)
O-rings	< 249
Valves	< 249
Cask Radial Outer Surface	185
Lead Gamma Shield	248
Inner Shell	249
Outer Shell	235
Basket	252
Liquid Neutron Shield	235
Maximum Cladding Temperature	358

Table 3.4-8 TRIGA Fuel Element Maximum Component Temperatures - Normal Conditions of Transport

Conditions: 100°F Ambient Temperature
Solar Insolation
1.05 Kilowatts Decay Heat Load

Condition 2: NAC-LWT (Transported via Truck Trailer)
Cavity Gas: Air

Component	Temperature (°F)
Liquid Neutron Shield	< 160
Outer Shell	< 161
Lead Gamma Shield	< 180
Inner Shell	< 181
Basket (maximum)	267[1]
Cladding (maximum)	326[1]

[1] As shown in Table 3.4-6, the Condition 2 analysis produces higher basket temperatures than Condition 1. Therefore, the Condition 2 analysis for TRIGA fuel bounds transport of the cask in an ISO container.

Table 3.4-9 TRIGA Fuel Cluster Rod Temperatures – Normal Conditions of Transport

Conditions: 100°F Ambient Temperature
Solar Insolation
1.05 Kilowatts Decay Heat Load

Condition 1: NAC-LWT (Transported in an ISO Container)
Cavity gas: Helium

Component	Temperature (°F)
Liquid Neutron Shield	207
Outer shell	207
Lead Gamma shield	221
Inner shell	222
Basket (maximum)	263
Aluminum insert tube	265
Cladding (maximum)	266

Condition 2: NAC-LWT (Transported via Truck Trailer)
Cavity gas: Air

Component	Temperature (°F)
Liquid Neutron Shield	159
Outer shell	160
Lead Gamma shield	177
Inner shell	178
Basket (maximum)	278
Aluminum insert tube	292
Cladding (maximum)	295

Table 3.4-10 PWR and BWR High Burnup Fuel Rods Maximum Component Temperatures – Normal Transport Condition

Conditions: 100°F Ambient Temperature Solar Insolation
2.1 Kilowatts Decay Heat Load
Condition 1: NAC-LWT (Transported in an ISO Container)
Cavity Gas: Helium

Component	Component Temperature (°F)	Allowable Temperature (°F)
Liquid Neutron Shield	306	N/A
Outer Shell	308	800
Lead Gamma Shield	375	600
Inner Shell	385	800
Lid Metallic Containment Shell	385	800
Port Cover Containment Shell	385	550
Basket (maximum)	387	800(1)
Cladding (maximum)	671	752(2)
Aluminum PWR Insert	394	700(3)
Stainless Steel Can Weldment	500	800(2)
Average Cavity Gas	506	N/A

(1) Allowable temperatures greater than 800°F for stainless steel can e used provided stress limits in ASME III, Subsection NH, are employed in the stress evaluations.

(2) The maximum allowable temperature under NCT for PWR, BWR and PWR MOX fuel rod cladding is 752°F (400°C) per ISG-11, Revision 3.

(3) The aluminum insert is not a structural component. The primary consideration in establishing the safe operating range of the aluminum is maintaining the integrity of the aluminum. According to MIL-HDBK-5F, it can be shown that aluminum at 700°F retains component performance.

Condition 2: NAC-LWT (Transported via Truck Trailer)
Cavity Gas: Air

Component	Temperature (°F)
Inner Shell	274
Basket (maximum)	280
Aluminum PWR Insert	286
Stainless Steel Can Weldment	538
Cladding (maximum)	896
Average Cavity Gas	541

Table 3.4-11 Fission Product Gas Inventories and Pressures for the Exxon 7 × 7 BWR Fuel Assembly

Fission Product	Inventory per Fuel Assembly (moles)	Initial Partial Pressure per Rod (psia)
H-3	7.670E-03	1.408E+00
Kr-80	0.000E+00	0.000E+00
Kr-81	0.000E+00	0.000E+00
Kr-82	8.110E-03	1.489E+00
Kr-83	1.270E-01	2.331E+01
Kr-84	7.060E-01	1.296E+02
Kr-85	9.590E-02	1.760E+01
Kr-86	9.330E-01	1.713E+02
I-127	1.770E-01	3.249E+01
Xe-128	3.000E-02	5.507E+00
I-129	7.030E-01	1.290E+02
Xe-129	4.260E-04	7.819E-02
Xe-130	9.040E-02	1.659E+01
Xe-131	9.710E-01	1.782E+02
Xe-132	5.030E+00	9.233E+02
Xe-134	5.690E+00	1.044E+03
Xe-136	8.590E+00	1.577E+03
Total	2.32E+01	4.251E+03

Table 3.4-12 DIDO Fuel Maximum Component Temperatures – Normal Transport Condition

Conditions: 100°F Ambient Temperature
Solar Insolation
1.05 Kilowatts Decay Heat Load

Condition 1: NAC-LWT (Transported in an ISO Container)
Cavity gas: Helium

Component	Temperature (°F)
	Design Basis Decay Heat Load
Liquid Neutron Shield	198[1,2]
Outer Shell	199[1,2]
Lead Gamma Shield	212[1,2]
Inner Shell	214[1,2]
Basket (maximum)	299[3]
Fuel (maximum)	306[3]

[1] Uniform 30-Watt/Assembly Configuration Heat Load for MTR fuel.
[2] Bounding values obtained from Table 3.4-6 for MTR fuel.
[3] Uniform 25-Watt/Assembly Configuration Heat Load for DIDO fuel.

Condition 2: NAC-LWT (Transported via Truck Trailer)
Cavity gas: Air

Component	Temperature (°F)
	Design Basis Decay Heat Load
Liquid Neutron Shield	160[1,2]
Outer Shell	161[1,2]
Lead Gamma Shield	180[1,2]
Inner Shell	181[1,2]
Basket (maximum)	327[3]
Fuel (maximum)	338[3]

[1] Uniform 30-Watt/Assembly Configuration Heat Load for MTR fuel.
[2] Bounding values obtained from Table 3.4-6 for MTR fuel.
[3] Uniform 25-Watt/Assembly Configuration Heat Load for DIDO fuel.

Table 3.4-13 General Atomics IFM Maximum Component Temperatures – Normal Transport Condition

Conditions: 100°F Ambient Temperature
Solar Insolation
13 W Decay Heat Load

NAC-LWT (Transported in an ISO Container)

Component	Temperature (°F)
	Design Basis Decay Heat Load
Liquid Neutron Shield	198[1]
Outer Shell	199[1]
Lead Gamma Shield	212[1]
Inner Shell	214[1]
Basket (maximum)	250[2]
FHU contents (maximum)	326[3]

[1] Bounding values obtained from Table 3.4-6 for MTR fuel.
[2] 13-Watt Configuration Heat Load for General Atomics fuel.
[3] Bounding value obtained from Table 3.4-8 for the 1.05 kW TRIGA fuel.

Table 3.4-14 PWR and BWR High Burnup Fuel Rods in a Fuel Assembly Lattice Maximum Component Temperatures—Normal Transport Condition

Conditions: 100°F Ambient Temperature
Solar Insolation
2.1 Kilowatts Decay Heat Load (BWR)
2.3 Kilowatts Decay Heat Load (PWR)
Transport Condition 2 (no ISO container) with air in the cavity

Component	Temperature (°F)
Inner Shell	274
Basket (maximum)	276
Aluminum PWR Insert	336
Cladding (maximum)	664
Average Cavity Gas	430

Table 3.4-15 Maximum Component Temperatures for High Burnup Fuel Rods with Damaged Fuel Rods in a Rod Holder

	Maximum Temperatures (°F)					
Case[1]	Basket	Aluminum Insert	Rod Holder Weldment	Fuel Rod Tube[2]	Fuel Cladding[3]	Cavity Gas Average
Damaged Rods at Locations #4, 5, 6, 7, 8, 9, 10, 11, 12	280	285	523	835	809	479
Damaged Rods at Locations #7, 8, 9, 10, 11, 12, 13, 14, 15	280	286	567	866	653	482
Damaged Rods at Locations #1, 2, 3, 4, 5, 6, 7, 8, 9	280	284	474	743	749	465

[1] See Figure 3.4-17 for fuel rod locations. The nine locations in the half-symmetry model correspond to fifteen actual fuel rod locations.
[2] The structural analysis of the fuel tubes in Section 2.6.7.10.2 uses a maximum temperature of 925°F.
[3] Maximum temperatures are reported for intact fuel rods only.

Table 3.4-16 Maximum Component Temperatures for TPBAR Shipment – Normal Conditions of Transport

Component	Temperature (°F)
Liquid Neutron Shield	207[1]
Outer Shell	207[1]
Lead Gamma Shield	221[1]
Inner Shell	222[1]
TPBARs	290
Aluminum Basket	228
Consolidation Canister	245
Gas (average)	246

[1] Cask component temperature conservatively obtained from Table 3.4-9, Condition 1 for TRIGA Fuel Cluster Rod.

Table 3.4-17 Maximum Component Temperatures - PULSTAR Fuel in MTR Basket

Conditions: 100°F Ambient Temperature
Solar Insolation
840 watts Decay Heat Load
(30 watts in Each Basket Cell)

Condition 1: NAC-LWT (Transported in an ISO Container)
Cavity gas: Helium

Component	Temperature (°F)
Liquid Neutron Shield	207
Outer shell	207
Lead Gamma shield	221
Inner shell	222
Basket (maximum)	263
Aluminum insert tube	265
Cladding (maximum)	266

Condition 2: NAC-LWT (Transported via Truck Trailer)
Cavity gas: Air

Component	Temperature (°F)
Liquid Neutron Shield	159
Outer shell	160
Lead Gamma shield	177
Inner shell	178
Basket (maximum)	278
Aluminum insert tube	292
Cladding (maximum)	295

Notes:
1. The temperatures in this table correspond to the temperatures in Table 3.4-9.
2. PULSTAR fuel can (if used) = 295°F (assume same as fuel cladding temperature).

Table 3.4-18 PULSTAR Fuel Dimensions

Description	Value
Fuel Assembly Height (inch)	38
Fuel Assembly Width (inch)	3.15 × 2.74
Active Fuel Region Height (inch)	24.1
Fuel Rod Diameter (inch)	0.47
Fuel Clad Thickness (inch)	0.0185
Fuel Pellet Diameter (inch)	0.423
Rod Length (inch)	26.2
Plenum Length (inch)	0.5
Number of Fuel Rods	25

Table 3.4-19 PULSTAR Payload Volume Summary

Description	Dimension[cm^3]
Fuel Volume (25 Elements)	1,860
Pellet to Clad Volume (25 Elements)	97
PULSTAR Can Free Volume	1,440
PULSTAR Can Total Volume	4,230
Assembly Envelope Volume	5,370
LWT Cavity Volume	409,300
MTR Basket Stack Volume	41,900

Table 3.4-20 PULSTAR Fuel Assembly Fission Product Gas Inventory

Isotope	Moles
^{4}He	2.28E-03
^{3}H	1.30E-04
^{82}Kr	6.32E-05
^{83}Kr	7.03E-03
^{84}Kr	1.66E-02
^{85}Kr	2.41E-03
^{86}Kr	2.81E-02
^{127}I	2.87E-03
^{128}Xe	1.27E-04
^{129}I	1.42E-02
^{130}Xe	3.11E-04
^{131}Xe	3.91E-02
^{132}Xe	8.49E-02
^{134}Xe	1.27E-01
^{136}Xe	1.23E-01
Total	4.48E-01

Table 3.4-21 PULSTAR Fuel Element Normal Condition Internal Pressure Summary

Description	Free Volume	Pressure		
	(liters)	(atm)	(psia)	(psig)
Cask Pressure -28 Intact Assemblies	217.0	1.4	21.3	6.6
Cask Pressure -14 Intact Assemblies and 14 Cans	233.0	1.8	27.2	12.5
Can Pressure - PULSTAR Failed Fuel Can	1.53	4.4	65.4	50.7

Table 3.4-22 Maximum Component Temperatures – MOATA Plate Fuel and Mark III Spiral Fuel in ANSTO Basket

Conditions: 100°F Ambient Temperature
Solar Insolation
Heat Load: 126 Watts – MOATA Plate Fuel; 756 Watts – Mark III Spiral Fuel

Component	Temperature (°F)
Liquid Neutron Shield[1]	207
Outer Shell[1]	207
Lead Gamma Shield[1]	221
Inner Shell[1]	222
Basket - MOATA Plate Fuel	230
Fuel Cladding – MOATA Plate Fuel	233
Basket – Mark III Spiral Fuel	248
Fuel Cladding – Mark III Spiral Fuel	250

[1] The cask component temperatures are conservatively obtain from Table 3.4-9 for the TRIGA Fuel Cluster Rod.

3.5 Hypothetical Accident Thermal Evaluation

The hypothetical accident scenario is a series of accidents that occur in a specified order as described in 10 CFR 71.73. The only thermal consequence as a result of the drop and puncture portions of the hypothetical accident is the assumption that the neutron shield is lost prior to the start of the fire. The remainder of the thermal analysis in this section consists of an evaluation of the thermal consequences of the fire portion of the hypothetical accident.

3.5.1 Finite Element Models

There are two finite element models used to evaluate the hypothetical fire accident condition. The axisymmetric thermal model, as described in Section 3.5.1.1, is used to evaluate all configurations except for the PWR and BWR high burnup fuel rod configuration. For the PWR and BWR high burnup fuel rod configuration, a two-dimensional planar finite element model is used. The planar model is described in Section 3.5.1.2.

3.5.1.1 Axisymmetric Thermal Model

The finite element code ANSYS (Revision 5.5) is used to generate a two-dimensional (2-D) axisymmetric finite element model and to perform thermal analyses for the pre-fire, fire and post-fire (cool down) conditions. The ANSYS finite element model is shown in Figure 3.5-1. Figure 3.5-2 and Figure 3.5-3 show the detail of the model at the locations where the thermal insulator is installed in the top and bottom regions. The ANSYS model uses thermal conductivity values for the thermal insulators that are conservative in that they are higher than the values shown in Table 3.2-6 and Table 3.2-8. The thermal insulator protects the lead gamma shield against localized melting during the fire event. As shown, the main components in the radial direction consist of the inner shell, the radial lead, the outer shell, the neutron shield tank and the expansion tank.

The model is constructed using the ANSYS thermal PLANE55 element. Thermal radiation and convection heat transfer at the cask surface is modeled using the PLANE55 and SURF19 elements. Radiation heat transfer across the neutron shield tank and neutron shield expansion tank is modeled using the ANSYS radiation LINK31 element.

The pre-fire condition is defined as the normal transport condition, and a steady-state analysis is performed to determine the temperature field of the cask body. This temperature field is used as the initial condition for the 30 minute fire transient analysis (fire condition), which is followed by a 50-hour cool down period (post-fire condition). Analysis of the 50-hour cool down period ensures that the maximum component temperatures are determined.

The pre-fire analysis considers the convection heat transfer of the liquid neutron shielding inside the shell, but convection heat transfer of the air inside the expansion tank is conservatively neglected. During the fire and post-fire conditions, the liquid neutron shielding is considered to be lost, due to either the pin puncture accident or the failure of the relief valve in the neutron shield tank resulting from high pressure steam produced by the fire. The convection heat transfer of the air in the tank is negligible compared to the radiation heat transfer. The radiation heat transfer across the air-filled tank, and expansion tank, is explicitly modeled using the ANSYS radiation LINK31 element. An emissivity of 0.36 is used for all inner surfaces of the stainless steel neutron shield tank and the expansion tank.

The impact limiters are not discretely modeled, but are represented as thermal boundary conditions. Before the fire accident, adiabatic thermal boundary conditions are conservatively applied to the interface regions between the cask and the impact limiters so that no heat is transferred out of the cask through the impact limiters. During the fire and post-fire periods, the impact limiters are assumed to be removed. In this time period, heat transfer by convection and radiation are modeled in the regions previously covered by the impact limiters. Solar insolation is considered in the model during the pre-fire and post-fire conditions, but neglected during the fire.

The heat input from the fire considers thermal radiation and convection heat transfer. A convection heat transfer coefficient of 0.02446 Btu/hr-in2-°F is applied to account for heat transfer to the cask surface. This value is twice the theoretical value (Wix) to account for uncertainties in the fire accident condition and the data from which the recommended value is derived. These assumptions lead to maximizing the material temperatures and are conservative.

The cask contents (basket and fuel) are not directly modeled. The decay heat generated from the fuel region inside the cask is simulated using an equivalent non-uniform heat flux applied to the inner surface of the cask cavity inner shell, corresponding to the height of the active fuel region. The analysis considers the bounding fuel heat load, 2.5 kW for PWR fuel, and applies the power distribution curve shown in Figure 3.4-2 with a peaking factor of 1.2.

ANSYS 5.5 was used to calculate the maximum post-fire accident temperatures at four new locations for the alternate port cover design. Temperatures calculated for comparable locations on the port cover body vary from those temperatures presented in Table 3.5-1. Changes in the ANSYS 5.5 version and computational solvers account for the differences in calculated results. The transient temperature analysis results are presented in Figure 3.5-12 and Figure 3.5-13.

Exactly the same model described above was rerun using ANSYS 5.5 for the alternate port cover to determine the bolt head and thread temperatures and the temperatures at both O-ring locations. The output is post-processed to determine the maximum average temperatures at specific locations of interest. The temperatures calculated are presented in Table 3.5-1.

3.5.1.2 Two-Dimensional Planar Thermal Model

Thermal analysis of the NAC-LWT cask loaded with PWR and BWR high burnup fuel rods is performed using a two-dimensional planar thermal model. The thermal model is identical to the model utilized to perform the steady state analysis (condition 2, Section 3.4.1.7) for the NAC-LWT cask loaded with PWR and BWR high burnup fuel rods. The detailed model description is contained in Section 3.4.1.7.2.

The Condition 2 model was selected since it initiates the thermal transient with clad temperatures 225°F higher (from Table 3.4-10, 896°F-671°F) than the Condition 1 model steady-state condition. This increase in the initial condition temperature for the cask cavity air-filled condition overcompensates for the higher conductivity of helium as the cavity gas. The effect of the higher helium conductivity heat input during the period of fire exposure is significantly less due to the influence of the parallel heat transfer paths by conduction through the metal contents and by radiation across the gas-filled space. This influence is seen in the transient maximum temperature difference from the higher steady-state temperature of 896°F to the maximum transient temperature of 1,014°F (a change of 118°F), which is significantly bounded by the steady-state temperature condition difference of 225°F, as stated previously. In addition to the conservative modeling introduced by the initial steady-state temperature, during the cooldown portion of the transient, the use of air thermal conductivity in the cavity retards the heat removal from the fuel (as compared to helium conductivity). This also results in a maximum transient temperature higher than when modeling helium as the cavity gas.

A thermal transient analysis for the design basis fuel is performed using the two-dimensional planar thermal model (see Figure 3.4-12). To impose the fire accident condition on this model, a temperature time history was applied to the outer surface of the model, which corresponds to the inner surface of the inner shell. This temperature time history at the inner shell inner surface near the axial midplane is obtained from the fire accident analysis (heat load of 2.5 kW and a peaking factor of 1.2, as described in Section 3.5.2) using the axisymmetric two-dimensional model described in Section 3.5.1.1.

Using a two-dimensional planar model of the cross-section, a 50.5-hour transient analysis is performed with a heat load of 2.1 kW with a peaking factor of 1.22. This represents the bounding heat load for the high burnup PWR and BWR fuel rods.

3.5.2 Package Conditions and Environment

The fire accident is preceded by the cask drop and cask puncture portions of the hypothetical accident. The only damage that occurs as a result of the drop and puncture accident events that are of importance to the cask thermal performance is the damage to the NAC-LWT cask neutron shield. As a result of these events, it is assumed that the integrity of the neutron shield has been damaged to such an extent that the entire contents of the neutron shield are no longer present.

The fuel heat load of 2.5 kW is applied using a nonuniform heat flux with a peaking factor of 1.2. Solar insolation is applied to the outer surfaces of the cask, including the area covered by the impact limiters, during the post-fire conditions, and neglected during the fire condition. The value of solar insolation, based on a 24-hour average to curved surfaces, is:

$$Q_{sun}=1,475/(24\times144) = 0.4268 \text{ BTU/hr-in}^2$$

Convection and radiation heat transfer at the outer surfaces of the cask were considered in the analysis. During the pre-fire (normal) and post-fire periods, the ambient temperature assumed is 100°F, and the cask outer surface emissivity is 0.36. During the fire, the ambient temperature is 1,475°F, and the cask surface emissivity is 0.9. The convection coefficient applied is 0.02446 Btu/hr-in^2-°F.

Using a decay heat of 2.5 kW, the conditions for the hypothetical fire accident are:

Analysis Condition	Loads and Boundary Conditions
Initial steady-state (pre-fire)	• Solar Insolation • Combined convection (using the film coefficent for the cask surface, $0.00125\Delta T^{0.33}$ Btu/hr-in^2-°F) and radiation heat transfer (as defined in Section 3.2.3) between the cask exterior (ε=0.36) and the ambient (100°F) • The surface of the cask in contact with the impact limiter is adiabatic
Fire transient (during fire)	• Ambient temperature 1,475°F with no solar insolation • Combined convective (additional coefficient of 0.02446 Btu/hr-in^2-°F) and radiative heat transfer using a film coefficient (as defined in Section 3.2.3) between the cask exterior (ε=0.9), including the area normally covered by impact limiters, and the fire • Neutron shield fluid lost
Cool down (post-fire)	• Ambient temperature 100°F with solar insolation • Combined convection (using the film coefficient for the cask surface, $0.00125\Delta T^{0.33}$ Btu/hr-in^2-°F) and radiation heat transfer (as defined in Section 3.2.3) between the cask exterior (ε=0.36), including the area covered by the impact limiters, and ambient • Neutron shield fluid lost

3.5.3 Package Temperatures

The temperatures of the cask body resulting from the fire are determined using ANSYS. The heat load used in the transient thermal analysis corresponds to the PWR fuel, since its heat load envelopes all other fuel types that can be transported in the NAC-LWT cask.

The maximum temperatures of the basket and fuel for the different fuel types are determined using the results of the fire transient analysis of the cask body and the maximum temperature differences between the basket and fuel and the inner shell of the cask body as computed in the steady state thermal evaluations.

3.5.3.1 Evaluation for PWR Fuel Contents

The maximum temperatures of the cask body and principal components are evaluated using the ANSYS model described in Section 3.5.1.1. A radial temperature profile is obtained during the postulated 30-minute fire and for a cooldown period of 50 hours. The maximum cask component temperatures for the hypothetical accident are presented in Table 3.5-1.

Maximum time dependent temperatures of different cask components, before, during and after the fire, are shown in Figure 3.5-4 and Figure 3.5-5. The temperatures of the components show a sharp increase during the fire and a sharp decrease that begins right after the fire. After the 50 hour cooling period, the temperatures of the components do not return to the normal conditions of transport values. This is attributed to the loss of the liquid neutron shield during the accident, which results in the loss of the (liquid) convection heat transfer across the tank.

As noted above, the fuel and the fuel basket were not directly modeled in the ANSYS analysis. To determine the maximum temperature of the components inside the basket, the following method is applied:

$$T_{max} = Tis_{max} + \Delta T_{comp}$$

where:

Tis_{max} is the maximum temperature of the inner shell, obtained in the ANSYS transient thermal analysis.

ΔT_{comp} is the difference in maximum temperatures from Table 3.4-2 between the inner shell and the fuel basket outer wall or the fuel rod cladding during normal transport.

The maximum temperatures of fuel cladding and basket wall are:

Component	ΔT_{comp} (°F) [1]	Tis_{max} (°F) [2]	T_{max} (°F)
Fuel basket outer wall	2 (276-274)	505	507
Fuel cladding	198 (472-274)	505	703

[1] Temperatures from Table 3.4-2.

[2] Temperatures obtained in the ANSYS evaluation.

As a result, the maximum average cavity gas temperature can be taken as the average of the maximum basket wall and maximum fuel cladding temperatures. This produces an average cavity gas temperature of 605°F.

As shown in Table 3.5-1, all of the cask component temperatures are within the allowable temperature limit during the fire accident event.

3.5.3.2 Evaluation of MTR Fuel Contents

The temperatures in the MTR fuel basket and MTR fuel plates produced during the fire accident were determined using the two ANSYS finite element models of the NAC-LWT cask for MTR fuel element discussed in Section 3.4.1.3.2. The gas in the NAC-LWT cask cavity is considered to be air. Other conditions applied to the model are the same as those described in Sections 3.5.1 and 3.5.2 for the axisymmetric fire transient model with respect to the liquid neutron shield and outer surface boundary conditions. The accident thermal models for MTR fuel are shown in Figure 3.5-6 and Figure 3.5-7, for the design basis decay heat loading and the variable decay heat loading, respectively. The type, form, design or enrichment of the MTR fuel assemblies has no effect as long as the decay heat load and other fuel characteristics are in compliance with the requirements of Table 1.2-4. The presence and/or use of axial fuel spacers and spacer plates to position the fuel assemblies for ease of handling have no effect on the thermal analyses of the MTR basket assembly.

The transient calculation is performed to determine the maximum temperatures in the MTR fuel elements only for the variable decay heat loading because this is the worst-case condition. The cask model is used to determine the temperature history of the cask components, including the basket. The fuel element model is used to determine the temperature rise between the basket and the hottest point in the fuel element. The capacitance of the fuel element is negligible compared to the very large capacitance of the cask assembly. Therefore, a constant ΔT between basket and fuel is used. The temperature history for the MTR fuel variable heat load fire accident analysis is

shown Figure 3.5-8. The temperature profile within the cask model at the time of the maximum fuel temperature is shown in Figure 3.5-9. The bounding case is an element with 10 fuel plates, a decay heat of 120W and with worst-case dimensions. The maximum temperatures of the components are presented in Table 3.5-2. These results demonstrate that the maximum MTR fuel plate temperature for the variable decay heat loading is 473°F. The MIL-HDBK-5F Specification for 6061-T6 aluminum alloy indicates that the material retains more than 35% of its room temperature yield and ultimate strengths during transient exposure to temperatures as high as 500°F. Therefore, the reduction in strength for the fuel cladding as a result of the fire transient is minor when compared to the values presented in Section 3.4.1.3.3 for aluminum at 400°F. Since the fuel cladding temperatures are maintained significantly below 500°F, it is concluded that the structural integrity of the fuel cladding is maintained. Furthermore, the aluminum cladding of the MTR fuel elements is heated to a temperature of approximately 900°F during the fabrication process and it is clear that the cladding integrity is maintained during that process.

3.5.3.3 Evaluation of TRIGA Fuel Contents

The accident condition temperatures are obtained by applying the temperature differential calculated for the MTR fuel configuration to the TRIGA fuel configuration. To determine the TRIGA accident condition maximum cladding temperature, the temperature difference between the maximum basket temperatures for the normal and accident component temperatures calculated for MTR fuel in Section 3.5.3.2, is added to the maximum cladding temperature calculated for TRIGA fuel in Section 3.4.1.5.

The maximum basket temperature for the MTR fuel design basis heat load fire accident analysis is 374°F, as reported in Table 3.5-2. This temperature is 107°F higher than the normal condition maximum temperature (267°F) reported in Table 3.4-6. The corresponding maximum TRIGA fuel cladding temperature for the fire accident condition is reported in Table 3.5-3 to be 433°F. The MIL-HDBK-5F Specification for 6061-T6 aluminum alloy indicates that the material retains more than 35% of its room temperature yield and ultimate strengths during transient exposure to temperatures as high as 500°F. Therefore, the reduction in strength for the aluminum-clad TRIGA fuel cladding as a result of the fire transient is minor when compared to the values presented in Section 3.4.1.3.3 for aluminum at 400°F. Since the fuel cladding temperatures are maintained significantly below 500°F, it is concluded that the structural integrity of the aluminum-clad TRIGA fuel is maintained. The allowable temperature for stainless steel-clad TRIGA fuel is significantly higher.

The TRIGA fuel generates small amounts of fission gases during reactor operations, but it contains no initial charge of helium gas. Consequently, the internal pressure developed in the accident condition is less for TRIGA fuel than for the design basis PWR fuel.

3.5.3.4 Evaluation of TRIGA Fuel Cluster Rod Contents

The temperatures in the TRIGA fuel cluster rod basket and cladding produced during the fire accident were determined using the ANSYS finite element model of the NAC-LWT for the TRIGA fuel discussed in Section 3.4.1.6 for Condition 2 (air in the cavity and without the ISO container). The gas in the NAC-LWT cask cavity is considered to be air. Other conditions applied to the model are the same as those described in Sections 3.5.1 and 3.5.2 for the axisymmetric fire transient model with respect to the liquid neutron shield and outer boundary conditions.

The temperatures in the basket are bounded by the maximum temperatures of the fuel region. The temperature time history for the fuel region is shown in Figure 3.5-10. The maximum temperature of the clad was determined to be 394°F. This value is below the 800°F limit for the clad or the 400°F limit for the aluminum specified in Section 3.4.1.6. Therefore, the components are determined to be acceptable for the fire accident condition.

3.5.3.5 Evaluation for PWR and BWR High Burnup Fuel Rod Contents in a Rod Holder

The maximum temperatures of the principal components are evaluated using the ANSYS model described in Section 3.5.1.2. The maximum cask component temperatures for the hypothetical accident are identical to those presented in Table 3.5-1 since the bounding temperature history from the analysis of NAC-LWT PWR contents is used as a boundary condition for the analysis for PWR and BWR high burnup fuel rod contents.

Maximum time dependent temperatures of different components, before, during and after the fire, are shown in Figure 3.5-11. For the maximum time dependent temperatures of cask components see Figure 3.5-4 and Figure 3.5-5.

As a result, the maximum average cavity gas temperature for fire accident is calculated as the average of the air contained inside the basket. This produces an average cavity gas temperature of 695°F.

Table 3.5-4 shows the can weldment and fuel rod cladding temperatures during the fire accident event.

3.5.3.6 Evaluation of DIDO Fuel Contents

The DIDO fuel maximum heat load is bounded by the maximum heat load of the MTR fuel. Therefore, in the accident condition, the maximum temperatures of the cask components for the MTR contents will bound the maximum temperatures for the cask components for the DIDO

contents. It is conservative to use the results of the fire transient evaluated in Section 3.5.3.2 for the cask inner shell temperature. The maximum basket and fuel temperatures (T_{max}) for the DIDO fuel for the accident conditions are determined by adding the increase in steady state temperature from the cask inner shell to the maximum temperature of the component ($\Delta T_{component}$) to the maximum cask inner shell temperature ($T_{inner\ shell}$) obtained from the MTR evaluation. The maximum temperatures of the fuel cladding and basket wall are:

Component	$\Delta T_{component}$ (°F)	$T_{inner\ shell}$[1] (°F)	T_{max} (°F)
Fuel basket	146 = 327[2]-181	334	480
Fuel cladding	157 = 338[2]-181	334	491

[1] Obtained from Table 3.5-2 for the uniform heat distribution.
[2] Obtained from Table 3.4-12, Condition 2.

The fuel cladding temperature previously listed is bounded by those determined for the MTR contents. It is concluded that the structural integrity of the fuel cladding is maintained for the fire accident condition.

3.5.3.7 Evaluation for General Atomics Fuel Contents

The General Atomics fuel maximum heat load is bounded by the maximum heat load of the DIDO and MTR fuels. Therefore, in the accident condition, the maximum temperatures of the cask components for the MTR contents will bound the maximum temperatures for the cask components with General Atomics fuel. It is conservative to use the results of the fire transient calculation evaluated in Section 3.5.3.2 for the cask inner shell temperature. The maximum basket temperature (T_{max}) for the General Atomics fuel for accident conditions is determined by adding the increase in steady-state temperature from the cask inner shell to the maximum temperature of the component ($\Delta T_{component}$) to the maximum cask inner shell temperature ($T_{inner\ shell}$) obtained from the MTR evaluation. The maximum temperature of the basket is:

$$T_{max} = (250 - 214) + 334 = 370^{\circ}F$$

where:

334°F is the maximum temperature of the LWT inner shell during a fire accident

This temperature is bounded by those determined for the MTR contents. It is concluded that the structural integrity of the General Atomics basket and contents is maintained for the fire accident condition.

3.5.3.8 Evaluation of PWR and BWR High Burnup Fuel Rods in Fuel Assembly Lattice

The total heat load of the PWR and BWR high burnup fuel rods (up to 25 rods) in a fuel assembly lattice is bounded by that for the PWR and BWR high burnup fuel in a rod holder as evaluated in Section 3.5.3.5. Therefore, in the accident condition, the maximum temperatures of the cask components for the design basis PWR configuration bound the maximum temperatures for the PWR or BWR high burnup fuel rods in the fuel assembly lattice. The fuel cladding is expected to have the same difference in temperature between normal conditions and the accident fire conditions as determined in Section 3.5.3.5. The temperature difference for the fuel cladding between normal and accident conditions for the high burnup fuel in a rod holder is 118°F (1,014°F – 896°F). The maximum fuel cladding temperature is 664°F for high burnup fuel rods in a fuel assembly lattice for normal conditions of transport as evaluated in Section 3.4.1.10 (Table 3.4-14). Therefore, the maximum temperature of the fuel cladding for the 25 fuel rods in the fuel assembly lattice for accident conditions is 782°F (664°F + 118°F).

3.5.3.9 Evaluation of PWR and BWR High Burnup Fuel in a Rod Holder with Damaged Rods

The damaged fuel maximum heat load is equal to the maximum heat load of the PWR and BWR high burnup fuel rods. To determine maximum temperatures of the fuel configuration with damaged fuel rods in the fire accident condition, temperatures from the normal and accident conditions for the PWR and BWR high burnup intact fuel rods (Table 3.4-10 and Table 3.5-4) are used to determine the temperature differentials that are caused by the fire accident. The increase in temperatures is added to the maximum normal conditions temperature for the fuel rods in a rod holder with damaged rods (Table 3.4-15) to compute the maximum fire temperatures. The maximum temperatures of the fuel cladding and stainless steel rod holder are shown in Table 3.5-5. The maximum temperatures for the cask components are bounded by those for the design basis PWR fuel assembly configuration.

3.5.3.10 Evaluation of TPBAR Contents

The maximum heat load of TPBARs is bounded by the maximum heat load of the MTR fuel. Therefore, in the accident condition, the maximum temperatures of the cask components for the MTR contents will bound the maximum temperatures for the cask components for the TPBAR contents. It is conservative to use the results of the fire transient evaluated in Section 3.5.3.2 for the cask inner shell temperature. The maximum component temperatures (T_{max}) for the TPBARs for the accident conditions are determined by adding the temperature difference ($\Delta T_{component}$)

between the cask inner shell and the maximum component temperature for normal conditions to the maximum accident cask inner shell temperature ($T_{inner\ shell}$) obtained from the MTR evaluation. The maximum component temperatures are computed as follows.

Component	$\Delta T_{component}$ (°F)	$T_{inner\ shell}$[2] (°F)	T_{max} (°F)
TPBAR	68 (290[1]-222[1])	334	402
Aluminum Basket	6 (228[1]-222[1])	334	340
Consolidation Canister	23 (245[1]-222[1])	334	357
Gas (average)	24 (246[1]-222[1])	334	358

[1] See Table 3.4-16
[2] See Table 3.5-2

The maximum temperatures of the components are presented in Table 3.5-6.

3.5.3.11 Evaluation of PULSTAR Fuel Elements in 28 MTR Basket

As described in Section 3.4.1.13, the thermal performance of the configuration of PULSTAR fuel elements in the 28 MTR basket is bounded by the thermal performance of the TRIGA fuel cluster rods, condition 2. The temperatures in the TRIGA fuel cluster rod basket and cladding produced during the fire accident were determined and described in Section 3.5.3.4. The temperatures in the basket are bounded by the maximum temperatures of the fuel region. The temperature time history for the fuel region is shown in Figure 3.5-11. The maximum temperature of the cladding was determined to be 394°F. This value is below the 1,058°F limit for the fuel cladding. Therefore, the components for PULSTAR fuel elements in the 28 MTR baskets are determined to be acceptable for the fire accident condition.

3.5.3.12 Evaluation of ANSTO Fuels

The maximum heat load of the spiral fuel assemblies (0.756 kW per cask) is bounded by the maximum heat load of the MTR fuel (1.05 kW per cask). Therefore, in the accident condition, the maximum temperatures of the cask components for the MTR contents will bound the maximum temperatures for the cask components for the ANSTO basket contents. It is conservative to use the results of the fire transient evaluated in Section 3.5.3.2 for the cask inner shell temperature. The maximum basket and fuel temperatures (T_{max}) for the ANSTO fuel contents for the accident condition are determined by adding the temperature difference ($\Delta T_{component}$) between the maximum temperature of the cask inner shell and the component (basket or fuel) for the normal condition to the maximum cask inner shell temperature ($T_{innershell}$)

for the accident condition obtained from the MTR evaluation. The maximum temperatures of the fuel cladding and basket are computed as follows.

Component	$\Delta T_{component}$ (°F)	$T_{innershell}$[1] (°F)	T_{max} (°F)
Fuel basket – MOATA Plate Fuel	8 = 230[2]-222[2]	334	342
Fuel cladding – MOATA Plate Fuel	11 = 233[2]-222[2]	334	345
Fuel basket – Mark III Spiral Fuel	26 = 248[2]-222[2]	334	360
Fuel cladding – Mark III Spiral Fuel	28 = 250[2]-222[2]	334	362

[1] Obtained from Table 3.5-2 for the uniform heat distribution
[2] Obtained from Table 3.4-22

3.5.3.13 Evaluation of 16 PWR MOX High Burnup Rods

The PWR/BWR Rod Transport Canister and 5 × 5 insert used for the transport of 16 PWR MOX high burnup rods is the same design as the one used for the BWR and PWR high burnup rods. The heat load used in the evaluation of the BWR high burnup rods, which includes the effect of the peaking factor, bounds that of the PWR MOX high burnup rods (see Section 3.4.1.15). As presented in Section 3.4.1.15, the reduced conductivity of the PWR MOX fuel rods does not affect the heat transfer through the canister or insert or, in the case of the transient, it does not affect the ability to absorb and retain heat. The initial temperatures of the fuel rods are conservative since the heat load used in the steady-state evaluation is for 25 rods of the design basis heat load (see Section 3.4.1.7), rather than the 16 PWR MOX high burnup rods. Therefore, the maximum component temperatures under the hypothetical accident condition (HAC) are identical to the results reported in Table 3.5-1 for the PWR assembly contents, which were used as the boundary condition for the analysis for PWR and BWR high burnup fuel rod contents and, therefore, are applicable to the PWR MOX fuel rod contents. Table 3.5-1 shows that the lid metallic seal, Alternate B port cover metallic face seal and lead gamma shield are below their respective temperature limits. In addition, the bounding temperatures for the PWR and BWR rod contents reported in Table 3.5-4, which are bounding for the PWR MOX fuel rod contents, show that the can weldment and fuel rod cladding temperatures under the HAC are below their respective limits.

3.5.4 Maximum Internal Pressure

3.5.4.1 Maximum Internal Pressure for Design Basis Fuel in Accident Conditions

The accident internal pressure is calculated assuming an accident with 100 percent fuel rod failure combined with the design basis fire described in 10 CFR 71. The fuel rod failure assumes 30 percent of the fission gas and 100 percent of the backfill gas escapes the ruptured fuel rods.

The internal pressure due to the 100 percent fuel rod rupture is calculated using the method described in Section 3.4.4. The total cask pressure of the cask backfill and failed fuel rods is calculated by a two step procedure. First, the pressures documented under normal conditions in Section 3.4.4 are adjusted to include the increased total free volume associated with 100% fuel rod failure. Then, the revised cask pressure at normal operating temperature is adjusted to accident condition temperatures.

Adjusting the partial pressure of the cask backfill:

$$P_{cask} = P_{initial}\left(\frac{V_{cask}}{V_{total}}\right)$$

where:

$P_{initial}$ = 25.8 psia (normal condition temperature adjusted cask backfill pressure)

V_{cask} = 5.196 ft^3 (147,134 cm^3) [Section 3.4.4]

$V_{rod\ void}$ = 8,123 cm^3 [Section 3.4.4]

V_{total} = 155,257 cm^3 ($V_{cask} + V_{rod\ void}$)

$$P_{cask} = 25.8\ \text{psia}\left(\frac{147{,}134\text{cm}^3}{155{,}257\text{cm}^3}\right)$$

$$P_{cask} = 24.4\ \text{psia}$$

Adjusting the partial pressure of the fuel rod backfill and fission gases:

$$P_{fuel\ rods} = P_{initial}\left(\frac{V_{rod\,void}}{V_{total}}\right)$$

where:

$P_{initial}$ = 1,521.3 psia (fuel rod backfill pressure of 989.8 psia plus fission gas pressure of 0.30 x 1771.5 psia)

$V_{rod\ void} = 8{,}123\ cm^3$

$V_{total} = 155{,}257\ cm^3$

$$P_{fuel\ rods} = 1{,}521.3\ psia\left(\frac{8{,}123.28 cm^3}{155{,}257 cm^3}\right)$$

$$P_{fuel\ rods} = 79.6\ psia$$

Summing the two partial pressures yields the total cask pressure at normal operating condition temperature:

$$P_{Total} = P_{cask} + P_{fuel\ rods}$$

$$P_{Total} = 24.4\ psia + 79.6\ psia$$

$$P_{Total} = 104.0\ psia$$

The fuel cladding has the highest temperature of any barrier with which the gas comes in contact during a design basis fire. As shown in Section 3.5.3.1, the maximum average cavity gas temperature is 605°F during the fire accident condition. For conservatism, a temperature of 667°F is used in the calculation of the maximum accident condition internal pressure. Given that the internal volume of the NAC-LWT Cask remains constant during the fire, the resultant pressure is proportional to the temperature change according to the ideal gas law:

$$P_2 = P_1\left(\frac{T_2}{T_1}\right)$$

Thus, for the design basis fire:

$$P_{fire} = 104.0\ psia\left(\frac{1127°R}{932°R}\right)$$

$$P_{fire} = 125.8\ psia$$

3.5.4.2 High Burnup Fuel Rod Canister Maximum Internal Pressure

The high burnup fuel rod canister maximum internal pressure in the accident conditions is calculated assuming 100 percent fuel rod failure combined with the design basis fire maximum temperature. The fuel rod failure assumes release of 30 percent of the fission gas and 100 percent of the backfill gas.

The canister internal pressure is calculated using the method described in Section 3.4.4.2, with the BWR used as the bounding fuel type for the analysis. The total canister pressure is calculated in two steps. First, the pressures documented under normal conditions in Section 3.4.4.2 are adjusted to include the increased total free volume associated with 100 percent fuel rod failure. Then, the canister pressure is adjusted to account for the accident condition temperature.

The partial pressure of the canister volume is calculated by:

$$P_{canister} = P_{initial}\left(\frac{V_{canister}}{V_{total}}\right)$$

where:

P_{inital} = 29.3 psia (from earlier)

$V_{canister}$ = 28.2 liters (from earlier)

V_{void} = 0.079 liter (from earlier)

V_{void} = $25*V_{void} + V_{canister} = 30.2$ liters

V_{total} = 30.2 liters

Therefore, $P_{canister}$ is equal to 27.4 psia. The partial pressure of the fuel rods is calculated by:

$$P_{fuel\ rods} = P_{initial}\left(\frac{V_{fuel\ rods}}{V_{total}}\right)$$

where:

$P_{initial}$ = 1,425 psia (earlier from Section 3.4.4.2)

$V_{fuel\ rods}$ = $25*V_{void}$

$V_{fuel\ rods}$ = ~1.97 liters (at 100% of the total fuel rod volume)

V_{total} = 30.2 liters ($V_{canister} + (25*V_{void})$)

then:

$$P_{fuel\ rods} = 1{,}425\ \text{psia}\left(\frac{1.97\ \text{liters}}{30.2\ \text{liters}}\right) = \sim 94\ \text{psia}$$

and

$$P_{total} = P_{canister} + P_{fuel\ rods} = 27.4\ \text{psia} + \sim 94\ \text{psia} = \sim 121\ \text{psia}\ (\sim 8.2\ \text{atm})$$

For the 100% fuel rod failure and the design basis fire accident temperature of 725°F, the pressure is calculated by multiplying the 100% rod failure pressure by the inverse ratio of the normal condition temperature (588.7 K) to the accident temperature (658.15 K). The pressure thus calculated is 135 psia (~9.2 atm)

3.5.4.3 25-Rod Maximum Internal Pressure-Cask Cavity

Using the same methodology used to calculate the cavity pressure in Section 3.5.4.2, the pressure from the 100% fuel rod failure and the design basis fire accident temperature of 725°F is calculated using the cask cavity free gas volume (89.32 liters from earlier). The resulting pressure in the cask cavity, assuming that the gases within the canister are released to the cask cavity, is 67 psia (~4.5 atm).

3.5.4.4 TPBAR Shipment Cask Cavity Internal Pressure-Accident Conditions

Employing the normal condition TPBAR result in Section 3.4.4.5 of 276 psig for the 300 production TPBAR content condition and adjusting system pressure to the average accident gas temperature of 358°F yields a maximum accident condition pressure of 322 psig. For a period of one year following the 90-day cooldown, the pressure for this content condition increases to 337 psig.

Utilizing the same assumptions as presented in Section 3.4.4.5 and the post-accident thermal conditions discussed above, the pressure for the 55 segmented TPBARs in the waste container will be less than 75 psia and, therefore, bounded by the 300 TPBAR content condition.

3.5.4.5 Maximum Internal Pressure for PULSTAR Fuel Payload

Maximum internal pressures under accident conditions are calculated using the same methodology as that employed in Section 3.4.4.6. The accident condition temperature is set to 394°F, and 100 percent of the fuel rods are assumed to fail. The resulting calculated pressures are summarized as follows.

Description	Free Volume (liters)	Pressure (atm)	Pressure (psia)	Pressure (psig)
Cask Pressure -28 Intact Assemblies	217.0	2.3	34.0	19.3
Cask Pressure -14 Intact Assemblies and 14 Cans	233.0	2.4	35.4	20.7
Can Pressure - PULSTAR Failed Fuel Can	1.53	5.0	73.9	59.2

3.5.4.6 Maximum Internal Pressure for 16 PWR MOX/UO_2 Fuel Rods in a Rod Holder

Using the same methodology used to calculate the cavity pressure in Section 3.4.4.4, the pressure from the 100% fuel rod failure with 100% gas release and the design basis fire accident temperature of 725°F is calculated. The resulting pressure in the cask cavity is 65.3 psig (80.0 psia, 5.4 atm).

3.5.5 Maximum Thermal Stresses

The most severe thermal stress conditions that occur during the fire test and subsequent cooldown have been evaluated. For conservatism, an internal pressure of 168 psig is used, in the analysis that is performed in Section 2.7.3. The temperatures corresponding to the maximum thermal stresses are reported in Table 3.5-1.

3.5.6 Evaluation of Package Performance for Hypothetical Accident Thermal Conditions

The NAC-LWT cask thermal performance has been assessed for the hypothetical accident, as specified in 10 CFR 71. The O-rings and the lead gamma shields remain within their safe operating ranges. The cask does not suffer any adverse structural consequences as a result of the thermal considerations of the hypothetical accident. The NAC-LWT cask maintains containment and does not exceed the dose rate limits of 49 CFR 173 as a result of the hypothetical accident.

3.5.7 Assessment of the Effects of the Fission Gas Release in the Fire Accident Condition

During the fire, the release of the fission gas is expected to reduce the effective thermal conductivity of the gas in the cavity or inside the sealed canisters. To assess the reduction of the thermal conductivity, the helium conductivity is factored by the ratio of the conservative initial fill pressure of 565 psia (Section 3.4.4) for the PWR fuel assemblies and the end of life pressure (which contains the fill gas plus the fission gas release) of 1,521 psia (Section 3.5.4). This ratio is computed to be 0.37. A conservative ratio of 0.24 is applied to the conductivity of helium, assuming that all fission product gases have a conductivity of zero.

For the temperatures shown, which envelope the maximum temperatures of the cavity gas in the accident condition, the reduced helium properties are larger than the thermal conductivity of air. This is bounding because, as shown in Table 4.2-2, the volume of fission product gas produced by the design basis PWR assembly is higher than that for any other fuel loading.

The data below (Krieth) reflects the comparison of the air conductivity and the factored helium conductivity.

Temperature (°F)	Air Conductivity (K_{air}) (Btu/hr-in-F)	Helium Conductivity (Btu/hr-in-F)	Factored Helium Conductivity (K_{He}) (Btu/hr-in-F)	Ratio K_{He}/K_{air}
300	0.00161	0.00883	0.00212	1.32
400	0.00177	0.00958	0.00230	1.30
500	0.00193	0.01017	0.00244	1.26
600	0.00208	0.01075	0.00258	1.24
700	0.00223	0.01113	0.00267	1.20
800	0.00238	0.01150	0.00276	1.16

The analyses performed for the contents employed air as the gas in the cavity and containers for the accident condition. This demonstrates that the evaluation of the accident condition using air bounds the "reduced helium properties" case.

Figure 3.5-1 Transient Thermal Analysis Finite Element Model of the NAC-LWT

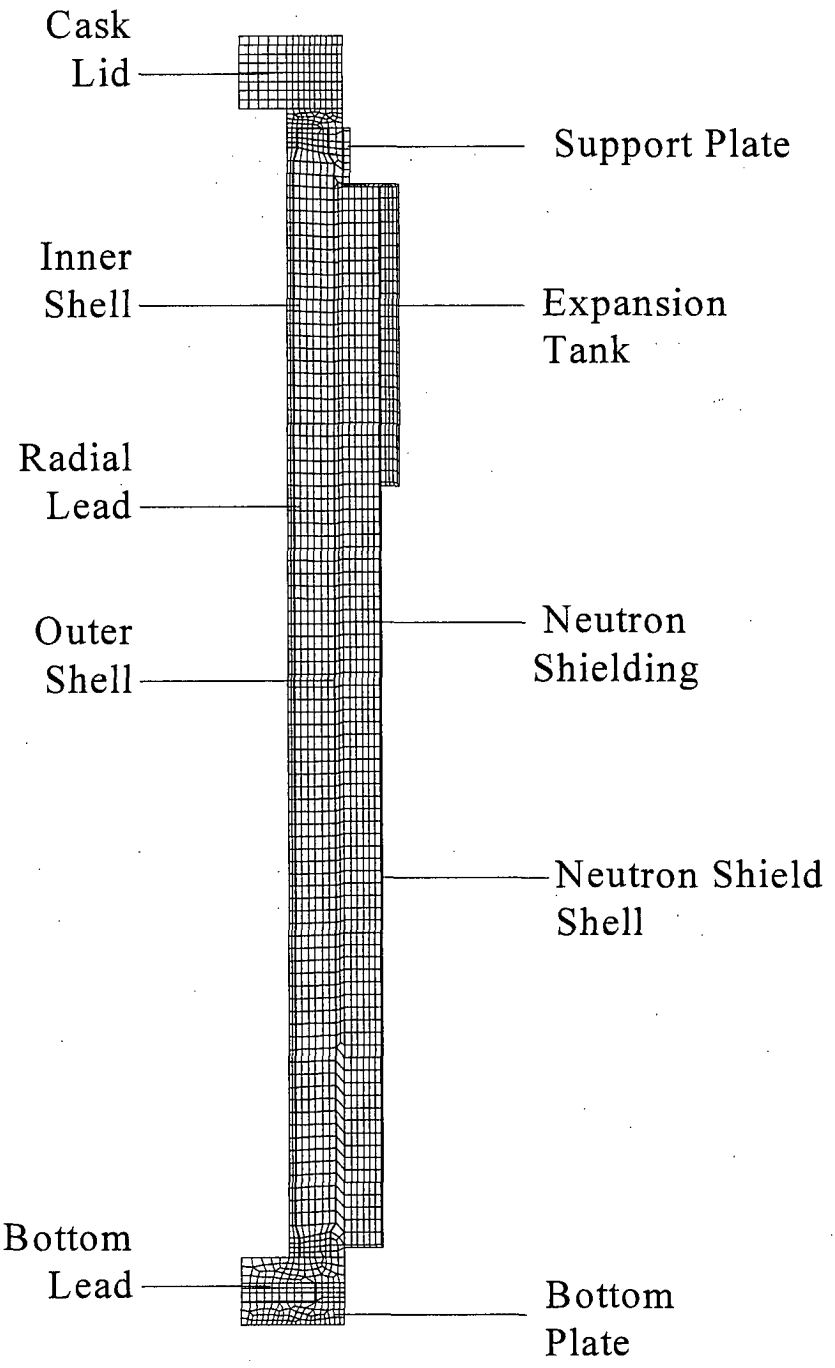

Figure 3.5-2 Top Region of the ANSYS Model

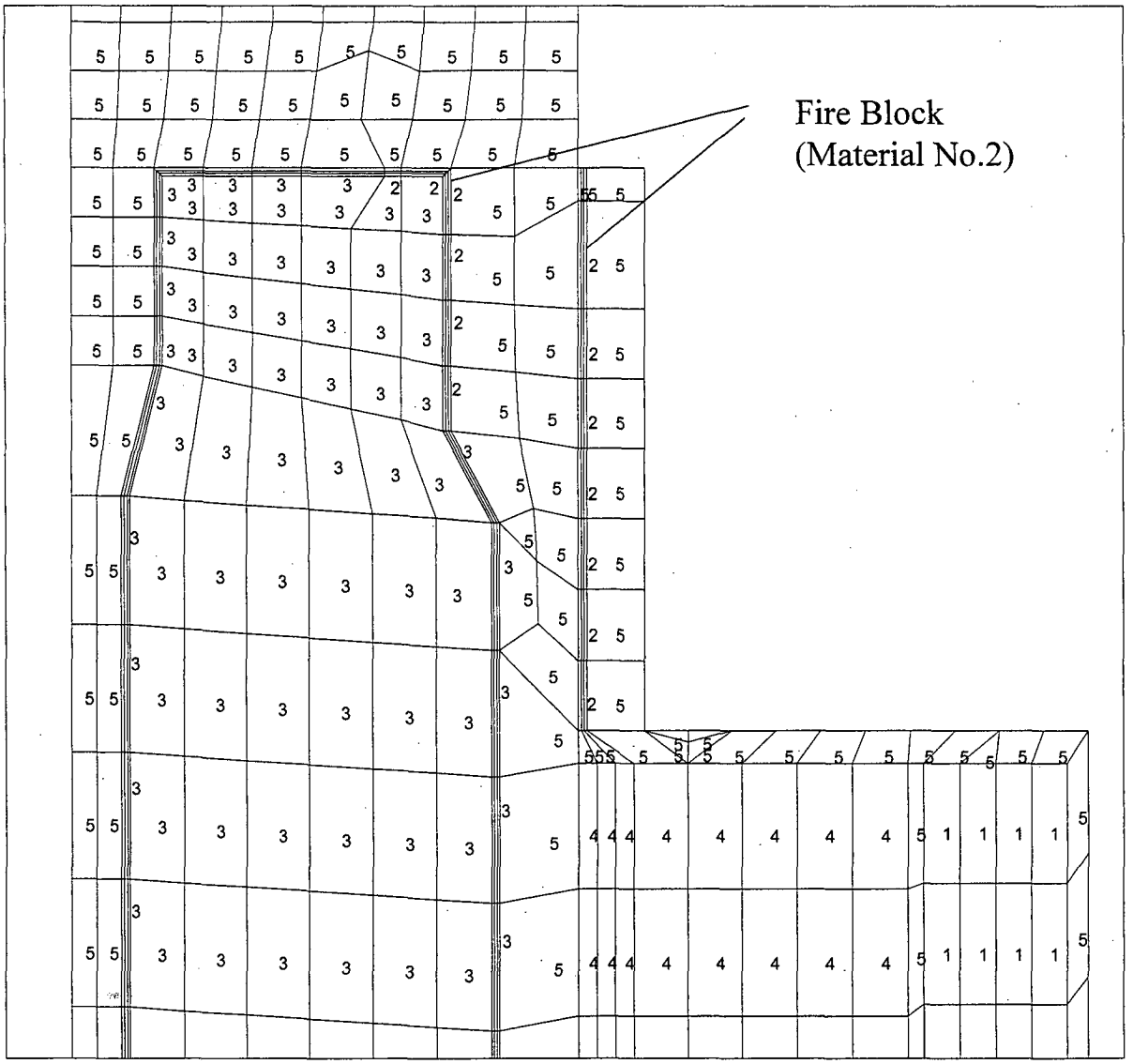

Note: Fire Block is either BISCO FPC or UNIFRAX Fiberfrax Ceramic Fiber Paper

Figure 3.5-3 Bottom Region of the ANSYS Model

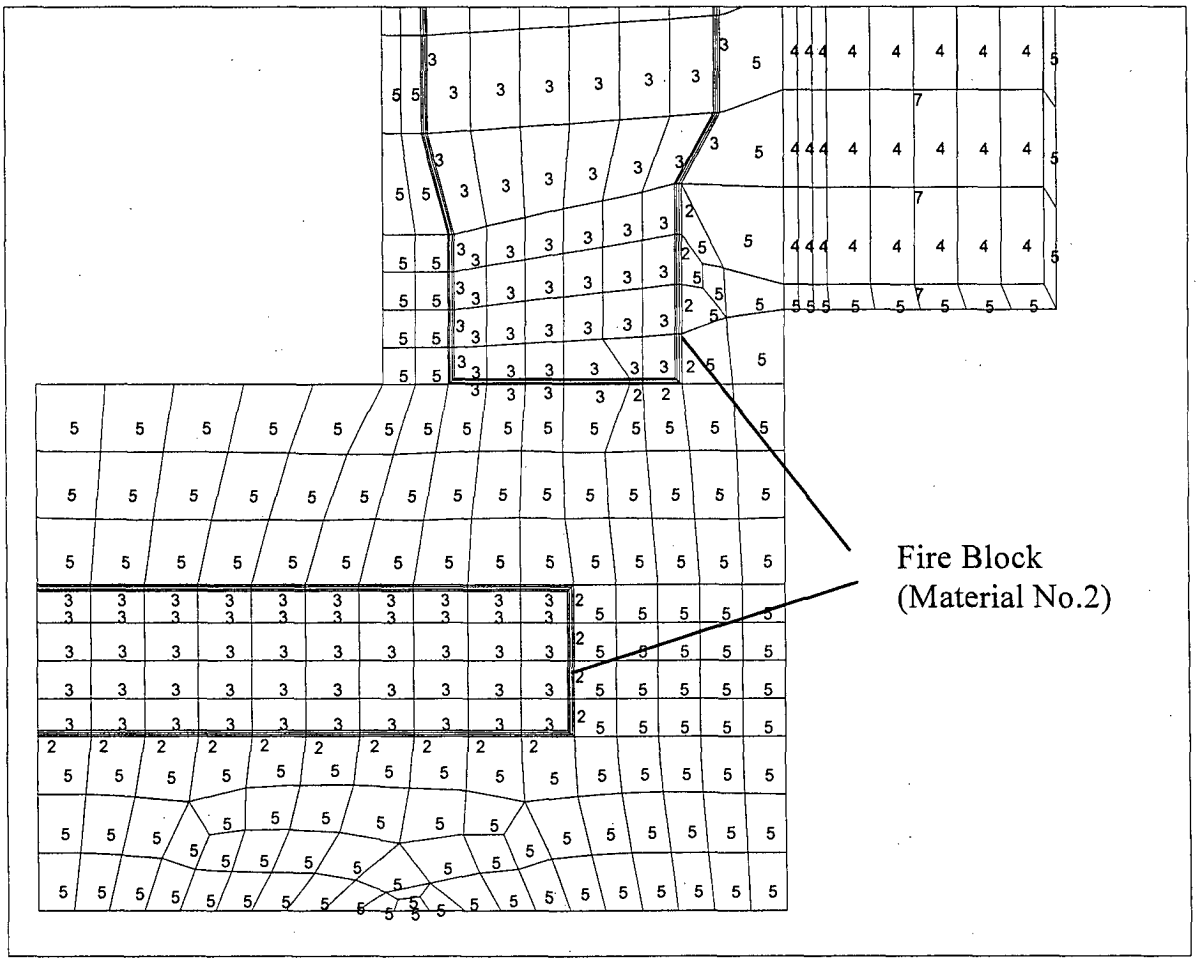

Note: Fire Block is either BISCO FPC or UNIFRAX Fiberfrax Ceramic Fiber Paper

Figure 3.5-4 Temperature History of NAC-LWT O-Rings and Valves in the Hypothetical Fire Event

1. Temperature of the Valves
2. Temperature of the O-Rings

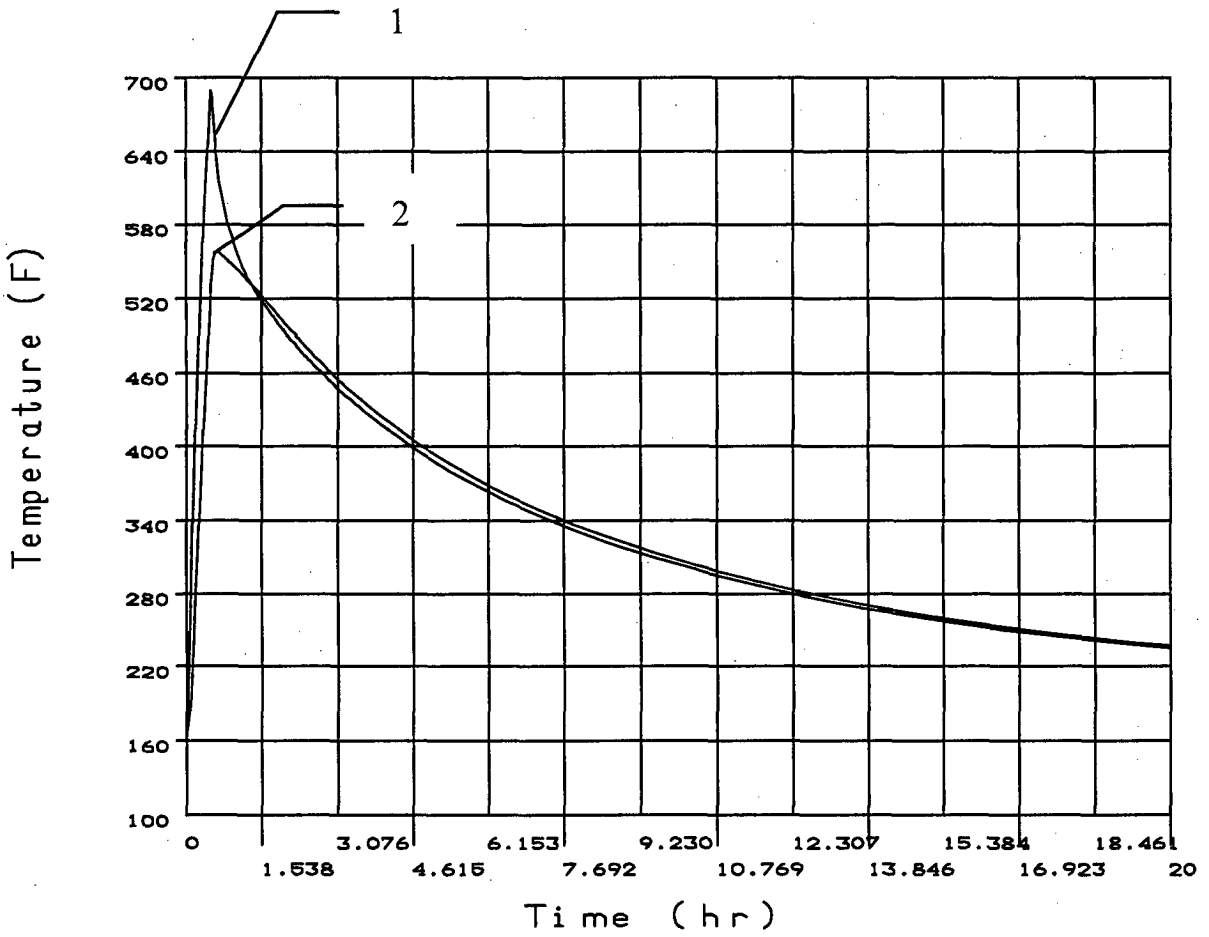

Figure 3.5-5 Temperature History of NAC-LWT Components in the Hypothetical Fire Event

1. Temperature of the Cask Outer Surface
2. Temperature of the Neutron Shield
3. Temperature of the Radial Lead Gamma Shield
4. Temperature of the Bottom Lead Gamma Shield
5. Temperature of the Inner Stainless Steel Shell

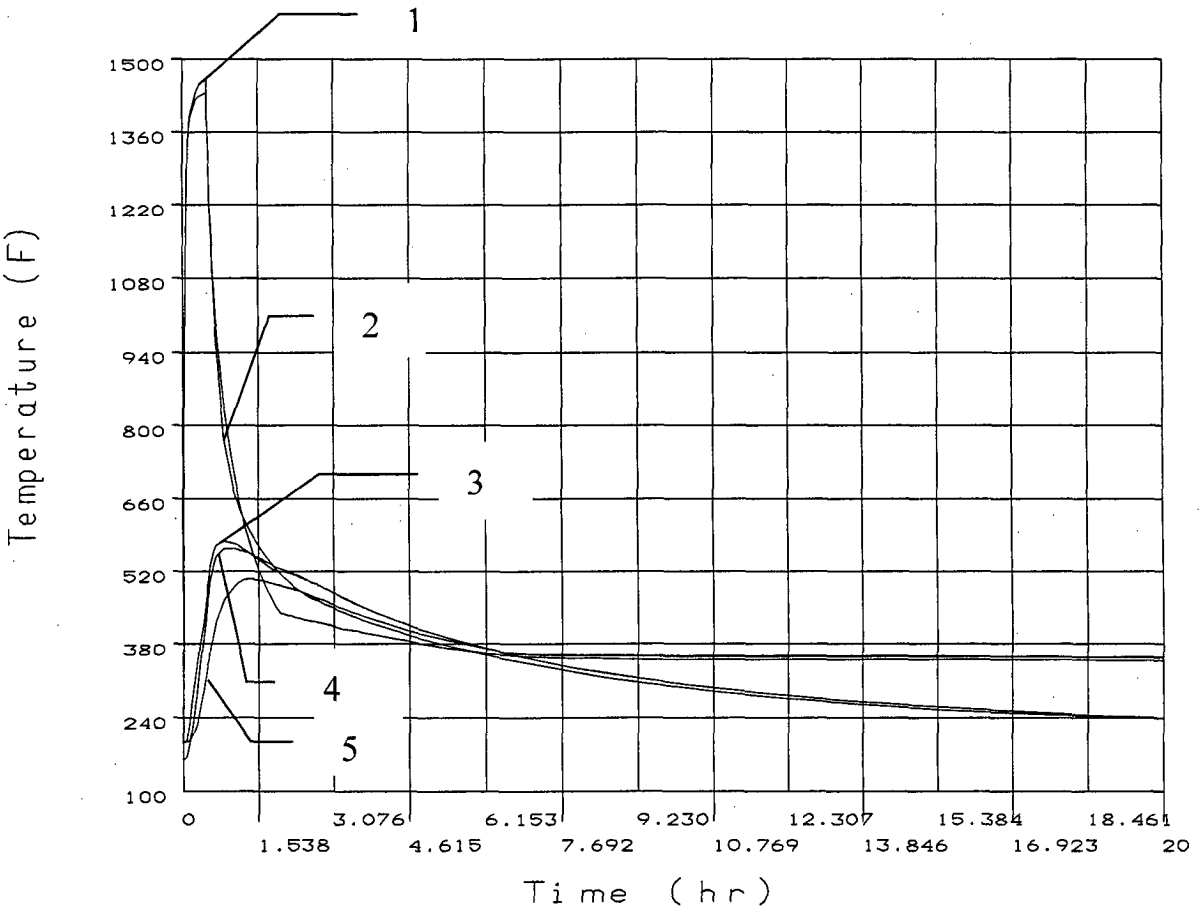

Figure 3.5-6 MTR Fuel Design Basis Heat Load Fire Accident ANSYS Thermal Model (Uniform 30-Watt/Element Configuration Heat Load)

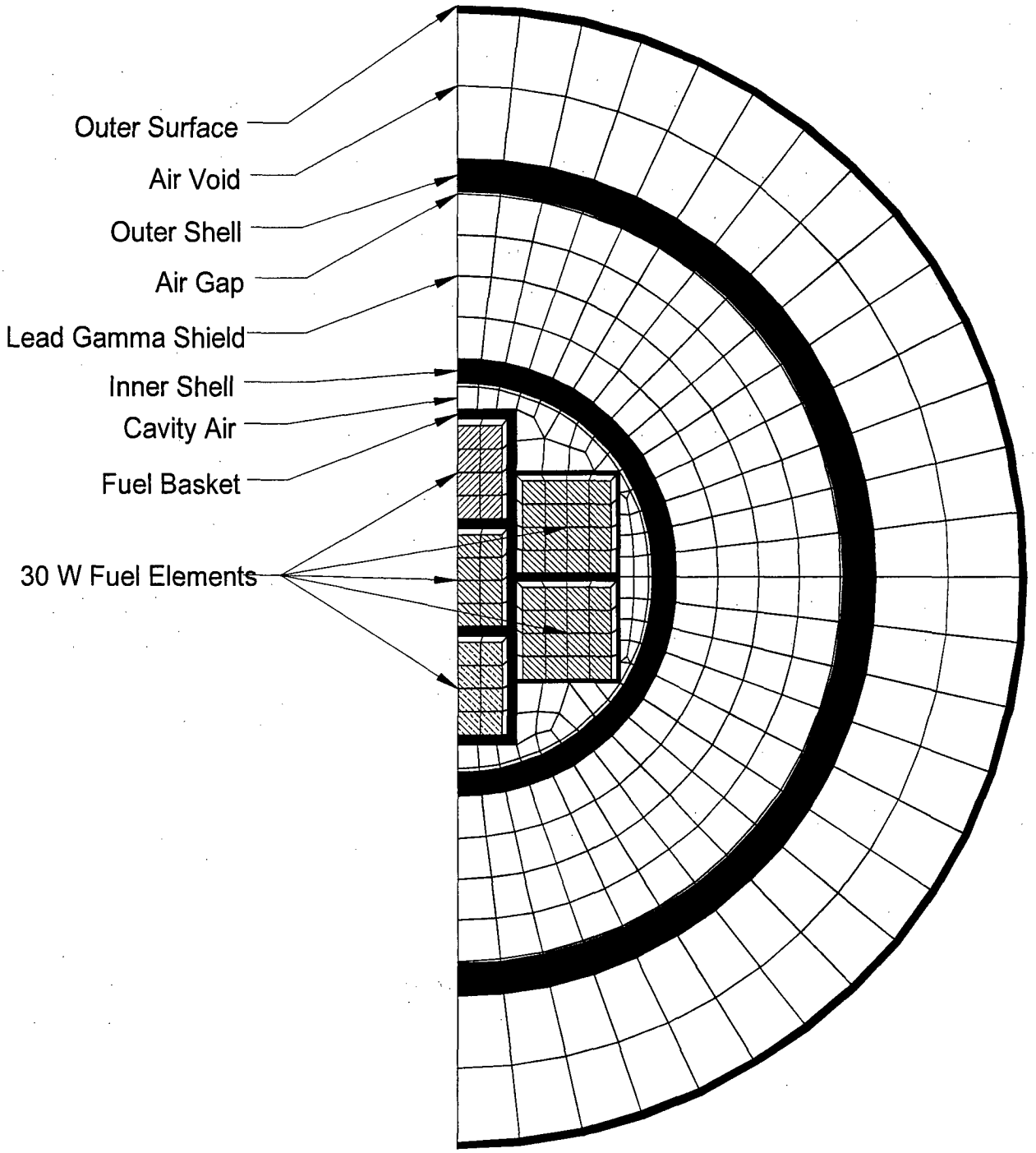

Figure 3.5-7 MTR Fuel Variable Heat Load Fire Accident ANSYS Thermal Model (120-Watt/70-Watt/20-Watt Configuration Heat Load)

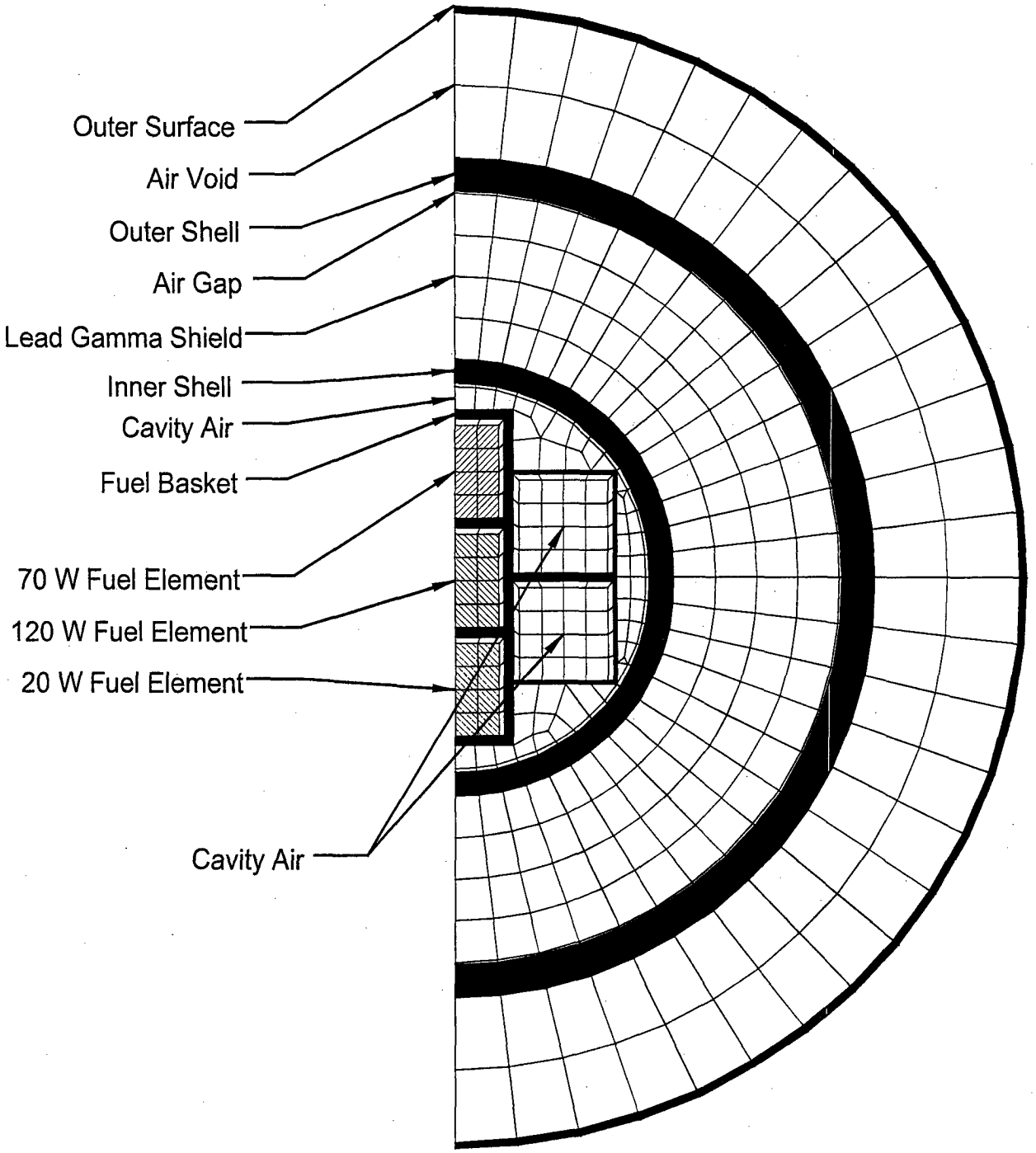

Figure 3.5-8 Temperature History in the MTR Fuel Variable Heat Load Fire Accident Analysis

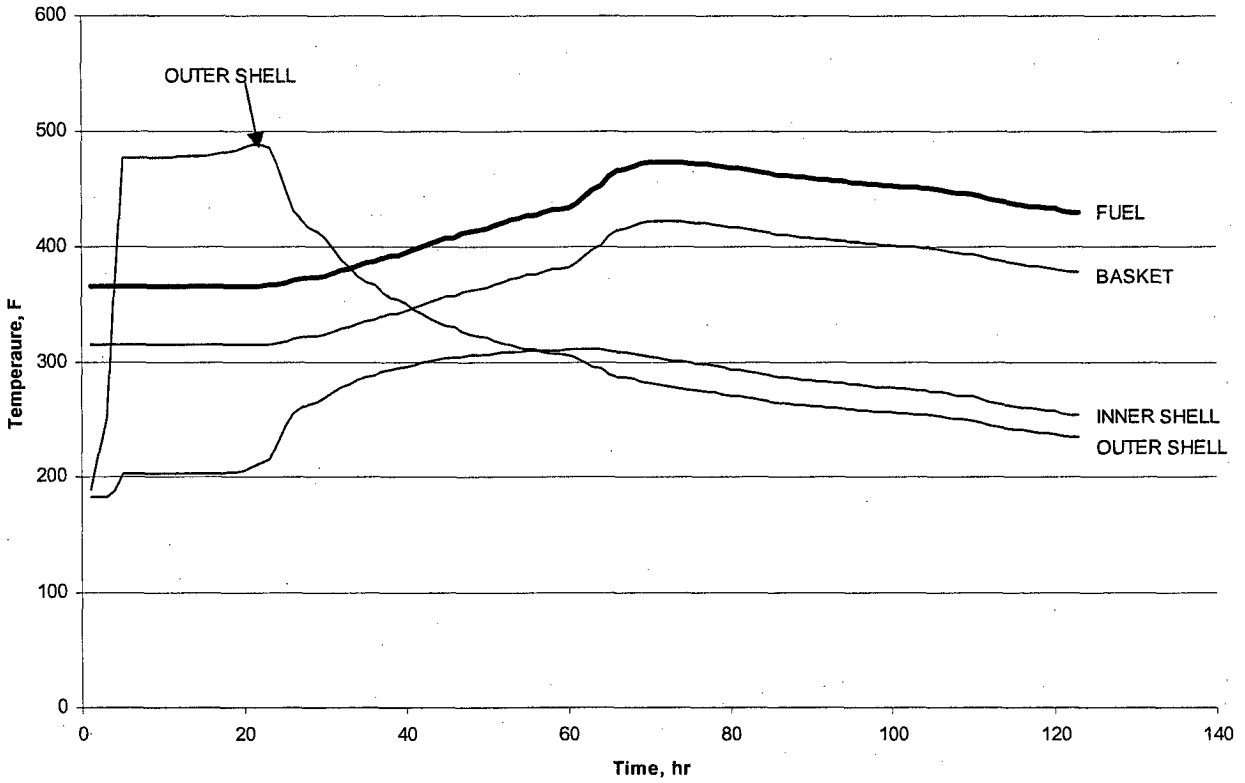

Note: 120-Watt / 70-Watt / 20-Watt Configuration Heat Load. Cavity gas is air with fire applied to cask surface.

Figure 3.5-9 Location of the Maximum Temperature in the MTR Fuel Variable Heat Load

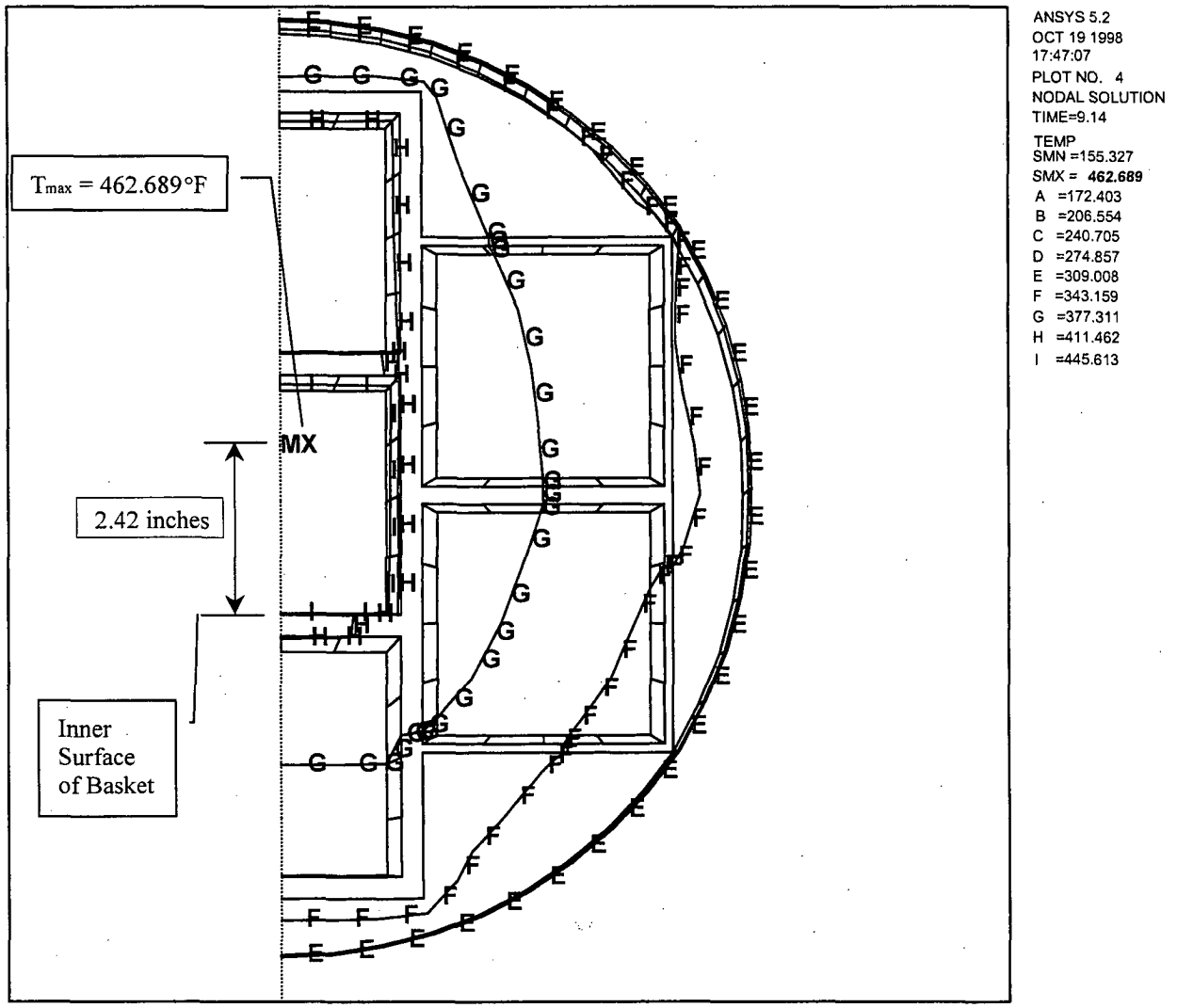

Figure 3.5-10 Temperature History for the TRIGA Fuel Cluster Rods Design Basis Heat Load Fire Accident Analysis

(Uniform 30 watt/basket cell or 210 watt/basket section or 1.05 kW total heat load)
(Cavity gas: Air, Fire is Applied to the Cask Surface)

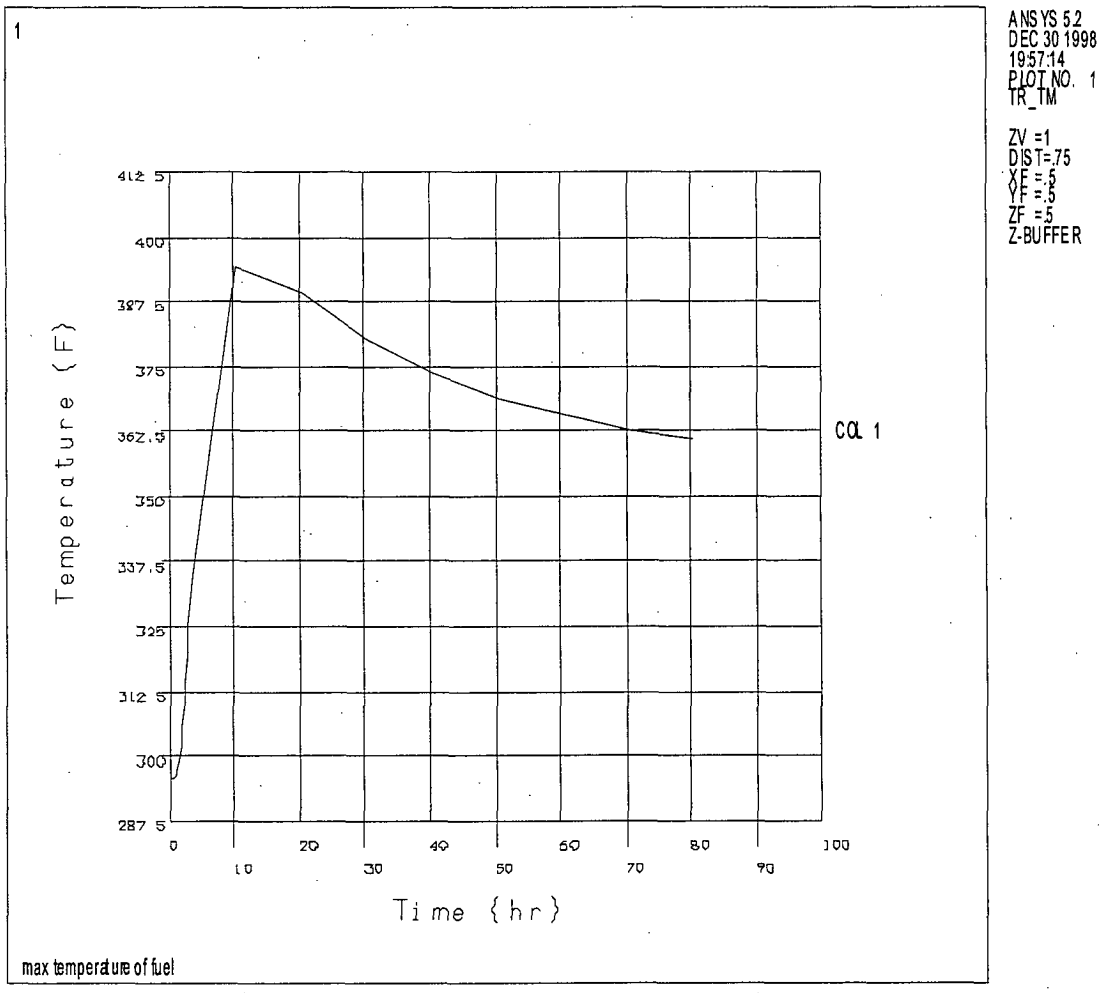

Figure 3.5-11 Temperature History of NAC-LWT Cask Components with PWR and BWR High Burnup Fuel Rods in the Hypothetical Fire Event

1. Average Temperature of Cask Cavity Gas
2. Temperature of the Fuel Cladding
3. Temperature of the Can Weldment
4. Temperature of the Aluminum Structural Component
5. Temperature of the Pin Tube

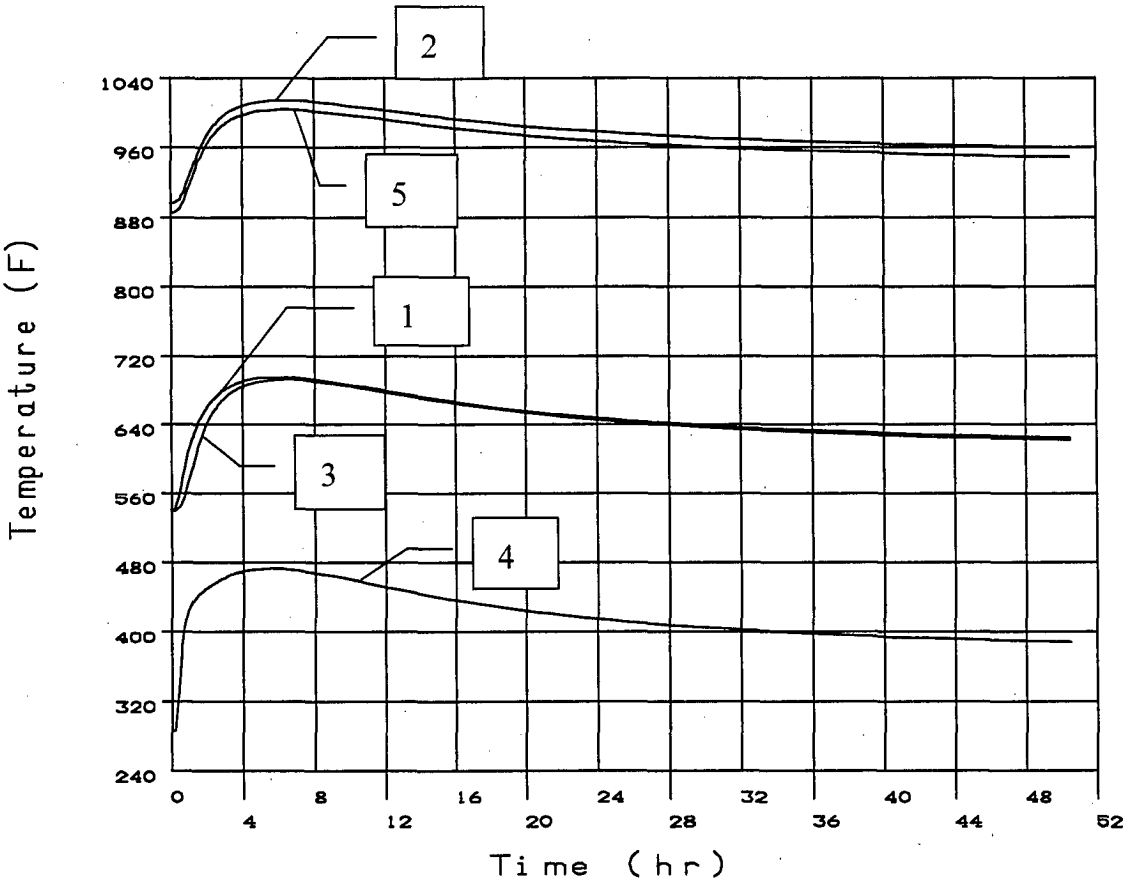

Figure 3.5-12 End of Fire Temperatures of the Alternate Port Cover Components

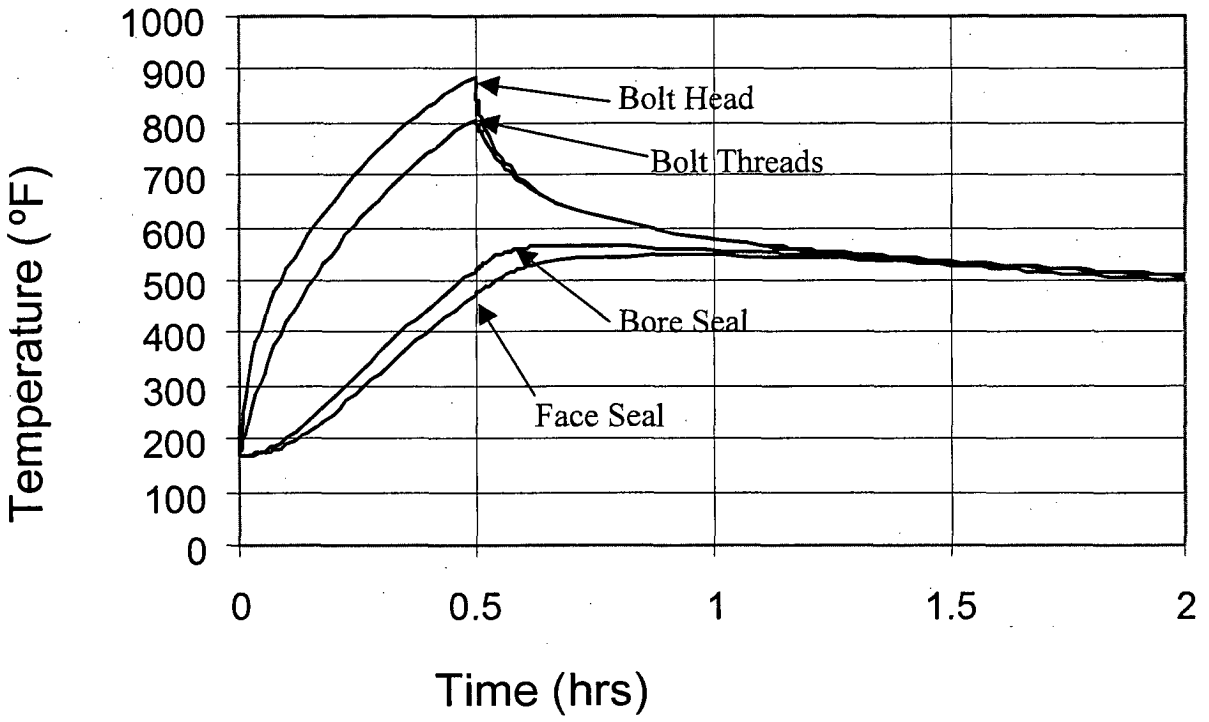

Figure 3.5-13 Transient Temperatures of the Alternate Port Cover Components

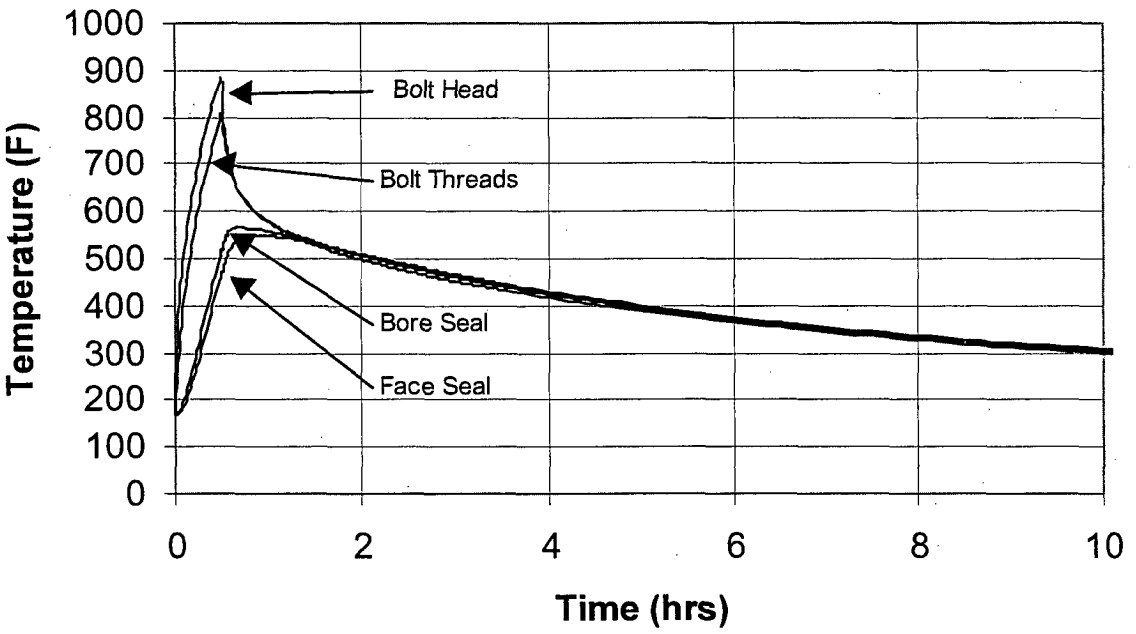

Table 3.5-1 Maximum Component Temperatures (°F) During the Fire Accident (Design Basis PWR Fuel, 2.5 kW Heat Load)

Component	Component Temperature (°F)	Temperature Limit (°F)
O-rings: TFE	558	735
Metallic	571(3)	800
Cask radial outer surface	1460	----(1)
Neutron shield region	1435	----(1)
Radial lead gamma shield	578	600
Bottom lead gamma shield	564	600
Inner stainless steel shell	505	800
Fuel basket outer wall	507	700(2)
Fuel rod cladding	703	1058
Alternate Port Cover	--	--
Bolt head	886	900
Bolt threads	807	900
Alternate Port Cover O-ring – bore	565(4)	550
Alternate Port Cover O-ring – face	547	550
Alternate B Port Cover metallic face seal	547	800

Notes:

(1) No upper limit established. The loss of the liquid neutron shield is assumed under HAC

(2) The primary consideration in establishing the safe operating range of the aluminum is maintaining the integrity of the aluminum. According to MIL-HDBK-5F, it can be shown that aluminum at 700°F retains component performance.

(3) The maximum port cover seal temperature is conservatively used to bound the maximum temperature of the metallic seal.

(4) Should the bore seal fail post-fire accident, containment would not be breached.

Table 3.5-2 MTR Fuel Fire Accident Maximum Temperatures (°F), 10 Fuel Plate/120W Element Case (Bounding Configuration)

Condition 2: NAC-LWT (Transported via Truck Trailer)
Cavity Gas: Air

Component	Design Basis Heat Loading*	Variable Decay Heat Loading**
Cask Radial Outer Surface	***	***
Lead Shield	***	***
Inner Shell	334	337
Fuel Basket	374	420
Fuel Cladding	385	473

* Uniform 30-Watt/Element Configuration Heat Load.

** 120-Watt/70-Watt/20-Watt Configuration Heat Load.

*** The maximum temperatures for these components are bounded by the design basis reported.

Table 3.5-3 TRIGA Fuel Fire Accident Maximum Temperatures (°F)

Component	Temperature
Fuel Basket	374
Fuel Cladding	433

Table 3.5-4 PWR and BWR High Burnup Fuel Rods Fire Accident Maximum Temperatures (°F)

NAC-LWT (Transported via Truck Trailer)
Cavity Gas: Air

Component	Component Temperature (°F)	Temperature Limit (°F)
Stainless steel Can Weldment	692	800
Fuel Rod Cladding	1,014	1,058[1]

[1] The maximum allowable temperature under HAC for PWR, BWR and PWR MOX fuel rod cladding is 1,058°F per ISG-11, Revision 3.

Table 3.5-5 Maximum Component Temperatures for High Burnup Fuel Rods in a Rod Holder with Damaged Fuel Rods for the Fire Accident

Component	Normal Conditions Temperature[1] (T_{norm})(°F)	Temperature Difference (ΔT) (°F)	Accident Temperature $T_{acc} = T_{norm} + \Delta T$(°F)
Rod Holder Weldment	567	692[2] – 538[3] = 154	721
Fuel Cladding	809	1014[2] – 896[3] = 118	927

[1] Table 3.4-14
[2] Table 3.5-4
[3] Table 3.4-10, Condition 2

Table 3.5-6 TPBAR Fire Accident Maximum Temperatures

Component	Temperature (°F)
TPBARs	402
Aluminum Basket	340
Consolidation Canister	357

August 2008

Revision LWT-08E

NAC-LWT

Legal Weight Truck Cask System

SAFETY ANALYSIS REPORT

Volume 2 of 2

Docket No. 71-9225

NAC INTERNATIONAL

Atlanta Corporate Headquarters: 3930 East Jones Bridge Road, Norcross, Georgia 30092 USA
Phone 770-447-1144, Fax 770-447-1797, www.nacintl.com

List of Effective Pages

LIST OF EFFECTIVE PAGES

Chapter 1

1-i thru 1-iv ..... Revision LWT-08A
1-1 thru 1-5 ..... Revision LWT-08A
1.1-1 thru 1.1-3 ..... Revision LWT-08E
1.2-1 thru 1.2-49 ..... Revision LWT-08A
1.3-1 ..... Revision 38
1.4-1 ..... Revision 38
1.5-1 ..... Revision 38

76 drawings in the
Chapter 1 List of Drawings

Chapter 1 Appendices 1-A
through 1-G

Chapter 2

2-i thru 2-xxiv ..... Revision LWT-08A
2-1 ..... Revision 38
2.1.1-1 thru 2.1.1-2 ..... Revision 38
2.1.2-1 thru 2.1.2-3 ..... Revision 38
2.1.3-1 thru 2.1.3-8 ..... Revision 38
2.2.1-1 thru 2.2.1-3 ..... Revision 38
2.3-1 ..... Revision 38
2.3.1-1 thru 2.3.1-13 ..... Revision 38
2.4-1 ..... Revision 38
2.4.1-1 ..... Revision 38
2.4.2-1 ..... Revision 38
2.4.3-1 ..... Revision 38
2.4.4-1 ..... Revision 38
2.4.5-1 ..... Revision 38
2.4.6-1 ..... Revision 38
2.5.1-1 thru 2.5.1-11 ..... Revision 38
2.5.2-1 thru 2.5.2-17 ..... Revision 38
2.6.1-1 thru 2.6.1-7 ..... Revision 38
2.6.2-1 thru 2.6.2-7 ..... Revision 38
2.6.3-1 ..... Revision 38
2.6.4-1 ..... Revision 38
2.6.5-1 thru 2.6.5-2 ..... Revision 38
2.6.6-1 ..... Revision 38
2.6.7-1 thru 2.6.7-136 ..... Revision 38
2.6.8-1 ..... Revision 38
2.6.9-1 ..... Revision 38
2.6.10-1 thru 2.6.10-15 ..... Revision 38
2.6.11-1 thru 2.6.11-12 ..... Revision 38
2.6.12-1 thru 2.6.12-91 ... Revision LWT-08A
2.7-1 ..... Revision 38
2.7.1-1 thru 2.7.1-117 ..... Revision 38
2.7.2-1 thru 2.7.2-23 ..... Revision 38
2.7.3-1 thru 2.7.3-5 ..... Revision 38
2.7.4-1 ..... Revision 38
2.7.5-1 thru 2.7.5-5 ..... Revision 38
2.7.6-1 thru 2.7.6-4 ..... Revision 38
2.7.7-1 thru 2.7.7-70 ..... Revision 38
2.8-1 ..... Revision 38
2.9-1 thru 2.9-13 ..... Revision 38
2.10.1-1 thru 2.10.1-3 ..... Revision 38
2.10.2-1 thru 2.10.2-49 ..... Revision 38
2.10.3-1 thru 2.10.3-18 ..... Revision 38
2.10.4-1 thru 2.10.4-11 ..... Revision 38
2.10.5-1 ..... Revision 38
2.10.6-1 thru 2.10.6-19 ..... Revision 38
2.10.7-1 thru 2.10.7-66 ..... Revision 38
2.10.8-1 thru 2.10.8-67 ..... Revision 38
2.10.9-1 thru 2.10.9-9 ..... Revision 38
2.10.10-1 thru 2.10.10-97 ..... Revision 38
2.10.11-1 thru 2.10.11-10 ..... Revision 38
2.10.12-1 thru 2.10.12-31 ..... Revision 38
2.10.13-1 thru 2.10.13-17 ..... Revision 38
2.10.14-1 thru 2.10.14-38 ..... Revision 38
2.10.15-1 thru 2.10.15-10 ..... Revision 38

LIST OF EFFECTIVE PAGES (Continued)

LIST OF EFFECTIVE PAGES (Continued)

Chapter 5

Table of Contents

List of Figures

List of Figures (continued)

List of Figures (continued)

List of Figures (continued)

List of Tables

List of Tables (continued)

List of Tables (continued)

List of Tables (continued)

List of Tables (continued)

List of Tables (continued)

5.1 Discussion and Results

The NAC-LWT cask is designed for the safe transport of spent nuclear fuel from various commercial nuclear installations and research reactors.

5.1.1 NAC-LWT Contents

The following contents constitute the design basis for transport in the NAC-LWT cask:

- one Westinghouse 15 × 15 Pressurized Water Reactor (PWR) assembly
- up to 25 PWR rods
- up to two General Electric 7 × 7 Boiling Water Reactor (BWR) assemblies
- fifteen intact metallic fuel rods or six failed metallic fuel rods
- up to 42 Materials Test Reactor (MTR) research reactor fuel elements
- up to 140 TRIGA fuel elements or up to 560 TRIGA fuel cluster rods
- up to 25 PWR or BWR UO_2 fueled high burnup (up to 80,000 MWd/MTU) rods
- up to 16 PWR MOX or UO_2 rods in any combination (up to 62,500 MWd/MTHM)
- up to 42 DIDO research reactor fuel assemblies
- two General Atomics (GA) Irradiated Fuel Material (IFM) Fuel Handling Units
- up to 300 TPBARs (of which two can be prefailed)
- up to 55 TPBARs segmented during PIE and associated segmentation debris
- up to 700 PULSTAR fuel elements (intact or damaged)
- up to 42 spiral fuel assemblies
- up to 42 MOATA plate bundles

The 25 high burnup PWR and BWR rods may be transported in three configurations: 1) a maximum of 25 intact fuel rods loaded in the rod holder; 2) a maximum of 25 fuel rods with up to 14 damaged fuel rods or rod fragments loaded in the rod holder; and 3) a maximum of 25 intact fuel rods housed in a fuel assembly lattice within the NAC-LWT PWR basket. The fuel assembly lattice may be irradiated up to an equivalent burnup of 80,000 MWd/MTU.

The metallic fuel consists of a single rod of uranium metal clad with aluminum. The intact metallic fuel rods are placed into a transport canister that will hold five intact rods. The cask can hold three transport canisters for a total of 15 intact metallic fuel rods. In the event the metallic fuel has failed or is suspected of having failed, each fuel rod is sealed in its own container. The failed metallic fuel is loaded into either one of the three holes in the metallic fuel basket or into one of the six openings in the failed metallic fuel basket.

MTR research reactor fuel elements are typically 33 to 57 inches long, including lower nozzle and upper handle. The fuel plates typically consist of U-Al, U_3O_8-Al, or USi-Al clad with aluminum. The fuel plates are held in a parallel arrangement with two thick aluminum slotted pieces to form a fuel element. Standard fuel elements have between 10 and 23 fuel plates. The active fuel region is typically 22.75 inches in height, and the fuel meat is typically 0.023-inch thick. The highly enriched uranium (HEU) fuel has been analyzed conservatively with an enrichment of 90 wt % ^{235}U and fuel loading per element up to 380 g ^{235}U, with a separate analysis performed to accommodate up to 460 g ^{235}U. The design basis fuel parameters are provided in Table 5.1.1-1. The fuel characteristics are presented in Table 5.1.1-2. The dose rates produced from the design basis 470 g ^{235}U and 640 g ^{235}U LEU and 380 g ^{235}U MEU MTR fuel are bounded by the HEU MTR design basis fuel. Therefore, a mixed loading of LEU, MEU and HEU MTR fuel elements are also bounded by a full HEU MTR fuel element loading.

The source term characteristics of the design basis PWR fuel assembly, BWR fuel assembly, metallic rods, 25 PWR rods, 16 PWR MOX rods, and MTR fuels are given in Table 5.1.1-3. The design basis PWR and BWR fuels require two years of cooling after discharge to meet the neutron and gamma source, and decay heat limits of the cask. The MOX rods require 90 days of cooling. The design basis metallic fuel requires one year cooling. The design basis MTR fuel requires a variable number of years cooling, after discharge, to meet the decay heat limits of the cask. Loading configurations must conform to the limits stated in Section 7.1.5.

DIDO research reactor fuel elements typically consist of U-Al, U_3O_8-Al, or U_3Si_2-Al that is aluminum clad. The fuel elements are held in a concentric arrangement inside an outer aluminum cylinder to form a fuel assembly. Fuel assemblies have 4 fuel elements. The active fuel region is typically 23.6 inches in height, and the fuel meat is typically 0.026 inch thick. The highly enriched uranium (HEU) fuel has been analyzed with a minimum enrichment of 90 wt % ^{235}U and fuel loading per assembly up to 190 g ^{235}U. Low enriched (LEU) and medium enriched (MEU) assemblies are evaluated at 190 g ^{235}U with minimum enrichments of 19 and 40 wt % ^{235}U, respectively. The design basis fuel parameters are provided in Table 5.1.1-1. The fuel characteristics are presented in Table 5.1.1-2. As discussed in Section 5, the dose rates produced from the design basis LEU and MEU DIDO fuel are bounded by the HEU DIDO design basis fuel. Therefore, a mixed loading of LEU, MEU and HEU DIDO fuel assemblies is also bounded by a full HEU DIDO fuel assembly loading.

Two GA IFM Fuel Handling Units (packages) are intended for a single shipment in the NAC-LWT. The first package is composed of Reduced-Enrichment Research and Test Reactor (RERTR) type fuel, which is an Incoloy clad TRIGA fuel. The second is composed of High-Temperature Gas-Cooled Reactor (HTGR) type fuel. Each set of IFM is packaged into stainless

steel weld-encapsulated primary and secondary enclosures. Design basis fuel parameters are summarized in Table 5.1.1-1, with fuel characteristics presented in Table 5.1.1-2. Design basis source terms are provided in Table 5.1.1-3. NAC-LWT combined dose rates for GA IFM are bounded by the dose rates for PWR fuel shown in Table 5.1.1-4 through Table 5.1.1-6.

An inventory of up to 300 production TPBARs (of which two can be prefailed) is intended for multiple shipments in the NAC-LWT. A separate content condition is for the transport of up to 55 segmented TPBARs and associated segmentation debris from PIE contained in a waste container. Each TPBAR is a Type 316 stainless steel rod with a 0.381-inch outer diameter and a 0.336-inch inner diameter and a post-irradiation length of approximately 154 inches. Tritium is produced by irradiation of ^{6}Li. Design basis fuel parameters are summarized in Table 5.1.1-1 with characteristics presented in Table 5.1.1-2. Design basis source terms are provided in Table 5.1.1-3. NAC-LWT dose rates for the payloads of up to 300 production TPBARs in a consolidation canister, or up to 55 segmented TPBARs in the waste container, are bounded by the dose rates for PWR fuel shown in Table 5.1.1-4 through Table 5.1.1-6.

Source terms for the high burnup PWR and BWR rods are developed using the SCALE SAS2H code package. Cask dose rates are evaluated using the SCALE SAS1 shielding analysis sequence. Results presented in Section 5.3.8 give the required cool time for PWR and BWR rods as a function of burnup for up to 25 intact fuel rods loaded in the NAC-LWT rod holder. The results presented in Sections 5.3.11 and 5.3.12 demonstrate that dose rate limits are met for the shipment of fuel rods in an irradiated fuel assembly lattice and damaged fuel rods in a rod holder, respectively.

Source terms for the 62,500 MWd/MTHM MOX rods, and the UO_2 rods evaluated in the same section, are developed using the SCALE 5.0 SAS2H code package. Source terms were conservatively calculated for a 70,000 MWd/MTHM burnup. Cask dose rates are evaluated using the MCNP5 Monte Carlo code. Results presented in Section 5.3.18 require the MOX and UO_2 rods to be cooled 90 days prior to shipment (low quality, power grade, MOX fuel requires 120 days to meet heat load limits, but produces dose rates below limits at 90 days).

As can be seen from Table 5.1.1-3, the PWR fuel assembly has the largest source terms and was used as the design basis fuel for shielding analysis of PWR and BWR fuel in the NAC-LWT presented in this section. The metallic fuel shielding analysis is presented in Section 5.3.3. Metallic fuel is shipped with the neutron shield drained and the analysis reflects this. The MTR fuel shielding analysis is presented in Section 5.3.4. The design basis source terms for 25 PWR rods at 60,000 MWd/MTU are well below the design basis PWR fuel assembly. However, the self shielding of 25 PWR rods is less than the 204 rod design basis PWR fuel assembly. Thus, a shielding evaluation of 25 design basis PWR rods is presented in Section 5.3.5. Similarly, the

self-shielding for either the 25 high burnup PWR or BWR rods at 80,000 MWd/MTU is lower than that of the design basis assemblies. Shielding evaluations for these rods are presented in Sections 5.3.8, 5.3.11 and 5.3.12.

The transport of up to 140 TRIGA fuel elements is evaluated in Section 5.3.6. TRIGA fuel is a solid metal hydride, U-ZrH and may be high enriched (70%), or low enriched (20%). The fuel clad is either aluminum or stainless steel. TRIGA fuel is fabricated in several configurations, as described in Section 1.2.3.1, that vary in weight, active fuel length and overall length. The typical fuel element length and weight is 28.3 inches and 8.82 pounds. The fuel follower control rod element (FFCR) establishes the upper bound weight (13.2 pounds) and length (approximately 45 inches). These elements can only be loaded in the top module of the TRIGA fuel basket. The design basis TRIGA fuel parameters are presented in Table 5.1.1-1 and Table 5.1.1-2. Source term characteristics are presented in Table 5.1.1-3. Cooling time for TRIGA fuel is variable, down to a minimum of 90 days, based on the time required for the decay heat to reach 7.5 watts.

In addition, the transport of TRIGA fuel cluster rods is evaluated in Section 5.3.7. These rods are obtained from the disassembly of the 5×5 (25 rod) arrays comprising the cluster-type TRIGA fuel as shown in Figure 1.2-6. Only the shipment of the fuel cluster rods is analyzed here; no other activated components of the TRIGA cluster assembly are considered for shipment in this analysis. The TRIGA fuel cluster rod is considered to contain a maximum design-basis fuel mass of 452 g of U-ZrH with an H to Zr ratio of 1.6 and a total uranium mass fraction of 10%. The fuel is highly enriched (93 wt. % ^{235}U). The rods are clad in Incoloy 800 and contain upper and lower stainless steel end plugs with a mass of approximately 60.5 g each. For shipment, each rod is placed inside an aluminum tube (ID 0.625 in, OD 0.750 in), with 16 rods occupying each LWT basket opening for a total of up to 112 rods per basket or 560 rods per cask.

The basis for the dose rate evaluation of the TRIGA fuel cluster rods is a source term and one-dimensional shielding analysis in which the minimum cooling time required for the dose rates produced by the TRIGA fuel cluster rods to fall below the dose rates produced by the design basis TRIGA fuel elements. Cooling time results are determined at a large number of fuel burnup values (at approximately every 2.5% increment in ^{235}U depletion).

PULSTAR fuel elements are zirconium alloy-clad UO_2 pellets with a physical design characteristic as listed in Table 5.1.1-1 and Table 5.1.1-2. PULSTAR fuel assemblies are a 5×5 rectangular array of elements surrounded by a zirconium alloy box, with aluminum upper and lower fittings. The element pitch is nominally 0.524 × 0.606 inch. PULSTAR fuel elements are analyzed at a loading of 32 grams ^{235}U per element, an initial enrichment of 6 wt % ^{235}U, and 45% ^{235}U burnup. For conservatism, a cool time of one year from discharge is employed in the

shielding analysis; a cool time of at least 1.5 years is required to meet the basket cell heat load limit of 30 W. Source term characteristics are presented in Table 5.1.1-3

Spiral fuel assemblies typically consist of 10 curved plates (also referred to as elements) of metallic U-Al fuel meat that is aluminum clad. The fuel elements are held in a spiral arrangement between an inner and outer aluminum cylinder to form a fuel assembly. The active fuel region is typically 60.325 cm in height, and the fuel meat is typically 0.061 cm thick. The elements are nominally enriched to 80 wt % ^{235}U and were conservatively evaluated at 75 wt % ^{235}U. Maximum fuel loading per assembly is evaluated at 160 g ^{235}U. The design basis fuel parameters are provided in Table 5.1.1-1. The fuel characteristics are presented in Table 5.1.1-2. Applying MEU DIDO fuel assembly minimum cool time curves, which are based on a 40 wt % ^{235}U enriched 190 g ^{235}U fuel assembly, to the spiral fuel elements produces source terms that are bounded by the DIDO MEU fuel. Given similar basket designs, the dose rates produced by the spiral fuel elements are bounded by the MEU DIDO evaluation set.

MOATA fuel bundles consist of a maximum of 14 flat MTR type fuel plates. The fuel plates are composed of a metallic U-Al fuel meat that is aluminum clad. The fuel elements are held in place with aluminum outer plates and pins through the top and bottom of the plate stack in their shipment configuration. The plates are held in a typical MTR plate (12 plates per assembly) with a comb side plate configuration during reactor operations. The active fuel region is typically 58.4 cm in height, and the fuel meat is typically 0.1016-cm thick. The elements are nominally enriched to 90 wt % ^{235}U and were conservatively evaluated at 80 wt % ^{235}U. Maximum fuel loading per plate is evaluated at 25 g ^{235}U (nominal loading is 22 g ^{235}U). The design basis fuel parameters are provided in Table 5.1.1-1. The fuel characteristics are presented in Table 5.1.1-2. The gamma radiation source for the 14 fuel plate bundle is approximately 2% of the DIDO MEU assembly. Since the basket designs are similar, the dose rates produced by the plate bundle are bounded by the MEU DIDO evaluation set.

The shield materials are selected and arranged to minimize cask weight while maintaining overall shield effectiveness. Lead and steel are chosen as effective gamma radiation shields, and a water tank on the outside of the cask is provided to efficiently moderate and absorb the neutron radiation.

The total neutron and gamma dose rates calculated for the normal operations conditions are shown in Table 5.1.1-4. Note that the maximum dose rate is on the cask lid surfaces at the top end of the cask and does not exceed the design limit of 200 mrem/hour for the surface of the cask. The 10 CFR 71 limits of 10 mrem/hour at two meters from the cask surface and the design limit of 200 mrem/hour on the cask surface are met. Table 5.1.1-4 contains the total dose rates for the hypothetical accident conditions. These dose rates are well under the 49 CFR 173 limit of

1000 mrem/hour at one meter from the cask surface. The dose rates for the lead slump accident are shown in Table 5.1.1-5. These dose rates show that even with the lead slumped, the hypothetical accident dose rate limits have not been exceeded and the cask is safe for transport.

The cask surface fuel centerline normal operations and hypothetical accident dose rates calculated include neutrons and gammas originating from the fuel, neutrons and gammas scattered from the ground and secondary gammas resulting from neutron capture in the neutron shield. All of the other dose locations also include the contribution from the ^{60}Co in the end-fittings.

Table 5.1.1-1 Type, Form, Quantity and Potential Sources of Design Basis Fuel

Fuel Type	-	PWR, Westinghouse 15 × 15
	-	3.7 wt % ^{235}U maximum initial enrichment
	-	35,000 MWd/MTU maximum burnup
	-	2.5 kW per assembly maximum decay heat
	-	2 years (or more) decay time after reactor discharge
Fuel Form	-	Intact assemblies
Quantity	-	1 design basis fuel assembly
Source of Fuel	-	Commercial PWR nuclear power reactors
Transport Index	-	35
Fuel Type	-	BWR, General Electric 7 × 7
	-	4.0 wt % ^{235}U maximum initial enrichment
	-	30,000 MWd/MTU maximum burnup
	-	1.1 kW per assembly maximum decay heat, 2.2 kW per cask for 2 assemblies
	-	2 years (or more) decay time after reactor discharge
Fuel Form	-	Intact assemblies
Quantity	-	2 design basis fuel assemblies
Source of Fuel	-	Commercial BWR nuclear power reactors
Transport Index	-	35
Fuel Type	-	High Burnup PWR or BWR rods
	-	5.0 wt % maximum ^{235}U initial enrichment
	-	80,000 MWd/MTU maximum average burnup
	-	2.3 kW /cask maximum decay heat
	-	Minimum cool time dependent on burnup (See Table 5.3.8-29)
Fuel Form	-	Intact rods in a fuel assembly lattice or rod holder and intact rods with up to 14 fuel rods classified as damaged in a rod holder
Quantity	-	Up to 25
Source of Fuel	-	Commercial PWR or BWR nuclear power reactor
Transport Index	-	36 (intact rods) 28 (intact rods in a fuel assembly lattice) 37 (intact rods with 14 rods classified as damaged)
Fuel Type	-	Uranium metal fuel rods
	-	Natural wt % ^{235}U
	-	1,600 MWd/MTU maximum burnup
	-	0.0357 kW per sound rod maximum decay heat, 0.54 kW per cask for 15 sound fuel rods
	-	1 year (or more) decay time after reactor discharge
Fuel Form	-	Intact or encapsulated failed fuel rods
Quantity	-	15 design basis fuel rods, or 6 design basis failed fuel rods
Source of Fuel	-	Research reactors
Transport Index	-	25

Table 5.1.1-1 Type, Form, Quantity and Potential Sources of Design Basis Fuel (cont'd)

Fuel Type	-	Material Test Reactor (MTR) Fuel Elements
	-	HEU: 90 wt % ^{235}U, Maximum burnup variable up to 660,000 MWd/MTU for 380 g ^{235}U and 577,500 MWd/MTU for 460 g ^{235}U
	-	MEU: 40 wt % ^{235}U, Maximum burnup variable up to 293,300 MWd/MTU for 380 g ^{235}U
	-	LEU: 19 wt % ^{235}U, Maximum burnup variable up to 139,300 MWd/MTU for 470 g ^{235}U and 640 g ^{235}U
	-	210 W per basket decay heat
	-	Variable cool time down to 90 days using the procedure in Section 7.1.5
Fuel Form	-	Intact aluminum clad parallel plates
Quantity	-	Up to 42 fuel elements
Source of Fuel	-	Research and Material Test Reactors
Transport Index	-	45
Fuel Type	-	TRIGA Fuel Element
	-	20 to 70 wt % ^{235}U
	-	80% ^{235}U depletion (approximately 151 GWd/MTU for LEU fuel and 460 GWd/MTU HEU fuel)
	-	7.5 watts per element decay heat
	-	Variable cool time down to 90 days
Fuel Form	-	Aluminum or stainless steel (304) clad rods, intact, failed or as debris
Quantity	-	Up to 140 fuel elements
Source of Fuel	-	Test, Research and Isotope Reactors
Transport Index	-	25
Fuel Type	-	TRIGA Fuel Cluster Rods
	-	93 wt % ^{235}U
	-	80% ^{235}U depletion (approximately 600 GWd/MTU)
	-	1.875 watts per rod decay heat
	-	Variable cool time down to 90 days
Fuel Form	-	Incoloy 800 clad rods, intact, failed or as debris
Quantity	-	Up to 560 fuel rods
Source of Fuel	-	Test, Research and Isotope Reactors
Transport Index	-	25
Fuel Type	-	DIDO Fuel Assemblies
	-	HEU: 90 wt % ^{235}U, Maximum burnup variable up to 577,460 MWd/MTU or 70% ^{235}U depletion
	-	MEU: 40 wt % ^{235}U, Maximum burnup variable up to 256,650 MWd/MTU or 70% ^{235}U depletion
	-	LEU: 19 wt % ^{235}U, Maximum burnup variable up to 121,910 MWd/MTU or 70% ^{235}U depletion
	-	175 or 126 W per basket decay heat
	-	Variable cool time down to 180 days using the procedure in Section 7.1.4

Table 5.1.1-1 Type, Form, Quantity and Potential Sources of Design Basis Fuel (cont'd)

Fuel Form	-	Intact aluminum clad concentric fuel tubes
Quantity	-	Up to 42 fuel assemblies
Source of Fuel	-	Research Reactors
Transport Index	-	40.1
Fuel Type	-	General Atomics (GA) Irradiated Fuel Material (IFM)
	-	RERTR (see activity inventory in Table 5.3.10-1)
	-	HTGR (see activity inventory in Table 5.3.10-1)
	-	<13.05 W
	-	Transport after 1/1/96
Fuel Form	-	RERTR: 13 intact TRIGA elements, 7 sectioned elements
	-	HTGR: Spherical loose fuel particles, cylindrical fuel rods, 2 fuel pebbles
Quantity	-	1 Fuel Handling Unit holding RERTR IFM and 1 Fuel Handling Unit holding HTGR IFM
Source of Fuel	-	Research reactors, commercial LWR reactors
Transport Index	-	<1
Maximum Activity	-	3403 Ci
Material Type	-	Tritium Producing Burnable Absorber Rods (TPBARs)
	-	3.35 W/TPBARs; 1.005 kW total[1]
	-	30 days minimum cool time
Material Form	-	Type 316 stainless steel clad TPBARs
Quantity	-	Up to 300 TPBARs (of which two can be prefailed)
Source of Material	-	Commercial LWR reactors
Transport Index	-	22
Maximum Activity	-	12,800 Ci/TPBAR; 3,840,000 Ci total[1]
Material Type	-	Tritium Producing Burnable Poison Rods (TPBARs)
	-	2.31 W/TPBAR, 127 W total
	-	90 days
Material Form	-	Type 316 stainless steel clad TPBARs segmented for PIE
Quantity	-	Up to 55 segmented TPBARs
Source of Material	-	Commercial LWRs
Transport Index	-	22[2]
Maximum Activity	-	12,000 Ci/TPBAR, 665,500 Ci total

[1] Conservatively calculated for 30-day minimum cooling time. Actual minimum cooling period for thermal requirements is 90 days.
[2] Conservatively applied 300 TPBAR shipment transport index.
[3] Conservatively evaluated at a one-year cool time and 38 watts per basket cell.

Table 5.1.1-1 Type, Form, Quantity and Potential Sources of Design Basis Fuel (cont'd)

Fuel Type	-	PULSTAR Fuel Elements
	-	6 wt % ^{235}U
	-	32 grams ^{235}U per element
	-	45% ^{235}U depletion (burnup)
	-	210 W per basket decay heat (30 watts per basket cell) × 4 = 840W
		Minimum cool time from discharge of 1.5 years[3]
Fuel Form	-	Intact assemblies; intact elements in fuel rod insert; canned intact or failed elements
Quantity	-	Up to 700 elements (25 elements per cell)
Sources of Fuel	-	Research reactors
Transport Index	-	25
Fuel Type	-	Spiral Fuel Assemblies
	-	75 wt % ^{235}U, maximum burnup variable up to 70% ^{235}U depletion
	-	18 W per assembly , 126 W per basket (at given cool time and burnup limits, maximum heat load is 15.7 W per assembly or 110 W per basket)
		Variable cool time down to 270 days using the procedure in Section 7.1.4 for 18 W DIDO MEU fuel
Fuel Form	-	Intact aluminum clad fuel plates within concentric aluminum inner and outer shells
Quantity	-	Up to 42 fuel assemblies
Sources of Fuel	-	Research reactors
Transport Index	-	40.1 (applied bounding MEU DIDO limit)
Fuel Type	-	MOATA Plate Bundles
	-	80 wt % ^{235}U, maximum burnup variable up to a 30,000 MWd/MTU or 4.1% ^{235}U depletion
Fuel Form	-	Intact aluminum-clad fuel plates
Quantity	-	Up to 42 bundles
Sources of Fuel	-	Research reactors
Transport Index	-	40.1 (applied bounding MEU DIDO limit)
Fuel Type	-	PWR MOX or UO_2 rods (including up to 9 BPRAs)
	-	5.0 wt % maximum ^{235}U initial enrichment for UO_2 rods 7.0 wt % fissile Pu for MOX rods
	-	62,500 MWd/MTHM maximum average burnup
	-	2.3 kW/cask maximum decay heat
	-	Minimum cool time 90 days (120 days for Power Grade MOX)
Fuel Form	-	Undamaged rods in a rod holder
Quantity	-	Up to 16 (any combination of UO_2 or MOX) fuel rods plus up to 9 BPRAs
Source of Fuel	-	Commercial PWR nuclear power reactor
Transport Index	-	28

Table 5.1.1-2 Design Basis Fuel for Shielding Evaluation

Parameter	PWR	BWR	Metallic	MTR (HEU)	MTR (MEU)	MTR (LEU)	DIDO
Assembly Array	15 × 15	7 × 7	N/A	Parallel Plates	Parallel Plates	Parallel Plates	Fuel Tubes
Assembly or Element Weight (lbs)	1650	750	1805 (15 rods)	13.0 (max)	13.0 (max)	13.0 (max)	15.0 (max)
Assembly/Element/Rod Length (in)	162	176	120.5	25.23[5]	26.14[5]	26.14[5]	24.6
Active Fuel Length (in)	144	144	120.0	24.80	25.59	25.59	23.6
No. Rods per Assembly	204	49	N/A	N/A	N/A	N/A	N/A
No. of Plates per Element	N/A	N/A	N/A	23	23	23	4
Fuel Rod Diameter/Plate Thickness (in)	0.422	0.563	1.36	0.050	0.050	0.050	0.059
Clad Material	Zr-4	Zr-4	Al	Al	Al	Al	Al
Clad Thickness (in)	0.0243	0.032	0.080	0.0150	0.0150	0.0150	0.0167
Pellet Diameter/Meat Thickness (in)	0.3659	0.487	1.36	0.020	0.020	0.020	0.026
Fuel Material	UO_2	UO_2	U metal	U_3O_8-Al; U-Al; or U_3Si_2-Al	U_3O_8-Al; U-Al; or U_3Si_2-Al	U_3O_8-Al; U-Al; oor U_3Si_2-Al	U_3O_8-Al; U-Al; or U_3Si_2-Al
Percent Theoretical Density	95	95	100	N/A	N/A	N/A	N/A
Enrichment (wt % ^{235}U)	3.7	4.0	Natural	90[8]	40[8]	19[8]	90 (HEU) 400 (MEU) 199 (LEU)
Maximum Average Burnup (MWd/MTU)	35,000	30,000	1,600	Variable up to 660,000[2,9]	Variable up to 293,300[2]	Variable up to 139,300[2]	Variable up to 577,460 (HEU) 256,650 (MEU) 121,910 (LEU)
Minimum Cool Time	2 Years	2 Years	1 Year	Variable down to 90 days[2]	Variable down to 90 days[2]	Variable down to 90 days[2]	Variable down to 180 days[10]
U Weight (kg/assembly)	475	198	N/A	N/A	N/A	N/A	N/A
U Weight (kg/element)	N/A	N/A	54.5	0.422 0.511	0.950	2.4737 3.3684	0.2111 (HEU) 0.4750 (MEU) 1.0000 (LEU)
UO_2 Weight (kg/assembly)	538.9	224.3	N/A	N/A	N/A	N/A	N/A

Notes:

1. Up to 2 of the PWR rods may have a maximum average burnup of 65,000 MWd/MTU.
2. Variable cool time down to 90 days using the procedure in Section 7.1.4.
3. Design Basis normal condition source term is for ACPR fuel with 86,100 MWd/MTU (50% ^{235}U depletion) and accident condition source term is for FLIP-LEU-II with 151,100 MWd/MTU (80% ^{235}U depletion).
4. Detailed fuel data is presented in Tables 1.2-1 and 6.2.5-1. The values presented here are the physical values for the bounding source terms of the ACPR and FLIP-LEU-II fuel types.
5. For MTR fuel assemblies, which are cut to remove non-fuel bearing hardware prior to transport, a nominal 0.28 inch of non-fuel hardware will remain above and below the active fuel region to allow for fuel handling operations
6. Minimum cool time varies with burnup such that maximum decay heat is 1.875 watts/rod.
7. Varies with burnup – see Table 5.3.8-29.
8. For the shielding evaluation, lower values are conservatively assumed.
9. Maximum burnup of 660,000 MWd/MTU for 380 g ^{235}U and 577,500 MWd/MTU for 460 g ^{235}U.
10. Variable cool time down to 180 days using the procedure in Section 7.1.4.

Table 5.1.1-2 Design Basis Fuel for Shielding Evaluation (continued)

Parameter	PWR Rods	High B/U PWR Rods	High B/U BWR Rods	PWR MOX/UO_2 Rods	TRIGA[4]	TRIGA Fuel Cluster Rods	TPBARs
Assembly Array	N/A	N/A	N/A	N/A	N/A	N/A	N/A
Assembly or Element Weight (lbs)	N/A	N/A	N/A	N/A	8.82 (nominal) 13.2 (max)		2.655
Assembly/Element/Rod Length (in)	162	162	176.1	162	45	31.0	153.035 (pre-irradiation)
Active Fuel Length (in)	144	150	150	153.5	15	22.5	N/A
No. Rods per Assembly per Shipment	25	25	25	16	1	1	300 Production or 55 Segmented
No. of Plates per Element	N/A	N/A	N/A	N/A	N/A	N/A	N/A
Fuel Rod Diameter/Plate Thickness (in)	0.422	0.440	0.570 (7×7) 0.4961 (other)	0.440	1.478	0.542	0.381
Clad Material	Zr-4	Zr-4	Zr-2	Zirc Alloy	304SS	Incoloy 800	316 SS
Clad Thickness (in)	0.242	0.026	0.036 (7×7) 0.0343 (other)	0.026	0.02	0.016	0.0225
Pellet Diameter/Meat Thickness (in)	0.3659	0.3805	0.4900 (7×7) 0.4213 (other)	0.3805	1.435 (max)	0.510	N/A
Fuel Material	UO2	UO2	UO2	UO_2 – PuO_2/ UO_2	U-ZrH	U-ZrH	N/A
Percent Theoretical Density	97	95	95	95	95	95	N/A
Enrichment (wt % ^{235}U)	5.0	5.0	5.0	5.0 (UO_2) 7.0 fissile Pu (MOX))	20	93.3	N/A
Maximum Average Burnup (MWd/MTHM)	60,000[1]	80,000	60,000 – 80,000	62,500	ACPR 86,100 (50% ^{235}U)[3] FLIP-LEU-II 151,100 (80% ^{235}U)[3]	Variable up to 600,000	N/A
Minimum Cool Time	150 days	150 days	Varies with burnup[7]	90 days (Power Grade MOX – 120 days)	ACPR 231 days FLIP-LEU-II 908 days	Varies with burnup[6]	30 days for production TPBAR; 90 days for PIE TPBAR
U Weight (kg/assembly)	58.2	65.6	108.8 (7×7) 91.3 (other)	N/A	N/A	N/A	N/A
HM Weight (kg/element)	N/A	N/A	N/A	2.63[11]	ACPR 0.280 FLIP-LEU-II 0.824	0.0452	N/A
UO_2 Weight (kg/assembly)	66.0	66.0	74.5	N/A	N/A	N/A	N/A

Notes:
1. Up to 2 of the PWR rods may have a maximum average burnup of 65,000 MWd/MTU.
2. Variable cool time down to 90 days using the procedure in Section 7.1.4.
3. Design Basis normal condition source term is for ACPR fuel with 86,100 MWd/MTU (50% ^{235}U depletion) and accident condition source term is for FLIP-LEU-II with 151,100 MWd/MTU (80% ^{235}U depletion).
4. Detailed fuel data is presented in Tables 1.2-1 and 6.2.5-1. The values presented here are the physical values for the bounding source terms of the ACPR and FLIP-LEU-II fuel types.
5. For MTR fuel assemblies, which are cut to remove nonfuel-bearing hardware prior to transport, a nominal 0.28 inch of nonfuel hardware will remain above and below the active fuel region to allow for fuel handling operations.
6. Minimum cool time varies with burnup such that maximum decay heat is 1.875 watts/rod.
7. Varies with burnup – see Table 5.3.8-29.
8. For the shielding evaluation, lower values are conservatively assumed.
9. Maximum burnup of 660,000 MWd/MTU for 380 g ^{235}U and 577,500 MWd/MTU for 460 g ^{235}U.
10. Variable cool time down to 180 days using the procedure in Section 7.1.4.
11. Heavy metal weight per rod.

Table 5.1.1-2 Design Basis Fuel for Shielding Evaluation (continued)

Parameter	GA IFM RERTR	GA IFM HTGR	PULSTAR Fuel	Spiral Fuel Assembly	MOATA Plate Bundle
Assembly Array	N/A	N/A	5×5	Spiral Plates	Parallel Plates
Assembly or Element Weight (lbs)	23.73	23.52	45 (assembly); 1.3 (element)	7.9	13.6[12]
Assembly/Element/Rod Length (in)	29.92	N/A	38 (assembly) 26.2 (element)	63.5 cm	58.4 cm[13]
Active Fuel Length (in)	22.05	N/A	24.1	60.325 cm	58.4 cm
No. Rods per Assembly	13 intact; 7 sectioned	N/A	25	N/A	N/A
No. of Plates per Element	N/A	N/A	N/A	10	Maximum 14
Fuel Rod Diameter/Plate Thickness (in)	0.543	N/A	0.47	0.147 cm	0.203 cm
Clad Material	Incoloy	N/A	Zirconium alloy	Al	Al
Clad Thickness (in)	0.031	N/A	0.0185	0.043 cm	N/A
Pellet Diameter/Meat Thickness (in)	0.512	N/A	0.423	0.061 cm	0.1016 cm
Fuel Material	U-ZrH	UC_2; UCO; UO_2; $(Th,U)C_2$; or $(Th,U)O_2$	UO_2	U-Al	U-Al
Percent Theoretical Density	N/A	N/A	94.9% (nominal); 99.5% (analyzed)	N/A	N/A
Enrichment (wt % ^{235}U)	19.7	93.15 (maximum)	6	75	80
Maximum Average Burnup (MWd/MTU)	N/A	N/A	45	70% ^{235}U depletion	30,000 MWd/MTU 4.1% ^{235}U depletion
Minimum Cool Time	None	None	1.0 Year	see MEU DIDO	10 yr
U Weight (kg/assembly)	8.49	0.45	13.33	0.213[14]	0.4375[15]
U Weight (kg/element)	0.42	N/A	0.53	0.0213[16]	0.03125[17]
UO_2 Weight (kg/assembly)	N/A	N/A	15.13	N/A	N/A

Notes: (cont'd)

12. For 14-fuel plate bundle.
13. Not available for in-core configuration. Analysis input restricted to active fuel length.
14. Based on a 160 g ^{235}U fissile material load and listed enrichment.
15. Based on fuel mass per plate multiplied by 14 plates.
16. Based on 10 plates per assembly.
17. Based on 25 g ^{235}U and listed enrichment.

Table 5.1.1-3 Nuclear and Thermal Source Parameters

Payload	Decay Heat (kW)	Gamma Source (MeV/sec) (g/sec)	Neutron Source (n/sec)	Top End-Fitting (g/sec)	Bottom End-Fitting (g/sec)
1 PWR Assembly	2.5	7.78E+15 1.27E+16	2.21E+08	1.49E+13	1.25E+13
2 BWR Assemblies	2.2	6.35E+15 1.04E+16	1.34E+08	1.16E+12	2.78E+12
15 Sound Metallic Fuel Rods[2]	0.532	8.81E+14 4.37E+15	1.61E+05	N/A	N/A
6 Failed Metallic Fuel Rods[1]	0.03	3.53E+14 1.75E+15	6.44E+04	N/A	N/A
42 HEU MTR Elements[3,9]	1.26	-- 7.42E+15	1.40E+08	N/A[15]	N/A[15]
42 MEU MTR Elements[3,8]	1.26	-- 7.86E+15	2.88E+07	N/A[15]	N/A[15]
42 LEU MTR Elements[3,8,14]	1.26	-- 7.51E+15	3.96E+07	N/A[15]	N/A[15]
42 DIDO Assemblies[10]	1.05	-- 6.07E+15	9.73E+04	N/A	N/A
25 PWR Rods[2]	1.41	3.47E+15 8.39E+15	1.40E+08	N/A	N/A
TRIGA (140 Elements)[7] Normal Condition	1.05	2.15E+15[4] 6.52E+15[4]	1.57E+06	Note 6	Note 6
TRIGA (140 Elements)[7] Accident Condition	1.05	2.60E+15[5] 5.97E+15[5]	1.06E+08	Note 6	Note 6
General Atomics Irradiated Fuel Material	0.013	-- 3.429E+13	1.279E+04	Note 11	Note 11
300 Production TPBARs	1.005	5.030E+15 6.681E+15	N/A	N/A	N/A
55 PIE TPBARs	0.127	– 7.54E+14	N/A	N/A	N/A
PULSTAR Fuel	1.05[12]	6.206E+15	2.115E+07	N/A	N/A
Spiral Fuel Assembly[13]	0.756	— 1.07E +14	4.54E+3	N/A	N/A
MOATA Plate Bundle	0.042	— 2.2E +12	< 1E+3	N/A	N/A
16 PWR MOX Rods	2.3	1.14E+16	1.17E+09	N/A	N/A

Notes:

1. Gamma and neutron source terms conservatively calculated based on design basis sound metallic fuel rods.
2. 23 rods with 60,000 MWd/MTU burnup and two rods with 65,000 MWd/MTU burnup. Source terms as a function of cool time for the 80,000 MWd/MTU burnup PWR and BWR rods are presented in Section 5.3.8.
3. Bounding values of the gamma and neutron source terms presented for 30W uniform loading for 80% burnup.
4. Based on TRIGA ACPR fuel (86,100 MWd/MTU, 231 days cooling, 50% ^{235}U depletion).
5. Based on TRIGA FLIP-LEU-II fuel (151,100 MWd/MTU, 908 days cooling, 80% ^{235}U depletion).
6. Total hardware gamma is 7.64E+14 gamma/second for ACPR fuel (86,100 MWd/MTU, 231 days cooling, 50% ^{235}U depletion).
7. TRIGA Fuel Elements are the bounding values used in dose determination for TRIGA cluster rods fuel type.
8. Moderator used is light water, H_20.
9. Moderator used is heavy water, D_20.
10. Bounding values of the gamma and neutron source terms presented for 25W uniform loading for 70% burnup HEU fuel.
11. Hardware activation, including end-fitting sources, for the TRIGA elements included in the total gamma source for GA IFM.
12. Cool time required to meet 30 watt per cell heat load limit is 1.5 years.
13. Based on 18 W per assembly heat load.
14. Fuel source represents maximum magnitude gamma source obtained from the 470 g ^{235}U analysis, and the maximum neutron source obtained from the 640 g ^{235}U analysis.
15. A maximum 100 grams of cadmium may be included as part of the MTR fuel element or plate construction. Activation of the cadmium produces no significant source per Section 5.3.4.

Table 5.1.1-4 Combined Dose Rates for Normal Operations Conditions

(1 PWR assembly, 35,000 MWd/MTU, 2-year cool time)

Location	Detector I.D.	Radiation	Normal Dose Rate (mrem/hr)
Radial at 2 m from personnel barrier, Fuel midplane	1	Neutron	1.25
		Secondary Gamma	0.18
		Primary Gamma	6.71
		TOTAL	8.14
Radial surface, Fuel midplane	2	Neutron	6.53
		Secondary Gamma	1.37
		Primary Gamma	43.44
		TOTAL	51.34
Bottom surface, Axial centerline	3	Neutron	0.33
		Primary Gamma	35.51
		End-fitting Gamma	17.02
		TOTAL	52.86
Bottom at 2 m from impact limiter, Axial centerline	4	Neutron	0.03
		Primary Gamma	2.19
		End-fitting Gamma	0.79
		TOTAL	3.01
Top surface, Axial centerline	5	Neutron	0.12
		Primary Gamma	54.17
		End-fitting Gamma	41.45
		TOTAL	95.74
Top at 2 m from impact limiter, Axial centerline	6	Neutron	0.01
		Primary Gamma	3.82
		End-fitting Gamma	2.17
		TOTAL	6.00
Top at Cab	7	Neutron	0.00135
		Primary Gamma	0.47
		End-fitting Gamma	0.25
		TOTAL	0.72

Table 5.1.1-5 Hypothetical Accident – Loss of Shielding Materials

(1 PWR assembly, 35,000 MWd/MTU, 2-year cool time)

Location	Detector I.D.	Radiation	Normal Dose Rate (mrem/hr)
Radial surface, Fuel midplane, With neutron shield	8	Neutron	6.53
		Secondary Gamma	1.37
		Primary Gamma	43.44
		TOTAL	51.34
Radial surface, Fuel midplane, Without neutron shield	9	Neutron	177.13
		Secondary Gamma	0.39
		Primary Gamma	75.00
		TOTAL	252.52
Radial at 1 m from surface, Fuel midplane, Without neutron shield	10	Neutron	50.93
		Secondary Gamma	1.52
		Primary Gamma	54.59
		TOTAL	107.04

Table 5.1.1-6 Hypothetical Accident –Lead Slump

Location	Detector I.D.	Radiation	Normal Dose Rate (mrem/hr)
Radial at 1 m from surface, PWR top end-fitting	11	End-fitting Gamma	3.60
		TOTAL	3.60
Radial at 1 m from surface, PWR top end-fitting	12	End-fitting Gamma	1.31
		TOTAL	1.31
Radial at 1 m from surface, PWR top end-fitting	13	End-fitting Gamma	0.80
		TOTAL	0.80
Radial at 1 m from surface, PWR bottom end-fitting	14	End-fitting Gamma	0.01
		TOTAL	0.01
Radial at 1 m from surface, PWR bottom end-fitting	15	End-fitting Gamma	0.35
		TOTAL	0.35
Radial at 1 m from surface, PWR bottom end-fitting	16	End-fitting Gamma	1.48
		TOTAL	1.48
Radial at 1 m from surface, BWR bottom end-fitting	17	End-fitting Gamma	0.10
		TOTAL	0.10
Radial at 1 m from surface, BWR bottom end-fitting	18	End-fitting Gamma	0.54
		TOTAL	0.54
Radial at 1 m from surface, BWR bottom end-fitting	19	End-fitting Gamma	0.84
		TOTAL	0.84

5.3.18 PWR MOX Rod Fuel Configuration

Results of a shielding and decay heat analysis for up to 16 high burnup PWR MOX fuel rods are presented in this section. The rods are conservatively evaluated with burnups up to 70 GWd/MTHM. MOX rods are limited in this licensing application to a burnup of 62.5 GWd/MTHM. The results are presented in terms of the cool time required for 16 rods to meet the cask total payload heat load limit of 2.3 kW established for PWR rods (including MOX rods). At this cool time, the package surface and 2-meter dose rate are calculated and shown to be below limits.

The shielding analysis is performed using the three-dimensional MCNP transport code. Source terms are generated based on a limiting description of PWR rods using the SCALE 5.0 SAS2H code. The limiting description of a PWR MOX fuel rod bounds MOX rods from all PWR assembly array sizes. Analyses compare various MOX plutonium compositions and the inclusion of UO_2 fuel rods (up to 80 GWd/MTHM burnup) to demonstrate licensing compliance for up to 16 MOX rods or UO_2 rods in any combination.

5.3.18.1 PWR MOX Rod Fuel Source Term

Source Term

Source terms are generated in a manner similar to those of the PWR rods described in Section 5.3.8. The limiting rod description is determined by developing a hybrid fuel rod model, which contains a conservatively bounding heavy metal loading. For a given burnup, the bounding heavy metal mass leads to bounding decay heat and radiation source terms. Fuel rod model parameters are shown in Table 5.3.18-1 in the "SAS2H" column. SAS2H models for the various MOX and UO_2 compositions are then developed based on the cycle parameters shown in Table 5.3.18-2. The rod exposure is conservatively assumed to occur over a typical number of reactor operating cycles: three for the PWR MOX rods. A down time of 60 days between cycles is assumed. Fuel rods are evaluated at an initial enrichment between 2 and 7 wt % ^{235}U for the UO_2 rods and between 2 and 7 wt % fissile plutonium for the four MOX fuel compositions shown in Table 5.3.18-3. Based on these compositions and the range of fissile plutonium contents analyzed, the resulting fractions of uranium and plutonium in the SAS2H fuel mixture are shown in Table 5.3.18-4. A sample SAS2H model for the MOX Services plutonium composition is shown in Figure 5.3.18-1. The SAS2H model adjusts the weight fractions in Table 5.3.18-4 by the modeled theoretical density factor shown in Table 5.3.18-1.

The SCALE 44-group library is employed in the source generation. For use in the MCNP shielding analysis, the gamma and neutron sources are rebinned within ORIGEN-S into the group

structure of the ANSWERS MCBEND code package. Gamma energy lines in this structure better reflect the gamma source lines around 1 MeV than the default energy lines generated by ORIGEN-S.

The amount of validation information on MOX fuel material depletion is limited, with public information restricted to SCALE benchmarks of San Onofre fuel [ORNL/TM-1999/326] with burnups up to 20 GWd/MTHM. To address this concern, calculations generated sources based on a conservative maximum burnup of 70 GWd/MTHM, while requesting a maximum burnup of 62.5 GWd/MTHM. Based on SAS2H results, this conservatism produces approximately 5% increases in heat load and gamma source (for gammas capable of penetrating the cask shields), and an increase of 20-25% in neutron source. As neutron source is most likely to be affected by uncertainties in the code libraries for MOX fuel at high burnups, a significant margin is built into the analysis. Further, the fuel rod evaluated in the NAC-LWT cask shielding calculations is based on a hybrid that contains approximately 2.6 kg of HM, while PWR fuel rods range up to 2.4 kg HM. The increased mass is the result of applying a 150-inch fuel height to a CE14×14 fuel rod type that is actually less than 140 inches in active height. The CE14×14 rod radius was chosen as the licensing basis because it is the largest diameter fuel pellet, which, in turn, produces maximum fuel mass per unit length. The increased fuel mass results in an 8% overestimation of total source when compared to the highest mass fuel rod for commercial PWRs (exempting South Texas rods). These conservatisms, in combination with the limited MOX validation information, and information available on benchmarking on SCALE SAS2H for standard and high burnup PWR rods [see ORNL references in Chapter 9], where the primary fissile isotopes in high burnup rods are plutonium (MOX) near end of life, justifies the acceptability of SCALE to generate the required MOX source terms.

Neutron and gamma sources and heat loads are summarized for the various compositions in Table 5.3.18-7. As the fissile plutonium content increases, heat loads increase and neutron source decreases. Minimum cool times required for the fuel rods to reach the maximum allowed heat load of 143.75 W/rod (2.3 kW/16 rods) are included in Table 5.3.18-8. The minimum cool time evaluated in the source term generation was 90 days. Therefore, any results indicating a less than 90-day cool time is permissible are listed as "< 90." The only evaluated material exceeding 90 days as the required cool time is Power Grade (low grade plutonium with a significant quantity of ^{240}Pu and ^{242}Pu). A minimum 120-day cool time for the Power Grade material ensures that heat load limits are met. For conservatism, shielding evaluations include the Power Grade material at 90 days' cool time source terms. Neutron and gamma source term spectra for a Power Grade MOX composition at the maximum burnup (70 GWd/MTHM), a 2% fissile plutonium content, and a cool time of 90 days are presented in Table 5.3.18-9 and Table 5.3.18-10, respectively.

The effect of subcritical neutron multiplication is directly computed in the MCNP analysis. As the k_{eff} of a dry transport configuration is extremely low ($k_{eff} < 0.1$), there is no significant subcritical multiplication in the system regardless of material composition. Comparison of k_{eff} as a function of fuel composition is included in Section 5.3.18.3. To simplify the analysis, all shielding results, with the exception of the subcritical multiplication studies, are based on using a standard uranium oxide fuel composition.

Axial Source Profile

The description of the axial source profile for PWR rods is based on bounding axial burnup profiles observed for fuel at much lower burnups. This description is conservative because the higher burned fuel of interest here will have a substantially lower axial peaking factor. The PWR axial source profiles are shown in Figure 5.3.18-2. Values are tabulated in Table 5.3.18-5.

The computed relation between source rate S and burnup B:

$$S = aB^b$$

implies that, in general, the average source rate is not equal to the source rate at the average burnup. The exponent b is determined based on SAS2H analyses of various fuel assemblies at different burnups. A design basis value of 4.22 is used for neutron source rate variation. The design basis exponent for photon source rates is 1.0.

Since SAS2H analyses are conducted at the average assembly burnup, a scale factor is required to relate the assembly average source rate to the source rate at the average burnup:

$$r = \frac{\overline{S}}{S(\overline{B})} = \frac{\int B^b dz}{a\overline{B}^b}$$

With the burnup profile normalized to one, this becomes

$$r = \frac{1}{H}\int B^b dz$$

where H is the height of the fuel region.

The integral is evaluated numerically using the trapezoid rule, and the resulting scale factors are shown in Table 5.3.18-6. Because MCNP normalizes the axial source profile by default, the scale factors are included in the MCNP runs in the tally multiplier cards.

The design basis scale factors were derived from UO_2 SAS2H calculations of source term versus burnup. To validate that the design basis factors are conservative, corresponding MOX factors are generated using SAS2H results. The revised factors are then used to calculate updated

"average source to source at average burnup" values. The results are shown in Table 5.3.18-6 and document that the factors used in the analysis produce conservative dose rates (i.e., the multiplication factor is higher based on the UO_2 derived values). For MOX material, both short (90 days) and long (2 years) cool times were evaluated to demonstrate that while factors increase with cool time, the 1.0 gamma and 4.22 factors for neutron are conservative. Note that for extended cool time, the source magnitude decreases significantly, and the licensing basis for the MOX material is 90 days.

5.3.18.2 MOX Fuel Shielding Model

MCNP three-dimensional shielding analysis allows detailed modeling of the fuel, canister, basket, and cask shield configurations. The fuel rod lattice (5×5 array of tubes containing up to 16 fuel rods) detail is conservatively omitted in the model. The remaining principal canister components and all shielding-related basket and cask body details are explicitly modeled, including the axial extents described by the applicable License Drawings.

The geometric description of a MCNP model is based on the combinatorial geometry system embedded in the code. In this system, bodies such as cylinders and rectangular parallelepipeds, and their logical intersections and unions, are used to describe the extent of material zones.

Source Models

The combination of 16 fuel rods, either UO_2 or MOX fissile material based, are loaded into a 5×5 tube array insert constructed from stainless steel. The insert in turn is located within a canister, placed into the LWT PWR basket insert. The 16 fuel rods are homogenized within the cross-sectional area of the canister internal spacer. No credit is taken for the stainless steel tubes in the fuel rod homogenization. While the array may contain additional material in the form of burnable poison rods (or other non-steel/inconel-based materials), these materials are not included in the homogenization and are not included as a source region as they are considered to have negligible activation when compared to the short cool time fuel source. Axial regions (elevations) are retained for the active fuel region, plenum region, and rod end-caps. The plenum region is modeled as a void for shielding purposes.

To minimize self-shielding, the MCNP fuel rod model has significantly less mass than the fuel rod model used to generate MOX source terms. Fuel rod parameters for this model are shown in Table 5.3.18-1 in the "MCNP" column. This column includes the axial extents of the active fuel, plenum and end-cap regions included in the three-dimensional model.

Also included in the evaluation set is a discrete fuel rod confirmatory model. The discrete fuel rod model validates the adequacy of the homogenized fuel region to provide accurate dose estimates. The discrete rod model is identical to the homogenized fuel model with the exception

of replacing the homogenized fuel region by an array that contains an exterior (outer layer) placement of 16 fuel rods rods in the 25 capacity rod holder. The remaining nine locations (interior nine cells of the 5×5 array) are modeled as void.

Canister and Basket Model

The canister model includes the steel internal spacer (represented as a steel box), steel can weldment (including can base, body and lid), the aluminum basket insert, and the aluminum PWR basket body. No credit is taken for canister internal aluminum shunts.

MCNP NAC-LWT Model

The three-dimensional model of the NAC-LWT cask is based on the following features.

Normal conditions:

- Radial neutron shield and shield shell
- Aluminum impact limiters with 0.5 g/cm^3 density (calculated based on the impact limiter weight and dimensions) and diameter equal to the neutron shield shell diameter

Accident conditions:

- Removal of radial neutron shield and shield shell
- Loss of upper and lower impact limiters

Common to both the normal and accident conditions models is a 0.1374 cm gap between the lead outer diameter and the cask outer shell. During normal conditions, the gap volume is represented as a radial uniform gap between the lead outer radius and the cask outer shell. During accident calculations, the lead is assumed to slump to form radial, top and bottom gaps. All three slump configurations are conservatively included in a single model. The use of an axial spacer prevents the fuel region source from approaching the top of the radial lead shield. Only the axial separation by the spacer is accounted for in the analysis. No credit is taken for spacer material.

Detailed model parameters used in creating the three-dimensional model are taken directly from the License Drawings. Elevations associated with the three-dimensional features are established with respect to the center bottom of the NAC-LWT cask cavity for the MCNP combinatorial model. The three-dimensional NAC-LWT models are shown in Figure 5.3.18-3 and Figure 5.3.18-4. A sample input file is provided in Figure 5.3.18-5. The sample input provides a complete source description used in the response function benchmark analysis.

Shield Regional Densities

Based on the homogenization described previously, fuel region material densities are shown in Table 5.3.18-11. The fuel region densities were conservatively calculated based on a minimum material mass fuel rod (1.62 kg HM, see Table 5.3.18-1) versus the maximum mass rod used in the source generation. Material compositions for the basket and cask materials are shown in Table 5.3.18-12.

5.3.18.3 MOX Fuel Shielding Evaluation

Calculational Methods

The shielding evaluation is performed using MCNP.

The MCNP shielding model described in Section 5.3.18.2 is utilized with the source terms described in Section 5.3.18.1 to estimate the dose rate profiles at various distances from the side, top and bottom of the cask for both normal and accident conditions. The method of solution is continuous energy Monte Carlo with a Monte Carlo based weight window generator to accelerate code convergence. Weight window and problem convergence is verified by the 10 statistical checks performed by MCNP. Radial or axial biasing is performed depending on the desired dose location.

Significant validation literature is available for MCNP as it is an industry standard tool for spent fuel cask evaluations. Available literature covers a range of shielding penetration problems ranging from slab geometry to spent fuel cask geometries. Confirmatory calculations against other validated shielding codes (SCALE and MCBEND) on NAC casks have further validated the use of MCNP for shielding evaluations.

MCNP Flux-to-Dose Conversion Factors

The ANSI/ANS 6.1.1-1977 flux-to-dose rate conversion factors are employed in the MCNP analysis. The ANSI/ANS neutron and gamma dose conversion factors are shown in Table 5.3.11-23 and Table 5.3.11-24.

Dose Response Method

In order to avoid the significant effort required to prepare and execute shielding runs for each material composition, a unique device is employed that permits the ready calculation of dose rates at a given location by use of a dose rate response function.

In general, the response method for dose rates is based on the decomposition of the respective quantity into a weighted sum over energy. A dose rate response function, $R_{tpg}(\vec{r})$, gives the response at a point $\vec{r}$ to source particles arising from energy group g from a fuel assembly

placed in basket position p. In practice, the spatial parameter, $\vec{r}$, is represented as discrete subsurface detectors on the cask surface. In addition, responses for detector average and maximum values may also be represented using this notation. In the case of a dose rate response, the response $R_{tpg}(\vec{r})$ is a scalar quantity.

For a given cask loading, the total response to radiation of type t with source spectrum f_{tp} is given by:

$$C_t(\vec{r}) = \sum_p \sum_{g'} R_{tpg'}(\vec{r}) f_{tpg'} w_{tp}$$

where:

$C_t(\vec{r})$ is the dose rate response to radiation of type t at location $\vec{r}$.

$R_{tpg'}(\vec{r})$ is the response to radiation of type t with energy g' emanating from position p at location $\vec{r}$.

$f_{tpg'}$ is the source strength for radiation of type t in group g' emanating from position p.

w_{tp} is a weight factor applied to radiation of type t in position p and is used to scale hardware source spectra that are provided on a per unit mass basis by the effective mass of activated material present in the source region.

The source type t refers to fuel gamma (Fg), fuel neutron (Fn), fuel n-gamma (Ng) and fuel hardware (Hw) source regions.

Response functions for the cask (generated using MCNP) solve the particle transport equations at each relevant spectrum line using Monte Carlo techniques. The results of the individual spectrum lines are then statistically summed. For the homogenized source region, a single source region exists for each source type, essentially eliminating the position portion of the summation. Response functions for a mixed load require two sets of runs (one for MOX, the other for UO_2 sources).

The response function method was used to calculate all relevant licensing dose rates, including normal condition cask surface, 1 meter, 2 meter, and accident condition 1 meter dose rates. The licensing dose rates were based on a 198 response function set for radial and axial normal and accident condition models. No interpolation was done on a precalculated data set. Further response functions were generated as part of the auxiliary calculations set (such as mixed payload analysis). Response functions rely on a fixed dose per unit source calculation, irrespective of fuel material compositions. Material substitution studies for the MOX/UO_2 materials have demonstatrated that there is no significant effect of fuel material choice on dose rates. This was expected as deep penetration NAC-LWT cask shielding problems are driven by material interaction within the shields and not within the small diameter payload volume. While MOX materials certainly contain significant differences in isotope cross-sections, within the confines of

the NAC-LWT cask evaluations, the small fissile material mass, the absence of moderator to reduce neutron energy to thermal or epithermal levels for increased material interaction, and the high neutron leakage (large height to diameter ratio) all contribute to the negligible effect of material properties.

To further document the acceptability of the response function approach, additional evaluations are performed comparing the result of the response approach (i.e., multiplication of source spectra by dose response at a given energy line) with a direct solution approach containing the full energy spectrum. The additional comparisons are based on both homogenized source region and the discrete fuel rod models. Discrete rod models allow mixed fuel to be explicitly accounted for. Results of the comparisons are shown in Figure 5.3.18-10 through Figure 5.3.18-12 and demonstrate that the results of the response and direct solutions are equivalent, independent of the source modeling employed (i.e., discrete fuel rods or homogenized). Differences between response method and direct calculation results are associated with significantly higher statistical uncertainties produced by the direct solution approach.

Fuel Material Effects

MCNP results documented in the dose rate section include subcritical neutron multiplication and isotope cross-section effects based on a 4 wt % enriched UO_2 (LEU) fuel description. To investigate potential dose increases due to a higher multiplication factor and isotope cross-sections associated with MOX material, dose rates are compared for a consistent source term of 4 wt % (4 wt % ^{235}U for UO_2 and 4 wt % fissile plutonium for MOX) at 80 GWd/MTHM (note that the burnup compared is above the 70 GWd/MTHM limit for MOX fuel and produces dose rates higher than 10 mrem/hr at 2 meters). Normal condition radial surface average neutron results are compared. As shown in Table 5.3.18-13, the difference between response function runs with UO_2 and direct solution runs with MOX is negligible. Therefore, use of UO_2 material composition runs is appropriate for computing MOX fuel dose rates.

To provide further evidence of the adequacy of the UO_2 material composition model to apply to mixed loading of UO_2 and MOX fuel, a mixed discrete fuel rod model is evaluated. The mixed fuel rod model contains a discrete set of eight UO_2 and eight MOX rods, each with its appropriate source and material definition. The result of the mixed rod analysis (see sample input file in Figure 5.3.18-9) is compared to the average dose result obtained from 16 UO_2 and 16 MOX rod evaluations and to a run containing the source of a mixed payload, but all fuel material defined is UO_2. As shown in Table 5.3.18-14, there is no significant difference between the results of a mixed payload description and that of a UO_2 fuel material. The results also illustrate that the code performs accurately for a mixed payload.

Discrete Fuel Rod Model Comparisons

To validate adequacy of the homogenized fuel model, when fuels rods are discrete volumes placed in a rod array, a comparison analysis is performed between homogenized and discrete rods. The discrete rods are placed into the exterior (outer layer) of the 25-rod array. As shown in Table 5.3.18-15 for a sample 80 GWd/MTHM, 90-day cooled source, the discrete model produces lower dose rates than the homogenized source model. Reduced dose rates are the result of the high-density fuel rod providing more shielding for the now compacted source region than the homogenized source.

Three-Dimensional Dose Rates for MOX Fuel

Dose rates are generated at the bounding 90-day minimum cool time for the various MOX plutonium compositions (and UO_2 fuel) at 2 percent fissile fuel material. Dose summaries for key conditions are listed in Table 5.3.18-16. As indicated by the source term magnitude and bounding heat load, the Power Grade MOX fuel produces bounding dose rates.

A summary of the maximum and average dose rates for the bounding power grade MOX fuel is shown in Table 5.3.18-17. All dose rates are below 10 CFR 71 limits. High uncertainties in the axial results are associated with the difficulty in axial biasing for a cask with a large ratio of length to diameter. Because dose rates in the axial locations are significantly below limits, no attempt is made to reduce the uncertainty in the results.

The axial elevation of the maximum cask surface and 2 meter dose rates are at the active fuel region midplane elevation. The cask surface dose rate profile is shown in Figure 5.3.18-6, with the 2 meter profile plotted in Figure 5.3.18-7. The normal condition maximum radial 2 meter dose rate is 9.2 mrem/hr. Accident condition radial 1 meter dose rates are well below the 1000 mrem/hr limit, with the radial 1 meter dose profile shown in Figure 5.3.18-8. The transport index (TI) for the MOX rod shipments is 28 based on the 1 meter normal condition dose rate.

Table 5.3.18-16 demonstrates that dose rate results for UO_2 (LEU) fuel at 80 GWd/MTHM are bounded by the results for the bounding Power Grade MOX fuel at 70 GWd/MTHM. Therefore, a mixed loading of UO_2 and MOX fuel rods is an acceptable payload for the NAC-LWT cask.

Figure 5.3.18-1 Sample SAS2H Input for PWR MOX Fuel

```
=SAS2H       PARM=(HALT06,SKIPSHIPDATA)
Power Grade, 2% Fissile, 70 GWd/MTHM, 90-150 days cooled
44GROUPNDF5 LATTICECELL
UO2          1 0.9254 811 92235 0.2 92238 99.8 END
PuO2         1 0.0246 811 94238 1 94239 62 94240 22 94241 12 94242 3 END
ZR           2 1.0 620 END
H2O          3 DEN=0.725 1.0 570 END
ARBM-BORMOD 0.725 1 1 0 0 5000 100 3 550.0E-6 570 END
END COMP
SQUAREPITCH 1.473 0.9665 1 3 1.118 2 0.986 0 END
NPIN/ASSM=176 FUELENGTH=389.9 NCYCLE=3 NLIB/CYC=2 PRINTLEVEL=6
LIGH=5 INPLEVEL=2 NUMZONES=4 END
3 1.3589 2 1.4605 3 1.6623 500 5.2039
POWER=19.36 BURN=556.8 DOWN=60 END
POWER=19.36 BURN=556.8 DOWN=60 END
POWER=19.36 BURN=556.8 DOWN=0 END
FE 0.6738 CR 0.1900 NI 0.1150 MN 0.0200 CO 0.0012
END
=ORIGENS
0$$  A4 21 A8 26 A10 51 71  E
1$$  1 1T
COOLING 90 TO 150 DAYS AND FISSION PRODUCT GAMMA REBIN
3$$  21 0 1 28 A33 22 E
54$$  A8 1 E T
35$$  0 T
56$$  0 7 A13 -2 4 3 E
57**  0.0 E T
COOLING 90 TO 150 DAYS AND FISSION PRODUCT GAMMA REBIN
SINGLE REACTOR ASSEMBLY
60** 90 100 110 120 130 140 150
65$$  A4 1 A7 1 A10 1 A25 1 A28 1 A31 1 A46 1 A49 1 A52 1 E
61**  F.00000001
81$$  2 51 26 1 E
82$$  F6
83**  1.40e+7  1.20e+7  1.00e+7  8.00e+6   6.50e+6  5.00e+6
      4.00e+6  3.00e+6  2.50e+6  2.00e+6   1.66e+6  1.44e+6
      1.22e+6  1.00e+6  0.80e+6  0.60e+6   0.40e+6  0.30e+6
      0.20e+6  0.10e+6  0.05e+6  0.02e+6   0.01e+6
84**  1.46e+7  1.36e+7  1.25e+7  1.125e+7  1.00e+7
      8.25e+6  7.00e+6  6.07e+6  4.72e+6   3.68e+6
      2.87e+6  1.74e+6  0.64e+6  0.39e+6   0.11e+6
      6.74e+4  2.48e+4  9.12e+3  2.95e+3   9.61e+2
      3.54e+2  1.66e+2  4.81e+1  1.60e+1   4.00e+0
      1.50e+0  5.50e-1  7.09e-2  1.00e-5   T
56$$ F0  T
END
```

Note: Only the fission product rebin section of the input file is shown. Identical rebins are performed for the actinide and light element sources.

Figure 5.3.18-2 PWR Rods Axial Burnup and Source Profiles

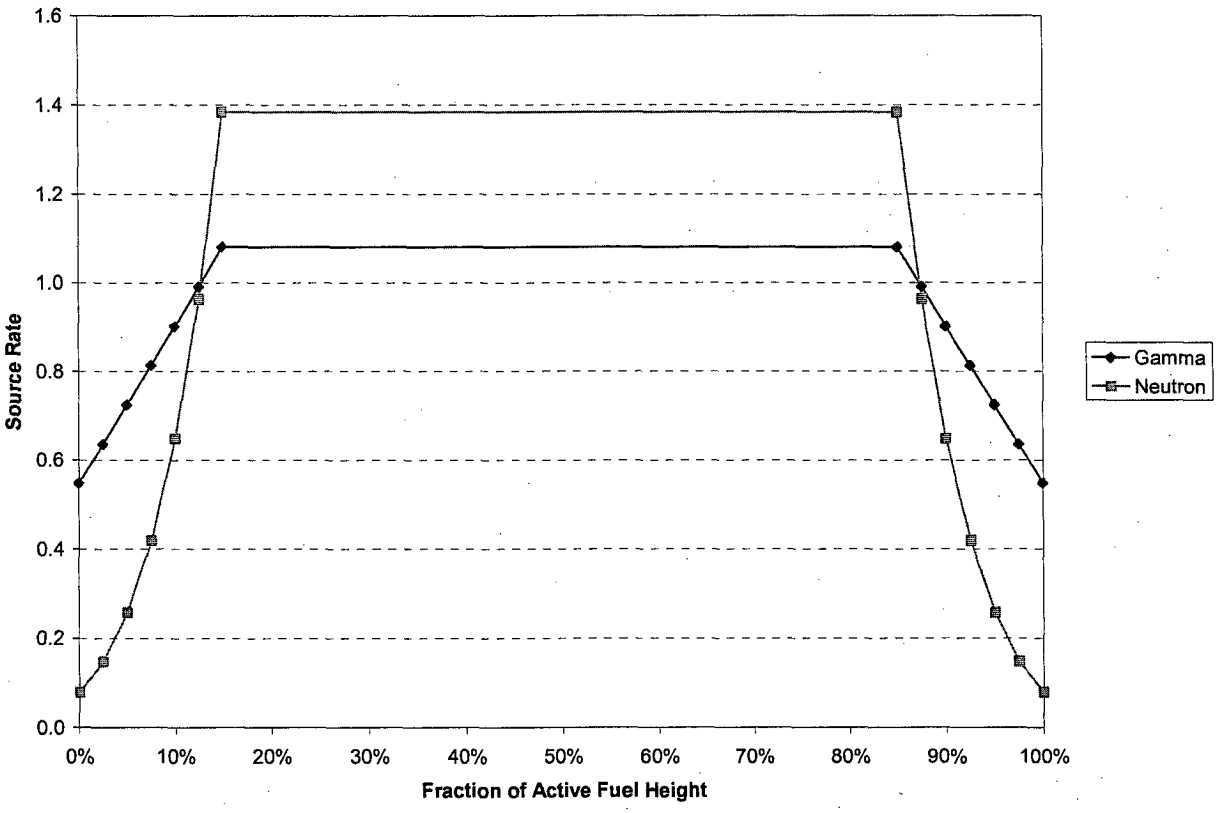

Figure 5.3.18-3 MCNP Model of NAC-LWT with PWR MOX Fuel – Axial Detail

Figure 5.3.18-4 MCNP Model of NAC-LWT with PWR MOX Fuel – Radial Detail

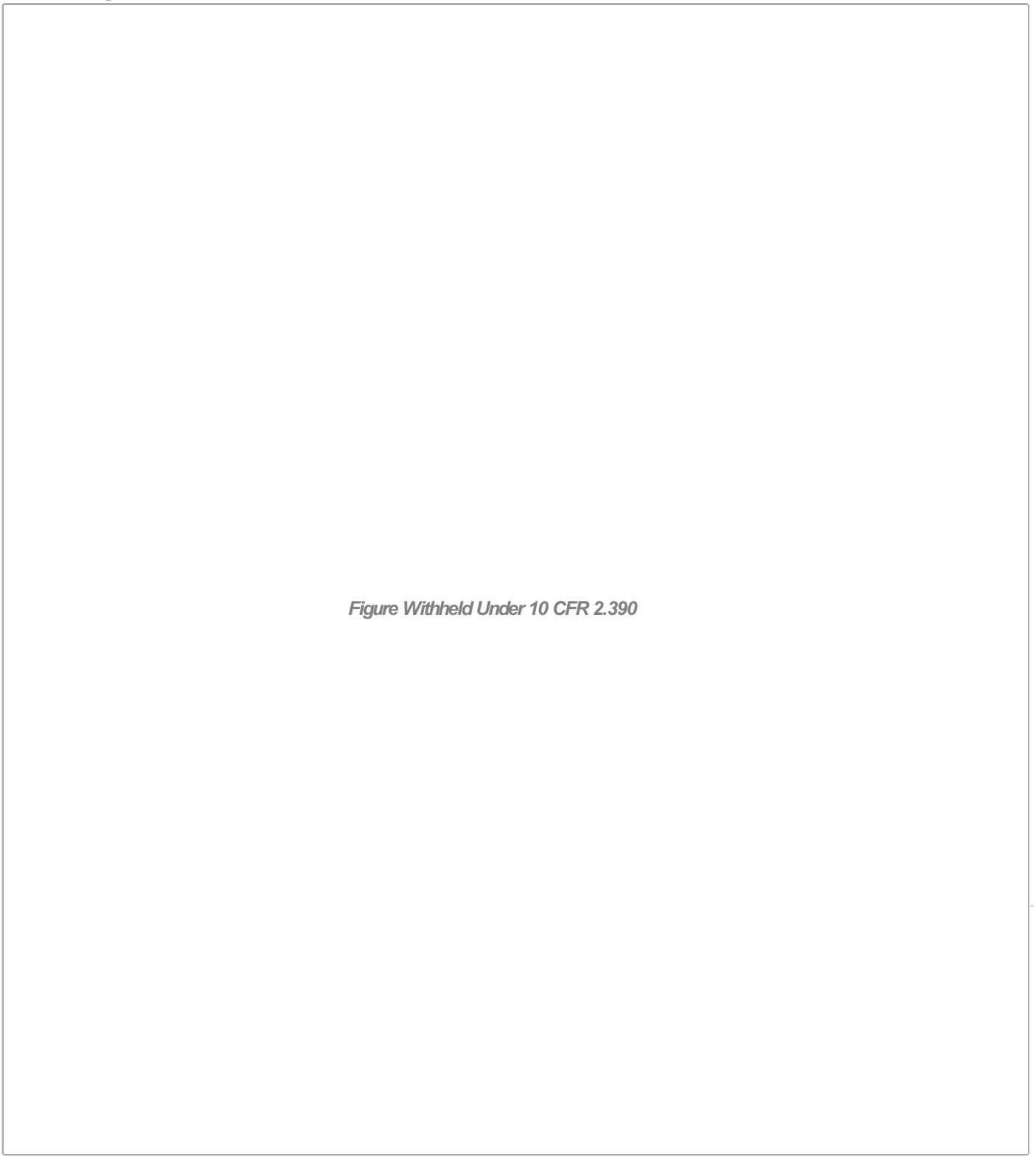

Figure 5.3.18-5 Sample MCNP Input File for PWR MOX Fuel (Response Method Benchmark Case)

```
NAC-LWT Cask - we17_leu_80b40e150d - Normal Transport Conditions
C Radial Biasing - Fuel Gamma Source
C 16 Rod Source & WE17x17 Fuel Homogenization
C Homogenized Rod Cells
1 2 -0.8430 -1  u=6 $ Bottom end cap
2 1 -1.2338 -2 +1 u=6 $ Fuel
3 0         -3 +2 u=6 $ Plenum
4 2 -0.8430 -4 +3 u=6 $ Top end cap
5 0         +4  u=6 $ Void
C Can Weldment Cells
10 0        -10 fill=6 ( 0.0000 0.0000 2.5400 )   u=5 $ Fuel Insert
11 5 -7.9400 -11 +10    u=5 $ Internal Spacer
12 0        -12 +11 +10   u=5 $ Can Weldment void
13 5 -7.9400 -13     u=5 $ Can Weldment base
14 5 -7.9400 -14 +13 +12 +10  u=5 $ Can Weldment body
15 5 -7.9400 -15 +14 +10   u=5 $ Can Weldment flange
16 5 -7.9400 -16 +15    u=5 $ Can Weldment lid
17 0         +16     u=5 $ Outside
C PWR Insert Cells
20 0        -20 fill=5 ( 0.0000 0.0000 1.2700 )   u=4 $ Can Weldment
21 7 -2.7020 -21 +20    u=4 $ PWR Insert Body
22 0         +21 +20    u=4 $ Outside
C PWR Basket Cells
30 0        -30 fill=4 ( 0.0000 0.0000 5.2070 )   u=3 $ PWR Insert
31 0  -32 -31    u=3 $ Offset
32 7 -2.7020 -32 +31 +30   u=3 $ Basket
33 0  +32 +30    u=3 $ Outside
C Cask Cavity Cells
40 0        -40 +41 fill=3   u=2 $ Cavity
41 5 -7.9400 -41     u=2 $ Spacer plate
42 0         +40 +41    u=2 $ Outside
C Cells - LWT Cask Normal Conditions
50 4 -11.344 -53     u=1 $ BotPb
51 0        -52 fill=2    u=1 $ Cavity
52 5 -7.9400 -50 -51 +53   u=1 $ Bottom
53 5 -7.9400 -50 +51 +55 +58 +52 u=1 $ OuterShell
54 5 -7.9400 -54 +57 +52   u=1 $ InnerShellTaper
55 5 -7.9400 -56 +52    u=1 $ InnerShell
56 4 -11.344 -57 +56    u=1 $ Lead
57 4 -11.344 -55 +54 +57   u=1 $ LeadTaper
58 0         -58 +57    u=1 $ LeadGap
59 3 -0.9669 -60 +50    u=1 $ NeutronShield
60 5 -7.9400 -59 +50 +60   u=1 $ NSShell
61 6 -0.4997 -61 +50    u=1 $ UpperLimiter
62 6 -0.4997 -62 +50    u=1 $ LowerLimiter
63 0         -63 +50 +59 +61 +62 u=1 $ Container
64 0         +63     u=1 $ Outside
C Detector Cells - Radial Biasing
100  0  -100  fill=1  $ Surface
150  0  -150  +100  $ SurfaceAzi
200  0  -200  +100  +150  $ 1ft
300  0  -300  +100  +150  +200  $ 1m
400  0  -400  +100  +150  +200  +300  $ 2m
500  0  -500  +100  +150  +200  +300  +400  $ 2m+Convey
600  0  +100  +150  +200  +300  +400  +500  $ Exterior

C Homogenized Rod Surfaces
1 PZ 1.7399    $ Bottom end cap
2 PZ 367.4999    $ Fuel
3 PZ 383.4003    $ Plenum
4 PZ 385.1402    $ Top end cap
C Can Weldment Surfaces
10 RPP -4.5212 4.5212 -4.5212 4.5212 2.5400 425.4500  $ Internal cavity
11 RPP -4.9975 4.9975 -4.9975 4.9975 2.5400 422.2750  $ Internal spacer
12 RPP -6.3500 6.3500 -6.3500 6.3500 2.5400 422.9100  $ Can weldment cavity
13 RPP -6.9850 6.9850 -6.9850 6.9850 0.0000 2.5400  $ Can weldment base
14 RPP -6.9850 6.9850 -6.9850 6.9850 0.0000 422.9100  $ Can weldment body
15 RPP -6.9850 6.9850 -6.9850 6.9850 0.0000 425.4500  $ Can weldment flange
16 RPP -6.9850 6.9850 -6.9850 6.9850 0.0000 426.7200  $ Can weldment lid
C PWR Insert Surfaces
20 RPP -7.2898 7.2898 -7.2898 7.2898 1.2700 427.9900  $ PWR Insert cavity
21 RPP -10.7950 10.7950 -10.7950 10.7950 0.0000 425.4500  $ PWR Insert body
C PWR Basket Surfaces
30 RPP -11.2713 11.2713 -11.2713 11.2713 5.2070 433.1970  $ Internal cavity
31 PZ 5.2070       $ Bottom offset
32 RCC 0.0000 0.0000 0.0000 0.0000 0.0000 415.4170 16.8273 $ Basket walls
C Cask Cavity Surfaces
40 RCC 0.0000 0.0000 0.0000 0.0000 0.0000 452.1199 16.9862 $ Cavity
41 RCC 0.0000 0.0000 438.7850 0.0000 0.0000 0.9525 11.1760 $ Spacer plate
C Surfaces - LWT Cask Normal Conditions
50 RCC 0.0000 0.0000 -26.6700 0.0000 0.0000 507.3650 36.5189 $ Lwt
51 RCC 0.0000 0.0000 -26.6700 0.0000 0.0000 26.6700 36.5189 $ Bottom
52 RCC 0.0000 0.0000 0.0000 0.0000 0.0000 452.1200 16.9863 $ Cavity
53 RCC 0.0000 0.0000 -17.7800 0.0000 0.0000 7.6200 26.3525 $ Bottom gamma shield
54 RCC 0.0000 0.0000 0.0000 0.0000 0.0000 444.5000 20.1740 $ Lead id - taper
55 RCC 0.0000 0.0000 0.0000 0.0000 0.0000 444.5000 31.5976 $ Lead od - taper
56 RCC 0.0000 0.0000 13.8176 0.0000 0.0000 416.8648 18.9103 $ Lead id
57 RCC 0.0000 0.0000 13.8176 0.0000 0.0000 416.8648 33.3271 $ Lead od
58 RCC 0.0000 0.0000 13.8176 0.0000 0.0000 416.8648 33.4645 $ Lead gap
59 RCC 0.0000 0.0000 3.8100 0.0000 0.0000 419.1000 49.8183 $ Neutron shield shell
60 RCC 0.0000 0.0000 5.0800 0.0000 0.0000 416.5600 49.2189 $ Neutron shield
61 RCC 0.0000 0.0000 450.2150 0.0000 0.0000 70.5612 49.8183 $ Upper limiter
62 RCC 0.0000 0.0000 -68.0212 0.0000 0.0000 71.8312 49.8183 $ Lower limiter
```

Figure 5.3.18-5 Sample MCNP Input File for PWR MOX Fuel (Response Method Benchmark Case)

```
63 RCC 0.0000 0.0000 -68.0212 0.0000 0.0000 588.7974 49.8183 $ Container
C Radial Detector DRA (Surface)
100  RCC  0.0000  0.0000  -68.1212  0.0000  0.0000  588.9974  49.9184
101  PZ  -38.6713
102  PZ  -9.2215
103  PZ  20.2284
104  PZ  49.6783
105  PZ  79.1282
106  PZ  108.5780
107  PZ  138.0279
108  PZ  167.4778
109  PZ  196.9276
110  PZ  226.3775
111  PZ  255.8274
112  PZ  285.2772
113  PZ  314.7271
114  PZ  344.1770
115  PZ  373.6269
116  PZ  403.0767
117  PZ  432.5266
118  PZ  461.9765
119  PZ  491.4263
C Radial Detector DRAA (SurfaceAzi)
150  RCC  0.0000  0.0000  211.3775  0.0000  0.0000  30.0000  50.0184
151     PX  0.0000
152  1  PX  0.0000
153  2  PX  0.0000
154  3  PX  0.0000
155  4  PX  0.0000
156  5  PX  0.0000
157  6  PX  0.0000
158  7  PX  0.0000
159  8  PX  0.0000
160     PY  0.0000
161  9  PX  0.0000
162  10  PX  0.0000
163  11  PX  0.0000
164  12  PX  0.0000
165  13  PX  0.0000
166  14  PX  0.0000
167  15  PX  0.0000
168  16  PX  0.0000
C Radial Detector DRB (1ft)
200  RCC  0.0000  0.0000  -98.6012  0.0000  0.0000  649.9574  80.2984
201  PZ  -66.1033
202  PZ  -33.6055
203  PZ  -1.1076
204  PZ  31.3903
205  PZ  63.8882
206  PZ  96.3860
207  PZ  128.8839
208  PZ  161.3818
209  PZ  193.8796
210  PZ  226.3775
211  PZ  258.8754
212  PZ  291.3732
213  PZ  323.8711
214  PZ  356.3690
215  PZ  388.8669
216  PZ  421.3647
217  PZ  453.8626
218  PZ  486.3605
219  PZ  518.8583
C Radial Detector DRC (1m)
300  RCC  0.0000  0.0000  -168.1212  0.0000  0.0000  788.9974  149.8184
301  PZ  -135.2463
302  PZ  -102.3714
303  PZ  -69.4965
304  PZ  -36.6216
305  PZ  -3.7467
306  PZ  29.1282
307  PZ  62.0030
308  PZ  94.8779
309  PZ  127.7528
310  PZ  160.6277
311  PZ  193.5026
312  PZ  226.3775
313  PZ  259.2524
314  PZ  292.1273
315  PZ  325.0022
316  PZ  357.8771
317  PZ  390.7520
318  PZ  423.6269
319  PZ  456.5017
320  PZ  489.3766
321  PZ  522.2515
322  PZ  555.1264
323  PZ  588.0013
C Radial Detector DRD (2m)
400  RCC  0.0000  0.0000  -268.1212  0.0000  0.0000  988.9974  249.8184
401  PZ  -226.9130
402  PZ  -185.7048
403  PZ  -144.4965
404  PZ  -103.2883
405  PZ  -62.0801
406  PZ  -20.8719
```

Figure 5.3.18-5 Sample MCNP Input File for PWR MOX Fuel (Response Method Benchmark Case)

```
407   PZ   20.3364
408   PZ   61.5446
409   PZ   102.7528
410   PZ   143.9611
411   PZ   185.1693
412   PZ   226.3775
413   PZ   267.5857
414   PZ   308.7940
415   PZ   350.0022
416   PZ   391.2104
417   PZ   432.4186
418   PZ   473.6269
419   PZ   514.8351
420   PZ   556.0433
421   PZ   597.2515
422   PZ   638.4598
423   PZ   679.6680
C Radial Detector DRE (2m+Convey)
500   RCC  0.0000  0.0000  -269.1212  0.0000  0.0000  990.9974  321.9200
501   PZ  -227.8296
502   PZ  -186.5381
503   PZ  -145.2465
504   PZ  -103.9550
505   PZ  -62.6634
506   PZ  -21.3719
507   PZ  19.9197
508   PZ  61.2113
509   PZ  102.5028
510   PZ  143.7944
511   PZ  185.0859
512   PZ  226.3775
513   PZ  267.6691
514   PZ  308.9606
515   PZ  350.2522
516   PZ  391.5437
517   PZ  432.8353
518   PZ  474.1269
519   PZ  515.4184
520   PZ  556.7100
521   PZ  598.0015
522   PZ  639.2931
523   PZ  680.5846

C
C Materials List
C
C Homogenized UO2 Fuel
m1     92235 -2.6740E-02
       92238 -6.4177E-01
        8016 -8.9904E-02
       40000 -2.3730E-01
       50000 -3.6238E-03
       26000 -3.0198E-04
       24000 -2.4158E-04
        7014 -1.2079E-04
C Fuel Rod End Cap (Zircaloy)
m2     40000 -9.8225E-01
       50000 -1.5000E-02
       26000 -1.2500E-03
       24000 -1.0000E-03
        7014 -5.0000E-04
C Water/Glycol
m3     1001 -1.03651E-01
       8016 -6.75619E-01
       6000 -2.20730E-01
mt3   lwtr.01
C Lead
m4     82000 -1.0
C Stainless Steel 304
m5     24000 -0.190
       25055 -0.020
       26000 -0.695
       28000 -0.095
C Aluminum (Impact Limiter)
m6     13027 -1.0
C Aluminum (Insert/Basket)
m7     13027 -1.0
phys:p 100 0 0 0 1
C
C Cell Importances
imp:p 1 43r 0
C
C Source Definition - Fuel Gamma
C LEU Basis - 80 GWd/MTHM, 4 wt % Fissile, 150 days cooled
sdef x=d1 y=d2 z=d3 erg=d4 cell=100:51:40:30:20:10:2
si1    -4.5212 4.5212
sp1    0 1
si2    -4.5212 4.5212
sp2    0 1
si3 a 1.7399 10.8839 20.0279 29.1719 38.3159 47.4599 56.6039
      312.6359 321.7799 330.9239 340.0679 349.2119 358.3559 367.4999
sp3 d 0.5470 0.6358 0.7247 0.8135 0.9023 0.9912 1.0800
      1.0800 0.9912 0.9023 0.8135 0.7247 0.6358 0.5470
si4    1.000E-02 2.000E-02 5.000E-02 1.000E-01 2.000E-01 3.000E-01
       4.000E-01 6.000E-01 8.000E-01 1.000E+00 1.220E+00 1.440E+00
       1.660E+00 2.000E+00 2.500E+00 3.000E+00 4.000E+00 5.000E+00
```

Figure 5.3.18-5 Sample MCNP Input File for PWR MOX Fuel (Response Method Benchmark Case)

```
      6.500E+00 8.000E+00 1.000E+01 1.200E+01 1.400E+01
sp4   0.0000E+00 6.5335E+13 8.3523E+13 4.2132E+13 4.2987E+13 1.0861E+13
      8.3438E+12 8.0750E+13 1.7401E+14 2.3085E+13 4.4177E+12 2.6664E+12
      8.9233E+11 3.0024E+11 7.9369E+11 2.1689E+10 1.8203E+09 7.5273E+05
      3.0209E+05 5.9261E+04 1.2582E+04 6.5057E+02 0.0000E+00
mode p
nps 40000000
C
C ANSI/ANS-6.1.1-1977 - Gamma Flux-to-Dose Conversion Factors
C (mrem/hr)/(photons/cm2-sec)
de0   0.01 0.03 0.05 0.07 0.1 0.15 0.2
      0.25 0.3 0.35 0.4 0.45 0.5 0.55
      0.6 0.65 0.7 0.8 1 1.4 1.8
      2.2 2.6 2.8 3.25 3.75 4.25 4.75
      5 5.25 5.75 6.25 6.75 7.5 9
      11 13 15
df0   3.96E-03 5.82E-04 2.90E-04 2.58E-04 2.83E-04 3.79E-04 5.01E-04
      6.31E-04 7.59E-04 8.78E-04 9.85E-04 1.08E-03 1.17E-03 1.27E-03
      1.36E-03 1.44E-03 1.52E-03 1.68E-03 1.98E-03 2.51E-03 2.99E-03
      3.42E-03 3.82E-03 4.01E-03 4.41E-03 4.83E-03 5.23E-03 5.60E-03
      5.80E-03 6.01E-03 6.37E-03 6.74E-03 7.11E-03 7.66E-03 8.77E-03
      1.03E-02 1.18E-02 1.33E-02
C
C Weight Window Generation - Radial
wwg 2 0 0 0 0
wwp:p 5 3 5 0 -1 0
mesh geom=cyl ref=0.0 6.3 193 origin=0.1 0.1 -568
     imesh 6.4 12.2 17.0 18.9 33.3 36.5 49.2 49.8 549.8
     iints 3 1 1 1 5 1 1 1 1
     jmesh 500 541 550 558 568 575 579 964 1020 1049 1089 1589
     jints 1 1 1 1 1 1 1 1 1 1 1 1
     kmesh 1
     kints 1
wwge:p  1e-3 1 20
fc2 Radial Surface Tally
f2:p +100.1
fm2 8.64200E+15
fs2  -101  -102  -103  -104  -105  -106
     -107  -108  -109  -110  -111  -112
     -113  -114  -115  -116  -117  -118
     -119  T
tf2
fc12 Radial SurfaceAzi Tally Q1 (+x+y)
f12:p +150.1
fm12 8.64200E+15
fs12 -151  -160
     +159  +158  +157  +156  +155  +154
     +153  +152  T
sd12 4.7141E+03  2.3571E+03  2.6190E+02  8r  9.4282E+03
tf12
fc22 Radial SurfaceAzi Tally Q2 (-x+y)
f22:p +150.1
fm22 8.64200E+15
fs22 +151  -160
     -168  -167  -166  -165  -164  -163
     -162  -161  T
sd22 4.7141E+03  2.3571E+03  2.6190E+02  8r  9.4282E+03
tf22
fc32 Radial SurfaceAzi Tally Q3 (-x-y)
f32:p +150.1
fm32 8.64200E+15
fs32 +151  +160
     -159  -158  -157  -156  -155  -154
     -153  -152  T
sd32 4.7141E+03  2.3571E+03  2.6190E+02  8r  9.4282E+03
tf32
fc42 Radial SurfaceAzi Tally Q4 (+x-y)
f42:p +150.1
fm42 8.64200E+15
fs42 -151  +160
     +168  +167  +166  +165  +164  +163
     +162  +161  T
sd42 4.7141E+03  2.3571E+03  2.6190E+02  8r  9.4282E+03
tf42
fc52 Radial 1ft Tally
f52:p +200.1
fm52 8.64200E+15
fs52  -201  -202  -203  -204  -205  -206
     -207  -208  -209  -210  -211  -212
     -213  -214  -215  -216  -217  -218
     -219  T
tf52
fc62 Radial 1m Tally
f62:p +300.1
fm62 8.64200E+15
fs62  -301  -302  -303  -304  -305  -306
     -307  -308  -309  -310  -311  -312
     -313  -314  -315  -316  -317  -318
     -319  -320  -321  -322  -323  T
tf62
fc72 Radial 2m Tally
f72:p +400.1
fm72 8.64200E+15
fs72  -401  -402  -403  -404  -405  -406
     -407  -408  -409  -410  -411  -412
     -413  -414  -415  -416  -417  -418
```

Figure 5.3.18-5 Sample MCNP Input File for PWR MOX Fuel (Response Method Benchmark Case)

```
     -419  -420  -421  -422  -423  T
tf72
fc82 Radial 2m+Convey Tally
f82:p +500.1
fm82 8.64200E+15
fs82  -501  -502  -503  -504  -505  -506
     -507  -508  -509  -510  -511  -512
     -513  -514  -515  -516  -517  -518
     -519  -520  -521  -522  -523  T
tf82
C
C Print Control
prdmp -15 -30 1 2
print
C Random Number Generator
rand gen=2 seed=19073486328125 stride=152917 hist=1
C
C Rotation Matrix
C
*TR1 0.0 0.0 0.0 10 100 90 -80 10 90 90 90 0
*TR2 0.0 0.0 0.0 20 110 90 -70 20 90 90 90 0
*TR3 0.0 0.0 0.0 30 120 90 -60 30 90 90 90 0
*TR4 0.0 0.0 0.0 40 130 90 -50 40 90 90 90 0
*TR5 0.0 0.0 0.0 50 140 90 -40 50 90 90 90 0
*TR6 0.0 0.0 0.0 60 150 90 -30 60 90 90 90 0
*TR7 0.0 0.0 0.0 70 160 90 -20 70 90 90 90 0
*TR8 0.0 0.0 0.0 80 170 90 -10 80 90 90 90 0
*TR9 0.0 0.0 0.0 100 190 90 10 100 90 90 90 0
*TR10 0.0 0.0 0.0 110 200 90 20 110 90 90 90 0
*TR11 0.0 0.0 0.0 120 210 90 30 120 90 90 90 0
*TR12 0.0 0.0 0.0 130 220 90 40 130 90 90 90 0
*TR13 0.0 0.0 0.0 140 230 90 50 140 90 90 90 0
*TR14 0.0 0.0 0.0 150 240 90 60 150 90 90 90 0
*TR15 0.0 0.0 0.0 160 250 90 70 160 90 90 90 0
*TR16 0.0 0.0 0.0 170 260 90 80 170 90 90 90 0
```

Figure 5.3.18-6 Normal Condition Axial Surface Dose Rate Profile by Source Type – Power Grade MOX at 70 GWd/MTHM, 2% Fissile Material, and 90 Days Cool Time

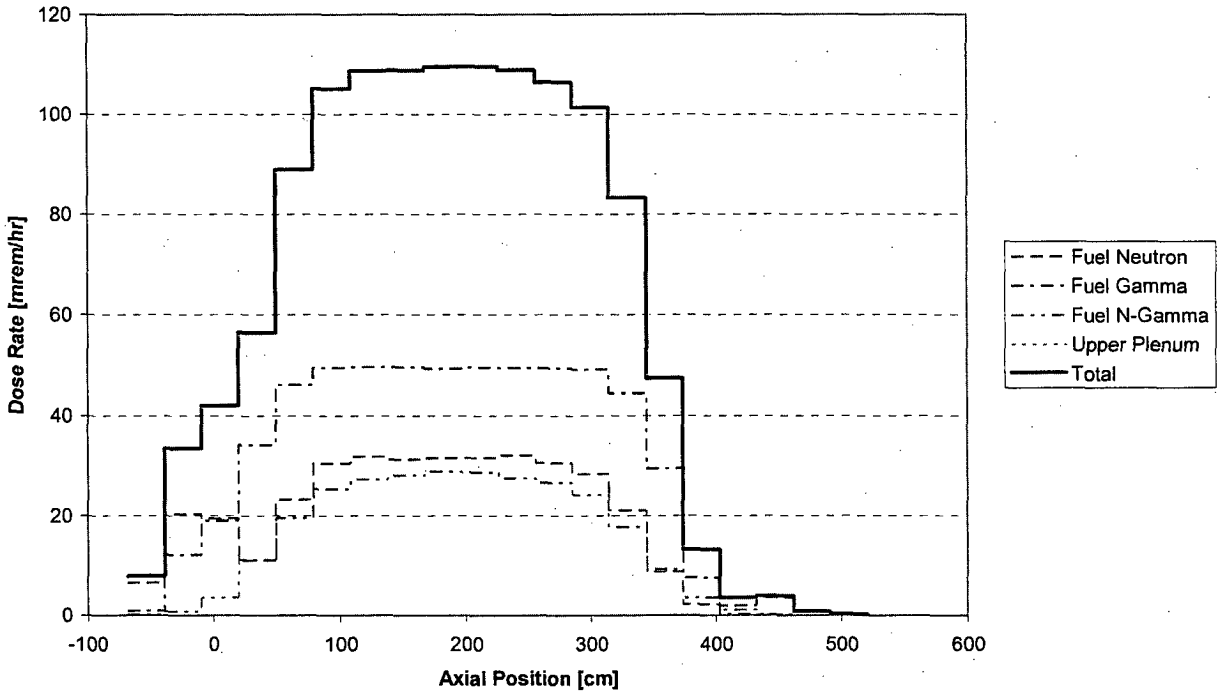

Figure 5.3.18-7 Normal Condition Radial 2m Dose Rate Profile by Source Type – Power Grade MOX at 70 GWd/MTHM, 2% Fissile Material, and 90 Days Cool Time

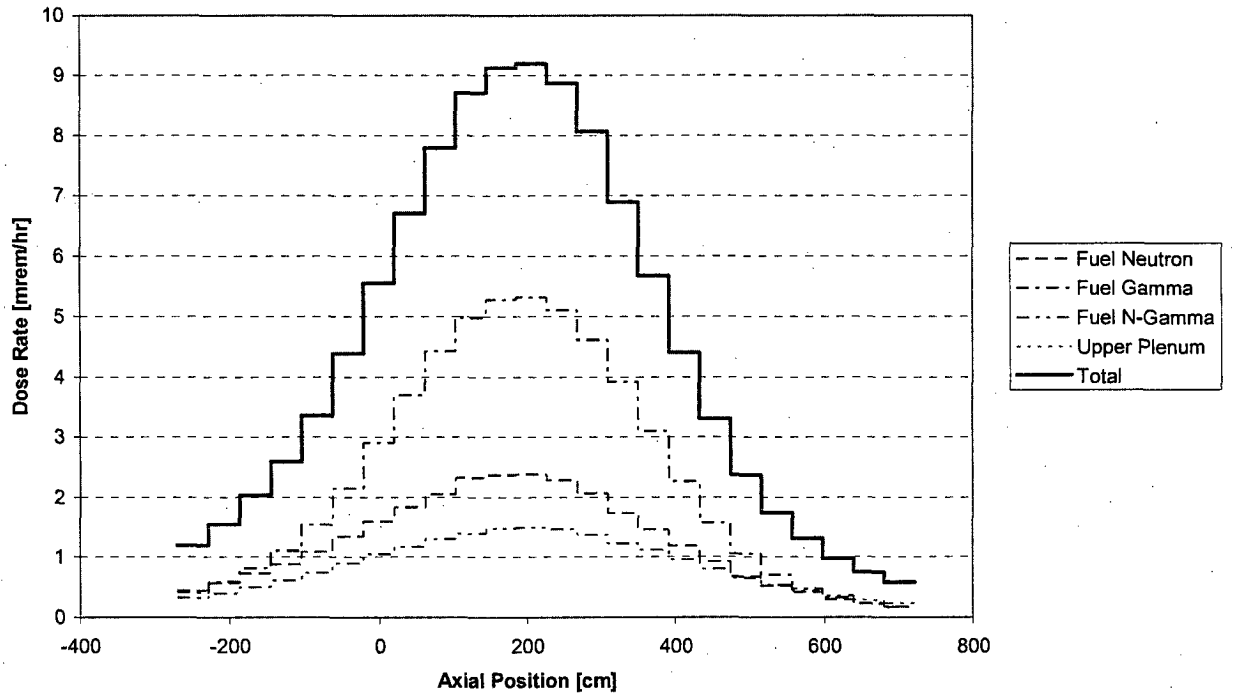

Figure 5.3.18-8 Accident Condition Radial 1m Dose Rate Profile by Source Type – Power Grade MOX at 70 GWd/MTHM, 2% Fissile Material, and 90 Days Cool Time

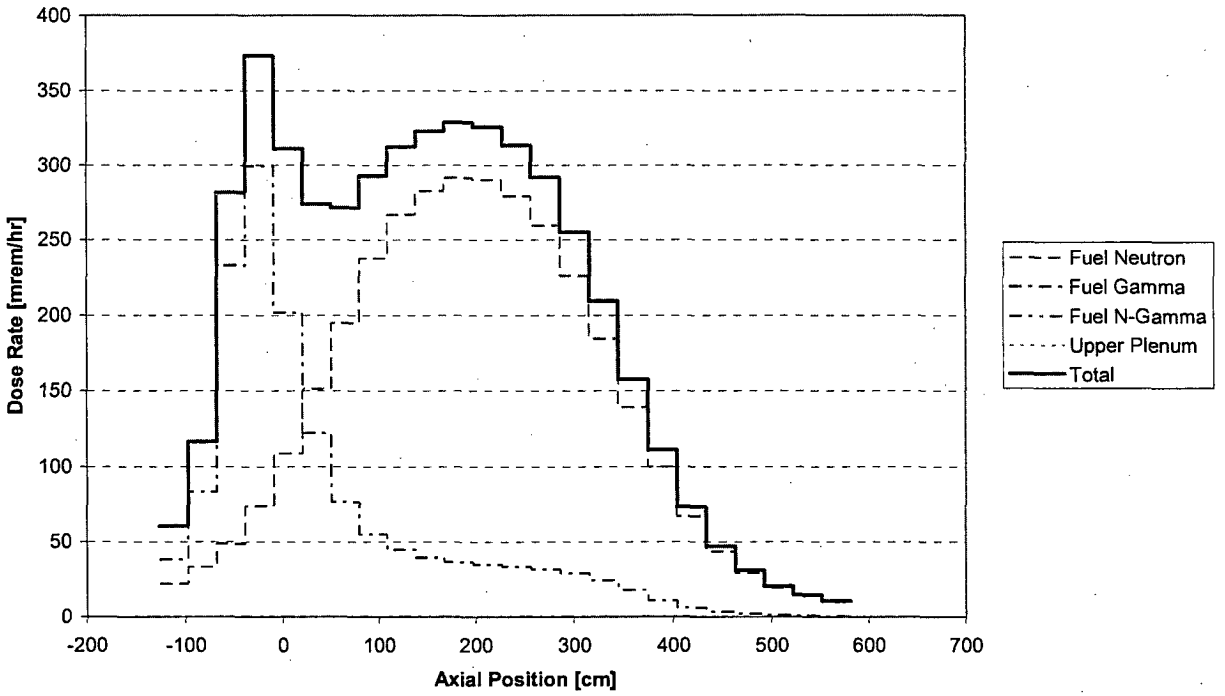

Figure 5.3.18-9 Sample MCNP Input File for Mixed PWR MOX/UO_2 Fuel

```
NAC-LWT Cask - we17pin_lw_80b40e090d - Normal Transport Conditions
C Radial Biasing - Fuel Gamma Source
C 16 Rod Source & WE17x17 Fuel
C Fuel Rod Cells
1 2 -6.5600 -1 -2    u=8 $ Bottom end cap
2 1 -10.960 -1 +2 -3 -5  u=8 $ Fuel
3 0         -1 +3 -4 -6  u=8 $ Plenum
4 2 -6.5600 -1 +4    u=8 $ Top end cap
5 0         -1 +2 -3 +5 -6 u=8 $ Annulus
6 2 -6.5600 -1 +2 -4 +6  u=8 $ Clad
7 0         +1     u=8 $ Outside fuel rod
C Fuel Rod Cells - Mixed Loading
8 2 -6.5600 -1 -2    u=7 $ Bottom end cap
9 8 -10.960 -1 +2 -3 -5  u=7 $ Fuel
10 0         -1 +3 -4 -6  u=7 $ Plenum
11 2 -6.5600 -1 +4    u=7 $ Top end cap
12 0         -1 +2 -3 +5 -6 u=7 $ Annulus
13 2 -6.5600 -1 +2 -4 +6  u=7 $ Clad
14 0         +1     u=7 $ Outside fuel rod
C Fuel Array Cells
15 0         -7 8 -9 10
       lat=1 u=6 fill=-3:3 -3:3 0:0
       6 6 6 6 6 6 6
       6 8 7 8 7 8 6
       6 7 6 6 6 7 6
       6 8 6 6 6 8 6
       6 7 6 6 6 7 6
       6 8 7 8 7 8 6
       6 6 6 6 6 6 6
C Can Weldment Cells
16 0         -11 fill=6 ( 0.0000 0.0000 2.5400 )   u=5 $ Fuel Insert
17 5 -7.9400 -12 +11    u=5 $ Internal Spacer
18 0         -13 +12 +11   u=5 $ Can Weldment void
19 5 -7.9400 -14     u=5 $ Can Weldment base
20 5 -7.9400 -15 +14 +13 +11  u=5 $ Can Weldment body
21 5 -7.9400 -16 +15 +11   u=5 $ Can Weldment flange
22 5 -7.9400 -17 +16    u=5 $ Can Weldment lid
23 0         +17     u=5 $ Outside
C PWR Insert Cells
24 0         -20 fill=5 ( 0.0000 0.0000 1.2700 )   u=4 $ Can Weldment
25 7 -2.7020 -21 +20    u=4 $ PWR Insert Body
26 0         +21 +20    u=4 $ Outside
C PWR Basket Cells
30 0         -30 fill=4 ( 0.0000 0.0000 5.2070 )   u=3 $ PWR Insert
31 0  -32 -31    u=3 $ Offset
32 7 -2.7020 -32 +31 +30   u=3 $ Basket
33 0  +32 +30    u=3 $ Outside
C Cask Cavity Cells
40 0         -40 +41 fill=3   u=2 $ Cavity
41 5 -7.9400 -41     u=2 $ Spacer plate
42 0         +40 +41    u=2 $ Outside
C Cells - LWT Cask Normal Conditions
50 4 -11.344 -53     u=1 $ BotPb
51 0         -52 fill=2    u=1 $ Cavity
52 5 -7.9400 -50 -51 +53   u=1 $ Bottom
53 5 -7.9400 -50 +51 +55 +58 +52 u=1 $ OuterShell
54 5 -7.9400 -54 +57 +52   u=1 $ InnerShellTaper
55 5 -7.9400 -56 +52    u=1 $ InnerShell
56 4 -11.344 -57 +56    u=1 $ Lead
57 4 -11.344 -55 +54 +57   u=1 $ LeadTaper
58 0         -58 +57    u=1 $ LeadGap
59 3 -0.9669 -60 +50    u=1 $ NeutronShield
60 5 -7.9400 -59 +50 +60   u=1 $ NSShell
61 6 -0.4997 -61 +50    u=1 $ UpperLimiter
62 6 -0.4997 -62 +50    u=1 $ LowerLimiter
63 0         -63 +50 +59 +61 +62 u=1 $ Container
64 0         +63     u=1 $ Outside
C Detector Cells - Radial Biasing
100  0  -100  fill=1  $ Surface
150  0  -150  +100  $ SurfaceAzi
200  0  -200  +100  +150  $ 1ft
300  0  -300  +100  +150  +200  $ 1m
```

```
400  0  -400  +100  +150  +200  +300  $ 2m
500  0  -500  +100  +150  +200  +300  +400  $ 2m+Convey
600  0  +100  +150  +200  +300  +400  +500  $ Exterior

C Fuel Rod Surfaces
1 RCC 0.0000 0.0000 0.0000 0.0000 0.0000 385.1402 0.4572 $ Fuel rod
2 PZ 1.7399
3 PZ 367.4999
4 PZ 383.4003
5 CZ 0.3922
6 CZ 0.4001
C Fuel Array Surfaces
7 PX 0.8731
8 PX -0.8731
9 PY 0.8731
10 PY -0.8731
C Can Weldment Surfaces
11 RPP -4.5212 4.5212 -4.5212 4.5212 2.5400 425.4500  $ Internal cavity
12 RPP -4.9975 4.9975 -4.9975 4.9975 2.5400 422.2750  $ Internal spacer
13 RPP -6.3500 6.3500 -6.3500 6.3500 2.5400 422.9100  $ Can weldment cavity
14 RPP -6.9850 6.9850 -6.9850 6.9850 0.0000 2.5400  $ Can weldment base
15 RPP -6.9850 6.9850 -6.9850 6.9850 0.0000 422.9100  $ Can weldment body
16 RPP -6.9850 6.9850 -6.9850 6.9850 0.0000 425.4500  $ Can weldment flange
17 RPP -6.9850 6.9850 -6.9850 6.9850 0.0000 426.7200  $ Can weldment lid
C PWR Insert Surfaces
20 RPP -7.2898 7.2898 -7.2898 7.2898 1.2700 427.9900  $ PWR Insert cavity
21 RPP -10.7950 10.7950 -10.7950 10.7950 0.0000 425.4500  $ PWR Insert body
C PWR Basket Surfaces
30 RPP -11.2713 11.2713 -11.2713 11.2713 5.2070 433.1970  $ Internal cavity
31 PZ 5.2070       $ Bottom offset
32 RCC 0.0000 0.0000 0.0000 0.0000 0.0000 415.4170 16.8273 $ Basket walls
C Cask Cavity Surfaces
40 RCC 0.0000 0.0000 0.0000 0.0000 0.0000 452.1199 16.9862 $ Cavity
41 RCC 0.0000 0.0000 438.7850 0.0000 0.0000 0.9525 11.1760 $ Spacer plate
C Surfaces - LWT Cask Normal Conditions
50 RCC 0.0000 0.0000 -26.6700 0.0000 0.0000 507.3650 36.5189 $ Lwt
51 RCC 0.0000 0.0000 -26.6700 0.0000 0.0000 26.6700 36.5189 $ Bottom
52 RCC 0.0000 0.0000 0.0000 0.0000 0.0000 452.1200 16.9863 $ Cavity
53 RCC 0.0000 0.0000 -17.7800 0.0000 0.0000 7.6200 26.3525 $ Bottom gamma shield
54 RCC 0.0000 0.0000 0.0000 0.0000 0.0000 444.5000 20.1740 $ Lead id - taper
55 RCC 0.0000 0.0000 0.0000 0.0000 0.0000 444.5000 31.5976 $ Lead od - taper
56 RCC 0.0000 0.0000 13.8176 0.0000 0.0000 416.8648 18.9103 $ Lead id
57 RCC 0.0000 0.0000 13.8176 0.0000 0.0000 416.8648 33.3271 $ Lead od
58 RCC 0.0000 0.0000 13.8176 0.0000 0.0000 416.8648 33.4645 $ Lead gap
59 RCC 0.0000 0.0000 3.8100 0.0000 0.0000 419.1000 49.8183 $ Neutron shield shell
60 RCC 0.0000 0.0000 5.0800 0.0000 0.0000 416.5600 49.2189 $ Neutron shield
61 RCC 0.0000 0.0000 450.2150 0.0000 0.0000 70.5612 49.8183 $ Upper limiter
62 RCC 0.0000 0.0000 -68.0212 0.0000 0.0000 71.8312 49.8183 $ Lower limiter
63 RCC 0.0000 0.0000 -68.0212 0.0000 0.0000 588.7974 49.8183 $ Container
C Radial Detector DRA (Surface)
100  RCC  0.0000  0.0000  -68.1212  0.0000  0.0000  588.9974  49.9184
101  PZ  -38.6713
102  PZ  -9.2215
103  PZ  20.2284
104  PZ  49.6783
105  PZ  79.1282
106  PZ  108.5780
107  PZ  138.0279
108  PZ  167.4778
109  PZ  196.9276
110  PZ  226.3775
111  PZ  255.8274
112  PZ  285.2772
113  PZ  314.7271
114  PZ  344.1770
115  PZ  373.6269
116  PZ  403.0767
117  PZ  432.5266
118  PZ  461.9765
119  PZ  491.4263
C Radial Detector DRAA (SurfaceAzi)
150  RCC  0.0000  0.0000  211.3775  0.0000  0.0000  30.0000  50.0184
151      PX  0.0000
152  1   PX  0.0000
153  2   PX  0.0000
154  3   PX  0.0000
```

```
155  4  PX  0.0000
156  5  PX  0.0000
157  6  PX  0.0000
158  7  PX  0.0000
159  8  PX  0.0000
160     PY  0.0000
161  9  PX  0.0000
162  10  PX  0.0000
163  11  PX  0.0000
164  12  PX  0.0000
165  13  PX  0.0000
166  14  PX  0.0000
167  15  PX  0.0000
168  16  PX  0.0000
C Radial Detector DRB (1ft)
200  RCC  0.0000  0.0000  -98.6012  0.0000  0.0000  649.9574  80.2984
201  PZ  -66.1033
202  PZ  -33.6055
203  PZ  -1.1076
204  PZ  31.3903
205  PZ  63.8882
206  PZ  96.3860
207  PZ  128.8839
208  PZ  161.3818
209  PZ  193.8796
210  PZ  226.3775
211  PZ  258.8754
212  PZ  291.3732
213  PZ  323.8711
214  PZ  356.3690
215  PZ  388.8669
216  PZ  421.3647
217  PZ  453.8626
218  PZ  486.3605
219  PZ  518.8583
C Radial Detector DRC (1m)
300  RCC  0.0000  0.0000  -168.1212  0.0000  0.0000  788.9974  149.8184
301  PZ  -135.2463
302  PZ  -102.3714
303  PZ  -69.4965
304  PZ  -36.6216
305  PZ  -3.7467
306  PZ  29.1282
307  PZ  62.0030
308  PZ  94.8779
309  PZ  127.7528
310  PZ  160.6277
311  PZ  193.5026
312  PZ  226.3775
313  PZ  259.2524
314  PZ  292.1273
315  PZ  325.0022
316  PZ  357.8771
317  PZ  390.7520
318  PZ  423.6269
319  PZ  456.5017
320  PZ  489.3766
321  PZ  522.2515
322  PZ  555.1264
323  PZ  588.0013
C Radial Detector DRD (2m)
400  RCC  0.0000  0.0000  -268.1212  0.0000  0.0000  988.9974  249.8184
401  PZ  -226.9130
402  PZ  -185.7048
403  PZ  -144.4965
404  PZ  -103.2883
405  PZ  -62.0801
406  PZ  -20.8719
407  PZ  20.3364
408  PZ  61.5446
409  PZ  102.7528
410  PZ  143.9611
411  PZ  185.1693
412  PZ  226.3775
413  PZ  267.5857
414  PZ  308.7940
```

```
415   PZ  350.0022
416   PZ  391.2104
417   PZ  432.4186
418   PZ  473.6269
419   PZ  514.8351
420   PZ  556.0433
421   PZ  597.2515
422   PZ  638.4598
423   PZ  679.6680
C Radial Detector DRE (2m+Convey)
500   RCC  0.0000  0.0000  -269.1212  0.0000  0.0000  990.9974  321.9200
501   PZ  -227.8296
502   PZ  -186.5381
503   PZ  -145.2465
504   PZ  -103.9550
505   PZ  -62.6634
506   PZ  -21.3719
507   PZ  19.9197
508   PZ  61.2113
509   PZ  102.5028
510   PZ  143.7944
511   PZ  185.0859
512   PZ  226.3775
513   PZ  267.6691
514   PZ  308.9606
515   PZ  350.2522
516   PZ  391.5437
517   PZ  432.8353
518   PZ  474.1269
519   PZ  515.4184
520   PZ  556.7100
521   PZ  598.0015
522   PZ  639.2931
523   PZ  680.5846

C
C Materials List
C
C UO2 Fuel
m1     92235 -2.6740E-02
       92238 -6.4177E-01
        8016 -8.9904E-02
C Fuel Rod End Cap (Zircaloy)
m2     40000 -9.8225E-01
       50000 -1.5000E-02
       26000 -1.2500E-03
       24000 -1.0000E-03
        7014 -5.0000E-04
C Water/Glycol
m3     1001 -1.03651E-01
       8016 -6.75619E-01
       6000 -2.20730E-01
mt3  lwtr.01
C Lead
m4     82000 -1.0
C Stainless Steel 304
m5     24000 -0.190
       25055 -0.020
       26000 -0.695
       28000 -0.095
C Aluminum (Impact Limiter)
m6     13027 -1.0
C Aluminum (Insert/Basket)
m7     13027 -1.0
C MOX Fuel
m8     92235 -1.2824E-03
       92238 -6.3994E-01
       94238 -1.3643E-05
       94239 -2.5513E-02
       94240 -1.6372E-03
       94241 -1.0914E-04
       94242 -1.3643E-05
        8016 -8.9904E-02
phys:p 100 0 0 0 1
C
C Cell Importances
```

```
imp:p 1 53r 0
C
C Source Definition - Fuel Gamma
C LEU/WG - 80 GWD/MTHM, 4 wt % Fissile, 90 days cooled
sdef cell=100:51:40:30:24:16:15:d4
     erg=d1
     pos= 0 0 1.7399
     rad=d2
     axs=0 0 1
     ext=d3
si1   1.000E-02 2.000E-02 5.000E-02 1.000E-01 2.000E-01 3.000E-01
      4.000E-01 6.000E-01 8.000E-01 1.000E+00 1.220E+00 1.440E+00
      1.660E+00 2.000E+00 2.500E+00 3.000E+00 4.000E+00 5.000E+00
      6.500E+00 8.000E+00 1.000E+01 1.200E+01 1.400E+01
sp1   0.0000E+00 8.0114E+13 1.0380E+14 5.0397E+13 5.8267E+13 1.2977E+13
      1.0169E+13 1.1443E+14 2.5269E+14 2.5656E+13 5.4103E+12 3.1422E+12
      2.4632E+12 4.7501E+11 1.1277E+12 7.2847E+10 2.4300E+09 7.7170E+05
      3.0970E+05 6.0750E+04 1.2899E+04 6.6693E+02 0.0000E+00
si2   0 0.3922
sp2   -21 1
si3 a 0.000 9.144 18.288 27.432 36.576 45.720 54.864
      310.896 320.040 329.184 338.328 347.472 356.616 365.760
sp3 d 0.5470 0.6358 0.7247 0.8135 0.9023 0.9912 1.0800
      1.0800 0.9912 0.9023 0.8135 0.7247 0.6358 0.5470
si4 l 2 9
sp4   1.0000 1.0258
mode p
nps 40000000
C
C ANSI/ANS-6.1.1-1977 - Gamma Flux-to-Dose Conversion Factors
C (mrem/hr)/(photons/cm2-sec)
de0   0.01 0.03 0.05 0.07 0.1 0.15 0.2
      0.25 0.3 0.35 0.4 0.45 0.5 0.55
      0.6 0.65 0.7 0.8 1 1.4 1.8
      2.2 2.6 2.8 3.25 3.75 4.25 4.75
      5 5.25 5.75 6.25 6.75 7.5 9
      11 13 15
df0   3.96E-03 5.82E-04 2.90E-04 2.58E-04 2.83E-04 3.79E-04 5.01E-04
      6.31E-04 7.59E-04 8.78E-04 9.85E-04 1.08E-03 1.17E-03 1.27E-03
      1.36E-03 1.44E-03 1.52E-03 1.68E-03 1.98E-03 2.51E-03 2.99E-03
      3.42E-03 3.82E-03 4.01E-03 4.41E-03 4.83E-03 5.23E-03 5.60E-03
      5.80E-03 6.01E-03 6.37E-03 6.74E-03 7.11E-03 7.66E-03 8.77E-03
      1.03E-02 1.18E-02 1.33E-02
C
C Weight Window Generation - Radial
wwg 2 0 0 0 0
wwp:p 5 3 5 0 -1 0
mesh geom=cyl ref=0.0 6.3 193 origin=0.1 0.1 -568
     imesh 6.4 12.2 17.0 18.9 33.3 36.5 49.2 49.8 549.8
     iints 3 1 1 1 5 1 1 1 1
     jmesh 500 541 550 558 568 575 579 964 1020 1049 1089 1589
     jints 1 1 1 1 1 1 1 1 1 1 1
     kmesh 1
     kints 1
wwge:p  1e-3 1 20
fc2 Radial Surface Tally
f2:p +100.1
fm2 1.16877E+16
fs2  -101  -102  -103  -104  -105  -106
     -107  -108  -109  -110  -111  -112
     -113  -114  -115  -116  -117  -118
     -119  T
tf2
fc12 Radial SurfaceAzi Tally Q1 (+x+y)
f12:p +150.1
fm12 1.16877E+16
fs12 -151  -160
     +159  +158  +157  +156  +155  +154
     +153  +152  T
sd12 4.7141E+03  2.3571E+03  2.6190E+02  8r  9.4282E+03
tf12
fc22 Radial SurfaceAzi Tally Q2 (-x+y)
f22:p +150.1
fm22 1.16877E+16
fs22 +151  -160
     -168  -167  -166  -165  -164  -163
```

```
     -162  -161  T
sd22 4.7141E+03  2.3571E+03  2.6190E+02  8r  9.4282E+03
tf22
fc32 Radial SurfaceAzi Tally Q3 (-x-y)
f32:p +150.1
fm32 1.16877E+16
fs32 +151  +160
     -159  -158  -157  -156  -155  -154
     -153  -152  T
sd32 4.7141E+03  2.3571E+03  2.6190E+02  8r  9.4282E+03
tf32
fc42 Radial SurfaceAzi Tally Q4 (+x-y)
f42:p +150.1
fm42 1.16877E+16
fs42 -151  +160
     +168  +167  +166  +165  +164  +163
     +162  +161  T
sd42 4.7141E+03  2.3571E+03  2.6190E+02  8r  9.4282E+03
tf42
fc52 Radial 1ft Tally
f52:p +200.1
fm52 1.16877E+16
fs52  -201  -202  -203  -204  -205  -206
     -207  -208  -209  -210  -211  -212
     -213  -214  -215  -216  -217  -218
     -219  T
tf52
fc62 Radial 1m Tally
f62:p +300.1
fm62 1.16877E+16
fs62  -301  -302  -303  -304  -305  -306
     -307  -308  -309  -310  -311  -312
     -313  -314  -315  -316  -317  -318
     -319  -320  -321  -322  -323  T
tf62
fc72 Radial 2m Tally
f72:p +400.1
fm72 1.16877E+16
fs72  -401  -402  -403  -404  -405  -406
     -407  -408  -409  -410  -411  -412
     -413  -414  -415  -416  -417  -418
     -419  -420  -421  -422  -423  T
tf72
fc82 Radial 2m+Convey Tally
f82:p +500.1
fm82 1.16877E+16
fs82  -501  -502  -503  -504  -505  -506
     -507  -508  -509  -510  -511  -512
     -513  -514  -515  -516  -517  -518
     -519  -520  -521  -522  -523  T
tf82
C
C Print Control
prdmp -15 -30 1 2
print
C Random Number Generator
rand gen=2 seed=19073486328125 stride=152917 hist=1
C
C Rotation Matrix
C
*TR1 0.0 0.0 0.0 10 100 90 -80 10 90 90 90 0
*TR2 0.0 0.0 0.0 20 110 90 -70 20 90 90 90 0
*TR3 0.0 0.0 0.0 30 120 90 -60 30 90 90 90 0
*TR4 0.0 0.0 0.0 40 130 90 -50 40 90 90 90 0
*TR5 0.0 0.0 0.0 50 140 90 -40 50 90 90 90 0
*TR6 0.0 0.0 0.0 60 150 90 -30 60 90 90 90 0
*TR7 0.0 0.0 0.0 70 160 90 -20 70 90 90 90 0
*TR8 0.0 0.0 0.0 80 170 90 -10 80 90 90 90 0
*TR9 0.0 0.0 0.0 100 190 90 10 100 90 90 90 0
*TR10 0.0 0.0 0.0 110 200 90 20 110 90 90 90 0
*TR11 0.0 0.0 0.0 120 210 90 30 120 90 90 90 0
*TR12 0.0 0.0 0.0 130 220 90 40 130 90 90 90 0
*TR13 0.0 0.0 0.0 140 230 90 50 140 90 90 90 0
*TR14 0.0 0.0 0.0 150 240 90 60 150 90 90 90 0
*TR15 0.0 0.0 0.0 160 250 90 70 160 90 90 90 0
*TR16 0.0 0.0 0.0 170 260 90 80 170 90 90 90 0
```

Figure 5.3.18-10 Comparison of Direct Solution and Response Function Results at Cask Surface for Normal Conditions Model for Discrete Rod Mixed Loading of 8 UO_2 Rods and 8 WG Rods

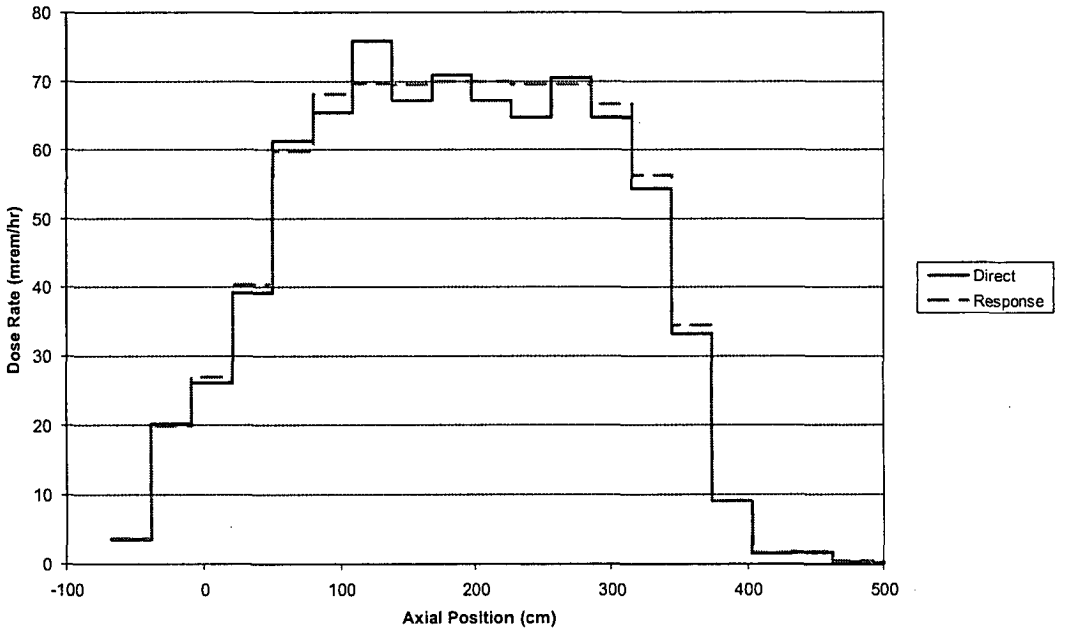

Figure 5.3.18-11 Comparison of Direct Solution and Response Function Results at Cask Surface for Normal Conditions Model for Homogenized WG Material

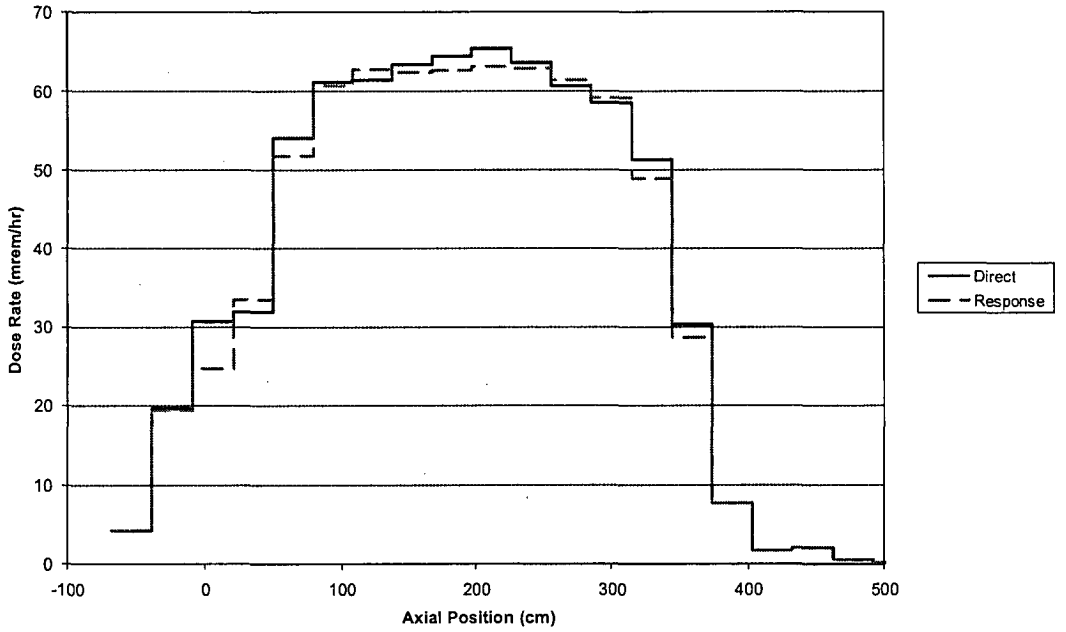

Figure 5.3.18-12 Comparison of Direct Solution and Response Function Results at Cask Surface for Normal Conditions Model for Homogenized LEU Material

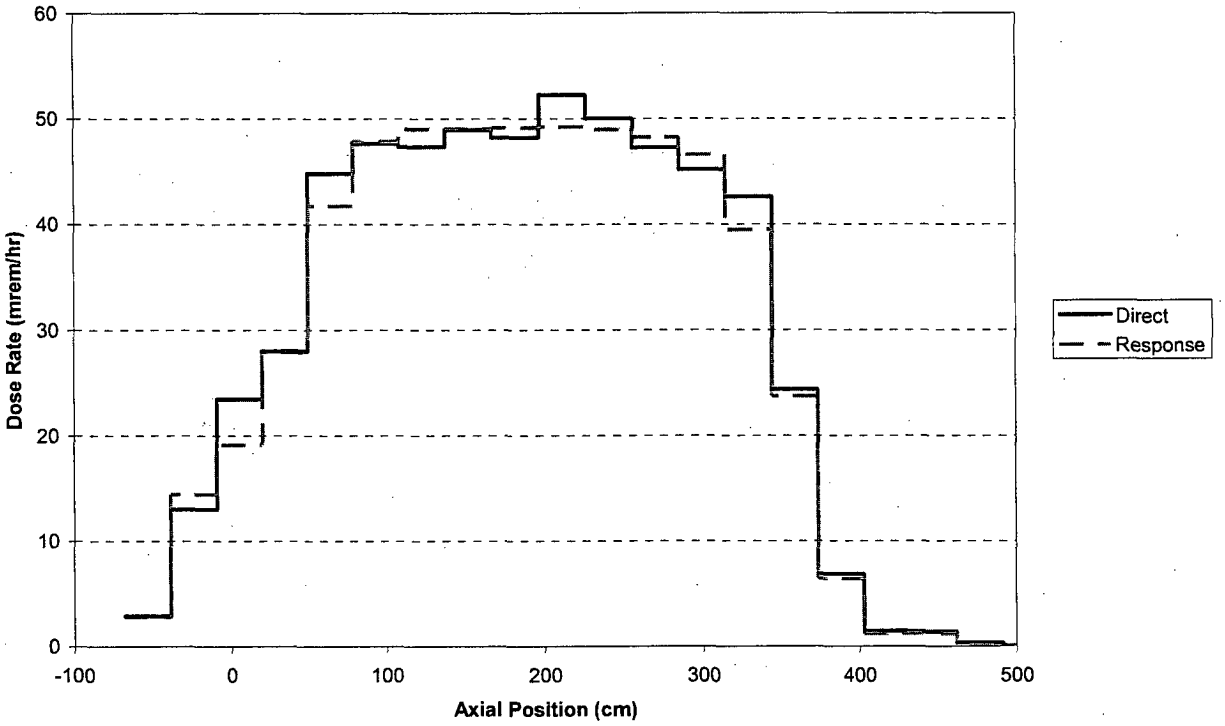

Table 5.3.18-1 High Burnup Fuel Rod Model Parameters

Parameter	Unit	SAS2H	MCNP
% Theoretical Density		95%	100%
Clad		Zirconium Alloy	Zirconium Alloy
Rod Diameter	[cm]	1.1180	0.9144
Clad Inner Diameter	[cm]	0.9860	0.8001
Pellet Diameter	[cm]	0.9665	0.7844
Active Length	[cm]	389.9	365.76
Heavy Metal Mass / Rod	[kg]	2.63[1]	1.62
Fuel Rods[2]		176	--
Pitch[2]	[cm]	1.4730	--
Plenum Height	[cm]	--	15.9004
End Cap Height	[cm]	--	1.7399
Number of Guide Tubes[3]		5	--
Guide Tube IR	[cm]	1.36	--
Guide Tube OR	[cm]	1.46	--

Table 5.3.18-2 High Burnup MOX Fuel Assembly Model Parameters[4]

Burnup [MWd/MTHM]	Number Cycles	Assembly Power [MW]	Cycle Length [d]
70,000	3	19.36	556.8

[1] Slight variations exist between various fuel material compositions due to density changes associated with Pu content.
[2] Only used for source generation to generate full assembly.
[3] Guide tube dimensions are required to construct the SAS2 Path B fuel model.
[4] UO_2 fuel evaluation employed same power density with increased cycle length (636.4 days) to achieve 80 GWd/MTHM burnup.

Table 5.3.18-3 MOX Fuel Material Compositions

Isotope	Isotopic Weight Fraction of U/Pu			
	Weapon Grade (WG)	Fuel Grade (FG)	Power Grade (PG)	MOX Services (MS)
^{235}U	0.2	0.2	0.2	0.2
^{238}U	99.8	99.8	99.8	99.8
^{238}Pu	0.05	0.1	1	0.05
^{239}Pu	93.5	86.1	62	89.85
^{240}Pu	6	12	22	9
^{241}Pu	0.4	1.6	12	1
^{242}Pu	0.05	0.2	3	0.1

Table 5.3.18-4 Uranium/Plutonium Fractions in MOX Fuel

Fissile Plutonium	Element	Element Weight Fraction in Fuel Composition			
		Weapon Grade (WG)	Fuel Grade (FG)	Power Grade (PG)	MOX Services (MS)
2%	U	97.96	97.82	97.41	97.89
	Pu	2.04	2.18	2.59	2.11
3%	U	96.94	96.72	96.12	96.84
	Pu	3.06	3.28	3.88	3.16
4%	U	95.92	95.63	94.82	95.77
	Pu	4.08	4.37	5.18	4.23
5%	U	94.90	94.53	93.52	94.72
	Pu	5.10	5.47	6.48	5.28
6%	U	93.87	93.44	92.22	93.67
	Pu	6.13	6.56	7.78	6.33
7%	U	92.85	92.34	90.92	92.61
	Pu	7.15	7.66	9.08	7.39

Table 5.3.18-5 PWR Fuel Axial Source Profile

% Active Fuel Height	Burnup Profile	Photon Source	Neutron Source
0.00%	0.5470	0.5470	7.840E-02
2.50%	0.6358	0.6358	1.479E-01
5.00%	0.7247	0.7247	2.569E-01
7.50%	0.8135	0.8135	4.185E-01
10.00%	0.9023	0.9023	6.481E-01
12.50%	0.9912	0.9912	9.633E-01
15.00%	1.0800	1.0800	1.384E+00
85.00%	1.0800	1.0800	1.384E+00
87.50%	0.9912	0.9912	9.633E-01
90.00%	0.9023	0.9023	6.481E-01
92.50%	0.8135	0.8135	4.185E-01
95.00%	0.7247	0.7247	2.569E-01
97.50%	0.6358	0.6358	1.479E-01
100.00%	0.5470	0.5470	7.840E-02

Table 5.3.18-6 Fuel Axial Source Profile Parameters

Description	Source	Exponent b	Average Source to Average Burnup
Design Basis (1.08 Peak)	Neutron	4.22	1.1269
	Gamma	1.00	1.000
MOX WG (1.08 Peak)	Neutron	2.702	1.0485
90 days cool time	Gamma	0.333	0.997
MOX WG (1.08 Peak)	Neutron	3.284	1.0752
2 years cool time	Gamma	0.766	0.998
MOX PG (1.08 Peak)	Neutron	1.708	1.0140
90 days cool time	Gamma	0.325	0.997
MOX PG (1.08 Peak)	Neutron	1.960	1.0213
2 years cool time	Gamma	0.735	0.998

Table 5.3.18-7 MOX Source Term Magnitudes at 70 GWd/MTHM and 90 Days Cool Time (per Rod Basis)

	Heat [watts/rod]				
Type	LEU	WG	FG	PG	MS
2% Fissile	111.4	118.1	119.5	125.2	118.8
3% Fissile	109.6	122.4	124.8	134.5	123.5
4% Fissile	108.0	126.7	130.1	144.2	128.3
5% Fissile	106.6	129.0	133.2	151.9	131.0
6% Fissile	105.2	129.3	134.3	157.5	131.7
7% Fissile	104.0	128.6	134.3	161.6	131.3
	Neutron [n/sec/rod]				
Type	LEU	WG	FG	PG	MS
2% Fissile	3.02E+07	4.34E+07	4.68E+07	7.33E+07	4.50E+07
3% Fissile	2.05E+07	3.28E+07	3.59E+07	5.99E+07	3.43E+07
4% Fissile	1.42E+07	2.59E+07	2.92E+07	5.29E+07	2.74E+07
5% Fissile	1.01E+07	2.14E+07	2.50E+07	4.94E+07	2.31E+07
6% Fissile	7.37E+06	1.83E+07	2.21E+07	4.73E+07	2.01E+07
7% Fissile	5.56E+06	1.60E+07	2.00E+07	4.58E+07	1.78E+07
	Gamma [γ/sec/rod]				
Type	LEU	WG	FG	PG	MS
2% Fissile	7.02E+14	7.11E+14	7.12E+14	7.12E+14	7.12E+14
3% Fissile	6.96E+14	7.12E+14	7.12E+14	7.13E+14	7.12E+14
4% Fissile	6.90E+14	7.09E+14	7.09E+14	7.11E+14	7.09E+14
5% Fissile	6.84E+14	7.06E+14	7.06E+14	7.09E+14	7.06E+14
6% Fissile	6.79E+14	7.03E+14	7.04E+14	7.08E+14	7.03E+14
7% Fissile	6.76E+14	7.00E+14	7.01E+14	7.06E+14	7.01E+14

Table 5.3.18-8 MOX Fuel Cool Time to Reach 143.75 W/Rod (Days)

Burnup (GWd/MTHM)	80	70	70	70	70
Fissile Material Type	LEU	WG	FG	PG	MS
7% Fissile Content	<90	<90	<90	120	<90
6% Fissile Content	<90	<90	<90	120	<90
5% Fissile Content	<90	<90	<90	110	<90
4% Fissile Content	<90	<90	<90	100	<90
3% Fissile Content	<90	<90	<90	<90	<90
2% Fissile Content	<90	<90	<90	<90	<90

Table 5.3.18-9 PWR Power Grade MOX Fuel Assembly Neutron Source Term for 70 GWd/MTHM, 2% Fissile Pu, and 90 Days Cooling (16 Rods)

Group	E Lower [MeV]	E Upper [MeV]	Source [neutrons/sec]
1	1.360E+01	1.460E+01	5.558E+04
2	1.250E+01	1.360E+01	1.419E+05
3	1.125E+01	1.250E+01	4.110E+05
4	1.000E+01	1.125E+01	1.086E+06
5	8.250E+00	1.000E+01	4.941E+06
6	7.000E+00	8.250E+00	1.036E+07
7	6.070E+00	7.000E+00	1.661E+07
8	4.720E+00	6.070E+00	5.380E+07
9	3.680E+00	4.720E+00	9.000E+07
10	2.870E+00	3.680E+00	1.220E+08
11	1.740E+00	2.870E+00	2.806E+08
12	6.400E-01	1.740E+00	4.000E+08
13	3.900E-01	6.400E-01	9.264E+07
14	1.100E-01	3.900E-01	8.346E+07
15	6.740E-02	1.100E-01	8.475E+06
16	2.480E-02	6.740E-02	6.216E+06
17	9.120E-03	2.480E-02	1.412E+06
18	2.950E-03	9.120E-03	3.328E+05
19	9.610E-04	2.950E-03	6.121E+04
20	3.540E-04	9.610E-04	1.086E+04
21	1.660E-04	3.540E-04	2.125E+03
22	4.810E-05	1.660E-04	8.485E+02
23	1.600E-05	4.810E-05	1.268E+02
24	4.000E-06	1.600E-05	2.625E+01
25	1.500E-06	4.000E-06	2.891E+00
26	5.500E-07	1.500E-06	6.710E-01
27	7.090E-08	5.500E-07	1.829E-01
28	1.000E-11	7.090E-08	9.100E-03
Total			1.173E+09

Table 5.3.18-10 PWR Power Grade MOX Fuel Assembly Gamma Source Term for 70 GWd/MTHM, 2% Fissile Pu, and 90 Days Cooling (16 Rods)

Group	E Lower [MeV]	E Upper [MeV]	Fuel Gamma [photons/sec]	Hardware Gamma[1] [photons/sec]
1	1.20E+01	1.40E+01	0.0000E+00	0.0000E+00
2	1.00E+01	1.20E+01	3.1246E+04	0.0000E+00
3	8.00E+00	1.00E+01	6.0432E+05	0.0000E+00
4	6.50E+00	8.00E+00	2.8462E+06	0.0000E+00
5	5.00E+00	6.50E+00	1.4508E+07	0.0000E+00
6	4.00E+00	5.00E+00	3.6147E+07	0.0000E+00
7	3.00E+00	4.00E+00	4.4686E+10	1.3138E-13
8	2.50E+00	3.00E+00	1.2211E+12	1.9460E+02
9	2.00E+00	2.50E+00	1.7739E+13	2.2777E+05
10	1.66E+00	2.00E+00	8.2987E+12	1.0318E+07
11	1.44E+00	1.66E+00	4.1253E+13	4.4657E+05
12	1.22E+00	1.44E+00	5.0438E+13	2.1733E+10
13	1.00E+00	1.22E+00	9.1018E+13	2.3000E+10
14	8.00E-01	1.00E+00	3.8442E+14	8.1955E+09
15	6.00E-01	8.00E-01	3.8492E+15	7.3117E+05
16	4.00E-01	6.00E-01	1.8316E+15	6.7064E+08
17	3.00E-01	4.00E-01	1.6843E+14	1.2419E+09
18	2.00E-01	3.00E-01	2.1407E+14	7.3205E+06
19	1.00E-01	2.00E-01	9.3336E+14	8.7699E+07
20	5.00E-02	1.00E-01	8.1935E+14	1.4913E+08
21	2.00E-02	5.00E-02	1.6657E+15	3.9420E+08
22	1.00E-02	2.00E-02	1.3199E+15	4.5530E+08
Total			1.1396E+16	5.5947E+10

[1] Reflects a 25 gram activated plenum spring. As indicated by the relative source magnitude differences between fuel and hardware gamma in any energy bin, there is no significant hardware source.

Table 5.3.18-11 Homogenization for PWR MOX Fuel Rod Regions

Material	Density [g/cm³]	Element	Number Density [atom/b-cm]
Homogenized Fuel Region (UO_2/MOX plus Clad)	1.23	Uranium-235	8.4528E-05
		Uranium-238	2.0031E-03
		Oxygen-16	4.1762E-03
		Zirconium	1.9328E-03
		Tin	2.2681E-05
		Iron	4.0176E-06
		Chromium	3.4521E-06
		Nitrogen-14	6.4091E-06
Fuel Rod End-Cap	0.84	Zirconium	5.4662E-03
		Tin	6.4146E-05
		Iron	1.1363E-05
		Chromium	9.7634E-06
		Nitrogen-14	1.8127E-05
Plenum Region[1]	0.0	N/A	0.0

[1] Plenum region modeled as void in the shielding evaluation.

Table 5.3.18-12 Cask/Basket Material Descriptions for PWR MOX Fuel

Material	Element	Density [g/cm³]	Number Density [atom/b-cm]
Stainless Steel 304	Fe	7.94	5.9505E-02
	Cr		1.7472E-02
	Ni		7.7392E-03
	Mn		1.7407E-03
Lead	Pb	11.34	3.2967E-02
Neutron Shield	H	0.97	5.9884E-02
	O		2.4595E-02
	C		1.0701E-02
Impact Limiter	Al	0.50	1.1153E-02
Aluminum	Al	2.70	6.0306E-02

Table 5.3.18-13 Material Composition Effect Study for PWR MOX Fuel

Fuel	Cool Time	Response (mrem/hr) Using UO_2 Composition	Direct (mrem/hr) Using Actual Composition	Diff
LEU	150 days	5.74	5.83	1.6%[1]
FG	90 days	10.72	10.86	1.3%
MS	90 days	10.16	10.29	1.3%
PG	90 days	18.44	18.70	1.4%
WG	90 days	9.72	9.86	1.4%

[1] Difference due to direct solution using the full spectrum of source in a single run versus response solution derived at by multiplication of the source spectrum by per energy line run results.

Table 5.3.18-14 Mixed Loading/Material Composition Effect Study for PWR MOX Fuel

Fuel Model	Fuel Material	Source	Dose Rate [mrem/hr]	FSD
LEU 16 Rods (MCNP Run)	UO_2	UO_2	36.3	1.2%
WG 16 Rods (MCNP Run)	WG	WG	44.0	1.0%
Numerical Avg. of LEU/WG 16 Rods	--	--	40.0	0.8%
Mixed Loading (MCNP Run)	UO_2/WG	UO_2/WG	40.0	1.1%
Mixed Loading (MCNP Run)	UO_2	UO_2/WG	39.7	1.1%

Table 5.3.18-15 MOX/UO_2 Fuel Material Configuration/Homogenization Study

Fuel	Surface Average (mrem/hr)			2m Average (mrem/hr)		
	Discrete	Homogenized	Difference	Discrete	Homogenized	Difference
LEU	36.3	39.8	9.7%	2.76	3.03	10.0%
FG	45.8	49.8	8.7%	3.38	3.71	9.8%
MS	44.7	48.9	9.4%	3.30	3.64	10.2%
PG	59.2	64.0	8.2%	4.23	4.61	8.8%
WG	44.0	48.2	9.6%	3.26	3.59	10.1%

Note: "Discrete" represents a model containing discrete 16 fuel rods placed in the outer cells of the 5×5 rod array, with void in the center 9 cells. "Homogenized" represents a smear or homogenized, material model.

Table 5.3.18-16 Maximum Radial Dose Rates for PWR MOX Fuel – 90 Days Cool Time, 2% Fissile Pu

Burnup (GWd/MTHM)	80	70	70	70	70
Fuel Material	LEU	WG	FG	PG	MS
Normal Surface	91.6	85.0	87.8	109.6	86.3
Normal 1 meter	23.6	22.1	22.7	27.5	22.4
Normal 2 meter	8.1	7.6	7.8	9.2	7.7
Accident 1 meter	362	344	347	373	345

Table 5.3.18-17 Detailed Dose Rates for Bounding Fuel – Power Grade PWR MOX Fuel, 2% Fissile Pu, 70 GWd/MTHM and 90 Days Cool Time

Transport Condition	Dose Rate Location	Maximum		Average	
		[mrem/hr]	FSD	[mrem/hr]	FSD
Normal	Side Surface of Cask	1.1E+02	0.5%	6.2E+01	0.2%
	Top Surface of Cask	8.6E-01	6.4%	4.3E-01	7.1%
	Bottom Surface of Cask	1.2E+01	8.2%	7.9E+00	6.3%
	Side 1m (Transport Index)	2.8E+01	0.4%	1.3E+01	0.1%
	2m from Truck - Radial	9.2E+00	0.3%	4.5E+00	0.1%
	2m from Top	3.3E-01	12.5%	2.1E-01	8.5%
	2m from Bottom	7.6E-01	8.5%	6.6E-01	5.9%
	Edge of Truck - Top	6.6E-02	30.6%	3.0E-02	13.7%
	Edge of Truck - Bottom	6.2E-01	21.2%	5.0E-01	7.0%
	Dose at Cab of Truck	2.3E-02	11.4%	1.6E-02	6.4%
Accident	Side Surface of Cask	4.1E+03	0.4%	1.4E+03	0.1%
	Top Surface of Cask	6.6E+00	16.7%	2.5E+00	11.9%
	Bottom Surface of Cask	6.5E+01	6.5%	3.8E+01	7.5%
	Side 1m	3.7E+02	0.3%	2.0E+02	0.1%
	Top 1m	1.3E+01	56.3%	5.5E+00	27.2%
	Bottom 1m	7.4E+01	29.5%	3.3E+01	17.6%

Chapter 6

6 CRITICALITY EVALUATION

The NAC-LWT cask is designed to transport either 1 pressurized water reactor (PWR) assembly; up to 25 intact PWR or BWR rods in a rod holder or fuel assembly lattice; up to 25 PWR or BWR fuel rods with a maximum of 14 of the rods classified as damaged in a rod holder; up to 16 PWR UO_2 or MOX rods in a rod holder; 2 boiling water reactor (BWR) assemblies; 15 sound metallic fuel rods; 6 failed metallic fuel rods; up to 42 high enriched uranium (HEU), medium enriched uranium (MEU) or low enriched uranium (LEU) Materials Test Reactor (MTR) fuel elements, or DIDO fuel assemblies; up to 140 TRIGA fuel elements; two packages of General Atomics Irradiated Fuel Material (GA IFM); up to 560 TRIGA fuel cluster rods; 1 consolidation canister with up to 300 TPBARs (including up to 2 damaged TPBARs); up to 700 PULSTAR fuel elements; up to 42 spiral fuel assemblies; or up to 42 MOATA plate bundles. This chapter illustrates that all packages meet the requirements of parts 71.55, 71.59 and 71.71 of 10 CFR 71.

In accordance with the requirements of 10 CFR 71.59 (b), the NAC-LWT cask is assigned a Criticality Safety Index (CSI) for criticality control for the authorized contents as follows:

Approved Contents	CSI
PWR fuel assemblies	100
BWR fuel assemblies	5.0
MTR fuel elements	0.0
Metallic fuel rods	0.0
TRIGA fuel elements (in poisoned TRIGA fuel baskets)	0.0
TRIGA fuel elements (in nonpoisoned TRIGA fuel baskets)	12.5
TRIGA fuel cluster rods	0.0
High burnup PWR (UO_2 or MOX) rods*	0.0
High burnup BWR rods*	0.0
DIDO fuel elements	12.5
General Atomic Irradiated Fuel Material (GA IFM)	0.0
TPBARS and segmented TPBARS	0.0
Intact (uncanned) PULSTAR fuel	0.0
Canned PULSTAR fuel	33.4
ANSTO fuel (spiral and/or MOATA)	0.0
Solid irradiated hardware	0.0

* up to 14 damaged rods

6.7 Payload Specific Details

This section contains NAC-LWT cask payload specific evaluation detail.

6.7.1 PWR Mixed Oxide Fuel Rods

This section includes input, analysis method, results, and critical benchmark evaluations for the NAC-LWT cask containing a payload of up to 16 PWR rods. The PWR rods may be composed of uranium oxide fuel pellets or mixed oxide fuel pellets (depleted or natural uranium oxide with plutonium oxide contributing the primary quantity of fissile material).

6.7.1.1 Package Fuel Loading

The NAC-LWT cask may transport up to 16 undamaged PWR fuel rods in a fuel rod holder. To bound all PWR MOX rods that may be transported in the NAC-LWT cask, UO_2 rods are evaluated with enrichments up to 5.0 wt % ^{235}U, while MOX rods were evaluated up to 7 wt % fissile plutonium. Characteristics of the design basis PWR rods are presented in Table 6.7.1-1 and Table 6.7.1-2. Given a fixed fissile material density, defined by a maximum UO_2 enrichment or fissile plutonium weight percent, the most reactive rod has the greatest fissile mass, i.e., the rod with the largest pellet radius. Therefore, the CE 14×14 pellet diameter of 0.3765 inch is chosen as the base radius for the most reactive PWR fuel rod evaluated here. A conservative maximum fissile material length of 153.5 inches is also applied. As a maximum reactivity fuel pitch is established, and the zirconium alloy is essentially transparent to neutrons, the clad thickness has no significant effect on the analysis.

6.7.1.2 Criticality Model Specifications

This section describes the models that are used in the criticality analyses for the NAC-LWT cask containing up to 16 PWR rods. PWR rods are either low enriched uranium oxide (maximum 5 wt % ^{235}U) fueled or MOX fueled. The models are analyzed separately under normal conditions and hypothetical accident conditions to ensure that all possible configurations are subcritical.

The model uses the MCNP5 code package with the ENDF/B-VI cross-section set. No cross-section pre-processing is required prior to MCNP implementation. MCNP uses the Monte Carlo technique to calculate the k_{eff} of a system. In these analyses, approximately 530 cycles with 1,000 neutron histories per cycle are tracked through the system.

Description of Calculational Models

The MCNP model of the NAC-LWT cask with 16 undamaged PWR rods includes triangular and square lattice formation of design basis rods centered in the cask cavity. No credit is taken for geometry control provided by the rod holder. The fuel rods, cask cavity and radial shields are explicitly modeled as shown in the Figure 6.7.1-1 model sketch.

The model of the NAC-LWT cask takes advantage of the universe structure of MCNP. Each universe defines an infinite space, bounded after its insertion into a containing cell. Four universes are employed herein. The "0" universe defines the cask universe. The remaining universes are discussed in the following sections. Each universe is developed independently as surfaces and cells. Fuel rod array surfaces and cells are configured to place the rods in either a rectangular (square) pitch array or a hex (triangular) pitch array. The rod pitch is a variable input into the model and is modified to achieve a maximum reactivity configuration. In the basket universe, the rod array is placed into a square (RPP) body that allows the moderator density outside the rod array to be adjusted independently.

The modeled accident condition completely removes the neutron shielding, the neutron shield tank and the cask impact limiters. In the normal conditions model, the impact limiter diameter is modeled as identical to the neutron shield tank diameter. This allows for closer packing for the cask array than physically possible.

VISED sketches of the assembled geometry are shown in Figure 6.7.1-2 through Figure 6.7.1-4. The cask outer surface is surrounded by a rectangular body with reflecting boundary conditions. The boundary conditions are imposed on the sides, top and bottom, which simulates an infinite array of casks.

Package Regional Densities

The composition densities (g/cc) and nuclide number densities (atm/b-cm) used in the subsequent criticality analyses are shown in Table 6.7.1-1. The various isotope weight compositions used in the MOX/UO_2 rod analysis are listed in Table 6.7.1-2.

Figure 6.7.1-1 MCNP Model Sketch of the NAC-LWT Cask with PWR MOX/UO_2 Rods

(Dimensions in centimeters)

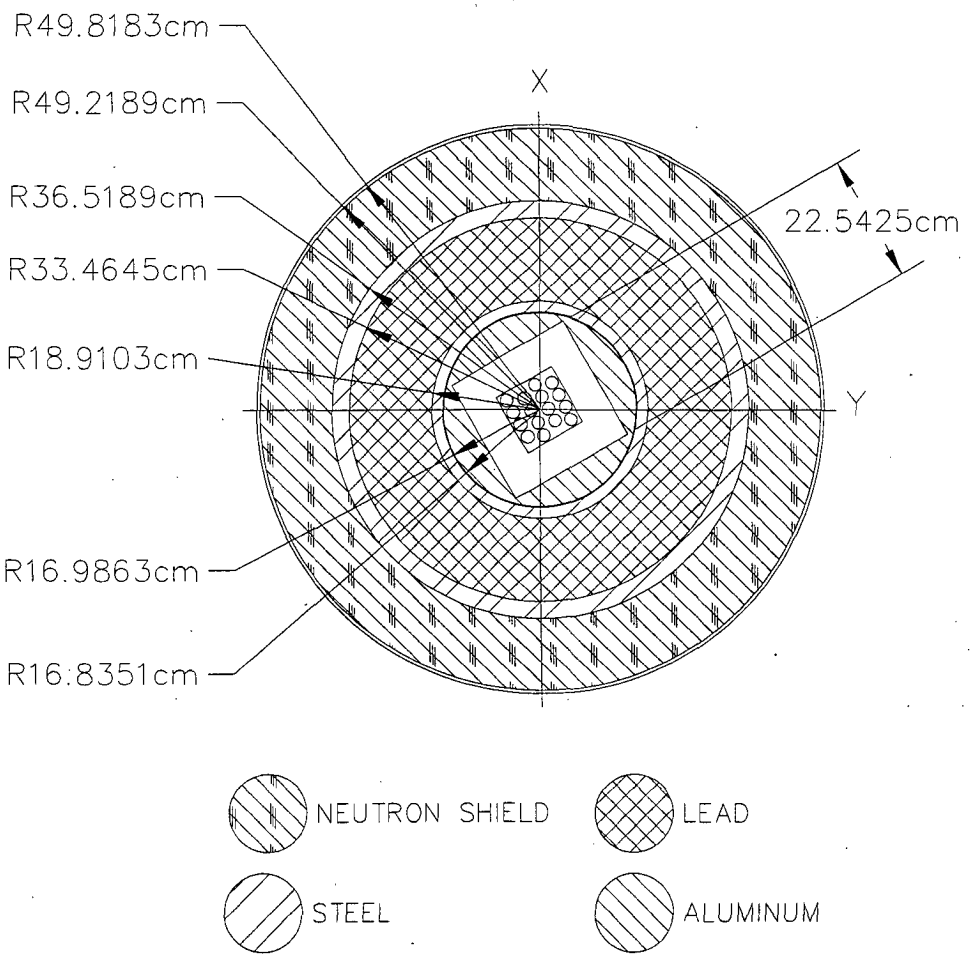

Figure 6.7.1-2 VISED Sketch of LWT Radial View – Hex Rod Array– Normal Conditions

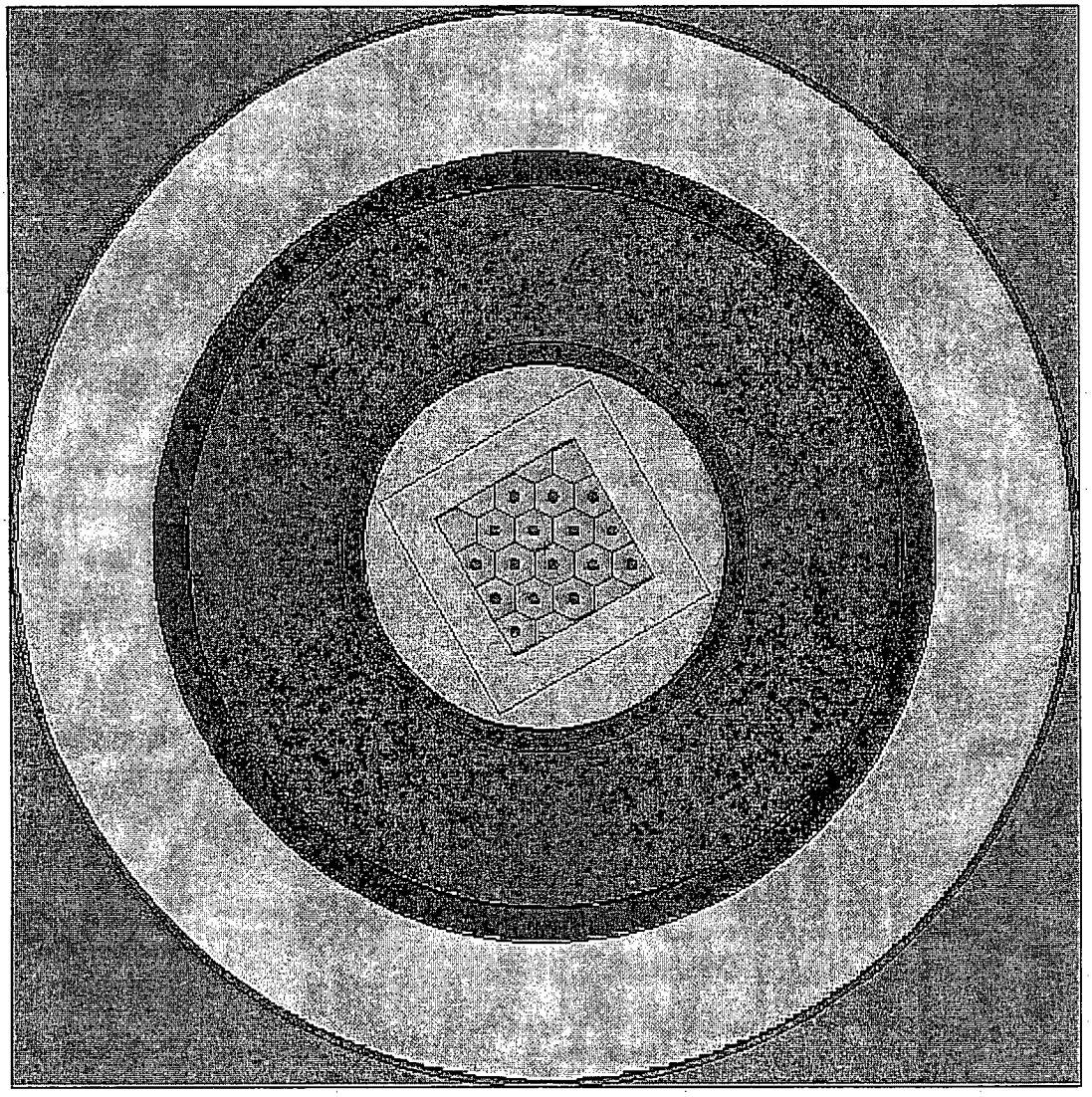

Figure 6.7.1-3 VISED Sketch of LWT Radial View – Square Rod Pitch - Accident Conditions

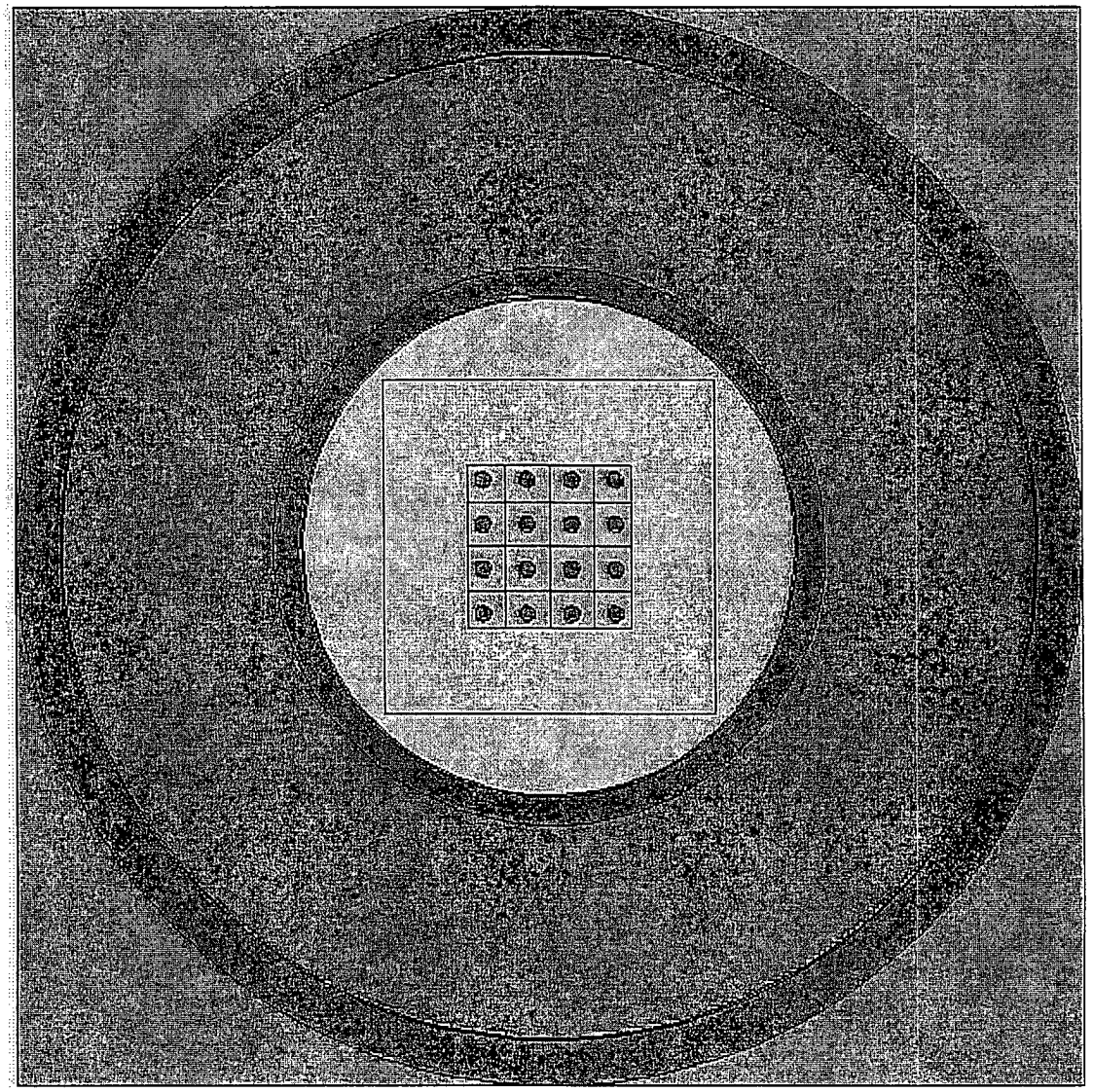

Figure 6.7.1-4 VISED Sketch of LWT Axial View – Accident Conditions

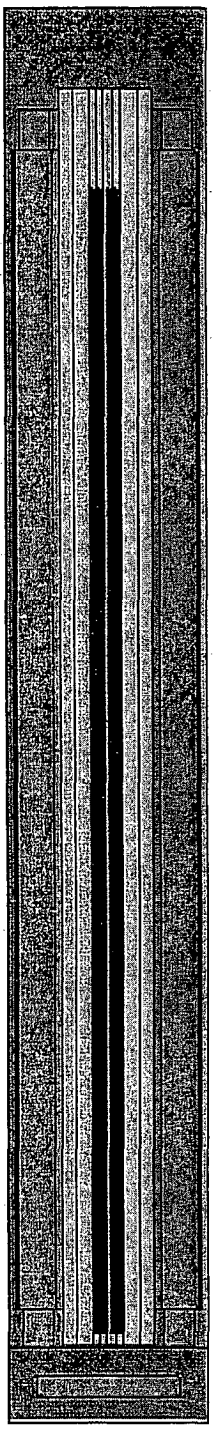

Table 6.7.1-1 PWR MOX Fuel Analysis Compositions and Number Densities

Material	5.0% Enriched UO_2	Weapons Grade (7 wt % Fissile Pu)[1]	Zirconium Alloy	H_2O	304 Stainless Steel	Pb	Al
Density, g/cc	10.522	10.556	6.56	0.9982	7.920	11.344	2.702
Density	atoms/b-cm						
Uranium-235	1.19E-03	1.54E-04					
Uranium-238	2.23E-02	2.16E-02					
Plutonium-238		9.15E-07					
Plutonium-239		1.70E-03					
Plutonium-240		1.09E-04					
Plutonium-241		7.23E-06					
Plutonium-242		9.00E-07					
Oxygen	4.70E-02	4.70E-02		3.338E-2			
Hydrogen				6.677E-2			
Zirconium Alloy			4.331E-2				
Iron					5.936E-2		
Chromium					1.743E-2		
Nickel					7.721E-3		
Manganese					1.736E-3		
Lead						3.297E-2	
Aluminum							6.031E-2

Table 6.7.1-2 PWR MOX Fuel Analysis Isotope Weight Fraction[2]

Isotope	UO_2	Weapon Grade	Fuel Grade	Power Grade	MOX Services
^{235}U	5	0.7	0.7	0.7	0.7
^{238}U	95	99.3	99.3	99.3	99.3
^{238}Pu	0	0.05	0.1	1	0.05
^{239}Pu	0	93.5	86.1	62	95
^{240}Pu	0	6	12	22	4.5
^{241}Pu	0	0.4	1.6	12	0.4
^{242}Pu	0	0.05	0.2	3	0.05

[1] Sample composition.
[2] Typical fresh fuel MOX material is composed of depleted uranium at 0.2 to 0.3 wt % ^{235}U. A bounding natural uranium enrichment of 0.7 wt % ^{235}U is used in the criticality evaluations.

6.7.1.3 Criticality Calculations

This section presents the criticality analysis for the NAC-LWT cask with up to 16 PWR UO_2 or MOX rods. UO_2 rods are enriched up to 5.0 wt % ^{235}U initial enrichment, while MOX rods contain up to 7 wt % fissile plutonium. No credit is taken for geometry control that is provided by the rod holder and no rod positions are specified for the rods in the lattice. Since various fuel rod arrangements may be shipped, the criticality of the PWR MOX rods in the NAC-LWT cask cavity is studied to determine the optimum pitch and, therefore, the maximum k_{eff} for the cask.

Criticality results are divided into individual sets of analyses.

- Evaluate the NAC-LWT accident configuration to demonstrate that, at a fixed fissile plutonium content, the maximum fissile percentage material (MOX Services definition) produces the maximum reactivity configuration.
- Determine the maximum reactivity pitch of the most reactive fuel material.
- Run the optimum moderator density evaluation.
- Evaluate normal condition and single cask "containment reflected" cases.

Included in all analyses are hypothetical plutonium compositions solely to justify the removal of the plutonium compositions as a licensing limit.

Rod Geometry and Material Composition Studies

Each of the material compositions is evaluated for the maximum fissile material mass rod. Fissile material in the uranium oxide rods is limited by the 5 wt % ^{235}U enrichment constraint, while the MOX material is limited by the 7 wt % fissile plutonium input. In addition to the physically realistic MOX material descriptions, three hypothetical MOX materials are evaluated: one containing all fissile plutonium (adding into ^{241}Pu the remaining plutonium weight fractions), an all ^{239}Pu material and an all ^{241}Pu material. The following nomenclature is used to describe the various plutonium fuel materials.

Abbreviation	Material
PG	Power grade plutonium isotopic distribution
FG	Fuel grade plutonium isotopic distribution
WG	Weapons grade plutonium isotopic distribution
MS	MOX Services "WG type" material
FP	Plutonium is modeled as all fissile plutonium
P9	Plutonium is modeled as all ^{239}Pu
P1	Plutonium is modeled as all ^{241}Pu

All cases are evaluated at a hexagonal pitch of 3.0 and 3.6 cm. Based on scoping evaluations, as validated in the following section, these fuel rod pitches approximate maximum reactivity configurations over a range of material composition.

As shown in later moderator density studies, maximum reactivity moderation is achieved by a preferentially flooded lattice with a void gap to the cask cavity. Fuel material and pitch studies are based on a flooded cask cavity. As these studies primarily rely on the interaction between rods in the lattice, rather than between casks, applying the results of the flooded cavity to the dry cavity/wet lattice is acceptable.

As seen in Table 6.7.1-3, maximum reactivity for physically realistic plutonium compositions is achieved by the MOX Services material. This result was expected as the MOX Services composition model contains the maximum fissile material within the plutonium oxide matrix. For the hypothetical compositions, the all ^{241}Pu case produces maximum reactivity. As the ^{241}Pu isotope has the highest fission cross-section, this result is to be expected.

Maximum Reactivity Rod Pitch Evaluation

The maximum fissile mass rod configuration is evaluated with uranium oxide, MOX Services (95 wt % ^{239}Pu in Pu), and 100% ^{241}Pu at a range of rod pitches to determine the maximum (optimum) pitch for a flooded cask cavity. This evaluation takes no credit for the actual pitch of the encapsulating stainless steel rod (11/16 inch at 1.75 cm OD) structure into which the rods are placed. As seen in Figure 6.7.1-5 and Table 6.7.1-4, the maximum reactivity pitch is approximately 3.4 to 3.6 cm for the MOX rods and around 3 cm for the uranium oxide rods, with a "flat" peak extending approximately 0.4 to 0.6 cm in width depending on material and configuration. Based on a three sigma uncertainty band, maximum reactivities do not statistically differ between hexagonal and square pitch configurations. The base case for the optimum moderator density studies will be the 3.6 cm hexagonal pitch for the MOX rods and the 3.0 cm hexagonal pitch for the UO_2 rods.

Optimum Moderator Density Evaluation

The maximum fissile mass rod is evaluated at various internal and external moderator densities, including preferential flooding of the fuel region. For the preferential flooding scenarios, the square container containing the rod array will be evaluated at a moderator density independent of that in the remainder of the cask cavity. Figure 6.7.1-6 through Figure 6.7.1-8 contain the moderator density plots of the uranium oxide, MOX Services, and all ^{241}Pu material configurations. All results produce identical trends in that maximum reactivity is achieved by a preferentially flooded fuel region and void cavity and cask exterior. This result was to be

expected as it provides maximum neutronic coupling within the reflective boundary (infinite array) model.

Maximum system reactivities are summarized in Table 6.7.1-5 for the UO_2 fuel compostion, the MOX Services defined fuel composition, and the hypothetical fissile material composition (100% ^{241}Pu) at the bounding fissile configuration—a maximum fuel material rod (0.3765-in pellet OD, 153.5-in active fuel length).

Single Cask Containment (Fully Reflected) and Normal Condition Array Evaluations

A single cask evaluation is performed to comply with 10 CFR 71.55(b)(3).

The containment for the NAC-LWT is the cask inner shell. While no operating condition results in a removal of the cask outer shell and lead gamma shield, the most reactive preferential flooded and fully flooded cases are reevaluated by removing the lead and outer shells (including neutron shield), and reflecting the system by 20 cm water at full density on the X, Y, and Z faces. Single cask, containment fully reflected reactivities are summarized in Table 6.7.1-6.

A normal condition infinite cask array is also evaluated. As indicated by the evaluations of the accident conditions array, including the radial neutron shield reduces system reactivity by eliminating neutronic interaction between casks. Normal condition cask array results are summarized in Table 6.7.1-7.

Maximum Reactivities and Comparison to USL

The maximum $k_{eff} + 2\sigma$ results for three primary analysis groups (single cask, normal array and accident array) are summarized in Table 6.7.1-8. Two normal condition array cases are included as the cask remains dry through all operating conditions, while 10 CFR 71 requires a normal condition maximum reactivity moderator density case. The listed values represent the maximum system reactivity adjusted for Monte Carlo run uncertainty and are significantly below the lower of system USL.

No benchmarks for mixed heterogeneous UO_2 and MOX rod systems are publically available. Therefore, individual benchmarks are established for UO_2 and MOX systems. The more limiting USL is applied to the results of the MOX/UO_2 rod calculations. Per Section 6.7.2, the USL for an array of UO_2 rods is 0.9376 and 0.9331 for an array of MOX rods for a Δk of 0.0045 between the two fuel types. The evaluations demonstrated that MCNP, with its associated cross-sections, accurately predicts system reactitities containing either fuel rod type.

The focus of the evaluations is a wet (flooded) system, as no reasonable extrapolation of the data provided would indicate a safety concern for a dry system at the requested fissile material levels.

While it is recognized that code performance and bias are potentially affected by the difference in the energy level of neutron causing fission, the benchmarks accounted for the basic phenomena, and the computer code is capable of tracking particles at their relevant energy levels.

Analyses have demonstrated that the UO_2 rod payload, calculated to be at maximum reactivity flooded with an EALCF of 0.13 eV (3.0 cm pitch study UO_2 case), are significantly lower in reactivity than the MOX payload with an EALCF of 0.13 eV (note systems have identical EALCF at optimum pitch). Insertion of the lower reactivity UO2 rods and corresponding replacement of higher reactivity MOX rods will reduce system reactivity.

Given the significant margin (Δk of 0.13) between maximum calculated reactivity for a hypothetical fuel material (all ^{241}Pu) at maximum reactivity pitch, without inclusion of the tube insert that retains the rods in a fixed position, the evaluations demonstrate that the system meets regulatory requirements. No mixed fuel evaluations are, therefore, performed and no mixed bias is discussed.

Table 6.7.1-9 compares the physical and hypothetical rod/material combinations to the area of applicability for the MOX material and maximum reactivity ^{241}Pu material. The MOX Services fuel material is within the area of applicability. No pure ^{241}Pu benchmark exists; therefore, the hypothetical configuration is significantly outside the area of applicability of the benchmark calculation. Compliance with regulatory limits is assured, as there is no significant reactivity trend versus plutonium isotopic composition. There is a significant margin to limits (0.13 Δk) versus a typical code bias in the 1-2% range, and the results are obtained from a hypothetical (conservative) isotope composition (all ^{241}Pu).

As the shipment includes uranium oxide rods, the maximum reactivity uranium oxide rod configuration characteristics are compared to the area of applicability in Table 6.7.1-10. The USL for UO_2 evaluations is 0.9372. Exceeding the area of applicability for enrichment and fuel to moderator ratios (expressed as rod pitch and H/U ratio) in the UO_2 benchmark cases is acceptable as neither function has a trend that is statistically significant and the margin to limits is large (> 0.4). A similar argument is applied to slightly lower fission energy for the maximum reactivity case than covered by the benchmark analysis. There is no statistically significant trend of reactivity versus energy, and any relative changes in USL postulated from the extrapolation is not significant versus the subcritical margin of the UO_2 rod shipment.

Evaluations of a mixed shipment of enriched UO_2 rods and MOX rods are not required, as the reactivity of the evaluated MOX rods are significantly higher than those of the UO_2 rods. Mixed shipments are, therefore, permitted.

Table 6.7.1-11 lists the bounding characteristics for the MOX/UO_2 PWR fuel rods evaluated in this section.

Figure 6.7.1-5 PWR MOX Rod Shipment - Reactivity versus Rod Pitch

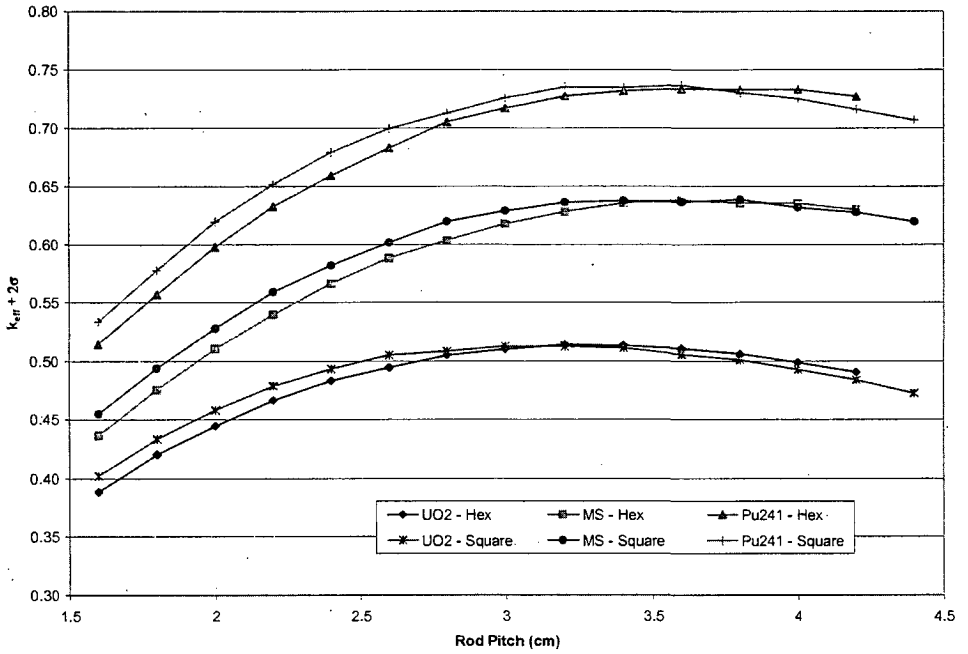

Figure 6.7.1-6 Moderator Density Study – UO_2 Fuel Material – 3.0 cm Rod Pitch

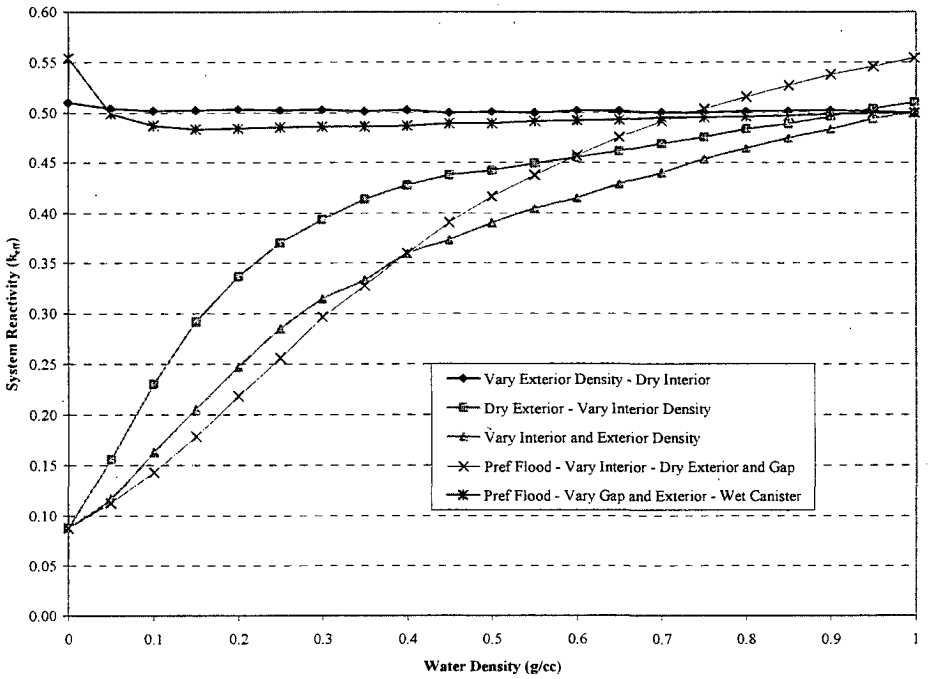

Figure 6.7.1-7 Moderator Density Study – MS Fuel Material – 3.6 cm Rod Pitch

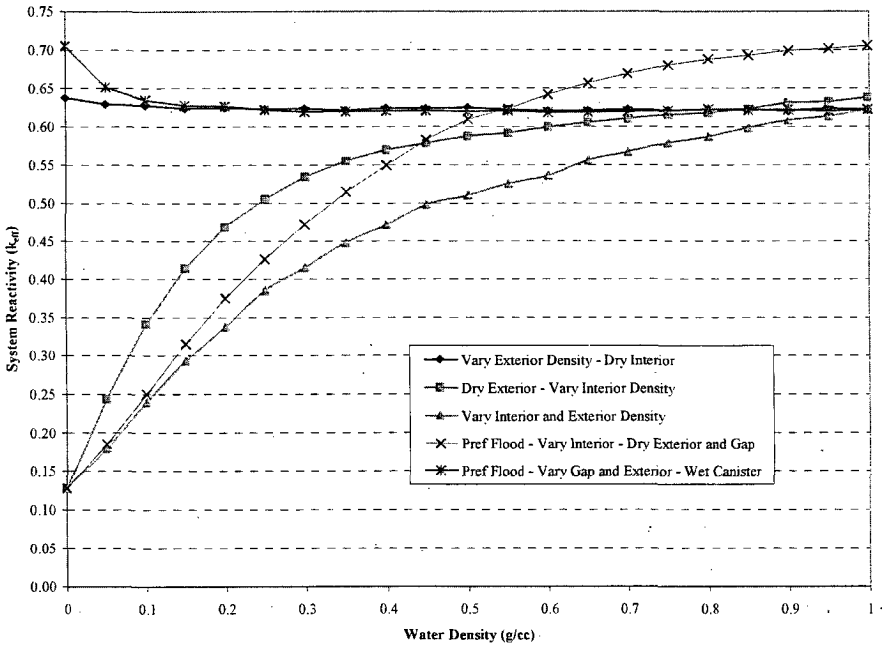

Figure 6.7.1-8 Moderator Density Study – PWR MOX ^{241}Pu Fuel Material – 3.6 cm Rod Pitch

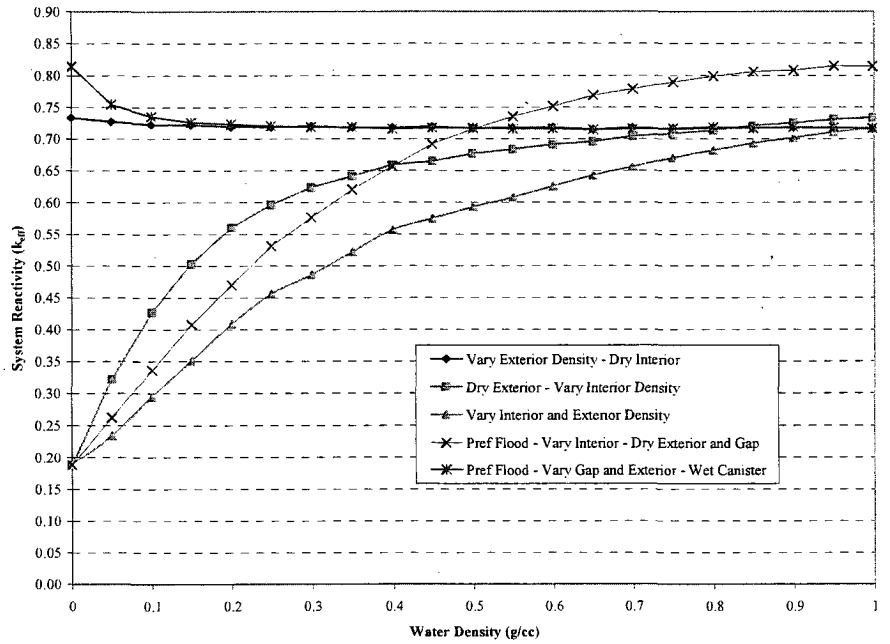

Table 6.7.1-3 PWR MOX Rod Shipment - Reactivity as a Function of Geometry and Material

Fuel Material	Rod Pitch	k_{eff}	σ	$k_{eff}+2\sigma$	vs. MS or P1 Composition	
					Δk_{eff}	$\Delta k_{eff}/\sigma$
UO_2	3.0	0.50837	0.00087	0.51011	-0.10728	-81.4
WG	3.0	0.61442	0.00106	0.61654	-0.00123	-0.8
FG	3.0	0.60516	0.00097	0.60710	-0.01049	-7.6
PG	3.0	0.59390	0.00104	0.59598	-0.02175	-15.1
MS	3.0	0.61565	0.00099	0.61763	--	--
FP	3.0	0.63359	0.00107	0.63573	-0.08132	-51.8
P9	3.0	0.62715	0.00111	0.62937	-0.08776	-54.9
P1	3.0	0.71491	0.00115	0.71721	--	--
UO_2	3.6	0.50911	0.00084	0.51079	-0.12688	-96.0
WG	3.6	0.63252	0.00098	0.63448	-0.00347	-2.5
FG	3.6	0.62282	0.00099	0.62480	-0.01317	-9.3
PG	3.6	0.61299	0.00105	0.61509	-0.02300	-15.7
MS	3.6	0.63599	0.00102	0.63803	--	--
FP	3.6	0.65225	0.00100	0.65425	-0.07909	-50.1
P9	3.6	0.64517	0.00107	0.64731	-0.08617	-53.1
P1	3.6	0.73134	0.00122	0.73378	--	--

Table 6.7.1-4 PWR MOX Fuel Shipment – Fuel Rod Pitch Study

Rod Pitch	Pitch Config	Fuel Material	k_{eff}	Fuel Material	k_{eff}	Fuel Material	k_{eff}
1.8	Hexagonal	UO_2	0.41843	MS	0.47357	^{241}Pu	0.55466
2.0	Hexagonal	UO_2	0.44262	MS	0.50841	^{241}Pu	0.59542
2.2	Hexagonal	UO_2	0.46448	MS	0.53761	^{241}Pu	0.63030
2.4	Hexagonal	UO_2	0.48147	MS	0.56403	^{241}Pu	0.65675
2.6	Hexagonal	UO_2	0.49260	MS	0.58626	^{241}Pu	0.68060
2.8	Hexagonal	UO_2	0.50325	MS	0.60145	^{241}Pu	0.70293
3.0	Hexagonal	UO_2	0.50837	MS	0.61565	^{241}Pu	0.71491
3.2	Hexagonal	UO_2	0.51224	MS	0.62593	^{241}Pu	0.72528
3.4	Hexagonal	UO_2	0.51156	MS	0.63376	^{241}Pu	0.72957
3.6	Hexagonal	UO_2	0.50911	MS	0.63599	^{241}Pu	0.73134
3.8	Hexagonal	UO_2	0.50464	MS	0.63360	^{241}Pu	0.73067
4.0	Hexagonal	UO_2	0.49718	MS	0.63359	^{241}Pu	0.73097
4.2	Hexagonal	UO_2	0.48894	MS	0.62789	^{241}Pu	0.72504
1.8	Square	UO_2	0.43146	MS	0.49220	^{241}Pu	0.57531
2.0	Square	UO_2	0.45613	MS	0.52574	^{241}Pu	0.61729
2.2	Square	UO_2	0.47678	MS	0.55687	^{241}Pu	0.64902
2.4	Square	UO_2	0.49150	MS	0.57989	^{241}Pu	0.67677
2.6	Square	UO_2	0.50343	MS	0.59949	^{241}Pu	0.69695
2.8	Square	UO_2	0.50669	MS	0.61768	^{241}Pu	0.71049
3.0	Square	UO_2	0.51090	MS	0.62688	^{241}Pu	0.72343
3.2	Square	UO_2	0.51089	MS	0.63415	^{241}Pu	0.73285
3.4	Square	UO_2	0.50965	MS	0.63544	^{241}Pu	0.73257
3.6	Square	UO_2	0.50429	MS	0.63440	^{241}Pu	0.73463
3.8	Square	UO_2	0.49939	MS	0.63658	^{241}Pu	0.72833
4.0	Square	UO_2	0.49120	MS	0.63003	^{241}Pu	0.72326
4.2	Square	UO_2	0.48232	MS	0.62576	^{241}Pu	0.71403

Table 6.7.1-5 PWR MOX Fuel Shipment – Optimum Moderator Study Maximum Reactivity Summary

Fuel Material	$k_{eff} + 2\sigma$
UO_2	0.55404
MOX Services	0.70523
^{241}Pu	0.81451

Table 6.7.1-6 PWR MOX Fuel Shipment Reactivity Summary for Single Cask Containment Fully Reflected Cases

Fuel Mat'l	Rod Gap (g/cc)	Array (g/cc)	Cavity (g/cc)	Exterior (g/cc)	k_{eff}	σ	$k_{eff} + 2\sigma$
UO_2	0.0001	0.0001	0.0001	0.9982	0.03394	0.00018	0.03430
UO_2	0.9982	0.9982	0.9982	0.9982	0.49629	0.00085	0.49799
UO_2	0.9982	0.9982	0.0001	0.9982	0.43536	0.00091	0.43718
MS	0.0001	0.0001	0.0001	0.9982	0.04527	0.00028	0.04583
MS	0.9982	0.9982	0.9982	0.9982	0.61686	0.00100	0.61886
MS	0.9982	0.9982	0.0001	0.9982	0.58689	0.00102	0.58893
^{241}Pu	0.0001	0.0001	0.0001	0.9982	0.04895	0.00036	0.04967
^{241}Pu	0.9982	0.9982	0.9982	0.9982	0.71168	0.00115	0.71398
^{241}Pu	0.9982	0.9982	0.0001	0.9982	0.67957	0.00121	0.68199

Table 6.7.1-7 PWR MOX Fuel Shipment Reactivity Summary for Normal Condition Array Cases

Fuel Mat'l	Rod Gap (g/cc)	Array (g/cc)	Cavity (g/cc)	Exterior (g/cc)	k_{eff}	σ	$k_{eff} + 2\sigma$
UO_2	0.0001	0.0001	0.0001	0.0001	0.03393	0.00016	0.03425
UO_2	0.9982	0.9982	0.9982	0.9982	0.49757	0.00089	0.49935
UO_2	0.9982	0.9982	0.9982	0.0001	0.49624	0.00092	0.49808
UO_2	0.9982	0.9982	0.0001	0.0001	0.43382	0.00087	0.43556
MS	0.0001	0.0001	0.0001	0.0001	0.04576	0.00025	0.04626
MS	0.9982	0.9982	0.9982	0.9982	0.61761	0.00101	0.61963
MS	0.9982	0.9982	0.9982	0.0001	0.61581	0.00102	0.61785
MS	0.9982	0.9982	0.0001	0.0001	0.58588	0.00099	0.58786
^{241}Pu	0.0001	0.0001	0.0001	0.0001	0.04905	0.00032	0.04969
^{241}Pu	0.9982	0.9982	0.9982	0.9982	0.71149	0.00112	0.71373
^{241}Pu	0.9982	0.9982	0.9982	0.0001	0.71256	0.0012	0.71496
^{241}Pu	0.9982	0.9982	0.0001	0.0001	0.68189	0.00118	0.68425

Table 6.7.1-8 PWR MOX Fuel Shipments - Summary of Maximum Reactivity Configurations

Fuel Material	Result	Accident Array – Preferentially Flooded	Normal Array – Preferentially Flooded	Normal Array – Dry	Single Cask Fully (Water) Reflected
UO_2	$k_{eff} + 2\sigma$	0.55404	0.49808	0.03425	0.49799
	EALCF (eV)	9.79E-02	8.83E-02	2.95E+05	8.81E-02
MS	$k_{eff} + 2\sigma$	0.70523	0.61963	0.04626	0.61886
	EALCF (eV)	1.25E-01	1.17E-01	2.14E+05	1.17E-01
^{241}Pu	$k_{eff} + 2\sigma$	0.81386	0.71496	0.04969	0.71398
	EALCF (eV)	1.33E-01	1.21E-01	8.72E+04	1.22E-01

Table 6.7.1-9 PWR MOX Fuel Shipments – PWR MOX Comparison to Area of Applicability

Parameter	Min	Max	MOX Services Materials	^{241}Pu Materials
EALCF (eV)	8.10E-02	8.99E-01	0.13	0.13
$^{235}U/^{238}U$ Weight Ratio	1.58E-03	1.51E+00	7.05E-03	7.05E-03
$^{238}Pu/^{238}U$ Weight Ratio	1.88E-06	1.54E-04	4.17E-05	0.0
$^{239}Pu/^{238}U$ Weight Ratio	1.39E-02	7.77E-01	7.92E-02	0.0
$^{240}Pu/^{238}U$ Weight Ratio	1.20E-03	8.48E-02	3.75E-03	0.0
$^{241}Pu/^{238}U$ Weight Ratio	7.90E-05	7.59E-03	3.34E-04	7.94E-02
$^{242}Pu/^{238}U$ Weight Ratio	4.63E-06	6.38E-04	4.17E-05	0.0
Water to Fuel Volume Ratio	1.10E+00	2.07E+01	1.43E+01	

Table 6.7.1-10 PWR MOX Fuel Shipments – UO_2 Comparison to Area of Applicability

Parameter	Min	Max	UO_2 Case
Enrichment (wt % ^{235}U)	2.35	4.738	5.0
Fuel rod pitch (cm)	1.3	2.54	3.0
Fuel pellet outer diameter (cm)	0.79	1.265	0.85/0.96
Fuel rod diameter (cm)	0.94	1.4172	0.93/1.12
H/^{235}U atom ratio	106.2	403.9	627 to 2140[1]
EALCF (eV)	0.09781	0.3447	0.0874

Table 6.7.1-11 Bounding Parameters for PWR MOX/UO_2 Rod Shipments

Parameter	Value
Fuel Form	Clad UO_2 or MOX rod
Number of Rods	16[2]
Clad Material	Zirconium Alloy
UO_2 Rods – Max. Enrichment (wt % ^{235}U)	5
MOX Rods – Max. Fissile Pu Content (wt %)	7[3]
Maximum Heavy Metal Content Per Rod (kg)	2.60
Maximum Pellet Diameter (inch)	0.3765
Maximum Active Fuel Length (inch)	153.5

[1] Dependent on pitch configuration (square or hexagonal).
[2] Mixture of UO_2 and MOX rods is permitted.
[3] Sum of ^{239}Pu and ^{241}Pu.

Table of Contents

List of Figures

List of Figures (continued)

6.6.15 PWR MOX Fuel Rods

This section contains truncated sample output files from the evaluation of MOX fuel rods in the NAC-LWT cask. The output files are shown in Figure 6.6.15-1 (MOX Services fuel composition in a hexagonal pitch) and Figure 6.6.15-2 (hexagonal pitch ^{241}Pu fuel composition). Included as Figure 6.6.15-3 is the MOX Services fuel composition case containing a square pitch rod lattice (3.8 cm pitch)..

Figure 6.6.15-1 Hexagonal Pitch MOX Rods – MOX Services Fuel Composition

```
        Thread Name & Version = MCNP5_RSICC, 1.30

 +---------------------------------------------------------------------+
 |   This program was prepared by the Regents of the University of     |
 |California at Los Alamos National Laboratory (the University) under  |
 |  contract number W-7405-ENG-36 with the U.S. Department of Energy    |
 |(DoE).  The University has certain rights in the program pursuant to|
 |  the contract and the program should not be copied or distributed    |
 | outside your organization.  All rights in the program are reserved  |
 |by the DoE and the University.  Neither the U.S. Government nor the  |
 | University makes any warranty, express or implied, or assumes any   |
 |     liability or responsibility for the use of this software.       |
 +---------------------------------------------------------------------+

1mcnp     version 5     ld=06212004                    10/25/07 21:05:56
 ********************************************************************                    probid =  10/25/07 21:05:56
 name=MS_Acc_NACCoC_c1.00_g0.00_e0.00_d0.01cm_HP_36mm.inp host=amdeng1-it1458

    1-       NAC-LWT Cask - MOX Experiments - Accident Transport Conditions
    2-       C
    3-       C EXCEL File Version: v2.00
    4-       C Run Version: v2.00
    5-       C
    6-       C Fissile Material Type: MOX Services
    7-       C Rod Interior Void Moderator Density: 0.9982 g/cc
    8-       C Canister Interior Moderator Density: 0.9982 g/cc
    9-       C Canister to Cask Gap Moderator Density: 0.0001 g/cc
   10-       C Cask Exterior Moderator Density: 0.0001 g/cc
   11-       C Boundary Condition / Distance:  Reflected / 0.01 cm
   12-       C
   13-       C Fuel Rod Pitch: 3.6 cm
   14-       C Fuel Rod Pitch Cofiguration: Hexagonal
   15-       C Number of Rods: 16
   16-       C
   17-       C Base Fuel Parameters: NACCoC
   18-       C
   19-       c Cells - Fuel Rod - NACCoC
   20-       1 1 -10.555 -1   u=3 $ Fuel
   21-       2 2 -0.9982 -2 +1  u=3 $ Plenum + Fuel to Clad Gap
   22-       3 3 -6.56 -3 +2  u=3 $ Clad + End Plugs
   23-       4 4 -0.9982 +3   u=3 $ Outside Fuel Rod
   24-       C 16 Rods - Hexagonal Pitch
   25-       10 4 -0.9982 -10
   26-                  *trcl=( 0.9000 -1.5588 0.0000 )
   27-                  lat=2 u=2 fill=-7:6 -5:5 0:0
   28-              2 2 2 2 2 2 2 2 2 2 2 2 2
   29-              2 2 2 2 2 2 2 2 2 2 2 2 2
   30-              2 2 2 2 2 2 2 2 2 2 2 2 2
   31-              2 2 2 2 2 2 2 3 2 2 2 2 2
   32-              2 2 2 2 2 2 3 3 3 2 2 2 2
   33-              2 2 2 2 2 3 3 3 3 3 2 2 2
   34-              2 2 2 2 2 3 3 3 3 3 2 2 2
   35-              2 2 2 2 2 3 3 3 3 2 2 2 2
   36-              2 2 2 2 2 2 2 2 2 2 2 2 2
   37-              2 2 2 2 2 2 2 2 2 2 2 2 2
   38-             2 2 2 2 2 2 2 2 2 2 2 2 2
   39-       C PWR Basket - Cells
   40-       20  4 -0.9982 -20   fill=2  u=1 $ Rod Array Container
   41-       21  5 -0.0001 +20 -21    u=1 $ Basket Cavity
   42-       22  7 -2.7020 -22 +21    u=1 $ Basket Body
   43-       23  5 -0.0001 +22     u=1 $ Outside
   44-       C Cells - LWT Cask Accident Conditions
   45-       40 8 -11.344 -43     u=0 $ BotPb
   46-       41 5 -0.0001 -42 fill=1    u=0 $ Cavity
   47-       42 9 -7.9400 -41 +43    u=0 $ Bottom
   48-       43 9 -7.9400 -40 +41 +45 +48 +42 u=0 $ OuterShell
   49-       44 9 -7.9400 -44 +47 +42   u=0 $ InnerShellTaper
   50-       45 9 -7.9400 -46 +42    u=0 $ InnerShell
   51-       46 8 -11.344 -47 +46    u=0 $ Lead
   52-       47 8 -11.344 -45 +44 +47   u=0 $ LeadTaper
   53-       48 0         -48 +47    u=0 $ LeadGap
   54-       49 6 -0.0001 -49 +40    u=0 $ Gap to Reflector
   55-       50 0          +49    u=0 $ Boundary
   56-
   57-       c Surfaces - Fuel Rod - NACCoC
   58-       1 RCC 0.0000 0.0000 10.5207 0.0000 0.0000 389.8900 0.4781   $ Fuel pellet stack
   59-       2 RCC 0.0000 0.0000 6.3990 0.0000 0.0000 409.4227 0.4876   $ Annulus + Plenum
   60-       3 RCC 0.0000 0.0000 5.0800 0.0000 0.0000 411.8226 0.5588   $ Clad + End-Caps
   61-       c Surfaces - Pitch - NACCoC
   62-       10 RHP 0.0000 0.0000 -1.0000 0.0000 0.0000 454.12 1.8000 0.0000 0.0000 $ Lattice
   63-       C PWR Basket - Surfaces
   64-       20 1 RPP -7.4148 7.4148 -7.4148 7.4148 0.0000 452.1200  $ Array Container
   65-       21 1 RPP -11.2713 11.2713 -11.2713 11.2713 0.0000 452.1200  $ Basket Opening
   66-       22  RCC 0.0000 0.0000 0.0000 0.0000 0.0000 452.1200 16.83512 $ Basket Outer Body
   67-       C Surfaces - LWT Cask Accident Conditions
   68-       40 RCC 0.0000 0.0000 -26.6700 0.0000 0.0000 507.3650 36.5189 $ Lwt Body
   69-       41 RCC 0.0000 0.0000 -26.6700 0.0000 0.0000 26.6700 36.5189 $ Bottom
   70-       42 RCC 0.0000 0.0000 0.0000 0.0000 0.0000 452.1200 16.9863 $ Cavity
```

```
 71-       43 RCC 0.0000 0.0000 -17.7800 0.0000 0.0000 7.6200 26.3525 $ Bottom gamma shield
 72-       44 RCC 0.0000 0.0000 0.0000 0.0000 0.0000 444.5000 20.1740 $ Lead id - taper
 73-       45 RCC 0.0000 0.0000 0.0000 0.0000 0.0000 444.5000 31.5976 $ Lead od - taper
 74-       46 RCC 0.0000 0.0000 13.8176 0.0000 0.0000 416.8648 18.9103 $ Lead id
 75-       47 RCC 0.0000 0.0000 13.8176 0.0000 0.0000 416.8648 33.3271 $ Lead od
 76-       48 RCC 0.0000 0.0000 13.8176 0.0000 0.0000 416.8648 33.4645 $ Lead gap
 77-       *49 RPP -36.5289 36.5289 -36.5289 36.5289 -26.6800 480.7050  $ Container
 78-
 79-       c
 80-       c Materials List
 81-       c
 82-       C MOX Material Composition Fuel
 83-       m1     92235 -5.6994E-03
 84-              92238 -8.0851E-01
 85-              94238 -3.3724E-05
 86-              94239 -6.4076E-02
 87-              94240 -3.0352E-03
 88-              94241 -2.6980E-04
 89-              94242 -3.3724E-05
 90-               8016 -1.1835E-01
 91-       C Rod Interior Void Material
 92-       m2     1001 2
 93-              8016 1
 94-       mt2      lwtr.01
 95-       c Clad Material
 96-       m3 26054 -7.063E-05 24050 -4.179E-05 7014 -4.980E-04
 97-              26056 -1.149E-03 24052 -8.370E-04 7015 -1.981E-06
 98-              26057 -2.702E-05 24053 -9.673E-05
 99-              26058 -3.631E-06 24054 -2.448E-05
100-              40000 -9.823E-01 50000 -1.500E-02
101-       C Canister Interior Non-Fuel Space
102-       m4     1001 2
103-              8016 1
104-       mt4      lwtr.01
105-       C Canister to Cask Gap Material
106-       m5     1001 2
107-              8016 1
108-       mt5      lwtr.01
109-       C Cask Exterior Material
110-       m6     1001 2
111-              8016 1
112-       mt6      lwtr.01
113-       c Aluminum
114-       m7 13027 -1.000E+00
115-       C Water/Glycol
116-       m10    1001 -1.03651E-01
warning. material  10 is not used in the problem.
117-              8016 -6.75619E-01
118-              6000 -2.20730E-01
119-       mt10     lwtr.01
warning. material  10 is not used in the problem.
120-       c Lead
121-       m8 82206 -2.534E-01
122-              82207 -2.207E-01
123-              82208 -5.259E-01
124-       c SS304
125-       m9 24050 -7.939E-03 26054 -3.927E-02 28058 -6.384E-02
126-              24052 -1.590E-01 26056 -6.387E-01 28060 -2.543E-02
127-              24053 -1.838E-02 26057 -1.502E-02 28061 -1.124E-03
128-              24054 -4.652E-03 26058 -2.019E-03 28062 -3.639E-03
129-                  28064 -9.623E-04
130-              25055 -2.000E-02
131-       C Aluminum Honeycomb Impact Limiter
132-       m11    13027 -1.0
warning. material  11 is not used in the problem.
133-       C Mode
134-       mode n
135-       C Cell Importances
136-       imp:n 1 18r 0
137-       C
138-       C Criticality Controls
139-       kcode 1000 0.80 30 530
140-       C
141-       C Starting Source Definition
142-       sdef cell=41:20:10:1
143-            erg=d1
144-            pos=0 0 10.5207
145-            rad=d2
146-            axs=0 0 1
147-            ext=d3
148-       sp1    -3
149-       si2 0.0000 0.4781
150-       sp2 -21 1
151-       si3 0.0000 389.8900
152-       sp3 0 1
153-       C Print Control
154-       print
155-       C Random Number Generator
156-       rand gen=2 seed=19073486328125 stride=152917 hist=1
157-       c
158-       c Rotation Matrix
159-       *TR1 0.0 0.0 0.0 -30 60 90 -120 -30 90 90 90 0  $ z-rotation -30 degrees

1source                                                                    print table 10

 values of defaulted or explicitly defined source variables
```

```
   sur         0.0000E+00
   tme         0.0000E+00
   dir         isotropic
   pos         0.0000E+00   0.0000E+00   1.0521E+01
   x           0.0000E+00
   y           0.0000E+00
   z           0.0000E+00
   axs         0.0000E+00   0.0000E+00   1.0000E+00
   vec         0.0000E+00   0.0000E+00   0.0000E+00
   ccc         0.0000E+00
   nrm         1.0000E+00
   ara         0.0000E+00
   wgt         1.0000E+00
   eff         1.0000E-02
   par         0.0000E+00
   tr          0.0000E+00


probability distribution   1 for source variable erg
energy function 3:  watt (fission) spectrum (endf law 10)

    f(e)=c*exp(-e/a)*sinh(sqrt(b*e))
    a = 9.6500E-01     b = 2.2900E+00     c = 4.5270E-01

    the mean of source distribution   1 is  1.9806E+00


probability distribution   2 for source variable rad
power law 21:     f(x)=c*abs(x)**k          k = 1.0000E+00


probability distribution   3 for source variable ext
unbiased histogram distribution

source        source           cumulative          probability
 entry         value           probability           of bin

   1       0.00000E+00        0.000000E+00        0.000000E+00
   2       3.89890E+02        1.000000E+00        1.000000E+00

    the mean of source distribution   3 is  1.9494E+02

order of sampling source variables.
cel axs rad ext pos erg tme

comment. total fission nubar data are being used.
1material composition                                                    print table 40

the sum of the fractions of material    2 was 3.000000E+00

the sum of the fractions of material    3 was 1.000050E+00

the sum of the fractions of material    4 was 3.000000E+00

the sum of the fractions of material    5 was 3.000000E+00

the sum of the fractions of material    6 was 3.000000E+00

the sum of the fractions of material    9 was 9.999753E-01

material
 number     component nuclide, atom fraction

    1           92235, 2.18414E-03      92238, 3.05926E-01      94238, 1.27607E-05      94239, 2.41437E-02
                94240, 1.13889E-03      94241, 1.00815E-04      94242, 1.25493E-05       8016, 6.66481E-01
    2            1001, 6.66667E-01       8016, 3.33333E-01
associated thermal s(a,b) data sets:    lwtr.01t
    3           26054, 1.19346E-04      24050, 7.62600E-05       7014, 3.24139E-03      26056, 1.87224E-03
                24052, 1.46874E-03       7015, 1.20369E-05      26057, 4.32542E-05      24053, 1.66532E-04
                26058, 5.71247E-06      24054, 4.13652E-05      40000, 9.81436E-01      50000, 1.15166E-02
    4            1001, 6.66667E-01       8016, 3.33333E-01
associated thermal s(a,b) data sets:    lwtr.01t
    5            1001, 6.66667E-01       8016, 3.33333E-01
associated thermal s(a,b) data sets:    lwtr.01t
    6            1001, 6.66667E-01       8016, 3.33333E-01
associated thermal s(a,b) data sets:    lwtr.01t
    7           13027, 1.00000E+00
    8           82206, 2.54963E-01      82207, 2.20987E-01      82208, 5.24050E-01
    9           24050, 8.79087E-03      26054, 4.02643E-02      28058, 6.09419E-02      24052, 1.69300E-01
                26056, 6.31511E-01      28060, 2.34673E-02      24053, 1.92010E-02      26057, 1.45900E-02
                28061, 1.02022E-03      24054, 4.76985E-03      26058, 1.92741E-03      28062, 3.24982E-03
                28064, 8.32505E-04      25055, 2.01337E-02
1material                                                                print table 40
 number     component nuclide, mass fraction

    1           92235, 5.69936E-03      92238, 8.08504E-01      94238, 3.37237E-05      94239, 6.40755E-02
                94240, 3.03518E-03      94241, 2.69798E-04      94242, 3.37237E-05       8016, 1.18349E-01
    2            1001, 1.11915E-01       8016, 8.88085E-01
    3           26054, 7.06265E-05      24050, 4.17879E-05       7014, 4.97975E-04      26056, 1.14894E-03
                24052, 8.36958E-04       7015, 1.98090E-06      26057, 2.70186E-05      24053, 9.67251E-05
                26058, 3.63082E-06      24054, 2.44788E-05      40000, 9.82251E-01      50000, 1.49992E-02
    4            1001, 1.11915E-01       8016, 8.88085E-01
    5            1001, 1.11915E-01       8016, 8.88085E-01
```

6	1001, 1.11915E-01	8016, 8.88085E-01		
7	13027, 1.00000E+00			
8	82206, 2.53400E-01	82207, 2.20700E-01	82208, 5.25900E-01	
9	24050, 7.93920E-03	26054, 3.92710E-02	28058, 6.38416E-02	24052, 1.59004E-01
	26056, 6.38716E-01	28060, 2.54306E-02	24053, 1.83805E-02	26057, 1.50204E-02
	28061, 1.12403E-03	24054, 4.65211E-03	26058, 2.01905E-03	28062, 3.63909E-03
	28064, 9.62324E-04	25055, 2.00005E-02		

warning. 6 materials had unnormalized fractions. print table 40.

1cell volumes and masses print table 50

cell	atom density	gram density	input volume	calculated volume	mass	pieces	reason volume not calculated
1	7.05663E-02	1.05550E+01	0.00000E+00	2.79982E+02	2.95521E+03	1	
2	1.00128E-01	9.98200E-01	0.00000E+00	2.58267E+01	2.57802E+01	1	
3	4.33411E-02	6.56000E+00	0.00000E+00	9.81838E+01	6.44086E+02	1	
4	1.00128E-01	9.98200E-01	0.00000E+00	0.00000E+00	0.00000E+00	0	infinite
5	1.00128E-01	9.98200E-01	0.00000E+00	5.09690E+03	5.08773E+03	0	
6	1.00128E-01	9.98200E-01	0.00000E+00	9.94289E+04	9.92499E+04	0	
7	1.00309E-05	1.00000E-04	0.00000E+00	1.30324E+05	1.30324E+01	0	
8	6.03063E-02	2.70200E+00	0.00000E+00	0.00000E+00	0.00000E+00	0	asymmetric
9	1.00309E-05	1.00000E-04	0.00000E+00	0.00000E+00	0.00000E+00	0	infinite
40	3.29629E-02	1.13440E+01	0.00000E+00	1.66245E+04	1.88588E+05	1	
41	1.00309E-05	1.00000E-04	0.00000E+00	4.09828E+05	4.09828E+01	1	
42	8.64586E-02	7.94000E+00	0.00000E+00	9.51154E+04	7.55216E+05	1	
43	8.64586E-02	7.94000E+00	0.00000E+00	4.53784E+05	3.60304E+06	1	
44	8.64586E-02	7.94000E+00	0.00000E+00	1.02842E+04	8.16563E+04	2	
45	8.64586E-02	7.94000E+00	0.00000E+00	9.04489E+04	7.18165E+05	1	
46	3.29629E-02	1.13440E+01	0.00000E+00	9.86269E+05	1.11882E+07	1	
47	3.29629E-02	1.13440E+01	0.00000E+00	5.13461E+04	5.82470E+05	2	
48	0.00000E+00	0.00000E+00	0.00000E+00	1.20186E+04	0.00000E+00	1	
49	1.00309E-05	1.00000E-04	0.00000E+00	0.00000E+00	0.00000E+00	0	asymmetric
50	0.00000E+00	0.00000E+00	0.00000E+00	0.00000E+00	0.00000E+00	0	infinite

warning. 2 cells appear to consist of more than one piece.

1surface areas print table 50

surface	input area	calculated area	reason area not calculated
1.1	0.00000E+00	1.17123E+03	
1.2	0.00000E+00	7.18104E-01	
1.3	0.00000E+00	7.18104E-01	
2.1	0.00000E+00	1.25434E+03	
2.2	0.00000E+00	7.46925E-01	
2.3	0.00000E+00	7.46925E-01	
3.1	0.00000E+00	1.44593E+03	
3.2	0.00000E+00	9.80986E-01	
3.3	0.00000E+00	9.80986E-01	
10.1	0.00000E+00	0.00000E+00	not a boundary
10.2	0.00000E+00	0.00000E+00	not a boundary
10.3	0.00000E+00	0.00000E+00	not a boundary
10.4	0.00000E+00	0.00000E+00	not a boundary
10.5	0.00000E+00	0.00000E+00	not a boundary
10.6	0.00000E+00	0.00000E+00	not a boundary
10.7	0.00000E+00	1.12237E+01	
10.8	0.00000E+00	1.12237E+01	
20.1	0.00000E+00	6.70476E+03	
20.2	0.00000E+00	6.70476E+03	
20.3	0.00000E+00	6.70476E+03	
20.4	0.00000E+00	6.70476E+03	
20.5	0.00000E+00	0.00000E+00	asymmetric
20.6	0.00000E+00	0.00000E+00	asymmetric
21.1	0.00000E+00	1.01920E+04	
21.2	0.00000E+00	1.01920E+04	
21.3	0.00000E+00	1.01920E+04	
21.4	0.00000E+00	1.01920E+04	
22.1	0.00000E+00	4.78244E+04	
40.1	0.00000E+00	1.16417E+05	
40.2	0.00000E+00	4.18972E+03	
40.3	0.00000E+00	4.18972E+03	
42.1	0.00000E+00	4.82539E+04	
43.1	0.00000E+00	1.26170E+03	
43.2	0.00000E+00	2.18169E+03	
43.3	0.00000E+00	2.18169E+03	
44.1	0.00000E+00	3.50295E+03	
44.2	0.00000E+00	2.23013E+03	
45.1	0.00000E+00	5.48652E+03	
46.1	0.00000E+00	4.95306E+04	
46.2	0.00000E+00	2.61173E+03	
46.3	0.00000E+00	2.61173E+03	
47.1	0.00000E+00	8.72916E+04	
48.1	0.00000E+00	8.76515E+04	
49.1	0.00000E+00	3.70684E+04	
49.2	0.00000E+00	3.70684E+04	
49.3	0.00000E+00	3.70684E+04	
49.4	0.00000E+00	3.70684E+04	
49.5	0.00000E+00	5.33744E+03	
49.6	0.00000E+00	5.33744E+03	
10010.1	0.00000E+00	9.43871E+02	
10010.2	0.00000E+00	9.43871E+02	
10010.3	0.00000E+00	9.43871E+02	
10010.4	0.00000E+00	9.43871E+02	
10010.5	0.00000E+00	9.43871E+02	
10010.6	0.00000E+00	9.43871E+02	

1cells print table 60

	cell	mat	atom density	gram density	volume	mass	pieces	neutron importance
1	1	1	7.05663E-02	1.05550E+01	2.79982E+02	2.95521E+03	1	1.0000E+00
2	2	2s	1.00128E-01	9.98200E-01	2.58267E+01	2.57802E+01	1	1.0000E+00
3	3	3	4.33411E-02	6.56000E+00	9.81838E+01	6.44086E+02	1	1.0000E+00
4	4	4s	1.00128E-01	9.98200E-01	0.00000E+00	0.00000E+00	0	1.0000E+00
5	10	4s	1.00128E-01	9.98200E-01	5.09690E+03	5.08773E+03	0	1.0000E+00
6	20	4s	1.00128E-01	9.98200E-01	9.94289E+04	9.92499E+04	0	1.0000E+00
7	21	5s	1.00309E-05	1.00000E-04	1.30324E+05	1.30324E+01	0	1.0000E+00
8	22	7	6.03063E-02	2.70200E+00	0.00000E+00	0.00000E+00	0	1.0000E+00
9	23	5s	1.00309E-05	1.00000E-04	0.00000E+00	0.00000E+00	0	1.0000E+00
10	40	8	3.29629E-02	1.13440E+01	1.66245E+04	1.88588E+05	1	1.0000E+00
11	41	5s	1.00309E-05	1.00000E-04	4.09828E+05	4.09828E+01	1	1.0000E+00
12	42	9	8.64586E-02	7.94000E+00	9.51154E+04	7.55216E+05	1	1.0000E+00
13	43	9	8.64586E-02	7.94000E+00	4.53784E+05	3.60304E+06	1	1.0000E+00
14	44	9	8.64586E-02	7.94000E+00	1.02842E+04	8.16563E+04	2	1.0000E+00
15	45	9	8.64586E-02	7.94000E+00	9.04489E+04	7.18165E+05	1	1.0000E+00
16	46	8	3.29629E-02	1.13440E+01	9.86269E+05	1.11882E+07	1	1.0000E+00
17	47	8	3.29629E-02	1.13440E+01	5.13461E+04	5.82470E+05	2	1.0000E+00
18	48	0	0.00000E+00	0.00000E+00	1.20186E+04	0.00000E+00	1	1.0000E+00
19	49	6s	1.00309E-05	1.00000E-04	0.00000E+00	0.00000E+00	0	1.0000E+00
20	50	0	0.00000E+00	0.00000E+00	0.00000E+00	0.00000E+00	0	0.0000E+00
total					2.36097E+06	1.72254E+07		

1surfaces print table 70

	surface	trans	type	surface coefficients			
1	1		rcc				
2	1.1		cz	4.7810000E-01			
3	1.2		pz	4.0041070E+02			
4	1.3		p	0.0000000E+00	0.0000000E+00	-1.0000000E+00	-1.0520700E+01
5	2		rcc				
6	2.1		cz	4.8760000E-01			
7	2.2		pz	4.1582170E+02			
8	2.3		p	0.0000000E+00	0.0000000E+00	-1.0000000E+00	-6.3990000E+00
9	3		rcc				
10	3.1		cz	5.5880000E-01			
11	3.2		pz	4.1690260E+02			
12	3.3		p	0.0000000E+00	0.0000000E+00	-1.0000000E+00	-5.0800000E+00
13	10		rhp				
14	10.1		px	1.8000000E+00			
15	10.2		p	-1.0000000E+00	0.0000000E+00	0.0000000E+00	1.8000000E+00
16	10.3		p	5.0000000E-01	8.6602540E-01	0.0000000E+00	1.8000000E+00
17	10.4		p	-5.0000000E-01	-8.6602540E-01	0.0000000E+00	1.8000000E+00
18	10.5		p	-5.0000000E-01	8.6602540E-01	0.0000000E+00	1.8000000E+00
19	10.6		p	5.0000000E-01	-8.6602540E-01	0.0000000E+00	1.8000000E+00
20	10.7		pz	4.5312000E+02			
21	10.8		p	0.0000000E+00	0.0000000E+00	-1.0000000E+00	1.0000000E+00
22	20		rpp				
23	20.1	1	p	8.6602540E-01	5.0000000E-01	0.0000000E+00	7.4148000E+00
24	20.2	1	p	-8.6602540E-01	-5.0000000E-01	0.0000000E+00	7.4148000E+00
25	20.3	1	p	-5.0000000E-01	8.6602540E-01	0.0000000E+00	7.4148000E+00
26	20.4	1	p	5.0000000E-01	-8.6602540E-01	0.0000000E+00	7.4148000E+00
27	20.5	1	pz	4.5212000E+02			
28	20.6	1	p	0.0000000E+00	0.0000000E+00	-1.0000000E+00	0.0000000E+00
29	21		rpp				
30	21.1	1	p	8.6602540E-01	5.0000000E-01	0.0000000E+00	1.1271300E+01
31	21.2	1	p	-8.6602540E-01	-5.0000000E-01	0.0000000E+00	1.1271300E+01
32	21.3	1	p	-5.0000000E-01	8.6602540E-01	0.0000000E+00	1.1271300E+01
33	21.4	1	p	5.0000000E-01	-8.6602540E-01	0.0000000E+00	1.1271300E+01
36	22		rcc				
37	22.1		cz	1.6835120E+01			
40	40		rcc				
41	40.1		cz	3.6518900E+01			
42	40.2		pz	4.8069500E+02			
43	40.3		p	0.0000000E+00	0.0000000E+00	-1.0000000E+00	2.6670000E+01
44	41		rcc				
48	42		rcc				
49	42.1		cz	1.6986300E+01			
52	43		rcc				
53	43.1		cz	2.6352500E+01			
54	43.2		pz	-1.0160000E+01			
55	43.3		p	0.0000000E+00	0.0000000E+00	-1.0000000E+00	1.7780000E+01
56	44		rcc				
57	44.1		cz	2.0174000E+01			
58	44.2		pz	4.4450000E+02			
60	45		rcc				
61	45.1		cz	3.1597600E+01			
64	46		rcc				
65	46.1		cz	1.8910300E+01			
66	46.2		pz	4.3068240E+02			
67	46.3		p	0.0000000E+00	0.0000000E+00	-1.0000000E+00	-1.3817600E+01
68	47		rcc				
69	47.1		cz	3.3327100E+01			
72	48		rcc				
73	48.1		cz	3.3464500E+01			
76	49	refl.	rpp				
77	49.1	refl.	px	3.6528900E+01			
78	49.2	refl.	p	-1.0000000E+00	0.0000000E+00	0.0000000E+00	3.6528900E+01
79	49.3	refl.	py	3.6528900E+01			
80	49.4	refl.	p	0.0000000E+00	-1.0000000E+00	0.0000000E+00	3.6528900E+01
81	49.5	refl.	pz	4.8070500E+02			
82	49.6	refl.	p	0.0000000E+00	0.0000000E+00	-1.0000000E+00	2.6680000E+01
83	10010		rhp				

```
    84  10010.1       1001   px    2.7000000E+00
    85  10010.2       1001   p    -1.0000000E+00   0.0000000E+00   0.0000000E+00   9.0000000E-01
    86  10010.3       1001   p     5.0000000E-01   8.6602540E-01   0.0000000E+00   9.0003960E-01
    87  10010.4       1001   p    -5.0000000E-01  -8.6602540E-01   0.0000000E+00   2.6999604E+00
    88  10010.5       1001   p    -5.0000000E-01   8.6602540E-01   0.0000000E+00   3.9600581E-05
    89  10010.6       1001   p     5.0000000E-01  -8.6602540E-01   0.0000000E+00   3.5999604E+00
1  identical surfaces                                                                    print table 70

   master surface     identical surfaces

       10.7           10010.7
       10.8           10010.8
       20.5              21.5      22.2      42.2
       20.6              21.6      22.3      41.2      42.3      44.3      45.3
       40.1              41.1
       40.3              41.3
       44.2              45.2
       46.2              47.2      48.2
       46.3              47.3      48.3


   surface coefficients for identical surfaces not used.

         surface     trans  type   surface coefficients

    90  10010.7       1001   pz    4.5312000E+02
    91  10010.8       1001   p     0.0000000E+00   0.0000000E+00  -1.0000000E+00   1.0000000E+00
    34     21.5          1   pz    4.5212000E+02
    38     22.2              pz    4.5212000E+02
    50     42.2              pz    4.5212000E+02
    35     21.6          1   p     0.0000000E+00   0.0000000E+00  -1.0000000E+00   0.0000000E+00
    39     22.3              p     0.0000000E+00   0.0000000E+00  -1.0000000E+00   0.0000000E+00
    46     41.2              pz    0.0000000E+00
    51     42.3              p     0.0000000E+00   0.0000000E+00  -1.0000000E+00   0.0000000E+00
    59     44.3              p     0.0000000E+00   0.0000000E+00  -1.0000000E+00   0.0000000E+00
    63     45.3              p     0.0000000E+00   0.0000000E+00  -1.0000000E+00   0.0000000E+00
    45     41.1              cz    3.6518900E+01
    47     41.3              p     0.0000000E+00   0.0000000E+00  -1.0000000E+00   2.6670000E+01
    62     45.2              pz    4.4450000E+02
    70     47.2              pz    4.3068240E+02
    74     48.2              pz    4.3068240E+02
    71     47.3              p     0.0000000E+00   0.0000000E+00  -1.0000000E+00  -1.3817600E+01
    75     48.3              p     0.0000000E+00   0.0000000E+00  -1.0000000E+00  -1.3817600E+01
1  cell temperatures in mev for the free-gas thermal neutron treatment.                  print table 72

   all non-zero importance cells with materials have a temperature for thermal neutrons of 2.5300E-08 mev.

 ************************************************
 * Random Number Generator  =                 2 *
 * Random Number Seed       =       19073486328125 *
 * Random Number Multiplier =  9219741426499971445 *
 * Random Number Adder      =                 1 *
 * Random Number Bits Used  =                63 *
 * Random Number Stride     =            152917 *
 ************************************************


        5 warning messages so far.
1physical constants                                                                     print table 98

   name                    value     description

   huge      1.0000000000000E+36     infinity
    pie      3.1415926535898E+00     pi
  euler      5.7721566490153E-01     euler constant
 avogad      6.0220434469282E+23     avogadro number (molecules/mole)
  aneut      1.0086649670000E+00     neutron mass (amu)
  avgdn      5.9703109000000E-01     avogadro number/neutron mass (1.e-24*molecules/mole/amu)
  slite      2.9979250000000E+02     speed of light (cm/shake)
 planck      4.1357320000000E-13     planck constant (mev shake)
  fscon      1.3703930000000E+02     inverse fine structure constant h*c/(2*pi*e**2)
 gpt(1)      9.3958000000000E+02     neutron mass (mev)
 gpt(3)      5.1100800000000E-01     electron mass (mev)


 fission q-values:     nuclide    q(mev)    nuclide    q(mev)
                         90232    171.91      91233    175.57
                         92233    180.84      92234    179.45
                         92235    180.88      92236    179.50
                         92237    180.40      92238    181.31
                         92239    180.40      92240    180.40
                         93237    183.67      94238    186.65
                         94239    189.44      94240    186.36
                         94241    188.99      94242    185.98
                         94243    187.48      95241    190.83
                         95242    190.54      95243    190.25
                         96242    190.49      96244    190.49
                         other    180.00


 the following compilation options were used:

     cheap
     dec
     plot
     mcplot
```

```
     xlib
     default datapath: C:\Program Files\LANL\MCNPDATA
                       C:\Progra~1\LANL\MCNPdata
1cross-section tables                                                                    print table 100

     table    length

                      tables from file actia

   1001.62c     5202  1-h-1 at 293.6K from endf-vi.8 njoy99.50                          mat 125      12/05/01
   7014.62c    67462  7-n-14 at 293.6K from endf-vi.8 njoy99.50                         mat 725      12/05/01
   8016.62c   170541  8-o-16 at 293.6K from endf-vi.8 njoy99.50                         mat 825      12/05/01
  13027.62c    75363  13-al-27 at 293.6K from endf-vi.8 njoy99.50                      mat1325      12/17/01
  24050.62c   194445  24-cr-50 at 293.6K from endf-vi.8 njoy99.50                      mat2425      12/20/01
  24052.62c   174773  24-cr-52 at 293.6K from endf-vi.8 njoy99.50                      mat2431      12/20/01
  24053.62c   147286  24-cr-53 at 293.6K from endf-vi.8 njoy99.50                      mat2434      12/20/01
  24054.62c   132737  24-cr-54 at 293.6K from endf-vi.8 njoy99.50                      mat2437      12/20/01
  25055.62c   134565  25-mn-55 at 293.6K from endf/b-vi.8 njoy99.50                    mat2525      02/11/02
  26054.62c   143370  26-fe-54 at 293.6K from endf-vi.8 njoy99.50                      mat2625      12/20/01
  26056.62c   230655  26-fe-56 at 293.6K from endf-vi.8 njoy99.50                      mat2631      12/20/01
  26057.62c   148842  26-fe-57 at 293.6K from endf-vi.8 njoy99.50                      mat2634      12/20/01
  26058.62c    87569  26-fe-58 at 293.6K from endf-vi.8 njoy99.50                      mat2637      12/20/01
  28058.62c   235403  28-ni-58 at 293.6K from endf-vi.8 njoy99.50                      mat2825      12/20/01
  28060.62c   158305  28-ni-60 at 293.6K from endf-vi.8 njoy99.50                      mat2831      12/20/01
  28061.62c   112032  28-ni-61 at 293.6K from endf-vi.8 njoy99.50                      mat2834      12/20/01
  28062.62c   104386  28-ni-62 at 293.6K from endf-vi.8 njoy99.50                      mat2837      12/20/01
  28064.62c    97689  28-ni-64 at 293.6K from endf-vi.8 njoy99.50                      mat2843      12/20/01

                      tables from file endf66a

   7015.66c    19013  7-n-15 at 293.6K from endf-vi.0 njoy99.50                         mat 728      07/13/01

                      tables from file endf66b

  40000.66c    98524  40-zr-0 at 293.6K from endf-vi.1 njoy99.50                        mat4000      07/24/01

                      tables from file endl92

  50000.42c   141628   ENDL library name:  nd920609  LANL/XTM modified:  951222                    911219
                     temperature = 2.5860E-08 adjusted to 2.5300E-08

                      tables from file endf66c

  82206.66c   219368  82-pb-206 at 293.6K from endf-vi.6 njoy99.50                       mat8231      08/13/01
  82207.66c   134389  82-pb-207 at 293.6K from endf-vi.6 njoy99.50                       mat8234      08/13/01
  82208.66c   135105  82-pb-208 at 293.6K from endf-vi.x njoy99.50                       mat8237      03/16/02
  94238.66c    53256  94-pu-238 at 293.6K from endf-vi.0 njoy99.50       total nu       mat9434      09/06/01
                     probability tables used from 2.0000E-04 to 1.0000E-02 mev.
  94240.66c   309518  94-pu-240 at 293.6K from endf-vi.2 njoy99.50       total nu       mat9440      09/06/01
                     probability tables used from 5.7000E-03 to 4.0000E-02 mev.
  94241.66c   126607  94-pu-241 at 293.6K from endf-vi.3 njoy99.50       total nu       mat9443      09/06/01
                     probability tables used from 3.0000E-04 to 4.0200E-02 mev.
  94242.66c   107114  94-pu-242 at 293.6K from endf-vi.0 njoy99.50       total nu       mat9446      09/06/01
                     probability tables used from 9.8600E-04 to 1.0000E-02 mev.

                      tables from file t16_2003

  92235.69c   587997  92-u-235 at 293.6K from t16 u2351a9d njoy99.50     total nu       mat9228      07/02/03
                     probability tables used from 2.2500E-03 to 2.5000E-02 mev.
  92238.69c   713320  92-u-238 at 293.6K from t16 u2381a8h njoy99.50     total nu       mat9237      07/02/03
                     probability tables used from 1.0000E-02 to 1.4903E-01 mev.
  94239.69c   506320  94-pu-239 at 293.6K from t16 pu2391a7d njoy99.50   total nu       mat9437      07/02/03
                     probability tables used from 2.5000E-03 to 3.0000E-02 mev.

                      tables from file tmccs

   lwtr.01t    10193  hydrogen in light water at 300 degrees kelvin                1001     0     010/22/85

  total      5582977

 warning. neutron energy cutoff is below some cross-section tables.

 comment.    1 cross sections modified by free gas thermal treatment.
1assignment of s(a,b) data to nuclides.                                                  print table 102

       mat        nuclide         s(a,b)
         2       1001.62c       lwtr.01t
         4       1001.62c       lwtr.01t
         5       1001.62c       lwtr.01t
         6       1001.62c       lwtr.01t

 ************************************************************************************************************************
 dump no.     1 on file MS_Acc_NACCoC_c1.00_g0.00_e0.00_d0.01cm_HP_36mm.inpr       nps =           0     coll =             0
ctm =        0.00   nrn =                0

        6 warning messages so far.
1estimated keff results by cycle                                                         print table 175

 cycle     1    k(collision)  0.662630    prompt removal lifetime(abs)  8.1191E+03    source points generated    844

 cycle     2    k(collision)  0.622585    prompt removal lifetime(abs)  8.6526E+03    source points generated    928

 cycle     3    k(collision)  0.744636    prompt removal lifetime(abs)  8.5012E+03    source points generated   1189

 cycle     4    k(collision)  0.686479    prompt removal lifetime(abs)  7.9407E+03    source points generated    916
```

```
cycle     5    k(collision)  0.671615    prompt removal lifetime(abs)  8.8591E+03    source points generated    972

cycle     6    k(collision)  0.675550    prompt removal lifetime(abs)  8.2834E+03    source points generated    999

cycle     7    k(collision)  0.693864    prompt removal lifetime(abs)  8.1740E+03    source points generated   1052

cycle     8    k(collision)  0.702859    prompt removal lifetime(abs)  8.6663E+03    source points generated   1006
```

estimator	cycle 526	ave of 496 cycles	combination	simple average	combined average	corr
k(collision)	0.741770	0.703646 0.0016	k(col/abs)	0.703392 0.0015	0.703372 0.0015	0.7953
k(absorption)	0.756647	0.703139 0.0016	k(abs/tk ln)	0.703262 0.0016	0.703196 0.0015	0.4218
k(trk length)	0.717143	0.703386 0.0022	k(tk ln/col)	0.703516 0.0017	0.703605 0.0016	0.5823
rem life(col)	8.4284E+03	8.4718E+03 0.0017	k(col/abs/tk ln)	0.703390 0.0015	0.703328 0.0015	
rem life(abs)	8.3911E+03	8.4726E+03 0.0016	life(col/abs/tl)	8.4742E+03 0.0015	8.4796E+03 0.0013	

source points generated 1046

estimator	cycle 527	ave of 497 cycles	combination	simple average	combined average	corr
k(collision)	0.643842	0.703525 0.0016	k(col/abs)	0.703297 0.0015	0.703275 0.0015	0.7960
k(absorption)	0.668059	0.703068 0.0016	k(abs/tk ln)	0.703158 0.0016	0.703110 0.0015	0.4250
k(trk length)	0.634707	0.703247 0.0022	k(tk ln/col)	0.703386 0.0017	0.703482 0.0016	0.5863
rem life(col)	8.2199E+03	8.4713E+03 0.0017	k(col/abs/tk ln)	0.703280 0.0015	0.703227 0.0015	
rem life(abs)	8.1559E+03	8.4720E+03 0.0016	life(col/abs/tl)	8.4737E+03 0.0015	8.4793E+03 0.0013	

source points generated 869

estimator	cycle 528	ave of 498 cycles	combination	simple average	combined average	corr
k(collision)	0.717239	0.703553 0.0016	k(col/abs)	0.703307 0.0015	0.703282 0.0015	0.7956
k(absorption)	0.699228	0.703060 0.0016	k(abs/tk ln)	0.703150 0.0016	0.703102 0.0015	0.4250
k(trk length)	0.699455	0.703240 0.0022	k(tk ln/col)	0.703396 0.0017	0.703504 0.0016	0.5860
rem life(col)	8.7750E+03	8.4719E+03 0.0017	k(col/abs/tk ln)	0.703284 0.0015	0.703229 0.0015	
rem life(abs)	8.6882E+03	8.4724E+03 0.0016	life(col/abs/tl)	8.4741E+03 0.0015	8.4795E+03 0.0013	

source points generated 1119

estimator	cycle 529	ave of 499 cycles	combination	simple average	combined average	corr
k(collision)	0.699031	0.703544 0.0016	k(col/abs)	0.703286 0.0015	0.703261 0.0015	0.7954
k(absorption)	0.686971	0.703028 0.0016	k(abs/tk ln)	0.703156 0.0016	0.703088 0.0015	0.4238
k(trk length)	0.725578	0.703285 0.0022	k(tk ln/col)	0.703414 0.0017	0.703503 0.0016	0.5854
rem life(col)	8.4836E+03	8.4719E+03 0.0017	k(col/abs/tk ln)	0.703286 0.0015	0.703216 0.0015	
rem life(abs)	8.6100E+03	8.4727E+03 0.0016	life(col/abs/tl)	8.4744E+03 0.0015	8.4804E+03 0.0013	

source points generated 961

estimator	cycle 530	ave of 500 cycles	combination	simple average	combined average	corr
k(collision)	0.702529	0.703542 0.0016	k(col/abs)	0.703276 0.0015	0.703251 0.0015	0.7954
k(absorption)	*0.694516*	*0.703011 0.0015*	*k(abs/tk ln)*	*0.703094 0.0016*	*0.703049 0.0015*	0.4238
k(trk length)	0.649825	0.703178 0.0022	k(tk ln/col)	0.703360 0.0017	0.703485 0.0016	0.5841
rem life(col)	8.2172E+03	8.4714E+03 0.0017	k(col/abs/tk ln)	0.703244 0.0015	0.703190 0.0015	
rem life(abs)	8.3284E+03	8.4724E+03 0.0016	life(col/abs/tl)	8.4741E+03 0.0015	8.4802E+03 0.0013	

source points generated 1018

```
 source distribution written to file MS_Acc_NACCoC_c1.00_g0.00_e0.00_d0.01cm_HP_36mm.inps          cycle =   530
1problem summary (active cycles only)              source particle weight for summary table normalization =       500000.00

      run terminated when   530   kcode cycles were done.
+                                                                                          10/25/07 21:18:09
      NAC-LWT Cask - MOX Experiments - Accident Transport Conditions                 probid =  10/25/07 21:05:56
0
```

neutron creation	tracks	weight (per source particle)	energy (per source particle)	neutron loss	tracks	weight (per source particle)	energy (per source particle)
source	500502	1.0000E+00	2.1043E+00	escape	0	0.	0.
				energy cutoff	0	0.	0.
				time cutoff	0	0.	0.
weight window	0	0.	0.	weight window	0	0.	0.
cell importance	0	0.	0.	cell importance	0	0.	0.
weight cutoff	0	1.0592E-01	4.8768E-06	weight cutoff	500977	1.0547E-01	4.3336E-06
e or t importance	0	0.	0.	e or t importance	0	0.	0.
dxtran	0	0.	0.	dxtran	0	0.	0.
forced collisions	0	0.	0.	forced collisions	0	0.	0.
exp. transform	0	0.	0.	exp. transform	0	0.	0.
upscattering	0	0.	2.2571E-07	downscattering	0	0.	2.0393E+00
photonuclear	0	0.	0.	capture	0	7.5486E-01	3.4580E-02
(n,xn)	949	1.6722E-03	1.5347E-03	loss to (n,xn)	474	8.3532E-04	8.0905E-03
prompt fission	0	0.	0.	loss to fission	0	2.4643E-01	2.3925E-02
delayed fission	0	0.	0.				
total	501451	1.1076E+00	2.1059E+00	total	501451	1.1076E+00	2.1059E+00

```
  number of neutrons banked                    501       average time of (shakes)            cutoffs
  neutron tracks per source particle     1.0029E+00        escape           0.0000E+00         tco   1.0000E+33
  neutron collisions per source particle 1.5353E+02        capture          9.4388E+03         eco   0.0000E+00
  total neutron collisions                 76766227        capture or escape 9.4388E+03        wc1  -5.0000E-01
  net multiplication              1.0008E+00 0.0000        any termination  9.7365E+03         wc2  -2.5000E-01

 computer time so far in this run    12.12 minutes        maximum number ever in bank        2
 computer time in mcrun              11.96 minutes        bank overflows to backup file      0
 source particles per minute            4.4359E+04
 random numbers generated                776053288        most random numbers used was       12401 in history      255214

 range of sampled source weights = 8.4104E-01 to 1.1848E+00

 source efficiency = 1.0000  in cell    1

 source efficiency = 0.1042  in cell    10

 source efficiency = 1.0000  in cell    20
```

source efficiency = 1.0000 in cell 41
1neutron activity in each cell print table 126

cell	tracks entering	population	collisions	collisions * weight (per history)	number weighted energy	flux weighted energy	average track weight (relative)	average track mfp (cm)
1	1255010	500853	588249	9.5138E-01	1.2434E-03	1.1278E+00	9.1668E-01	2.6471E+00
2	1783820	500855	71781	1.0077E-01	4.1502E-04	8.2308E-01	8.3190E-01	1.8137E+00
3	1923591	500862	78833	1.3909E-01	5.6258E-04	8.8063E-01	8.8178E-01	3.8130E+00
4	4738894	500933	23063782	3.3926E+01	1.9840E-04	5.3541E-01	8.2904E-01	1.3620E+00
5	1421751	373841	6076166	8.6070E+00	1.3853E-04	3.5425E-01	7.9418E-01	1.1032E+00
6	0	0	0	0.0000E+00	0.0000E+00	0.0000E+00	0.0000E+00	0.0000E+00
7	1663380	374111	1888	2.7445E-03	4.9624E-04	4.1450E-01	8.2621E-01	1.3160E+04
8	2075969	374082	2123010	3.6862E+00	5.4141E-04	3.4564E-01	8.1935E-01	9.7325E+00
9	2178870	357717	98	1.4370E-04	5.9979E-04	3.0426E-01	8.1703E-01	1.1977E+04
10	26756	5352	105825	1.4813E-01	3.0621E-03	1.0020E-01	7.1747E-01	3.2033E+00
11	0	0	0	0.0000E+00	0.0000E+00	0.0000E+00	0.0000E+00	0.0000E+00
12	117397	15536	1374254	1.8224E+00	2.6104E-03	1.0374E-01	7.2074E-01	2.5082E+00
13	3367057	211757	13287925	1.9309E+01	3.4664E-03	1.7878E-01	7.8829E-01	2.7581E+00
14	42780	15974	147895	2.0621E-01	8.2779E-04	1.6867E-01	7.5443E-01	2.3675E+00
15	2192206	356597	5325642	8.0534E+00	9.0372E-04	3.0289E-01	8.1723E-01	2.5854E+00
16	2661735	296813	24149944	3.7756E+01	1.6531E-03	2.2215E-01	8.0496E-01	3.5572E+00
17	88453	20419	366868	5.3434E-01	1.7669E-03	1.3640E-01	7.4778E-01	3.3059E+00
18	3155968	210444	0	0.0000E+00	2.8143E-03	1.8703E-01	7.9827E-01	0.0000E+00
19	1754788	180075	4067	6.0877E-03	3.8995E-03	1.8293E-01	7.8977E-01	1.0874E+04
total	30448425	4796221	76766227	1.1525E+02				

print table 128 requires 1067 decimal words of dynamically allocated storage.
1neutron weight balance in each cell print table 130

cell index	1	2	3	4	5	6	7	8	9
cell number	1	2	3	4	10	20	21	22	23
external events:									
entering	1.2681E+00	3.1938E+00	3.4204E+00	7.9797E+00	2.3195E+00	0.0000E+00	2.7616E+00	3.4266E+00	3.5712E+00
source	1.0000E+00	0.0000E+00	0.0000E+00	0.0000E+00	0.0000E+00	0.0000E+00	0.0000E+00	0.0000E+00	0.0000E+00
energy cutoff	0.0000E+00	0.0000E+00	0.0000E+00	0.0000E+00	0.0000E+00	0.0000E+00	0.0000E+00	0.0000E+00	0.0000E+00
time cutoff	0.0000E+00	0.0000E+00	0.0000E+00	0.0000E+00	0.0000E+00	0.0000E+00	0.0000E+00	0.0000E+00	0.0000E+00
exiting	-1.8832E+00	-3.1934E+00	-3.4192E+00	-7.8425E+00	-2.2857E+00	0.0000E+00	-2.7616E+00	-3.3873E+00	-3.5712E+00
total	3.8488E-01	3.6018E-04	1.1827E-03	1.3724E-01	3.3874E-02	0.0000E+00	6.3609E-06	3.9247E-02	2.1550E-07
variance reduction events:									
weight window	0.0000E+00	0.0000E+00	0.0000E+00	0.0000E+00	0.0000E+00	0.0000E+00	0.0000E+00	0.0000E+00	0.0000E+00
cell importance	0.0000E+00	0.0000E+00	0.0000E+00	0.0000E+00	0.0000E+00	0.0000E+00	0.0000E+00	0.0000E+00	0.0000E+00
weight cutoff	2.8229E-05	2.7032E-06	-9.7040E-06	-1.9749E-05	-4.7973E-05	0.0000E+00	-9.9564E-07	5.7430E-05	0.0000E+00
e or t importance	0.0000E+00	0.0000E+00	0.0000E+00	0.0000E+00	0.0000E+00	0.0000E+00	0.0000E+00	0.0000E+00	0.0000E+00
dxtran	0.0000E+00	0.0000E+00	0.0000E+00	0.0000E+00	0.0000E+00	0.0000E+00	0.0000E+00	0.0000E+00	0.0000E+00
forced collisions	0.0000E+00	0.0000E+00	0.0000E+00	0.0000E+00	0.0000E+00	0.0000E+00	0.0000E+00	0.0000E+00	0.0000E+00
exp. transform	0.0000E+00	0.0000E+00	0.0000E+00	0.0000E+00	0.0000E+00	0.0000E+00	0.0000E+00	0.0000E+00	0.0000E+00
total	2.8229E-05	2.7032E-06	-9.7040E-06	-1.9749E-05	-4.7973E-05	0.0000E+00	-9.9564E-07	5.7430E-05	0.0000E+00
physical events:									
capture	-1.3879E-01	-3.6289E-04	-1.1985E-03	-1.3722E-01	-3.3826E-02	0.0000E+00	-5.3652E-06	-3.9305E-02	-2.1550E-07
(n,xn)	6.2341E-04	0.0000E+00	5.0860E-05	0.0000E+00	0.0000E+00	0.0000E+00	0.0000E+00	0.0000E+00	0.0000E+00
loss to (n,xn)	-3.1093E-04	0.0000E+00	-2.5430E-05	0.0000E+00	0.0000E+00	0.0000E+00	0.0000E+00	0.0000E+00	0.0000E+00
fission	0.0000E+00	0.0000E+00	0.0000E+00	0.0000E+00	0.0000E+00	0.0000E+00	0.0000E+00	0.0000E+00	0.0000E+00
loss to fission	-2.4643E-01	0.0000E+00	0.0000E+00	0.0000E+00	0.0000E+00	0.0000E+00	0.0000E+00	0.0000E+00	0.0000E+00
photonuclear	0.0000E+00	0.0000E+00	0.0000E+00	0.0000E+00	0.0000E+00	0.0000E+00	0.0000E+00	0.0000E+00	0.0000E+00
total	-3.8491E-01	-3.6289E-04	-1.1730E-03	-1.3722E-01	-3.3826E-02	0.0000E+00	-5.3652E-06	-3.9305E-02	-2.1550E-07
total	0.0000E+00	0.0000E+00	0.0000E+00	0.0000E+00	0.0000E+00	0.0000E+00	0.0000E+00	0.0000E+00	0.0000E+00

cell index	10	11	12	13	14	15	16	17	18
cell number	40	41	42	43	44	45	46	47	48
external events:									
entering	3.8410E-02	0.0000E+00	1.7109E-01	5.3543E+00	6.4450E-02	3.6004E+00	4.2962E+00	1.3246E-01	5.0388E+00
source	0.0000E+00	0.0000E+00	0.0000E+00	0.0000E+00	0.0000E+00	0.0000E+00	0.0000E+00	0.0000E+00	0.0000E+00
energy cutoff	0.0000E+00	0.0000E+00	0.0000E+00	0.0000E+00	0.0000E+00	0.0000E+00	0.0000E+00	0.0000E+00	0.0000E+00
time cutoff	0.0000E+00	0.0000E+00	0.0000E+00	0.0000E+00	0.0000E+00	0.0000E+00	0.0000E+00	0.0000E+00	0.0000E+00
exiting	-3.8338E-02	0.0000E+00	-1.5873E-01	-5.2124E+00	-6.0345E-02	-3.3858E+00	-4.2663E+00	-1.3214E-01	-5.0388E+00
total	7.1248E-05	0.0000E+00	1.2354E-02	1.4185E-01	4.1045E-03	2.1458E-01	2.9932E-02	3.1701E-04	0.0000E+00
variance reduction events:									
weight window	0.0000E+00	0.0000E+00	0.0000E+00	0.0000E+00	0.0000E+00	0.0000E+00	0.0000E+00	0.0000E+00	0.0000E+00
cell importance	0.0000E+00	0.0000E+00	0.0000E+00	0.0000E+00	0.0000E+00	0.0000E+00	0.0000E+00	0.0000E+00	0.0000E+00
weight cutoff	5.9575E-07	0.0000E+00	-3.9444E-05	1.7827E-04	8.9663E-06	2.2838E-04	5.6942E-05	7.6461E-06	0.0000E+00
e or t importance	0.0000E+00	0.0000E+00	0.0000E+00	0.0000E+00	0.0000E+00	0.0000E+00	0.0000E+00	0.0000E+00	0.0000E+00
dxtran	0.0000E+00	0.0000E+00	0.0000E+00	0.0000E+00	0.0000E+00	0.0000E+00	0.0000E+00	0.0000E+00	0.0000E+00
forced collisions	0.0000E+00	0.0000E+00	0.0000E+00	0.0000E+00	0.0000E+00	0.0000E+00	0.0000E+00	0.0000E+00	0.0000E+00
exp. transform	0.0000E+00	0.0000E+00	0.0000E+00	0.0000E+00	0.0000E+00	0.0000E+00	0.0000E+00	0.0000E+00	0.0000E+00
total	5.9575E-07	0.0000E+00	-3.9444E-05	1.7827E-04	8.9663E-06	2.2838E-04	5.6942E-05	7.6461E-06	0.0000E+00
physical events:									
capture	-7.1844E-05	0.0000E+00	-1.2315E-02	-1.4204E-01	-4.1135E-03	-2.1481E-01	-3.0482E-02	-3.2465E-04	0.0000E+00
(n,xn)	0.0000E+00	0.0000E+00	0.0000E+00	6.9717E-06	0.0000E+00	6.6859E-06	9.8428E-04	0.0000E+00	0.0000E+00
loss to (n,xn)	0.0000E+00	0.0000E+00	0.0000E+00	-3.4859E-06	0.0000E+00	-3.3429E-06	-4.9214E-04	0.0000E+00	0.0000E+00

fission	0.0000E+00	0.0000E+00	0.0000E+00	0.0000E+00	0.0000E+00	0.0000E+00	0.0000E+00	0.0000E+00	0.0000E+00
loss to fission	0.0000E+00	0.0000E+00	0.0000E+00	0.0000E+00	0.0000E+00	0.0000E+00	0.0000E+00	0.0000E+00	0.0000E+00
photonuclear	0.0000E+00	0.0000E+00	0.0000E+00	0.0000E+00	0.0000E+00	0.0000E+00	0.0000E+00	0.0000E+00	0.0000E+00
total	-7.1844E-05	0.0000E+00	-1.2315E-02	-1.4203E-01	-4.1135E-03	-2.1481E-01	-2.9989E-02	-3.2465E-04	0.0000E+00
total	0.0000E+00	0.0000E+00	0.0000E+00	0.0000E+00	0.0000E+00	0.0000E+00	0.0000E+00	0.0000E+00	0.0000E+00

cell index	19	
cell number	49	total
external events:		
entering	2.7677E+00	4.9405E+01
source	0.0000E+00	1.0000E+00
energy cutoff	0.0000E+00	0.0000E+00
time cutoff	0.0000E+00	0.0000E+00
exiting	-2.7677E+00	-4.9405E+01
total	9.6082E-07	1.0000E+00
variance reduction events:		
weight window	0.0000E+00	0.0000E+00
cell importance	0.0000E+00	0.0000E+00
weight cutoff	5.0063E-07	4.5179E-04
e or t importance	0.0000E+00	0.0000E+00
dxtran	0.0000E+00	0.0000E+00
forced collisions	0.0000E+00	0.0000E+00
exp. transform	0.0000E+00	0.0000E+00
total	5.0063E-07	4.5179E-04
physical events:		
capture	-1.4614E-06	-7.5486E-01
(n,xn)	0.0000E+00	1.6722E-03
loss to (n,xn)	0.0000E+00	-8.3532E-04
fission	0.0000E+00	0.0000E+00
loss to fission	0.0000E+00	-2.4643E-01
photonuclear	0.0000E+00	0.0000E+00
total	-1.4614E-06	-1.0005E+00
total	0.0000E+00	0.0000E+00

1neutron activity of each nuclide in each cell, per source particle print table 140

cell index	cell name	nuclides	atom fraction	total collisions	collisions * weight	wgt. lost to capture	wgt. gain by fission	wgt. gain by (n,xn)	photons produced	photon wgt produced	avg photon energy
1	1	92235.69c	2.18E-03	13149	1.8238E-02	2.6523E-03	1.3545E-02	0.0000E+00	0	0.0000E+00	0.0000E+00
		92238.69c	3.06E-01	186994	3.3548E-01	2.5440E-02	5.4986E-03	3.0727E-04	0	0.0000E+00	0.0000E+00
		94238.66c	1.28E-05	67	9.7812E-05	7.8916E-05	4.0561E-06	0.0000E+00	0	0.0000E+00	0.0000E+00
		94239.69c	2.41E-02	247900	3.4650E-01	9.9448E-02	2.2599E-01	5.2057E-06	0	0.0000E+00	0.0000E+00
		94240.66c	1.14E-03	7457	1.1940E-02	1.0232E-02	1.0428E-04	0.0000E+00	0	0.0000E+00	0.0000E+00
		94241.66c	1.01E-04	1305	1.8084E-03	4.2713E-04	1.2840E-03	0.0000E+00	0	0.0000E+00	0.0000E+00
		94242.66c	1.25E-05	36	6.0894E-05	3.7138E-05	1.8504E-06	0.0000E+00	0	0.0000E+00	0.0000E+00
		8016.62c	6.66E-01	131341	2.3725E-01	4.7184E-04	0.0000E+00	0.0000E+00	0	0.0000E+00	0.0000E+00
2	2	1001.62c	6.67E-01	66694	9.2467E-02	3.5248E-04	0.0000E+00	0.0000E+00	0	0.0000E+00	0.0000E+00
		8016.62c	3.33E-01	5087	8.3067E-03	1.0409E-05	0.0000E+00	0.0000E+00	0	0.0000E+00	0.0000E+00
3	3	26054.62c	1.19E-04	4	7.4446E-06	8.2238E-07	0.0000E+00	0.0000E+00	0	0.0000E+00	0.0000E+00
		24050.62c	7.63E-05	8	1.1117E-05	5.2938E-06	0.0000E+00	0.0000E+00	0	0.0000E+00	0.0000E+00
		7014.62c	3.24E-03	270	4.2214E-04	2.9134E-05	0.0000E+00	0.0000E+00	0	0.0000E+00	0.0000E+00
		26056.62c	1.87E-03	172	2.7365E-04	1.5704E-05	0.0000E+00	0.0000E+00	0	0.0000E+00	0.0000E+00
		24052.62c	1.47E-03	60	1.0627E-04	4.4084E-06	0.0000E+00	0.0000E+00	0	0.0000E+00	0.0000E+00
		7015.66c	1.20E-05	1	2.0715E-06	4.3673E-12	0.0000E+00	0.0000E+00	0	0.0000E+00	0.0000E+00
		26057.62c	4.33E-05	3	5.7570E-06	2.7967E-09	0.0000E+00	0.0000E+00	0	0.0000E+00	0.0000E+00
		24053.62c	1.67E-04	20	3.0965E-05	7.3217E-06	0.0000E+00	0.0000E+00	0	0.0000E+00	0.0000E+00
		26058.62c	5.71E-06	1	1.4554E-06	3.1973E-07	0.0000E+00	0.0000E+00	0	0.0000E+00	0.0000E+00
		24054.62c	4.14E-05	1	2.0725E-06	6.0645E-10	0.0000E+00	0.0000E+00	0	0.0000E+00	0.0000E+00
		40000.66c	9.81E-01	77568	1.3693E-01	1.0679E-03	0.0000E+00	2.5430E-05	0	0.0000E+00	0.0000E+00
		50000.42c	1.15E-02	725	1.2911E-03	6.7541E-05	0.0000E+00	0.0000E+00	0	0.0000E+00	0.0000E+00
4	4	1001.62c	6.67E-01	21628102	3.1581E+01	1.3528E-01	0.0000E+00	0.0000E+00	0	0.0000E+00	0.0000E+00
		8016.62c	3.33E-01	1435680	2.3453E+00	1.9355E-03	0.0000E+00	0.0000E+00	0	0.0000E+00	0.0000E+00
5	10	1001.62c	6.67E-01	5707107	8.0275E+00	3.3538E-02	0.0000E+00	0.0000E+00	0	0.0000E+00	0.0000E+00
		8016.62c	3.33E-01	369059	5.7955E-01	2.8754E-04	0.0000E+00	0.0000E+00	0	0.0000E+00	0.0000E+00
6	20	1001.62c	6.67E-01	0	0.0000E+00	0.0000E+00	0.0000E+00	0.0000E+00	0	0.0000E+00	0.0000E+00
		8016.62c	3.33E-01	0	0.0000E+00	0.0000E+00	0.0000E+00	0.0000E+00	0	0.0000E+00	0.0000E+00
7	21	1001.62c	6.67E-01	1732	2.5018E-03	5.3619E-06	0.0000E+00	0.0000E+00	0	0.0000E+00	0.0000E+00
		8016.62c	3.33E-01	156	2.4270E-04	3.2713E-09	0.0000E+00	0.0000E+00	0	0.0000E+00	0.0000E+00
8	22	13027.62c	1.00E+00	2123010	3.6862E+00	3.9305E-02	0.0000E+00	0.0000E+00	0	0.0000E+00	0.0000E+00
9	23	1001.62c	6.67E-01	88	1.2864E-04	2.1542E-07	0.0000E+00	0.0000E+00	0	0.0000E+00	0.0000E+00
		8016.62c	3.33E-01	10	1.5062E-05	8.2269E-11	0.0000E+00	0.0000E+00	0	0.0000E+00	0.0000E+00
10	40	82206.66c	2.55E-01	25173	3.4731E-02	2.7307E-05	0.0000E+00	0.0000E+00	0	0.0000E+00	0.0000E+00
		82207.66c	2.21E-01	23283	3.2961E-02	4.1971E-05	0.0000E+00	0.0000E+00	0	0.0000E+00	0.0000E+00
		82208.66c	5.24E-01	57369	8.0440E-02	2.5667E-06	0.0000E+00	0.0000E+00	0	0.0000E+00	0.0000E+00

11	41	1001.62c 6.67E-01	0	0.0000E+00	0.0000E+00	0.0000E+00	0.0000E+00	0	0.0000E+00	0.0000E+00
		8016.62c 3.33E-01	0	0.0000E+00	0.0000E+00	0.0000E+00	0.0000E+00	0	0.0000E+00	0.0000E+00
12	42	24050.62c 8.79E-03	22634	3.5886E-02	5.0283E-04	0.0000E+00	0.0000E+00	0	0.0000E+00	0.0000E+00
		26054.62c 4.03E-02	43963	7.0549E-02	4.1183E-04	0.0000E+00	0.0000E+00	0	0.0000E+00	0.0000E+00
		28058.62c 6.09E-02	185596	2.3990E-01	1.0944E-03	0.0000E+00	0.0000E+00	0	0.0000E+00	0.0000E+00
		24052.62c 1.69E-01	95848	1.4109E-01	7.2604E-04	0.0000E+00	0.0000E+00	0	0.0000E+00	0.0000E+00
		26056.62c 6.32E-01	808702	1.0013E+00	6.0096E-03	0.0000E+00	0.0000E+00	0	0.0000E+00	0.0000E+00
		28060.62c 2.35E-02	27885	4.6516E-02	2.8672E-04	0.0000E+00	0.0000E+00	0	0.0000E+00	0.0000E+00
		24053.62c 1.92E-02	65788	9.9650E-02	1.2037E-03	0.0000E+00	0.0000E+00	0	0.0000E+00	0.0000E+00
		26057.62c 1.46E-02	17938	2.8790E-02	2.1264E-04	0.0000E+00	0.0000E+00	0	0.0000E+00	0.0000E+00
		28061.62c 1.02E-03	1327	1.8701E-03	1.6196E-05	0.0000E+00	0.0000E+00	0	0.0000E+00	0.0000E+00
		24054.62c 4.77E-03	3571	5.5204E-03	1.2960E-05	0.0000E+00	0.0000E+00	0	0.0000E+00	0.0000E+00
		26058.62c 1.93E-03	1926	3.0589E-03	2.7125E-05	0.0000E+00	0.0000E+00	0	0.0000E+00	0.0000E+00
		28062.62c 3.25E-03	14955	2.2767E-02	1.4098E-04	0.0000E+00	0.0000E+00	0	0.0000E+00	0.0000E+00
		28064.62c 8.33E-04	1172	2.0355E-03	5.1368E-06	0.0000E+00	0.0000E+00	0	0.0000E+00	0.0000E+00
		25055.62c 2.01E-02	82949	1.2342E-01	1.6648E-03	0.0000E+00	0.0000E+00	0	0.0000E+00	0.0000E+00
13	43	24050.62c 8.79E-03	224394	3.7208E-01	5.8811E-03	0.0000E+00	0.0000E+00	0	0.0000E+00	0.0000E+00
		26054.62c 4.03E-02	457333	7.7117E-01	4.8990E-03	0.0000E+00	0.0000E+00	0	0.0000E+00	0.0000E+00
		28058.62c 6.09E-02	1729500	2.4409E+00	1.3150E-02	0.0000E+00	0.0000E+00	0	0.0000E+00	0.0000E+00
		24052.62c 1.69E-01	1032660	1.6563E+00	8.0696E-03	0.0000E+00	0.0000E+00	0	0.0000E+00	0.0000E+00
		26056.62c 6.32E-01	7735666	1.0652E+01	7.0255E-02	0.0000E+00	1.5751E-06	0	0.0000E+00	0.0000E+00
		28060.62c 2.35E-02	284768	4.9380E-01	3.3119E-03	0.0000E+00	0.0000E+00	0	0.0000E+00	0.0000E+00
		24053.62c 1.92E-02	635953	1.0153E+00	1.4020E-02	0.0000E+00	0.0000E+00	0	0.0000E+00	0.0000E+00
		26057.62c 1.46E-02	187135	3.1564E-01	2.2517E-03	0.0000E+00	1.9108E-06	0	0.0000E+00	0.0000E+00
		28061.62c 1.02E-03	13567	2.0961E-02	1.7693E-04	0.0000E+00	0.0000E+00	0	0.0000E+00	0.0000E+00
		24054.62c 4.77E-03	37002	6.1565E-02	1.1488E-04	0.0000E+00	0.0000E+00	0	0.0000E+00	0.0000E+00
		26058.62c 1.93E-03	19846	3.3234E-02	2.9139E-04	0.0000E+00	0.0000E+00	0	0.0000E+00	0.0000E+00
		28062.62c 3.25E-03	144771	2.3200E-01	1.7147E-03	0.0000E+00	0.0000E+00	0	0.0000E+00	0.0000E+00
		28064.62c 8.33E-04	12360	2.2167E-02	6.2663E-05	0.0000E+00	0.0000E+00	0	0.0000E+00	0.0000E+00
		25055.62c 2.01E-02	772970	1.2215E+00	1.7836E-02	0.0000E+00	0.0000E+00	0	0.0000E+00	0.0000E+00
14	44	24050.62c 8.79E-03	2257	3.6357E-03	1.7986E-04	0.0000E+00	0.0000E+00	0	0.0000E+00	0.0000E+00
		26054.62c 4.03E-02	4235	6.9394E-03	1.3937E-04	0.0000E+00	0.0000E+00	0	0.0000E+00	0.0000E+00
		28058.62c 6.09E-02	19754	2.6772E-02	3.8375E-04	0.0000E+00	0.0000E+00	0	0.0000E+00	0.0000E+00
		24052.62c 1.69E-01	10363	1.5850E-02	2.0913E-04	0.0000E+00	0.0000E+00	0	0.0000E+00	0.0000E+00
		26056.62c 6.32E-01	90447	1.1985E-01	2.1525E-03	0.0000E+00	0.0000E+00	0	0.0000E+00	0.0000E+00
		28060.62c 2.35E-02	2541	4.3191E-03	8.9712E-05	0.0000E+00	0.0000E+00	0	0.0000E+00	0.0000E+00
		24053.62c 1.92E-02	6508	1.0115E-02	4.1602E-04	0.0000E+00	0.0000E+00	0	0.0000E+00	0.0000E+00
		26057.62c 1.46E-02	1792	2.9469E-03	5.7133E-05	0.0000E+00	0.0000E+00	0	0.0000E+00	0.0000E+00
		28061.62c 1.02E-03	113	1.6337E-04	2.9738E-06	0.0000E+00	0.0000E+00	0	0.0000E+00	0.0000E+00
		24054.62c 4.77E-03	329	5.3342E-04	2.5471E-06	0.0000E+00	0.0000E+00	0	0.0000E+00	0.0000E+00
		26058.62c 1.93E-03	182	2.8460E-04	4.0371E-06	0.0000E+00	0.0000E+00	0	0.0000E+00	0.0000E+00
		28062.62c 3.25E-03	1520	2.4171E-03	5.6784E-05	0.0000E+00	0.0000E+00	0	0.0000E+00	0.0000E+00
		28064.62c 8.33E-04	111	1.9873E-04	2.0767E-07	0.0000E+00	0.0000E+00	0	0.0000E+00	0.0000E+00
		25055.62c 2.01E-02	7743	1.2184E-02	4.1947E-04	0.0000E+00	0.0000E+00	0	0.0000E+00	0.0000E+00
15	45	24050.62c 8.79E-03	81095	1.3624E-01	9.6184E-03	0.0000E+00	0.0000E+00	0	0.0000E+00	0.0000E+00
		26054.62c 4.03E-02	163277	2.8221E-01	6.7571E-03	0.0000E+00	0.0000E+00	0	0.0000E+00	0.0000E+00
		28058.62c 6.09E-02	685869	1.0095E+00	2.0192E-02	0.0000E+00	0.0000E+00	0	0.0000E+00	0.0000E+00
		24052.62c 1.69E-01	396986	6.5384E-01	9.5378E-03	0.0000E+00	0.0000E+00	0	0.0000E+00	0.0000E+00
		26056.62c 6.32E-01	3259168	4.7321E+00	1.1291E-01	0.0000E+00	3.3429E-06	0	0.0000E+00	0.0000E+00
		28060.62c 2.35E-02	92241	1.6289E-01	4.6046E-03	0.0000E+00	0.0000E+00	0	0.0000E+00	0.0000E+00
		24053.62c 1.92E-02	232819	3.7911E-01	2.3610E-02	0.0000E+00	0.0000E+00	0	0.0000E+00	0.0000E+00
		26057.62c 1.46E-02	66241	1.1455E-01	2.6634E-03	0.0000E+00	0.0000E+00	0	0.0000E+00	0.0000E+00
		28061.62c 1.02E-03	5093	8.0726E-03	1.8482E-04	0.0000E+00	0.0000E+00	0	0.0000E+00	0.0000E+00
		24054.62c 4.77E-03	12749	2.1779E-02	1.3347E-04	0.0000E+00	0.0000E+00	0	0.0000E+00	0.0000E+00
		26058.62c 1.93E-03	6698	1.1451E-02	2.0600E-04	0.0000E+00	0.0000E+00	0	0.0000E+00	0.0000E+00
		28062.62c 3.25E-03	51276	8.5061E-02	3.1530E-03	0.0000E+00	0.0000E+00	0	0.0000E+00	0.0000E+00
		28064.62c 8.33E-04	3626	6.6497E-03	8.9188E-05	0.0000E+00	0.0000E+00	0	0.0000E+00	0.0000E+00
		25055.62c 2.01E-02	268504	4.4997E-01	2.1151E-02	0.0000E+00	0.0000E+00	0	0.0000E+00	0.0000E+00
16	46	82206.66c 2.55E-01	5804104	8.9875E+00	6.8570E-03	0.0000E+00	6.0193E-05	0	0.0000E+00	0.0000E+00
		82207.66c 2.21E-01	5361381	8.4381E+00	2.2860E-02	0.0000E+00	1.4604E-04	0	0.0000E+00	0.0000E+00
		82208.66c 5.24E-01	12984459	2.0331E+01	7.6484E-04	0.0000E+00	2.8591E-04	0	0.0000E+00	0.0000E+00
17	47	82206.66c 2.55E-01	88291	1.2688E-01	7.9354E-05	0.0000E+00	0.0000E+00	0	0.0000E+00	0.0000E+00
		82207.66c 2.21E-01	80596	1.1838E-01	2.3687E-04	0.0000E+00	0.0000E+00	0	0.0000E+00	0.0000E+00
		82208.66c 5.24E-01	197981	2.8908E-01	8.4289E-06	0.0000E+00	0.0000E+00	0	0.0000E+00	0.0000E+00
19	49	1001.62c 6.67E-01	3648	5.4226E-03	1.4610E-06	0.0000E+00	0.0000E+00	0	0.0000E+00	0.0000E+00
		8016.62c 3.33E-01	419	6.6504E-04	3.9930E-10	0.0000E+00	0.0000E+00	0	0.0000E+00	0.0000E+00
	total		76766227	1.1525E+02	7.5486E-01	2.4643E-01	8.3688E-04	0	0.0000E+00	0.0000E+00

total over all cells by nuclide	total collisions	collisions * weight	wgt. lost to capture	wgt. gain by fission	wgt. gain by (n,xn)	photons produced	photon wgt produced	avg photon energy
1001.62c	27407371	3.9709E+01	1.6918E-01	0.0000E+00	0.0000E+00	0	0.0000E+00	0.0000E+00
7014.62c	270	4.2214E-04	2.9134E-05	0.0000E+00	0.0000E+00	0	0.0000E+00	0.0000E+00
7015.66c	1	2.0715E-06	4.3673E-12	0.0000E+00	0.0000E+00	0	0.0000E+00	0.0000E+00
8016.62c	1941752	3.1714E+00	2.7053E-03	0.0000E+00	0.0000E+00	0	0.0000E+00	0.0000E+00
13027.62c	2123010	3.6862E+00	3.9305E-02	0.0000E+00	0.0000E+00	0	0.0000E+00	0.0000E+00
24050.62c	330388	5.4785E-01	1.6187E-02	0.0000E+00	0.0000E+00	0	0.0000E+00	0.0000E+00
24052.62c	1535917	2.4672E+00	1.8547E-02	0.0000E+00	0.0000E+00	0	0.0000E+00	0.0000E+00
24053.62c	941088	1.5042E+00	3.9257E-02	0.0000E+00	0.0000E+00	0	0.0000E+00	0.0000E+00
24054.62c	53652	8.9400E-02	2.6385E-04	0.0000E+00	0.0000E+00	0	0.0000E+00	0.0000E+00
25055.62c	1132166	1.8071E+00	4.1071E-02	0.0000E+00	0.0000E+00	0	0.0000E+00	0.0000E+00
26054.62c	668812	1.1309E+00	1.2208E-02	0.0000E+00	0.0000E+00	0	0.0000E+00	0.0000E+00
26056.62c	11894155	1.6506E+01	1.9134E-01	0.0000E+00	4.9180E-06	0	0.0000E+00	0.0000E+00
26057.62c	273109	4.6193E-01	5.1849E-03	0.0000E+00	1.9108E-06	0	0.0000E+00	0.0000E+00
26058.62c	28653	4.8030E-02	5.2887E-04	0.0000E+00	0.0000E+00	0	0.0000E+00	0.0000E+00
28058.62c	2620719	3.7171E+00	3.4821E-02	0.0000E+00	0.0000E+00	0	0.0000E+00	0.0000E+00
28060.62c	407435	7.0753E-01	8.2929E-03	0.0000E+00	0.0000E+00	0	0.0000E+00	0.0000E+00
28061.62c	20100	3.1067E-02	3.8093E-04	0.0000E+00	0.0000E+00	0	0.0000E+00	0.0000E+00

28062.62c	212522	3.4224E-01	5.0655E-03	0.0000E+00	0.0000E+00	0	0.0000E+00	0.0000E+00
28064.62c	17269	3.1051E-02	1.5720E-04	0.0000E+00	0.0000E+00	0	0.0000E+00	0.0000E+00
40000.66c	77568	1.3693E-01	1.0679E-03	0.0000E+00	2.5430E-05	0	0.0000E+00	0.0000E+00
50000.42c	725	1.2911E-03	6.7541E-05	0.0000E+00	0.0000E+00	0	0.0000E+00	0.0000E+00
82206.66c	5917568	9.1491E+00	6.9637E-03	0.0000E+00	6.0193E-05	0	0.0000E+00	0.0000E+00
82207.66c	5465260	8.5894E+00	2.3138E-02	0.0000E+00	1.4604E-04	0	0.0000E+00	0.0000E+00
82208.66c	13239809	2.0700E+01	7.7584E-04	0.0000E+00	2.8591E-04	0	0.0000E+00	0.0000E+00
92235.69c	13149	1.8238E-02	2.6523E-03	1.3545E-02	0.0000E+00	0	0.0000E+00	0.0000E+00
92238.69c	186994	3.3548E-01	2.5440E-02	5.4986E-03	3.0727E-04	0	0.0000E+00	0.0000E+00
94238.66c	67	9.7812E-05	7.8916E-05	4.0561E-06	0.0000E+00	0	0.0000E+00	0.0000E+00
94239.69c	247900	3.4650E-01	9.9448E-02	2.2599E-01	5.2057E-06	0	0.0000E+00	0.0000E+00
94240.66c	7457	1.1940E-02	1.0232E-02	1.0428E-04	0.0000E+00	0	0.0000E+00	0.0000E+00
94241.66c	1305	1.8084E-03	4.2713E-04	1.2840E-03	0.0000E+00	0	0.0000E+00	0.0000E+00
94242.66c	36	6.0894E-05	3.7138E-05	1.8504E-06	0.0000E+00	0	0.0000E+00	0.0000E+00

1keff results for: NAC-LWT Cask - MOX Experiments - Accident Transport Conditions probid = 10/25/07 21:05:56

the initial fission neutron source distribution was generated from a general sdef source description.
the criticality problem was scheduled to skip 30 cycles and run a total of 530 cycles with nominally 1000 neutrons per cycle.
this problem has run 30 inactive cycles with 29983 neutron histories and 500 active cycles with 500502 neutron histories.

this calculation has completed the requested number of keff cycles using a total of 530485 fission neutron source histories.
all cells with fissionable material were sampled and had fission neutron source points.

the results of the w test for normality applied to the individual collision, absorption, and track-length keff cycle values are:

the k(collision) cycle values appear normally distributed at the 95 percent confidence level
the k(absorption) cycle values appear normally distributed at the 95 percent confidence level
the k(trk length) cycle values appear normally distributed at the 95 percent confidence level

---

| the final estimated combined collision/absorption/track-length keff = 0.70319 with an estimated standard deviation of 0.00102

| the estimated 68, 95, & 99 percent keff confidence intervals are 0.70216 to 0.70422, 0.70115 to 0.70523, and 0.70048 to 0.70590 |

| the final combined (col/abs/tl) prompt removal lifetime = 8.4802E-05 seconds with an estimated standard deviation of 1.0633E-07 |

| the average neutron energy causing fission = 9.7087E-02 mev

| the energy corresponding to the average neutron lethargy causing fission = 1.2505E-07 mev

| the percentages of fissions caused by neutrons in the thermal, intermediate, and fast neutron ranges are:

| (<0.625 ev): 91.72% (0.625 ev - 100 kev): 4.76% (>100 kev): 3.52%

| the average fission neutrons produced per neutron absorbed (capture + fission) in all cells with fission = 1.8263E+00

| the average fission neutrons produced per neutron absorbed (capture + fission) in all the geometry cells = 7.0264E-01

| the average number of neutrons produced per fission = 2.855

---

the estimated average keffs, one standard deviations, and 68, 95, and 99 percent confidence intervals are:

keff estimator	keff	standard deviation	68% confidence	95% confidence	99% confidence	corr
collision	0.70354	0.00111	0.70243 to 0.70465	0.70133 to 0.70575	0.70061 to 0.70648	
absorption	0.70301	0.00109	0.70192 to 0.70410	0.70084 to 0.70518	0.70013 to 0.70589	
track length	0.70318	0.00152	0.70165 to 0.70470	0.70014 to 0.70621	0.69915 to 0.70720	
col/absorp	0.70325	0.00104	0.70221 to 0.70430	0.70117 to 0.70533	0.70049 to 0.70601	0.7954
abs/trk len	0.70305	0.00104	0.70201 to 0.70409	0.70098 to 0.70512	0.70031 to 0.70579	0.4238
col/trk len	0.70349	0.00109	0.70239 to 0.70458	0.70130 to 0.70567	0.70059 to 0.70638	0.5841
col/abs/trk len	0.70319	0.00102	0.70216 to 0.70422	0.70115 to 0.70523	0.70048 to 0.70590	

if the largest of each keff occurred on the next cycle, the keff results and 68, 95, and 99 percent confidence intervals would be:

keff estimator	keff	standard deviation	68% confidence	95% confidence	99% confidence
collision	0.70369	0.00112	0.70257 to 0.70481	0.70146 to 0.70592	0.70073 to 0.70664
absorption	0.70314	0.00110	0.70205 to 0.70424	0.70096 to 0.70532	0.70025 to 0.70604
track length	0.70339	0.00154	0.70186 to 0.70493	0.70034 to 0.70645	0.69934 to 0.70745
col/abs/trk len	0.70334	0.00103	0.70231 to 0.70437	0.70128 to 0.70540	0.70061 to 0.70607

the estimated average prompt removal lifetimes, one standard deviations, and 68, 95, and 99 percent confidence intervals are (sec):

estimator	lifetime	std. dev.	68% confidence	95% confidence	99% confidence	corr
collision	8.47143E-05	1.42417E-07	8.4572E-05 to 8.4857E-05	8.4431E-05 to 8.4998E-05	8.4338E-05 to 8.5091E-05	
absorption	8.47241E-05	1.37731E-07	8.4586E-05 to 8.4862E-05	8.4450E-05 to 8.4998E-05	8.4360E-05 to 8.5088E-05	
track length	8.47846E-05	1.07925E-07	8.4677E-05 to 8.4893E-05	8.4570E-05 to 8.5000E-05	8.4499E-05 to 8.5070E-05	
col/absorp	8.47240E-05	1.37879E-07	8.4586E-05 to 8.4862E-05	8.4449E-05 to 8.4999E-05	8.4360E-05 to 8.5088E-05	0.9665
abs/trk len	8.48024E-05	1.06263E-07	8.4696E-05 to 8.4909E-05	8.4591E-05 to 8.5014E-05	8.4522E-05 to 8.5083E-05	0.8746
col/trk len	8.47991E-05	1.06906E-07	8.4692E-05 to 8.4906E-05	8.4586E-05 to 8.5012E-05	8.4517E-05 to 8.5082E-05	0.8399
col/abs/trk len	8.48016E-05	1.06329E-07	8.4695E-05 to 8.4908E-05	8.4590E-05 to 8.5013E-05	8.4521E-05 to 8.5083E-05	

absorption estimates of prompt lifetimes (sec):

	escape	capture	fission	removal
fraction	0.00000E+00	7.53886E-01	2.46114E-01	1.00000E+00
lifetime(abs)	0.00000E+00	1.12383E-04	3.44248E-04	8.47241E-05
lifetime(c/a/t)	0.00000E+00	1.12486E-04	3.44563E-04	8.48016E-05

1average keff results summed over 10 cycles each to form 50 batch values of keff print table 178

batch number	start cycle	end cycle	keff estimators by batch k(coll)	k(abs)	k(track)	average keff estimators and deviations k(coll)	st dev	k(abs)	st dev	k(track)	st dev	col/abs/tl k(c/a/t)	st dev
1	31	40	0.69464	0.70858	0.69703								
2	41	50	0.69991	0.69995	0.71175	0.69728	0.00264	0.70427	0.00431	0.70439	0.00736		
3	51	60	0.69908	0.70175	0.71143	0.69788	0.00164	0.70343	0.00263	0.70674	0.00485		
4	61	70	0.70512	0.70586	0.70015	0.69969	0.00215	0.70404	0.00195	0.70509	0.00381	0.70399	0.00052
5	71	80	0.70990	0.71146	0.70550	0.70173	0.00263	0.70552	0.00212	0.70517	0.00295	0.70603	0.00173
6	81	90	0.70562	0.70888	0.70384	0.70238	0.00225	0.70608	0.00182	0.70495	0.00242	0.70627	0.00132
7	91	100	0.69488	0.69474	0.70383	0.70131	0.00218	0.70446	0.00223	0.70479	0.00205	0.70515	0.00189
8	101	110	0.70672	0.69958	0.71642	0.70198	0.00201	0.70385	0.00203	0.70624	0.00229	0.70565	0.00159
9	111	120	0.70039	0.70157	0.69025	0.70181	0.00178	0.70360	0.00181	0.70447	0.00269	0.70369	0.00169
10	121	130	0.70465	0.70223	0.69620	0.70209	0.00162	0.70346	0.00162	0.70364	0.00255	0.70323	0.00141
11	131	140	0.70238	0.70619	0.69735	0.70212	0.00146	0.70371	0.00149	0.70307	0.00237	0.70321	0.00127
12	141	150	0.70607	0.70232	0.71159	0.70245	0.00137	0.70359	0.00136	0.70378	0.00228	0.70344	0.00115
13	151	160	0.70037	0.70040	0.70984	0.70229	0.00127	0.70335	0.00128	0.70424	0.00215	0.70340	0.00107
14	161	170	0.72037	0.71651	0.71747	0.70358	0.00175	0.70429	0.00151	0.70519	0.00220	0.70471	0.00143
15	171	180	0.69433	0.69238	0.70387	0.70296	0.00174	0.70349	0.00162	0.70510	0.00205	0.70426	0.00148
16	181	190	0.70269	0.70088	0.69643	0.70295	0.00163	0.70333	0.00152	0.70456	0.00199	0.70381	0.00139
17	191	200	0.70976	0.70864	0.70773	0.70335	0.00158	0.70364	0.00146	0.70475	0.00188	0.70410	0.00132
18	201	210	0.70393	0.71074	0.69819	0.70338	0.00149	0.70404	0.00143	0.70438	0.00181	0.70423	0.00125
19	211	220	0.70859	0.70134	0.70737	0.70365	0.00144	0.70389	0.00136	0.70454	0.00172	0.70417	0.00117
20	221	230	0.69003	0.68724	0.68572	0.70297	0.00152	0.70306	0.00154	0.70360	0.00188	0.70321	0.00143
21	231	240	0.69404	0.69697	0.70617	0.70255	0.00151	0.70277	0.00149	0.70372	0.00180	0.70307	0.00138
22	241	250	0.70290	0.70303	0.70274	0.70256	0.00144	0.70278	0.00142	0.70368	0.00171	0.70307	0.00131
23	251	260	0.69744	0.70080	0.69572	0.70234	0.00139	0.70270	0.00136	0.70333	0.00167	0.70288	0.00127
24	261	270	0.68944	0.68842	0.69940	0.70180	0.00144	0.70210	0.00143	0.70317	0.00161	0.70253	0.00130
25	271	280	0.71173	0.70875	0.69470	0.70220	0.00144	0.70237	0.00140	0.70283	0.00158	0.70256	0.00123
26	281	290	0.69046	0.69795	0.68252	0.70175	0.00145	0.70220	0.00136	0.70205	0.00171	0.70218	0.00125

```
    27   291   300   0.69890  0.70547  0.69782      0.70164 0.00140   0.70232 0.00131   0.70189 0.00165      0.70221
0.00121
    28   301   310   0.72067  0.71493  0.72845      0.70232 0.00151   0.70277 0.00134   0.70284 0.00185      0.70287
0.00131
    29   311   320   0.71248  0.71290  0.70837      0.70267 0.00150   0.70312 0.00134   0.70303 0.00180      0.70318
0.00130
    30   321   330   0.70552  0.71034  0.68928      0.70277 0.00145   0.70336 0.00132   0.70257 0.00180      0.70322
0.00126
 ------------------------------------------------------------------------------------------------------------------------
---
    31   331   340   0.70673  0.70583  0.72029      0.70290 0.00141   0.70344 0.00128   0.70314 0.00183      0.70344
0.00124
    32   341   350   0.71397  0.70181  0.72231      0.70324 0.00141   0.70339 0.00124   0.70374 0.00187      0.70352
0.00119
    33   351   360   0.69317  0.69015  0.70837      0.70294 0.00140   0.70299 0.00126   0.70388 0.00182      0.70330
0.00119
    34   361   370   0.70051  0.70177  0.69207      0.70287 0.00136   0.70295 0.00123   0.70353 0.00180      0.70316
0.00116
    35   371   380   0.72093  0.70273  0.70370      0.70338 0.00142   0.70295 0.00119   0.70354 0.00174      0.70307
0.00112
    36   381   390   0.70896  0.71222  0.71827      0.70354 0.00139   0.70320 0.00119   0.70395 0.00174      0.70338
0.00114
    37   391   400   0.70283  0.69897  0.68309      0.70352 0.00135   0.70309 0.00116   0.70339 0.00179      0.70316
0.00113
    38   401   410   0.71038  0.71680  0.71233      0.70370 0.00132   0.70345 0.00118   0.70362 0.00176      0.70351
0.00114
    39   411   420   0.70453  0.69894  0.71991      0.70372 0.00129   0.70333 0.00116   0.70404 0.00176      0.70351
0.00112
    40   421   430   0.71224  0.71442  0.70680      0.70393 0.00128   0.70361 0.00116   0.70411 0.00172      0.70375
0.00111
 ------------------------------------------------------------------------------------------------------------------------
---
    41   431   440   0.71180  0.70908  0.70762      0.70412 0.00126   0.70374 0.00114   0.70419 0.00168      0.70388
0.00109
    42   441   450   0.69886  0.70084  0.70113      0.70400 0.00123   0.70368 0.00112   0.70412 0.00164      0.70380
0.00107
    43   451   460   0.70033  0.69292  0.70745      0.70391 0.00121   0.70343 0.00112   0.70420 0.00160      0.70366
0.00106
    44   461   470   0.70894  0.70544  0.69422      0.70403 0.00119   0.70347 0.00109   0.70397 0.00158      0.70365
0.00103
    45   471   480   0.70260  0.70505  0.69236      0.70400 0.00116   0.70351 0.00107   0.70371 0.00157      0.70361
0.00101
    46   481   490   0.69987  0.69934  0.69771      0.70391 0.00114   0.70342 0.00105   0.70358 0.00154      0.70351
0.00099
    47   491   500   0.70292  0.70173  0.71993      0.70389 0.00111   0.70338 0.00103   0.70393 0.00154      0.70356
0.00097
    48   501   510   0.69558  0.69375  0.68100      0.70371 0.00110   0.70318 0.00103   0.70345 0.00159      0.70332
0.00099
    49   511   520   0.69737  0.69503  0.71016      0.70358 0.00109   0.70301 0.00102   0.70359 0.00156      0.70322
0.00097
    50   521   530   0.70154  0.70293  0.68301      0.70354 0.00107   0.70301 0.00100   0.70318 0.00158      0.70313
0.00096
```

average keff results summed over 20 cycles each to form 25 batch values of keff

```
  batch  start   end     keff estimators by batch          average keff estimators and deviations                col/abs/tl
keff
 number  cycle  cycle    k(coll)  k(abs)  k(track)     k(coll)  st dev    k(abs)  st dev   k(track) st dev      k(c/a/t) st
dev
      1     31     50   0.69728  0.70427  0.70439
      2     51     70   0.70210  0.70381  0.70579     0.69969 0.00241   0.70404 0.00023   0.70509 0.00070
      3     71     90   0.70776  0.71017  0.70467     0.70238 0.00303   0.70608 0.00205   0.70495 0.00043
      4     91    110   0.70080  0.69716  0.71013     0.70198 0.00218   0.70385 0.00266   0.70624 0.00133      0.70631
0.00037
      5    111    130   0.70252  0.70190  0.69323     0.70209 0.00169   0.70346 0.00210   0.70364 0.00280      0.70281
0.00204
      6    131    150   0.70423  0.70425  0.70447     0.70245 0.00143   0.70359 0.00172   0.70378 0.00229      0.70309
0.00154
      7    151    170   0.71037  0.70846  0.71366     0.70358 0.00165   0.70429 0.00161   0.70519 0.00240      0.70431
0.00181
      8    171    190   0.69851  0.69663  0.70015     0.70295 0.00157   0.70333 0.00169   0.70456 0.00217      0.70344
0.00178
      9    191    210   0.70685  0.70969  0.70296     0.70338 0.00145   0.70404 0.00165   0.70438 0.00192      0.70383
0.00158
     10    211    230   0.69931  0.69429  0.69654     0.70297 0.00136   0.70306 0.00177   0.70360 0.00189      0.70311
0.00148
 ------------------------------------------------------------------------------------------------------------------------
---
     11    231    250   0.69847  0.70000  0.70446     0.70256 0.00129   0.70278 0.00162   0.70368 0.00171      0.70287
0.00138
     12    251    270   0.69344  0.69461  0.69756     0.70180 0.00140   0.70210 0.00163   0.70317 0.00164      0.70228
0.00149
     13    271    290   0.70110  0.70335  0.68861     0.70175 0.00129   0.70220 0.00150   0.70205 0.00188      0.70186
0.00137
     14    291    310   0.70978  0.71020  0.71314     0.70232 0.00133   0.70277 0.00150   0.70284 0.00191      0.70245
0.00143
     15    311    330   0.70900  0.71162  0.69883     0.70277 0.00131   0.70336 0.00152   0.70257 0.00180      0.70275
0.00138
     16    331    350   0.71035  0.70382  0.72130     0.70324 0.00132   0.70339 0.00142   0.70374 0.00205      0.70337
0.00137
     17    351    370   0.69684  0.69596  0.70022     0.70287 0.00129   0.70295 0.00141   0.70353 0.00194      0.70300
0.00135
     18    371    390   0.71494  0.70748  0.71099     0.70354 0.00139   0.70320 0.00135   0.70395 0.00187      0.70342
0.00133
```

19	391	410	0.70660	0.70788	0.69771	0.70370	0.00133	0.70345	0.00130	0.70362	0.00180	0.70352	0.00126
20	411	430	0.70839	0.70668	0.71336	0.70393	0.00128	0.70361	0.00124	0.70411	0.00178	0.70376	0.00122
21	431	450	0.70533	0.70496	0.70437	0.70400	0.00122	0.70368	0.00118	0.70412	0.00169	0.70381	0.00116
22	451	470	0.70464	0.69918	0.70084	0.70403	0.00116	0.70347	0.00115	0.70397	0.00162	0.70369	0.00112
23	471	490	0.70124	0.70219	0.69504	0.70391	0.00112	0.70342	0.00110	0.70358	0.00159	0.70355	0.00108
24	491	510	0.69925	0.69774	0.70046	0.70371	0.00109	0.70318	0.00108	0.70345	0.00153	0.70335	0.00106
25	511	530	0.69946	0.69898	0.69658	0.70354	0.00106	0.70301	0.00105	0.70318	0.00150	0.70317	0.00103

average keff results summed over 25 cycles each to form 20 batch values of keff

batch number	start cycle	end cycle	keff estimators by batch k(coll)	k(abs)	k(track)	average keff estimators and deviations k(coll)	st dev	k(abs)	st dev	k(track)	st dev	col/abs/tl k(c/a/t)	st dev
1	31	55	0.69657	0.70340	0.70573								
2	56	80	0.70689	0.70764	0.70461	0.70173	0.00516	0.70552	0.00212	0.70517	0.00056		
3	81	105	0.70330	0.70294	0.70696	0.70225	0.00303	0.70466	0.00150	0.70577	0.00068		
4	106	130	0.70161	0.69985	0.69725	0.70209	0.00215	0.70346	0.00160	0.70364	0.00218	0.70307	0.00279
5	131	155	0.70351	0.70440	0.70454	0.70238	0.00169	0.70365	0.00125	0.70382	0.00170	0.70330	0.00181
6	156	180	0.70590	0.70272	0.71151	0.70296	0.00150	0.70349	0.00104	0.70510	0.00189	0.70355	0.00140
7	181	205	0.70925	0.70930	0.70200	0.70386	0.00155	0.70432	0.00121	0.70466	0.00166	0.70439	0.00124
8	206	230	0.69675	0.69424	0.69617	0.70297	0.00161	0.70306	0.00164	0.70360	0.00178	0.70322	0.00165
9	231	255	0.69816	0.69762	0.70089	0.70244	0.00152	0.70246	0.00157	0.70330	0.00160	0.70281	0.00153
10	256	280	0.70007	0.70157	0.69860	0.70220	0.00138	0.70237	0.00140	0.70283	0.00151	0.70247	0.00138
11	281	305	0.69993	0.70605	0.69500	0.70199	0.00126	0.70270	0.00131	0.70212	0.00154	0.70230	0.00127
12	306	330	0.71128	0.71058	0.70758	0.70277	0.00139	0.70336	0.00137	0.70257	0.00148	0.70296	0.00134
13	331	355	0.70623	0.70055	0.71508	0.70303	0.00131	0.70314	0.00128	0.70353	0.00166	0.70325	0.00123
14	356	380	0.70789	0.70037	0.70362	0.70338	0.00126	0.70295	0.00120	0.70354	0.00154	0.70318	0.00113
15	381	405	0.70582	0.70761	0.70172	0.70354	0.00118	0.70326	0.00116	0.70342	0.00144	0.70335	0.00106
16	406	430	0.70975	0.70893	0.71445	0.70393	0.00117	0.70361	0.00114	0.70411	0.00151	0.70379	0.00110
17	431	455	0.70786	0.70519	0.71145	0.70416	0.00112	0.70370	0.00107	0.70454	0.00149	0.70397	0.00106
18	456	480	0.70116	0.70015	0.68966	0.70400	0.00107	0.70351	0.00103	0.70371	0.00163	0.70369	0.00104
19	481	505	0.70176	0.70044	0.70559	0.70388	0.00102	0.70334	0.00099	0.70381	0.00154	0.70357	0.00099
20	506	530	0.69715	0.69667	0.69113	0.70354	0.00103	0.70301	0.00100	0.70318	0.00159	0.70324	0.00101

average keff results summed over 50 cycles each to form 10 batch values of keff

batch number	start cycle	end cycle	keff estimators by batch k(coll)	k(abs)	k(track)	average keff estimators and deviations k(coll)	st dev	k(abs)	st dev	k(track)	st dev	col/abs/tl k(c/a/t)	st dev
1	31	80	0.70173	0.70552	0.70517								
2	81	130	0.70245	0.70140	0.70211	0.70209	0.00036	0.70346	0.00206	0.70364	0.00153		
3	131	180	0.70471	0.70356	0.70803	0.70296	0.00090	0.70349	0.00119	0.70510	0.00171		
4	181	230	0.70300	0.70177	0.69909	0.70297	0.00063	0.70306	0.00095	0.70360	0.00193	0.70287	0.00055
5	231	280	0.69911	0.69960	0.69975	0.70220	0.00092	0.70237	0.00101	0.70283	0.00168	0.70213	0.00111
6	281	330	0.70561	0.70832	0.70129	0.70277	0.00094	0.70336	0.00129	0.70257	0.00140	0.70271	0.00120
7	331	380	0.70706	0.70046	0.70935	0.70338	0.00100	0.70295	0.00117	0.70354	0.00153	0.70322	0.00106
8	381	430	0.70779	0.70827	0.70808	0.70393	0.00103	0.70361	0.00121	0.70411	0.00144	0.70384	0.00113
9	431	480	0.70451	0.70267	0.70056	0.70400	0.00091	0.70351	0.00107	0.70371	0.00133	0.70380	0.00099
10	481	530	0.69946	0.69855	0.69836	0.70354	0.00093	0.70301	0.00108	0.70318	0.00130	0.70336	0.00104

average keff results summed over 100 cycles each to form 5 batch values of keff

batch number	start cycle	end cycle	keff estimators by batch k(coll)	k(abs)	k(track)	average keff estimators and deviations k(coll)	st dev	k(abs)	st dev	k(track)	st dev	col/abs/tl k(c/a/t)	st dev
1	31	130	0.70209	0.70346	0.70364								
2	131	230	0.70385	0.70266	0.70356	0.70297	0.00088	0.70306	0.00040	0.70360	0.00004		
3	231	330	0.70236	0.70396	0.70052	0.70277	0.00055	0.70336	0.00038	0.70257	0.00103		
4	331	430	0.70742	0.70436	0.70872	0.70393	0.00123	0.70361	0.00037	0.70411	0.00170	0.70359	0.00063
5	431	530	0.70198	0.70061	0.69946	0.70354	0.00103	0.70301	0.00066	0.70318	0.00161	0.70330	0.00075

average keff results summed over 125 cycles each to form 4 batch values of keff

batch number	start cycle	end cycle	keff estimators by batch k(coll)	k(abs)	k(track)	average keff estimators and deviations k(coll)	st dev	k(abs)	st dev	k(track)	st dev	col/abs/tl k(c/a/t)	st dev
1	31	155	0.70238	0.70365	0.70382								
2	156	280	0.70202	0.70109	0.70183	0.70220	0.00018	0.70237	0.00128	0.70283	0.00099		
3	281	405	0.70623	0.70503	0.70460	0.70354	0.00135	0.70326	0.00115	0.70342	0.00082		
4	406	530	0.70354	0.70227	0.70246	0.70354	0.00095	0.70301	0.00085	0.70318	0.00063	0.70379	0.00031

average keff results summed over 250 cycles each to form 2 batch values of keff

batch number	start cycle	end cycle	keff estimators by batch k(coll)	k(abs)	k(track)	average keff estimators and deviations k(coll)	st dev	k(abs)	st dev	k(track)	st dev
1	31	280	0.70220	0.70237	0.70283						
2	281	530	0.70488	0.70365	0.70353	0.70354	0.00134	0.70301	0.00064	0.70318	0.00035

laverage individual and combined collision/absorption/track-length keff results for 10 different batch sizes

cycles per keff batch	number of k batches	average keff estimators and deviations k(col) st dev	k(abs) st dev	k(trk) st dev	normality co/ab/trk	average k(c/a/t) k(c/a/t) st dev	k(c/a/t) confidence 95% confidence	99% confidence
1	500	0.7035 0.0011	0.7030 0.0011	0.7032 0.0015	95/95/95	0.70319 0.00102	0.70115-0.70523	0.70048-0.70590
2	250	0.7035 0.0011	0.7030 0.0010	0.7032 0.0016	95/95/95	0.70319 0.00101	0.70119-0.70520	0.70054-0.70585
4	125	0.7035 0.0010	0.7030 0.0010	0.7032 0.0015	99/95/95	0.70316 0.00096	0.70125-0.70507	0.70063-0.70570
5	100	0.7035 0.0010	0.7030 0.0010	0.7032 0.0016	95/95/95	0.70315 0.00096	0.70125-0.70506	0.70063-0.70568
10	50	0.7035 0.0011	0.7030 0.0010	0.7032 0.0016	95/95/95	0.70313 0.00096	0.70121-0.70506	0.70057-0.70570
20	25	0.7035 0.0011	0.7030 0.0010	0.7032 0.0015	95/95/95	0.70317 0.00103	0.70102-0.70531	0.70025-0.70608
25	20	0.7035 0.0010	0.7030 0.0010	0.7032 0.0016	95/95/95	0.70324 0.00101	0.70110-0.70537	0.70031-0.70616
50	10	0.7035 0.0009	0.7030 0.0011	0.7032 0.0013	95/95/95	0.70336 0.00104	0.70091-0.70581	0.69973-0.70699
100	5	0.7035 0.0010	0.7030 0.0007	0.7032 0.0016	95/95/95	0.70330 0.00075	0.70010-0.70651	0.69591-0.71070
125	4	0.7035 0.0010	0.7030 0.0009	0.7032 0.0006	95/95/95	0.70379 0.00031	0.69989-0.70769	0.68426-0.72332

lindividual and average keff estimator results by cycle

keff cycle	neutron histories	keff estimators by cycle k(coll)	k(abs)	k(track)	average keff estimators and deviations k(coll) st dev	k(abs) st dev	k(track) st dev	average k(c/a/t) k(c/a/t)	st dev	fom
1	1000	0.66263	0.67157	0.66002						
2	844	0.62259	0.63335	0.60633						
3	928	0.74464	0.73878	0.73698						
4	1189	0.68648	0.69320	0.71005						
5	916	0.67162	0.67449	0.66605						
6	972	0.67555	0.69125	0.65326						
7	999	0.69386	0.68906	0.66118						
8	1052	0.70286	0.67585	0.73216						
9	1006	0.69990	0.70969	0.76966						
10	1024	0.69455	0.70359	0.71872						
11	992	0.71945	0.72461	0.77486						
12	1044	0.74157	0.74571	0.71944						
13	1026	0.71667	0.70198	0.67162						
14	971	0.68381	0.69304	0.65735						
15	972	0.67127	0.68589	0.70914						
16	980	0.70348	0.68749	0.72402						
17	1075	0.67107	0.68658	0.63445						
18	942	0.69601	0.70231	0.71773						
19	1027	0.70549	0.71679	0.64485						
20	1045	0.77572	0.74148	0.75166						
21	1103	0.69297	0.68583	0.72338						
22	898	0.67206	0.66187	0.67595						

```
    23         949 | 0.71079  0.69071  0.73845  |
    24        1052 | 0.68395  0.66337  0.74105  |
    25         970 | 0.68790  0.69966  0.67099  |
    26        1010 | 0.70855  0.69614  0.70095  |
    27        1009 | 0.67223  0.64488  0.68232  |
    28         973 | 0.73330  0.74610  0.69315  |
    29        1080 | 0.69622  0.71162  0.68492  |
    30         935 | 0.73041  0.69416  0.74775  |
 ------------------  begin active keff cycles  ----------------------------------------------------------------------------------------------------
---
    31        1047 | 0.71428  0.73079  0.71371  |
    32         971 | 0.69249  0.71990  0.70235  | 0.70338 0.01089   0.72534 0.00544   0.70803 0.00568  |
    33         981 | 0.69778  0.70563  0.66827  | 0.70151 0.00656   0.71877 0.00728   0.69478 0.01365  |
    34         994 | 0.68924  0.69195  0.69822  | 0.69845 0.00556   0.71207 0.00846   0.69564 0.00969  | 0.69375 0.01721
8655
    35         994 | 0.68162  0.70872  0.64083  | 0.69508 0.00547   0.71140 0.00658   0.68468 0.01329  | 0.69941 0.01388
10969
    36         977 | 0.71544  0.70426  0.72827  | 0.69847 0.00561   0.71021 0.00551   0.69194 0.01306  | 0.70431 0.00742
33097
    37        1037 | 0.73287  0.74246  0.72458  | 0.70339 0.00683   0.71481 0.00655   0.69660 0.01198  | 0.70980 0.01000
16163
    38        1015 | 0.69058  0.70612  0.77117  | 0.70179 0.00612   0.71373 0.00577   0.70593 0.01395  | 0.70945 0.00924
16573
    39         956 | 0.66418  0.66719  0.62670  | 0.69761 0.00683   0.70856 0.00726   0.69712 0.01513  | 0.70110 0.01044
10967
    40         956 | 0.66792  0.70877  0.69622  | 0.69464 0.00679   0.70858 0.00649   0.69703 0.01353  | 0.70301 0.00977
11412
 ----------------------------------------------------------------------------------------------------------------------------------------------
---
.
.
.
 ----------------------------------------------------------------------------------------------------------------------------------------------
--
   511         928 | 0.75910  0.74259  0.75416  | 0.70383 0.00113   0.70326 0.00111   0.70356 0.00154  | 0.70348 0.00104
20679
   512        1183 | 0.67984  0.69205  0.72746  | 0.70378 0.00113   0.70324 0.00111   0.70361 0.00154  | 0.70346 0.00104
20711
   513         882 | 0.68107  0.68076  0.70320  | 0.70373 0.00113   0.70319 0.00111   0.70361 0.00153  | 0.70342 0.00104
20724
   514        1007 | 0.69072  0.68108  0.70462  | 0.70370 0.00112   0.70315 0.00111   0.70361 0.00153  | 0.70339 0.00104
20741
   515        1027 | 0.64762  0.66328  0.62331  | 0.70359 0.00113   0.70306 0.00111   0.70344 0.00154  | 0.70328 0.00104
20556
   516         932 | 0.68972  0.68472  0.71744  | 0.70356 0.00113   0.70303 0.00111   0.70347 0.00153  | 0.70326 0.00104
20586
   517        1052 | 0.74062  0.71731  0.75135  | 0.70364 0.00113   0.70305 0.00111   0.70357 0.00153  | 0.70331 0.00104
20573
   518        1053 | 0.70672  0.69771  0.68843  | 0.70364 0.00112   0.70304 0.00110   0.70354 0.00153  | 0.70330 0.00104
20612
   519         938 | 0.67005  0.67215  0.67557  | 0.70357 0.00112   0.70298 0.00110   0.70348 0.00153  | 0.70323 0.00104
20571
   520         937 | 0.70825  0.71869  0.75603  | 0.70358 0.00112   0.70301 0.00110   0.70359 0.00153  | 0.70327 0.00104
20596
 ----------------------------------------------------------------------------------------------------------------------------------------------
---
   521        1058 | 0.71063  0.71456  0.63479  | 0.70360 0.00112   0.70304 0.00110   0.70345 0.00153  | 0.70327 0.00103
20634
   522        1009 | 0.68556  0.69318  0.65900  | 0.70356 0.00112   0.70302 0.00110   0.70336 0.00153  | 0.70323 0.00103
20648
   523         969 | 0.67996  0.70849  0.66781  | 0.70351 0.00112   0.70303 0.00110   0.70329 0.00153  | 0.70321 0.00103
20690
   524         978 | 0.72088  0.70570  0.70327  | 0.70355 0.00111   0.70303 0.00109   0.70329 0.00153  | 0.70322 0.00103
20730
   525        1035 | 0.71400  0.70193  0.73850  | 0.70357 0.00111   0.70303 0.00109   0.70336 0.00153  | 0.70324 0.00103
20767
   526        1006 | 0.74177  0.75665  0.71714  | 0.70365 0.00111   0.70314 0.00110   0.70339 0.00152  | 0.70333 0.00103
20676
   527        1046 | 0.64384  0.66806  0.63471  | 0.70353 0.00112   0.70307 0.00110   0.70325 0.00153  | 0.70323 0.00103
20527
   528         869 | 0.71724  0.69923  0.69946  | 0.70355 0.00112   0.70306 0.00109   0.70324 0.00152  | 0.70323 0.00103
20572
   529        1119 | 0.69903  0.68697  0.72558  | 0.70354 0.00111   0.70303 0.00109   0.70328 0.00152  | 0.70322 0.00103
20601
   530         961 | 0.70253  0.69452  0.64982  | 0.70354 0.00111   0.70301 0.00109   0.70318 0.00152  | 0.70319 0.00102
20625
 ----------------------------------------------------------------------------------------------------------------------------------------------
---

  the largest active cycle keffs by estimator are:                                  the smallest active cycle keffs by estimator
are:

                  collision 0.77667 on cycle 250                                              collision 0.63361 on cycle 397
                absorption 0.76931 on cycle 201                                             absorption 0.63388 on cycle 510
              track length 0.81127 on cycle 331                                           track length 0.60593 on cycle 445
1plot of the estimated col/abs/track-length keff one standard deviation interval versus cycle number (| = final keff =  0.70319)

    cycle   active 0.69                          0.70                          0.71                          0.72
   number   cycles  |----------------------------|-----------------------------|-----------------------------|
      40       10  |        (-------------------------------k-----------------------------)                   |
      45       15  |                    (-----------------k-|--------------)                                  |
      50       20  |                  (--------------k------|------)                                         |
      55       25  |                  (------------k--------|--)                                             |
      60       30  |                 (-------------k--------|---)                                            |
      65       35  |                    (-----------k--------|--)                                             |
```

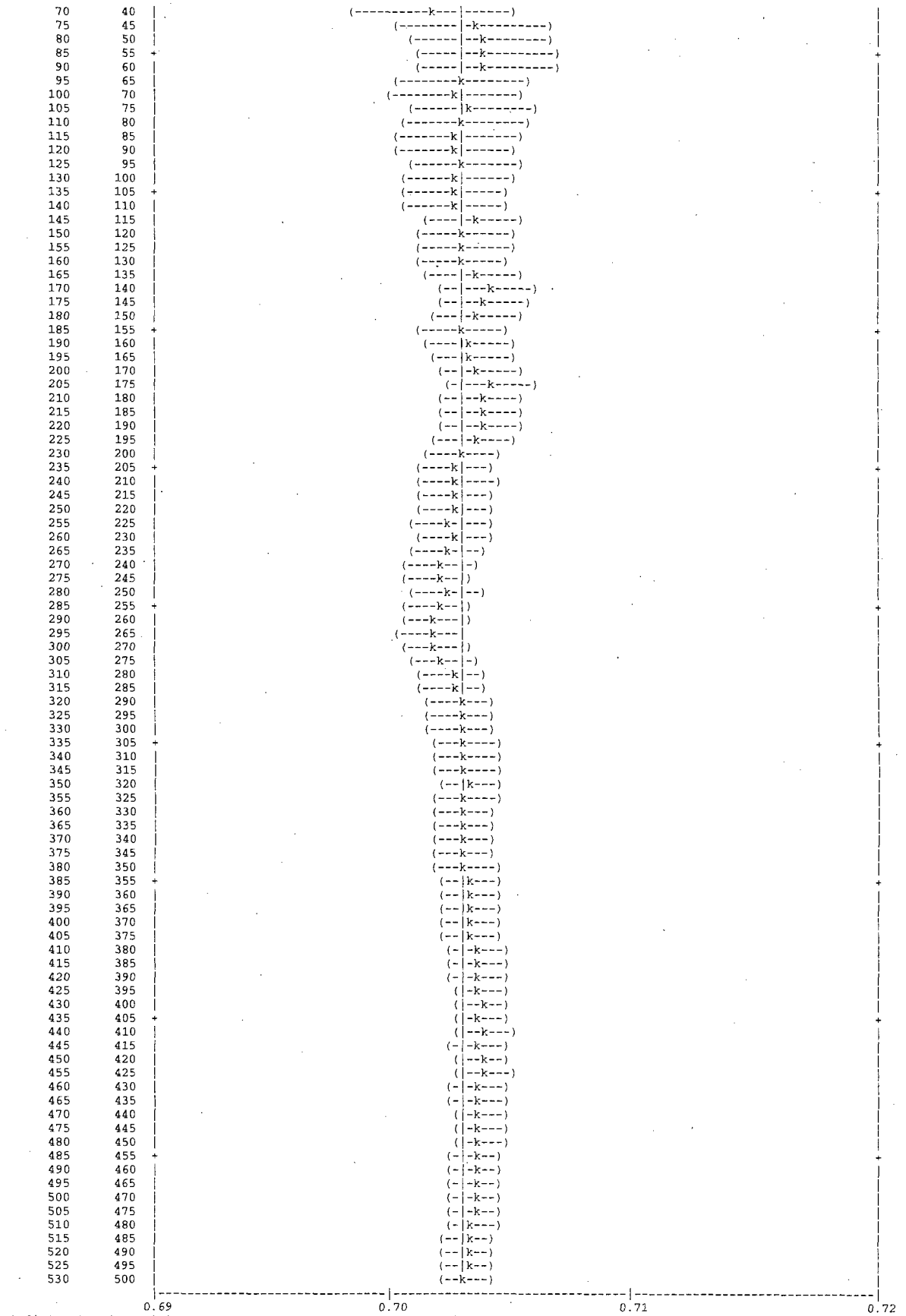

1individual and collision/absorption/track-length keffs for different numbers of inactive cycles skipped for fission source settling

skip cycles	active cycles	active neutrons	average keff estimators and deviations k(col)	st dev	k(abs)	st dev	k(trk)	st dev	normality co/ab/tl	average k(c/a/t)	st dev	k(c/a/t) confidence 95% confidence	99% confidence intervals
0	530	530485	0.7032	0.0011	0.7026	0.0011	0.7030	0.0015	95/95/95	0.70281	0.00101	0.70081-0.70482	0.70015-0.70547
1	529	529485	0.7033	0.0011	0.7026	0.0011	0.7030	0.0015	95/95/95	0.70288	0.00101	0.70088-0.70488	0.70022-0.70554
2	528	528641	0.7034	0.0011	0.7028	0.0011	0.7032	0.0015	95/95/95	0.70303	0.00100	0.70104-0.70502	0.70039-0.70566
3	527	527713	0.7034	0.0011	0.7027	0.0011	0.7032	0.0015	95/95/95	0.70296	0.00100	0.70097-0.70495	0.70033-0.70559
4	526	526524	0.7034	0.0011	0.7027	0.0011	0.7031	0.0015	95/95/95	0.70298	0.00100	0.70099-0.70497	0.70034-0.70562
5	525	525608	0.7034	0.0011	0.7028	0.0011	0.7032	0.0015	95/95/95	0.70304	0.00100	0.70105-0.70503	0.70040-0.70568
6	524	524636	0.7035	0.0011	0.7028	0.0011	0.7033	0.0015	95/95/95	0.70308	0.00100	0.70109-0.70507	0.70044-0.70572
7	523	523637	0.7035	0.0011	0.7028	0.0011	0.7034	0.0015	95/95/95	0.70311	0.00100	0.70112-0.70511	0.70047-0.70576
8	522	522585	0.7035	0.0011	0.7029	0.0011	0.7033	0.0015	95/95/95	0.70313	0.00100	0.70113-0.70513	0.70048-0.70578
9	521	521579	0.7035	0.0011	0.7029	0.0011	0.7032	0.0015	95/95/95	0.70310	0.00100	0.70110-0.70510	0.70045-0.70576
10	520	520555	0.7035	0.0011	0.7029	0.0011	0.7032	0.0015	95/95/95	0.70310	0.00101	0.70110-0.70511	0.70044-0.70576
11	519	519563	0.7035	0.0011	0.7028	0.0011	0.7030	0.0015	95/95/95	0.70305	0.00101	0.70104-0.70505	0.70038-0.70571
12	518	518519	0.7034	0.0011	0.7027	0.0011	0.7030	0.0015	95/95/95	0.70297	0.00101	0.70097-0.70498	0.70031-0.70563
13	517	517493	0.7034	0.0011	0.7027	0.0011	0.7031	0.0015	95/95/95	0.70298	0.00101	0.70097-0.70499	0.70031-0.70564
14	516	516522	0.7035	0.0011	0.7028	0.0011	0.7032	0.0015	95/95/95	0.70301	0.00101	0.70100-0.70502	0.70035-0.70568
15	515	515550	0.7035	0.0011	0.7028	0.0011	0.7031	0.0015	95/95/95	0.70305	0.00101	0.70104-0.70506	0.70038-0.70572
16	514	514570	0.7035	0.0011	0.7028	0.0011	0.7031	0.0015	95/95/95	0.70306	0.00101	0.70104-0.70508	0.70038-0.70573
17	513	513495	0.7036	0.0011	0.7028	0.0011	0.7032	0.0015	95/95/95	0.70312	0.00101	0.70110-0.70514	0.70044-0.70580
18	512	512553	0.7036	0.0011	0.7028	0.0011	0.7032	0.0015	95/95/95	0.70312	0.00102	0.70110-0.70514	0.70044-0.70580
19	511	511526	0.7036	0.0011	0.7028	0.0011	0.7033	0.0015	95/95/95	0.70312	0.00102	0.70109-0.70515	0.70043-0.70581
20	510	510481	0.7034	0.0011	0.7027	0.0011	0.7032	0.0015	95/95/95	0.70303	0.00101	0.70101-0.70505	0.70035-0.70571
.													
.													
.													
.													
475	55	55110	0.6995	0.0033	0.6991	0.0032	0.6982	0.0046	95/95/95	0.69904	0.00308	0.69285-0.70523	0.69079-0.70729
480	50	50070	0.6995	0.0034	0.6986	0.0034	0.6984	0.0049	95/95/95	0.69873	0.00330	0.69209-0.70538	0.68986-0.70761
485	45	45025	0.6998	0.0038	0.6990	0.0037	0.6998	0.0053	95/95/95	0.69932	0.00362	0.69201-0.70663	0.68955-0.70909
490	40	40100	0.6994	0.0039	0.6984	0.0038	0.6985	0.0056	95/95/95	0.69858	0.00374	0.69100-0.70617	0.68842-0.70875
495	35	34999	0.6989	0.0043	0.6970	0.0041	0.6955	0.0062	95/95/95	0.69704	0.00414	0.68861-0.70547	0.68571-0.70838
500	30	29990	0.6982	0.0049	0.6972	0.0046	0.6914	0.0068	95/95/95	0.69647	0.00484	0.68655-0.70640	0.68307-0.70987
505	25	25031	0.6972	0.0057	0.6967	0.0053	0.6911	0.0079	95/95/95	0.69586	0.00554	0.68436-0.70735	0.68023-0.71148
510	20	19989	0.6995	0.0066	0.6990	0.0052	0.6966	0.0092	95/95/95	0.69852	0.00542	0.68707-0.70996	0.68279-0.71424
515	15	14962	0.7021	0.0066	0.7013	0.0055	0.6946	0.0104	95/95/95	0.70061	0.00608	0.68736-0.71386	0.68203-0.71919
520	10	10050	0.7015	0.0085	0.7029	0.0072	0.6830	0.0122	95/95/95	0.69931	0.00934	0.67722-0.72141	0.66662-0.73201
525	5	5001	0.7009	0.0161	0.7011	0.0149	0.6853	0.0182	95/95/95	0.69614	0.02351	0.59496-0.79732	0.46277-0.92951
527	3	2949	0.7063	0.0056	0.6936	0.0036	0.6916	0.0222					
528	2	2080	0.7008	0.0017	0.6907	0.0038	0.6877	0.0379					

the minimum estimated standard deviation for the col/abs/tl keff estimator occurs with 3 inactive cycles and 527 active cycles.

the first active half of the problem skips 30 cycles and uses 250 active cycles; the second half skips 280 and uses 250 cycles.
the col/abs/trk-len keff, one standard deviation, and 68, 95, and 99 percent intervals for each active half of the problem are:

problem	keff	standard deviation	68% confidence	95% confidence	99% confidence
first half	0.70239	0.00143	0.70096 to 0.70381	0.69954 to 0.70523	0.69862 to 0.70616

second half	0.70385	0.00147	0.70238 to 0.70532	0.70092 to 0.70678	0.69997 to 0.70773
final result	0.70319	0.00102	0.70216 to 0.70422	0.70115 to 0.70523	0.70048 to 0.70590

the first and second half values of k(collision/absorption/track length) appear to be the same at the 68 percent confidence level.

1plot of the estimated col/abs/track-length keff one standard deviation interval by active cycle number (| = final keff = 0.70319)

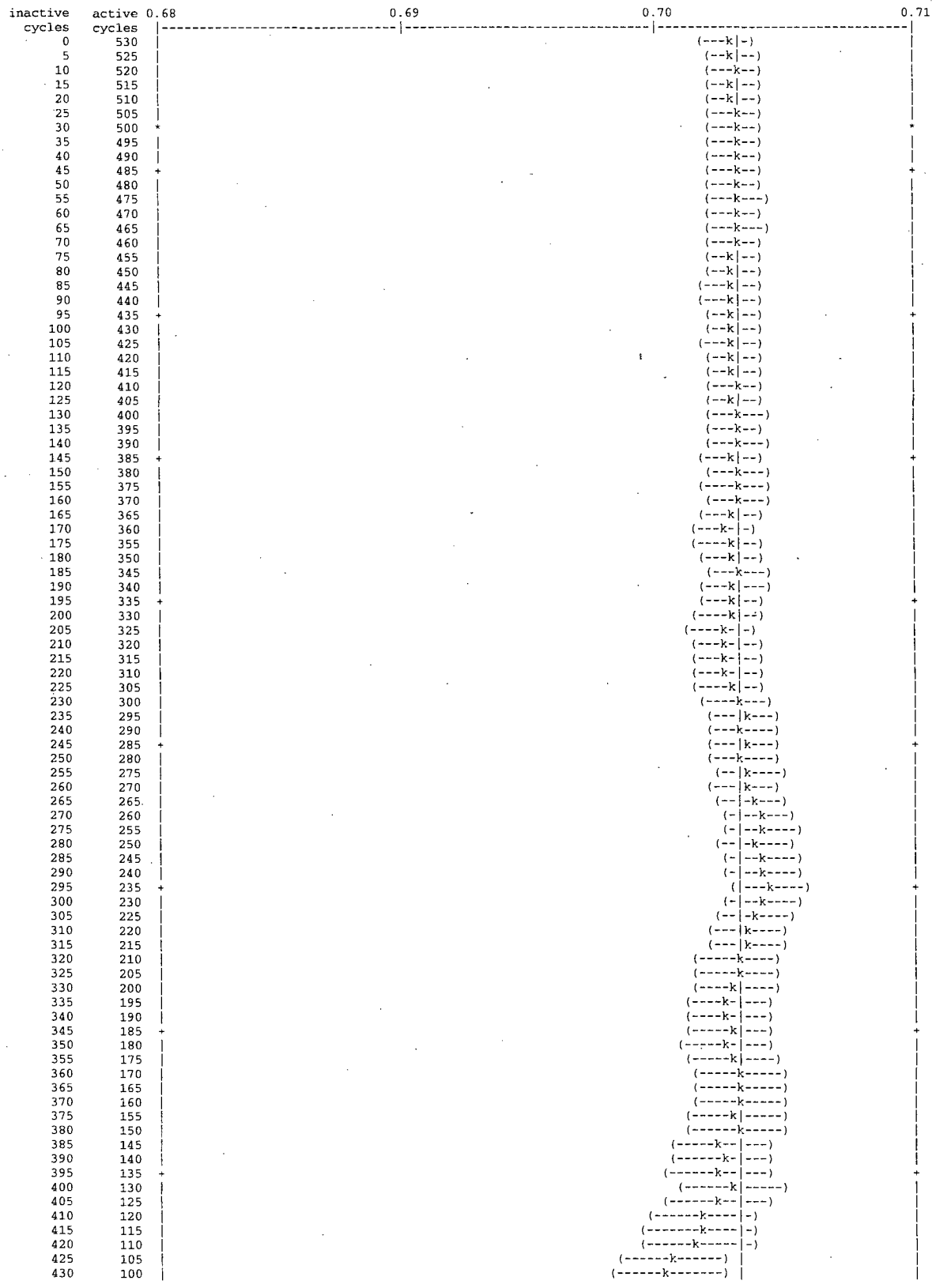

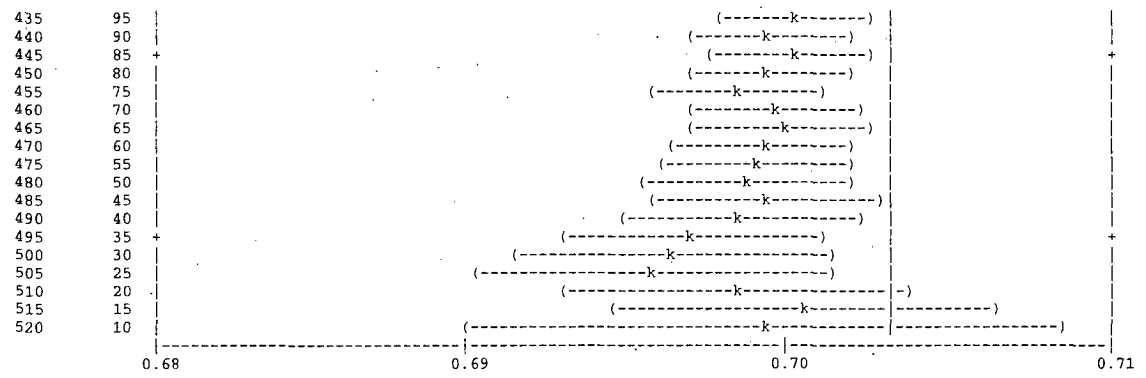


```
 ************************************************************************************************************************
 dump no.     2 on file MS_Acc_NACCoC_c1.00_g0.00_e0.00_d0.01cm_HP_36mm.inpr       nps =      530485     coll =       76766227
ctm =       11.96    nrn =          776053288

        6 warning messages so far.

 run terminated when    530    kcode cycles were done.

 computer time =    12.12 minutes

 mcnp      version 5      06212004                  10/25/07 21:18:09                  probid =  10/25/07 21:05:56
```

Figure 6.6.15-2 Hexagonal Pitch MOX Rods – ^{241}Pu Fuel Composition

```
Thread Name & Version = MCNP5_RSICC, 1.30

+-------------------------------------------------------------------+
|   This program was prepared by the Regents of the University of   |
|California at Los Alamos National Laboratory (the University) under |
|  contract number W-7405-ENG-36 with the U.S. Department of Energy  |
|(DoE).  The University has certain rights in the program pursuant to|
|  the contract and the program should not be copied or distributed  |
| outside your organization.  All rights in the program are reserved |
|by the DoE and the University.  Neither the U.S. Government nor the |
| University makes any warranty, express or implied, or assumes any  |
|     liability or responsibility for the use of this software.      |
+-------------------------------------------------------------------+

1mcnp     version 5     ld=06212004                    10/25/07 23:04:59
*************************************************************************                 probid =  10/25/07 23:04:59
 name=P1_Acc_NACCoC_c1.00_g0.00_e0.00_d0.01cm_HP_36mm.inp host=amdeng2-it1459

NAC-LWT Cask - MOX Experiments - Accident Transport Conditions
C
C EXCEL File Version: v2.00
C Run Version: v2.00
C
C Fissile Material Type: All Pu-241
C Rod Interior Void Moderator Density: 0.9982 g/cc
C Canister Interior Moderator Density: 0.9982 g/cc
C Canister to Cask Gap Moderator Density: 0.0001 g/cc
C Cask Exterior Moderator Density: 0.0001 g/cc
C Boundary Condition / Distance:  Reflected / 0.01 cm
C
C Fuel Rod Pitch: 3.6 cm
C Fuel Rod Pitch Cofiguration: Hexagonal
C Number of Rods: 16
C
C Base Fuel Parameters: NACCoC
C
c Cells - Fuel Rod - NACCoC
1 1 -10.554 -1   u=3 $ Fuel
2 2 -0.9982 -2 +1  u=3 $ Plenum + Fuel to Clad Gap
3 3 -6.56 -3 +2  u=3 $ Clad + End Plugs
4 4 -0.9982 +3   u=3 $ Outside Fuel Rod
C 16 Rods - Hexagonal Pitch
10 4 -0.9982 -10
           *trcl=( 0.9000 -1.5588 0.0000 )
           lat=2 u=2 fill=-7:6 -5:5 0:0
      2 2 2 2 2 2 2 2 2 2 2 2 2 2
      2 2 2 2 2 2 2 2 2 2 2 2 2 2
      2 2 2 2 2 2 2 2 2 2 2 2 2 2
      2 2 2 2 2 2 2 3 2 2 2 2 2 2
      2 2 2 2 2 2 3 3 3 2 2 2 2 2
      2 2 2 2 2 3 3 3 3 3 2 2 2 2
      2 2 2 2 2 3 3 3 3 2 2 2 2 2
      2 2 2 2 2 3 3 3 2 2 2 2 2 2
      2 2 2 2 2 2 2 2 2 2 2 2 2 2
      2 2 2 2 2 2 2 2 2 2 2 2 2 2
      2 2 2 2 2 2 2 2 2 2 2 2 2 2
C PWR Basket - Cells
20  4 -0.9982 -20   fill=2  u=1 $ Rod Array Container
21  5 -0.0001 +20 -21     u=1 $ Basket Cavity
22  7 -2.7020 -22 +21     u=1 $ Basket Body
23  5 -0.0001 +22      u=1 $ Outside
C Cells - LWT Cask Accident Conditions
40 8 -11.344 -43      u=0 $ BotPb
41 5 -0.0001 -42 fill=1    u=0 $ Cavity
42 9 -7.9400 -41 +43    u=0 $ Bottom
43 9 -7.9400 -40 +41 +45 +48 +42 u=0 $ OuterShell
44 9 -7.9400 -44 +47 +42   u=0 $ InnerShellTaper
45 9 -7.9400 -46 +42    u=0 $ InnerShell
46 8 -11.344 -47 +46    u=0 $ Lead
47 8 -11.344 -45 +44 +47   u=0 $ LeadTaper
48 0         -48 +47    u=0 $ LeadGap
49 6 -0.0001 -49 +40    u=0 $ Gap to Reflector
50 0          +49    u=0 $ Boundary

c Surfaces - Fuel Rod - NACCoC
1 RCC 0.0000 0.0000 10.5207 0.0000 0.0000 389.8900 0.4781   $ Fuel pellet stack
2 RCC 0.0000 0.0000 6.3990 0.0000 0.0000 409.4227 0.4876   $ Annulus + Plenum
3 RCC 0.0000 0.0000 5.0800 0.0000 0.0000 411.8226 0.5588   $ Clad + End-Caps
c Surfaces - Pitch - NACCoC
10 RHP 0.0000 0.0000 -1.0000 0.0000 0.0000 454.12 1.8000 0.0000 0.0000 $ Lattice
C PWR Basket - Surfaces
20 1 RPP -7.4148 7.4148 -7.4148 7.4148 0.0000 452.1200  $ Array Container
21 1 RPP -11.2713 11.2713 -11.2713 11.2713 0.0000 452.1200  $ Basket Opening
22  RCC 0.0000 0.0000 0.0000 0.0000 0.0000 452.1200 16.83512 $ Basket Outer Body
C Surfaces - LWT Cask Accident Conditions
40 RCC 0.0000 0.0000 -26.6700 0.0000 0.0000 507.3650 36.5189 $ Lwt Body
41 RCC 0.0000 0.0000 -26.6700 0.0000 0.0000 26.6700 36.5189 $ Bottom
```

```
 70-       42 RCC 0.0000 0.0000 0.0000 0.0000 0.0000 452.1200 16.9863 $ Cavity
 71-       43 RCC 0.0000 0.0000 -17.7800 0.0000 0.0000 7.6200 26.3525 $ Bottom gamma shield
 72-       44 RCC 0.0000 0.0000 0.0000 0.0000 0.0000 444.5000 20.1740 $ Lead id - taper
 73-       45 RCC 0.0000 0.0000 0.0000 0.0000 0.0000 444.5000 31.5976 $ Lead od - taper
 74-       46 RCC 0.0000 0.0000 13.8176 0.0000 0.0000 416.8648 18.9103 $ Lead id
 75-       47 RCC 0.0000 0.0000 13.8176 0.0000 0.0000 416.8648 33.3271 $ Lead od
 76-       48 RCC 0.0000 0.0000 13.8176 0.0000 0.0000 416.8648 33.4645 $ Lead gap
 77-       *49 RPP -36.5289 36.5289 -36.5289 36.5289 -26.6800 480.7050  $ Container
 78-
 79-       c
 80-       c Materials List
 81-       c
 82-       C MOX Material Composition Fuel
 83-       m1     92235 -5.7210E-03
 84-              92238 -8.1157E-01
 85-              94238 -6.4417E-10
 86-              94239 -6.4417E-10
 87-              94240 -6.4417E-10
 88-              94241 -6.4417E-02
 89-              94242 -6.4417E-10
 90-               8016 -1.1829E-01
 91-       C Rod Interior Void Material
 92-       m2     1001 2
 93-              8016 1
 94-       mt2      lwtr.01
 95-       c Clad Material
 96-       m3 26054 -7.063E-05 24050 -4.179E-05 7014 -4.980E-04
 97-              26056 -1.149E-03 24052 -8.370E-04 7015 -1.981E-06
 98-              26057 -2.702E-05 24053 -9.673E-05
 99-              26058 -3.631E-06 24054 -2.448E-05
100-              40000 -9.823E-01 50000 -1.500E-02
101-       C Canister Interior Non-Fuel Space
102-       m4     1001 2
103-              8016 1
104-       mt4      lwtr.01
105-       C Canister to Cask Gap Material
106-       m5     1001 2
107-              8016 1
108-       mt5      lwtr.01
109-       C Cask Exterior Material
110-       m6     1001 2
111-              8016 1
112-       mt6      lwtr.01
113-       c Aluminum
114-       m7 13027 -1.000E+00
115-       C Water/Glycol
116-       m10    1001 -1.03651E-01
warning. material  10 is not used in the problem.
117-              8016 -6.75619E-01
118-              6000 -2.20730E-01
119-       mt10     lwtr.01
warning. material  10 is not used in the problem.
120-       c Lead
121-       m8 82206 -2.534E-01
122-              82207 -2.207E-01
123-              82208 -5.259E-01
124-       c SS304
125-       m9 24050 -7.939E-03 26054 -3.927E-02 28058 -6.384E-02
126-              24052 -1.590E-01 26056 -6.387E-01 28060 -2.543E-02
127-              24053 -1.838E-02 26057 -1.502E-02 28061 -1.124E-03
128-              24054 -4.652E-03 26058 -2.019E-03 28062 -3.639E-03
129-                  28064 -9.623E-04
130-              25055 -2.000E-02
131-       C Aluminum Honeycomb Impact Limiter
132-       m11    13027 -1.0
warning. material  11 is not used in the problem.
133-       C Mode
134-       mode n
135-       C Cell Importances
136-       imp:n 1 18r 0
137-       C
138-       C Criticality Controls
139-       kcode 1000 0.80 30 530
140-       C
141-       C Starting Source Definition
142-       sdef cell=41:20:10:1
143-            erg=d1
144-            pos=0 0 10.5207
145-            rad=d2
146-            axs=0 0 1
147-            ext=d3
148-       sp1   -3
149-       si2 0.0000 0.4781
150-       sp2 -21 1
151-       si3 0.0000 389.8900
152-       sp3 0 1
153-       C Print Control
154-       print
155-       C Random Number Generator
156-       rand gen=2 seed=19073486328125 stride=152917 hist=1
157-       c
158-       c Rotation Matrix
159-       *TR1 0.0 0.0 0.0 -30 60 90 -120 -30 90 90 90 0  $ z-rotation -30 degrees

1source                                                                    print table 10

 values of defaulted or explicitly defined source variables
```

```
   sur        0.0000E+00
   tme        0.0000E+00
   dir        isotropic
   pos        0.0000E+00   0.0000E+00   1.0521E+01
   x          0.0000E+00
   y          0.0000E+00
   z          0.0000E+00
   axs        0.0000E+00   0.0000E+00   1.0000E+00
   vec        0.0000E+00   0.0000E+00   0.0000E+00
   ccc        0.0000E+00
   nrm        1.0000E+00
   ara        0.0000E+00
   wgt        1.0000E+00
   eff        1.0000E-02
   par        0.0000E+00
   tr         0.0000E+00


probability distribution   1 for source variable erg
energy function 3:  watt (fission) spectrum (endf law 10)

    f(e)=c*exp(-e/a)*sinh(sqrt(b*e))
    a = 9.6500E-01     b = 2.2900E+00     c = 4.5270E-01

   the mean of source distribution   1 is  1.9806E+00


probability distribution   2 for source variable rad
power law 21:     f(x)=c*abs(x)**k          k = 1.0000E+00


probability distribution   3 for source variable ext
unbiased histogram distribution

source        source          cumulative          probability
 entry         value          probability           of bin

   1       0.00000E+00        0.000000E+00        0.000000E+00
   2       3.89890E+02        1.000000E+00        1.000000E+00

    the mean of source distribution   3 is  1.9494E+02


order of sampling source variables.
cel axs rad ext pos erg tme

 comment. total fission nubar data are being used.
1material composition                                                    print table 40

 the sum of the fractions of material    2 was 3.000000E+00

 the sum of the fractions of material    3 was 1.000050E+00

 the sum of the fractions of material    4 was 3.000000E+00

 the sum of the fractions of material    5 was 3.000000E+00

 the sum of the fractions of material    6 was 3.000000E+00

 the sum of the fractions of material    9 was 9.999753E-01

 material
  number     component nuclide, atom fraction

    1           92235, 2.19354E-03      92238, 3.07241E-01      94238, 2.43869E-10      94239, 2.42846E-10
                94240, 2.41833E-10      94241, 2.40826E-02      94242, 2.39829E-10       8016, 6.66483E-01
    2            1001, 6.66667E-01       8016, 3.33333E-01
 associated thermal s(a,b) data sets:    lwtr.01t
    3           26054, 1.19346E-04      24050, 7.62600E-05       7014, 3.24139E-03      26056, 1.87224E-03
                24052, 1.46874E-03       7015, 1.20369E-05      26057, 4.32542E-05      24053, 1.66532E-04
                26058, 5.71247E-06      24054, 4.13652E-05      40000, 9.81436E-01      50000, 1.15166E-02
    4            1001, 6.66667E-01       8016, 3.33333E-01
 associated thermal s(a,b) data sets:    lwtr.01t
    5            1001, 6.66667E-01       8016, 3.33333E-01
 associated thermal s(a,b) data sets:    lwtr.01t
    6            1001, 6.66667E-01       8016, 3.33333E-01
 associated thermal s(a,b) data sets:    lwtr.01t
    7           13027, 1.00000E+00
    8           82206, 2.54963E-01      82207, 2.20987E-01      82208, 5.24050E-01
    9           24050, 8.79087E-03      26054, 4.02643E-02      28058, 6.09419E-02      24052, 1.69300E-01
                26056, 6.31511E-01      28060, 2.34673E-02      24053, 1.92010E-02      26057, 1.45900E-02
                28061, 1.02022E-03      24054, 4.76985E-03      26058, 1.92741E-03      28062, 3.24982E-03
                28064, 8.32505E-04      25055, 2.01337E-02
1material                                                                                print table 40
  number     component nuclide, mass fraction

    1           92235, 5.72101E-03      92238, 8.11572E-01      94238, 6.44171E-10      94239, 6.44171E-10
                94240, 6.44171E-10      94241, 6.44171E-02      94242, 6.44171E-10       8016, 1.18290E-01
    2            1001, 1.11915E-01       8016, 8.88085E-01
    3           26054, 7.06265E-05      24050, 4.17879E-05       7014, 4.97975E-04      26056, 1.14894E-03
                24052, 8.36958E-04       7015, 1.98090E-06      26057, 2.70186E-05      24053, 9.67251E-05
                26058, 3.63082E-06      24054, 2.44788E-05      40000, 9.82251E-01      50000, 1.49992E-02
    4            1001, 1.11915E-01       8016, 8.88085E-01
```

5	1001, 1.11915E-01	8016, 8.88085E-01		
6	1001, 1.11915E-01	8016, 8.88085E-01		
7	13027, 1.00000E+00			
8	82206, 2.53400E-01	82207, 2.20700E-01	82208, 5.25900E-01	
9	24050, 7.93920E-03	26054, 3.92710E-02	28058, 6.38416E-02	24052, 1.59004E-01
	26056, 6.38716E-01	28060, 2.54306E-02	24053, 1.83805E-02	26057, 1.50204E-02
	28061, 1.12403E-03	24054, 4.65211E-03	26058, 2.01905E-03	28062, 3.63909E-03
	28064, 9.62324E-04	25055, 2.00005E-02		

warning. 6 materials had unnormalized fractions. print table 40.

1cell volumes and masses print table 50

	cell	atom density	gram density	input volume	calculated volume	mass	pieces	reason volume not calculated
1	1	7.05243E-02	1.05540E+01	0.00000E+00	2.79982E+02	2.95493E+03	1	
2	2	1.00128E-01	9.98200E-01	0.00000E+00	2.58267E+01	2.57802E+01	1	
3	3	4.33411E-02	6.56000E+00	0.00000E+00	9.81838E+01	6.44086E+02	1	
4	4	1.00128E-01	9.98200E-01	0.00000E+00	0.00000E+00	0.00000E+00	0	infinite
5	10	1.00128E-01	9.98200E-01	0.00000E+00	5.09690E+03	5.08773E+03	0	
6	20	1.00128E-01	9.98200E-01	0.00000E+00	9.94289E+04	9.92499E+04	0	
7	21	1.00309E-05	1.00000E-04	0.00000E+00	1.30324E+05	1.30324E+01	0	
8	22	6.03063E-02	2.70200E+00	0.00000E+00	0.00000E+00	0.00000E+00	0	asymmetric
9	23	1.00309E-05	1.00000E-04	0.00000E+00	0.00000E+00	0.00000E+00	0	infinite
10	40	3.29629E-02	1.13440E+01	0.00000E+00	1.66245E+04	1.88588E+05	1	
11	41	1.00309E-05	1.00000E-04	0.00000E+00	4.09828E+05	4.09828E+01	1	
12	42	8.64586E-02	7.94000E+00	0.00000E+00	9.51154E+04	7.55216E+05	1	
13	43	8.64586E-02	7.94000E+00	0.00000E+00	4.53784E+05	3.60304E+06	1	
14	44	8.64586E-02	7.94000E+00	0.00000E+00	1.02842E+04	8.16563E+04	2	
15	45	8.64586E-02	7.94000E+00	0.00000E+00	9.04489E+04	7.18165E+05	1	
16	46	3.29629E-02	1.13440E+01	0.00000E+00	9.86269E+05	1.11882E+07	1	
17	47	3.29629E-02	1.13440E+01	0.00000E+00	5.13461E+04	5.82470E+05	2	
18	48	0.00000E+00	0.00000E+00	0.00000E+00	1.20186E+04	0.00000E+00	1	
19	49	1.00309E-05	1.00000E-04	0.00000E+00	0.00000E+00	0.00000E+00	0	asymmetric
20	50	0.00000E+00	0.00000E+00	0.00000E+00	0.00000E+00	0.00000E+00	0	infinite

warning. 2 cells appear to consist of more than one piece.

1surface areas print table 50

	surface	input area	calculated area	reason area not calculated
2	1.1	0.00000E+00	1.17123E+03	
3	1.2	0.00000E+00	7.18104E-01	
4	1.3	0.00000E+00	7.18104E-01	
6	2.1	0.00000E+00	1.25434E+03	
7	2.2	0.00000E+00	7.46925E-01	
8	2.3	0.00000E+00	7.46925E-01	
10	3.1	0.00000E+00	1.44593E+03	
11	3.2	0.00000E+00	9.80986E-01	
12	3.3	0.00000E+00	9.80986E-01	
14	10.1	0.00000E+00	0.00000E+00	not a boundary
15	10.2	0.00000E+00	0.00000E+00	not a boundary
16	10.3	0.00000E+00	0.00000E+00	not a boundary
17	10.4	0.00000E+00	0.00000E+00	not a boundary
18	10.5	0.00000E+00	0.00000E+00	not a boundary
19	10.6	0.00000E+00	0.00000E+00	not a boundary
20	10.7	0.00000E+00	1.12237E+01	
21	10.8	0.00000E+00	1.12237E+01	
23	20.1	0.00000E+00	6.70476E+03	
24	20.2	0.00000E+00	6.70476E+03	
25	20.3	0.00000E+00	6.70476E+03	
26	20.4	0.00000E+00	6.70476E+03	
27	20.5	0.00000E+00	0.00000E+00	asymmetric
28	20.6	0.00000E+00	0.00000E+00	asymmetric
30	21.1	0.00000E+00	1.01920E+04	
31	21.2	0.00000E+00	1.01920E+04	
32	21.3	0.00000E+00	1.01920E+04	
33	21.4	0.00000E+00	1.01920E+04	
37	22.1	0.00000E+00	4.78244E+04	
41	40.1	0.00000E+00	1.16417E+05	
42	40.2	0.00000E+00	4.18972E+03	
43	40.3	0.00000E+00	4.18972E+03	
49	42.1	0.00000E+00	4.82539E+04	
53	43.1	0.00000E+00	1.26170E+03	
54	43.2	0.00000E+00	2.18169E+03	
55	43.3	0.00000E+00	2.18169E+03	
57	44.1	0.00000E+00	3.50295E+03	
58	44.2	0.00000E+00	2.23013E+03	
61	45.1	0.00000E+00	5.48652E+03	
65	46.1	0.00000E+00	4.95306E+04	
66	46.2	0.00000E+00	2.61173E+03	
67	46.3	0.00000E+00	2.61173E+03	
69	47.1	0.00000E+00	8.72916E+04	
73	48.1	0.00000E+00	8.76515E+04	
77	49.1	0.00000E+00	3.70684E+04	
78	49.2	0.00000E+00	3.70684E+04	
79	49.3	0.00000E+00	3.70684E+04	
80	49.4	0.00000E+00	3.70684E+04	
81	49.5	0.00000E+00	5.33744E+03	
82	49.6	0.00000E+00	5.33744E+03	
84	10010.1	0.00000E+00	9.43871E+02	
85	10010.2	0.00000E+00	9.43871E+02	
86	10010.3	0.00000E+00	9.43871E+02	
87	10010.4	0.00000E+00	9.43871E+02	
88	10010.5	0.00000E+00	9.43871E+02	
89	10010.6	0.00000E+00	9.43871E+02	

1cells print table 60

	cell	mat	atom density	gram density	volume	mass	pieces	neutron importance
1	1	1	7.05243E-02	1.05540E+01	2.79982E+02	2.95493E+03	1	1.0000E+00
2	2	2s	1.00128E-01	9.98200E-01	2.58267E+01	2.57802E+01	1	1.0000E+00
3	3	3	4.33411E-02	6.56000E+00	9.81838E+01	6.44086E+02	1	1.0000E+00
4	4	4s	1.00128E-01	9.98200E-01	0.00000E+00	0.00000E+00	0	1.0000E+00
5	10	4s	1.00128E-01	9.98200E-01	5.09690E+03	5.08773E+03	0	1.0000E+00
6	20	4s	1.00128E-01	9.98200E-01	9.94289E+04	9.92499E+04	0	1.0000E+00
7	21	5s	1.00309E-05	1.00000E-04	1.30324E+05	1.30324E+01	0	1.0000E+00
8	22	7	6.03063E-02	2.70200E+00	0.00000E+00	0.00000E+00	0	1.0000E+00
9	23	5s	1.00309E-05	1.00000E-04	0.00000E+00	0.00000E+00	0	1.0000E+00
10	40	8	3.29629E-02	1.13440E+01	1.66245E+04	1.88588E+05	1	1.0000E+00
11	41	5s	1.00309E-05	1.00000E-04	4.09828E+05	4.09828E+01	1	1.0000E+00
12	42	9	8.64586E-02	7.94000E+00	9.51154E+04	7.55216E+05	1	1.0000E+00
13	43	9	8.64586E-02	7.94000E+00	4.53784E+05	3.60304E+06	1	1.0000E+00
14	44	9	8.64586E-02	7.94000E+00	1.02842E+04	8.16563E+04	2	1.0000E+00
15	45	9	8.64586E-02	7.94000E+00	9.04489E+04	7.18165E+05	1	1.0000E+00
16	46	8	3.29629E-02	1.13440E+01	9.86269E+05	1.11882E+07	1	1.0000E+00
17	47	8	3.29629E-02	1.13440E+01	5.13461E+04	5.82470E+05	2	1.0000E+00
18	48	0	0.00000E+00	0.00000E+00	1.20186E+04	0.00000E+00	1	1.0000E+00
19	49	6s	1.00309E-05	1.00000E-04	0.00000E+00	0.00000E+00	0	1.0000E+00
20	50	0	0.00000E+00	0.00000E+00	0.00000E+00	0.00000E+00	0	0.0000E+00
total					2.36097E+06	1.72254E+07		

1surfaces print table 70

	surface	trans	type	surface coefficients			
1	1		rcc				
2	1.1		cz	4.7810000E-01			
3	1.2		pz	4.0041070E+02			
4	1.3		p	0.0000000E+00	0.0000000E+00	-1.0000000E+00	-1.0520700E+01
5	2		rcc				
6	2.1		cz	4.8760000E-01			
7	2.2		pz	4.1582170E+02			
8	2.3		p	0.0000000E+00	0.0000000E+00	-1.0000000E+00	-6.3990000E+00
9	3		rcc				
10	3.1		cz	5.5880000E-01			
11	3.2		pz	4.1690260E+02			
12	3.3		p	0.0000000E+00	0.0000000E+00	-1.0000000E+00	-5.0800000E+00
13	10		rhp				
14	10.1		px	1.8000000E+00			
15	10.2		p	-1.0000000E+00	0.0000000E+00	0.0000000E+00	1.8000000E+00
16	10.3		p	5.0000000E-01	8.6602540E-01	0.0000000E+00	1.8000000E+00
17	10.4		p	-5.0000000E-01	-8.6602540E-01	0.0000000E+00	1.8000000E+00
18	10.5		p	-5.0000000E-01	8.6602540E-01	0.0000000E+00	1.8000000E+00
19	10.6		p	5.0000000E-01	-8.6602540E-01	0.0000000E+00	1.8000000E+00
20	10.7		pz	4.5312000E+02			
21	10.8		p	0.0000000E+00	0.0000000E+00	-1.0000000E+00	1.0000000E+00
22	20		rpp				
23	20.1	1	p	8.6602540E-01	5.0000000E-01	0.0000000E+00	7.4148000E+00
24	20.2	1	p	-8.6602540E-01	-5.0000000E-01	0.0000000E+00	7.4148000E+00
25	20.3	1	p	-5.0000000E-01	8.6602540E-01	0.0000000E+00	7.4148000E+00
26	20.4	1	p	5.0000000E-01	-8.6602540E-01	0.0000000E+00	7.4148000E+00
27	20.5	1	pz	4.5212000E+02			
28	20.6	1	p	0.0000000E+00	0.0000000E+00	-1.0000000E+00	0.0000000E+00
29	21		rpp				
30	21.1	1	p	8.6602540E-01	5.0000000E-01	0.0000000E+00	1.1271300E+01
31	21.2	1	p	-8.6602540E-01	-5.0000000E-01	0.0000000E+00	1.1271300E+01
32	21.3	1	p	-5.0000000E-01	8.6602540E-01	0.0000000E+00	1.1271300E+01
33	21.4	1	p	5.0000000E-01	-8.6602540E-01	0.0000000E+00	1.1271300E+01
36	22		rcc				
37	22.1		cz	1.6835120E+01			
40	40		rcc				
41	40.1		cz	3.6518900E+01			
42	40.2		pz	4.8069500E+02			
43	40.3		p	0.0000000E+00	0.0000000E+00	-1.0000000E+00	2.6670000E+01
44	41		rcc				
48	42		rcc				
49	42.1		cz	1.6986300E+01			
52	43		rcc				
53	43.1		cz	2.6352500E+01			
54	43.2		pz	-1.0160000E+01			
55	43.3		p	0.0000000E+00	0.0000000E+00	-1.0000000E+00	1.7780000E+01
56	44		rcc				
57	44.1		cz	2.0174000E+01			
58	44.2		pz	4.4450000E+02			
60	45		rcc				
61	45.1		cz	3.1597600E+01			
64	46		rcc				
65	46.1		cz	1.8910300E+01			
66	46.2		pz	4.3068240E+02			
67	46.3		p	0.0000000E+00	0.0000000E+00	-1.0000000E+00	-1.3817600E+01
68	47		rcc				
69	47.1		cz	3.3327100E+01			
72	48		rcc				
73	48.1		cz	3.3464500E+01			
76	49	refl.	rpp				
77	49.1	refl.	px	3.6528900E+01			
78	49.2	refl.	p	-1.0000000E+00	0.0000000E+00	0.0000000E+00	3.6528900E+01
79	49.3	refl.	py	3.6528900E+01			
80	49.4	refl.	p	0.0000000E+00	-1.0000000E+00	0.0000000E+00	3.6528900E+01
81	49.5	refl.	pz	4.8070500E+02			
82	49.6	refl.	p	0.0000000E+00	0.0000000E+00	-1.0000000E+00	2.6680000E+01

```
    83  10010                rhp
    84  10010.1       1001   px    2.7000000E+00
    85  10010.2       1001   p    -1.0000000E+00   0.0000000E+00   0.0000000E+00   9.0000000E-01
    86  10010.3       1001   p     5.0000000E-01   8.6602540E-01   0.0000000E+00   9.0003960E-01
    87  10010.4       1001   p    -5.0000000E-01  -8.6602540E-01   0.0000000E+00   2.6999604E+00
    88  10010.5       1001   p    -5.0000000E-01   8.6602540E-01   0.0000000E+00   3.9600581E-05
    89  10010.6       1001   p     5.0000000E-01  -8.6602540E-01   0.0000000E+00   3.5999604E+00
1  identical surfaces                                                                  print table 70

   master surface     identical surfaces

       10.7           10010.7
       10.8           10010.8
       20.5             21.5      22.2      42.2
       20.6             21.6      22.3      41.2      42.3      44.3      45.3
       40.1             41.1
       40.3             41.3
       44.2             45.2
       46.2             47.2      48.2
       46.3             47.3      48.3


   surface coefficients for identical surfaces not used.

         surface     trans  type   surface coefficients

    90  10010.7       1001   pz    4.5312000E+02
    91  10010.8       1001   p     0.0000000E+00   0.0000000E+00  -1.0000000E+00   1.0000000E+00
    34     21.5          1   pz    4.5212000E+02
    38     22.2              pz    4.5212000E+02
    50     42.2              pz    4.5212000E+02
    35     21.6          1   p     0.0000000E+00   0.0000000E+00  -1.0000000E+00   0.0000000E+00
    39     22.3              p     0.0000000E+00   0.0000000E+00  -1.0000000E+00   0.0000000E+00
    46     41.2              pz    0.0000000E+00
    51     42.3              p     0.0000000E+00   0.0000000E+00  -1.0000000E+00   0.0000000E+00
    59     44.3              p     0.0000000E+00   0.0000000E+00  -1.0000000E+00   0.0000000E+00
    63     45.3              p     0.0000000E+00   0.0000000E+00  -1.0000000E+00   0.0000000E+00
    45     41.1              cz    3.6518900E+01
    47     41.3              p     0.0000000E+00   0.0000000E+00  -1.0000000E+00   2.6670000E+01
    62     45.2              pz    4.4450000E+02
    70     47.2              pz    4.3068240E+02
    74     48.2              pz    4.3068240E+02
    71     47.3              p     0.0000000E+00   0.0000000E+00  -1.0000000E+00  -1.3817600E+01
    75     48.3              p     0.0000000E+00   0.0000000E+00  -1.0000000E+00  -1.3817600E+01
1  cell temperatures in mev for the free-gas thermal neutron treatment.                print table 72

   all non-zero importance cells with materials have a temperature for thermal neutrons of 2.5300E-08 mev.

 ************************************************
 * Random Number Generator  =                  2 *
 * Random Number Seed       =       19073486328125 *
 * Random Number Multiplier =  9219741426499971445 *
 * Random Number Adder      =                  1 *
 * Random Number Bits Used  =                 63 *
 * Random Number Stride     =             152917 *
 ************************************************


        5 warning messages so far.
 1physical constants                                                                  print table 98


   name                    value     description

   huge      1.0000000000000E+36     infinity
    pie      3.1415926535898E+00     pi
  euler      5.7721566490153E-01     euler constant
 avogad      6.0220434469282E+23     avogadro number (molecules/mole)
  aneut      1.0086649670000E+00     neutron mass (amu)
  avgdn      5.9703109000000E-01     avogadro number/neutron mass (1.e-24*molecules/mole/amu)
  slite      2.9979250000000E+02     speed of light (cm/shake)
 planck      4.1357320000000E-13     planck constant (mev shake)
  fscon      1.3703930000000E+02     inverse fine structure constant h*c/(2*pi*e**2)
 gpt(1)      9.3958000000000E+02     neutron mass (mev)
 gpt(3)      5.1100800000000E-01     electron mass (mev)


 fission q-values:     nuclide    q(mev)    nuclide    q(mev)
                         90232    171.91      91233    175.57
                         92233    180.84      92234    179.45
                         92235    180.88      92236    179.50
                         92237    180.40      92238    181.31
                         92239    180.40      92240    180.40
                         93237    183.67      94238    186.65
                         94239    189.44      94240    186.36
                         94241    188.99      94242    185.98
                         94243    187.48      95241    190.83
                         95242    190.54      95243    190.25
                         96242    190.49      96244    190.49
                         other    180.00


 the following compilation options were used:

    cheap
    dec
    plot
```

```
     mcplot
     xlib
     default datapath: C:\Program Files\LANL\MCNPDATA
                       C:\Progra~1\LANL\MCNPdata
1cross-section tables                                                    print table 100

     table    length

                       tables from file actia

   1001.62c     5202  1-h-1 at 293.6K from endf-vi.8 njoy99.50                  mat 125      12/05/01
   7014.62c    67462  7-n-14 at 293.6K from endf-vi.8 njoy99.50                 mat 725      12/05/01
   8016.62c   170541  8-o-16 at 293.6K from endf-vi.8 njoy99.50                 mat 825      12/05/01
  13027.62c    75363  13-al-27 at 293.6K from endf-vi.8 njoy99.50              mat1325      12/17/01
  24050.62c   194445  24-cr-50 at 293.6K from endf-vi.8 njoy99.50              mat2425      12/20/01
  24052.62c   174773  24-cr-52 at 293.6K from endf-vi.8 njoy99.50              mat2431      12/20/01
  24053.62c   147286  24-cr-53 at 293.6K from endf-vi.8 njoy99.50              mat2434      12/20/01
  24054.62c   132737  24-cr-54 at 293.6K from endf-vi.8 njoy99.50              mat2437      12/20/01
  25055.62c   134565  25-mn-55 at 293.6K from endf/b-vi.8 njoy99.50           mat2525      02/11/02
  26054.62c   143370  26-fe-54 at 293.6K from endf-vi.8 njoy99.50              mat2625      12/20/01
  26056.62c   230655  26-fe-56 at 293.6K from endf-vi.8 njoy99.50              mat2631      12/20/01
  26057.62c   148842  26-fe-57 at 293.6K from endf-vi.8 njoy99.50              mat2634      12/20/01
  26058.62c    87569  26-fe-58 at 293.6K from endf-vi.8 njoy99.50              mat2637      12/20/01
  28058.62c   235403  28-ni-58 at 293.6K from endf-vi.8 njoy99.50              mat2825      12/20/01
  28060.62c   158305  28-ni-60 at 293.6K from endf-vi.8 njoy99.50              mat2831      12/20/01
  28061.62c   112032  28-ni-61 at 293.6K from endf-vi.8 njoy99.50              mat2834      12/20/01
  28062.62c   104386  28-ni-62 at 293.6K from endf-vi.8 njoy99.50              mat2837      12/20/01
  28064.62c    97689  28-ni-64 at 293.6K from endf-vi.8 njoy99.50              mat2843      12/20/01

                       tables from file endf66a

   7015.66c    19013  7-n-15 at 293.6K from endf-vi.0 njoy99.50                 mat 728      07/13/01

                       tables from file endf66b

  40000.66c    98524  40-zr-0 at 293.6K from endf-vi.1 njoy99.50                mat4000      07/24/01

                       tables from file endl92

  50000.42c   141628   ENDL library name:  nd920609  LANL/XTM modified:  951222                    911219
                      temperature = 2.5860E-08 adjusted to 2.5300E-08

                       tables from file endf66c

  82206.66c   219368  82-pb-206 at 293.6K from endf-vi.6 njoy99.50               mat8231      08/13/01
  82207.66c   134389  82-pb-207 at 293.6K from endf-vi.6 njoy99.50               mat8234      08/13/01
  82208.66c   135105  82-pb-208 at 293.6K from endf-vi.x njoy99.50               mat8237      03/16/02
  94238.66c    53256  94-pu-238 at 293.6K from endf-vi.0 njoy99.50      total nu  mat9434      09/06/01
                      probability tables used from 2.0000E-04 to 1.0000E-02 mev.
  94240.66c   309518  94-pu-240 at 293.6K from endf-vi.2 njoy99.50      total nu  mat9440      09/06/01
                      probability tables used from 5.7000E-03 to 4.0000E-02 mev.
  94241.66c   126607  94-pu-241 at 293.6K from endf-vi.3 njoy99.50      total nu  mat9443      09/06/01
                      probability tables used from 3.0000E-04 to 4.0200E-02 mev.
  94242.66c   107114  94-pu-242 at 293.6K from endf-vi.0 njoy99.50      total nu  mat9446      09/06/01
                      probability tables used from 9.8600E-04 to 1.0000E-02 mev.

                       tables from file t16_2003

  92235.69c   587997  92-u-235 at 293.6K from t16 u235la9d njoy99.50   total nu  mat9228      07/02/03
                      probability tables used from 2.2500E-03 to 2.5000E-02 mev.
  92238.69c   713320  92-u-238 at 293.6K from t16 u238la8h njoy99.50   total nu  mat9237      07/02/03
                      probability tables used from 1.0000E-02 to 1.4903E-01 mev.
  94239.69c   506320  94-pu-239 at 293.6K from t16 pu239la7d njoy99.50 total nu  mat9437      07/02/03
                      probability tables used from 2.5000E-03 to 3.0000E-02 mev.

                       tables from file tmccs

   lwtr.01t    10193  hydrogen in light water at 300 degrees kelvin          1001     0     010/22/85

  total      5582977

 warning. neutron energy cutoff is below some cross-section tables.

 comment.    1 cross sections modified by free gas thermal treatment.
1assignment of s(a,b) data to nuclides.                                  print table 102

       mat        nuclide         s(a,b)
         2       1001.62c       lwtr.01t
         4       1001.62c       lwtr.01t
         5       1001.62c       lwtr.01t
         6       1001.62c       lwtr.01t


1estimated keff results by cycle                                         print table 175

 cycle     1    k(collision)  0.773576    prompt removal lifetime(abs)  7.9159E+03    source points generated    986

 cycle     2    k(collision)  0.761973    prompt removal lifetime(abs)  8.7479E+03    source points generated   1002

 cycle     3    k(collision)  0.792952    prompt removal lifetime(abs)  8.6388E+03    source points generated   1019

 cycle     4    k(collision)  0.798553    prompt removal lifetime(abs)  8.0609E+03    source points generated   1013

 cycle     5    k(collision)  0.846007    prompt removal lifetime(abs)  8.0978E+03    source points generated   1058

 cycle     6    k(collision)  0.778445    prompt removal lifetime(abs)  8.7756E+03    source points generated    927
```

```
 cycle     7    k(collision)  0.852315    prompt removal lifetime(abs)  8.2963E+03    source points generated   1086

 cycle     8    k(collision)  0.776196    prompt removal lifetime(abs)  8.4369E+03    source points generated    916
```

estimator	cycle 526	ave of 496 cycles	combination	simple average	combined average	corr
k(collision)	0.813156	0.812679 0.0016	k(col/abs)	0.811904 0.0015	0.811535 0.0015	0.8154
k(absorption)	0.811817	0.811128 0.0015	k(abs/tk ln)	0.811770 0.0015	0.811387 0.0014	0.4631
k(trk length)	0.745849	0.812412 0.0021	k(tk ln/col)	0.812546 0.0017	0.812633 0.0016	0.6279
rem life(col)	8.6684E+03	8.3853E+03 0.0016	k(col/abs/tk ln)	0.812073 0.0015	0.811477 0.0014	
rem life(abs)	8.6270E+03	8.3849E+03 0.0016	life(col/abs/tl)	8.3888E+03 0.0014	8.3982E+03 0.0012	

source points generated 1039

estimator	cycle 527	ave of 497 cycles	combination	simple average	combined average	corr
k(collision)	0.809185	0.812672 0.0016	k(col/abs)	0.811898 0.0015	0.811530 0.0015	0.8154
k(absorption)	0.809090	0.811124 0.0015	k(abs/tk ln)	0.811777 0.0015	0.811387 0.0014	0.4630
k(trk length)	0.821169	0.812430 0.0021	k(tk ln/col)	0.812551 0.0017	0.812630 0.0016	0.6278
rem life(col)	8.0102E+03	8.3845E+03 0.0016	k(col/abs/tk ln)	0.812075 0.0015	0.811477 0.0014	
rem life(abs)	8.0245E+03	8.3841E+03 0.0016	life(col/abs/tl)	8.3881E+03 0.0014	8.3977E+03 0.0012	

source points generated 1005

estimator	cycle 528	ave of 498 cycles	combination	simple average	combined average	corr
k(collision)	0.821391	0.812690 0.0016	k(col/abs)	0.811905 0.0015	0.811532 0.0015	0.8153
k(absorption)	0.809602	0.811121 0.0015	k(abs/tk ln)	0.811753 0.0015	0.811376 0.0014	0.4629
k(trk length)	0.790409	0.812386 0.0021	k(tk ln/col)	0.812538 0.0017	0.812636 0.0016	0.6272
rem life(col)	7.9693E+03	8.3837E+03 0.0016	k(col/abs/tk ln)	0.812066 0.0015	0.811468 0.0014	
rem life(abs)	8.0772E+03	8.3835E+03 0.0016	life(col/abs/tl)	8.3875E+03 0.0014	8.3975E+03 0.0012	

source points generated 1027

estimator	cycle 529	ave of 499 cycles	combination	simple average	combined average	corr
k(collision)	0.788892	0.812642 0.0016	k(col/abs)	0.811869 0.0015	0.811499 0.0015	0.8154
k(absorption)	0.798522	0.811096 0.0015	k(abs/tk ln)	0.811733 0.0015	0.811352 0.0014	0.4630
k(trk length)	0.804736	0.812370 0.0021	k(tk ln/col)	0.812506 0.0017	0.812594 0.0016	0.6271
rem life(col)	8.4590E+03	8.3839E+03 0.0016	k(col/abs/tk ln)	0.812036 0.0015	0.811442 0.0014	
rem life(abs)	8.4459E+03	8.3837E+03 0.0016	life(col/abs/tl)	8.3878E+03 0.0014	8.3979E+03 0.0012	

source points generated 969

estimator	cycle 530	ave of 500 cycles	combination	simple average	combined average	corr
k(collision)	0.864442	0.812746 0.0016	k(col/abs)	0.811973 0.0015	0.811603 0.0015	0.8166
k(absorption)	0.862854	0.811199 0.0015	k(abs/tk ln)	0.811816 0.0015	0.811450 0.0014	0.4642
k(trk length)	0.843483	0.812433 0.0021	k(tk ln/col)	0.812589 0.0017	0.812690 0.0016	0.6276
rem life(col)	8.0058E+03	8.3831E+03 0.0016	k(col/abs/tk ln)	0.812126 0.0015	0.811537 0.0014	
rem life(abs)	8.0790E+03	8.3830E+03 0.0016	life(col/abs/tl)	8.3872E+03 0.0014	8.3977E+03 0.0012	

source points generated 1088

```
 source distribution written to file P1_Acc_NACCoC_c1.00_g0.00_e0.00_d0.01cm_HP_36mm.inps        cycle =    530
1problem summary (active cycles only)              source particle weight for summary table normalization =        500000.00

      run terminated when   530   kcode cycles were done.
+                                                                                          10/25/07 23:17:01
      NAC-LWT Cask - MOX Experiments - Accident Transport Conditions                 probid =  10/25/07 23:04:59
0
```

neutron creation	tracks	weight (per source particle)	energy (per source particle)	neutron loss	tracks	weight (per source particle)	energy (per source particle)
source	500798	1.0000E+00	2.0304E+00	escape	0	0.	0.
				energy cutoff	0	0.	0.
				time cutoff	0	0.	0.
weight window	0	0.	0.	weight window	0	0.	0.
cell importance	0	0.	0.	cell importance	0	0.	0.
weight cutoff	0	1.0507E-01	4.7424E-06	weight cutoff	501256	1.0507E-01	4.2477E-06
e or t importance	0	0.	0.	e or t importance	0	0.	0.
dxtran	0	0.	0.	dxtran	0	0.	0.
forced collisions	0	0.	0.	forced collisions	0	0.	0.
exp. transform	0	0.	0.	exp. transform	0	0.	0.
upscattering	0	0.	2.2358E-07	downscattering	0	0.	1.9694E+00
photonuclear	0	0.	0.	capture	0	7.2325E-01	3.3293E-02
(n,xn)	914	1.5938E-03	1.3448E-03	loss to (n,xn)	456	7.9510E-04	7.6641E-03
prompt fission	0	0.	0.	loss to fission	0	2.7755E-01	2.1466E-02
delayed fission	0	0.	0.				
total	501712	1.1067E+00	2.0318E+00	total	501712	1.1067E+00	2.0318E+00

```
  number of neutrons banked                    487       average time of (shakes)          cutoffs
  neutron tracks per source particle     1.0034E+00        escape          0.0000E+00        tco   1.0000E+33
  neutron collisions per source particle 1.5178E+02        capture         9.5720E+03        eco   0.0000E+00
  total neutron collisions                 75888898        capture or escape 9.5720E+03      wc1  -5.0000E-01
  net multiplication              1.0008E+00 0.0000        any termination   9.6263E+03      wc2  -2.5000E-01

 computer time so far in this run    11.91 minutes        maximum number ever in bank        2
 computer time in mcrun              11.75 minutes        bank overflows to backup file      0
 source particles per minute            4.5171E+04
 random numbers generated               769937194        most random numbers used was       12106 in history      314654

 range of sampled source weights = 8.5106E-01 to 1.1655E+00

 source efficiency = 1.0000  in cell     1

 source efficiency = 0.1042  in cell    10

 source efficiency = 1.0000  in cell    20

 source efficiency = 1.0000  in cell    41
1neutron  activity in each cell                                                    print table 126
```

	cell	tracks entering	population	collisions	collisions * weight (per history)	number weighted energy	flux weighted energy	average track weight (relative)	average track mfp (cm)
1	1	1241569	501146	586077	9.5153E-01	1.3646E-03	1.1014E+00	9.2286E-01	2.6348E+00
2	2	1753661	501152	72734	1.0239E-01	4.0488E-04	7.9744E-01	8.3249E-01	1.7794E+00
3	3	1892568	501155	78060	1.3835E-01	5.6811E-04	8.5842E-01	8.8595E-01	3.7904E+00
4	4	4675755	501209	22767197	3.3677E+01	1.9441E-04	5.2073E-01	8.3143E-01	1.3415E+00
5	10	1405445	371543	6018259	8.5610E+00	1.3456E-04	3.4232E-01	7.9570E-01	1.0857E+00
6	20	0	0	0	0.0000E+00	0.0000E+00	0.0000E+00	0.0000E+00	0.0000E+00
7	21	1643189	371205	1813	2.6501E-03	4.8443E-04	4.0398E-01	8.2611E-01	1.3004E+04
8	22	2050981	371181	2086136	3.6199E+00	5.2913E-04	3.3678E-01	8.1901E-01	9.7847E+00
9	23	2153778	354933	90	1.4430E-04	5.8421E-04	2.9581E-01	8.1614E-01	1.1843E+04
10	40	25792	5252	101677	1.4356E-01	3.2300E-03	1.0644E-01	7.2359E-01	3.2337E+00
11	41	0	0	0	0.0000E+00	0.0000E+00	0.0000E+00	0.0000E+00	0.0000E+00
12	42	115694	15185	1342637	1.7759E+00	2.6306E-03	1.0677E-01	7.2112E-01	2.5371E+00
13	43	3325425	208962	13169115	1.9143E+01	3.4252E-03	1.7553E-01	7.8816E-01	2.7485E+00
14	44	42149	15682	143930	2.0099E-01	8.1919E-04	1.6869E-01	7.5553E-01	2.3693E+00
15	45	2163315	353876	5282663	7.9853E+00	8.7776E-04	2.9482E-01	8.1629E-01	2.5676E+00
16	46	2626045	293982	23873147	3.7303E+01	1.6270E-03	2.1773E-01	8.0445E-01	3.5473E+00
17	47	87444	20018	361275	5.2806E-01	1.8325E-03	1.3891E-01	7.5094E-01	3.3232E+00
18	48	3117979	207568	0	0.0000E+00	2.7619E-03	1.8387E-01	7.9764E-01	0.0000E+00
19	49	1731775	177414	4088	6.0903E-03	3.8532E-03	1.7945E-01	7.8941E-01	1.0816E+04
total		30052564	4771463	75888898	1.1414E+02				

1neutron weight balance in each cell print table 130

cell index	1	2	3	4	5	6	7	8	9
cell number	1	2	3	4	10	20	21	22	23
external events:									
entering	1.2512E+00	3.1557E+00	3.3816E+00	7.8956E+00	2.2976E+00	0.0000E+00	2.7283E+00	3.3845E+00	3.5279E+00
source	1.0000E+00	0.0000E+00	0.0000E+00	0.0000E+00	0.0000E+00	0.0000E+00	0.0000E+00	0.0000E+00	0.0000E+00
energy cutoff	0.0000E+00	0.0000E+00	0.0000E+00	0.0000E+00	0.0000E+00	0.0000E+00	0.0000E+00	0.0000E+00	0.0000E+00
time cutoff	0.0000E+00	0.0000E+00	0.0000E+00	0.0000E+00	0.0000E+00	0.0000E+00	0.0000E+00	0.0000E+00	0.0000E+00
exiting	-1.8614E+00	-3.1553E+00	-3.3804E+00	-7.7598E+00	-2.2640E+00	0.0000E+00	-2.7283E+00	-3.3455E+00	-3.5279E+00
total	3.8978E-01	3.6619E-04	1.1670E-03	1.3572E-01	3.3608E-02	0.0000E+00	6.9143E-06	3.9023E-02	1.3065E-07
variance reduction events:									
weight window	0.0000E+00	0.0000E+00	0.0000E+00	0.0000E+00	0.0000E+00	0.0000E+00	0.0000E+00	0.0000E+00	0.0000E+00
cell importance	0.0000E+00	0.0000E+00	0.0000E+00	0.0000E+00	0.0000E+00	0.0000E+00	0.0000E+00	0.0000E+00	0.0000E+00
weight cutoff	1.1135E-04	3.7032E-06	1.9991E-06	4.5624E-05	-1.5941E-05	0.0000E+00	-1.4890E-06	-4.0693E-05	0.0000E+00
e or t importance	0.0000E+00	0.0000E+00	0.0000E+00	0.0000E+00	0.0000E+00	0.0000E+00	0.0000E+00	0.0000E+00	0.0000E+00
dxtran	0.0000E+00	0.0000E+00	0.0000E+00	0.0000E+00	0.0000E+00	0.0000E+00	0.0000E+00	0.0000E+00	0.0000E+00
forced collisions	0.0000E+00	0.0000E+00	0.0000E+00	0.0000E+00	0.0000E+00	0.0000E+00	0.0000E+00	0.0000E+00	0.0000E+00
exp. transform	0.0000E+00	0.0000E+00	0.0000E+00	0.0000E+00	0.0000E+00	0.0000E+00	0.0000E+00	0.0000E+00	0.0000E+00
total	1.1135E-04	3.7032E-06	1.9991E-06	4.5624E-05	-1.5941E-05	0.0000E+00	-1.4890E-06	-4.0693E-05	0.0000E+00
physical events:									
capture	-1.1266E-01	-3.6990E-04	-1.1822E-03	-1.3576E-01	-3.3593E-02	0.0000E+00	-5.4253E-06	-3.8983E-02	-1.3065E-07
(n,xn)	6.2734E-04	0.0000E+00	2.6371E-05	0.0000E+00	0.0000E+00	0.0000E+00	0.0000E+00	0.0000E+00	0.0000E+00
loss to (n,xn)	-3.1285E-04	0.0000E+00	-1.3185E-05	0.0000E+00	0.0000E+00	0.0000E+00	0.0000E+00	0.0000E+00	0.0000E+00
fission	0.0000E+00	0.0000E+00	0.0000E+00	0.0000E+00	0.0000E+00	0.0000E+00	0.0000E+00	0.0000E+00	0.0000E+00
loss to fission	-2.7755E-01	0.0000E+00	0.0000E+00	0.0000E+00	0.0000E+00	0.0000E+00	0.0000E+00	0.0000E+00	0.0000E+00
photonuclear	0.0000E+00	0.0000E+00	0.0000E+00	0.0000E+00	0.0000E+00	0.0000E+00	0.0000E+00	0.0000E+00	0.0000E+00
total	-3.8989E-01	-3.6990E-04	-1.1690E-03	-1.3576E-01	-3.3593E-02	0.0000E+00	-5.4253E-06	-3.8983E-02	-1.3065E-07
total	0.0000E+00	0.0000E+00	0.0000E+00	0.0000E+00	0.0000E+00	0.0000E+00	0.0000E+00	0.0000E+00	0.0000E+00

cell index	10	11	12	13	14	15	16	17	18
cell number	40	41	42	43	44	45	46	47	48
external events:									
entering	3.7341E-02	0.0000E+00	1.6904E-01	5.2877E+00	6.3487E-02	3.5504E+00	4.2362E+00	1.3150E-01	4.9768E+00
source	0.0000E+00	0.0000E+00	0.0000E+00	0.0000E+00	0.0000E+00	0.0000E+00	0.0000E+00	0.0000E+00	0.0000E+00
energy cutoff	0.0000E+00	0.0000E+00	0.0000E+00	0.0000E+00	0.0000E+00	0.0000E+00	0.0000E+00	0.0000E+00	0.0000E+00
time cutoff	0.0000E+00	0.0000E+00	0.0000E+00	0.0000E+00	0.0000E+00	0.0000E+00	0.0000E+00	0.0000E+00	0.0000E+00
exiting	-3.7270E-02	0.0000E+00	-1.5693E-01	-5.1469E+00	-5.9514E-02	-3.3370E+00	-4.2065E+00	-1.3116E-01	-4.9768E+00
total	7.0996E-05	0.0000E+00	1.2111E-02	1.4074E-01	3.9735E-03	2.1336E-01	2.9727E-02	3.4420E-04	0.0000E+00
variance reduction events:									
weight window	0.0000E+00	0.0000E+00	0.0000E+00	0.0000E+00	0.0000E+00	0.0000E+00	0.0000E+00	0.0000E+00	0.0000E+00
cell importance	0.0000E+00	0.0000E+00	0.0000E+00	0.0000E+00	0.0000E+00	0.0000E+00	0.0000E+00	0.0000E+00	0.0000E+00
weight cutoff	-2.4210E-06	0.0000E+00	9.0859E-05	-3.1358E-04	-1.0418E-05	1.3278E-04	2.2441E-05	-1.8057E-05	0.0000E+00
e or t importance	0.0000E+00	0.0000E+00	0.0000E+00	0.0000E+00	0.0000E+00	0.0000E+00	0.0000E+00	0.0000E+00	0.0000E+00
dxtran	0.0000E+00	0.0000E+00	0.0000E+00	0.0000E+00	0.0000E+00	0.0000E+00	0.0000E+00	0.0000E+00	0.0000E+00
forced collisions	0.0000E+00	0.0000E+00	0.0000E+00	0.0000E+00	0.0000E+00	0.0000E+00	0.0000E+00	0.0000E+00	0.0000E+00
exp. transform	0.0000E+00	0.0000E+00	0.0000E+00	0.0000E+00	0.0000E+00	0.0000E+00	0.0000E+00	0.0000E+00	0.0000E+00
total	-2.4210E-06	0.0000E+00	9.0859E-05	-3.1358E-04	-1.0418E-05	1.3278E-04	2.2441E-05	-1.8057E-05	0.0000E+00
physical events:									
capture	-6.8575E-05	0.0000E+00	-1.2202E-02	-1.4044E-01	-3.9631E-03	-2.1350E-01	-3.0195E-02	-3.2989E-04	0.0000E+00
(n,xn)	0.0000E+00	0.0000E+00	0.0000E+00	1.4057E-05	0.0000E+00	2.9429E-05	8.8912E-04	7.4907E-06	0.0000E+00
loss to (n,xn)	0.0000E+00	0.0000E+00	0.0000E+00	-7.0285E-06	0.0000E+00	-1.4715E-05	-4.4358E-04	-3.7454E-06	0.0000E+00
fission	0.0000E+00	0.0000E+00	0.0000E+00	0.0000E+00	0.0000E+00	0.0000E+00	0.0000E+00	0.0000E+00	0.0000E+00
loss to fission	0.0000E+00	0.0000E+00	0.0000E+00	0.0000E+00	0.0000E+00	0.0000E+00	0.0000E+00	0.0000E+00	0.0000E+00
photonuclear	0.0000E+00	0.0000E+00	0.0000E+00	0.0000E+00	0.0000E+00	0.0000E+00	0.0000E+00	0.0000E+00	0.0000E+00
total	-6.8575E-05	0.0000E+00	-1.2202E-02	-1.4043E-01	-3.9631E-03	-2.1349E-01	-2.9750E-02	-3.2614E-04	0.0000E+00

total	0.0000E+00	0.0000E+00	0.0000E+00	0.0000E+00	0.0000E+00	0.0000E+00	0.0000E+00	0.0000E+00	0.0000E+00

cell index 19
cell number 49 total

external events:		
entering	2.7311E+00	4.8806E+01
source	0.0000E+00	1.0000E+00
energy cutoff	0.0000E+00	0.0000E+00
time cutoff	0.0000E+00	0.0000E+00
exiting	-2.7311E+00	-4.8806E+01
total	1.4036E-06	1.0000E+00
variance reduction events:		
weight window	0.0000E+00	0.0000E+00
cell importance	0.0000E+00	0.0000E+00
weight cutoff	0.0000E+00	6.1524E-06
e or t importance	0.0000E+00	0.0000E+00
dxtran	0.0000E+00	0.0000E+00
forced collisions	0.0000E+00	0.0000E+00
exp. transform	0.0000E+00	0.0000E+00
total	0.0000E+00	6.1524E-06
physical events:		
capture	-1.4036E-06	-7.2325E-01
(n,xn)	0.0000E+00	1.5938E-03
loss to (n,xn)	0.0000E+00	-7.9510E-04
fission	0.0000E+00	0.0000E+00
loss to fission	0.0000E+00	-2.7755E-01
photonuclear	0.0000E+00	0.0000E+00
total	-1.4036E-06	-1.0000E+00
total	0.0000E+00	0.0000E+00

1neutron activity of each nuclide in each cell, per source particle print table 140

cell index	cell name	nuclides	atom fraction	total collisions	collisions * weight	wgt. lost to capture	wgt. gain by fission	wgt. gain by (n,xn)	photons produced	photon wgt produced	avg photon energy
1	1	92235.69c	2.19E-03	11604	1.6516E-02	2.3773E-03	1.2018E-02	1.2382E-06	0	0.0000E+00	0.0000E+00
		92238.69c	3.07E-01	182793	3.3056E-01	2.3571E-02	5.1778E-03	2.8296E-04	0	0.0000E+00	0.0000E+00
		94238.66c	2.44E-10	0	0.0000E+00	0.0000E+00	0.0000E+00	0.0000E+00	0	0.0000E+00	0.0000E+00
		94239.69c	2.43E-10	0	0.0000E+00	0.0000E+00	0.0000E+00	0.0000E+00	0	0.0000E+00	0.0000E+00
		94240.66c	2.42E-10	0	0.0000E+00	0.0000E+00	0.0000E+00	0.0000E+00	0	0.0000E+00	0.0000E+00
		94241.66c	2.41E-02	261894	3.6794E-01	8.6289E-02	2.6036E-01	3.0294E-05	0	0.0000E+00	0.0000E+00
		94242.66c	2.40E-10	0	0.0000E+00	0.0000E+00	0.0000E+00	0.0000E+00	0	0.0000E+00	0.0000E+00
		8016.62c	6.66E-01	129786	2.3652E-01	4.2088E-04	0.0000E+00	0.0000E+00	0	0.0000E+00	0.0000E+00
2	2	1001.62c	6.67E-01	67564	9.4009E-02	3.5973E-04	0.0000E+00	0.0000E+00	0	0.0000E+00	0.0000E+00
		8016.62c	3.33E-01	5170	8.3772E-03	1.0168E-05	0.0000E+00	0.0000E+00	0	0.0000E+00	0.0000E+00
3	3	26054.62c	1.19E-04	8	1.3417E-05	2.1703E-06	0.0000E+00	0.0000E+00	0	0.0000E+00	0.0000E+00
		24050.62c	7.63E-05	8	1.5666E-05	3.9708E-06	0.0000E+00	0.0000E+00	0	0.0000E+00	0.0000E+00
		7014.62c	3.24E-03	267	4.4474E-04	2.3671E-05	0.0000E+00	0.0000E+00	0	0.0000E+00	0.0000E+00
		26056.62c	1.87E-03	192	3.0462E-04	2.1713E-05	0.0000E+00	0.0000E+00	0	0.0000E+00	0.0000E+00
		24052.62c	1.47E-03	61	1.1116E-04	3.5581E-06	0.0000E+00	0.0000E+00	0	0.0000E+00	0.0000E+00
		7015.66c	1.20E-05	1	2.0596E-06	1.1114E-12	0.0000E+00	0.0000E+00	0	0.0000E+00	0.0000E+00
		26057.62c	4.33E-05	9	1.5459E-05	1.0398E-06	0.0000E+00	0.0000E+00	0	0.0000E+00	0.0000E+00
		24053.62c	1.67E-04	32	4.9398E-05	9.4886E-06	0.0000E+00	0.0000E+00	0	0.0000E+00	0.0000E+00
		26058.62c	5.71E-06	0	0.0000E+00	0.0000E+00	0.0000E+00	0.0000E+00	0	0.0000E+00	0.0000E+00
		24054.62c	4.14E-05	2	4.1326E-06	3.8278E-08	0.0000E+00	0.0000E+00	0	0.0000E+00	0.0000E+00
		40000.66c	9.81E-01	76724	1.3605E-01	1.0591E-03	0.0000E+00	1.3185E-05	0	0.0000E+00	0.0000E+00
		50000.42c	1.15E-02	756	1.3400E-03	5.7434E-05	0.0000E+00	0.0000E+00	0	0.0000E+00	0.0000E+00
4	4	1001.62c	6.67E-01	21345331	3.1346E+01	1.3390E-01	0.0000E+00	0.0000E+00	0	0.0000E+00	0.0000E+00
		8016.62c	3.33E-01	1421866	2.3311E+00	1.8663E-03	0.0000E+00	0.0000E+00	0	0.0000E+00	0.0000E+00
5	10	1001.62c	6.67E-01	5653062	7.9858E+00	3.3326E-02	0.0000E+00	0.0000E+00	0	0.0000E+00	0.0000E+00
		8016.62c	3.33E-01	365197	5.7522E-01	2.6681E-04	0.0000E+00	0.0000E+00	0	0.0000E+00	0.0000E+00
6	20	1001.62c	6.67E-01	0	0.0000E+00	0.0000E+00	0.0000E+00	0.0000E+00	0	0.0000E+00	0.0000E+00
		8016.62c	3.33E-01	0	0.0000E+00	0.0000E+00	0.0000E+00	0.0000E+00	0	0.0000E+00	0.0000E+00
7	21	1001.62c	6.67E-01	1675	2.4240E-03	5.4231E-06	0.0000E+00	0.0000E+00	0	0.0000E+00	0.0000E+00
		8016.62c	3.33E-01	138	2.2604E-04	2.2451E-09	0.0000E+00	0.0000E+00	0	0.0000E+00	0.0000E+00
8	22	13027.62c	1.00E+00	2086136	3.6199E+00	3.8983E-02	0.0000E+00	0.0000E+00	0	0.0000E+00	0.0000E+00
9	23	1001.62c	6.67E-01	83	1.3264E-04	1.3062E-07	0.0000E+00	0.0000E+00	0	0.0000E+00	0.0000E+00
		8016.62c	3.33E-01	7	1.1663E-05	2.8285E-11	0.0000E+00	0.0000E+00	0	0.0000E+00	0.0000E+00
10	40	82206.66c	2.55E-01	24516	3.4087E-02	2.7874E-05	0.0000E+00	0.0000E+00	0	0.0000E+00	0.0000E+00
		82207.66c	2.21E-01	22486	3.2056E-02	3.8462E-05	0.0000E+00	0.0000E+00	0	0.0000E+00	0.0000E+00
		82208.66c	5.24E-01	54675	7.7416E-02	2.2389E-06	0.0000E+00	0.0000E+00	0	0.0000E+00	0.0000E+00
11	41	1001.62c	6.67E-01	0	0.0000E+00	0.0000E+00	0.0000E+00	0.0000E+00	0	0.0000E+00	0.0000E+00
		8016.62c	3.33E-01	0	0.0000E+00	0.0000E+00	0.0000E+00	0.0000E+00	0	0.0000E+00	0.0000E+00
12	42	24050.62c	8.79E-03	21758	3.4511E-02	4.7860E-04	0.0000E+00	0.0000E+00	0	0.0000E+00	0.0000E+00
		26054.62c	4.03E-02	42532	6.8094E-02	4.1345E-04	0.0000E+00	0.0000E+00	0	0.0000E+00	0.0000E+00

		28058.62c	6.09E-02	181784	2.3443E-01	1.0840E-03	0.0000E+00	0.0000E+00	0	0.0000E+00	0.0000E+00
		24052.62c	1.69E-01	93120	1.3676E-01	6.9642E-04	0.0000E+00	0.0000E+00	0	0.0000E+00	0.0000E+00
		26056.62c	6.32E-01	791641	9.7764E-01	6.0022E-03	0.0000E+00	0.0000E+00	0	0.0000E+00	0.0000E+00
		28060.62c	2.35E-02	26722	4.4624E-02	2.8130E-04	0.0000E+00	0.0000E+00	0	0.0000E+00	0.0000E+00
		24053.62c	1.92E-02	64103	9.6929E-02	1.1944E-03	0.0000E+00	0.0000E+00	0	0.0000E+00	0.0000E+00
		26057.62c	1.46E-02	17618	2.8309E-02	2.0807E-04	0.0000E+00	0.0000E+00	0	0.0000E+00	0.0000E+00
		28061.62c	1.02E-03	1322	1.8890E-03	1.4576E-05	0.0000E+00	0.0000E+00	0	0.0000E+00	0.0000E+00
		24054.62c	4.77E-03	3470	5.4180E-03	9.0993E-06	0.0000E+00	0.0000E+00	0	0.0000E+00	0.0000E+00
		26058.62c	1.93E-03	1803	2.8359E-03	2.7057E-05	0.0000E+00	0.0000E+00	0	0.0000E+00	0.0000E+00
		28062.62c	3.25E-03	14741	2.2397E-02	1.4380E-04	0.0000E+00	0.0000E+00	0	0.0000E+00	0.0000E+00
		28064.62c	8.33E-04	1134	1.9718E-03	6.5208E-06	0.0000E+00	0.0000E+00	0	0.0000E+00	0.0000E+00
		25055.62c	2.01E-02	80889	1.2014E-01	1.6420E-03	0.0000E+00	0.0000E+00	0	0.0000E+00	0.0000E+00
13	43	24050.62c	8.79E-03	221175	3.6703E-01	5.7475E-03	0.0000E+00	0.0000E+00	0	0.0000E+00	0.0000E+00
		26054.62c	4.03E-02	451871	7.6283E-01	4.7802E-03	0.0000E+00	0.0000E+00	0	0.0000E+00	0.0000E+00
		28058.62c	6.09E-02	1715612	2.4243E+00	1.2971E-02	0.0000E+00	0.0000E+00	0	0.0000E+00	0.0000E+00
		24052.62c	1.69E-01	1019845	1.6356E+00	7.9758E-03	0.0000E+00	1.8340E-06	0	0.0000E+00	0.0000E+00
		26056.62c	*6.32E-01*	7666679	*1.0557E+01*	*6.9499E-02*	*0.0000E+00*	*2.0166E-06*	*0*	*0.0000E+00*	*0.0000E+00*
		28060.62c	2.35E-02	283261	4.9171E-01	3.2930E-03	0.0000E+00	0.0000E+00	0	0.0000E+00	0.0000E+00
		24053.62c	1.92E-02	630863	1.0081E+00	1.3984E-02	0.0000E+00	1.5387E-06	0	0.0000E+00	0.0000E+00
		26057.62c	1.46E-02	185000	3.1223E-01	2.2263E-03	0.0000E+00	1.6393E-06	0	0.0000E+00	0.0000E+00
		28061.62c	1.02E-03	13468	2.0832E-02	1.7934E-04	0.0000E+00	0.0000E+00	0	0.0000E+00	0.0000E+00
		24054.62c	4.77E-03	36356	6.0531E-02	1.2171E-04	0.0000E+00	0.0000E+00	0	0.0000E+00	0.0000E+00
		26058.62c	1.93E-03	19406	3.2608E-02	2.6030E-04	0.0000E+00	0.0000E+00	0	0.0000E+00	0.0000E+00
		28062.62c	3.25E-03	144976	2.3288E-01	1.6922E-03	0.0000E+00	0.0000E+00	0	0.0000E+00	0.0000E+00
		28064.62c	8.33E-04	12230	2.1954E-02	7.1773E-05	0.0000E+00	0.0000E+00	0	0.0000E+00	0.0000E+00
		25055.62c	2.01E-02	768373	1.2152E+00	1.7635E-02	0.0000E+00	0.0000E+00	0	0.0000E+00	0.0000E+00
14	44	24050.62c	8.79E-03	2269	3.6509E-03	1.8711E-04	0.0000E+00	0.0000E+00	0	0.0000E+00	0.0000E+00
		26054.62c	4.03E-02	4128	6.7625E-03	1.1885E-04	0.0000E+00	0.0000E+00	0	0.0000E+00	0.0000E+00
		28058.62c	6.09E-02	19305	2.6369E-02	3.6453E-04	0.0000E+00	0.0000E+00	0	0.0000E+00	0.0000E+00
		24052.62c	1.69E-01	9781	1.5040E-02	1.7043E-04	0.0000E+00	0.0000E+00	0	0.0000E+00	0.0000E+00
		26056.62c	6.32E-01	87969	1.1668E-01	2.1107E-03	0.0000E+00	0.0000E+00	0	0.0000E+00	0.0000E+00
		28060.62c	2.35E-02	2542	4.3148E-03	8.3706E-05	0.0000E+00	0.0000E+00	0	0.0000E+00	0.0000E+00
		24053.62c	1.92E-02	6286	9.7393E-03	4.0739E-04	0.0000E+00	0.0000E+00	0	0.0000E+00	0.0000E+00
		26057.62c	1.46E-02	1769	2.9096E-03	5.1876E-05	0.0000E+00	0.0000E+00	0	0.0000E+00	0.0000E+00
		28061.62c	1.02E-03	127	1.8882E-04	4.4798E-06	0.0000E+00	0.0000E+00	0	0.0000E+00	0.0000E+00
		24054.62c	4.77E-03	325	5.1374E-04	2.4205E-06	0.0000E+00	0.0000E+00	0	0.0000E+00	0.0000E+00
		26058.62c	1.93E-03	178	2.8855E-04	2.4763E-06	0.0000E+00	0.0000E+00	0	0.0000E+00	0.0000E+00
		28062.62c	3.25E-03	1408	2.2061E-03	5.8112E-05	0.0000E+00	0.0000E+00	0	0.0000E+00	0.0000E+00
		28064.62c	8.33E-04	92	1.6133E-04	2.3044E-06	0.0000E+00	0.0000E+00	0	0.0000E+00	0.0000E+00
		25055.62c	2.01E-02	7751	1.2164E-02	3.9874E-04	*0.0000E+00*	*0.0000E+00*	*0*	*0.0000E+00*	*0.0000E+00*
15	45	24050.62c	8.79E-03	80564	1.3531E-01	9.5234E-03	0.0000E+00	0.0000E+00	0	0.0000E+00	0.0000E+00
		26054.62c	4.03E-02	160789	2.7759E-01	6.8030E-03	0.0000E+00	0.0000E+00	0	0.0000E+00	0.0000E+00
		28058.62c	6.09E-02	681315	1.0027E+00	2.0061E-02	0.0000E+00	0.0000E+00	0	0.0000E+00	0.0000E+00
		24052.62c	1.69E-01	391001	6.4399E-01	9.4778E-03	0.0000E+00	1.6111E-06	0	0.0000E+00	0.0000E+00
		26056.62c	6.32E-01	3234714	4.6943E+00	1.1239E-01	0.0000E+00	8.7451E-06	0	0.0000E+00	0.0000E+00
		28060.62c	2.35E-02	91514	1.6155E-01	4.5728E-03	0.0000E+00	0.0000E+00	0	0.0000E+00	0.0000E+00
		24053.62c	1.92E-02	231983	3.7789E-01	2.3538E-02	0.0000E+00	0.0000E+00	0	0.0000E+00	0.0000E+00
		26057.62c	1.46E-02	64846	1.1199E-01	2.6033E-03	0.0000E+00	0.0000E+00	0	0.0000E+00	0.0000E+00
		28061.62c	1.02E-03	5128	8.0158E-03	2.0266E-04	0.0000E+00	0.0000E+00	0	0.0000E+00	0.0000E+00
		24054.62c	4.77E-03	12710	2.1748E-02	1.3227E-04	0.0000E+00	4.3583E-06	0	0.0000E+00	0.0000E+00
		26058.62c	1.93E-03	6657	1.1330E-02	1.9784E-04	0.0000E+00	0.0000E+00	0	0.0000E+00	0.0000E+00
		28062.62c	3.25E-03	51037	8.4785E-02	3.0676E-03	0.0000E+00	0.0000E+00	0	0.0000E+00	0.0000E+00
		28064.62c	8.33E-04	3627	6.6572E-03	7.6507E-05	0.0000E+00	0.0000E+00	0	0.0000E+00	0.0000E+00
		25055.62c	2.01E-02	266778	4.4741E-01	2.0862E-02	0.0000E+00	0.0000E+00	0	0.0000E+00	0.0000E+00
16	46	82206.66c	2.55E-01	5741763	8.8860E+00	6.7912E-03	0.0000E+00	6.4064E-05	0	0.0000E+00	0.0000E+00
		82207.66c	2.21E-01	5300449	8.3363E+00	2.2654E-02	0.0000E+00	1.2740E-04	0	0.0000E+00	0.0000E+00
		82208.66c	5.24E-01	12830935	2.0081E+01	7.5043E-04	0.0000E+00	2.5407E-04	0	0.0000E+00	0.0000E+00
17	47	82206.66c	2.55E-01	86445	1.2471E-01	8.9207E-05	0.0000E+00	1.9156E-06	0	0.0000E+00	0.0000E+00
		82207.66c	2.21E-01	79902	1.1779E-01	2.3046E-04	0.0000E+00	0.0000E+00	0	0.0000E+00	0.0000E+00
		82208.66c	5.24E-01	194928	2.8556E-01	1.0224E-05	0.0000E+00	1.8298E-06	0	0.0000E+00	0.0000E+00
19	49	1001.62c	6.67E-01	3653	5.3988E-03	1.4029E-06	0.0000E+00	0.0000E+00	0	0.0000E+00	0.0000E+00
		8016.62c	3.33E-01	435	6.9146E-04	6.3757E-10	0.0000E+00	0.0000E+00	0	0.0000E+00	0.0000E+00
	total			75888898	1.1414E+02	7.2325E-01	2.7755E-01	7.9870E-04	0	0.0000E+00	0.0000E+00

total over all cells by nuclide	total collisions	collisions * weight	wgt. lost to capture	wgt. gain by fission	wgt. gain by (n,xn)	photons produced	photon wgt produced	avg photon energy
1001.62c	27071368	3.9433E+01	1.6759E-01	0.0000E+00	0.0000E+00	0	0.0000E+00	0.0000E+00
7014.62c	267	4.4474E-04	2.3671E-05	0.0000E+00	0.0000E+00	0	0.0000E+00	0.0000E+00
7015.66c	1	2.0596E-06	1.1114E-12	0.0000E+00	0.0000E+00	0	0.0000E+00	0.0000E+00
8016.62c	1922599	3.1521E+00	2.5641E-03	0.0000E+00	0.0000E+00	0	0.0000E+00	0.0000E+00
13027.62c	2086136	3.6199E+00	3.8983E-02	0.0000E+00	0.0000E+00	0	0.0000E+00	0.0000E+00
24050.62c	325774	5.4051E-01	1.5941E-02	0.0000E+00	0.0000E+00	0	0.0000E+00	0.0000E+00
24052.62c	1513808	2.4315E+00	1.8324E-02	0.0000E+00	3.4452E-06	0	0.0000E+00	0.0000E+00
24053.62c	933267	1.4927E+00	3.9133E-02	0.0000E+00	1.5387E-06	0	0.0000E+00	0.0000E+00
24054.62c	52863	8.8215E-02	2.6554E-04	0.0000E+00	4.3583E-06	0	0.0000E+00	0.0000E+00
25055.62c	1123791	1.7949E+00	4.0537E-02	0.0000E+00	0.0000E+00	0	0.0000E+00	0.0000E+00
26054.62c	659328	1.1153E+00	1.2118E-02	0.0000E+00	0.0000E+00	0	0.0000E+00	0.0000E+00
26056.62c	11781195	1.6346E+01	1.9002E-01	0.0000E+00	1.0762E-05	0	0.0000E+00	0.0000E+00
26057.62c	269242	4.5546E-01	5.0906E-03	0.0000E+00	1.6393E-06	0	0.0000E+00	0.0000E+00
26058.62c	28044	4.7062E-02	4.8768E-04	0.0000E+00	0.0000E+00	0	0.0000E+00	0.0000E+00
28058.62c	2598016	3.6878E+00	3.4481E-02	0.0000E+00	0.0000E+00	0	0.0000E+00	0.0000E+00
28060.62c	404039	7.0220E-01	8.2308E-03	0.0000E+00	0.0000E+00	0	0.0000E+00	0.0000E+00
28061.62c	20045	3.0926E-02	4.0105E-04	0.0000E+00	0.0000E+00	0	0.0000E+00	0.0000E+00
28062.62c	212162	3.4226E-01	4.9617E-03	0.0000E+00	0.0000E+00	0	0.0000E+00	0.0000E+00
28064.62c	17083	3.0744E-02	1.5711E-04	0.0000E+00	0.0000E+00	0	0.0000E+00	0.0000E+00
40000.66c	76724	1.3605E-01	1.0591E-03	0.0000E+00	1.3185E-05	0	0.0000E+00	0.0000E+00
50000.42c	756	1.3400E-03	5.7434E-05	0.0000E+00	0.0000E+00	0	0.0000E+00	0.0000E+00
82206.66c	5852724	9.0448E+00	6.9083E-03	0.0000E+00	6.5980E-05	0	0.0000E+00	0.0000E+00

82207.66c	5402837	8.4862E+00	2.2923E-02	0.0000E+00	1.2740E-04	0	0.0000E+00	0.0000E+00
82208.66c	13080538	2.0444E+01	7.6289E-04	0.0000E+00	2.5590E-04	0	0.0000E+00	0.0000E+00
92235.69c	11604	1.6516E-02	2.3773E-03	1.2018E-02	1.2382E-06	0	0.0000E+00	0.0000E+00
92238.69c	182793	3.3056E-01	2.3571E-02	5.1778E-03	2.8296E-04	0	0.0000E+00	0.0000E+00
94238.66c	0	0.0000E+00	0.0000E+00	0.0000E+00	0.0000E+00	0	0.0000E+00	0.0000E+00
94239.69c	0	0.0000E+00	0.0000E+00	0.0000E+00	0.0000E+00	0	0.0000E+00	0.0000E+00
94240.66c	0	0.0000E+00	0.0000E+00	0.0000E+00	0.0000E+00	0	0.0000E+00	0.0000E+00
94241.66c	261894	3.6794E-01	8.6289E-02	2.6036E-01	3.0294E-05	0	0.0000E+00	0.0000E+00
94242.66c	0	0.0000E+00	0.0000E+00	0.0000E+00	0.0000E+00	0	0.0000E+00	0.0000E+00

1keff results for: NAC-LWT Cask - MOX Experiments - Accident Transport Conditions probid = 10/25/07 23:04:59

the initial fission neutron source distribution was generated from a general sdef source description.
the criticality problem was scheduled to skip 30 cycles and run a total of 530 cycles with nominally 1000 neutrons per cycle.
this problem has run 30 inactive cycles with 30072 neutron histories and 500 active cycles with 500798 neutron histories.

this calculation has completed the requested number of keff cycles using a total of 530870 fission neutron source histories.
all cells with fissionable material were sampled and had fission neutron source points.

the results of the w test for normality applied to the individual collision, absorption, and track-length keff cycle values are:

the k(collision) cycle values appear normally distributed at the 95 percent confidence level
the k(absorption) cycle values appear normally distributed at the 95 percent confidence level
the k(trk length) cycle values appear normally distributed at the 95 percent confidence level

---

the final estimated combined collision/absorption/track-length keff = 0.81154 with an estimated standard deviation of 0.00116

the estimated 68, 95, & 99 percent keff confidence intervals are 0.81038 to 0.81269, 0.80923 to 0.81384, and 0.80848 to 0.81459

the final combined (col/abs/tl) prompt removal lifetime = 8.3977E-05 seconds with an estimated standard deviation of 1.0227E-07

the average neutron energy causing fission = 7.7342E-02 mev

the energy corresponding to the average neutron lethargy causing fission = 1.3304E-07 mev

the percentages of fissions caused by neutrons in the thermal, intermediate, and fast neutron ranges are:

(<0.625 ev): 89.17% (0.625 ev - 100 kev): 7.97% (>100 kev): 2.86%

the average fission neutrons produced per neutron absorbed (capture + fission) in all cells with fission = 2.0828E+00

the average fission neutrons produced per neutron absorbed (capture + fission) in all the geometry cells = 8.1209E-01

the average number of neutrons produced per fission = 2.928

---

the estimated average keffs, one standard deviations, and 68, 95, and 99 percent confidence intervals are:

keff estimator	keff	standard deviation	68% confidence	95% confidence	99% confidence	corr
collision	0.81275	0.00130	0.81144 to 0.81405	0.81015 to 0.81534	0.80930 to 0.81619	
absorption	0.81120	0.00119	0.81001 to 0.81239	0.80883 to 0.81357	0.80805 to 0.81435	
track length	0.81243	0.00169	0.81074 to 0.81412	0.80907 to 0.81579	0.80797 to 0.81689	
col/absorp	0.81160	0.00118	0.81042 to 0.81279	0.80925 to 0.81396	0.80848 to 0.81472	0.8166
abs/trk len	0.81145	0.00115	0.81030 to 0.81260	0.80916 to 0.81374	0.80841 to 0.81449	0.4642
col/trk len	0.81269	0.00128	0.81141 to 0.81397	0.81013 to 0.81525	0.80930 to 0.81608	0.6276
col/abs/trk len	0.81154	0.00116	0.81038 to 0.81269	0.80923 to 0.81384	0.80848 to 0.81459	

if the largest of each keff occurred on the next cycle, the keff results and 68, 95, and 99 percent confidence intervals would be:

keff estimator	keff	standard deviation	68% confidence	95% confidence	99% confidence
collision	0.81294	0.00132	0.81162 to 0.81426	0.81032 to 0.81556	0.80947 to 0.81642

absorption	0.81135	0.00120	0.81015 to 0.81255	0.80896 to 0.81374	0.80818 to 0.81452
track length	0.81269	0.00170	0.81098 to 0.81439	0.80929 to 0.81608	0.80819 to 0.81719
col/abs/trk len	0.81169	0.00117	0.81053 to 0.81286	0.80937 to 0.81402	0.80861 to 0.81478

the estimated average prompt removal lifetimes, one standard deviations, and 68, 95, and 99 percent confidence intervals are (sec):

estimator	lifetime	std. dev.	68% confidence	95% confidence	99% confidence	corr
collision	8.38310E-05	1.35781E-07	8.3695E-05 to 8.3967E-05	8.3561E-05 to 8.4102E-05	8.3472E-05 to 8.4190E-05	
absorption	8.38304E-05	1.31414E-07	8.3699E-05 to 8.3962E-05	8.3569E-05 to 8.4092E-05	8.3483E-05 to 8.4178E-05	
track length	8.39544E-05	1.02540E-07	8.3852E-05 to 8.4057E-05	8.3750E-05 to 8.4159E-05	8.3684E-05 to 8.4225E-05	
col/absorp	8.38305E-05	1.31533E-07	8.3699E-05 to 8.3962E-05	8.3568E-05 to 8.4092E-05	8.3483E-05 to 8.4178E-05	0.9641
abs/trk len	8.39766E-05	1.02177E-07	8.3874E-05 to 8.4079E-05	8.3773E-05 to 8.4180E-05	8.3707E-05 to 8.4247E-05	0.8463
col/trk len	8.39708E-05	1.02352E-07	8.3868E-05 to 8.4073E-05	8.3767E-05 to 8.4175E-05	8.3700E-05 to 8.4241E-05	0.8149
col/abs/trk len	8.39767E-05	1.02267E-07	8.3874E-05 to 8.4079E-05	8.3773E-05 to 8.4180E-05	8.3706E-05 to 8.4247E-05	

absorption estimates of prompt lifetimes (sec):

	escape	capture	fission	removal
fraction	0.00000E+00	7.22671E-01	2.77329E-01	1.00000E+00
lifetime(abs)	0.00000E+00	1.16001E-04	3.02278E-04	8.38304E-05
lifetime(c/a/t)	0.00000E+00	1.16203E-04	3.02805E-04	8.39767E-05

laverage keff results summed over 10 cycles each to form 50 batch values of keff print table 178

batch number	start cycle	end cycle	keff estimators by batch k(coll)	k(abs)	k(track)	average keff estimators and deviations k(coll)	st dev	k(abs)	st dev	k(track)	st dev	col/abs/tl k(c/a/t)	st dev
1	31	40	0.82966	0.83432	0.81935								
2	41	50	0.81388	0.81282	0.81550	0.82177	0.00789	0.82357	0.01075	0.81743	0.00193		
3	51	60	0.81591	0.81479	0.81007	0.81981	0.00496	0.82065	0.00686	0.81497	0.00269		
4	61	70	0.82413	0.82314	0.81926	0.82089	0.00367	0.82127	0.00489	0.81605	0.00218	0.81694	0.00574
5	71	80	0.82191	0.82228	0.81994	0.82110	0.00285	0.82147	0.00379	0.81683	0.00186	0.81825	0.00362
6	81	90	0.81341	0.81903	0.80153	0.81982	0.00265	0.82107	0.00312	0.81428	0.00297	0.81800	0.00617
7	91	100	0.81570	0.80876	0.80207	0.81923	0.00232	0.81931	0.00317	0.81253	0.00306	0.81900	0.00447
8	101	110	0.82256	0.81550	0.81347	0.81964	0.00205	0.81883	0.00279	0.81265	0.00265	0.81916	0.00422
9	111	120	0.82739	0.81588	0.82961	0.82050	0.00200	0.81850	0.00248	0.81453	0.00300	0.82101	0.00377
10	121	130	0.81189	0.80694	0.79886	0.81964	0.00199	0.81735	0.00250	0.81297	0.00311	0.82178	0.00370
11	131	140	0.81512	0.81798	0.81439	0.81923	0.00184	0.81741	0.00226	0.81310	0.00282	0.82030	0.00312
12	141	150	0.81892	0.80779	0.81619	0.81921	0.00168	0.81660	0.00222	0.81335	0.00258	0.82018	0.00294
13	151	160	0.81253	0.80385	0.81782	0.81869	0.00163	0.81562	0.00226	0.81370	0.00240	0.81873	0.00276
14	161	170	0.82293	0.81659	0.81584	0.81900	0.00154	0.81569	0.00210	0.81385	0.00223	0.81876	0.00269
15	171	180	0.81782	0.81307	0.81272	0.81892	0.00144	0.81552	0.00196	0.81378	0.00208	0.81870	0.00256
16	181	190	0.81490	0.80501	0.83582	0.81867	0.00137	0.81486	0.00195	0.81515	0.00238	0.81813	0.00211
17	191	200	0.80059	0.80287	0.80113	0.81760	0.00167	0.81416	0.00196	0.81433	0.00238	0.81579	0.00232
18	201	210	0.80941	0.79895	0.80353	0.81715	0.00164	0.81331	0.00203	0.81373	0.00233	0.81600	0.00240
19	211	220	0.81458	0.82191	0.81115	0.81701	0.00155	0.81376	0.00197	0.81359	0.00220	0.81590	0.00210
20	221	230	0.79879	0.80440	0.80211	0.81610	0.00173	0.81330	0.00193	0.81302	0.00217	0.81416	0.00206
21	231	240	0.82474	0.82558	0.81525	0.81651	0.00170	0.81388	0.00193	0.81312	0.00207	0.81450	0.00204
22	241	250	0.80621	0.81448	0.80174	0.81604	0.00169	0.81391	0.00184	0.81261	0.00204	0.81398	0.00192
23	251	260	0.80096	0.81176	0.80767	0.81539	0.00174	0.81381	0.00176	0.81239	0.00196	0.81344	0.00172
24	261	270	0.81023	0.80779	0.80387	0.81517	0.00168	0.81356	0.00170	0.81204	0.00191	0.81322	0.00170
25	271	280	0.82492	0.81865	0.82710	0.81556	0.00166	0.81377	0.00165	0.81264	0.00193	0.81362	0.00168
26	281	290	0.80925	0.81282	0.80933	0.81532	0.00161	0.81373	0.00158	0.81251	0.00186	0.81349	0.00160
27	291	300	0.81000	0.80975	0.80467	0.81512	0.00156	0.81358	0.00153	0.81222	0.00181	0.81331	0.00156
28	301	310	0.79874	0.79355	0.81099	0.81454	0.00162	0.81287	0.00164	0.81218	0.00174	0.81258	0.00155
29	311	320	0.81086	0.81598	0.80630	0.81441	0.00156	0.81298	0.00158	0.81197	0.00169	0.81254	0.00149

30	321	330	0.80031	0.80718	0.80098	0.81394	0.00158	0.81278	0.00154	0.81161	0.00168	0.81215	0.00145
31	331	340	0.80388	0.79876	0.81420	0.81362	0.00156	0.81233	0.00156	0.81169	0.00162	0.81188	0.00140
32	341	350	0.81724	0.82617	0.81614	0.81373	0.00152	0.81276	0.00157	0.81183	0.00158	0.81229	0.00138
33	351	360	0.83520	0.81845	0.85451	0.81438	0.00161	0.81293	0.00153	0.81312	0.00200	0.81299	0.00149
34	361	370	0.80886	0.80069	0.80539	0.81422	0.00157	0.81257	0.00153	0.81290	0.00196	0.81279	0.00150
35	371	380	0.81531	0.81537	0.82615	0.81425	0.00152	0.81265	0.00149	0.81328	0.00194	0.81301	0.00145
36	381	390	0.81009	0.80545	0.81262	0.81413	0.00149	0.81245	0.00146	0.81326	0.00188	0.81287	0.00142
37	391	400	0.81143	0.80964	0.80847	0.81406	0.00145	0.81238	0.00142	0.81313	0.00184	0.81279	0.00138
38	401	410	0.82492	0.81788	0.80537	0.81435	0.00144	0.81252	0.00139	0.81292	0.00180	0.81280	0.00136
39	411	420	0.80586	0.80407	0.81463	0.81413	0.00142	0.81231	0.00137	0.81297	0.00175	0.81263	0.00133
40	421	430	0.80978	0.79689	0.81285	0.81402	0.00139	0.81192	0.00139	0.81296	0.00171	0.81250	0.00133
41	431	440	0.80815	0.81161	0.81895	0.81388	0.00136	0.81191	0.00136	0.81311	0.00167	0.81253	0.00128
42	441	450	0.79458	0.80377	0.79193	0.81342	0.00140	0.81172	0.00134	0.81261	0.00171	0.81208	0.00128
43	451	460	0.81535	0.81672	0.81120	0.81346	0.00137	0.81184	0.00131	0.81257	0.00167	0.81215	0.00125
44	461	470	0.80700	0.81373	0.79954	0.81332	0.00135	0.81188	0.00128	0.81228	0.00166	0.81206	0.00122
45	471	480	0.79961	0.80600	0.81020	0.81301	0.00135	0.81175	0.00126	0.81223	0.00162	0.81191	0.00118
46	481	490	0.80546	0.79821	0.80770	0.81285	0.00133	0.81145	0.00127	0.81213	0.00159	0.81171	0.00119
47	491	500	0.82768	0.80894	0.82950	0.81316	0.00134	0.81140	0.00124	0.81250	0.00160	0.81175	0.00117
48	501	510	0.79942	0.80020	0.81243	0.81288	0.00134	0.81117	0.00124	0.81250	0.00156	0.81156	0.00115
49	511	520	0.81145	0.80954	0.81694	0.81285	0.00132	0.81113	0.00121	0.81259	0.00153	0.81157	0.00113
50	521	530	0.80779	0.81443	0.80466	0.81275	0.00129	0.81120	0.00119	0.81243	0.00151	0.81156	0.00110

average keff results summed over 20 cycles each to form 25 batch values of keff

batch number	start cycle	end cycle	keff estimators by batch k(coll)	k(abs)	k(track)	average keff estimators and deviations k(coll)	st dev	k(abs)	st dev	k(track)	st dev	col/abs/tl k(c/a/t)	st dev
1	31	50	0.82177	0.82357	0.81743								
2	51	70	0.82002	0.81897	0.81466	0.82089	0.00088	0.82127	0.00230	0.81605	0.00138		
3	71	90	0.81766	0.82066	0.81074	0.81982	0.00119	0.82107	0.00135	0.81428	0.00194		
4	91	110	0.81913	0.81213	0.80777	0.81964	0.00086	0.81883	0.00243	0.81265	0.00213	0.82491	0.00351
5	111	130	0.81964	0.81141	0.81424	0.81964	0.00067	0.81735	0.00240	0.81297	0.00168	0.82164	0.00234
6	131	150	0.81702	0.81289	0.81529	0.81921	0.00070	0.81660	0.00209	0.81335	0.00142	0.81897	0.00199
7	151	170	0.81773	0.81022	0.81683	0.81900	0.00063	0.81569	0.00199	0.81385	0.00130	0.81868	0.00149
8	171	190	0.81636	0.80904	0.82427	0.81867	0.00063	0.81486	0.00191	0.81515	0.00172	0.81847	0.00100
9	191	210	0.80500	0.80091	0.80233	0.81715	0.00162	0.81331	0.00229	0.81373	0.00208	0.81685	0.00310
10	211	230	0.80668	0.81316	0.80663	0.81610	0.00179	0.81330	0.00205	0.81302	0.00199	0.81400	0.00245
11	231	250	0.81547	0.82003	0.80849	0.81604	0.00162	0.81391	0.00195	0.81261	0.00185	0.81404	0.00220
12	251	270	0.80559	0.80977	0.80577	0.81517	0.00171	0.81356	0.00181	0.81204	0.00178	0.81292	0.00199
13	271	290	0.81708	0.81574	0.81822	0.81532	0.00158	0.81373	0.00168	0.81251	0.00171	0.81341	0.00181
14	291	310	0.80437	0.80165	0.80783	0.81454	0.00166	0.81287	0.00178	0.81218	0.00162	0.81242	0.00178
15	311	330	0.80558	0.81158	0.80364	0.81394	0.00166	0.81278	0.00166	0.81161	0.00161	0.81191	0.00166
16	331	350	0.81056	0.81246	0.81517	0.81373	0.00157	0.81276	0.00155	0.81183	0.00152	0.81217	0.00147
17	351	370	0.82203	0.80957	0.82995	0.81422	0.00155	0.81257	0.00147	0.81290	0.00178	0.81256	0.00144
18	371	390	0.81270	0.81041	0.81938	0.81413	0.00146	0.81245	0.00139	0.81326	0.00172	0.81267	0.00133
19	391	410	0.81817	0.81376	0.80692	0.81435	0.00140	0.81252	0.00132	0.81292	0.00166	0.81265	0.00129
20	411	430	0.80782	0.80048	0.81374	0.81402	0.00137	0.81192	0.00139	0.81296	0.00157	0.81232	0.00130

21	431	450	0.80137	0.80769	0.80544	0.81342	0.00143	0.81172	0.00133	0.81261	0.00154	0.81189
0.00121												
22	451	470	0.81117	0.81523	0.80537	0.81332	0.00137	0.81188	0.00128	0.81228	0.00150	0.81185
0.00114												
23	471	490	0.80253	0.80211	0.80895	0.81285	0.00139	0.81145	0.00130	0.81213	0.00145	0.81149
0.00112												
24	491	510	0.81355	0.80457	0.82096	0.81288	0.00133	0.81117	0.00127	0.81250	0.00143	0.81149
0.00108												
25	511	530	0.80962	0.81198	0.81080	0.81275	0.00128	0.81120	0.00122	0.81243	0.00137	0.81151
0.00102												

average keff results summed over 25 cycles each to form 20 batch values of keff

batch number	start cycle	end cycle	keff estimators by batch k(coll)	k(abs)	k(track)	average keff estimators and deviations k(coll)	st dev	k(abs)	st dev	k(track)	st dev	col/abs/tl k(c/a/t)	st dev
1	31	55	0.82053	0.82250	0.81285								
2	56	80	0.82167	0.82044	0.82080	0.82110	0.00057	0.82147	0.00103	0.81683	0.00397		
3	81	105	0.81838	0.81434	0.80979	0.82019	0.00096	0.81909	0.00245	0.81448	0.00328		
4	106	130	0.81800	0.81211	0.80842	0.81964	0.00087	0.81735	0.00246	0.81297	0.00277	0.82224	
0.00032													
5	131	155	0.81447	0.81041	0.81672	0.81861	0.00124	0.81596	0.00236	0.81372	0.00227	0.81922	
0.00207													
6	156	180	0.82046	0.81331	0.81407	0.81892	0.00106	0.81552	0.00198	0.81378	0.00186	0.81883	
0.00216													
7	181	205	0.80757	0.80137	0.81314	0.81730	0.00185	0.81350	0.00262	0.81368	0.00157	0.81729	
0.00252													
8	206	230	0.80773	0.81189	0.80835	0.81610	0.00200	0.81330	0.00228	0.81302	0.00152	0.81355	
0.00221													
9	231	255	0.81254	0.81725	0.80802	0.81571	0.00181	0.81374	0.00206	0.81246	0.00145	0.81295	
0.00186													
10	256	280	0.81428	0.81405	0.81423	0.81556	0.00162	0.81377	0.00184	0.81264	0.00131	0.81313	
0.00159													

11	281	305	0.80535	0.80546	0.80570	0.81463	0.00174	0.81301	0.00183	0.81201	0.00134	0.81211	
0.00165													
12	306	330	0.80631	0.81025	0.80721	0.81394	0.00173	0.81278	0.00168	0.81161	0.00129	0.81160	
0.00145													
13	331	355	0.81434	0.81294	0.82462	0.81397	0.00159	0.81279	0.00155	0.81261	0.00155	0.81274	
0.00144													
14	356	380	0.81786	0.81084	0.82194	0.81425	0.00150	0.81265	0.00144	0.81328	0.00158	0.81291	
0.00138													
15	381	405	0.81727	0.81240	0.81194	0.81445	0.00141	0.81264	0.00134	0.81319	0.00148	0.81288	
0.00131													
16	406	430	0.80757	0.80117	0.80963	0.81402	0.00139	0.81192	0.00145	0.81296	0.00140	0.81260	
0.00138													
17	431	455	0.80436	0.80922	0.80511	0.81345	0.00142	0.81176	0.00137	0.81250	0.00139	0.81203	
0.00128													
18	456	480	0.80551	0.81151	0.80762	0.81301	0.00141	0.81175	0.00129	0.81223	0.00134	0.81185	
0.00116													
19	481	505	0.81200	0.80345	0.81795	0.81296	0.00134	0.81131	0.00130	0.81253	0.00130	0.81180	
0.00112													
20	506	530	0.80872	0.80907	0.81054	0.81275	0.00129	0.81120	0.00123	0.81243	0.00124	0.81169	
0.00105													

average keff results summed over 50 cycles each to form 10 batch values of keff

batch number	start cycle	end cycle	keff estimators by batch k(coll)	k(abs)	k(track)	average keff estimators and deviations k(coll)	st dev	k(abs)	st dev	k(track)	st dev	col/abs/tl k(c/a/t)	st dev
1	31	80	0.82110	0.82147	0.81683								
2	81	130	0.81819	0.81322	0.80911	0.81964	0.00145	0.81735	0.00412	0.81297	0.00386		
3	131	180	0.81746	0.81186	0.81539	0.81892	0.00111	0.81552	0.00300	0.81378	0.00237		
4	181	230	0.80765	0.80663	0.81075	0.81610	0.00292	0.81330	0.00307	0.81302	0.00184	0.81410	
0.00461													
5	231	280	0.81341	0.81565	0.81112	0.81556	0.00233	0.81377	0.00243	0.81264	0.00147	0.81288	
0.00269													
6	281	330	0.80583	0.80786	0.80646	0.81394	0.00250	0.81278	0.00221	0.81161	0.00158	0.81120	
0.00232													
7	331	380	0.81610	0.81189	0.82328	0.81425	0.00213	0.81265	0.00187	0.81328	0.00214	0.81255	
0.00226													
8	381	430	0.81242	0.80678	0.81079	0.81402	0.00186	0.81192	0.00178	0.81296	0.00188	0.81238	
0.00219													
9	431	480	0.80494	0.81037	0.80636	0.81301	0.00193	0.81175	0.00158	0.81223	0.00181	0.81170	
0.00170													
10	481	530	0.81036	0.80626	0.81424	0.81275	0.00174	0.81120	0.00152	0.81243	0.00163	0.81151	
0.00155													

average keff results summed over 100 cycles each to form 5 batch values of keff

batch number	start cycle	end cycle	keff estimators by batch k(coll)	k(abs)	k(track)	average keff estimators and deviations k(coll)	st dev	k(abs)	st dev	k(track)	st dev	col/abs/tl k(c/a/t)	st dev
1	31	130	0.81964	0.81735	0.81297								

```
      2    131    230      0.81256  0.80924  0.81307        0.81610 0.00354    0.81330 0.00405    0.81302 0.00005
      3    231    330      0.80962  0.81175  0.80879        0.81394 0.00297    0.81278 0.00240    0.81161 0.00141
      4    331    430      0.81426  0.80934  0.81703        0.81402 0.00210    0.81192 0.00190    0.81296 0.00168        0.81086
0.00109
      5    431    530      0.80765  0.80831  0.81030        0.81275 0.00207    0.81120 0.00164    0.81243 0.00141        0.81084
0.00058


 average keff results summed over 125 cycles each to form  4 batch values of keff

  batch  start    end      keff estimators by batch              average keff estimators and deviations                col/abs/tl
keff
 number  cycle   cycle      k(coll)  k(abs)  k(track)        k(coll)  st dev    k(abs)  st dev    k(track) st dev        k(c/a/t) st
dev

      1     31    155      0.81861  0.81596  0.81372
      2    156    280      0.81252  0.81157  0.81156        0.81556 0.00305    0.81377 0.00219    0.81264 0.00108
      3    281    405      0.81223  0.81038  0.81428        0.81445 0.00208    0.81264 0.00170    0.81319 0.00083
      4    406    530      0.80763  0.80689  0.81017        0.81275 0.00225    0.81120 0.00187    0.81243 0.00095        0.80866
0.00201


 average keff results summed over 250 cycles each to form  2 batch values of keff

  batch  start    end      keff estimators by batch              average keff estimators and deviations
 number  cycle   cycle      k(coll)  k(abs)  k(track)        k(coll)  st dev    k(abs)  st dev    k(track) st dev

      1     31    280      0.81556  0.81377  0.81264
      2    281    530      0.80993  0.80863  0.81223        0.81275 0.00282    0.81120 0.00257    0.81243 0.00021
1average individual and combined collision/absorption/track-length keff results for 10 different batch sizes

 cycles per  number of    average keff estimators and deviations      normality  average k(c/a/t)    k(c/a/t) confidence
intervals
 keff batch  k batches  k(col) st dev  k(abs) st dev  k(trk) st dev   co/ab/trk  k(c/a/t) st dev    95% confidence    99%
confidence

       1        500  |  0.8127 0.0013  0.8112 0.0012  0.8124 0.0017  |95/95/95|  0.81154 0.00116   0.80923-0.81384   0.80848-
0.81459
       2        250  |  0.8127 0.0013  0.8112 0.0012  0.8124 0.0016  |95/95/95|  0.81152 0.00115   0.80924-0.81381   0.80849-
0.81456
       4        125  |  0.8127 0.0012  0.8112 0.0011  0.8124 0.0016  |95/95/95|  0.81150 0.00104   0.80943-0.81356   0.80876-
0.81424
       5        100  |  0.8127 0.0013  0.8112 0.0011  0.8124 0.0016  |95/95/95|  0.81156 0.00109   0.80939-0.81373   0.80868-
0.81444
      10         50  |  0.8127 0.0013  0.8112 0.0012  0.8124 0.0015  |95/95/no|  0.81156 0.00110   0.80935-0.81378   0.80861-
0.81452
      20         25  |  0.8127 0.0013  0.8112 0.0012  0.8124 0.0014  |95/95/95|  0.81151 0.00102   0.80939-0.81363   0.80863-
0.81439
      25         20  |  0.8127 0.0013  0.8112 0.0012  0.8124 0.0012  |95/95/95|  0.81169 0.00105   0.80946-0.81391   0.80863-
0.81475
      50         10  |  0.8127 0.0017  0.8112 0.0015  0.8124 0.0016  |95/95/95|  0.81151 0.00155   0.80785-0.81518   0.80610-
0.81693
     100          5  |  0.8127 0.0021  0.8112 0.0016  0.8124 0.0014  |95/95/95|  0.81084 0.00058   0.80835-0.81333   0.80510-
0.81658
     125          4  |  0.8127 0.0023  0.8112 0.0019  0.8124 0.0010  |95/95/95|  0.80866 0.00201   0.78307-0.83424   0.68049-
0.93682
 ------------------------------------------------------------------------------------------------------------------------------
---
1individual and average keff estimator results by cycle

  keff      neutron     keff estimators by cycle          average keff estimators and deviations              average k(c/a/t)
 cycle    histories    k(coll)  k(abs)  k(track)     k(coll)  st dev    k(abs)  st dev    k(track) st dev    k(c/a/t)  st dev    fom

      1         1000 |  0.77358  0.79932  0.74740  |
      2          986 |  0.76197  0.79060  0.75265  |
      3         1002 |  0.79295  0.77210  0.82091  |
      4         1019 |  0.79855  0.80426  0.80619  |
      5         1013 |  0.84601  0.85820  0.82484  |
      6         1058 |  0.77844  0.75337  0.72031  |
      7          927 |  0.85231  0.84192  0.83283  |
      8         1086 |  0.77620  0.80320  0.77936  |
      9          916 |  0.79294  0.79449  0.78476  |
     10         1021 |  0.81179  0.81686  0.82052  |
 ------------------------------------------------------------------------------------------------------------------------------
---
     11         1034 |  0.77867  0.78231  0.75394  |
     12          960 |  0.81982  0.81026  0.73652  |
     13         1046 |  0.80821  0.82129  0.79494  |
     14          986 |  0.78548  0.78599  0.78331  |
     15          966 |  0.85796  0.85715  0.80780  |
     16         1101 |  0.79257  0.77507  0.78607  |
     17          912 |  0.82974  0.83238  0.82775  |
     18         1038 |  0.80387  0.79760  0.88017  |
     19          966 |  0.81923  0.79387  0.86437  |
     20         1014 |  0.82715  0.80886  0.80226  |
 ------------------------------------------------------------------------------------------------------------------------------
---
     21         1014 |  0.82259  0.85874  0.80640  |
     22          992 |  0.86693  0.86026  0.84444  |
     23         1050 |  0.84547  0.83464  0.84392  |
     24          963 |  0.76921  0.78385  0.77723  |
     25          914 |  0.86921  0.85248  0.88038  |
     26         1121 |  0.80505  0.83543  0.81121  |
     27          939 |  0.83546  0.81099  0.88213  |
     28         1027 |  0.80724  0.82815  0.77292  |
```

```
    29         976 | 0.83872  0.81914  0.85585  |
    30        1025 | 0.79872  0.80144  0.84044  |
 ------------------  begin active keff cycles  ----------------------------------------------------------------------------------------
---
    31         985 | 0.79769  0.81254  0.77994  |
    32        1003 | 0.78199  0.79373  0.78218  |  0.78984 0.00785   0.80313 0.00940   0.78106 0.00112  |
    33         999 | 0.82857  0.82168  0.80760  |  0.80275 0.01368   0.80931 0.00823   0.78991 0.00887  |
    34        1051 | 0.82903  0.85712  0.80382  |  0.80932 0.01170   0.82127 0.01329   0.79339 0.00717  |  0.78247 0.01718
14266
    35        1009 | 0.83682  0.82981  0.86441  |  0.81482 0.01060   0.82298 0.01044   0.80759 0.01525  |  0.81913 0.01641
14997
    36        1023 | 0.84764  0.83567  0.83147  |  0.82029 0.01024   0.82509 0.00878   0.81157 0.01307  |  0.82250 0.01228
22601
    37        1023 | 0.82213  0.82044  0.81896  |  0.82055 0.00866   0.82443 0.00745   0.81263 0.01110  |  0.82202 0.00976
30546
    38         974 | 0.83130  0.84804  0.85184  |  0.82190 0.00762   0.82738 0.00710   0.81753 0.01079  |  0.82559 0.00890
32910
    39        1015 | 0.82956  0.84174  0.80362  |  0.82275 0.00677   0.82897 0.00646   0.81598 0.00964  |  0.82631 0.00820
34663
    40         969 | 0.89183  0.88243  0.84970  |  0.82966 0.00919   0.83432 0.00787   0.81935 0.00926  |  0.82988 0.00961
23195
 ----------------------------------------------------------------------------------------------------------------------------------
---
.
.
.
.
.
 ----------------------------------------------------------------------------------------------------------------------------------
---
   511        1007 | 0.81678  0.82585  0.81586  |  0.81288 0.00132   0.81120 0.00120   0.81251 0.00170  |  0.81156 0.00116
30004
   512        1001 | 0.76297  0.75270  0.73827  |  0.81278 0.00132   0.81108 0.00121   0.81235 0.00171  |  0.81144 0.00117
29684
   513         943 | 0.80793  0.79311  0.77191  |  0.81277 0.00132   0.81104 0.00120   0.81227 0.00170  |  0.81140 0.00117
29688
   514        1074 | 0.84159  0.85901  0.82520  |  0.81283 0.00131   0.81114 0.00121   0.81230 0.00170  |  0.81149 0.00117
29623
   515        1059 | 0.79077  0.77557  0.83553  |  0.81278 0.00131   0.81106 0.00121   0.81234 0.00170  |  0.81145 0.00117
29618
   516         943 | 0.83794  0.82702  0.82522  |  0.81284 0.00131   0.81110 0.00120   0.81237 0.00170  |  0.81148 0.00116
29655
   517        1087 | 0.80995  0.82004  0.78851  |  0.81283 0.00131   0.81112 0.00120   0.81232 0.00169  |  0.81148 0.00116
29721
   518         968 | 0.89895  0.87356  0.93949  |  0.81301 0.00132   0.81124 0.00121   0.81258 0.00171  |  0.81162 0.00117
29252
   519        1102 | 0.78411  0.80850  0.85787  |  0.81295 0.00132   0.81124 0.00120   0.81268 0.00171  |  0.81163 0.00117
29329
   520         875 | 0.76352  0.75999  0.77152  |  0.81285 0.00132   0.81113 0.00121   0.81259 0.00171  |  0.81153 0.00117
29162
 ----------------------------------------------------------------------------------------------------------------------------------
---
   521         989 | 0.80518  0.81700  0.80918  |  0.81283 0.00131   0.81115 0.00120   0.81258 0.00170  |  0.81154 0.00117
29234
   522        1062 | 0.82496  0.84155  0.83930  |  0.81286 0.00131   0.81121 0.00120   0.81264 0.00170  |  0.81160 0.00117
29242
   523        1036 | 0.82159  0.83155  0.85448  |  0.81287 0.00131   0.81125 0.00120   0.81272 0.00170  |  0.81165 0.00116
29266
   524         975 | 0.75715  0.77727  0.77199  |  0.81276 0.00131   0.81118 0.00120   0.81264 0.00170  |  0.81157 0.00116
29207
   525         920 | 0.77191  0.78500  0.76597  |  0.81268 0.00131   0.81113 0.00120   0.81255 0.00170  |  0.81150 0.00116
29183
   526        1036 | 0.81316  0.81182  0.74585  |  0.81268 0.00131   0.81113 0.00120   0.81241 0.00170  |  0.81148 0.00116
29223
   527        1039 | 0.80919  0.80909  0.82117  |  0.81267 0.00131   0.81112 0.00119   0.81243 0.00170  |  0.81148 0.00116
29277
   528        1005 | 0.82139  0.80960  0.79041  |  0.81269 0.00130   0.81112 0.00119   0.81239 0.00169  |  0.81147 0.00116
29327
   529        1027 | 0.78889  0.79852  0.80474  |  0.81264 0.00130   0.81110 0.00119   0.81237 0.00169  |  0.81144 0.00115
29371
   530         969 | 0.86444  0.86285  0.84348  |  0.81275 0.00130   0.81120 0.00119   0.81243 0.00169  |  0.81154 0.00116
29242
 ----------------------------------------------------------------------------------------------------------------------------------
---

  the largest active cycle keffs by estimator are:                    the smallest active cycle keffs by estimator
are:

                collision 0.91061 on cycle 312                                  collision 0.73198 on cycle 226
               absorption 0.88814 on cycle 312                                 absorption 0.72474 on cycle 226
             track length 0.93949 on cycle 518                               track length 0.71577 on cycle 390
1plot of the estimated col/abs/track-length keff one standard deviation interval versus cycle number (| = final keff =  0.81154)

   cycle   active 0.81                          0.82                          0.83                          0.84
  number   cycles  |----------------------------|-----------------------------|-----------------------------|
      40       10  |  |                          (-----------------------------k-----------------------------)  |
      45       15  |  |                  (-------------------------k-------------------------)                 |
      50       20  |  |          (-----------------------k-----------------------)                             |
      55       25  |  |    (---------------------k---------------------)                                       |
      60       30  |  |      (-----------------k-----------------)                                             |
      65       35  |  |            (---------------k---------------)                                           |
      70       40  |  |            (--------------k--------------)                                             |
      75       45  |  |               (-------------k-------------)                                             |
      80       50  |  |              (-------------k------------)                                               |
      85       55  +  |             (------------k------------)                                                 +
      90       60  |  |             (------------k-----------)                                                  |
```

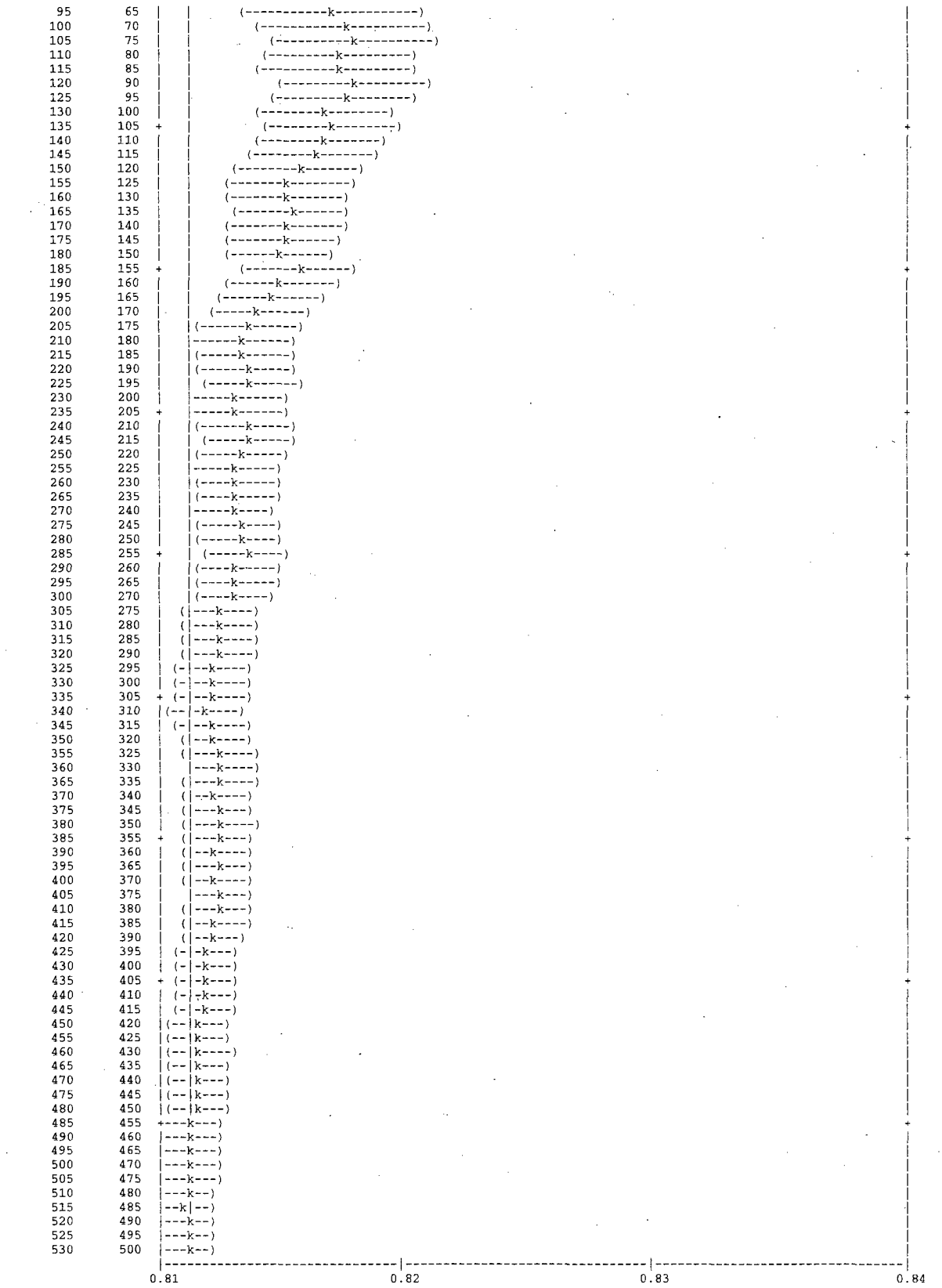

1individual and collision/absorption/track-length keffs for different numbers of inactive cycles skipped for fission source settling

skip cycles	active cycles	active neutrons	average keff estimators and deviations k(col)	st dev	k(abs)	st dev	k(trk)	st dev	co/ab/tl	normality average k(c/a/t)	st dev	k(c/a/t) confidence intervals 95% confidence	99% confidence

```
    0    530       530870| 0.8127 0.0013  0.8113 0.0012  0.8122 0.0017 |95/95/95| 0.81157 0.00113  0.80932-0.81381  0.80859-
0.81454
    1    529       529870| 0.8128 0.0013  0.8113 0.0012  0.8123 0.0017 |95/95/95| 0.81162 0.00113  0.80937-0.81386  0.80864-
0.81459
    2    528       528884| 0.8129 0.0013  0.8114 0.0012  0.8124 0.0016 |95/95/95| 0.81168 0.00113  0.80943-0.81393  0.80870-
0.81466
    3    527       527882| 0.8129 0.0013  0.8114 0.0012  0.8124 0.0017 |95/95/95| 0.81173 0.00113  0.80948-0.81398  0.80875-
0.81471
    4    526       526863| 0.8130 0.0013  0.8114 0.0012  0.8124 0.0017 |95/95/95| 0.81175 0.00113  0.80949-0.81400  0.80876-
0.81473
    5    525       525850| 0.8129 0.0013  0.8114 0.0012  0.8124 0.0017 |95/95/95| 0.81167 0.00113  0.80941-0.81392  0.80868-
0.81465
    6    524       524792| 0.8130 0.0013  0.8115 0.0012  0.8126 0.0017 |95/95/95| 0.81177 0.00113  0.80952-0.81401  0.80879-
0.81474
    7    523       523865| 0.8129 0.0013  0.8114 0.0012  0.8125 0.0017 |95/95/95| 0.81172 0.00113  0.80947-0.81396  0.80874-
0.81469
    8    522       522779| 0.8129 0.0013  0.8114 0.0012  0.8126 0.0017 |95/95/95| 0.81175 0.00113  0.80950-0.81400  0.80877-
0.81473
    9    521       521863| 0.8130 0.0013  0.8115 0.0012  0.8126 0.0017 |95/95/95| 0.81179 0.00113  0.80953-0.81404  0.80880-
0.81477
   10    520       520842| 0.8130 0.0013  0.8114 0.0012  0.8126 0.0017 |95/95/95| 0.81177 0.00113  0.80952-0.81403  0.80878-
0.81477
 ------------------------------------------------------------------------------------------------------------------------------
---
   11    519       519808| 0.8131 0.0013  0.8115 0.0012  0.8127 0.0017 |95/95/95| 0.81184 0.00113  0.80959-0.81410  0.80885-
0.81484
   12    518       518848| 0.8130 0.0013  0.8115 0.0012  0.8129 0.0017 |95/95/95| 0.81187 0.00113  0.80961-0.81413  0.80887-
0.81487
   13    517       517802| 0.8131 0.0013  0.8115 0.0012  0.8129 0.0017 |95/95/95| 0.81186 0.00114  0.80960-0.81413  0.80886-
0.81487
   14    516       516816| 0.8131 0.0013  0.8115 0.0012  0.8130 0.0017 |95/95/95| 0.81191 0.00114  0.80965-0.81418  0.80891-
0.81492
   15    515       515850| 0.8130 0.0013  0.8114 0.0012  0.8130 0.0017 |95/95/95| 0.81184 0.00114  0.80958-0.81411  0.80884-
0.81485
   16    514       514749| 0.8131 0.0013  0.8115 0.0012  0.8130 0.0017 |95/95/95| 0.81190 0.00114  0.80964-0.81417  0.80890-
0.81491
   17    513       513837| 0.8130 0.0013  0.8115 0.0012  0.8130 0.0017 |95/95/95| 0.81187 0.00114  0.80959-0.81414  0.80885-
0.81488
   18    512       512799| 0.8130 0.0013  0.8115 0.0012  0.8129 0.0017 |95/95/95| 0.81186 0.00114  0.80959-0.81414  0.80885-
0.81488
   19    511       511833| 0.8130 0.0013  0.8115 0.0012  0.8128 0.0017 |95/95/95| 0.81187 0.00114  0.80959-0.81415  0.80885-
0.81489
   20    510       510819| 0.8130 0.0013  0.8115 0.0012  0.8128 0.0017 |95/95/95| 0.81187 0.00115  0.80959-0.81416  0.80885-
0.81490
 ------------------------------------------------------------------------------------------------------------------------------
---
.
.
.
.
 ------------------------------------------------------------------------------------------------------------------------------
---
  475    55        55160| 0.8091 0.0040  0.8061 0.0037  0.8134 0.0053 |95/95/95| 0.80765 0.00368  0.80025-0.81504  0.79780-
0.81750
  480    50        50124| 0.8104 0.0043  0.8063 0.0039  0.8142 0.0058 |95/95/95| 0.80785 0.00405  0.79971-0.81599  0.79698-
0.81871
  485    45        45138| 0.8117 0.0047  0.8075 0.0042  0.8169 0.0058 |95/95/95| 0.80926 0.00443  0.80032-0.81820  0.79731-
0.82121
  490    40        40182| 0.8116 0.0051  0.8083 0.0044  0.8159 0.0064 |95/95/95| 0.80894 0.00466  0.79949-0.81839  0.79628-
0.82160
  495    35        35116| 0.8117 0.0056  0.8094 0.0049  0.8181 0.0071 |95/95/95| 0.81015 0.00517  0.79962-0.82067  0.79600-
0.82429
  500    30        30049| 0.8062 0.0056  0.8081 0.0053  0.8113 0.0074 |95/95/95| 0.80779 0.00552  0.79646-0.81911  0.79250-
0.82308
  505    25        25133| 0.8087 0.0064  0.8091 0.0061  0.8105 0.0086 |95/95/95| 0.80898 0.00634  0.79583-0.82214  0.79110-
0.82687
  510    20        20117| 0.8096 0.0078  0.8120 0.0073  0.8108 0.0104 |95/95/95| 0.81175 0.00785  0.79518-0.82833  0.78898-
0.83452
  515    15        15033| 0.8115 0.0097  0.8156 0.0077  0.8153 0.0125 |95/95/95| 0.81902 0.00788  0.80185-0.83620  0.79494-
0.84311
  520    10        10058| 0.8078 0.0095  0.8144 0.0081  0.8047 0.0114 |95/95/95| 0.82210 0.01244  0.79269-0.85152  0.77857-
0.86564
 ------------------------------------------------------------------------------------------------------------------------------
---
  525     5         5076| 0.8194 0.0125  0.8184 0.0114  0.8011 0.0164 |95/99/95| 0.81633 0.01852  0.73663-0.89603  0.63251-
1.00015
  527     3         3001| 0.8249 0.0219  0.8237 0.0199  0.8129 0.0159 |
  528     2         1996| 0.8267 0.0378  0.8307 0.0322  0.8241 0.0194 |
```

the minimum estimated standard deviation for the col/abs/tl keff estimator occurs with 0 inactive cycles and 530 active cycles.

the first active half of the problem skips 30 cycles and uses 250 active cycles; the second half skips 280 and uses 250 cycles.
the col/abs/trk-len keff, one standard deviation, and 68, 95, and 99 percent intervals for each active half of the problem are:

problem	keff	standard deviation	68% confidence	95% confidence	99% confidence
first half	0.81362	0.00164	0.81198 to 0.81526	0.81035 to 0.81688	0.80929 to 0.81794
second half	0.80936	0.00164	0.80771 to 0.81100	0.80608 to 0.81263	0.80501 to 0.81370
final result	0.81154	0.00116	0.81038 to 0.81269	0.80923 to 0.81384	0.80848 to 0.81459

the first and second half values of k(collision/absorption/track length) appear to be the same at the 95 percent confidence level.

1plot of the estimated col/abs/track-length keff one standard deviation interval by active cycle number (| = final keff = 0.81154)

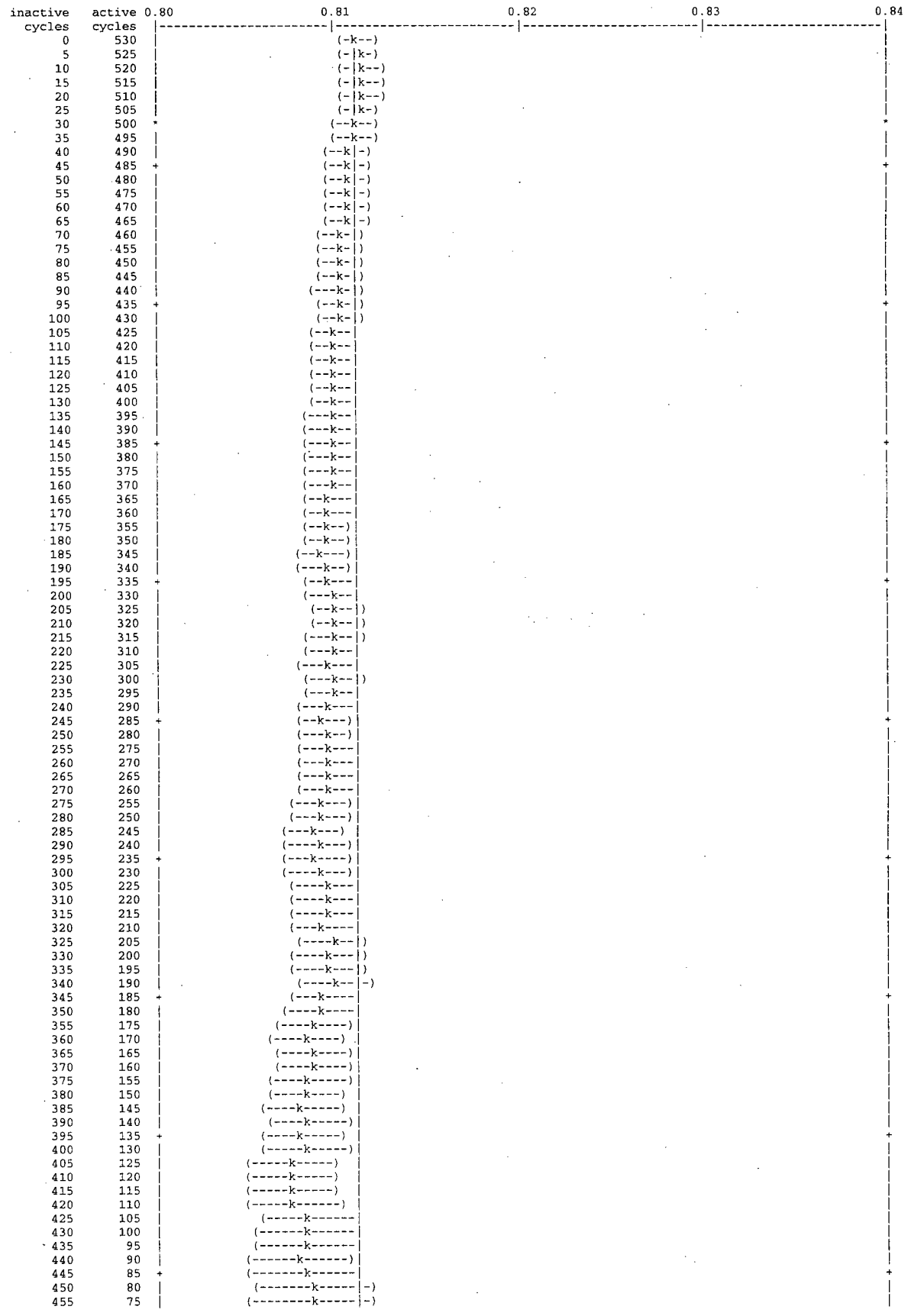

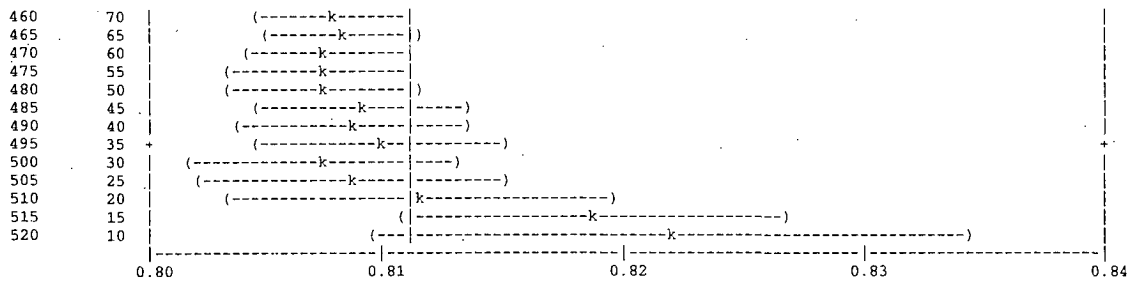


```
 ****************************************************************************************************************************
 dump no.     2 on file P1_Acc_NACCoC_c1.00_g0.00_e0.00_d0.01cm_HP_36mm.inpr     nps =       530870     coll =        75888898
ctm =        11.75   nrn =          769937194

        6 warning messages so far.

 run terminated when    530    kcode cycles were done.

 computer time =    11.91 minutes

 mcnp      version 5     06212004                    10/25/07 23:17:01                    probid =  10/25/07 23:04:59
```

Figure 6.6.15-3 Square Pitch MOX Rods – MOX Services Fuel Composition

```
NAC-LWT Cask - MOX Experiments - Accident Transport Conditions
C
C EXCEL File Version: v2.00
C Run Version: v2.00
C
C Fissile Material Type: MOX Services
C Rod Interior Void Moderator Density: 0.9982 g/cc
C Canister Interior Moderator Density: 0.9982 g/cc
C Canister to Cask Gap Moderator Density: 0.9982 g/cc
C Cask Exterior Moderator Density: 0.0001 g/cc
C Boundary Condition / Distance:  Reflected / 0.01 cm
C
C Fuel Rod Pitch: 3.8 cm
C Fuel Rod Pitch Cofiguration: Square
C Number of Rods: 16
C
C Base Fuel Parameters: NACCoC
C
c Cells - Fuel Rod - NACCoC
1 1 -10.555 -1    u=3 $ Fuel
2 2 -0.9982 -2 +1  u=3 $ Plenum + Fuel to Clad Gap
3 3 -6.56 -3 +2   u=3 $ Clad + End Plugs
4 4 -0.9982 +3    u=3 $ Outside Fuel Rod
C 16 Rods - Square Pitch
10 4 -0.9982 -10
           *trcl=( 1.9000 1.9000 0.0000 )
           lat=1 u=2 fill=-3:3 -3:3 0:0
      2 2 2 2 2 2 2
      2 3 3 3 3 2 2
      2 3 3 3 3 2 2
      2 3 3 3 3 2 2
      2 3 3 3 3 2 2
      2 2 2 2 2 2 2
      2 2 2 2 2 2 2
C PWR Basket - Cells
20  4 -0.9982 -20    fill=2  u=1 $ Rod Array Container
21  5 -0.9982 +20 -21    u=1 $ Basket Cavity
22  7 -2.7020 -22 +21    u=1 $ Basket Body
23  5 -0.9982 +22     u=1 $ Outside
C Cells - LWT Cask Accident Conditions
40 8 -11.344 -43     u=0 $ BotPb
41 5 -0.9982 -42 fill=1    u=0 $ Cavity
42 9 -7.9400 -41 +43    u=0 $ Bottom
43 9 -7.9400 -40 +41 +45 +48 +42 u=0 $ OuterShell
44 9 -7.9400 -44 +47 +42   u=0 $ InnerShellTaper
45 9 -7.9400 -46 +42    u=0 $ InnerShell
46 8 -11.344 -47 +46    u=0 $ Lead
47 8 -11.344 -45 +44 +47   u=0 $ LeadTaper
48 0         -48 +47    u=0 $ LeadGap
49 6 -0.0001 -49 +40    u=0 $ Gap to Reflector
50 0          +49    u=0 $ Boundary

c Surfaces - Fuel Rod - NACCoC
1 RCC 0.0000 0.0000 10.5207 0.0000 0.0000 389.8900 0.4781   $ Fuel pellet stack
2 RCC 0.0000 0.0000 6.3990 0.0000 0.0000 409.4227 0.4876   $ Annulus + Plenum
3 RCC 0.0000 0.0000 5.0800 0.0000 0.0000 411.8226 0.5588   $ Clad + End Caps
c Surfaces - Pitch - NACCoC
10 RPP -1.9000 1.9000 -1.9000 1.9000 -1.0000 453.12    $ Lattice Cell Boundaries
C PWR Basket - Surfaces
20  RPP -6.9294 6.9294 -6.9294 6.9294 0.0000 452.1200  $ Array Container
21  RPP -11.2713 11.2713 -11.2713 11.2713 0.0000 452.1200  $ Basket Opening
22  RCC 0.0000 0.0000 0.0000 0.0000 0.0000 452.1200 16.83512 $ Basket Outer Body
C Surfaces - LWT Cask Accident Conditions
40 RCC 0.0000 0.0000 -26.6700 0.0000 0.0000 507.3650 36.5189 $ Lwt Body
41 RCC 0.0000 0.0000 -26.6700 0.0000 0.0000 26.6700 36.5189 $ Bottom
42 RCC 0.0000 0.0000 0.0000 0.0000 0.0000 452.1200 16.9863 $ Cavity
43 RCC 0.0000 0.0000 -17.7800 0.0000 0.0000 7.6200 26.3525 $ Bottom gamma shield
44 RCC 0.0000 0.0000 0.0000 0.0000 0.0000 444.5000 20.1740 $ Lead id - taper
45 RCC 0.0000 0.0000 0.0000 0.0000 0.0000 444.5000 31.5976 $ Lead od - taper
46 RCC 0.0000 0.0000 13.8176 0.0000 0.0000 416.8648 18.9103 $ Lead id
47 RCC 0.0000 0.0000 13.8176 0.0000 0.0000 416.8648 33.3271 $ Lead od
48 RCC 0.0000 0.0000 13.8176 0.0000 0.0000 416.8648 33.4645 $ Lead gap
*49 RPP -36.5289 36.5289 -36.5289 36.5289 -26.6800 480.7050  $ Container

c
c Materials List
c
C MOX Material Composition Fuel
m1    92235 -5.6994E-03
      92238 -8.0851E-01
      94238 -3.3724E-05
      94239 -6.4076E-02
      94240 -3.0352E-03
      94241 -2.6980E-04
      94242 -3.3724E-05
       8016 -1.1835E-01
C Rod Interior Void Material
m2    1001 2
      8016 1
mt2     lwtr.01
```

```
c Clad Material
m3 26054 -7.063E-05 24050 -4.179E-05 7014 -4.980E-04
      26056 -1.149E-03 24052 -8.370E-04 7015 -1.981E-06
      26057 -2.702E-05 24053 -9.673E-05
      26058 -3.631E-06 24054 -2.448E-05
      40000 -9.823E-01 50000 -1.500E-02
C Canister Interior Non-Fuel Space
m4    1001 2
      8016 1
mt4     lwtr.01
C Canister to Cask Gap Material
m5    1001 2
      8016 1
mt5     lwtr.01
C Cask Exterior Material
m6    1001 2
      8016 1
mt6     lwtr.01
c Aluminum
m7 13027 -1.000E+00
C Water/Glycol
m10   1001 -1.03651E-01
      8016 -6.75619E-01
      6000 -2.20730E-01
mt10    lwtr.01
c Lead
m8 82206 -2.534E-01
      82207 -2.207E-01
      82208 -5.259E-01
c SS304
m9 24050 -7.939E-03 26054 -3.927E-02 28058 -6.384E-02
      24052 -1.590E-01 26056 -6.387E-01 28060 -2.543E-02
      24053 -1.838E-02 26057 -1.502E-02 28061 -1.124E-03
      24054 -4.652E-03 26058 -2.019E-03 28062 -3.639E-03
          28064 -9.623E-04
      25055 -2.000E-02
C Aluminum Honeycomb Impact Limiter
m11   13027 -1.0
C Mode
mode n
C Cell Importances
imp:n 1 18r 0
C
C Criticality Controls
kcode 1000 0.80 30 530
C
C Starting Source Definition
sdef cell=41:20:10:1
      erg=d1
      pos=0 0 10.5207
      rad=d2
      axs=0 0 1
      ext=d3
sp1   -3
si2 0.0000 0.4781
sp2 -21 1
si3 0.0000 389.8900
sp3 0 1
C Print Control
print
C Random Number Generator
rand gen=2 seed=19073486328125 stride=152917 hist=1
c
c Rotation Matrix
*TR1 0.0 0.0 0.0 -30 60 90 -120 -30 90 90 90 0  $ z-rotation -30 degrees
```

Chapter 7

7.1.11 Procedure for Dry Loading of TPBAR Waste Container

This section describes the procedure for the loading of a TPBAR Waste Container into a NAC-LWT cask in a dry loading facility. Appropriate radiological controls and procedures addressing tritium shall be utilized by the licensee, including appropriate monitoring for tritium exposure.

NAC-LWT casks to be used for the transport of TPBARs shall be configured as shown on Drawing No. 315-40-128, including Alternate B port covers.

1. Perform a receiving survey of the ISO and trailer, and inspect for damage.
2. Position the trailer in the designated cask unloading area. Set the trailer brakes and chock the wheels to prevent unintended movement. If site-specific conditions exist that require the trailer to move to allow the cask to be uprighted on its rotation trunnions, release the brakes and remove the chocks when required to complete the uprighting operations. If necessary, the ISO container may be removed from the trailer and secured in the unloading area.
3. Licensees shall receive and survey the package for radiation and removable contamination (for both gross beta-gamma and tritium) per 10 CFR 20 and 49 CFR 173. Record the survey results. If radiation or contamination levels exceed the limits of 49 CFR 173.441 or 173.443, respectively, the licensee shall notify the shipper and ensure the appropriate notifications are completed.
4. Remove the roof from the ISO container and open the front and rear ISO doors. Remove the ISO roof cross members, if installed.
5. Remove the top and bottom impact limiters.
6. Remove the cask tie-down strap. Complete the radiation and contamination surveys of the package as additional surfaces become accessible. Clean the cask surfaces as required for entry into the dry loading facility.
7. Using the cask lifting yoke with lift yoke arm guides removed, engage the lifting trunnions of the front end of the cask. Raise the cask to a vertical position on the rear cask supports, moving the crane and/or trailer, as required, to keep the cask engaged in the rear cask supports and the crane cable vertical. When the cask is vertical, block the trailer wheels and lift the cask from the container.
8. Place the cask in a transfer cart or a loading fixture. Disengage the lifting yoke.
9. Remove the Alternate B vent and drain valve port covers. Replace the metallic seal with an approved spare and inspect the Viton® O-ring seal on each cover. If the Viton® O-ring shows any damage, replace it. Ensure the replacement O-rings are properly installed and seated. Store the port cover to protect the seal surfaces. Visually inspect the vent and drain valved quick-disconnect nipples and replace, if necessary.
10. Loosen and remove all closure lid bolts.
11. Attach the lid removal fixture to the closure lid.

12. Use a transfer cart or loading fixture and move the cask into the loading position.
13. Remove the closure lid and set it on a support that is suitable for radiological control and for maintaining the cleanliness of the closure lid. Carefully inspect the Teflon O-ring seal in the underside of the closure lid. If the O-ring shows any damage, replace it. Remove the metallic O-ring and replace it with an approved spare. Ensure the replacement
    O-rings are properly installed and seated. Inspect the lid bolts and replace any that are damaged. Verify that the TPBAR spacer is installed on the bottom of the cask lid and not damaged when the lid is set down.
14. Install the seal surface protector in the lid cavity, if required.
15. Load the TPBAR Waste Container into the TPBAR basket positioned in the cask cavity using the required grapple or handling system. Verify the contents of the Waste Container comply with the CoC content conditions.
16. Remove the cask seal surface protector, if used, and install the cask closure lid.
17. Use the transfer cart or loading fixture and remove the cask from the loading area.
18. Inspect, install and tighten all 12 closure lid bolts to 260 ± 20 ft-lbs in three passes using the torque sequence indicated on the closure lid.
19. Connect a vacuum pump to the cask vent valve.
20. Install the drain port cover, if drain valve is not required for operations, and torque the port cover bolts to 285 ± 15 in-lbs.
21. Perform the helium mass spectrometer maintenance leakage rate test on the cask lid to leaktight criteria in accordance with the requirements of Section 8.1.3.1, Steps 3 through 10.
22. Following successful completion of the helium backfill and helium leak testing of the lid seal, monitor the cavity volume for tritium and record the results.

    Note: Tritium monitoring system shall have a minimum sensitivity of 5×10^{-3} micro curies/cc.
23. Install Alternate B port covers on the vent and drain openings and torque each port cover bolt to 285 ± 15 in-lbs. Perform a helium leakage rate test on each port cover to leaktight criteria in accordance with Section 8.1.3.3.
24. Decontaminate the cask. Survey the cask surface for gross beta-gamma and tritium removable contamination levels, and radiation dose rates.

    Note: Removable contamination levels and radiation levels shall comply with 49 CFR 173.443 and 173.441, respectively.
25. Using the cask lifting yoke with the guide arms removed, lift and position the cask in the rear cask supports on the ISO/trailer. Engage the trunnion pockets in the bottom end of the cask with the rotation trunnions. Lower the cask to rest on the front tiedown

saddle, moving the crane, and/or trailer, as required, to keep the crane cables vertical. Disengage the cask lifting yoke from the cask lifting trunnions and set it aside.

26. Install and attach the cask tiedown strap. Install the cask top and bottom impact limiters.

27. Install a tamper-indicating seal to one of the top impact limiter ball lock pins.

28. Install roof cross members, close ISO container doors, and replace ISO container roof.

29. Complete a Health Physics survey on the external surface of the package and record the results. Complete dose rate measurements at the cask surface, at 1 meter from the cask surface, and at 2 meters from the vertical plane of the side of the transport vehicle. The maximum dose rate at 1 meter from the cask is the transport index (TI). Ensure compliance with 10 CFR 71.87(i) and observe the following criteria.

    - If the dose rate is less than 2 mSv/h (200 mrem/hr) at all accessible points on the external surface of the cask, and the TI is less than 10, the package must meet the requirements of 10 CFR 71.47 (a).
    - If the dose rate is greater than 2 mSv/h (200 mrem/hr), but is less than 10 mSv/h (1000 mrem/hr) at any point on the external surface of the package, or the TI is greater than 10, the package must be shipped as "exclusive use" and meet the requirements of 10 CFR 71.47 (b), (c) and (d). If the dose rate and shipping requirements of 10 CFR 71.47 (b), (1), (2), (3) and (4) cannot be met, the package cannot be shipped.

    Note: 10 CFR 71.47 (c) and (d) require the shipper to provide the carrier with written instructions for maintenance of the exclusive use shipment. The instructions must be included with the shipping paper information. The instructions must be sufficient so that, when followed, they cause the carrier to avoid actions that unnecessarily delay delivery or unnecessarily result in increased radiation levels or radiation exposures to transport workers or members of the general public.

    - If the dose rate is > 10 mSv/h (1000 mrem/hr) at any point on the external surface of the cask, the cask exceeds the limits of 10 CFR 71.47 and cannot be shipped.

30. Complete the shipping document, carrier instructions (if required), and apply appropriate placards and labels.

7.1.12 Procedure for Wet Loading PWR MOX Fuel Rods in a Transport Canister Into the NAC-LWT Cask

PWR MOX fuel rods (or combinations of PWR MOX and UO_2 PWR fuel rods) are required to be loaded into a screened or free flow PWR/BWR Rod Transport Canister prior to loading into the NAC-LWT cask for transport. Although a maximum quantity of 16 MOX fuel rods may be shipped, it is required that the 5 × 5 rod insert be used to position the rods in the transport canister (i.e., the 4 × 4 insert is not authorized for use for the transport of MOX fuel rods).

In order to satisfy the increased potential for release of significant quantities of radioactive materials, and as recommended by NUREG-1617, Supplement 1, the NAC-LWT cask assembly specified for the transport of PWR MOX fuel rods contained in a transport canister provides a leaktight containment boundary (e.g., Alternate B port covers with metallic seals are utilized in combination with the closure lid and its metallic seal). All cask penetrations are individually helium leakage tested to meet the leaktight containment testing requirements of ANSI N14.5-1997.

The screened or free flow transport canister with a 5 × 5 rod insert will be loaded with up to 16 PWR MOX fuel rods (or a combination of up to 16 PWR MOX and UO_2 PWR fuel rods). In addition to the 16 PWR MOX fuel rods, up to 9 zirconium alloy-based burnable poison rods (BPRs) may be loaded into the unused insert openings.

NAC-LWT casks to be used for the transport of MOX fuel rods shall be configured as shown on Drawing No. 315-40-104, Assembly 97, including Alternate B port covers.

1. Perform a receiving survey of the empty cask and inspect for damage.
2. Position a trailer in the designated cask unloading area. Set the trailer brakes and chock the wheels to prevent unintended movement. If site-specific conditions exist that require the trailer to move to allow the cask to be uprighted on its rotation trunnions, release brakes and remove the chocks when required to complete uprighting operations. If an ISO is used, it may be removed from the trailer and secured in the unloading area.
3. Remove the roof from the ISO container and open the front and rear ISO doors. Remove roof cross-members, if installed.

   Note: Verify that the package nameplate displays the package identification number, USA/9225/B(U)F-96, as required by the CoC for PWR MOX fuel rods.

4. Perform a Health Physics survey of the cask and adjacent surfaces of the trailer.

   Note: A receiving survey of the cask and transporter must be performed as soon as practical after arrival at the site to assure compliance with 10 CFR 71.87(i) and 10 CFR 71.47, and to assure timely reporting of any reportable noncompliance.

5. Remove the top and bottom impact limiters.
6. Remove the cask tie-down strap.
7. Using the lifting yoke with the guides removed, engage the lifting trunnions. Raise the cask to vertical by rotating the cask rotation sockets on the rear cask supports, moving the crane and/or trailer as required to maintain the lift yoke engaged to the trunnions and the cask engaged in the rear supports. When the cask is fully vertical, lift the cask from the supports and remove it from the trailer/container.
8. Place the cask in the decontamination pit or other designated area. Disengage the lifting yoke. Clean cask surfaces of road dirt, as required, for entry into the spent fuel pool.
9. Visually inspect the neutron shield tank fill, drain and level inspection plugs for signs of neutron shield fluid leakage. If leakage is detected, verify shield tank fluid level and correct, as required.
10. Remove the Alternate B vent and drain valve port covers. Prior to reinstallation of the port covers, replace the metallic O-ring seal with an approved spare and inspect the Viton® O-ring seal for each port cover. If the Viton® O-ring shows any damage, replace it. Ensure that the replacement O-rings are properly installed and seated. Store the port covers to protect the seal surfaces. Visually inspect the valved quick-disconnect nipples and replace them, if necessary.
11. Remove closure lid bolts. Attach the lid lift slings to the closure lid. Remove the closure lid and set it on a support that is suitable for radiological control and for maintaining the cleanliness of the closure lid. Prior to reinstallation of the lid, carefully inspect the Teflon O-ring seal in the underside of the closure lid. If the O-ring shows any damage, replace it. Remove the metallic O-ring and replace it with an approved spare. Ensure that the replacement O-ring(s) is properly installed and seated. Inspect the lid bolts and replace any that are damaged. Ensure that the Rod Transport Canister spacer is not damaged when the lid is set down.
12. Visually inspect the inner cavity for foreign material or damage. Install or verify the presence of the drain tube and the PWR basket assembly.
13 Fill the cask cavity with clean water. Install lift yoke arm guides and remote actuation components on the cask lifting yoke.
14. Engage the cask lifting yoke with the cask lifting trunnions and pick up the cask. Carefully lower the cask to the bottom of the cask loading area while spraying the cask down with clean water.
15. Disengage the lifting yoke from the cask and remove the yoke from the pool.
16. Identify the PWR/BWR Rod Transport Canister to be loaded and verify that a 5 × 5 rod insert is located in the canister.
17. Identify the PWR MOX fuel rods (and standard PWR rods and BPRs, as applicable) to be loaded into the PWR/BWR Rod Transport Canister. Verify that the fuel rods and BPRs comply with the content type, form, heat load, minimum cooling time and

quantity conditions of the NAC-LWT CoC. Load the screened or free flow PWR/BWR transport canister with up to 16 PWR MOX fuel rods, a combination of MOX and standard PWR rods, and up to 9 BPRs in the open tube locations in the 5 × 5 insert. Perform an independent verification of the fuel rod selection and loading process.

18. Install the transport canister lid and torque the lid bolts to 35 ± 5 inch-pounds.

19. Position the loaded PWR/BWR Rod Transport Canister over the cask and then carefully lower it into the cask to avoid damage to the cask sealing surfaces. Note that the transport canister may be loaded into the cask with the PWR basket insert.

20. Position the cask lifting yoke over the cask closure lid. Attach the slings to the closure lid and cask lifting yoke. Lower the yoke over the cask.

21. Position the closure lid over the cask and verify that the appropriate lid spacer is installed per the approved PWR MOX fuel rod transport arrangement in Drawing 315-40-104, Section 1.4. Lower the closure lid into the lid recess using the lid match marks as guides to align the lid. Visually confirm that the closure lid is flush with the top of the cask and properly seated.

22. Lower the cask handling yoke to slack the closure lid cables. Engage the lift yoke to the lifting trunnions and begin lifting the cask.

    Note: Visually verify the yoke engagement before lifting the cask.

23. Raise the cask until the lid is slightly above the surface of the pool. At the option of the licensee/user, a number of closure lid bolts (4 to 12) may be installed hand tight.

24. Raise the cask clear of the pool, rinsing the yoke and cask with clean water and transfer the cask to the decontamination pit or other work area. Remove the yoke and lid lift slings.

25. Install and tighten the 12 closure lid bolts to 260 ± 20 ft-lb in three passes, using the torque sequence stamped on the closure lid.

26. At the option of the licensee/user, a 25 to 50 gallon clean water flush of the cask cavity may be performed by connecting a valved clean water line to the drain valve and a valved drain line to the vent valve. After the cavity flushing is completed, if performed, disconnect the water supply and drain lines.

27. Connect a nitrogen or helium gas supply line to the vent valve and the drain line to the drain valve.

28. Open the nitrogen or helium gas supply valve and pressurize the cask cavity (<30 psig) to force out the water. Continue to supply pressurized helium to the cask for a minimum of five minutes after the last residual free water discharges from the drain line. Remove the drain and gas supply lines and attach a vacuum drying system (VDS) to the cask vent valve.

29. Evacuate the cask cavity to a vacuum pressure of less than 10 torr (13 mbar) and continue vacuum pumping for a minimum of 15 minutes.

30. At the end of the vacuum pumping period, isolate the cask cavity from the vacuum pump and stop the pump. Monitor the cask cavity pressure for a minimum of 10 minutes. If the pressure rise is less than 5 torr (6.7 mbar), the cavity is verified as dry of free water. If the pressure rise is greater than 5 torr (6.7 mbar), repeat vacuum drying until the dryness verification results are satisfactory.

31. Backfill the cask cavity with helium to 0 psig (1 atmosphere, absolute), +2, -0 psi. Disconnect the VDS.

32. Perform the helium leakage test of the closure lid containment O-ring using a Helium Mass Spectrometer Leak Detector (He MSLD) in accordance with the requirements of Section 8.1.3.1, Steps 6 through 10, with leakage rate acceptance criteria per 8.1.3.1, Step 9(b).

33. Install, torque the high-strength bolts to 285 ± 15 inch-pounds, and helium leakage test the Alternate B vent and drain port covers to leaktight criteria in accordance with Section 8.1.3.3.2, Steps 1-10.

34. Decontaminate the cask. Survey the cask for surface contamination and radiation dose rates.

    Note: Ensure compliance with 10 CFR 71.87(i) and 10 CFR 71.47.

35. Remove lift yoke arm guides. Engage the cask lifting yoke to the lifting trunnions.

36. Lift the cask and position the cask rotation sockets in the rear rotation trunnions of the rear support structure. Carefully lower the cask to the horizontal transport orientation resting on the front saddle by moving the crane and/or trailer, as required, to maintain cask engagement to the rear supports.

37. Disengage the cask lifting yoke from the cask lifting trunnions and remove it from the area.

38. Install the cask tie-down strap. Install the top and bottom impact limiters.

39. Install tamper seal wire and number seal on the top attachment point of the top impact limiter.

40. Install roof cross-members, close ISO container doors, and replace ISO container roof.

41. Complete radiation and contamination surveys of the external surfaces of the package and record the data. Ensure removable contamination and radiation dose rate survey results comply with the limits specified in 10 CFR 71.87(i) and (j).

42. Measure the dose rate in millirems per hour at one meter from the package surface to determine the Transport Index (TI). Indicate the TI on the Radioactive Material labels applied to the package in accordance with 49 CFR 172, Subpart E.

43. Determine the appropriate Criticality Safety Index (CSI) assigned to the package contents in accordance with the CoC, and indicate the correct CSI on the Fissile Material label applied to the package per 49 CFR 172, Subpart E.

44. Apply appropriate placards to the transport vehicle in accordance with 49 CFR 172, Subpart F.

45. Complete the shipping documents and provide the carrier with instructions regarding the requirements for maintaining an exclusive use shipment.

Chapter 9

Table of Contents

9 REFERENCES

"AISC Manual of Steel Construction," 8th Edition, The American Institute of Steel Construction, Inc., 1990.

Alcoa Aluminum Handbook, Pittsburgh, PA, Aluminum Company of America, 1959.

"Aluminum Construction Manual," 2nd Edition, Section 3, The Aluminum Association, Washington, D.C., 1972.

"Annual Book of ASTM Standards," Section 3, Volume 03.01, American Society for Testing and Materials, 1986.

"ANSYS' Computer Code for Large-Scale General Purpose Engineering Analysis," Swanson Analysis Systems, Inc., Houston, PA.

"ASME Boiler and Pressure Vessel Code," Section III, Subsection NG – Core Support Structures and Subsection NH – Class 1 – Components in Elevated Temperature Service, The American Society of Mechanical Engineers, 1995 with Addenda through 1997.

Baker, E.H., L. Kovalevsky, and F.L. Rish, Structural Analysis of Shells, New York, McGraw-Hill Book Co., December 1966.

Bates, O.K., "Thermal Conductivities of Aqueous Ethylene Glycol Solutions," St. Lawrence University, Canton, NY.

Baumeister, T. and L.S. Marks, Standard Handbook for Mechanical Engineers, 7th Edition, New York, McGraw-Hill Book Co., December 1966.

BAW-246, "NULIF – A Neutron Spectrum Generator, Few-Group Constant Calculator, and Depletion Code," Babcock & Wilcox, August 1976.

Bevington, P.R., Data Reduction and Error Analysis for the Physical Sciences, New York, McGraw-Hill Book Company.

Biggs, J.M., Introduction to Structural Dynamics, New York, McGraw-Hill Book Co., 1964.

Blake, A., "Charts Simplify Calculations for Moments and Deflections of Circular Arches," Machine Design, Cleveland, Penton Publishing Co., December 25, 1958.

Blodgett, O.W., Design of Welded Structures, Cleveland, James F. Lincoln Arc Welding Foundation, 1972.

Book of Standards, Part 7, American Society for Testing and Materials, 1970.

Bruhn, E.F., Analysis and Design of Flight Vehicle Structures, 1st Edition, Cincinnati, Tri-State Offset, Co., 1965.

Bucholz, J.A., "Scoping Design Analyses for Optimized Shipping Casks Containing 1-, 2-, 3-, 5-, 7-, or 10-year old PWR Spent Fuel," Oak Ridge National Laboratory, ORNL/CSD/TM-149, January 1983.

Bucholz, J.A., "XSDOSE: A Module for Calculating Fluxes and Dose Rates at Points Outside A Shield," Vol. 2, Sect. F4 of SCALE-4, August 1981.

Bucholz, J.A., et. Al., "SAS1: A One-Dimensional Shielding Analysis Module."

Cain, V.R. and R.E. Malenfant, "QAD-CG, The Combinatorial Geometry Version of the QAD-P5A Point Kernam Shielding Code," Bechtel Power Corporation, July 1977.

CCC-545, "SCALE-4, A Modular Code System for Performing Standardized Computer Analysis of Licensing Evaluation," ORNL, June 1990.

Chun, R., M. Witte, and M. Schwartz, "Dynamic Impact Effects on Spent Fuel Assemblies," UCID-21246, Lawrence Livermore National Laboratory, October 1987.

"Coefficient of Cubical Expansion for Glycol, Water, and Glycol-Water Solutions," E.I. du Pont de Nemours & Co., Inc., Wilmington, DE, 1963.

Cook, I. And R.S. Peckover, "Effective Thermal Conductivity of Debris Beds," Post Accident Debris Cooling, Proceedings of the Fifth Post Accident Heat Removal Information Exchange Meeting, 40-45, 1982.

Cragoe, C.S., "Properties of Ethylene Glycol and Its Aqueous Solutions," National Bureau of Standards.

DOE/ET/34014-10, "Extended Fuel Burnup Demonstration Program," U.S. Department of Energy, September 1983.

Gallagher, C., "NL Industries Internal Test Report on Tensile Properties of Chemical Lead at Elevated Temperatures," Central Research Laboratory, Highstown, NJ, February 1976.

Gerard, G. and H. Becker, "Handbook of Structural Stability," Part III, TN3783, National Advisory Committee for Aeronautics, 1957.

Greene, N.M., J.L. Lucius, L.M. Petrie, W.E. Ford III, J.E. White, and R.Q. Wright, "AMPX – A Modular Code System for Generating Multigroup Neutron-Gamma Libraries from ENDF/B," ORNL/TM-3706, Oak Ridge National Laboratory, March 1976.

Greene, N.M. and L.M. Petrie, "XSDRNPM-S: A One-Dimensional Discrete Ordinates Code for Transport Analysis," Vol. 2, Sect. F3 of SCALE-4, January 1983.

Handbook of Chemistry and Physics, 49th Edition, Cleveland, OH, The Chemical Rubber Company, 1968.

Hermann, O.W. and R.M. Westfall, "ORIGEN-S: SCALE System Module to Calculate Fuel Depletion, Actinide Transmutation, Fission Product Buildup and Decay and Associated Radiation Source Terms," Vol. 2, Sect. F7 of SCALE-4, February 1989.

Hermann, O.W., "SAS2(H): A Coupled One-Dimensional Depletion and Shielding Analysis Code," Vol. 1, Sect. S2 of SCALE-4, June 1990.

IAEA Transportation Safety Standards (TS-R-1), "Regulations for the Safe Transport of Radioactive Material," June 2000.

Johnson, E.B. and R.K. Reedy, "Critical Experiments with SPERT-D Fuel Elements," ORNL-TM-1207, July 14, 1965.

Jordan, W.C., N.F. Landers, and L.M. Petrie, "Validation of KENO-Va Comparison with Critical Experiments," ORNL/CSD/TM-238, December 1986.

Juvinall, R.C., Stress, Strain, and Strength, New York, McGraw-Hill Book Co., 1967.

Kinsey, R., "Data Formats and Procedures for the Evaluated Nuclear Data File, ENDF," ENDF-102, Second Edition, Brookhaven National Laboratory, 1979.

Kreith, F., Principles of Heat Transfer,2nd Edition, Scranton, PA, International Textbook Company, 1965.

Manual of Steel Construction, 8th Edition, New York, American Institute of Steel Construction, Inc., 1990.

Mark's Standard Handbook for Mechanical Engineers, 9th Edition, McGraw-Hill Book Company, New York.

Merritt, F.S., Standard Handbook for Civil Engineers, McGraw-Hill Book Company, New York, 1968.

Metals Handbook, 9th Edition, American Society of Metals.

MIL-HDBK-5A, "Metallic Materials and Elements for Aerospace Vehicle Structures," Department of Defense, February 1966.

MIL-HDBK-5C, "Metallic Materials and Elements for Aerospace Vehicle Structures," Department of Defense, December 1978.

MIL-HDBK-5E, "Metallic Materials and Elements for Aerospace Vehicle Structures," Department of Defense, May 1989.

Nelms, H.A., "Effects of Jacket Physical Properties and Curvature on Puncture Resistance," Structural Analysis of Shipping Casks, Volume 3, ORNL/TM-1312, Oak Ridge National Laboratory, June 1968.

"Nuclear Systems Materials Handbook," Volume 1, Revision 1, Hanford Engineering Development Laboratories, Richland, WA, March 10, 1976.

NUREG-0612, "Control of Heavy Loads at Nuclear Power Plants," U.S. Nuclear Regulatory Commission, July 1980.

NUREG-1617, Supplement 1, "Standard Review Plan for Transportation Packages for MOX Spent Nuclear Fuel," U.S. Nuclear Regulatory Commission, September 2005.

NUREG/CR-0733, "Critical Separation Between Sub-Critical Clusters of 4.29 w/o U^{235} Enriched UO_2 Rods in Water with Fixed Neutron Poisons," S.R. Bierman, B.M. Durst, E.D. Clayton, Battelle Pacific Northwest Laboratories, May 1978.

NUREG/CR-0200, Volume 2, Section F2, "SCALE-2 NITAWL-S, Resonance Self-Shielding by the Nordheim Method," N. M. Green and L. M. Petrie, Oak Ridge National Laboratory, October 1981.

NUREG/CR-6361, "Criticality Benchmark Guide for Light-Water-Reactor Fuel in Transportation and Storage Packages," U.S. Nuclear Regulatory Commission, March 1997.

NUREG/CR-6487, Anderson, B.L., Carlson, R.W., and Fisher, L.E., "Containment Analysis for Type B Packages Used to Transport Various Contents," Lawrence Livermore Laboratory, 1996.

NUREG/CR-0200, Volume 2, Section F3, "SCALE-2 XSDRNMP-S, A One Dimensional Discrete Ordinates Program for Transport Analysis," R.M. Westfall, L.M. Petrie, N.M. Greene, J.L. Lucius, Oak Ridge National Laboratory, June 1983.

NUREG/CR-0481, "An Assessment of Stress-Strain Data Suitable for Finite-Element Elastic-Plastic Analysis of Shipping Containers," H.J. Rack and G.A. Knorovsky, Sandia Laboratories, SAND77-1872, September 1978.

NUREG/CR-0796 PNL-2827, "Criticality Experiments with Sub-Critical Clusters of 2.35 and 4.29 w/o U^{235} Enriched $U0_2$ Rods in Water with Uranium or Lead Reflecting Walls," S.R. Bierman, B.M. Durst, E.D. Clayton, Battelle Pacific Northwest Laboratories, April 1979.

Paxton, H.C., Critical Dimensions of Systems Containing U^{235}, Pu^{239}, and U^{233}," TID-7028, June 1964.

Peery, D.J., Aircraft Structures, New York, McGraw-Hill Book Company, 1950.

Petrie, L.M. and N.F. Cross, "KENO-IV: An Improved Monte Carlo Criticality Program," ORNL-4938, Oak Ridge National Laboratory, November 1975.

PNL-2438, "Critical Separation Between Sub-Critical Clusters of 2.35 w/o U^{235} Enriched UO_2, Rods in Water with Fixed Neutron Poisons," S.R. Bierman, E.D. Clayton, B.M. Durst, Battelle Pacific Northwest Laboratories, October 1977.

Radiological Health Handbook, U.S. Department of Health, Education and Welfare, Rockville, MD, January 1970.

"Regulations for the Safe Transport of Radioactive Materials," Safety Series No. 6, Revised Edition, International Atomic Energy Agency, 1973.

"Research and Advanced Development Applied Mechanics," Volume 1, Engineering Data Sheets, Avco Corporation, 1962.

Resnick, R. and D. Halliday, Physics, 3rd Edition, Part 1, New York, John Wiley & Sons, 1977.

Roark, R.J., Formulas for Stress and Strain, 4th Edition, New York, McGraw-Hill, Inc., 1965.

Roark, R.J., and W.C. Young, Formulas for Stress and Strain, 5th Edition, New York, McGraw-Hill, Inc., 1975; 6th Edition, 1989.

Roddy, J.W., H.C. Claiborne, R.C. Ashline, P.J. Johnson, B.T. Rhyne, "Physical and Decay Characteristics of Commercial LWR Spent Fuel," ORNL/TM-9591/Vl-Rl, Oak Ridge National Laboratory, January 1986.

"Safety Analysis Report for the NLI-1/2 Spent Fuel Shipping Cask," Nuclear Assurance Corporation, USA/9010/B()F, December 12, 1985.

Schaeffer, N.M., Reactor Engineering for Nuclear Engineers, Springfield, VA, 1984.

"Screw-Thread Standards for Federal Services," U.S. Department of Commerce, 1957.

Shamban TFE O-Ring Seals, Spec. 22-53, Part No. S11214-460, W.S. Shamban & Co., Fort Wayne, IN, 1966.

Shappert, L.B., "Cask Designer's Guide: A Guide for the Design, Fabrication, and Operation of Shipping Casks for Nuclear Applications," ORNL-NSIC-68, Oak Ridge National Laboratories, February 1970.

Shappert, L.B., and W.D. Box, "The Drop Test Facility at the Oak Ridge National Laboratory: A Facility Available to Private Industry," Oak Ridge National Laboratory, Oak Ridge, TN.

Shigley, J.E., Mechanical Engineering Design, 3rd Edition, New York, McGraw-Hill, Inc., 1977.

Shigley, J.E., and C.R. Mischke, Standard Handbook of Machine Design, New York, 1986.

Singer, F.L., Strength of Materials, New York, Harper & Brothers, 1951.

"Table Speeds Calculation of Strength of Threads," Product Engineering, November 27, 1961.

Tang, J.S. "SAS4: A Monte Carlo Cask Shielding Analysis Module Using An Automated Biasing Procedure," March 1989.

"Test Plan: LWT Quarter-Scale Model Drop Tests," Document No. 315-P-01. Nuclear Assurance Corporation, May 31, 1988.

Tietz, T.E., "Determination of the Mechanical Properties of High Purity Lead and a 0.058% Copper-Lead Alloy," Stanford Research Institute, Menlo Park, CA, WADC Technical Report 57-695, ASTIA Document No. 151165, April 1958.

Timoshenko, S., Strength of Materials, 3rd Edition, New York, R. E. Krieger Publishing Co., 1976.

Timoshenko, S., Theory of Plates and Shells, 1st Edition, New York, McGraw-Hill Book Co., 1940.

Timoshenko and Gere, Theory of Elastic Stability, 2nd Edition, New York, McGraw-Hill, Inc., 1961.

Timoshenko, S. and Young, Theory of Structures, New York, McGraw-Hill Book Co., 1965.

Turner, W.D., D.C. Elrod, and I.I. Simon-Tov, "HEATING 5 - An IBM 360 Heat Conduction Program," Oak Ridge National Laboratory, ORNL/CSD/TM-15, March 1977.

Williamson, R.A. and R.R. Alvy, "Impact Effect of Fragments Striking Structural Elements," Holmes and Harver, Inc., 1973.

Childs, K.W., HEATING 7.2 User's Manual, Oak Ridge National Laboratory, ORNL/NUREG/CSD-2/V2/R5, September 1995.

Avallone, E. and T. Baumeister, Marks' Standard Handbook for Mechanical Engineers, 9th Edition, New York, McGraw-Hill Book Company, 1987.

"SCALE 4.3 Modular Code System for Performing Standardized Computer Analyses for Licensing Evaluation for Workstations and Personal Computers," CCC-545, September 1995.

Herman, O.W., "SAS2H: A Coupled One-Dimensional Depletion and Shielding Analysis Module," and C.V. Parks, ORNL/NUREG/CSD-2/V1/R5, Volume 1, Section S2, September. 1995.

Tang, S., "SAS4: A Monte Carlo Cask Shielding Analysis Module Using an Automated Biasing Procedure," ORNL/NUREG/CSD-2/V1/R5, Volume 1, Section S4, September, 1995.

Bucholz, J.A., Landers, N.F., and Petrie, L.M., ORNL/NUREG/CSD-2/V3/R5, Section M7, "The Material Information Processor For Scale," September 1995.

Greene, M., Westfall, R.M., and L.M. Petrie, ORNL/NUREG/CSD-2/V2/R5, "NITAWL-II: Scale System Module For Performing Resonance Shielding And Working Library Production" September 1995.

Jordan, W.C., ORNL/NUREG/CSD-2/V3/R5, Section M4, "Scale Cross-Section Libraries," September 1995.

Landers, N. F., and Petrie L.M, ORNL/NUREG/CSD-2/V1/R5, Section C4, "CSAS: Control Module For Enhanced Criticality Safety Analysis Sequences," September 1995.

Mele, Ravink and Trkov, "TRIGA Mark II Benchmark Experiment, Part I Steady State Operation," Jozef Stefan Institute, Nuclear Technology, Vol. 105, January 1994.

Petrie L.M., and Landers, N.F., ORNL/NUREG/CSD-2/V2/R5, Section F11, "KENO-Va: An Improved Monte Carlo Criticality Program with Supergrouping," September 1995.

Tomsio, M., "Characterization of Triga Fuel," ORNL/Sub/86-22047/3, GA-C18542, Oak Ridge National Laboratory, Oak Ridge, Tennessee, October 1986.

Krieth, F., and Bohn, M.S., "Principals of Heat Transfer," 5th Edition, West Publishing Company, 1993.

Incropera, F.P., and DeWitt, D.P., "Fundamentals of Heat and Mass Transfer," 4th Edition, John Wiley and Sons, 1996.

Owen, D.B., "Factors for One-Sided Tolerance Limits and for Variables Sampling Plans," SCR-607, 1963.

ANSI N14.5-1987, "American National Standard for Radioactive Materials - Leakage Tests on Packages for Shipment," American National Standards Institute, 1987.

ANSI/ANS - 8.1-1983, "Nuclear Criticality Safety in Operations with Fissionable Materials Outside Reactors."

ANSI/ANS - 8.17-1984, "Criticality Safety Criteria for the Handling, Storage, and Transportation of LWR Fuel Outside Reactors."

Bierman, S.R., Clayton, E.D., "Criticality Experiments with Subcritical Clusters of 2.35 w/o and 4.31 w/o ^{235}U Enriched UO_2 Rods in Water at a Water-to-Fuel Volume Ratio of 1.6," NUREG/CR-1547, July 1980.

Baldwin, N.M., Hoovler, G.S., Eng, R.L., and Welfare, F.G., "Critical Experiments Supporting Close Proximity Water Storage of Power Reactor Fuel," B&W-1484-7, July 1979.

Bierman, S.R., and E.D. Clayton, "Criticality Experiments with Subcritical Clusters of 2.35 w/o and 4.31 w/o ^{235}U Enriched UO_2 Rods in Water with Steel Reflecting Walls," Nuclear Technology, Volume 54, pp. 131-144, August 1981.

Bierman, S.R., Durst, B.M., and Clayton, E.D., "Criticality Experiments with Subcritical Clusters of 2.35 and 4.31 w/o ^{235}U Enriched UO_2 Rods in Water with Uranium or Lead Reflecting Walls," NUREG/CR-0796, April 1979.

Bierman, S.R., "Criticality Experiments to Provide Benchmark Data on Neutron Flux Traps," PNL-6205/UC-714, June 1988.

Manaranche, J.C. et al, "Dissolution and Storage Experiment with 4.75 w/o ^{235}U Enriched UO_2 Rods," Nuclear Technology, Volume 50, September 1980.

Machinery's Handbook, 25th Edition, Industrial Press, Inc., New York, NY, 1996.

BISCO Products Data, "FPC Fireblock Silicone Foam," BISCO Products, Inc., Park Ridge, IL, February 1988.

Letter from Rogers Corporation, Bisco Materials Unit, dated February 2, 1999, from Daniel J. Kubrick.

Interim Staff Guidance (ISG)-11, Revision 3, "Cladding Considerations for the Transportation and Storage of Spent Fuel," U.S. Nuclear Regulatory Commission, November 2003.

Holometrix Micromet test report NCN-2, dated May 2000.

Ugural, A.C. and Fenster, S.K., "Advanced Strength and Applied Elasticity," Second Edition, Elsevier Science Publishing Company, New York, New York, 1987.

NAC Specification 315-S-09, "O-Ring Temperature Testing for the LWT Alternate Port Cover," Revision 0, February 2000.

"HTGR/RERTR Fuel Materials Characterization and Packaging Report," PC-00384/1, General Atomics, San Diego, CA, April 2002.

UNIFRAX Product Specifications, Fiberfrax® Ceramic Fiber Paper, C-1423, Unifrax Corporation, Niagara Falls, NY, June 1996.

LLNL Report UCRL-53441, "Review of Hydrogen Isotope Permeability Through Materials"

RSIC Computer Code Collection, *ORIGEN2.1; Isotope Generation and Depletion Code – Matrix Exponential Method,* CCC-371, Oak Ridge National Laboratory, Oak Ridge TN, 1996.

Y.K. Sakamoto and M. Sugisaki, "Fusion Science and Technology," Vol. 41, pp 912-914, May 2002.

"Aluminum Standards and Data," Table 2.2, The Aluminum Association, Washington, DC, 1997.

Blake, Alexander, "Practical Stress Analysis in Engineering Design," 2nd Edition, Marcel Dekker Inc., New York, 1990.

ORNL/TM-12667, "Validation of the SCALE System for PWR Spent Fuel Isotopic Composition Analyses," Oak Ridge National Laboratory, March 1995.

ORNL/TM-13317, "An Extension of the Validation of SCALE (SAS2H) Isotopic Prediction for PWR Spent Fuel," Oak Ridge National Laboratory, September 1996.

NUREG/CR-6798, "Isotopic Analysis of High Burnup PWR Spent Fuel Samples from the Takahama-3 Reactor," US Nuclear Regulatory Commission, January 2003.

ORNL/TM-13315, "Validation of SCALE (SAS2H) Isotopic Predictions for BWR Spent Fuel," Oak Ridge National Laboratory, September 1998.

ORNL/TM-13687, "Prediction of the Isotopic Composition of UO_2 Fuel from a BWR: Analysis of the DU1 Sample from the Dodewaard Reactor," Oak Ridge National Laboratory, October 1998.